#234037
P.483

(NASA-CR-185902) SPACE SHUTTLE THERMAL PROTECTION SYSTEM DEVELOPMENT Midterm Summary Report, 1 Jul. - 12 Nov. 1971 (Lockheed Missiles and Space Co.) 483 p

N90-70119

Unclas
00/16 0234037

Lockheed

**MISSILES & SPACE COMPANY**

A GROUP DIVISION OF LOCKHEED AIRCRAFT CORPORATION

SUNNYVALE, CALIFORNIA

NAS 9-12083
DRL-11, DRD-MA-067T
LMSC-A997045
12 November 1971

# MIDTERM SUMMARY REPORT FOR SPACE SHUTTLE THERMAL PROTECTION SYSTEM DEVELOPMENT

For the Period From
1 July 1971 to 12 November 1971
to
National Aeronautics and Space Administration
Manned Spacecraft Center
Houston, Texas

Approved by:

R. D. Buttram, Project Leader

K. J. Forsberg, Manager
Structures Technology

J. F. Milton, Director
Manned Space Programs

LOCKHEED MISSILES & SPACE COMPANY

# DISTRIBUTION SHEET

One copy to:

NASA Manned Spacecraft Center
Orbiter Procurement Section
Houston, Texas 77058
Attention: Paul W. Liebhardt/BC42

NASA Manned Spacecraft Center
Technology Utilization Office
Houston, Texas 77058
Attention: John Wheeler, JM7

NASA Ames Research Center
Mail Stop 234-1
Moffett Field, California 94035
Attention: Howard Larson

Langley Research Center
MD-Thermal Protection
Mail Stop 206
Hampton, Virginia 23365
Attention: Andrew J. Chapman

George C. Marshall Space Flight Center
S&E-ASTN-M
Huntsville, Alabama 35812
Attention: Wilbur A. Riehl

Twenty (20) copies and one (1) reproducible to:

NASA Manned Spacecraft Center
Structures and Mechanics Division
Houston, Texas 77058
Attention: ES5/Don Tillian

# FOREWORD

This is the Mid-Term Report prepared by Lockheed Missiles & Space Company, Inc. (LMSC) for NASA Contract NAS9-12083, Space Shuttle Thermal Protection System Development. Documented in this report are the LMSC efforts performed to date for the National Aeronautics and Space Administration Manned Spacecraft Center, under the direction of the Thermal Technology Branch of the Structures and Mechanics Division, D. J. Tillian, COR.

The general arrangement of this report is in accordance with the specific task efforts described in the contract statement of work. Pertinent information derived from related contract and in-house efforts is included in the applicable sections.

CONTENTS


| Section | | Page |
|---|---|---|
| 1 | PROGRAM PLAN | 1-1 |
| 2 | DESIGN | 2-1 |
| | 2.1 Criteria Requirements and Environments | 2-1 |
| | TASK 2.2 Design Methods | 2-24 |
| 3 | MATERIALS OPTIMIZATION | 3-1 |
| | 3.1 Coating Evaluation | 3-1 |
| | 3.2 Potential Failure Modes | 3-18 |
| | 3.3 Attachment Methods | 3-24 |
| | 3.4 Non-Destructive Evaluation (NDE) Methods | 3-29 |
| 4 | PROPERTY CHARACTERIZATION | 4-1 |
| | 4.1 Thermophysical Properties | 4-1 |
| | 4.2 Mechanical Properties | 4-27 |
| 5 | ENVIRONMENTAL RESPONSE BEHAVIOR | 5-1 |
| | 5.1 Material/Substrate Evaluation | 5-1 |
| | 5.2 Design Details Evaluation | 5-3 |
| | 5.3 Specialized Environmental Tests | 5-3 |
| 6 | PROTOTYPE PANELS AND MATERIAL SPECIMENS | 6-1 |
| | 6.1 Prototype Panels | 6-1 |
| | 6.2 Material Specimens | 6-13 |

| Appendix | | |
|---|---|---|
| A | Design and Analysis of Primary Candidate Structure Configuration | A-1 |
| B | Stress Analysis of Substrate for Prototype Panel No. 1 | B-1 |
| C | Stress Analysis of Substrates for Prototype Panel Nos. 2 through 4 | C-1 |
| D | Dynamic Analysis of Prototype Panel Substrates | D-1 |
| E | Venting Characteristics of LI-1500 Tiles With Strain Isolation | E-1 |
| F | Environmental Test Plan | F-1 |
| G | Non-Destructive Evaluation of LI-1500 | G-1 |

# INTRODUCTION AND SUMMARY

The successful operation of the Space Shuttle vehicle is dependent upon design and development of a reliable, low cost, reusable thermal protection system (TPS). Current NASA planning defines an ablative one-use TPS on the MARK I orbiter to be followed by a MARK II system utilizing reusable rigid surface insulation (RSI) as the TPS. The LMSC candidate RSI material system is an all-silica system designated as LI-1500 (15 $lb/ft^3$). LMSC considers the LI-1500 material system to be sufficiently well developed to be considered as the primary TPS for the MARK I shuttle phase.

The basic objective of this contract is to establish materials and design technology of LI-1500 rigidized surface insulation. LMSC's approach to accomplishing this program objective is based on executing the following tasks as specified in the negotiated contract statement of work:

- Task 1.0 – Program Plan
- Task 2.0 – Design
  - 2.1 – Design Criteria, Environments and Requirements
  - 2.2 – Design Applications
- Task 3.0 – Material Optimization
- Task 4.0 – Property Characterization
- Task 5.0 – Environmental Response Behavior
  - 5.1 – Material Substrate Evaluation
  - 5.2 – Design Details Evaluation
  - 5.3 – Specialized Environmental Tests
- Task 6.0 – Prototype Panels and Specimen Deliverables
  - 6.1 – Prototype Panels – Orbiter and Booster
  - 6.2 – Material Samples

LMSC exercised the option to extend this contract Midterm Report and the prototype panel review from 4 October to 12 November. A midterm review of the contract was presented on 4 October in addition to eight prototype panel designs utilizing the LI-0025 $Cr_2O_3$ coating. During the interim, LMSC has conducted an intensive test

program to establish a more advanced coating system. This effort was successful and culminated in a 100-cycle test series at 2500°F, as described in Section 3.1.

Eight new prototype panel designs have been completed and are reported here. Four test panels were designed, using LI-1500 conductivity properties as a function of temperature only (1 atmosphere) and four flight panels considering the effects of reentry ambient pressure conditions also. The flight panel LI-1500 requirements are less than test panel thicknesses by 25 to 38 percent for the specific vehicle areas and environments considered. The efforts involved in establishing the total of 16 prototype panel designs have resulted in a large data base from which the contract Design Methods Report can be formalized.

The majority of planned test efforts under Task 4.0 have been completed and are reported in this document. The tests under Task 5.0, however, are largely influenced by the LI-1500 coating system. Therefore, this testing is being conducted during the month of November instead of October, as originally planned.

# Section 1
# PROGRAM PLAN

LMSC presented the contractually required Program Plan (LMSC-A991130) to NASA/MSC on 16 July 1971. This plan conformed with the contract Data Requirements List (DRL) and the Data Requirements Description (DRD, MA-020T). The major topics presented in detail were:

- Program Description
- Management Procedures, Organization, and Facilities
- Detail Task Description and Related Manpower
- Program Phasing
- Technical Statement of Work
- Submittal of Data

LMSC's master schedule (Fig. 1-1) has been updated to reflect the current contract position. All program milestones have been met on schedule, including the storage of NASA/MSC material samples. LMSC has exercised the option of extending the Midterm Report and prototype panel CDR one month as prescribed in the NASA TWX received 29 September. This extension was offered to provide a maximum technology interchange between current Development and Improvement Programs. Tasks relating to the design, fabrication, and test of the prototype panels and details have been extended to reflect this change. Panel delivery dates have been postponed to the first week of January 1972. The details of the booster prototype panels and design conditions have not been received per contract schedule. This task has also been extended to the end of the contract.

The Organization Chart (LMSC-A991223) was submitted to NASA/MSC under a separate cover on 30 July. LMSC's management policy is to assign executive management responsibility for all programs to "line-of-business" managers reporting directly to a division General Manager. Because the thermal protection system is a critical subsystem for manned reentry vehicles, TPS work is managed as a major subsystem program within the Manned Space Programs line-of-business. LMSC has assigned prime

# PROGRAM MASTER SCHEDULE

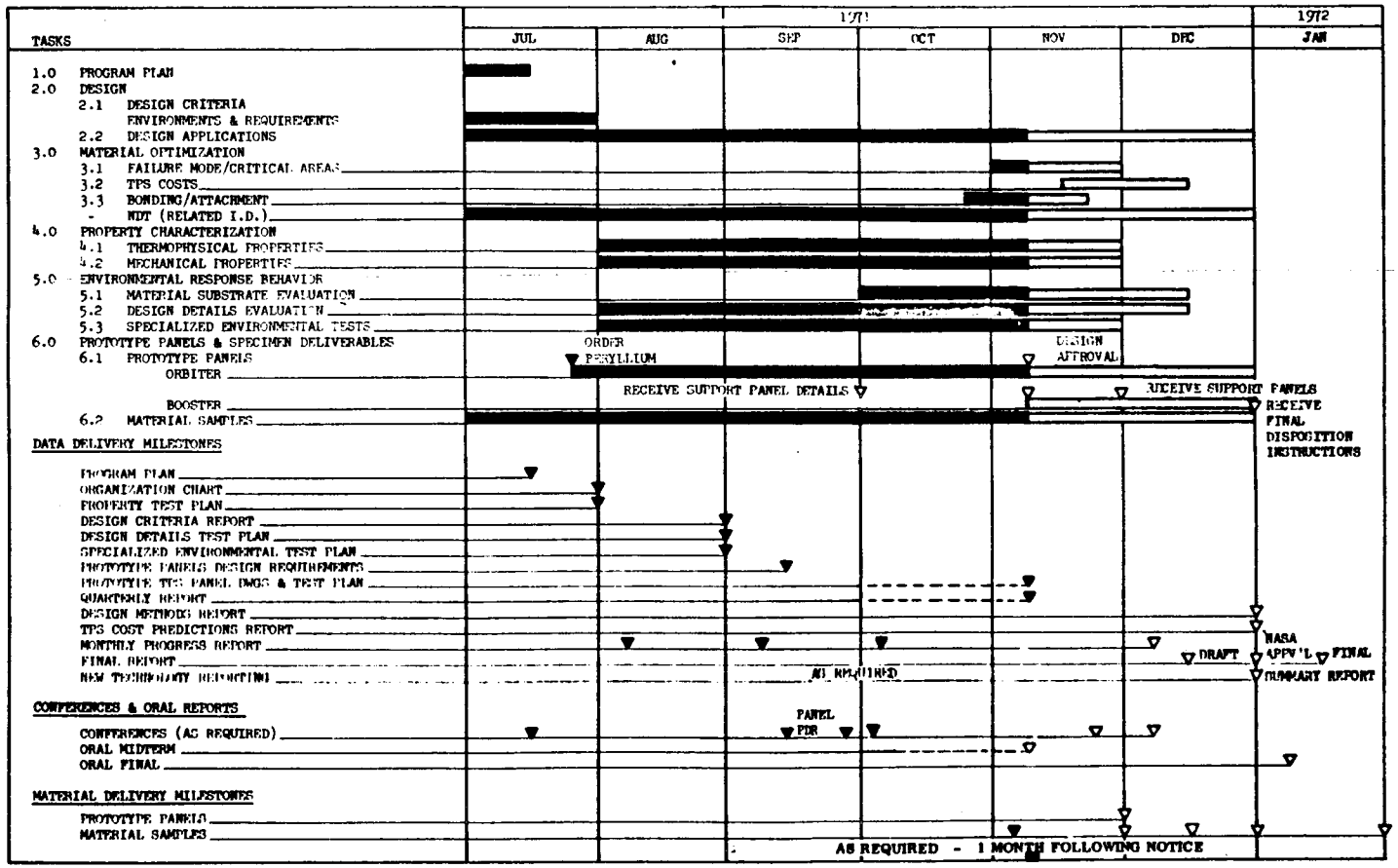


Fig. 1-1

responsibility for the NAS 9-12083 development program to the Thermal Protection Systems organization in the Manned Space Programs Office of the Space Shuttle Division. This organization has participated in all phases of LMSC's Space Shuttle efforts and is intimately familiar with the requirements of the TPS. Individuals assigned to this project have assisted in both the development of LI-1500 and the past related contract activities. The project organization and its position in the overall LMSC organization is shown in Fig. 1-2. Key personnel and their respective LMSC department numbers are shown under each task. The project organization position in the overall LMSC organization and the line departments furnishing project support were shown in the Organization Chart document.

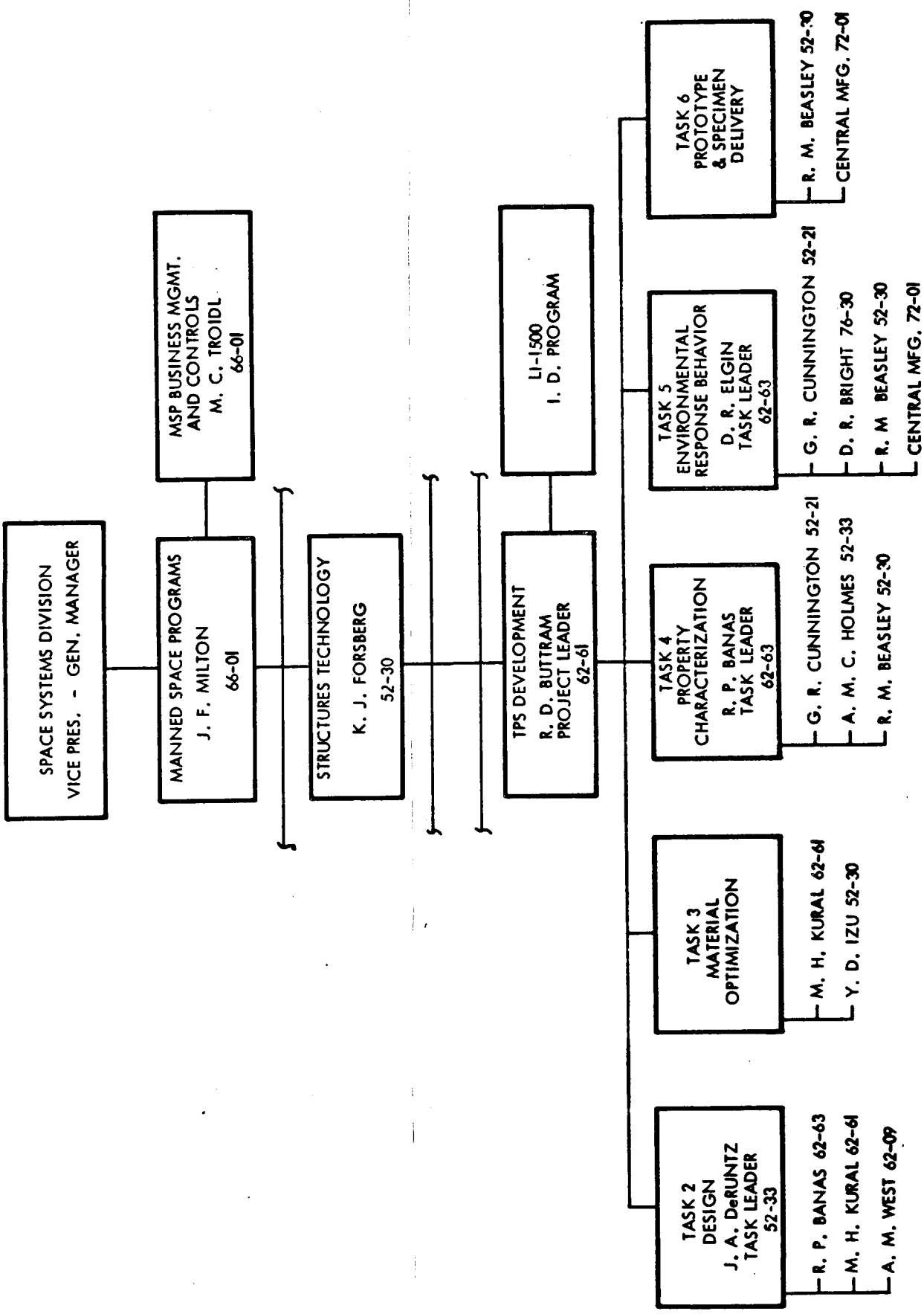


Fig. 1-2 Project Organization Chart

# Section 2
# DESIGN

The development of rigidized surface insulation for shuttle application includes the establishment of rationale, methods of analyses, techniques, and design. This key contract task defines the criteria/methodology required for shuttle usage of LI-1500 RSI. The effort is divided into two subtasks. The first defines the criteria, requirements, and environments applicable to the shuttle TPS work that has been completed. The second subtask is design applications and methodology establishment. Most of the effort in this subtask has also been completed but not yet documented in usable form.

## 2.1 CRITERIA REQUIREMENTS AND ENVIRONMENTS

Space Shuttle requirements applicable to the design of the Thermal Protection Systems (TPS) are delineated, together with design criteria and primary design conditions to be utilized in the development of the TPS. Applicable loads and thermal environments are provided for both the orbiter and booster, based on the vehicle design data available at the time of the study. Requirements and criteria for accomplishing "proof of design" are also included. These data* are briefly summarized in the following subsections.

The results of the study summarized herein are considered to represent a basis for initiating TPS detail design/analysis efforts in a Phase C Space Shuttle development program. In the course of the present TPS technology development program, and other concurrent space shuttle studies, some changes to requirements and design criteria will naturally evolve. These are not expected to be extensive in scope and, in most cases, of only minor consequence to the designs.

In the areas of loads and thermal environments, considerable changes can be expected for the following reasons:

---

*LMSC-A991379/SS-1108, "Design Criteria for Space Shuttle Thermal Protection System Development," dated Sep 1, 1971

- Improved knowledge of the environments to be encountered, and the time-dependent thermal effects within the TPS.
- Changed space shuttle configurations and design details.
- Improved knowledgeability of material-characteristics effects and related implications on the design criteria.
- Augmented detail analyses of the TPS subsystems, and of the detail design areas within each subsystem.

A major element of TPS design criteria, which is dependent upon specific Space Shuttle System concepts and baseline mission presumptions, is the definition of the optimization criteria between TPS weight and cost. A basis for definitizing these criteria is provided.

The criteria and loads specified by NASA/MSC for prototype panel design are included as subsection 2.1.6.

### 2.1.1 Objectives and Scope

The thermal protection systems for the space shuttle must protect the primary vehicle substructure and other vehicle subsystems during various phases of mission environments. The TPS on the orbiter, and (where required) on the booster, must perform this function with a high level of reliability. Extensive failure of the TPS systems is likely to lead to loss of, or major damage to, the vehicle system. In that sense, TPS is somewhat like a pressure vessel wherein structural integrity of all its elements is essential to achieve normal or safe operation. It has one major handicap compared to a pressure vessel, in that pressure vessels can readily be proof-tested, even on a flight article, whereas the total TPS cannot. On the orbiter, it must be capable of successfully performing its function in 100 operational missions.

The high level of reliability must be achieved while minimizing weight and cost. On the orbiter, a typical total weight of the TPS can lie between 20,000 and 50,000 pounds, with weight uncertainties in the order of 5,000 to 10,000 pounds. In space shuttle Missions 2 and 3, this uncertainty (7,500 pounds nominal) represents approximately 30 percent and 20 percent, respectively, of the total payload. Thus, the system is quite weight-critical as well as being reliability sensitive.

A primary objective of the space shuttle program is – "development of an economical general purpose transportation system." Development and operation of the TPS of the orbiter vehicle system is roughly estimated to represent 5 to 10 percent of total orbiter program costs. Thus, the TPS has major influence on total-program economy, and at the same time technologically represents one of the most uncertain subsystems in the Space Shuttle System. Minimizing cost, therefore, is a primary consideration during the TPS design selection process. Since a major portion of TPS program costs is expected to be encountered in the maintenance and refurbishment operational activities, the TPS life-cycle costs must be utilized as the cost basis for trade-study comparisons.

Requirements and criteria that influence design/development of the TPS are defined in a variety of NASA and contractor documents. The following criteria elements are summarized in LMSC-A991379, which also identifies the sources by reference to the applicable documents:

- Space shuttle program requirements and criteria applicable to TPS
- Space shuttle structural design criteria applicable to TPS
- Design/development optimization criteria applicable to TPS
- Spacecraft criteria and standards applicable to TPS
- Loads and thermal environment data applicable to orbiter and booster TPS

The "applicable documents" are: (1) primary applicable space shuttle directives or documents, (2) related space shuttle design criteria studies, and (3) space vehicle or other potentially applicable design documents. The documents listed in these three groupings are identified in the text of LMSC-A991379, where applicable. The same requirement/criterion items often appear in two or more cited references.

### 2.1.2 Design Requirements

Space Shuttle System requirements applicable to the TPS have been extracted primarily from the Space Shuttle draft "Statement of Work" and its technical requirement Appendices. These are described in LMSC-A991379, in the fullest detail available as determined from the applicable studies and documents resulting therefrom, under the following groupings: (1) System Requirements, (2) General Technical Requirements,

(3) Thermal Protection and Control, (4) Natural Environment Design Requirements, and (5) Manned Spacecraft Criteria and Standards.

Requirements that are especially pertinent to this development program are listed below.

- The combined storage and operational service life of the Space Shuttle System shall be a minimum of 10 years after the first manned orbital flight. Each Space Shuttle System flight article shall be capable, with a cost-effective level of refurbishment and maintenance, of a minimum operational lifetime of 100 missions.
- The Space Shuttle System flight hardware turn-around time from landing at the launch facility to launch readiness shall be less than 14 calendar days.
- The orbiter vehicle and booster vehicle shall be insensitive to weather conditions during pad preparations and standby periods.
- All TPS materials/systems will sustain 100 design missions. TPS design for all missions shall assure crew safety for worst case abort entry.
- The TPS shall be designed to the same criteria as the primary structure of the airframe.
- External thermal coatings shall have a reuse capability of 100 flights without significant deterioration or degradation. Coating systems requiring refurbishment shall be consistent with other repair/replacement/maintenance requirements.
- The space shuttle shall be designed for 0.95 probability of no puncture during the maximum total time-in-orbit, using the meteoroid model defined in par. 2.5.1 of TM-X-53957.

### 2.1.3 Structural Design Criteria

The basic structural design criteria applicable to the space shuttle TPS are specified in the draft Space Shuttle Statement-of-Work, Appendix B, and explained (at least in part) in NASA SP 8057. These criteria have been extracted and set forth in the fullest detail available in LMSC-A991379 under the following groupings: (1) Strength Requirements, (2) Strength Allowables, (3) Design Load Criteria, (4) Rigidity Criteria, and (5) Optimization Criteria. Structural criteria which are especially pertinent to this development program are listed below.

- Combined Stresses. The structural design shall exclude the use of pressure-stabilized structures, with the exception of main propulsion tanks when exposed to ascent flight loads. When the stresses due to internal pressure and thermal

conditions are additive to the external flight loads, the ultimate external load will be combined with the maximum regulated internal pressure and the thermally induced load, times a factor of 1.5. When the stresses due to internal pressure and thermal conditions are relieving (subtractive) the external flight loads, the minimum thermally induced load and the minimum regulated pressure (or zero pressure, if the operational capability of the vehicle is not affected by the loss of pressure) will be combined with the ultimate external load. No load conditions outside the crew safety envelope shall be considered. In no case shall the ratios of allowable stress to combined limit stress be less than 1.35.

- The design loads used for final vehicle design shall be based on a Monte Carlo analysis in which the vehicle is flown analytically through a sufficient number of profiles to statistically define the 99 percentile loads.
- Aeroelasticity. Static and dynamic structural deformations and responses under all conditions and environments shall not cause (1) a structural failure or system malfunction, (2) impair the stability and control characteristics of the vehicle, or (3) cause unintentional contact between adjacent bodies.
- Dynamic Aeroelasticity. The orbiter vehicle shall be free from classical flutter, stall flutter, and control-surface buzz at dynamic pressures up to 1.32 times the maximum dynamic pressure expected during flight. External panels shall be free of panel flutter at 1.5 times the local dynamic pressure at the appropriate temperature and Mach number for all flight regimes including aborts.
- Basic Optimization Criteria. Three primary value elements are involved in design-optimization and development-program-optimization of the TPS: (1) structural integrity reliability, (2) system weight, and (3) life-cycle costs. All three of these have major influence on the Space Shuttle System total cost-effectiveness. Trade studies invariably must involve two of the three elements, and very often all three.
- A level of structural integrity reliability comparable to that achieved in a commercial air transport is essential. Therefore, this element is presumed constant, and at a level, which to all intents and purposes, is equal to 1.0. Design-configuration and program optimizations, therefore, are not concerned about the numerical value of reliability, but rather the cost in dollars and weight to achieve it. Safe-life designs may be traded off against fail-safe designs to determine which produces the required level of structural integrity assurance at the best combination of weight and cost.
- To achieve a balanced design, the dollars expended to reduce weight enough for increasing payload by one pound should be the same for all elements of the Space Shuttle Vehicle Systems, provided that the technological (and cost) uncertainties are essentially equivalent. If payload can be increased by weight reductions in primary airframe (by use of exotic materials) at the same cost as for a comparable change in the TPS, but with less uncertainty, then the trade is in favor of the change in the airframe. Also, quite obviously, if it requires 6 pounds of weight removed from the booster to increase payload by 1 pound, and it requires only 1 pound off of the orbiter to do the same thing, then six times as much money can be spent for weight reduction on the orbiter than on the booster.

### 2.1.4 Environmental Data

Environmental data are presented in the following categories: ascent trajectory, entry trajectory, peak temperature isotherms, differential pressures, and vibration/acoustics. Attachment of RSI directly to primary structure may be the final TPS design. In this application, the strains and deflections of the structure will dictate the TPS attachment design. Strains and deflections are dependent on vehicle loadings and configurations as well as structural geometry. Primary vehicle loadings are not included due to this dependence. Design for this application will be based on representative strains and deflections derived from specific configurations and loading conditions, which do not differ appreciably for the various vehicles and environments currently proposed.

Design environments for the prototype panels are not included in this section. These conditions will be transmitted separately as specified in the contract.

Ascent trajectories for the mated system booster and orbiter are shown in LMSC-A991379 for the LMSC, MDAC, and NAR configurations, respectively. All trajectories result in orbiter injection to a 50 X 100 nm orbit with an inclination-angle of 28.5 deg. The final design reference orbit was a circular orbit at 270 nm with an inclination-angle of 55 deg.

Orbiter entry trajectories from a 270-nm orbit (LMSC) and a 100-nm polar orbit (MDAC and NAR) are shown in LMSC-A991379. The LMSC orbiter shown is a delta-body configuration, while both the NAR and MDAC orbiters are of the delta-wing category. All trajectories generate about 1,100 nm of aerodynamic crossrange, but the LMSC trajectory takes 1,350 sec to reach 100,000 ft while the MDAC and NAR trajectories take about 2,100 sec. The impact of longer reentry time is to increase the insulation requirements of the TPS. All trajectories were generated under what essentially appears to be the same philosophy. A choice of TPS material is made and heating boundaries are generated for the orbiter lower centerline based on the temperature capability of the chosen TPS material(s). An entry trajectory is generated using the appropriate aerodynamic characteristics for each orbiter. The trajectory is maintained above the heating boundary by use of bank angle and angle-of-attack modulation while attaining

1,100 nm of aerodynamic crossrange. Orbiter peak-temperature isotherms corresponding to the entry trajectories are depicted for the LMSC, MDAC, NAR and GAC orbiters in LMSC-A991379.

The orbiter shell differential pressures have been obtained for three critical flight phases for the delta-body orbiter maximum $\alpha q$ on ascent, during a 2.5 g subsonic maneuver. These pressures are shown in LMSC-A991379. To account for venting uncertainties, ±0.25 psi has been added to the differential pressures shown in this document.

The orbiter and booster thermal protection system will be subjected to various acoustic and aerodynamic buffeting as well as mechanically induced random-vibration responses during the mission profile. During liftoff, intense acoustic pressures are generated by the booster engine exhaust turbulence. During transonic and maximum dynamic pressure portion of flight, high unsteady aerodynamic pressures are experienced due to turbulent boundary layer noise, separated flow, oscillating shock waves, and interaction of shock waves and boundary layer. During reentry, both hypersonic and low-speed aerodynamic noise is present. Acoustic environments encountered by flight test vehicles during takeoff, landing, cruise, and maneuvers must also be considered. The acoustic environments presented in LMSC-A991379 are for launch, maximum dynamic pressure, and reentry phases of the mission.

Typical booster entry trajectories, peak temperatures, and design loads are shown in a series of six Figures in LMSC-A991379.

### 2.1.5 Proof of Design

A properly balanced development program will include some combination of the following engineering activities: analysis, design, development testing, qualification testing, acceptance testing, operational (flight and ground) testing, and/or special testing. The scope of work undertaken in each of these activities influences to some extent the level-of-effort warranted in the other activities, to achieve adequate proof of design. Therefore, definition of the basic requirements for proof of design is an integral part of design criteria. The responsibility for planning proof of design overall rests with the vehicle contractor. Proof of structural adequacy of the TPS under all anticipated loads and environmental conditions shall be provided by appropriate analyses and tests.

Reports shall be prepared on analyses and tests conducted to verify the structural adequacy of the design. Assumptions, methods, and data used shall be defined. An integrated plan, early in the Phase C Space Shuttle Program, shall describe the total plan for verifying structural adequacy and shall include schedules for accomplishment. The plan shall be revised as necessary to reflect changes in schedules, requirements, objectives, design characteristics, and operational usage.

Reports shall be prepared to provide the following information concerning the TPS: operating restrictions (limitations on preparation testing and operational use), inspection and repair, and operational-usage measurements (systems for evaluating structural adequacy during operational usage).

Analyses in the areas listed below shall be performed to verify structural adequacy in compliance with the design criteria defined in previous sections. Where adequate theoretical analysis does not exist or where experimental correlation with theory is inadequate, the analysis shall be supplemented by tests.

- Design criteria (i.e., LMSC-A991379 and its subsequent revisions)
- Design loads
- Thermal analysis
- Stress analysis

The stress analyses shall verify structural adequacy in terms of the optimization criteria defined in subsection 2.1.3.

Tests shall be conducted to assist in defining or verifying static and dynamic design loads, pressures, and environments that the TPS will encounter through its service life.

When structural material characteristics, including physical and allowable mechanical properties and failure mechanisms, are not available in NASA-approved references, tests shall be performed to characterize the materials in accordance with the specified design criteria.

Development tests represented in part by the present program, shall be performed as necessary to:

- Evaluate design concepts
- Verify analytical techniques
- Evaluate structural modifications for achieving desirable structural characteristics
- Obtain data for reliability predictions
- Determine failure modes or causes of failure

Qualification tests shall be conducted on flight-quality hardware to demonstrate structural adequacy under more stringent loads than the worst expected loads. In defining the number and types of qualification tests, the highest practical level of assembly shall be used. Test conditions shall be selected to demonstrate clearly that all elements of the structure satisfy design criteria. Tests shall be performed on representative sections of each of the TPS subsystems, to verify the following:

- Detrimental deflections do not occur under deformation-critical combined limit-load/limit-pressure and thermal conditions.
- Rupture or collapse does not occur under critical combined ultimate-load/ultimate-pressure and thermal conditions.
- Neither detrimental deflections nor rupture occur under limit-load/thermal exposure to specified life-cycle criteria.

The foregoing tests shall demonstrate, as closely as is practicable, the structural integrity for the primary design conditions, including demonstrations of cumulative damage tolerance where applicable.

Acceptance tests shall be conducted on flight hardware to verify that the materials, manufacturing processes, and workmanship meet design specifications.

Flight tests conducted for purposes of structural integrity evaluation shall include verification of limit-load/thermal conditions used in the design of the TPS and in the test conditions used in the TPS qualification tests. These tests shall specifically include tests, with appropriate instrumentation, to collect data permitting evaluation of at least critical heating and of refurbishment techniques. Prior to or in conjunction with these tests, techniques for inspection of the TPS subsystems shall be developed to locate hidden defects, deteriorations, and fatigue effects.

### 2.1.6 Prototype Panel Design Conditions

The point design requirements for the prototype panels have been specified by NASA/MSC. LMSC has complied with these requirements in the design effort (Section 2.2).

#### 2.1.6.1 Structural Design Requirements

| | |
|---|---|
| Ultimate Factor of Safety: | 1.5 |
| Combined Loading: | Summation of ratio of the allowable load to combined limit loads ≥ 1.35 |
| Panel Flutter: | Flutter free for 1.5 times local dynamic pressures at any flight mach number |

2.1.6.2 Thermal Design Requirements. Design factors of safety are not applied to the heating rates for the specified vehicle areas shown in Fig. 2.1.6-1. The heating rate for Area 2 has been perturbed to result in a maximum surface temperature of 2300°F, as shown on Fig. 2.1.6-2. Adiabatic conditions have been assumed for the panels in insulation sizing efforts.

2.1.6.3 Environments. Figures 2.1.6-3 through 2.1.6-12 show the trajectories, loading, and environments to which the prototype panels have been designed and/or analyzed. The combination of conditions considered and the critical design conditions are discussed in detail in Section 2.2.

*D. J. Tillian, NASA/MSC, to R. D. Buttram, LMSC, "Point Design Requirements for Two Orbiter Design Areas-Reusable Surface Insulation TPS Development, Phase 2," U. S. Government Two-Way Memo, 21 July 1971

# TPS DESIGN AREAS FOR ORBITER LOWER SURFACE

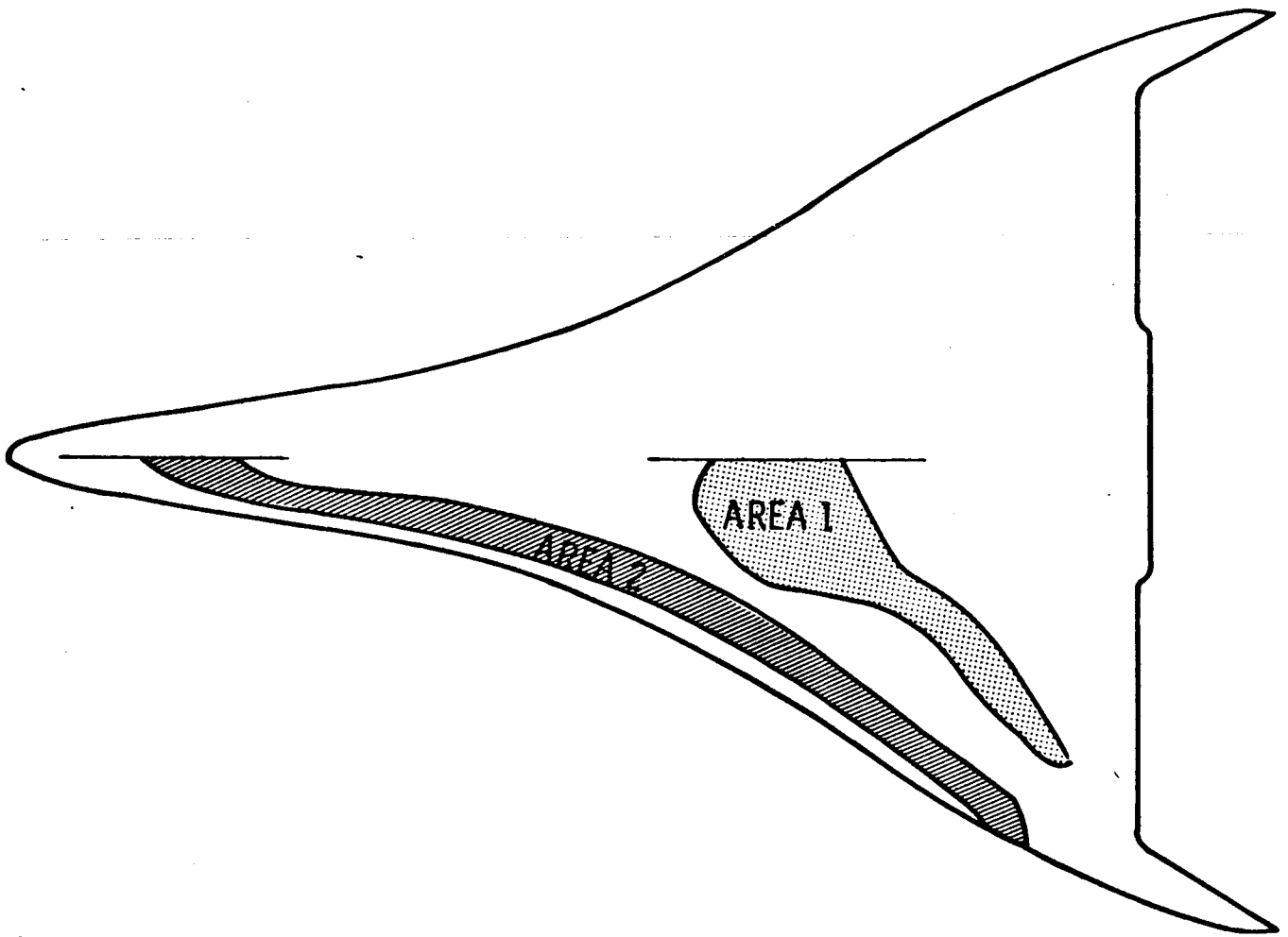


D04980
RDB

Fig. 2.1.6-1

# LOCAL HEATING RATE AND STAGNATION TEMPERATURE HISTORIES FOR ORBITER DURING ENTRY

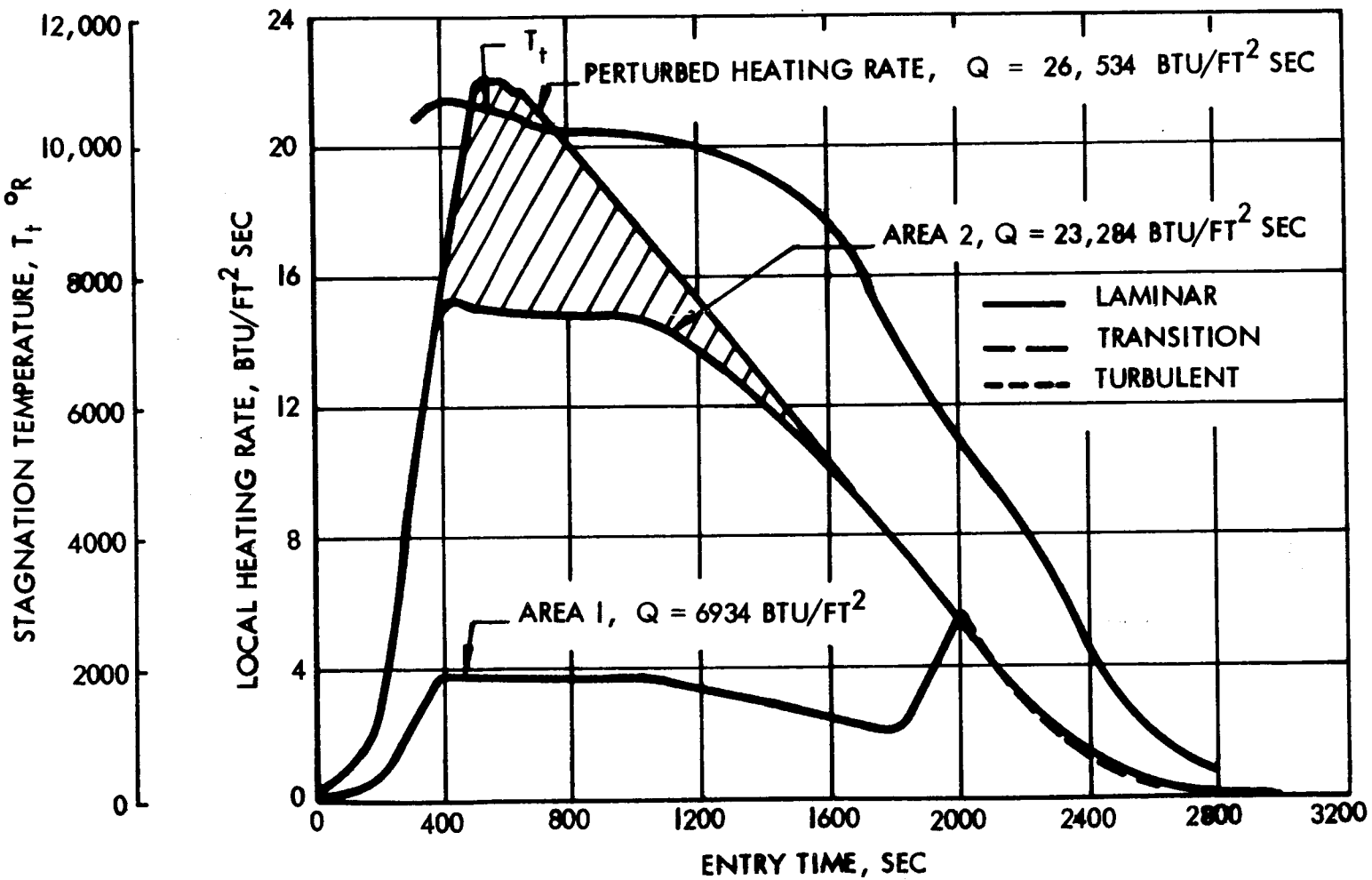


Fig. 2.1.6-2

# ENTRY TRAJECTORY

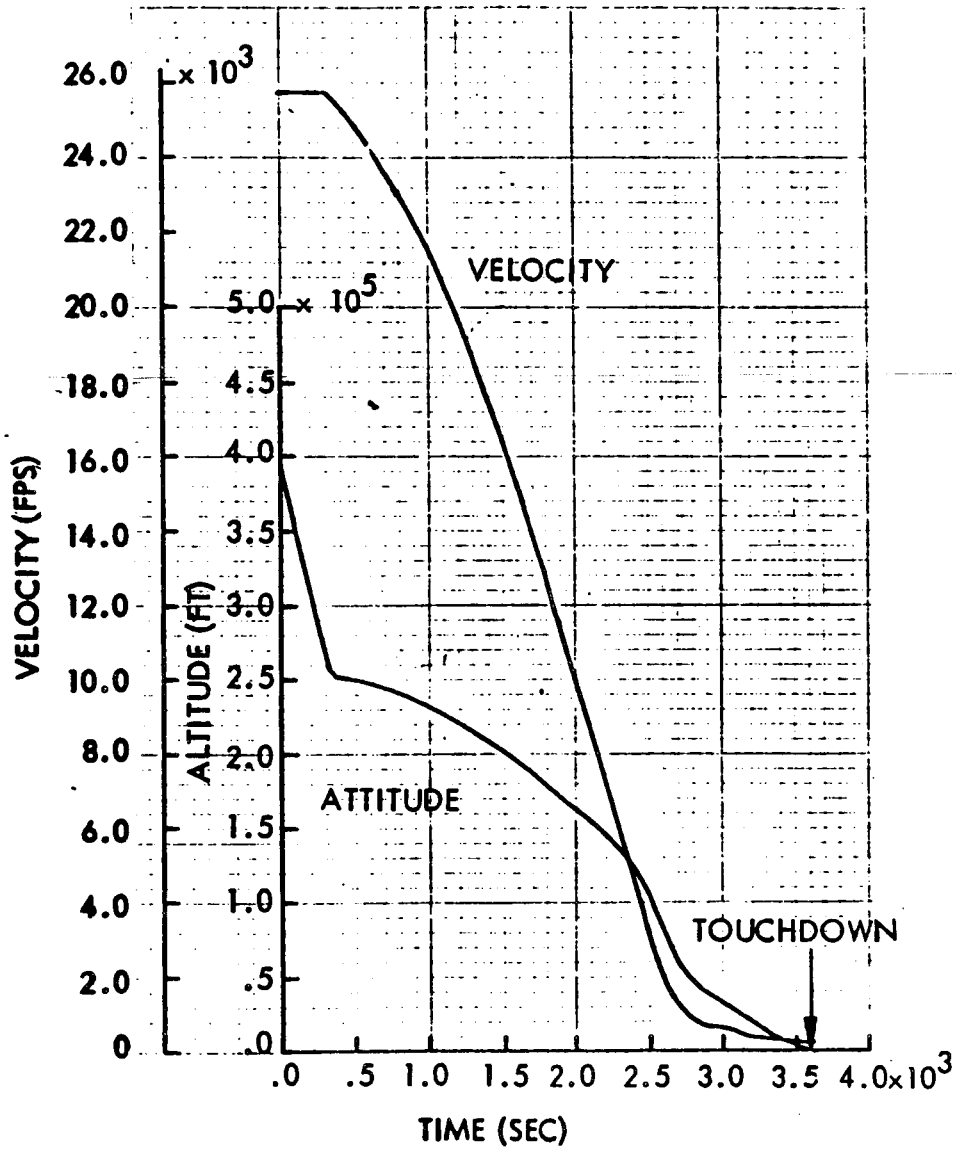


Fig. 2.1.6-3





rdb

# LOCAL AND FREE-STREAM STATIC PRESSURE HISTORIES ON ORBITER FUSELAGE DURING LAUNCH

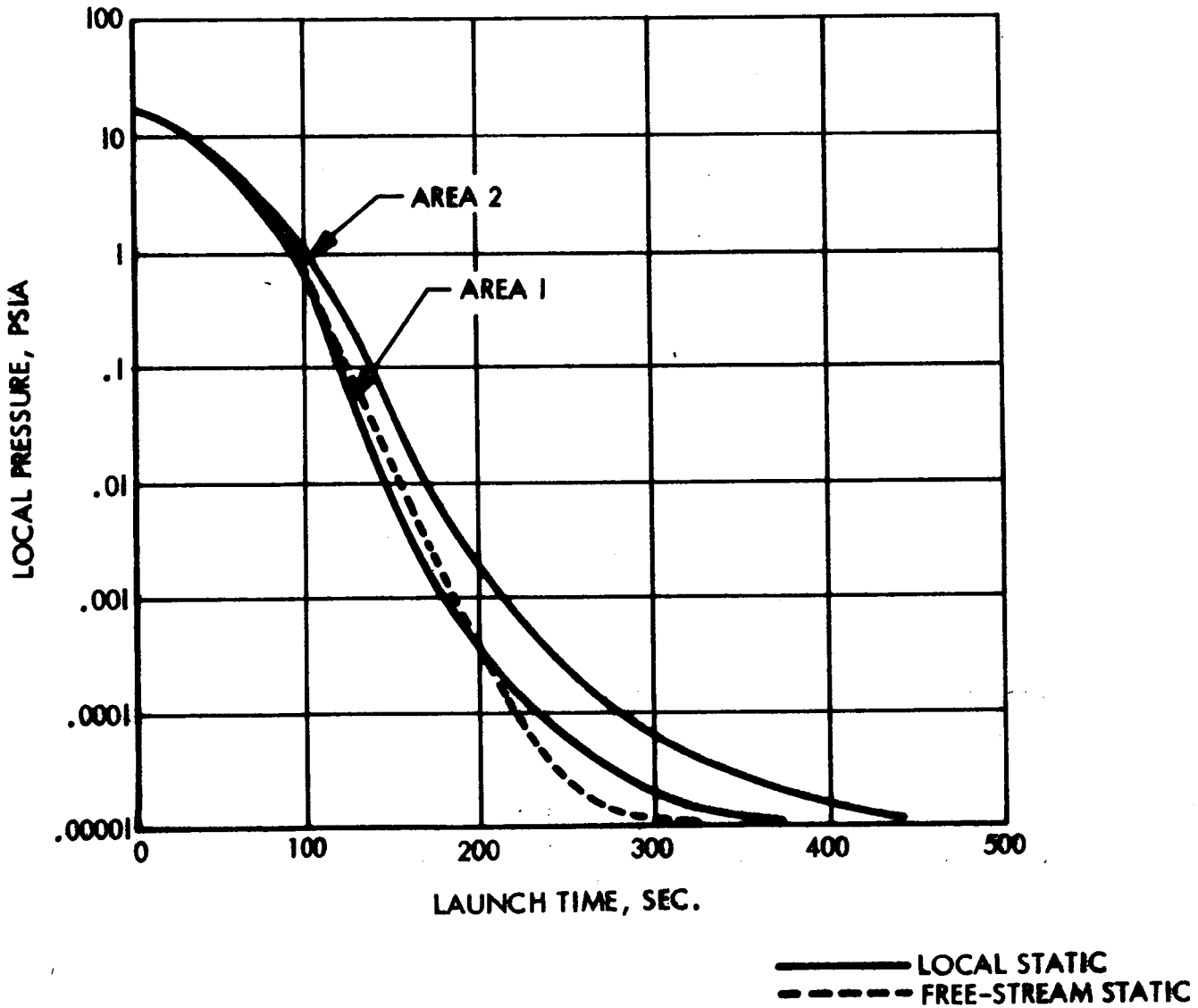


DO6017

Fig. 2.1.6-4

# FREE-STREAM AND LOCAL PRESSURE HISTORIES ON ORBITER CENTERLINE DURING ENTRY

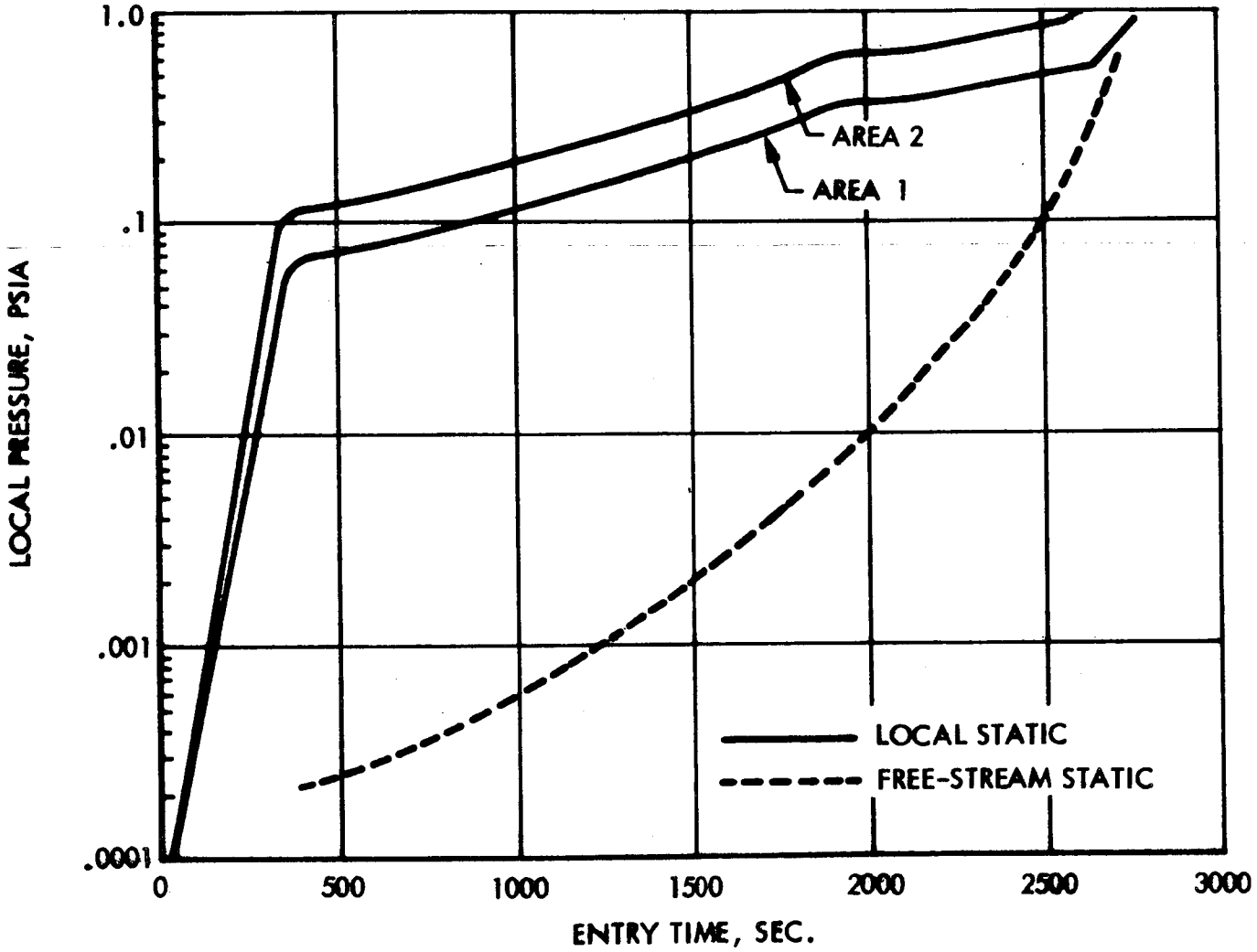


Fig. 2.1.6-5

DO6042

# LOCAL HEATING RATE AND STAGNATION TEMPERATURE HISTORY FOR ORBITER DURING LAUNCH

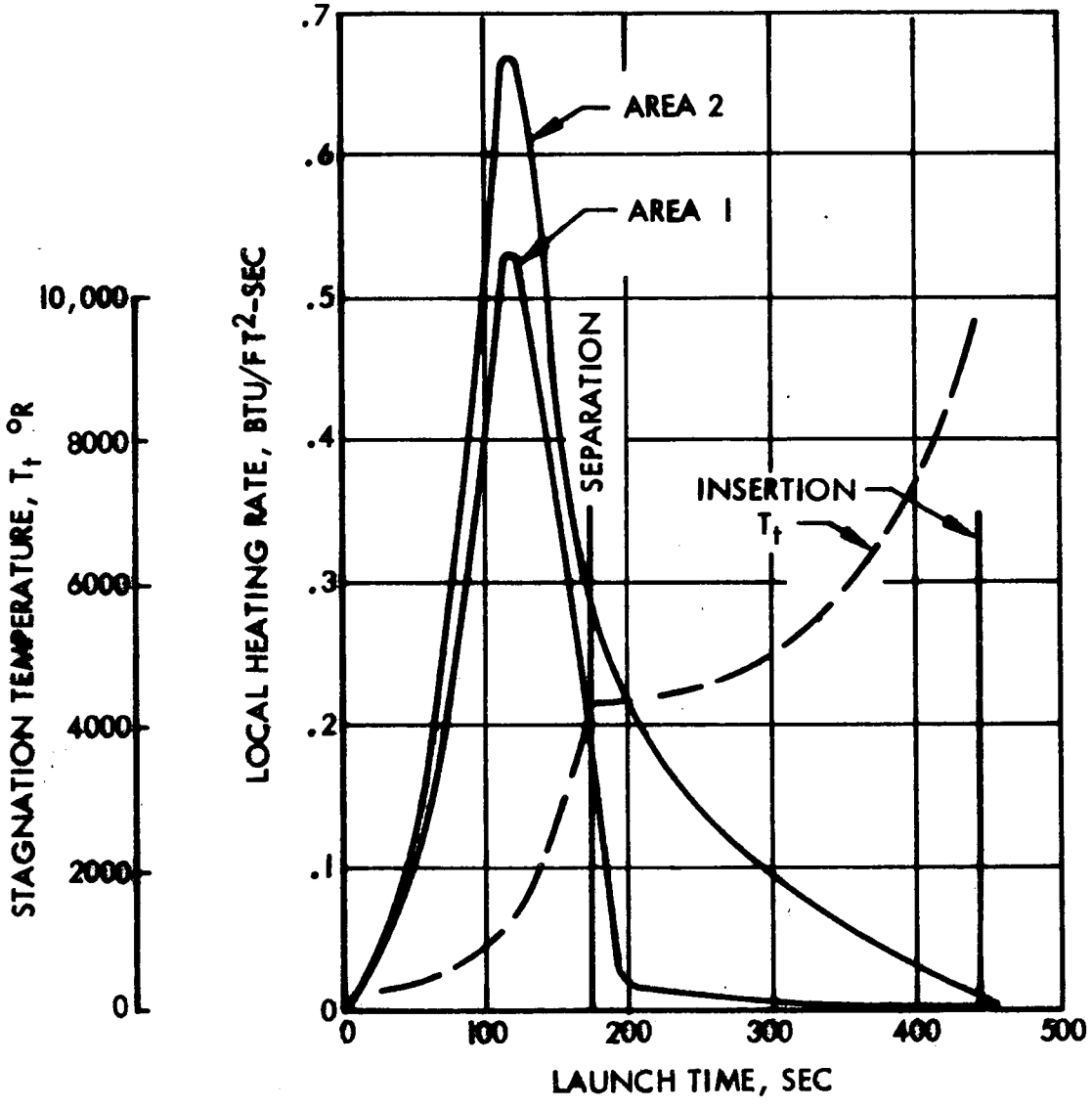


DO6016

Fig. 2.1.6-6

# LIMIT DIFFERENTIAL PANEL PRESSURES FOR ASCENT

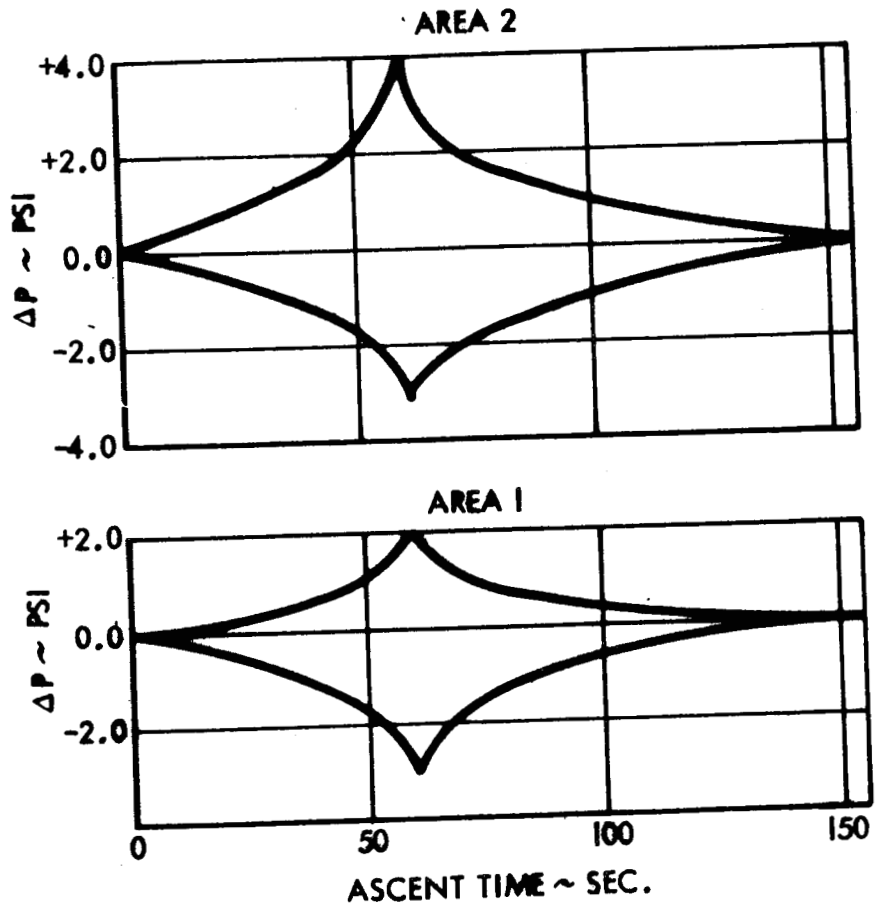


Fig. 2.1.6-7

# LIMIT DIFFERENTIAL PANEL PRESSURES FOR ENTRY

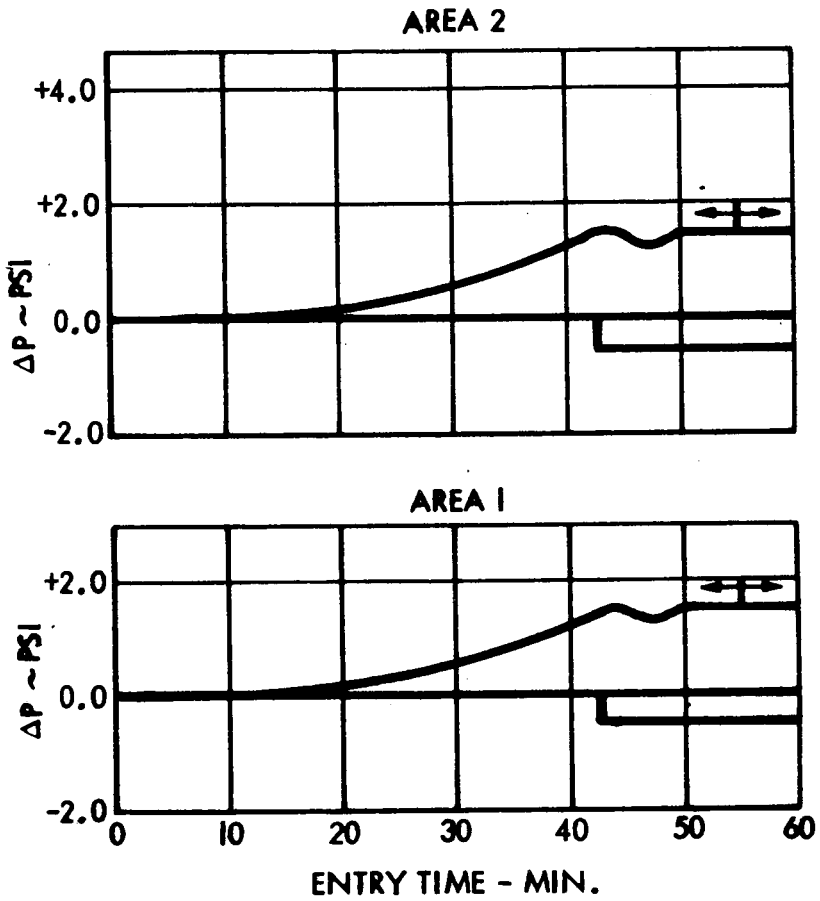


Fig. 2.1.6-8

# ASCENT AND ENTRY DYNAMIC PRESSURES

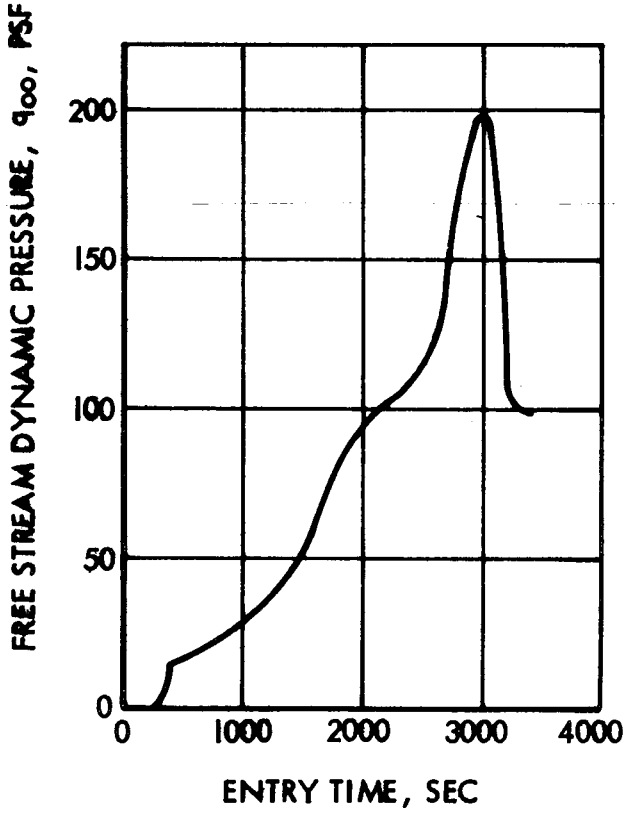


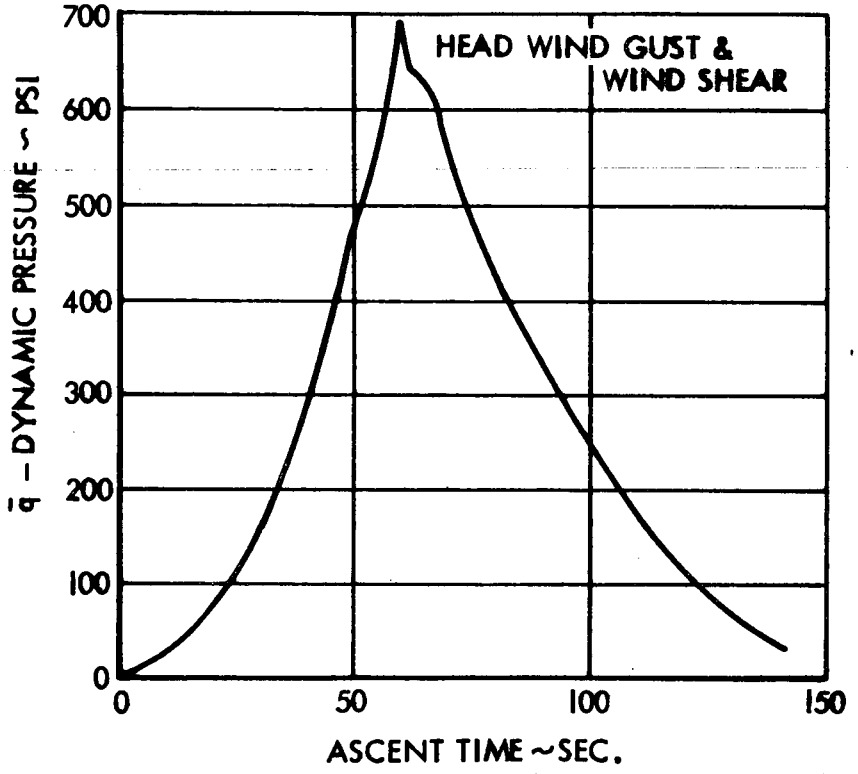


DO6132

Fig. 2.1.6-9

# AREA 1 - ASCENT AND ENTRY LINELOADS

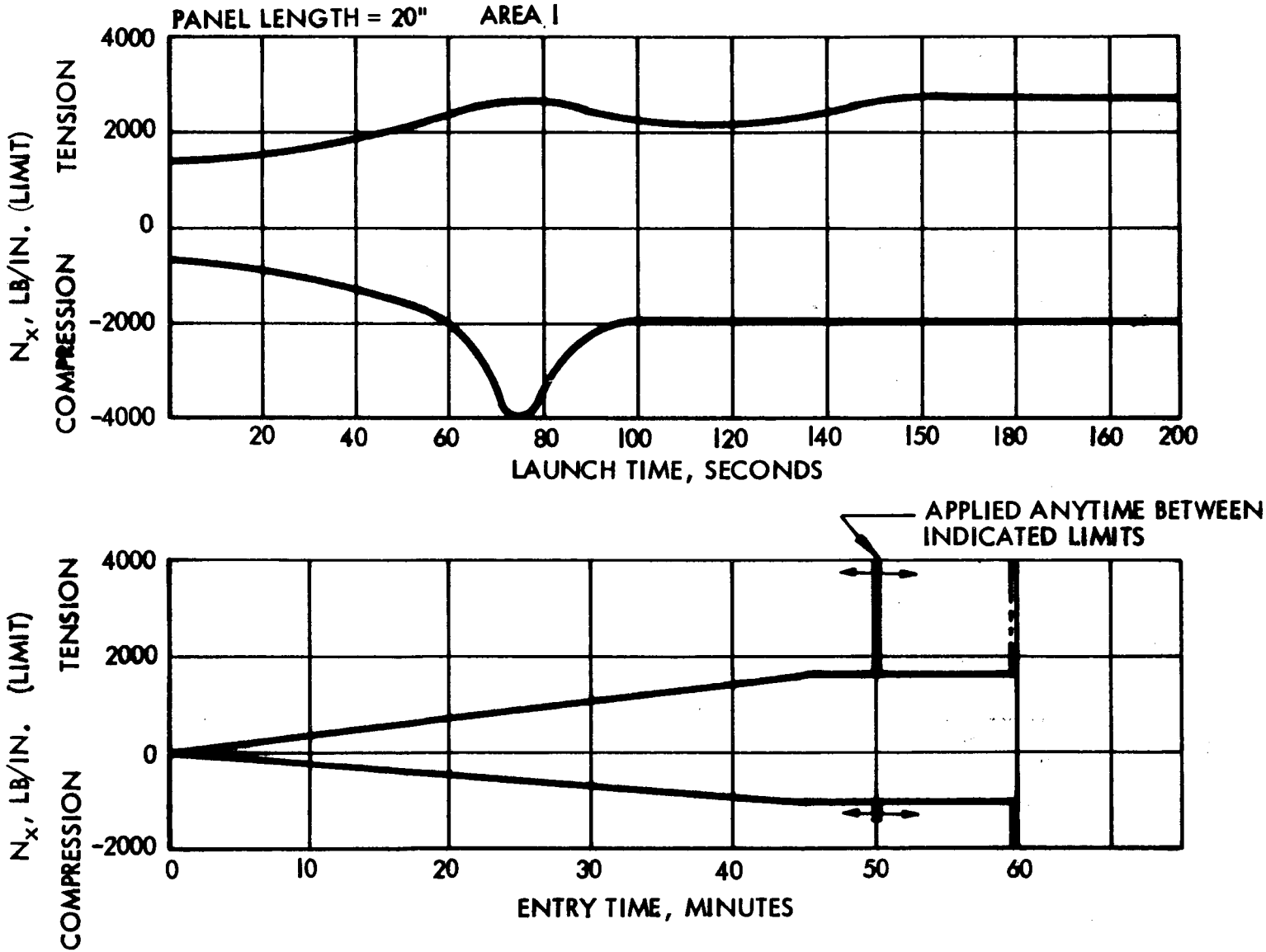


DO6131

Fig. 2.1.6-10

# AREA 2 - ASCENT AND ENTRY LINELOADS

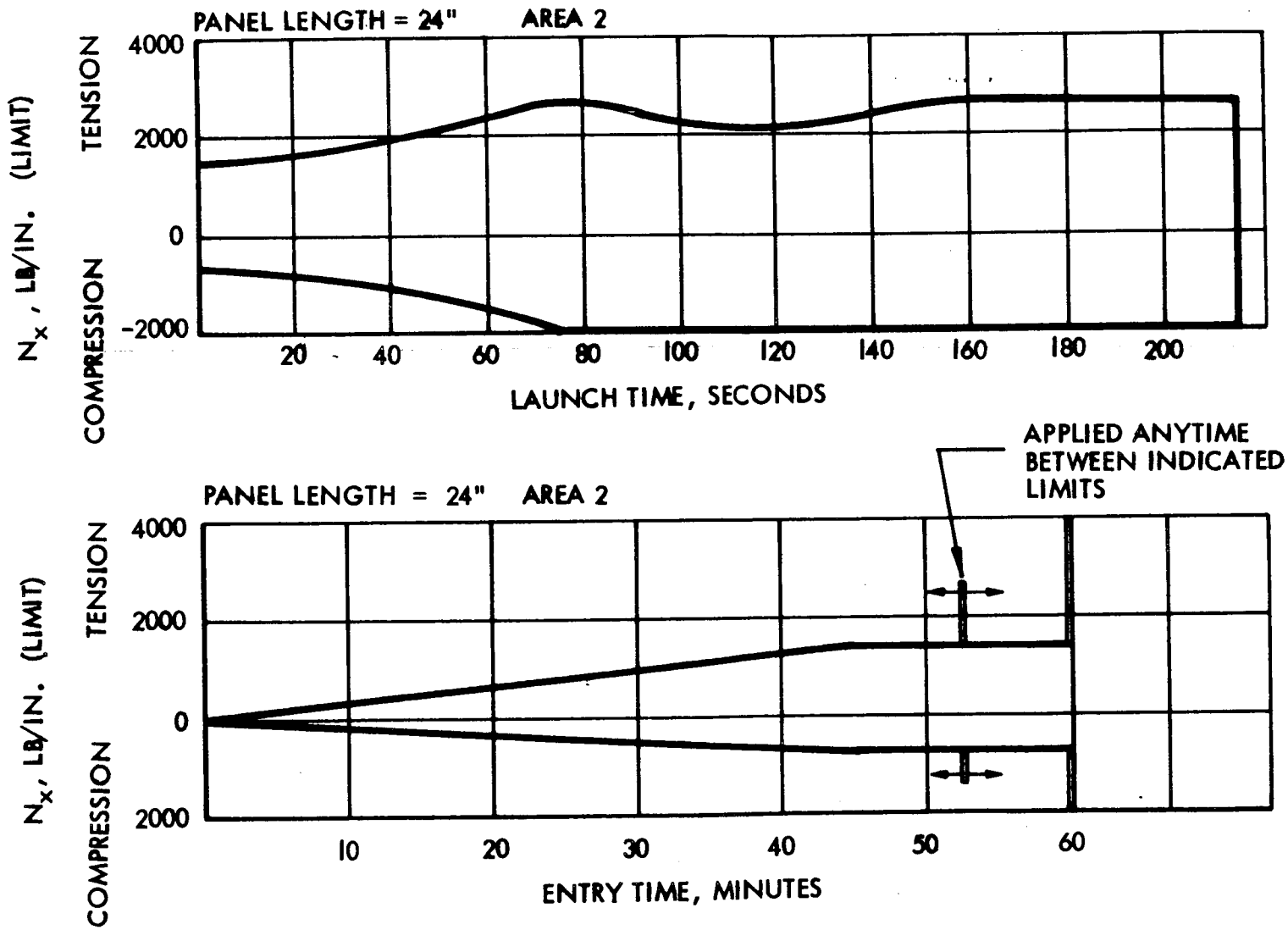






Fig. 2.1.6-11

# OVERALL SPL VS. TIME – TYPICAL ORBITER MISSION

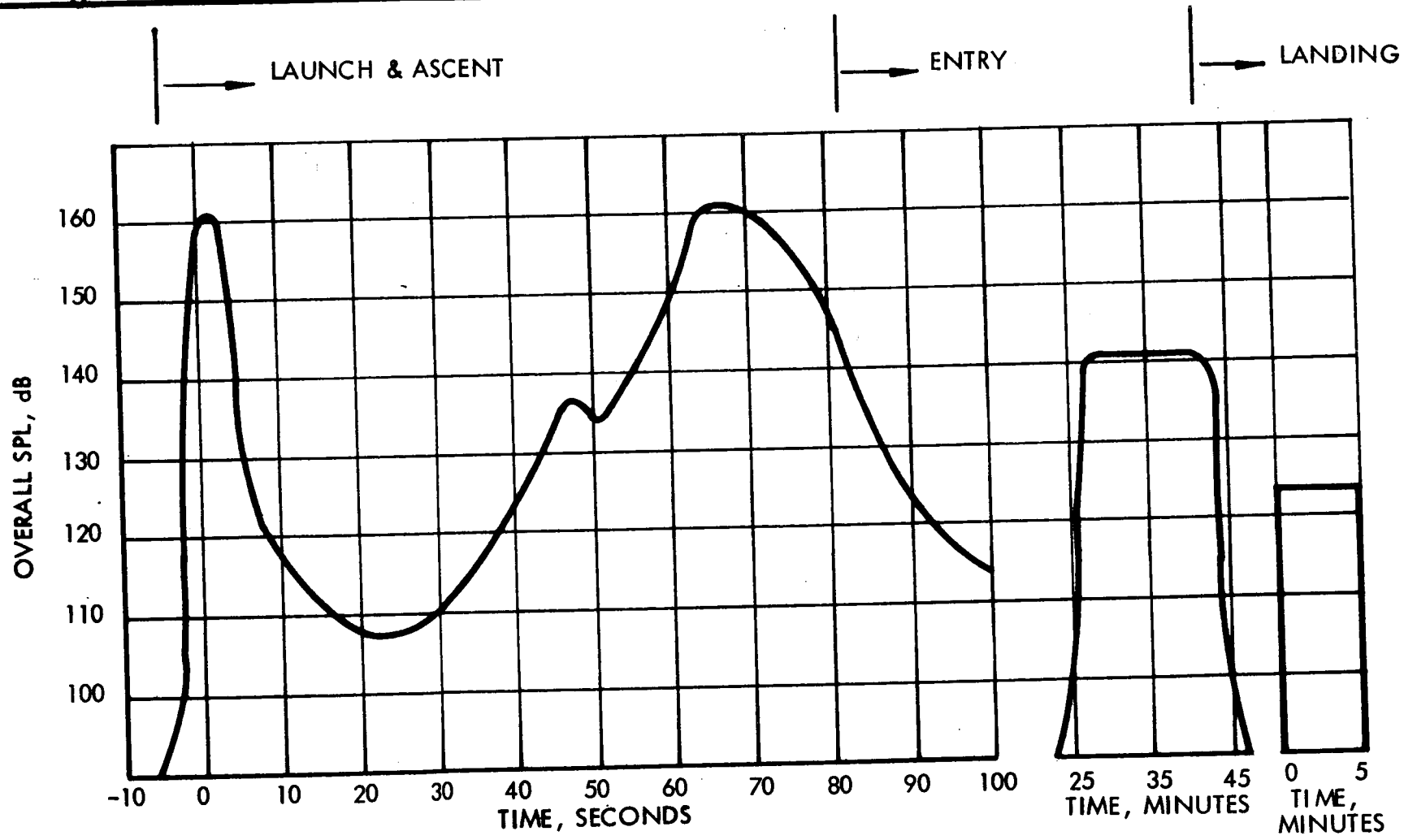


Fig. 2.1.6-12

## TASK 2.2 DESIGN METHODS

The objective of this task is to develop a logical path through the TPS system variables and, thereby, arrive at an optimum thermal/structural design. In the following paragraphs, the methods of analysis are identified and relationships between the RSI/booster/orbiter parameters are established. Detail guidelines are presented to substantiate the design of the prototype panels fabricated and delivered under this contract. LMSC has identified the effect of atmospheric testing on RSI systems, i.e., LI-1500 heat conductivity dependence upon environmental pressure. The so-called "test" and "flight" prototypes are defined; these differ in required LI-1500 thickness.

In establishing the design methods, effort has been concentrated on:

- Metallic substrate design
- Thermal sizing of RSI
- RSI tile stress analysis
- RSI attachment methods

Based on these studies, prototype panels designed to NASA specified conditions are compared with metallic heat shield designs. Flutter and acoustic analyses are also presented for the prototype panels.

The design sequence is best illustrated in Fig. 2.2-1. First, the basic structural sizing is done in conjunction with a thermal analysis that establishes required RSI thickness. This optimization loop considers the tradeoff between heat sink effect of structure versus insulation thickness. Next, the RSI system stress levels are determined through a second optimization loop in which bond thickness is varied to ensure acceptable RSI stress levels under the environmental design conditions. Finally, a complete verification of the design is made.

# LOGIC SEQUENCE - PROTOTYPE PANEL DESIGN

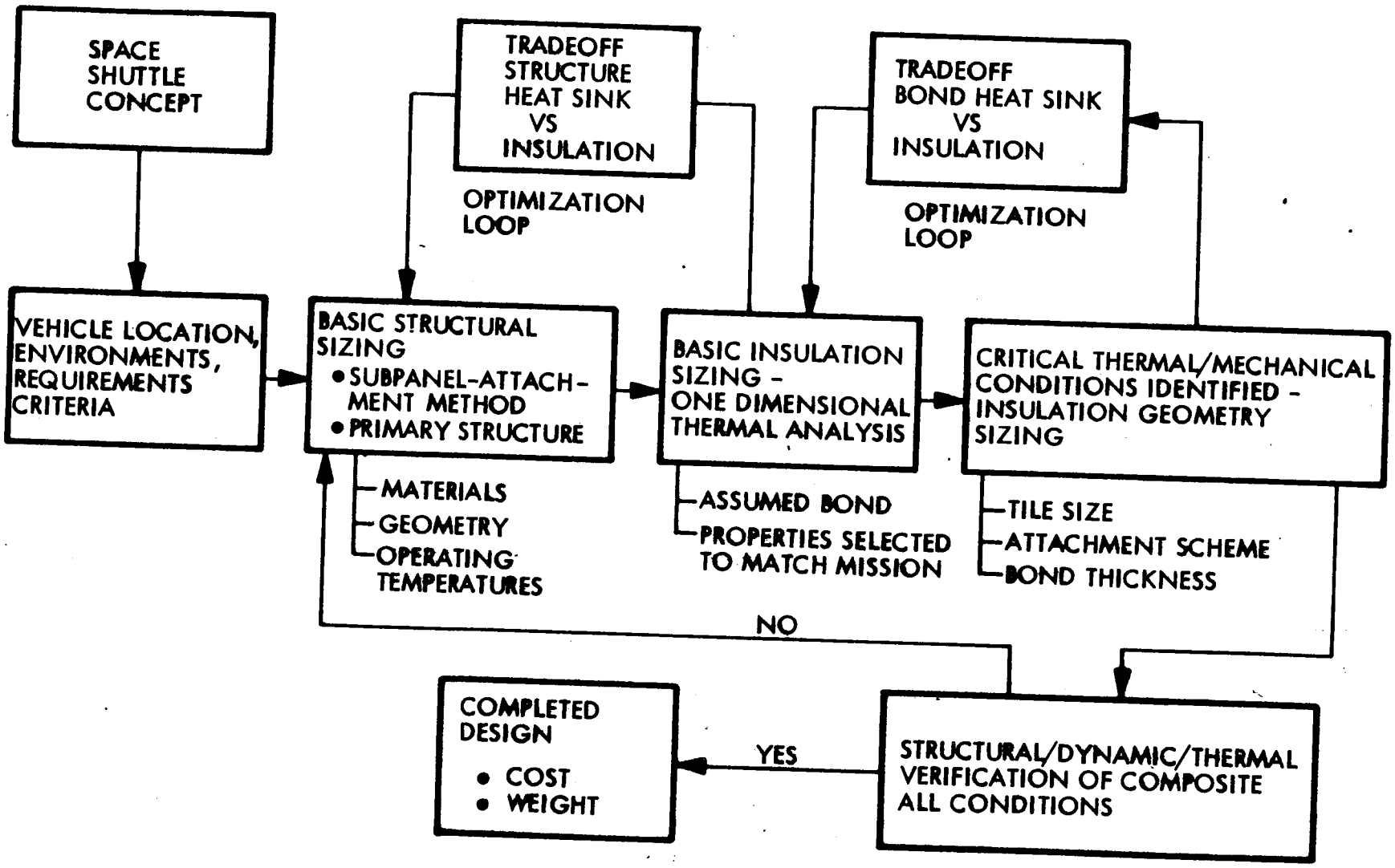


Fig. 2.2-1

### 2.2.1 Structural Considerations for LI-1500 Substrates

#### 2.2.1.1 Methods of Optimization and Analysis.

Subpanels. This TPS concept consists of a subpanel with LI-1500 attached. The subpanel is easily removable as a unit from the vehicle primary structure. The subpanels are designed to carry only airloads over spans which generally correspond to major frame or rib spacings. Because only minor support is provided at the panel edges, which are perpendicular to the frames or ribs, simple beam analysis is used in the design and analysis. Bending stresses obtained in this manner, based on simply supported edge conditions, are compared with local instability allowables for the extreme fiber elements in compression and with the material ultimate tensile properties for the extreme fiber elements in tension. Attention is also directed to the maximum deflection of the panel and the effect of this deflection upon the design of the LI-1500 tiles.

This type of analysis is easily coded for the computer to perform structural optimization studies. LMSC has developed a code, called SUBPAN, which has been used in the present program. This code may be used to optimize several subpanel material/configuration combinations. Mechanical properties for a number of materials are stored in the program as a function of temperature. These materials include titanium, beryllium, graphite-epoxy, and aluminum. Alternately, mechanical properties for other materials may be read in. The configurations that may be called include zee-stiffened subpanels, trapezoidal corrugation-stiffened subpanels, honeycomb-sandwich subpanels, integral L-stiffened subpanels, and plane trapezoidal corrugation subpanels. Data needed to operate this code include panel length, design temperature and pressure (burst and/or collapse), plus definition of the practical restraints involved and the selection of material and configuration. The practical restraints generally include specification of the minimum gages permissible, and the widths of section elements which are fixed by practical considerations (e.g., zee-stiffener attach-flange width).

The code is patterned after work reported in the literature on the optimization of beams, which has shown that, for practical designs, the analysis must be set in terms of both

permissible deflection and permissible bending stress. Beams optimized to a deflection criterion alone tend to be deep with thin sections, while beams optimized to a stress criterion alone tend to be shallow and flexible. In the LMSC code, the deflection criterion is stated as a maximum permitted for limit loads at the center of the panel, which may be varied as desired. Because the subpanels must have a capability for carrying burst pressures as well as collapse pressures, and some configurations are unsymmetrical, both tensile and compressive outer-fiber stresses are computed to ensure that allowable stresses are not exceeded. The search for the lightest design meeting the criteria established, while satisfying the constraints imposed, is limited to standard sheet gages. Also, properties for a number of standard commercially available honeycomb cores have been stored in the program to ensure this standardization feature for honeycomb sandwich subpanel optimization.

Primary Structure. LI-1500 is also proposed for direct application to primary structure. These panels carry direct axial loads, either tension or compression, in addition to airloads. For the purposes of this program, the primary structure panels are considered to be very wide in comparison to their length; therefore, the conditions along the unloaded edges are not important and the panels may be analyzed as beam columns. An appropriate closed-form solution for uniformly loaded, simply supported, beam columns of uniform cross-section may be found in Timoshenko's "Theory of Elastic Stability." This type of edge support is probably conservative for most applications, particularly those in which the panels are continuous over intermediate supports. However, the use of more realistic edge conditions depends upon the detail definition of the intermediate supports and their resistance to rotation under load. Stresses applied to the cross section are equal to the sum of the direct stress plus bending stress due to the beam-column action. These stresses are compared with compressive and tensile stress allowables at the section outer fibers as described above for subpanels. In a similar way, the effect of deflection due to beam-column action upon the LI-1500 tile design is also considered.

Data for use in the design of beam-columns are shown in Fig. 2.2.1-1. This figure yields moment of inertia requirements as a function of the uniformly applied pressure and axial line load on a 7075-T6 aluminum panel at 250°F. The panel length is 24 inches, and the maximum deflection is limited to 0.10 inch. Intercept points along the ordinate

# BEAM COLUMN REQUIRED MOMENT-OF-INERTIA FOR DEFLECTION CRITERION

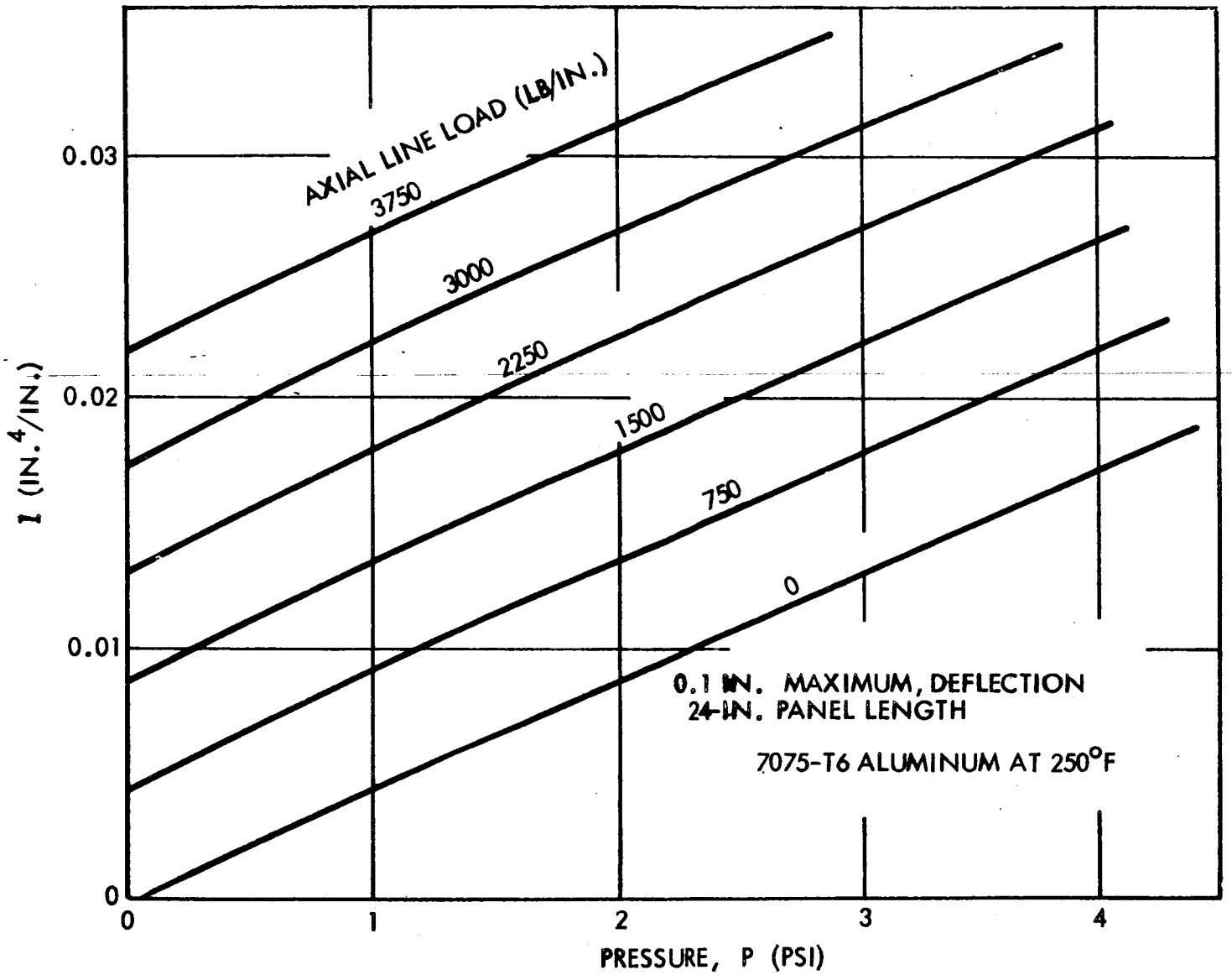


D05121
RDB

Fig. 2.2.1-1

correspond to Euler column stiffness values; the bottom curve represents a beam subject to uniform lateral pressure alone.

Beam-column analysis has been computerized at LMSC and used in the design and analysis of the prototype panels. This code may be intergrated into the existing code for the structural optimization of subpanels by merely redefining the stiffness requirements for the section and utilizing the existing search techniques. While this work is being completed, structural optimization of primary structure panels is being performed using wide column minimum weight solutions that have been perturbed according to a fixed interaction equation to account for pressure effects. Beam column analysis checks are subsequently performed to verify and/or modify the resulting designs.

2.2.1.2 Substrate Optimization Parametric Studies. The studies performed for Contract NAS9-11222 and for the present contract indicate that subpanel and primary structure configurations and materials may be qualitatively compared, utilizing wide column structural optimization data that have been reported in the literature. These data are of the general form:

$$\frac{Nx}{l\bar{\eta}E} = \varepsilon \left(\frac{\bar{t}}{l}\right)^n$$

where $\varepsilon$ is a measure of the efficiency of a given configuration. The value of the exponent n is usually 2.0 for conventionally stiffened configurations composed of straight elements but is smaller for configurations with curved elements.

Several configurations are shown in Fig. 2.2.1-2. It may be seen that the configurations that do not possess a flat sheet or skin are more efficient (lighter weight) than those that do. Also, configurations with curved stiffening elements are more efficient (lighter weight) than those with straight stiffening elements. However, only those configurations that do include a flat sheet or skin are studied here in view of the need for a flat surface to which the LI-1500 may be attached. Among these configurations, the zee-stiffened configuration is most efficient. Other configurations that are more efficient than the zee-stiffened configuration may be identified, for example, the integral tee configuration, but the increase in efficiency is rather small. Likewise, honeycomb sandwich construction is less efficient than zee-stiffened construction, principally because of the difference between the true optimum core weight and that which is practical to handle and fabricate.

The data in Fig. 2.2.1-2 may be replotted in a way that is more useful in providing insight into the selection of materials for optimum subpanels and primary structure. Weight ratios are derived in the form:

$$\frac{W_x}{W_i} = \frac{\rho_x}{\rho_i} \left(\frac{\eta . E_i}{\eta . E_x}\right)^{\frac{1}{n}}$$

where $W = \bar{t} . \rho$

# COMPARISON OF WIDE COLUMN CONFIGURATIONS

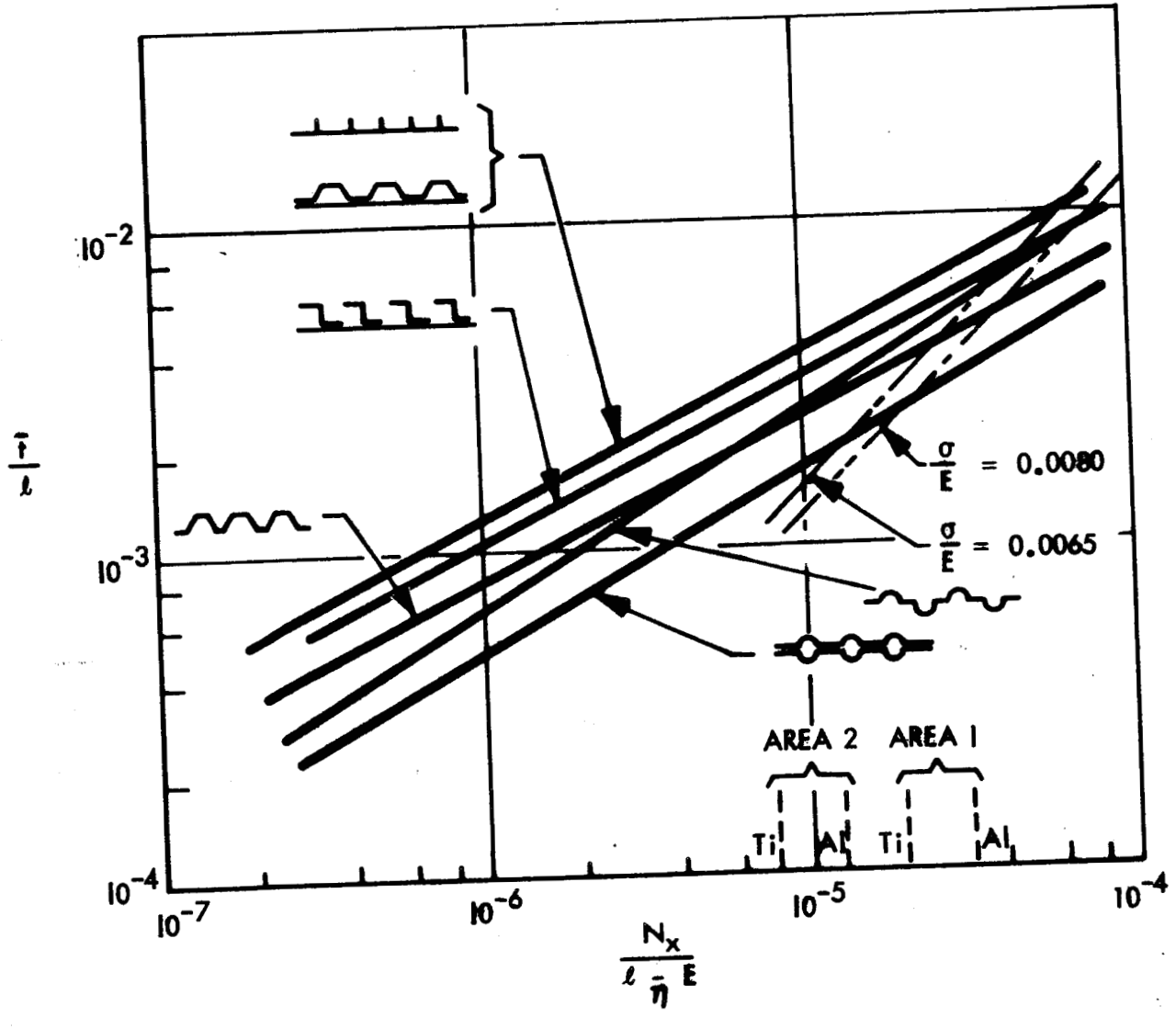


Fig. 2.2.1-2

This equation may be rewritten using beryllium as the base material:

$$\frac{W_x}{W_{Be}} = \frac{\rho_x}{\rho_{Be}} \left(\frac{E_{T_{Be}}}{E_{T_x}}\right)^{\frac{1}{n}}$$

$$\text{where } \eta = {}^{E_T}/_{E}$$

The above form of the equation permits the comparison of a number of materials in both the elastic and plastic stress ranges for a given value of n. Using $n = 2$, which corresponds to conventionally stiffened configurations, yields the results shown in Figs. 2.2.1-3 and 2.2.1-4. These figures have been developed for room temperature and 600°F material properties, respectively.

Parallel lines in the figures represent complimentary areas of elasticity in the materials while curved lines represent plasticity effects. The majority of the curved lines are in a downward direction indicating plasticity in the beryllium. The lone exception is HM21A-T8 magnesium, curving upward, indicating plasticity in the magnesium at corresponding stresses in the beryllium which are elastic. It is clear from the figures that beryllium is the most efficient material among those studied, particularly for applications wherein the optimum stress is below the proportional limit for beryllium. At optimum stresses above this point, beryllium's advantage drops off rather rapidly.

The data of Figs. 2.2.1-2 through -4 must of course be interpreted qualitatively inasmuch as subpanels and primary structure panels are not classed as wide columns. However, in primary structure panels the difference lies only in the added bending due to air loads; thus, it would seem logical to view Figs. 2.2.1-3 and -4 in terms of the maximum outer fiber compressive stress rather than a uniform compressive stress. The same analogy may be applied to subpanels.

In the case of primary structure panels under moderate axial loads (1500-3000 ppi), the stress corresponding to optimum design for panel lengths of about 25 in. is above the proportional limit for beryllium. The additional compressive stress due to bending

# BERYLLIUM - BASED WEIGHT RATIOS FOR ELASTIC-PLASTIC CONVENTIONALLY STIFFENED WIDE COLUMNS AT ROOM TEMPERATURE

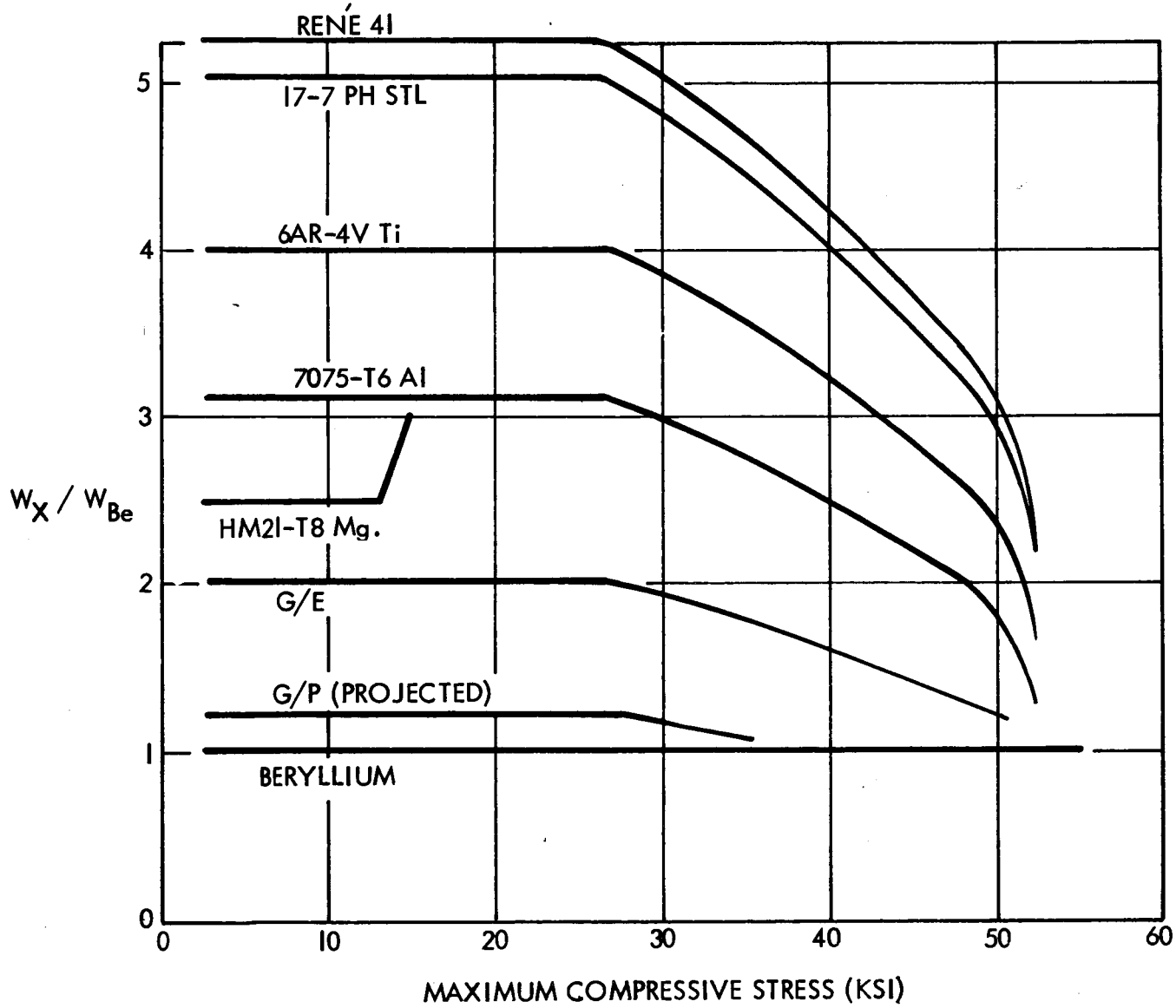


DO6027

Fig. 2.2.1-3

# BERYLLIUM - BASED WEIGHT RATIOS FOR ELASTIC-PLASTIC CONVENTIONALLY STIFFENED WIDE COLUMNS AT 600°F

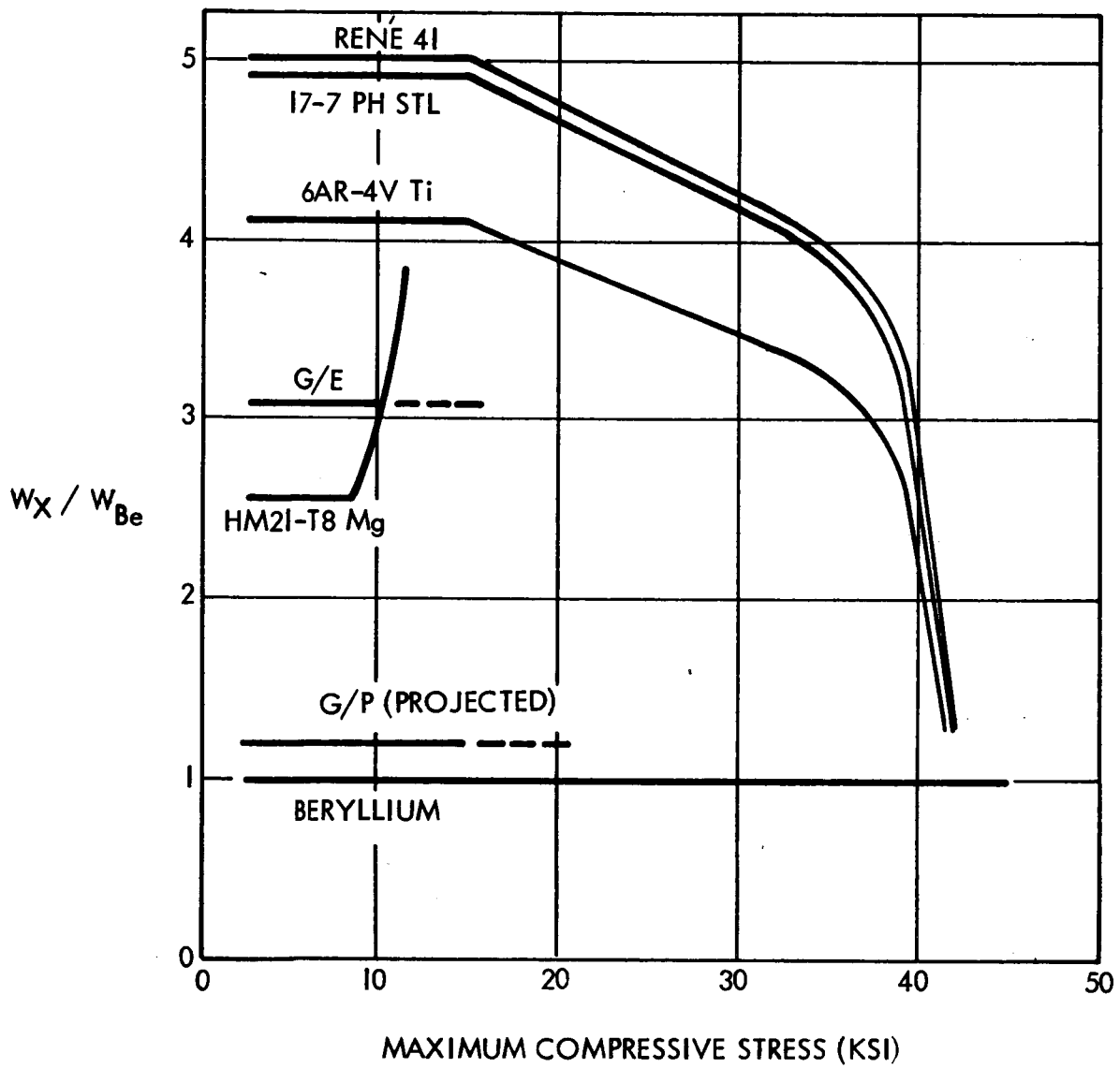


DO6026

Fig. 2.2.1-4

under air loads essentially eliminates beryllium from consideration due to the high degree of plasticity. Figure 2.2.1-3 shows that fibrous graphite systems are better candidates in these applications at room temperature, followed by aluminum, titanium, and steels in that order. For immediate design use, aluminum and titanium are prime choices.

The situation with regard to subpanels is different in that the total compressive stress is due to bending from airloads. In this case, stresses for optimum design, while usually in the plastic range for beryllium, are sufficiently low that beryllium is the best choice of material. The stress level for optimum design is controlled to some degree by the constraint on maximum deflection which prevents shallow, highly stressed designs. The curves in Figs. 2.2.1-3 and -4 show that graphite polyimide is projected to be very competitive with beryllium in this application; however, G/P is not considered a production material at the present time.

It is of interest to note that charts of the type of Fig. 2.2.1-3 show greater spread between curves when drawn to represent more efficient structural configurations (see Ref. 3). Thus, the position of beryllium in the elastic stress range improves relative to other materials for configurations, without flat sheets as shown in Fig. 2.2.1-2.

2.2.1.3 Selection of Optimum Substrate Configurations for Four Prototype Panels. Four prototype panels are to be optimumly designed, analyzed, fabricated and delivered to NASA/MSC under this program. These panels are to meet the point design requirements specified by NASA/MSC and shown in Section 2.1.6. In addition, the four panels are to represent the application of LI-1500 to both subpanels and primary structure. The panels are to be nominally 24 x 25 in. in overall size in order to be compatible with existing NASA/MSC test fixtures.

The material to be used in the substrate for each panel, and the application to be represented by each panel, are shown below. These selections have been based on prior studies performed at LMSC and NASA/MSC with regard to materials and the anticipated usage of reusable surface insulation material on the space shuttle orbiter vehicle:

| Prototype Panel No. | Application | Material | Vehicle Area Location | Max. Substrate Temperature |
|---|---|---|---|---|
| 1 | Subpanel | Beryllium | 2 | 600°F |
| 2 | Primary Structure | Aluminum | 2 | 300°F |
| 3 | Primary Structure | Aluminum | 1 | 300°F |
| 4 | Primary Structure | Titanium | 2 | 600°F |

The point design requirements of Section 2.1.6 are summarized in Fig. 2.2.1-5. Note that maximum differential pressures occur during ascent while the substrate back-face surface is at room temperature, and that the maximum back-face temperatures noted above are not developed until after landing. The maximum in-plane loads in vehicle Area 2 occur during landing; this is also true of Area 1 except that maximum compression load occurs during ascent. It may be observed that the in-plane tension loads exceed the in-plane compression loads in vehicle Area 2 by a considerable amount; thus, the selection of substrate configuration will probably not have impact upon weight for prototype panels 2 and 4.

The design/analysis process leading to a completely verified, optimum, LI-1500-substrate system is comprised of a number of specific steps which are interrelated with each other. The logic sequence for this process is presented in Fig. 2.2.1-6. As indicated in this figure, the design/analysis process begins with basic structural optimization (sizing) of the panel substrates, which includes selection of the substrate configuration. This portion of the process will be described in the following paragraphs. Note that these results are preliminary results in that they are used as input to a thermo-structural optimization loop for basic sizing of the LI-1500. Included in this loop is a consideration of the heat-sink properties of the substrate. It will be shown subsequently that the LI-1500/beryllium subpanel combination for optimum thermo-structural design utilizes a beryllium subpanel which is somewhat heavier than the beryllium subpanel developed on the basis of structural optimization principles alone. This situation occurs due to the unique heat-sink properties of beryllium. Other materials do not exhibit the same phenomenon, and thus the results of material-configuration studies for the prototype panels which are based on structural optimization techniques alone are valid for application in the final design selection process.

# ORBITER SHELL DESIGN CONDITIONS

| OPERATION | AREA | ELAPSED TIME | DIFFERENTIAL PRESSURE (LIMIT) (PSI) | IN-PLANE LOAD (LIMIT) (PPI) | SPL (dB) | MAX SURFACE TEMP (°F) | MAXIMUM BACKFACE TEMP (AMBIENT) (°F) | |
|---|---|---|---|---|---|---|---|---|
| | | | | | | | ALUMINUM | TITANIUM |
| LAUNCH | 1,2 | —— | —— | —— | 160 | | R.T. | R.T. |
| ASCENT | 1 | 60 SEC | + 2.0, - 3.0 | + 2400, - 2100 | 150 | ≈ 200 | R.T. | R.T. |
| | | 67 | —— | —— | 161 | | R.T. | R.T. |
| | | 75 | + 0.9, - 1.5 | + 2700, - 4000 | 155 | | R.T. | R.T. |
| | 2 | 60 | + 4.0, - 3.0 | + 2300, - 1500 | 150 | ≈ 200 | R.T. | R.T. |
| | | 67 | —— | —— | 161 | | R.T. | R.T. |
| | | 75 | + 1.8, - 1.9 | + 2700, - 2000 | 155 | | R.T. | R.T. |
| ENTRY | 1 | 10 MIN | + 0.1, - 0.0 | + 300, - 200 | —— | 1480 | -150 | -150 |
| | 2 | 10 MIN | + 0.1, - 0.0 | + 300, - 200 | —— | 2300 | -150 | -150 |
| | 1 | 25-45 MIN | + 1.5, - 0.5 | + 1600, - 1000 | 141 | 1200 - 400 | < 300 | < 600 |
| | 2 | 25-45 MIN | + 1.5, - 0.5 | + 1400, - 700 | 141 | 1850 - 400 | < 300 | < 600 |
| POST-ENTRY CRUISE | 1 | 45-60 MIN | + 2.0, - 0.5 | + 4000, - 1400 | 124 | ≈ 100 | < 300 | < 600 |
| | 2 | 45-60 MIN | + 2.0, - 0.5 | + 2700, - 1400 | 124 | ≈ 100 | < 300 | < 600 |
| LANDING | 1,2 | 60 MIN | + 0.5, - 0.5 | + 4000, - 2000 | 124 | ≈ 100 | < 300 | < 600 |
| DEAD STOP | 1,2 | > 60 MIN | —— | —— | | ≈ 100 | 300 | 600 |

(COLLAPSE) (BURST) (TENSION) (COMP.)

- PLUS PRESSURE IS COLLAPSE (VENTING ALLOWANCE INCLUDED)
- PLUS IN-PLANE LOAD IS TENSION
- FACTOR-OF-SAFETY BETWEEN LIMIT AND ULTIMATE IS 1.5

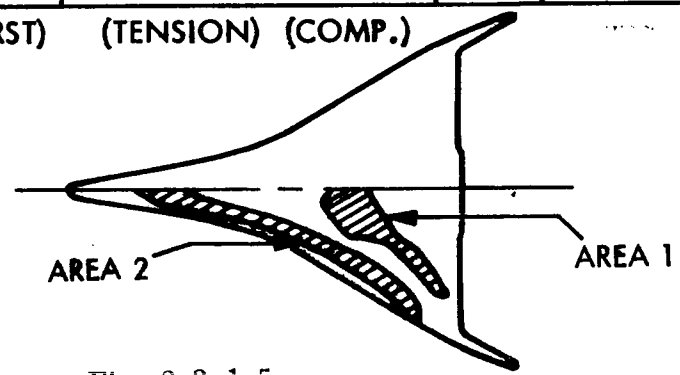


Fig. 2.2.1-5

rdb

D04947 (1)

# LOGIC SEQUENCE - PROTOTYPE PANEL DESIGN

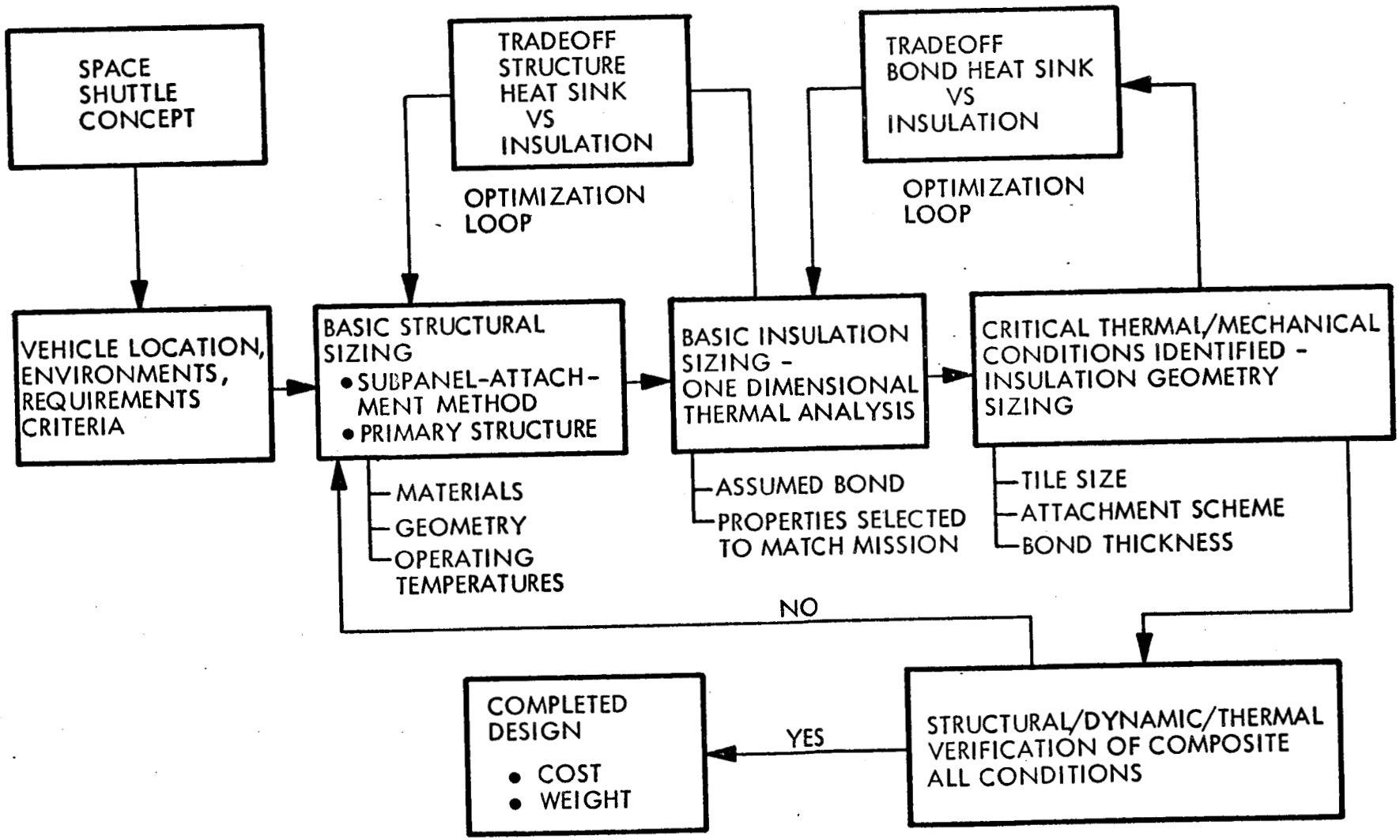


Fig. 2.2.1-6

Selection of Optimum Subpanel Configuration for Prototype Panel No. 1. A comparison of several material/configuration combinations structurally optimized to sustain the design loads for prototype panel No. 1 when utilized as a subpanel is shown in Fig. 2.2.1-7. These results were obtained from the SUBPAN computer code which was discussed in Sec. 2.2.1.1. All designs have been optimized for the burst/collapse pressures shown, which, as noted previously, occur during ascent when the subpanel is at room temperature. The panel span has been kept constant at 25 in., and a maximum allowable deflection constraint at limit load of 0.10 in. has been employed. Note that graphite epoxy is included for comparative purposes even though its acceptability under lower loads at temperatures approaching the maximum backface temperature of 600°F is doubtful. Graphite-polyimide was not included because it is not considered to be a material which is sufficiently developed for the manufacture of panels for this program. However, graphite-epoxy and graphite-polyimide designs at room temperature may be currently considered similar, with the graphite polyimide having potential for satisfactory use at 600°F.

Most of the designs shown in the figure have been constrained by minimum gage requirements specified in the computer code input. This gage for beryllium is 0.016 in. except in the honeycomb designs, where it is 0.010 in. The minimum gage for titanium and graphite-epoxy is 0.012 in. in the conventional constructions and 0.008 in. in honeycomb sandwich construction. Because of the thin gages involved, the graphite-epoxy properties have been selected to represent quasi-isotropic lay-ups rather than uni-directional lay-ups. Note also that the attach-flange widths have been assigned fixed, realistic values, and that commercially available honeycomb sandwich cores have been specified (with the exception of the beryllium honeycomb core). These cores are the lightest which experience has demonstrated can be handled and utilized without adverse structural effects.

The maximum compressive stresses due to bending are considerably higher for the beryllium designs than for either the titanium or graphite-epoxy designs. This indicates that beryllium satisfies stiffness requirements with less material volume than its competitors. The maximum compressive stress for beryllium is in the range

# COMPARISON OF LI-1500 SUBPANELS DESIGNED FOR STRENGTH AND STIFFNESS

COLLAPSE PRESSURE: 4.0 LB/IN.$^2$ (LIMIT), 6.0 LB/IN.$^2$ (ULTIMATE)

BURST PRESSURE: 3.0 LB/IN.$^2$ (LIMIT), 4.5 LB/IN.$^2$ (ULTIMATE)

MAXIMUM ALLOWABLE DEFLECTION AT LIMIT LOAD = 0.10 IN.

SPAN LENGTH = 25 IN.

DESIGN TEMPERATURE: 70°F

| CONFIGURATIONS | WEIGHT (LB/FT$^2$) |
|---|---|
| 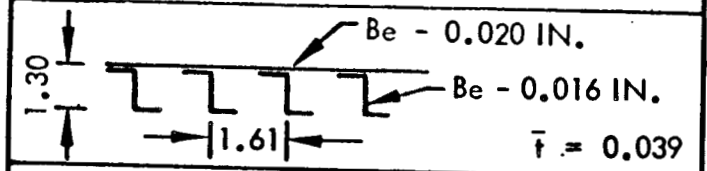  | 0.387* |
| 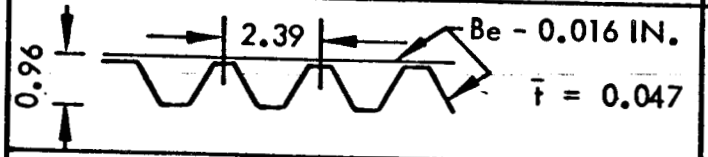  | 0.472 |
| 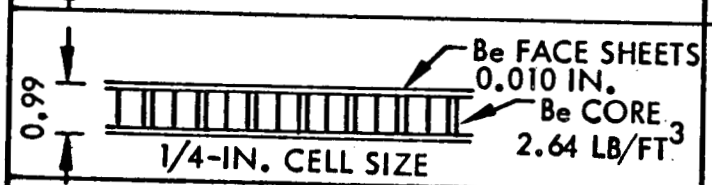  | 0.427 |
| 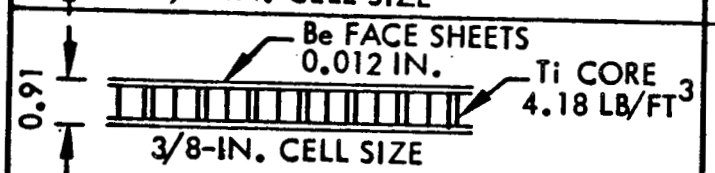  | 0.568 |
| 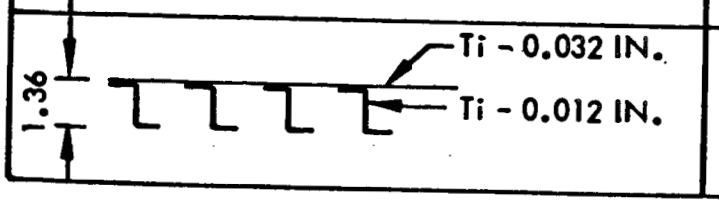  | 1.505 |

| CONFIGURATIONS | WEIGHT (LB/FT$^2$) |
|---|---|
| 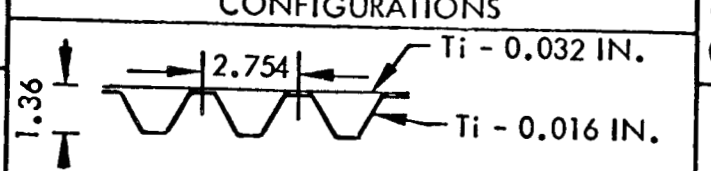  | 1.374 |
| 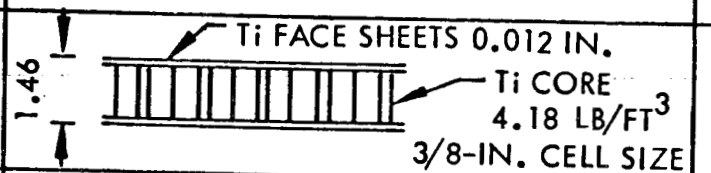  | 1.107 |
| 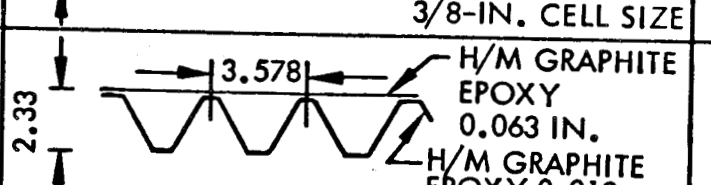  | 0.721 |
| 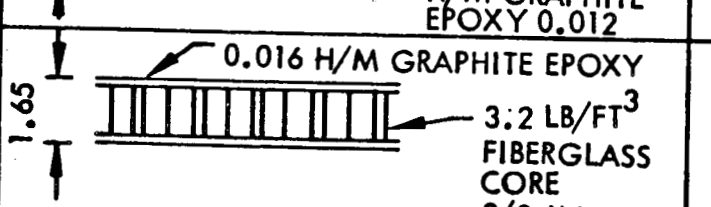  | 0.734 |

*THERMAL OPTIMUM $\bar{t}$ = 0.06 IN., OR 0.57 LB/FT$^2$ BASED ON 0.10-IN. BOND THICKNESS

D04992 (1)
RDB

Fig. 2.2.1-7

44-52 Ksi for the four beryllium configurations, generally increasing as weight decreases. This stress is in the range 27-33 Ksi for titanium, and 18-24 Ksi for graphite epoxy. Referring back to Fig. 2.2.1-3, it may be seen that the material weight ratios illustrated in this figure are reasonably accurate for a given configuration. Scatter in the ratios is present but this is due in part to the effect of the constraints in reducing ideal configuration structural efficiency. It should also be pointed out that while Fig. 2.2.1-3 assumes the same maximum compressive stress in the two materials being compared, this situation does not develop in the comparison presented here. Thus, Fig. 2.2.1-3 tends to yield conservative weight ratios. In a similar manner, the configurations comparison shown in Fig. 2.2.1-2 is also seen to yield reasonably accurate, qualitative projections for a given material.

In summary, this comparison shows that zee-stiffened beryllium construction is the optimum configuration for the substrate of prototype panel No. 1. This configuration, therefore, has been selected as a basis for subsequent steps in the design/analysis process. Other beryllium configurations are competitive; however, these competitors are more difficult to manufacture in addition to being heavier. The present comparison is probably somewhat a function of the loads, constraints and panel span specified here. Interchanges in the position of various material/configuration combinations may occur for other loads and constraints, but no significant changes are anticipated in the range of orbiter airloads currently cited.

The effect of panel span upon weight may be studied through charts of the type shown in Figs. 2.2.1-8 and -9. These charts show total system weight as a function of the sum of the weights of the individual parts. Here the aluminum primary structure has been sized using optimum wide column analysis to carry the in-plane loads in Area 2 listed in Fig. 2.2.1-5. Note the effect of the tension load requirement in over-riding the compression load requirement in Fig. 2.2.1-8. Fuselage frame weights have been calculated using the criterion presented in Ref. 2 for inertia requirements together with web and flange stability criteria for establishing area. These data do not consider curvature effects; in addition, they are dependent upon intermediate support points which for example might be provided by keels, longerons, floors, spars or struts.

# FRAME SPACING VS TPS/STRUCTURE WEIGHT SUBPANEL CONCEPT – AREA 2 FLIGHT DESIGN

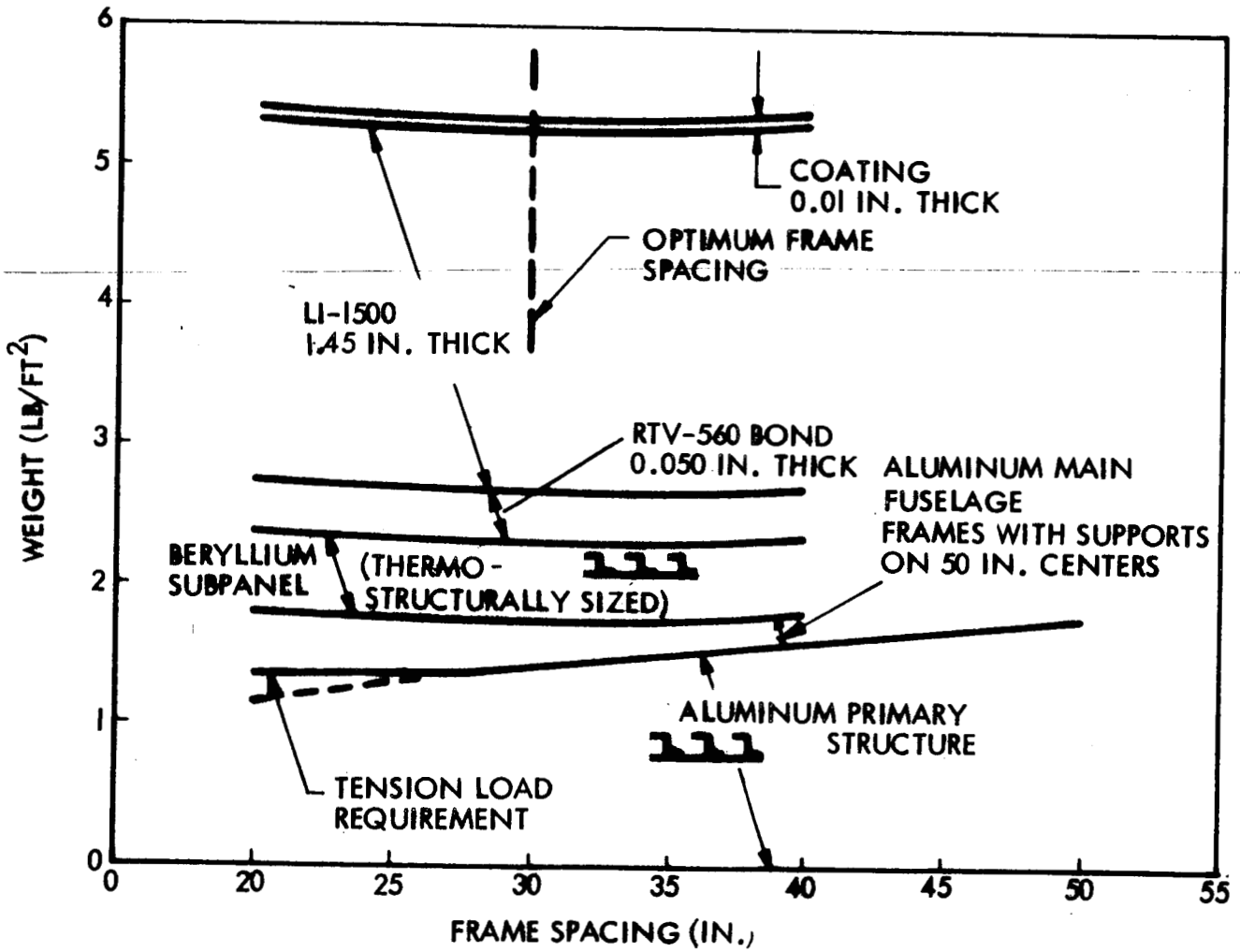


Fig. 2.2.1-8

D05164
rdb

# FRAME SPACING VS TPS/STRUCTURE WEIGHT SUBPANEL CONCEPT – AREA 2 FLIGHT DESIGN WITH CORRUGATED PRIMARY STRUCTURE

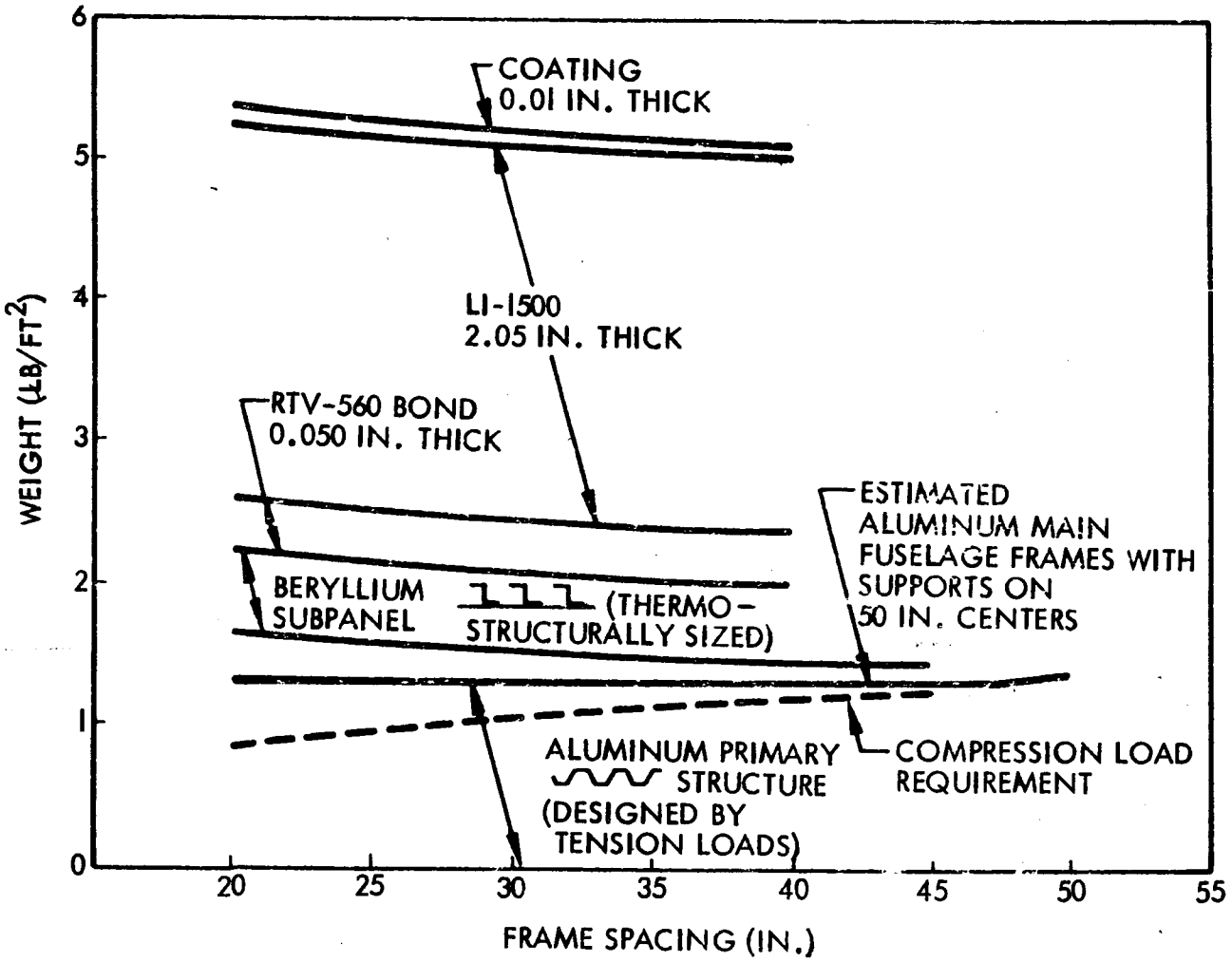


Fig. 2.2.1-9

D05154 (1)
rdb

The assumed support point spacing of 50 in. in the figures has been arbitrarily selected to result in a reasonable frame weight while maintaining an acceptably large support point spacing.

The beryllium subpanel weight shown in the figures is constant over the span of frame spacings of interest because it is a thermo-structurally optimized weight. As noted previously, and discussed elsewhere in this report, lower total system weights are obtained when beryllium in excess of that required for structural purposes is added to the system, used as a heat sink, and traded off against LI-1500 weight. Structural requirements do not exceed the thermo-structural optimization requirement until frame spacings greater than 40 in. are studied.

The LI-1500 thickness shown in Fig. 2.2.1-8 has been sized to limit the in-flight temperature of the aluminum primary structure to 300°F. The beryllium subpanel temperature, while capable of temperatures to 600°F, does not reach this temperature because of the limitation on the maximum temperature in the aluminum.

Figure 2.2.1-8 shows that the optimum frame spacing is about 30 inches. The total weight curve, however, is rather flat with respect to frame spacing in the range of values shown. It is therefore concluded that a span of approximately 25 in. for prototype panel No. 1 is representative of optimum frame spacing under the present design conditions.

In comparing Figs. 2.2.1-8 and -9, it is apparent that for the present design conditions, the use of more efficient primary structure configurations does not produce a more efficient design because of the in-plane tension loads. The influence of these loads tilts the total weight curve so that the optimum frame spacing is in excess of 40 inches. Again, however, the total weight curve is rather flat with respect to frame spacing. These charts demonstrate that optimum frame spacing is highly dependent upon the vehicle loads, and the character of the parts which compose the system. Note also that the weight of the LI-1500 material is roughly equivalent to the weight of the remaining parts. Thus, efforts to minimize structural weight must be dramatically effective if substantial overall weight reductions are to be obtained.

Selection of Optimum Primary Structure Configuration for Prototype Panel Nos. 2-4. Using the analytical techniques described in Section 2.2.1.1, several candidate primary structure configurations were optimized as beam columns. The design loads for vehicle area 2 were used in this study; all configurations were assumed to be fabricated from 7075-T6 aluminum inasmuch as material selection was not an open parameter. Also, a design temperature of 250°F was used since this is the maximum temperature the panels are subjected to in flight. See Appendix A for the detail analysis of each configuration.

The results, presented in Fig. 2.2.1-10, show the zee-stiffened configuration to be the lightest configuration. Again, the relative standing of the four configurations is reasonably well predicted by Fig. 2.2.1-2. Of interest in Fig. 2.2.1-10 are the maximum compressive stresses in the various configurations. The trapezoidal corrugation stiffened configuration maximum stress is apparently the result of the relatively shallow section in bending. Such a section is necessitated by b/t limitations on the greater number of thinner elements making up the section. The high maximum stress in the honeycomb sandwich configuration is, of course, somewhat misleading since the core does not sustain any direct load although it comprises one-third of the weight of the configuration.

The conclusions to be drawn from Fig. 2.2.1-10 apply specifically to prototype panel No. 2 but they may also be applied to prototype panels 3 and 4 as well. The stresses may be seen to be essentially unaffected by plasticity; therefore, the same ordering of the configurations may be anticipated for titanium optimum designs for prototype panel No. 4. Prototype panel No. 3, however, must be designed for the considerably higher in-plane compressive line loads in vehicle area 1. As shown in Fig. 2.2.1-2, these loads result in highly plastic stresses in optimum designs, with the result that weight becomes a function of total available load-carrying material without particular regard to its geometric destribution. In this situation, the honeycomb sandwich configuration does not improve in standing because of the non-load-carrying status of the core. However, the remaining configurations tend to have equal weights. For reasons of material procurement and simplicity of manufacture, therefore, the zee-stiffened configuration is again selected.

# COMPARISON OF CONFIGURATIONS FOR DIRECT-TO-PRIMARY STRUCTURE LI-1500 APPLICATIONS

- RESULTS BASED ON BEAM-COLUMN ANALYSIS (ALL DESIGNS STABLE)
- ALL DESIGNS USE 7075-T6 ALUMINUM AT 250°F
- DESIGNS BASED ON AREA 2 VEHICLE LOADS; CRITICAL ULTIMATE LOAD

FOR MAXIMUM DEFLECTION IN ALL DESIGNS ARE: $N_{x_{COMP}}$ = 2250 PPI, $P_{COLLAPSE}$ = 6 PSI

| CONFIGURATION | WT/FT$^2$ (LB) | MAXIMUM DEFLECTION (IN.) | | MAX OUTER FIBER STRESS (PSI) |
|---|---|---|---|---|
| | | BENDING ALONE | BEAM COLUMN | |
| 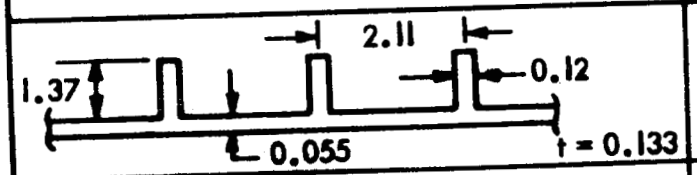  | 1.99 | 0.093 | 0.180 | 38,624* |
| 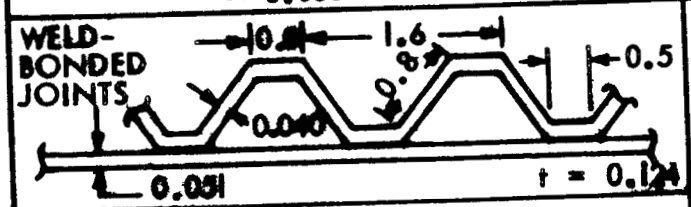  | 1.78 | 0.120 | 0.306 | 43,580* |
| 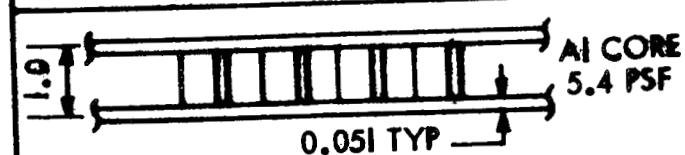  | 2.12 | 0.104 | 0.222 | 44,746* |
| 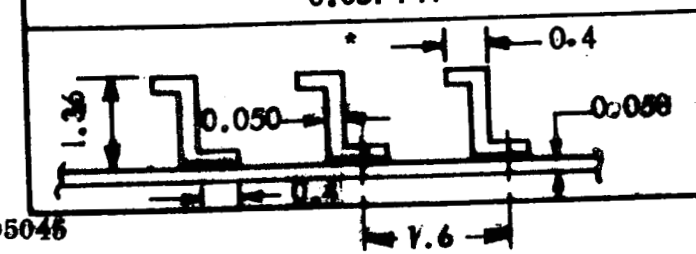  | 1.65 | 0.089 | 0.163 | 39,449* |

* OCCURS UNDER MAXIMUM LINE LOAD CONDITION

Fig. 2.2.1-10

DO5046

rdb

It should be pointed out that the configurations considered in this comparison have been limited to those with one or more flat surfaces on the premise that such a surface is required for the attachment of LI-1500. This decision may involve an arbitrary weight penalty to the system in those designs which are not critical for in-plane tension loads (see Fig. 2.2.1-2). In prototype panels 2-4, the relative magnitudes of the in-plane tension and compression loads result in little or no weight penalty, but there may be other vehicle areas where this situation is not the case. Also, note should be made of the maximum deflections associated with the various configurations in Fig. 2.2.1-10. Values up to 0.31 in. are shown, which appear high for compatibility with LI-1500 tiles. While these values are based on simply-supported edge conditions, and thus may be unrealistically high, it is apparent that some limiting deflection should be considered in primary structure panels with direct-bonded LI-1500 tiles. The zee-stiffened configuration in Fig. 2.2.1-10, notably, has the lowest maximum deflection of the configurations studies.

Charts of the type of Figs. 2.2.1-8 and -9 may be prepared which illustrate the effect of frame spacing upon total system weight when LI-1500 is attached directly to primary structure. An example chart is shown in Fig. 2.2.1-11. This chart represents a vehicle area 2 design, using aluminum primary structure and frames. The frames have been sized and supported in the same way described in the previous section. It may be seen that the optimum frame spacing in this case is approximately 25 in. which agrees favorably with the span specified for the prototype panels. The total weight curve is again rather flat, indicating some variation in the frame spacing will not affect system weight significantly.

The LI-1500 thickness shown in Fig. 2.2.1-11 has been sized to maintain the aluminum primary structure at temperatures of 300$^{\circ}$F or less. As a result, the weight of the LI-1500 is somewhat in excess of the weight of the rest of the system. It may be observed that the total system weight in Fig. 2.2.1-11 is greater than that in comparable designs utilizing subpanels as shown previously in Figs. 2.2.1-8 and -9. The difference appears to be due principally to greater LI-1500 weight, if the combined primary structure/frame/subpanel weight in Figs. 2.2.1-8 and -9 is traded off against the primary structure/frame weight in Fig. 2.2.1-11.

# FRAME SPACING VS TPS/STRUCTURE WEIGHT
## DIRECT-TO-PRIMARY STRUCTURE ATTACH CONCEPT - AREA 2 FLIGHT DESIGN

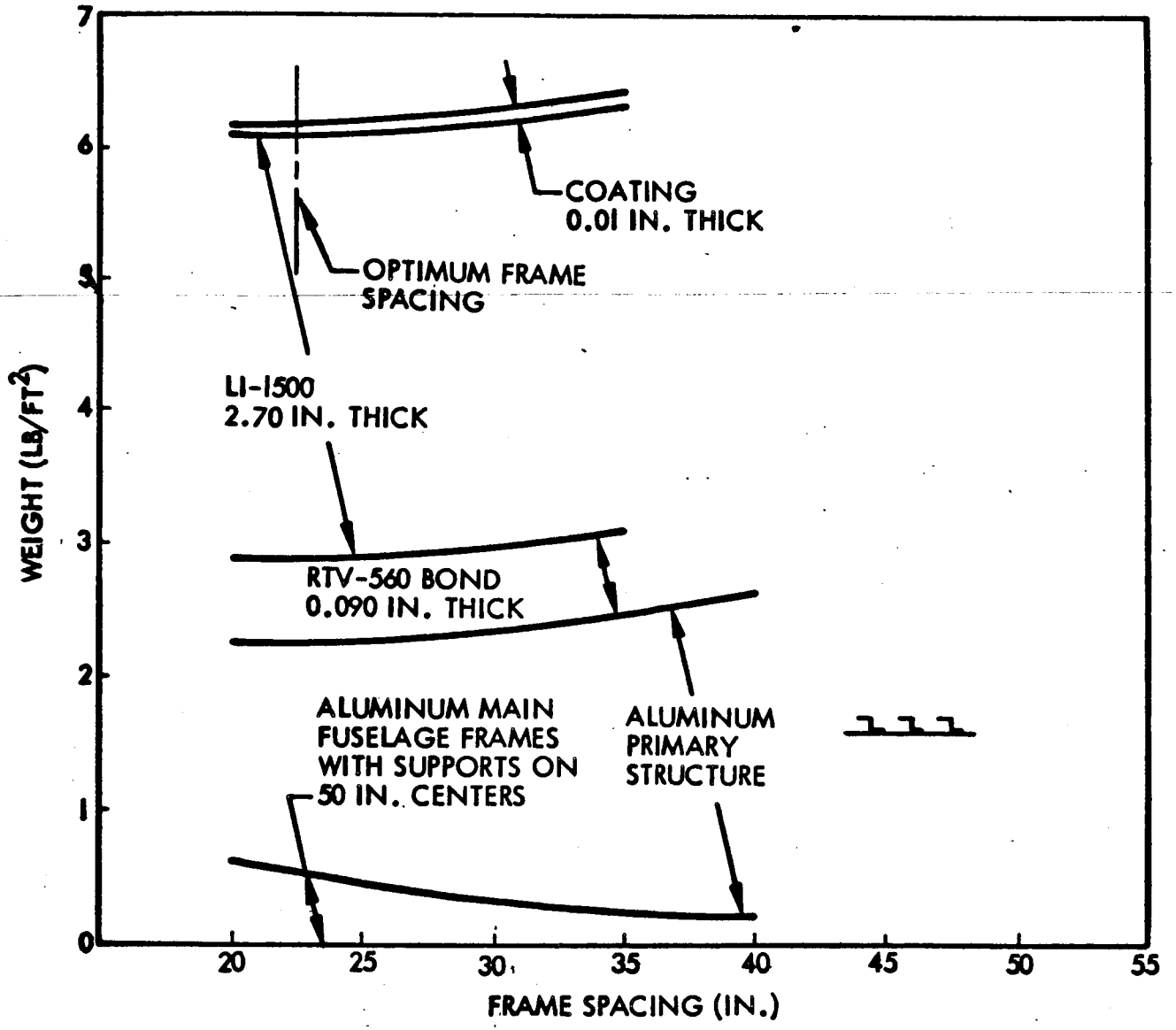


Fig. 2.2.1-11



D05146
rdb

41

Of further interest in Fig. 2.2.1-11 is the trend in frame weight with frame spacing. The downward trend with increased spacing is due to the fact that the frames are fewer in number and their weight is being distributed over greater surface areas. However, the trend is also influenced by the fact that the frame stiffness requirement is inversely proportional to panel length; that is, increasing panel stiffness with increasing panel length tends to reduce frame stiffness requirements.

2.2.1.4 Design and Analysis of Prototype Panel Substrates. On the basis of the data and results presented in the preceding sections of this report, the following material/configuration selections have been established for the four prototype panels:

| Panel No. | Vehicle Area No. | Type | Material | Configuration |
|---|---|---|---|---|
| 1 | 2 | Subpanel | Beryllium | Zee-Stiffened |
| 2 | 2 | Primary Structure | Aluminum | Zee-Stiffened |
| 3 | 1 | Primary Structure | Aluminum | Zee-Stiffened |
| 4 | 2 | Primary Structure | Titanium | Zee-Stiffened |

Detailed optimum design and analysis studies for the specific design requirements of NASA/MSC have been performed on each of these selections and are discussed below.

The orbiter design conditions presented in Fig. 2.2.1-5 may be summarized for purposes of the present analysis in the form shown in Fig. 2.2.1-12. Three load conditions are shown for each vehicle area. Load conditions I and II occur when the substrates are at room temperature, and load condition III occurs when the substrates are at or near the maximum temperatures shown in Note 1 to the figure. It has been conservatively assumed in these studies that any combination of line load and pressure for a given load condition may be applied simultaneously to the panel.

Optimum sizing of the four prototype panels was performed using the structural optimization computer codes previously discussed, followed by perturbations on these proportions as required for thermo-structural optimization. The latter optimization produced modifications only to the substrate for prototype panel No. 1. The designs were subsequently subjected to a detailed stress analysis to determine minimum margins of safety. These analyses are presented in Appendixes B and C, for prototype panel No. 1 and panel Nos. 2 through 4, respectively. Note that panel No. 3, representing Vehicle Area 1, has been sized for a panel span of 20 in., whereas the remaining panels have been sized for a panel span of 24 in. (see Section 2.1.6).

# PROTOTYPE PANELS DESIGN LOADS - SUMMARY

| LOAD COND | IN-PLANE LINE LOAD (LB/IN.) TENSION LIM | TENSION ULT | COMPRESSION LIM | COMPRESSION ULT | DIFFERENTIAL PRESSURE (LB/IN.$^2$) BURST LIM | BURST ULT | COLLAPSE LIM | COLLAPSE ULT |
|---|---|---|---|---|---|---|---|---|
| **AREA 1 PANELS** | | | | | | | | |
| I | 2400 | 3600 | 2100 | 3150 | 3.0 | 4.5 | 2.0 | 3.0 |
| II | 2700 | 4050 | 4000 | 6000 | 1.5 | 2.25 | 0.9 | 1.35 |
| III | 4000 | 6000 | 2000 | 3000 | 0.5 | 0.75 | 2.0 | 3.0 |
| **AREA 2 PANELS** | | | | | | | | |
| I | 2300 | 3450 | 1500 | 2250 | 3.0 | 4.5 | 4.0 | 6.0 |
| II | 2700 | 4050 | 2000 | 3000 | 1.9 | 2.85 | 1.8 | 2.7 |
| III | 4000 | 6000 | 2000 | 3000 | 0.5 | 0.75 | 2.0 | 3.0 |

NOTES:

1.

| PROTOTYPE PANEL CONFIGURATION NO. | LOAD AREA NO. | MAX TEMP COND III (°F) | PANEL SPAN (IN.) |
|---|---|---|---|
| 1 | TWO-PRESSURE ONLY | 600 | 24 |
| 2 | 2 | 250 | 24 |
| 3 | 1 | 250 | 20 |
| 4 | 2 | 600 | 24 |

2. LOAD CONDITIONS I AND II AT ROOM TEMPERATURE
3. LINE LOADS AND PRESSURES ACT IN ANY COMBINATION ON PANEL CONFIGURATIONS 2, 3, AND 4
4. FACTOR OF SAFETY = 1.5

DO6163

Fig. 2.2.1-12

The minimum margins of safety for the four panels are 10 percent or less, as shown in Fig. 2.2.1-13. Note that the minimum margin of safety for Prototype Panel No. 1 occurs for Loading Condition I when the panel is at room temperature. The minimum margin of safety for Panel No. 2 also occurs when the panel is at room temperature, but in the remaining two panels the minimum margin of safety occurs when the panels are at or near the maximum temperature permitted.

Results of the beam-column analysis performed on Panels 2 through 4 are summarized in Fig. 2.2.1-14. It may be seen that maximum deflections between approximately 0.09 in. and 0.19 in. are predicted. Approximately one-half of the deflection is caused by bending due to airloads in Prototype Panels 2 and 4, which represent Vehicle Area 2. Panel No. 3, representing Vehicle Area 1, is subject to much higher axial loads over a shorter span; thus, the deflection due to airloads is a much smaller proportion of the total deflection in this case.

Dynamic analyses are also required and were performed on the prototype panels as indicated in the analysis logic sequence diagram of Fig. 2.2.1-6. These analyses consisted of checks of each panel design for flutter stability and also for sonic fatigue. Analysis details are presented in Appendix D, and results are summarized in Figs. 2.2.1-15 and -16. Figure 2.2.1-15 shows the interstiffener panel flutter boundary for the weakest prototype panel, which is Panel No. 4. It may be observed that this panel is clearly flutter free when compared to the dynamic pressures expected on the vehicle during launch and reentry. Flutter of the complete panel was also investigated and found to yield significantly higher flutter boundaries for all panels than that shown in Fig. 2.2.1-15.

Sonic fatigue analysis results are presented in Fig. 2.2.1-16. These results are based on an experimentally determined LI-1500 damping ratio of 0.02. The data points shown on the figure represent the anticipated life cycle of the panels multiplied by a safe-life margin of four. As may be seen, all four prototype panel points fall below their respective allowable stress curves.

# MINIMUM MARGINS OF SAFETY SUMMARY - PROTOTYPE PANELS

| CONFIGURATION NO. | ELEMENT | M.S. | FAILURE MODE | CRITICAL LOAD COND |
|---|---|---|---|---|
| 1 | PANEL ASSEMBLY | + 0.34 | TENSION - ULTIMATE | 1 |
| | STIFFENER ONLY | + 0.05 | LOCAL BUCKLING | 1 |
| | FACE SHEET | + 0.41 | BENDING - ULTIMATE | 1 |
| | CLOSURE ANGLE | + 0.12 | LOCAL BUCKLING | 1 |
| | STIFFENER LEG | + 0.34 | LOCAL BUCKLING | 1 |
| 2 | PANEL ASS'Y | + 0.82 | COLUMN BUCKLING | 111 |
| | STIFFENER LEG | + 0.15 | CRIPPLING | 11 |
| | STIFFENER LEG | + 0.06 | TENSION - ULTIMATE | 111 |
| | STIFFENER LEG | + 0.28 | BEARING - ULTIMATE | 111 |
| | FACE SHEET | + 0.59 | LOCAL BUCKLING | 111 |
| 3 | PANEL ASS'Y | + 0.45 | COLUMN BUCKLING | 11 |
| | STIFFENER LEG | + 0.10 | CRIPPLING | 11 |
| | STIFFENER LEG | + 0.36 | TENSION - ULTIMATE | 111 |
| | STIFFENER LEG | + 0.62 | BEARING - ULTIMATE | 111 |
| | FACE SHEET | + 0.49 | LOCAL BUCKLING | 11 |
| 4 | PANEL ASS'Y | + 0.67 | COLUMN BUCKLING | 111 |
| | STIFFENER LEG | + 0.18 | CRIPPLING | 111 |
| | STIFFENER LEG | + 0.29 | TENSION - ULTIMATE | 111 |
| | STIFFENER LEG | + 0.62 | BEARING - ULTIMATE | 111 |
| | FACE SHEET | + 0.01 | LOCAL BUCKLING | 111 |
| | FASTENERS | + 1.2 | SHEAR - ULTIMATE | 111 |

$$M.S = \frac{\text{ALLOWABLE LOAD}}{\text{ULTIMATE LOAD}} - 1$$

Fig. 2.2.1-13

# BEAM – COLUMN ANALYSIS RESULTS FOR PANELS 2-4

| PANEL NO. | MAXIMUM DEFLECTION (IN.) | | MAX OUTER FIBER STRESS (PSI) | CRITICAL LOAD CONDITION |
|---|---|---|---|---|
| | BENDING ALONE | BEAM COLUMN | | |
| 2 ($\ell$ = 24 IN.) | 0.089 | 0.163 | 30,924 | 1 (COLLAPSE PRESSURE) |
| | 0.067 | 0.122 | 39,449 | 1 (BURST PRESSURE) |
| 3 ($\ell$ = 20 IN.) | 0.016 | 0.087 | 60,246 | 1 (BURST PRESSURE) |
| 4 ($\ell$ = 24 IN.) | 0.096 | 0.186 | 40,338 | 1 (COLLAPSE PRESSURE) |
| | 0.072 | 0.140 | 52,561 | 1 (BURST PRESSURE) |

DO5024
RDB

Fig. 2.2.1-14

# TPS CRITICAL PANEL FLUTTER STABILITY

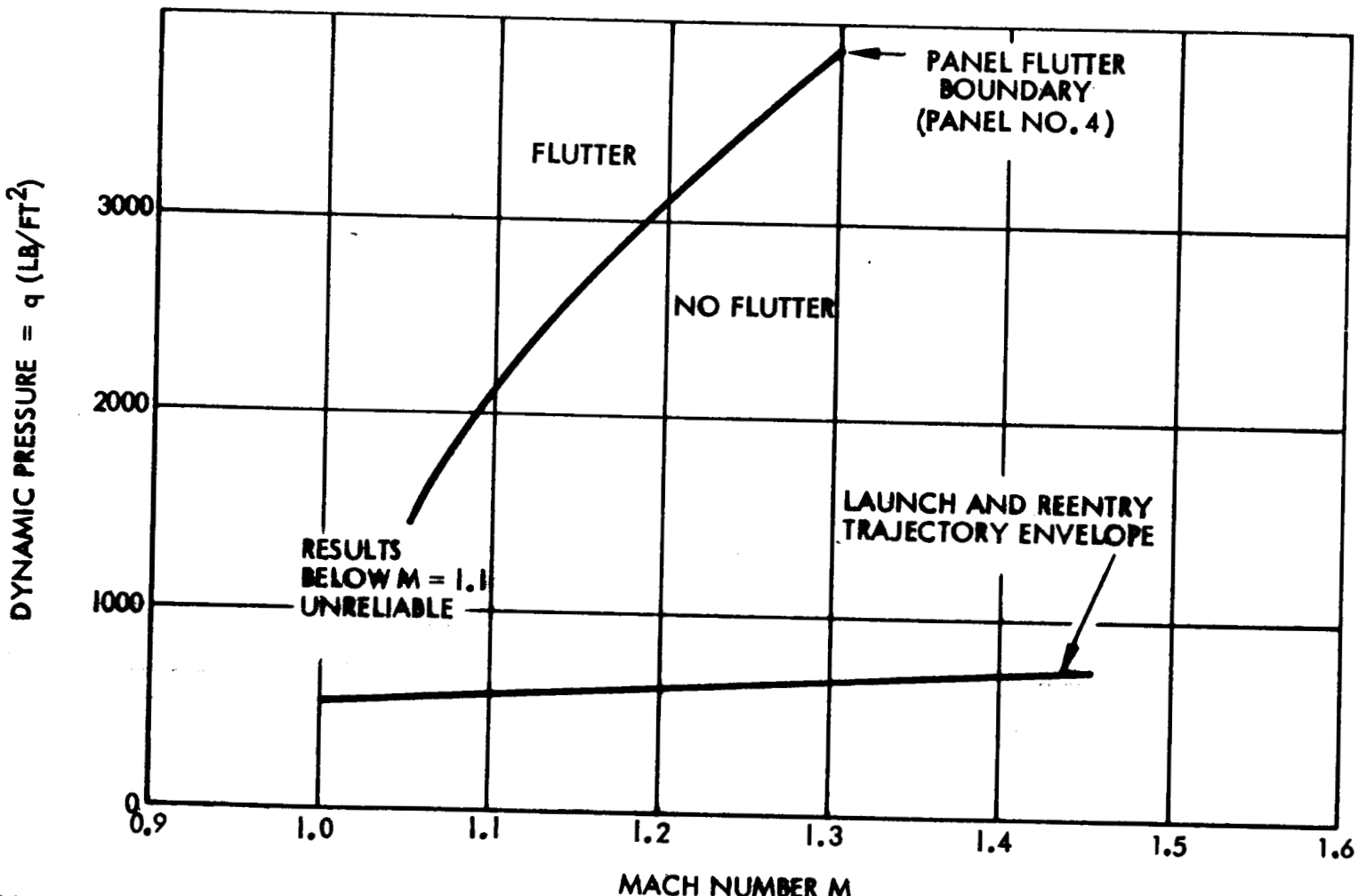


DO5042(1)
RDB

Fig. 2.2.1-15

# SONIC FATIGUE ANALYSIS OF TPS PANELS

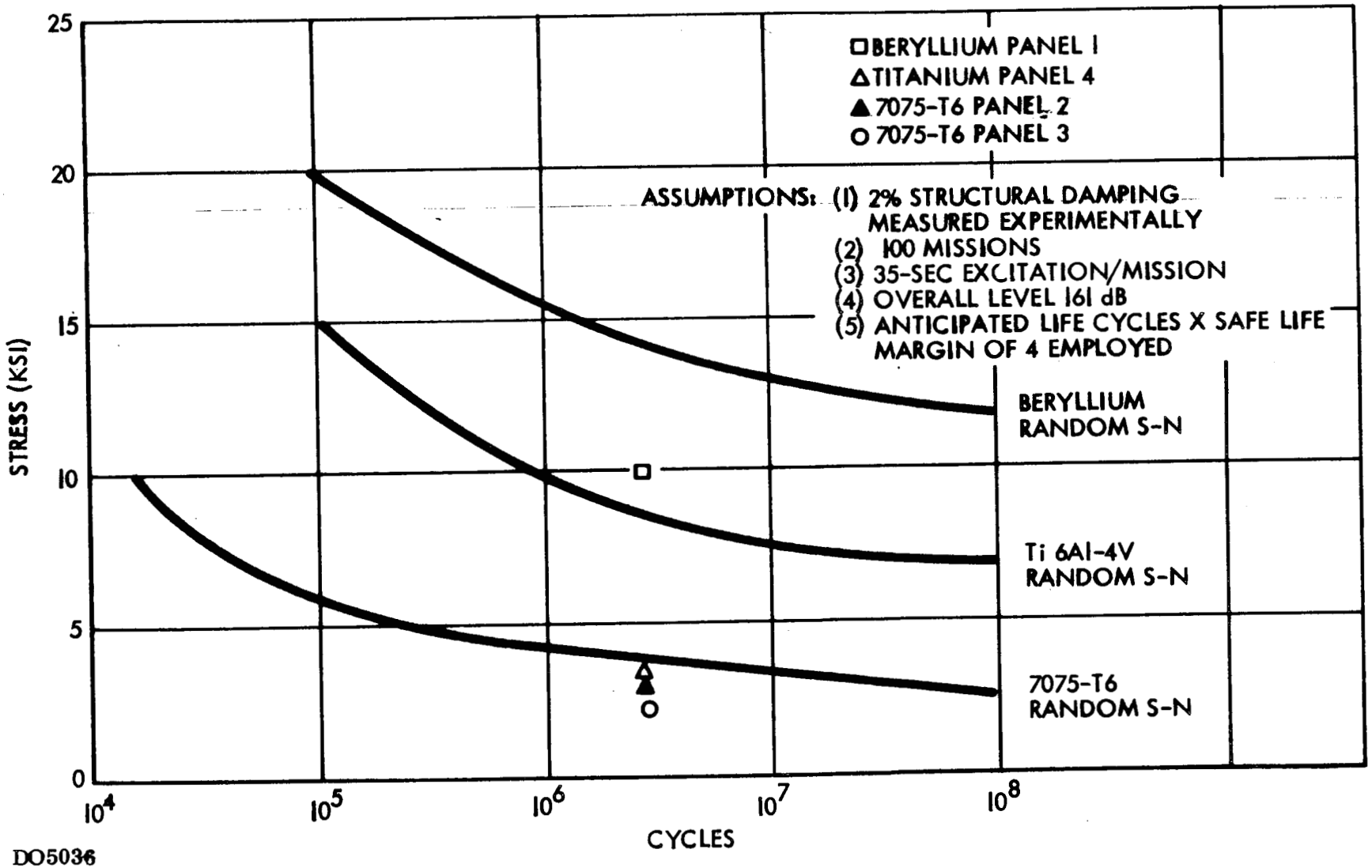


DO5036

Fig. 2.2.1-16

The four prototype panel substrate final designs are shown in Figs. 6.1-1 through -4 for Panel Nos. 1 through 4, respectively, as verified by static and dynamic analyses. The weights of the metallic portion of these panels (with no allowance for fasteners or closeouts) are summarized below:

| Panel No. | $\bar{t}$ (in.) | $Wt/Ft^2$ (lb) |
|---|---|---|
| 1 | 0.061 | 0.57 |
| 2 | 0.114 | 1.66 |
| 3 | 0.143 | 2.08 |
| 4 | 0.090 | 2.07 |

2.2.1.5 Comparison of LI-1500 Panel Designs Vs Metallic Heat Shield Designs. The prototype panels proposed herein for fabrication and test must be shown to be lighter than comparable metallic heat shield designs that have been developed at LMSC. In this subsection, metallic heat shield designs are described and weight comparisons are presented.

Two approaches to the design of metallic heat shields have been studied at LMSC. In one, the metallic heat shield is supported by relatively closely spaced standoffs which are attached to a subpanel with span equal to the frame spacing. Flexible insulation is placed between the heat shield and the subpanel; the depth of the standoffs is the optimum derived from a consideration of the materials specified for the design, the design environment, and the insulation properties. In the second approach, the heat shield is designed with sufficient stiffness to span the distance between frames directly; insulation and packaging is placed underneath, between the heat shield and the primary structure. Typical designs utilizing a coated columbium heat shield are shown in Fig. 2.2.1-17. These designs have been developed for a short pulse trajectory with maximum temperature of 2300°F, as utilized in on-going LMSC space-shuttle orbiter studies. As shown in the figure, the subpanel approach yields the lightest metallic heat shield weight.

# METALLIC HEAT SHIELD WEIGHT COMPARISON

(LS 400-7 TWO-STAGE ORBITER WITH FRAME SPACING = 25 IN.
SHORT PULSE TRAJECTORY AT MAXIMUM TEMPERATURE OF 2300°F)

| CONCEPTS | DESCRIPTIONS | TPS WEIGHT LB/FT$^2$ |
|---|---|---|
| 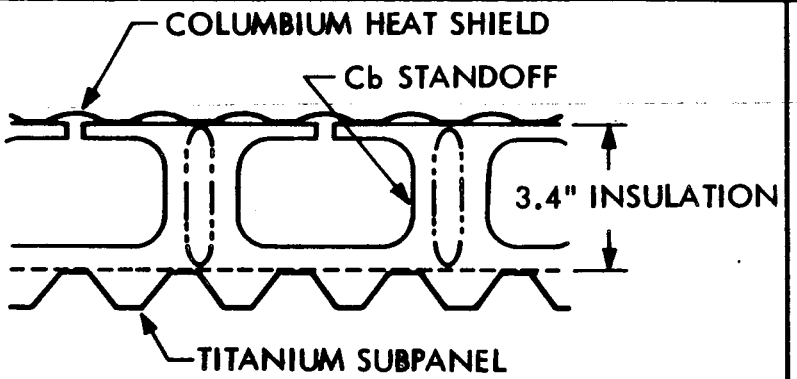 | WEIGHT OF METALLIC HEATSHIELD, STANDOFFS, AND TITANIUM SUBPANEL<br>WEIGHT OF FLEXIBLE INSULATION AND PACKAGING<br>TOTAL WEIGHT | 2.361<br>1.997<br>4.358 |
| 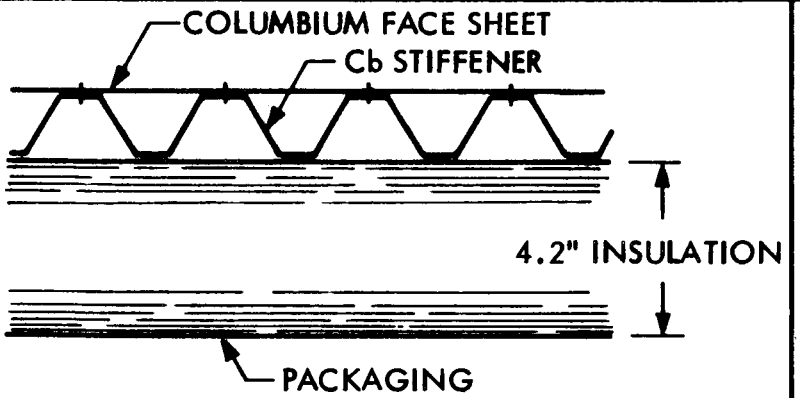 | WEIGHT OF METALLIC HEATSHIELD WITHOUT SUBPANEL<br>WEIGHT OF FLEXIBLE INSULATION AND PACKAGING<br>TOTAL WEIGHT | 3.654<br>2.417<br>6.071 |

- LMSC's BEST METALLIC HEATSHIELD FOR 2300°F APPLICATIONS UTILIZES SUBPANEL CONCEPT

D05172
rdb

Fig. 2.2.1-17

The short-pulse trajectory is characterized by a substantially lower total heat input than the trajectory for which the prototype panels have been designed. Selecting the subpanel approach as the optimum approach, heat shield weights for other total heat inputs have been determined as shown in Fig. 2.2.1-18. Noted on this figure are total heat inputs for the NASA-MSC trajectory, both perturbed to 2300°F and unperturbed, for Vehicle Area 2. Weights are shown for LI-1500 panel designs as well as metallic heat shield designs. As a check on these results, a metallic heat shield data point obtained from a MDAC reference report is also shown. Good agreement in terms of unit panel weight may be observed. The curves in Fig. 2.2.1-18 emphasize the weight penalty involved with the longer pulse trajectories as well as the relative efficiency of metallic heat shields vs LI-1500.

It is apparent from Fig. 2.2.1-18 that care must be exercised to compare TPS designs based on identical heat pulses. Several such comparisons are presented in Fig. 2.2.1-19; these relate to the heat-pulses presented in Fig. 2.2.1-20. Heat-pulses are shown in Fig. 2.2.1-20 for the LMSC delta wing orbiter protected by LI-1500 and by metallic TPS. Note that the LI-1500 heat pulse is of short duration and peaks at 2300°F, while the metallic TPS heat pulse is of long duration in order to limit the peak temperature to 2000°F. The NASA-MSC heat pulse, also shown, is seen to combine the higher maximum temperature with the long duration heat pulse.

The data in Fig. 2.2.1-19 relate to both Vehicle Areas 1 and 2. Area 2 results are presented for both metallic and LI-1500 TPS designs for the following heat-pulses:

a. LMSC delta wing orbiter, 2300°F maximum temperature flight heat pulse (RE214)

b. NASA-MSC unperturbed, 2050°F maximum temperature flight heat pulse

c. NASA-MSC perturbed 2300°F maximum temperature flight heat pulse

d. NASA-MSC perturbed, 2300°F maximum temperature test heat pulse

The significant differences in these heat pulses are: (1) the designs for flight heat pulses account for radiation to the primary structure in those designs specifying sub-panels, whereas the test heat pulse designs are based on an adiabatic back-face

# COMPARISON OF TPS UNIT WEIGHTS

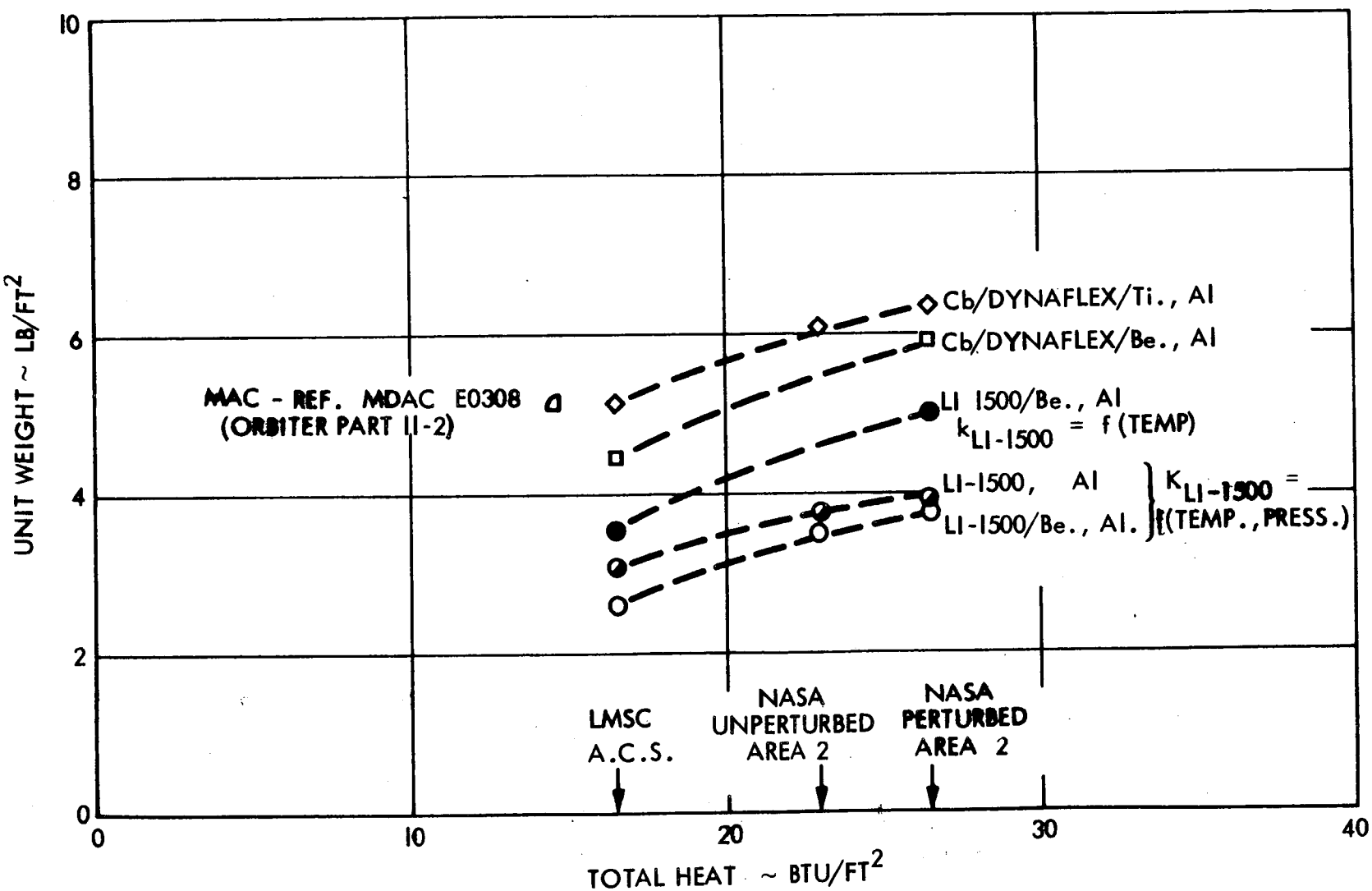


Fig. 2.2.1-18

# COMPARISON OF METALLIC TPS VS LI-1500 TPS

| CONCEPTS | DESCRIPTION | AREA 2 PANEL LENGTH = 24 IN. | | | | AREA 1 PANEL LENGTH = 20 IN. | |
|---|---|---|---|---|---|---|---|
| | | $P_{COLLAPSE}$ = 6 LB/IN.$^2$, $P_{BURST}$ = 4.5 LB/IN.$^2$, $-N_x$ = [illegible] LB/IN., $N_x$ = [illegible] LB/IN. | | | | $P_{LAPSE}$ = 3 LB/IN.$^2$, $P_{BURST}$ = 4.5 LB/IN.$^2$, $N_x$ = [illegible] LB/IN. | |
| | | (1) 2300°F LMSC-RE214 | (2) 2050°F NASA (UNPERTURBED) | (3) 2300°F NASA (PERTURBED) | (4) 2300°F NASA (TEST) | (5) 1480°F FLIGHT | (6) 1480°F TEST |
| 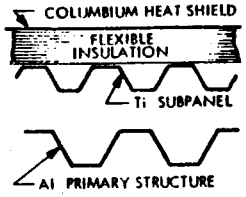 | METALLIC TPS | | | | | | |
| | ●METALLIC HEATSHIELD WITH Ti SUBPANEL | 3.489* | 2.615* | 2.645* | 2.521* | 1.606** | 1.573** |
| | ●FLEXIBLE INSULATION: | 2.680 | 3.467 | 3.625 | 2.942 | 2.102 | 1.787 |
| | -METALLIC HEATSHIELD AND INSULATION. | 6.169 | 6,082 | 6,270 | 5.463 | 3.708 | 3.360 |
| | -CORRUGATED ALUMINUM PRIMARY STRUCTURE | 1.486 (T) | 1.486 | 1.486 | 1.486 | 1.595 (C) | 1.595 |
| | ●WEIGHT OF TPS AND PRIMARY STRUCTURE, LB/FT$^2$ | 7.655 | 7.568 | 7.756 | 6.949 | 5.303 | 4.955 |
| 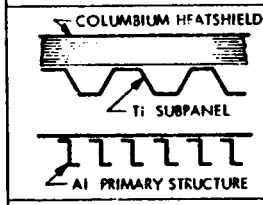 | METALLIC TPS | | | | | | |
| | ●METALLIC HEATSHIELD WITH Ti SUBPANEL | 3.489* | 2.615* | 2.645* | 2.521* | 1.606** | 1.573** |
| | ●FLEXIBLE INSULATION: | 2.680 | 3.467 | 3.625 | 2.942 | 2.102 | 1.787 |
| | - METALLIC HEATSHIELD AND INSULATION | 6.169 | 6.082 | 6.270 | 5.463 | 3.708 | 3.360 |
| | - Z-STIFFNED ALUMINUM PRIMARY STRUCTURE | 1.486 (T) | 1.486 | 1.486 | 1.486 | 1.726 (C) | 1.726 |
| | ●WEIGHT OF TPS AND PRIMARY STRUCTURE, LB/FT$^2$ | 7.655 | 7.560 | 7.756 | 6.949 | 5.434 | 5.086 |
| 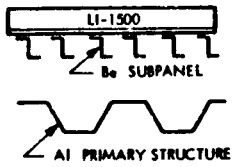 | RSI TPS WITH SUBPANEL | | | | | | |
| | ●BERYLLIUM SUBPANEL | 0.630 | 0.630 | 0.630 | 0.630 | 0.630 | 0.630 |
| | ●LI-1500 AND BOND | 2.171 | 2.880 | 3.076 | 3.142 | 1.764 | 1.961 |
| | - LI-1500, BOND AND SUBPANEL | 2.801 | 3.510 | 3.706 | 3.772 | 2.394 | 2.591 |
| | - CORRUGATED ALUMINUM PRIMARY STRUCTURE | 1.486 (T) | 1.486 | 1.486 | 1.486 | 1.595 (C) | 1.595 |
| | ●WEIGHT OF TPS AND PRIMARY STRUCTURE, LB/FT$^2$ | 4.287 | 4.996 | 5.192 | 5.258 | 3.989 | 4.186 |
| 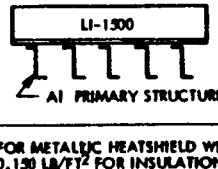 | RSI TPS ATTACHED DIRECTLY TO PRIMARY STRUCTURE | 2.05 | | | | | 3.169 |
| | ● LI-1500 AND BOND | 3.077 | 3.733 | 3.930 | 5.045 | 2.722 | 3.273 |
| | ● Z-STIFFENED ALUMINUM PRIMARY STRUCTURE | 1.747 | 1.747 | 1.747 | 1.747 | 2.183 | 2.183 |
| | ●WEIGHT OF TPS AND PRIMARY STRUCTURE, LB/FT$^2$ | 4.824 | 5.480 | 5.677 | 6.792 | 4.905 | 5.352 |

*FOR METALLIC HEATSHIELD WITH Be SUBPANEL, DEDUCT 0.262 LB/FT FOR SUBPANEL AND 0.150 LB/FT$^2$ FOR INSULATION
**RENE' 41 HEATSHIELD

Fig. 2.2.1-19

# COMPARISON OF LMSC - MSC RADIANT - HEAT PULSES FOR 1100 - NM CROSSRANGE TRAJECTORY

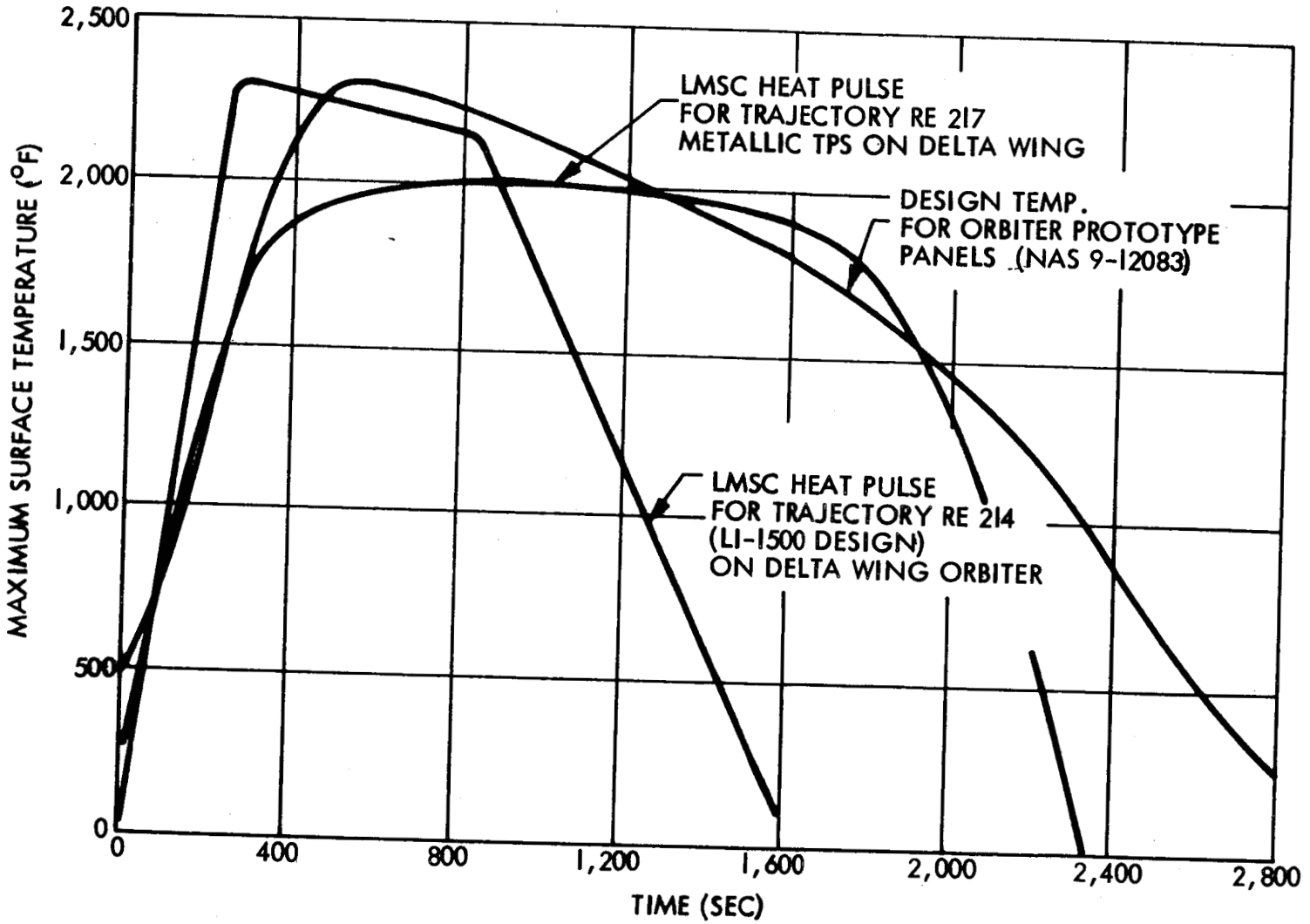


Fig. 2.2.1-20

temperature; (2) the flight heat pulse LI-1500 designs utilize the lower thermal conductivity of LI-1500 in vacuum, whereas the test heat pulse designs do not; and (3) the LMSC-RE214 heat pulse involves significantly lower total heat input. Because Area 1 experiences a much lower maximum surface temperature, only two heat pulses are considered; these correspond to the NASA-MSC flight and test heat pulses.

In Vehicle Area 2, it can be seen that the adiabatic back-face temperature stipulation for test is advantageous for the metallic TPS designs but disadvantageous for the LI-1500 TPS designs. In the latter designs, the lower thermal conductivity of LI-1500 in vacuum cannot be utilized in the one atmosphere tests. The lower thermal conductivity of LI-1500 in vacuum is noted to over-compensate for weight penalties in maintaining the aluminum primary structure temperature at or below 300°F in flight; note that this radiation factor results in a weight penalty to the metallic TPS flight designs. Thus, the test heat pulse comparison of LI-1500 and metallic TPS designs results in a close comparison that is misleading in terms of the true flight environment. The same phenomenon is observed in the results for Vehicle Area 1.

The NASA-MSC 2050°F and 2300°F heat pulses yield metallic TPS designs which are not significantly different from the designs for the LMSC-RE214 heat pulse. The LI-1500 TPS designs show weight increases due principally to the need for more material to absorb the added heat of the longer heat pulse.

It should be noted, in comparing the data of Figs. 2.2.1-8 and -9 and Fig. 2.2.1-11 with the data of Fig. 2.2.1-19, that frame weights have been included in the former but not in the latter. Also, the subpanel and primary structure weights calculated previously have been multiplied by a non-optimum factor to account for fasteners, closeouts, and other details.

In summary, the data presented here show the LI-1500 TPS designs to be lighter than comparable metallic TPS designs, when both are designed to the same heat pulse. LI-1500 TPS designs based on a 2300°F maximum temperature flight heat pulse are also lighter than metallic TPS designs based on a 2050°F maximum temperature flight heat pulse. The desirability of designing and testing LI-1500 TPS designs in the true vacuum environment of flight when maximum temperatures are attained has also been established.

### 2.2.2 Thermal Analysis

The basic insulation sizing of the design methodology logic sequence is presented in terms of the design iterations performed for the four prototype panels to be supplied under Task 6. The thermodynamics effort starts with the given heat rate and pressure environments for Areas 1 and 2, and concludes with two dimensional thermal modeling of the test panels to verify the one dimensional thermal sizing analyses.

2.2.2.1 Ascent and Reentry Heating Environment. The ascent and reentry heat rates provided by NASA for Areas 1 and 2 of the delta wing orbiter, Fig. 2.2.2-1, are shown in Figs. 2.2.2-2 and -3. The perturbed heat rate of Area 2 was used in these analyses. Calculation of ascent temperature histories was based on a surface emittance of 0.8, the LMSC THERM computer code, and a one-dimensional thermal model (see Figs. 2.2.2-4 and -5). Maximum surface temperatures of 495$^{\circ}$F and 565$^{\circ}$F are experienced by Areas 1 and 2, respectively. The ascent heating environment is very mild, as evidenced by the temperature distributions at orbit injection, shown in Fig. 2.2.2-6. The substrate temperature has not increased from its initial value of 75$^{\circ}$F.

The reentry heating and pressure environment for Areas 1 and 2 is shown in Figs. 2.2.2-7 and -8. The temperatures shown are radiation equilibrium temperatures calculated with an emittance of 0.8 and the heat rate histories of Figs. 2.2.2-2 and -3. The maximum surface temperatures are 2300$^{\circ}$F and 1480$^{\circ}$F for Areas 2 and 1, respectively. The difference in the times of peak temperature for Areas 1 and 2 is associated with the occurrence of boundary layer transition for Area 1 at about 2000 sec. into the reentry. As noted in Figs. 2.2.2-7 and -8, most of the reentry heat pulse occurs while the local static pressure is less than 0.1 ATM. Hence, the pressure dependence of the thermal conductivity of the LI-1500 rigid surface insulation will significantly affect the thermal sizing of the RSI.

2.2.2.2 Thermal/Structural Optimization for Test Panels. Lockheed's THERM computer code was used to size the prototype panels. The THERM code is a highly efficient thermal analyzer code that utilizes finite difference techniques to solve the transient

# LOWER SURFACE OF DELTA WING ORBITER

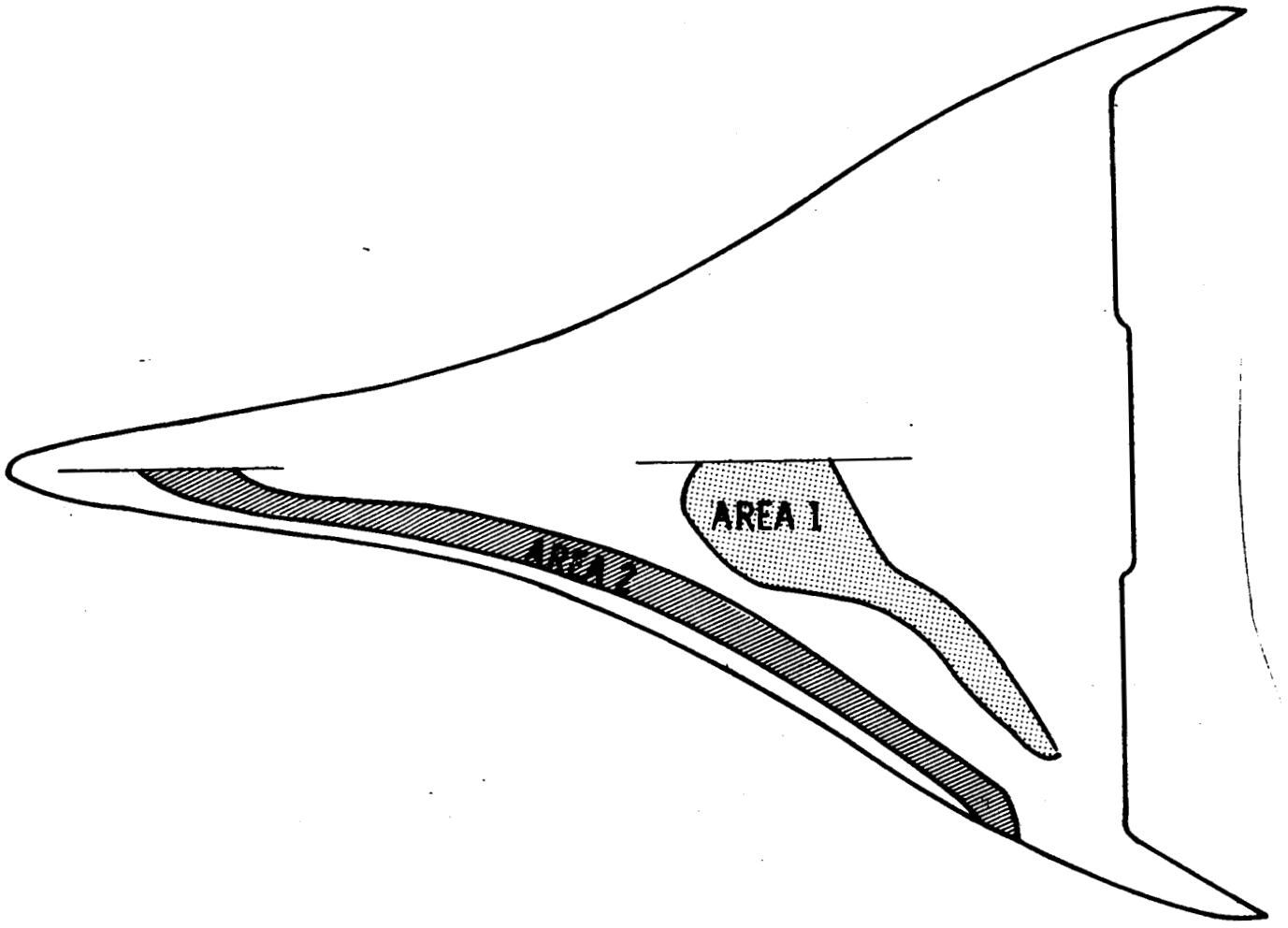


Fig. 2.2.2-1

DO5997

# ASCENT TRAJECTORY AND HEAT RATE HISTORIES

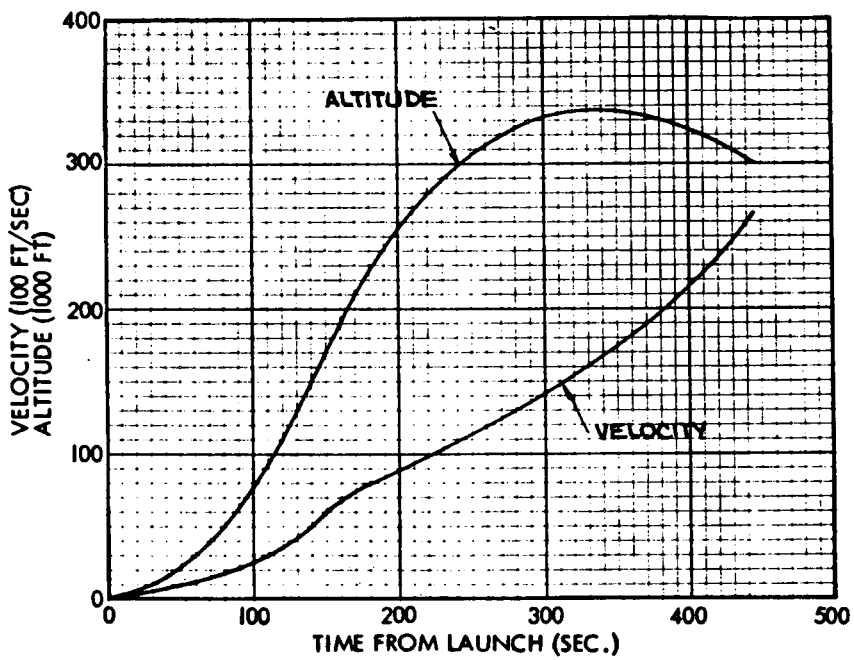


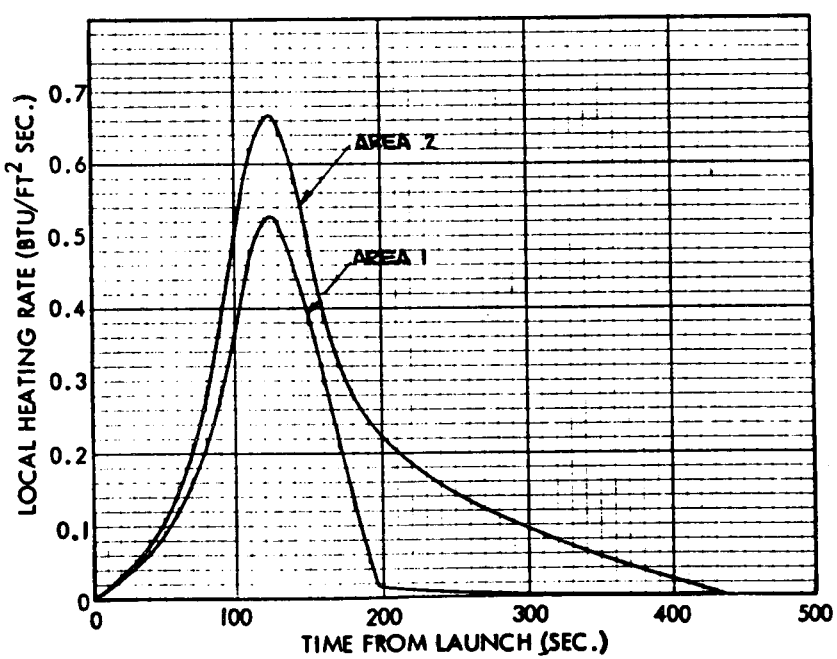


DO6150

Fig. 2.2.2-2

# REENTRY TRAJECTORY AND HEAT RATE HISTORIES

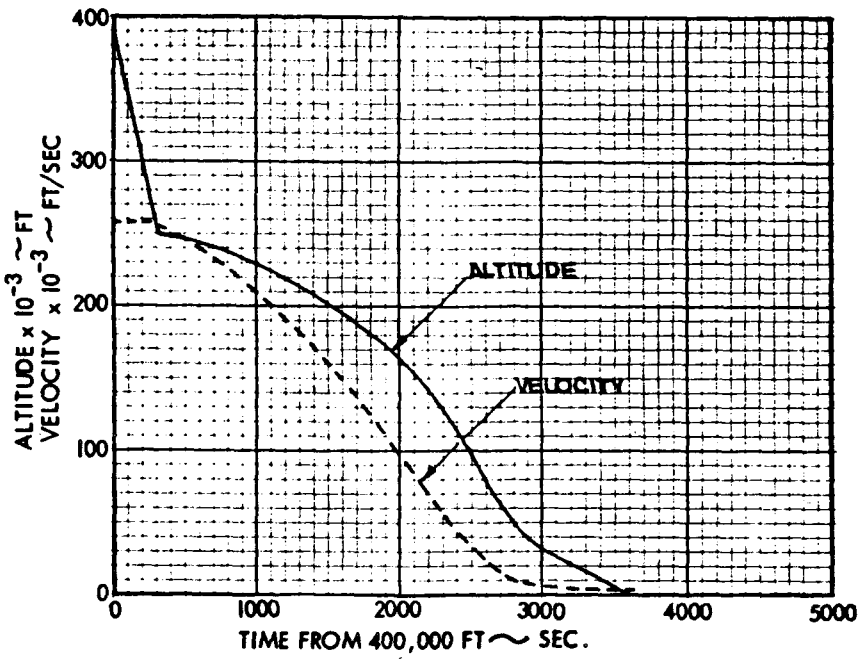


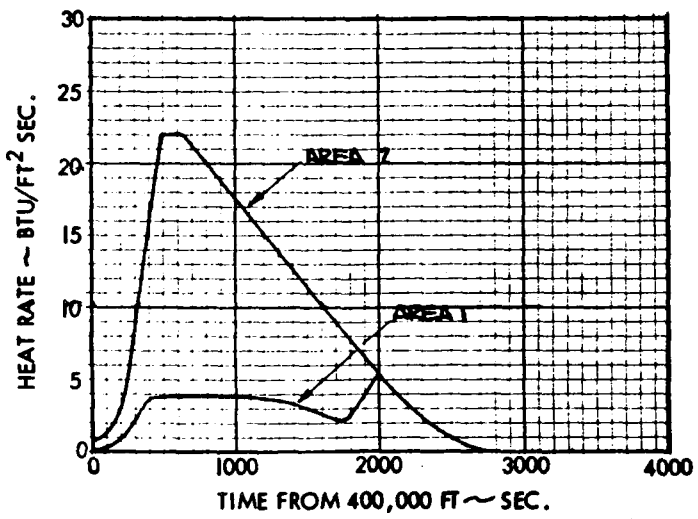


DO6149

Fig. 2.2.2-3

# ASCENT TEMP. HISTORIES FOR AREA I

ASCENT TEMPS. NASA AREA I

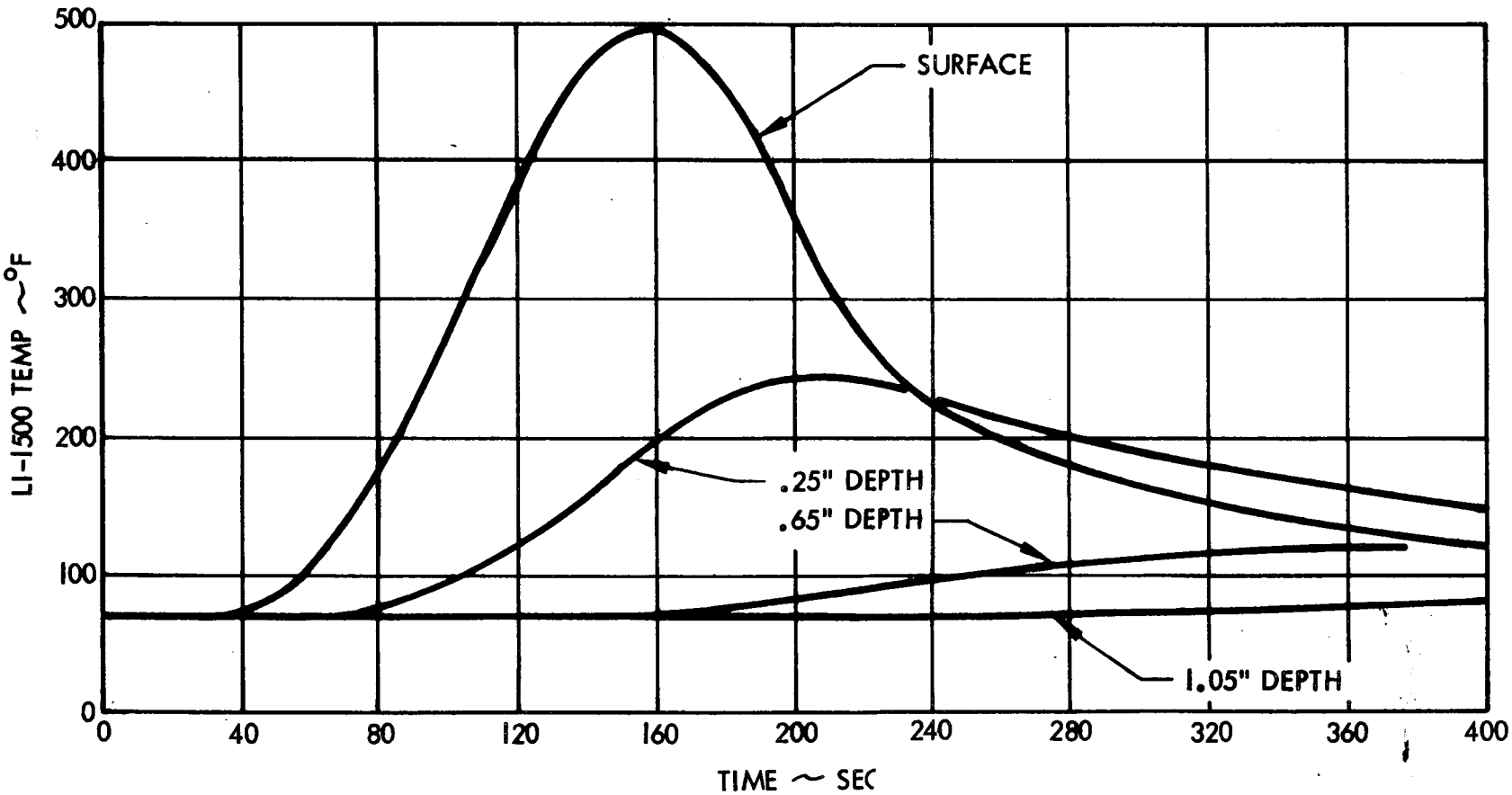


Fig. 2.2.2-4

# ASCENT TEMP. HISTORIES FOR AREA 2

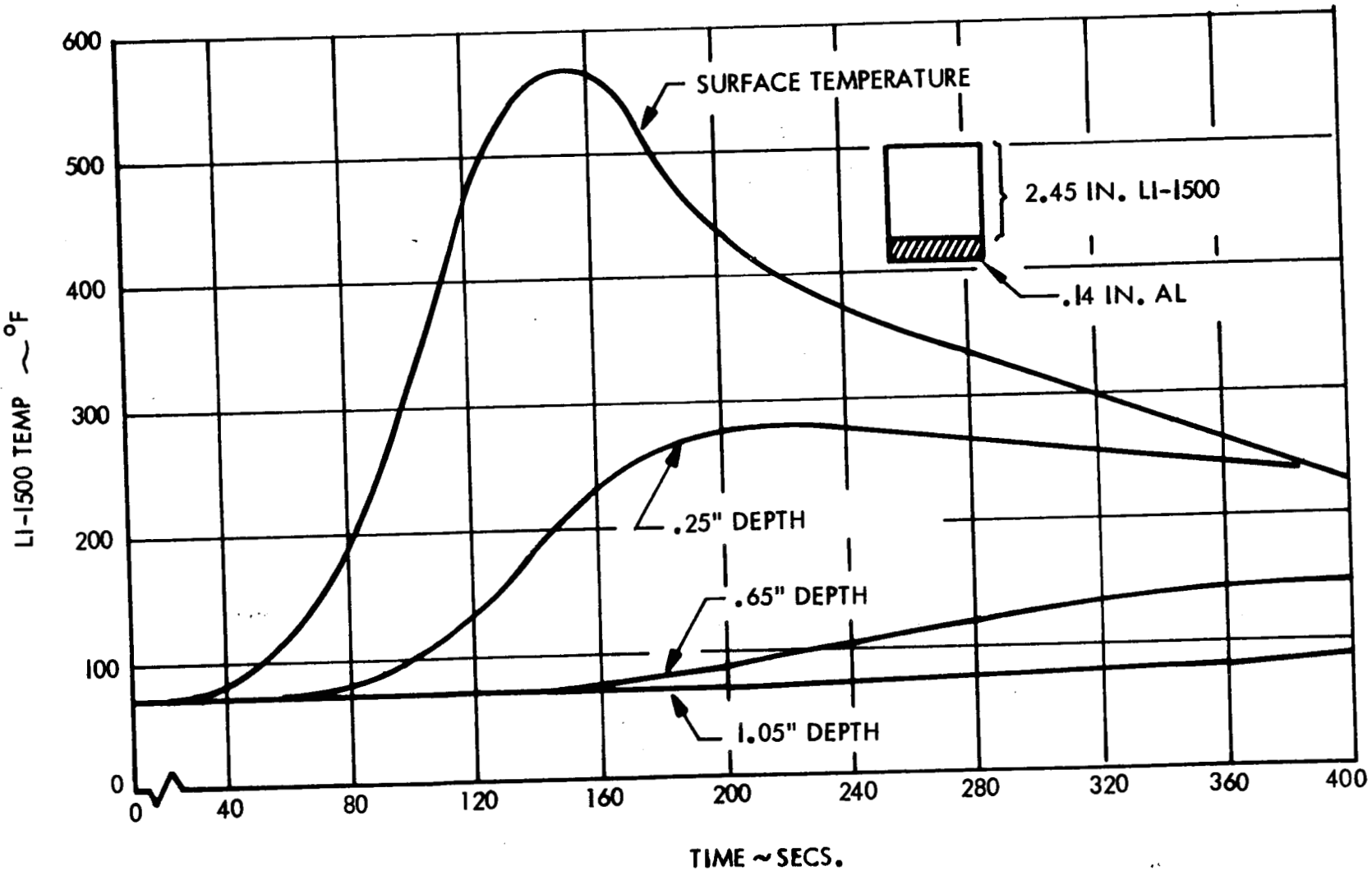


DO6057

Fig. 2.2.2-5

# ASCENT TEMPERATURE DISTRIBUTIONS
## AREA 2

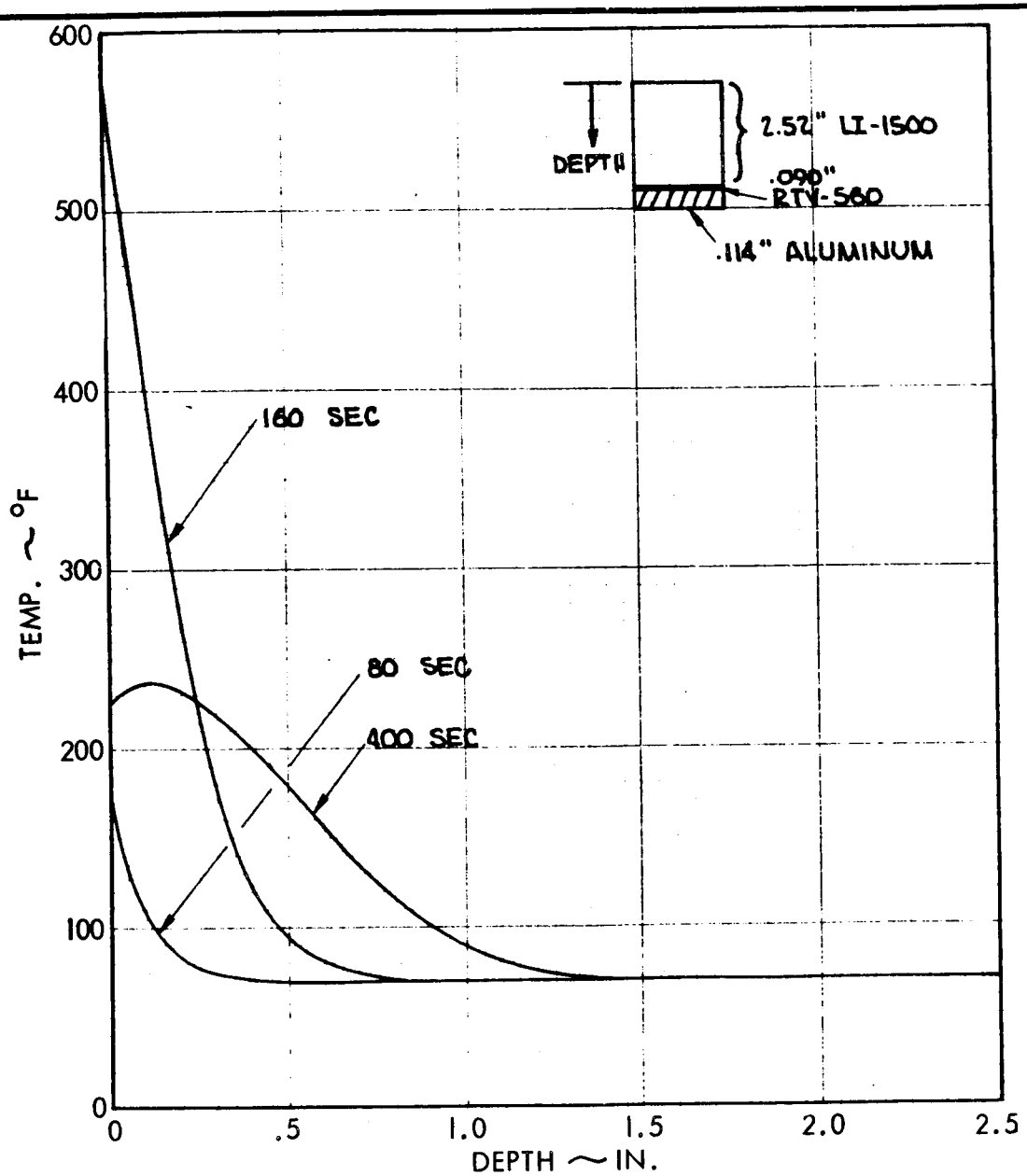


Fig. 2.2.2-6

# REENTRY TEMPERATURE AND PRESSURE HISTORIES - AREA 1

EMITTANCE = 0.8

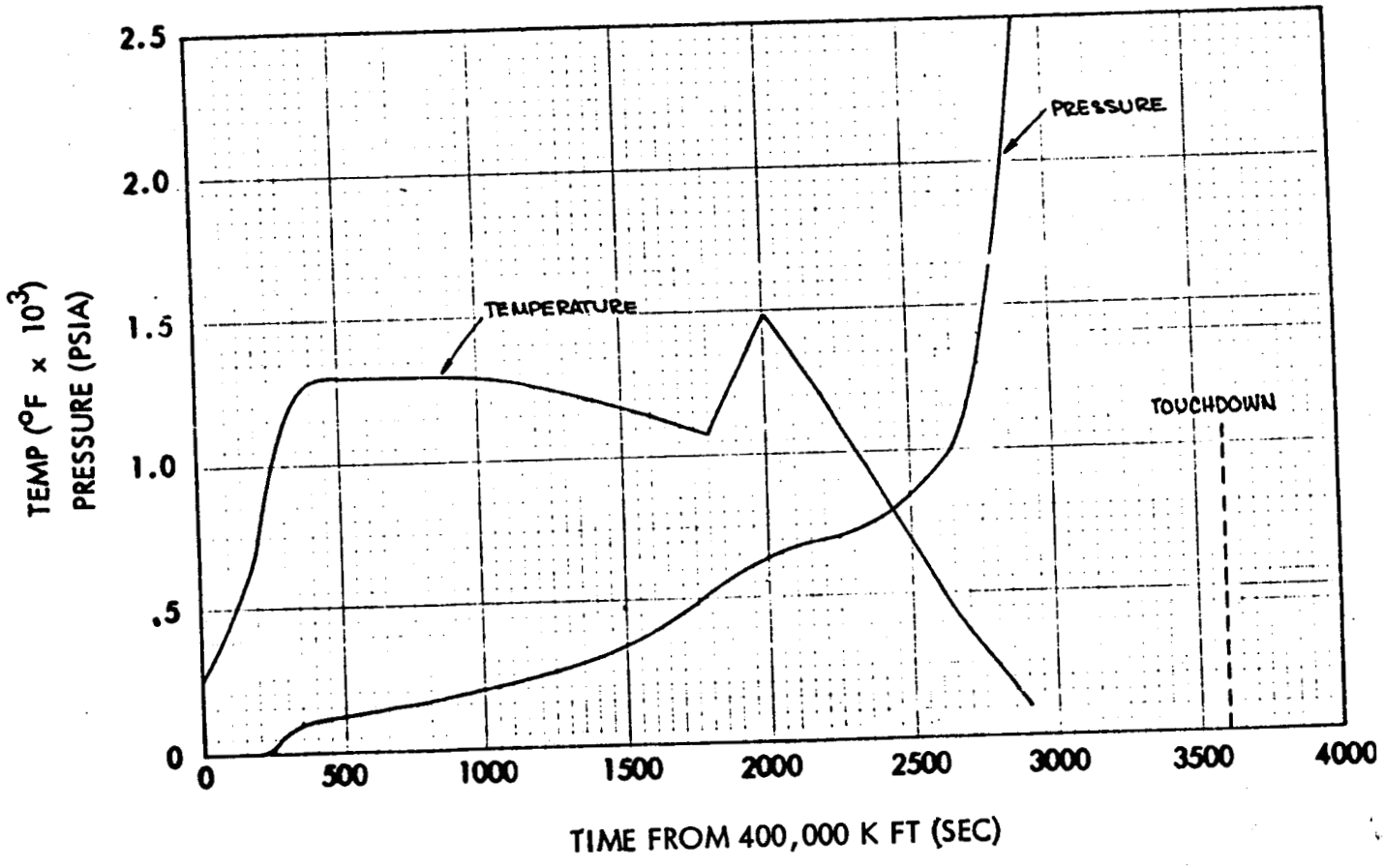


Fig. 2.2.2-7

# REENTRY TEMPERATURE AND PRESSURE HISTORIES
## AREA 2

EMITTANCE = 0.8

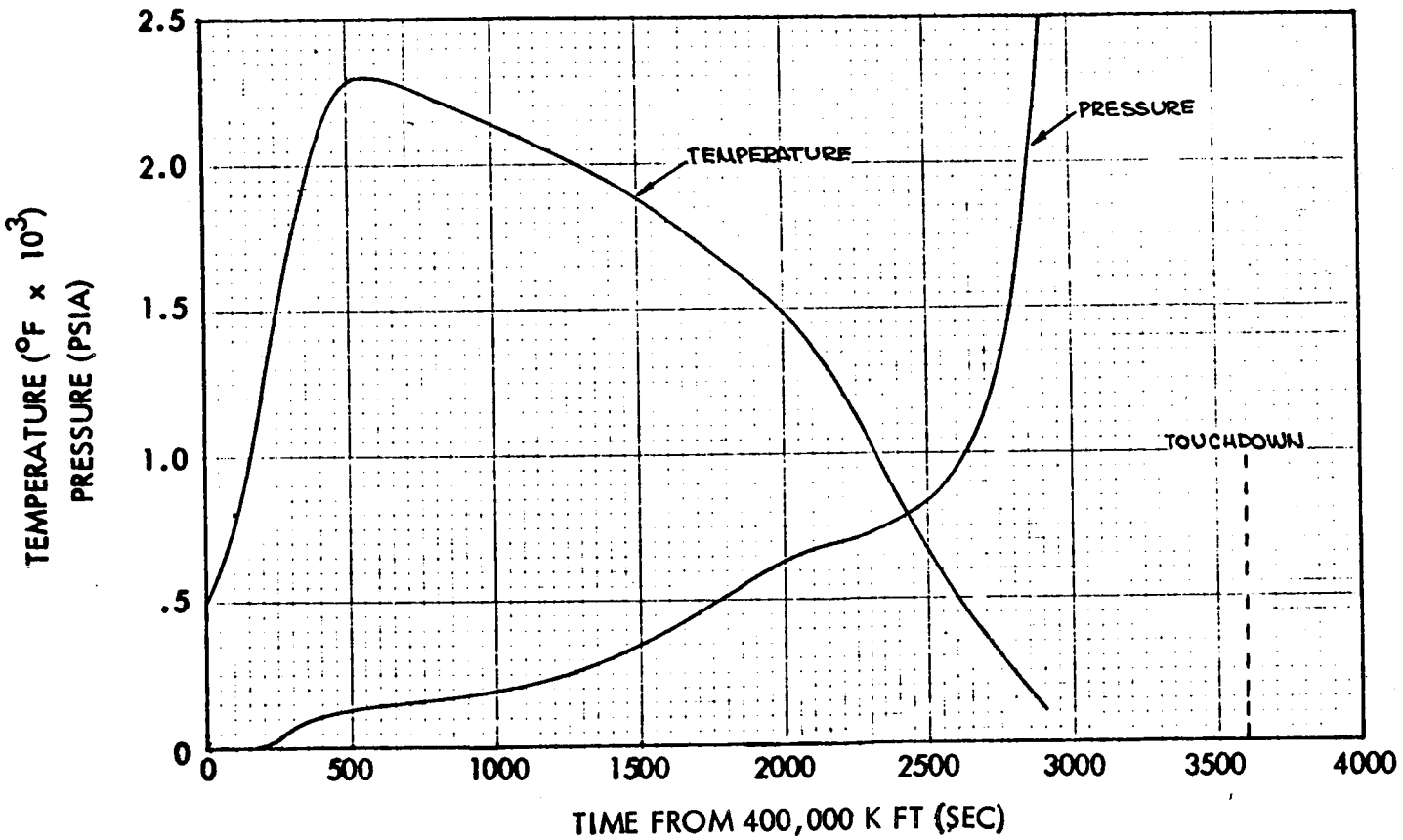


Fig. 2.2.2-8

conduction equation for a one-, two-, or three-dimensional problem. The code has an automatic plotting routine available to the user. The code handles other modes of heat transfer such as convection and radiation.

The heat balance at each node, as programmed in the computer code, is given by:

$$\Delta V \, \rho \, C_P \frac{\partial T_i}{\partial \theta} = \dot{q}_{in} - \dot{q}_{out} = \sum_{j=1}^{n} \left( \frac{T_i - T_j}{R_{i-j}} \right)$$

where:

$\Delta V$ = node volume
$\rho$ = density
$C_P$ = specific heat
$T$ = temperature
$\theta$ = time
$q$ = heat rate
$R_{i-j}$ = thermal resistance between nodes i and j
$i, j$ = node numbers

$\dot{q}_{in}$ is the heat conducted to the node from adjacent higher temperature nodes and $\dot{q}_{out}$ is the heat lost by conduction to adjacent lower temperature nodes. The temperature of the surface node is driven to follow the temperature history of the desired orbiter location, as obtained from Figs. 2.2.2-7 and -8.

The equations for determining resistor and capacitor values are shown in Table 2.2.2-1. These equations are evaluated during each computer iteration, thereby changing resistor and capacitor values as the node temperatures change. These values are then used to calculate the temperature response of the network.

Table 2.2.2-1

THERMAL RESISTOR AND CAPACITOR METHODOLOGY

| TYPE | VALUE | COMMENTS |
|---|---|---|
| RESISTOR DESCRIPTION | | |
| Conduction | $R = \ell / kA$ | $k = f(\text{Temp, Pressure})$ |
| Radiation | $R = \dfrac{1}{\sigma (RADK)\,(T_i^2 + T_j^2)\,(T_i + T_j)}$<br>Where:<br>$RADK = \epsilon_{ij}\, A_i\, F_i$<br>and:<br>$\epsilon_{ij} = \dfrac{1}{\frac{1}{\epsilon_i} + \frac{1}{\epsilon_j} - 1}$ | T in $^{o}R$<br><br>Parallel Plate View Factor |
| Air Convection | $R = \dfrac{1}{hA}$ | $h = \dfrac{0.14k_A}{\ell}(G_R\, P_R)^{1/3}$ |
| CAPACITOR DESCRIPTION | | |
| All | $C = \rho \ell A C_P$ | $C_P = f\,(\text{Temp})$ |

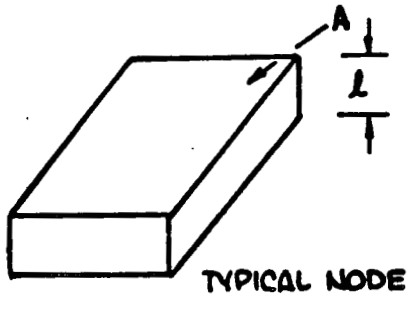


$\ell$ = Depth or length of conduction path

A = Area of node perpendicular to conduction path

The following ground rules and assumptions were used in conjunction with the THERM code for the basic insulation sizing of the prototype panel:

a. One-dimensional analysis
b. Radiation equilibrium temperature used as a surface temperature boundary condition
c. Adiabatic substrate
d. No ground cart cooling of substrate in either primary structure application or subpanel application
e. Thermal model includes a node for adhesive
f. Prototype panel tests will be performed at 1 ATM pressure

The thermal models considered for the sizing are shown in Fig. 2.2.2-9. The models were divided into seven nodes. The effect of lumping both the adhesive and substrate as one node was investigated. It was found that for adhesive thickness (with RTV-560 conductivity of 0.18 Btu/ft-hr-$^{o}$F) up to 0.20 in., the maximum transient difference between the LI-1500 adhesive interface temperature and the adhesive substrate interface temperature is about 20$^{o}$F. Since it was desirable to compare transient temperature differences between interfaces, the thermal model with the adhesive and substrate modelled individually was used. For adhesives with lower thermal conductivity or thicknesses greater than 0.20 in., the adhesive node should be included in the thermal model.

# THERMAL MODEL CONSIDERED FOR LI-1500 SIZING

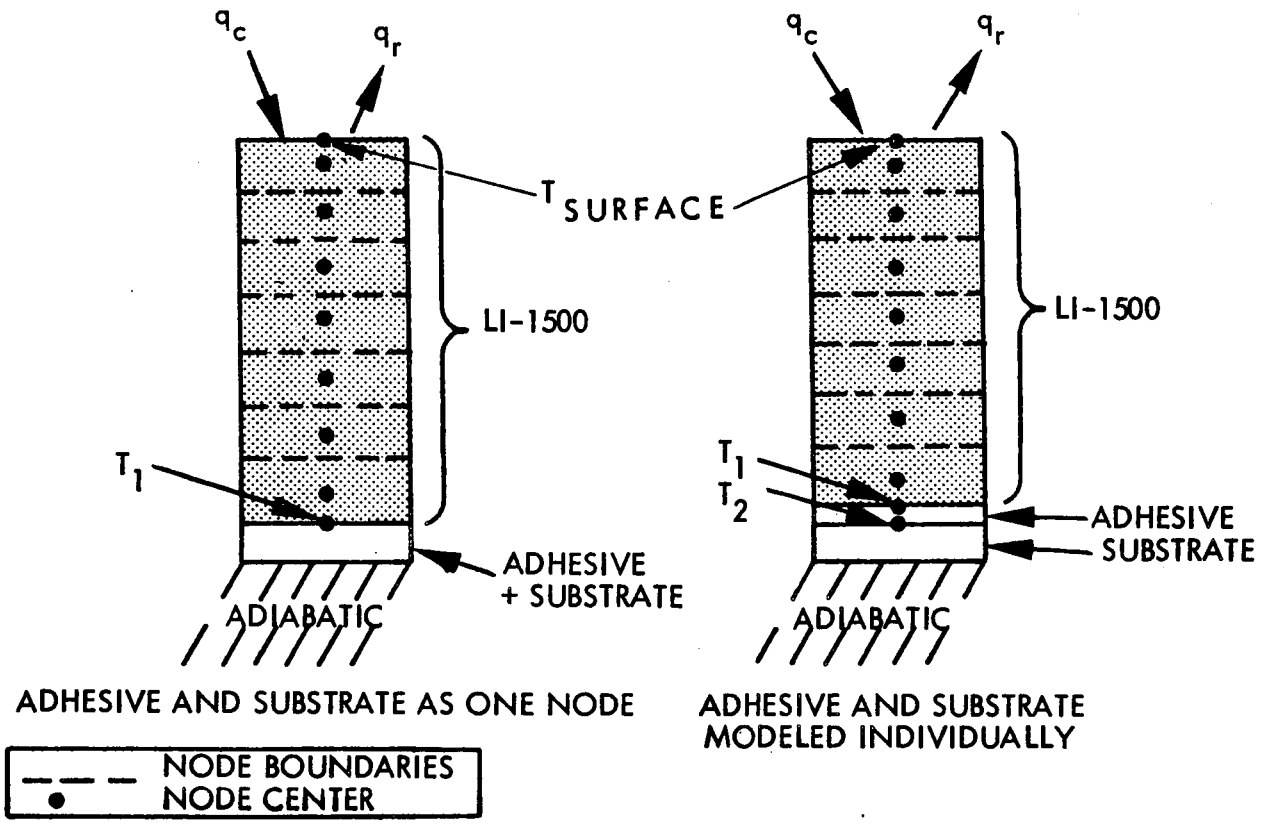


)O6000

Fig. 2.2.2-9

To accomplish the basic sizing for the test panels, the thermal properties of LI-1500 at 1 ATM pressure (from Section 4.1) were used. These data can also be found in Ref. 1. The thermal properties of the panel materials are listed in Table 2.2.2-2. The effective thicknesses for the test panels are listed below.

| Panel No. | Material | Area | Max. Surface Temp ($^{o}$F) | Max. Substrate Temp ($^{o}$F) | Effective Thickness (in.) |
|---|---|---|---|---|---|
| 1 | beryllium | 2 | 2300 | 600 | 0.064 |
| 2 | aluminum | 2 | 2300 | 300 | 0.114 |
| 3 | aluminum | 1 | 1480 | 300 | 0.143 |
| 4 | titanium | 2 | 2300 | 600 | 0.090 |

Typical parametric sizing data for the beryllium panel for a constant adhesive thickness are shown in Fig. 2.2.2-10. The data indicate the effect of beryllium substrate thickness on the required insulation thickness. Parametric data for the titanium test panel are shown in Fig. 2.2.2-11.

The data from Fig. 2.2.2-10 are used as the basis for TPS optimization for the beryllium panel shown in Fig. 2.2.2-12. The total unit weight, consisting of beryllium, LI-1500, and adhesive, is plotted against the beryllium effective thickness for a maximum beryllium temperature of 600$^{o}$F. The unit weight of the surface coating (approximately 0.10 lb/ft$^{2}$) is not included in the total unit weight.

While the strength requirement dictates a beryllium thickness of 0.040 in., the minimum weight system occurs at a thickness of about 0.090 in. Although the total unit weight curve is flat, the data indicate a lower weight system can be achieved at beryllium effective thicknesses up to 0.16 in. Hence, for beryllium a stronger and lighter TPS is attainable at larger effective thicknesses.

Figure 2.2.2-13 shows the effect of beryllium effective thickness on the total unit weight for various RTV 560 adhesive thicknesses. Although a highly expanded ordinate is used for total TPS weight, a larger adhesive thickness tends to shift the minimum

Table 2.2.2-2

THERMOPHYSICAL PROPERTIES OF SELECTED MATERIALS

| Beryllium $\rho = 115$ lb/ft$^3$ | | |
|---|---|---|
| T ~ $^oF$ | C ~ Btu/lb $^oF$ | k ~ Btu/ft sec $^oF$ |
| 40 | 0.425 | $2.94 \times 10^{-2}$ |
| 200 | 0.500 | 2.750 |
| 400 | 0.570 | 2.500 |
| 600 | 0.615 | 2.250 |
| 1000 | 0.675 | 1.780 |
| 1500 | 0.745 | 1.250 |
| 2200 | 0.845 | 0.778 |
| **Titanium $\rho = 276$ lb/ft$^3$** | | |
| T ~ $^oF$ | C ~ Btu/lb $^oF$ | k ~ Btu/ft sec $^oF$ |
| 40 | 0.125 | $0.116 \times 10^{-2}$ |
| 200 | 0.135 | 0.119 |
| 300 | 0.140 | 0.153 |
| 1000 | 0.180 | 0.222 |
| **Aluminum 7075 $\rho = 276$ lb/ft$^3$** | | |
| T ~ $^oF$ | C ~ Btu/lb $^oF$ | k ~ Btu/ft sec $^oF$ |
| 0 | 0.195 | $2.14 \times 10^{-2}$ |
| 200 | 0.218 | 2.22 |
| 400 | 0.240 | 2.78 |
| 600 | 0.262 | 2.84 |
| 800 | 0.288 | 2.78 |

# TYPICAL PARAMETRIC SIZING DATA

## BERYLLIUM FLIGHT PANEL NO. 1

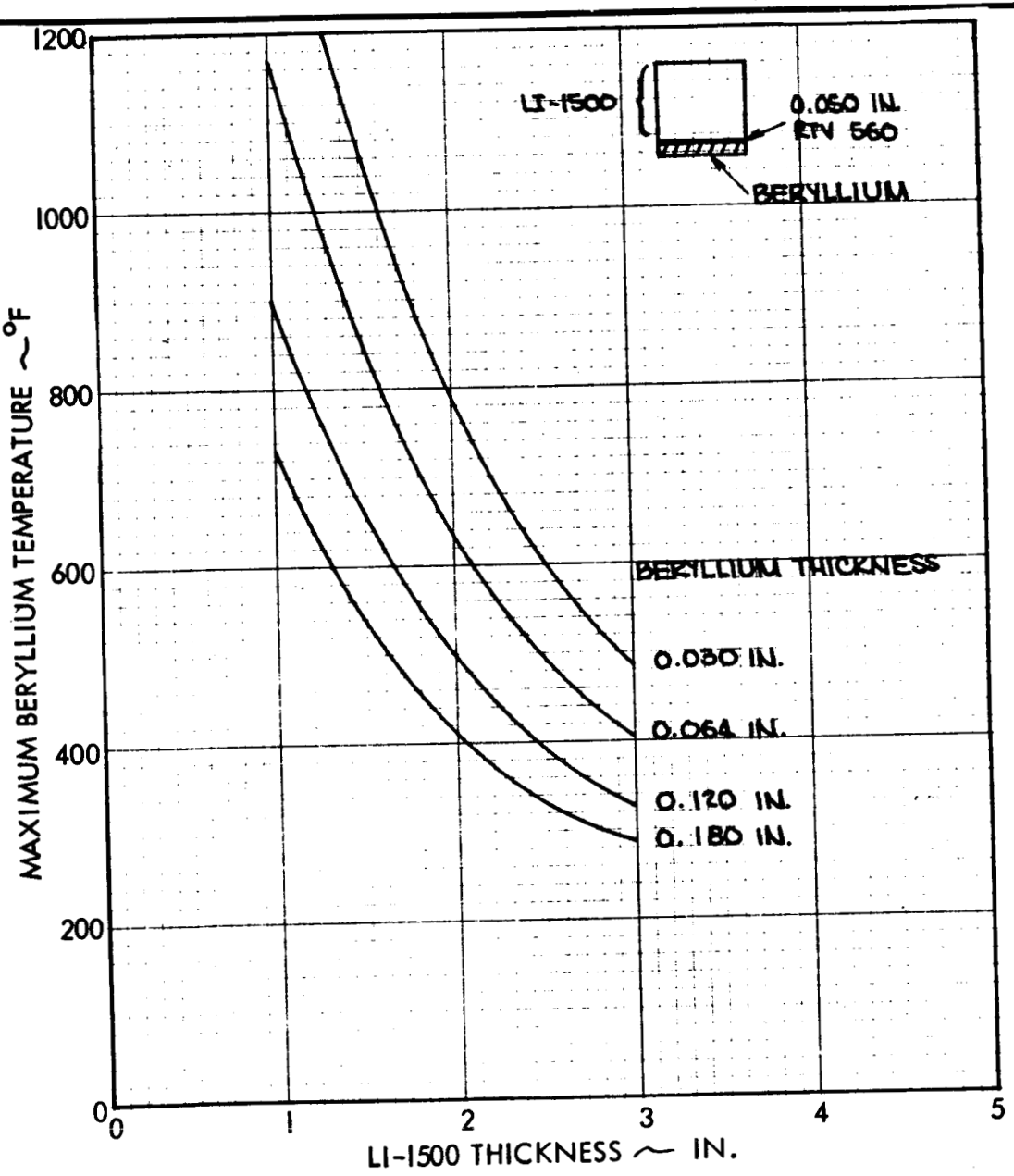


Fig. 2.2.2-10

# TYPICAL LI-1500 PARAMETRIC SIZING DATA

## TITANIUM TEST PANEL NO. 4

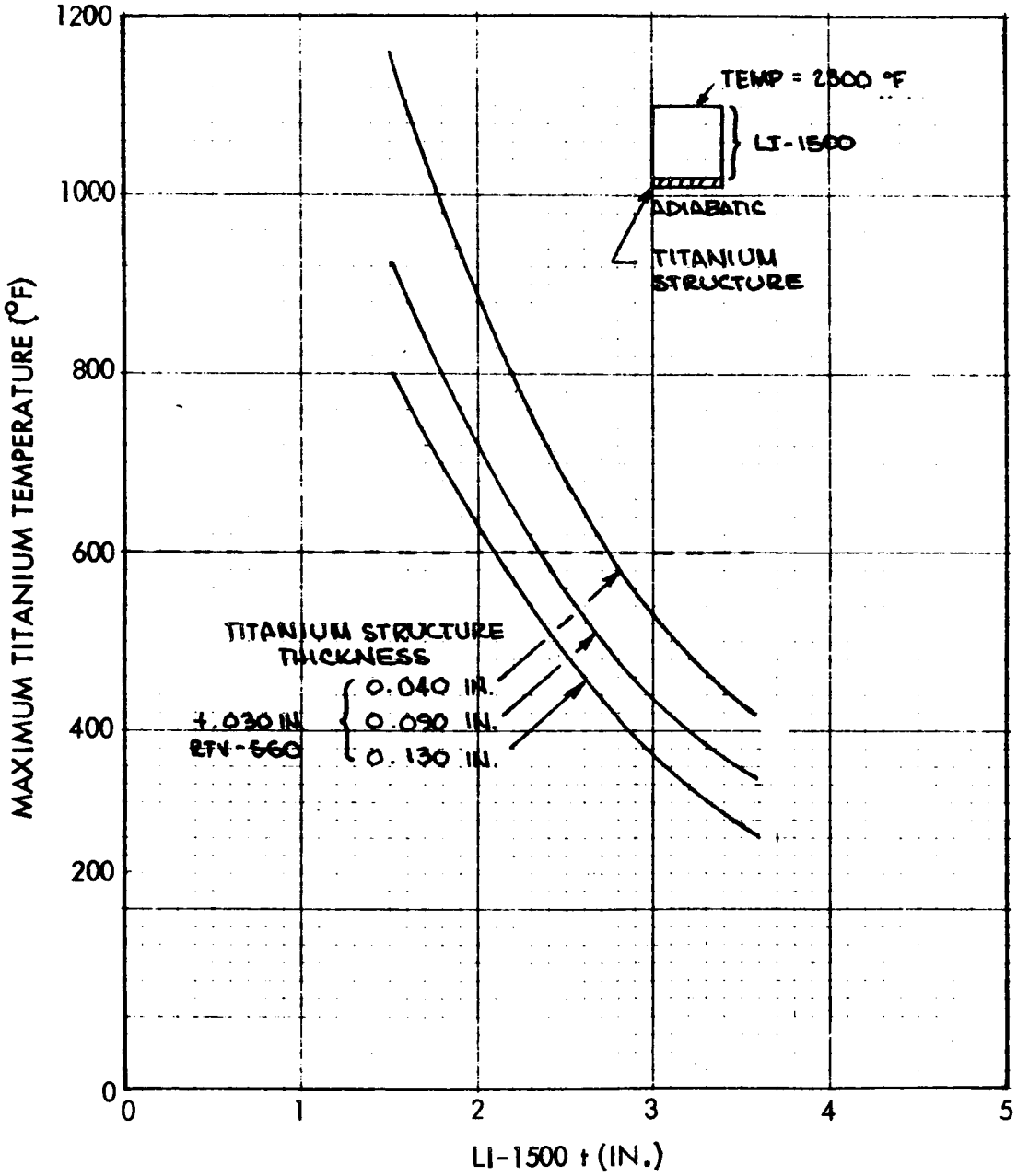


Fig. 2.2.2-11

# TPS THERMAL-STRUCTURAL OPTIMIZATION FOR TEST PANEL NO. 1

AREA 2 – MAXIMUM Be TEMP = 600°F, SURFACE TEMP = 2300°F

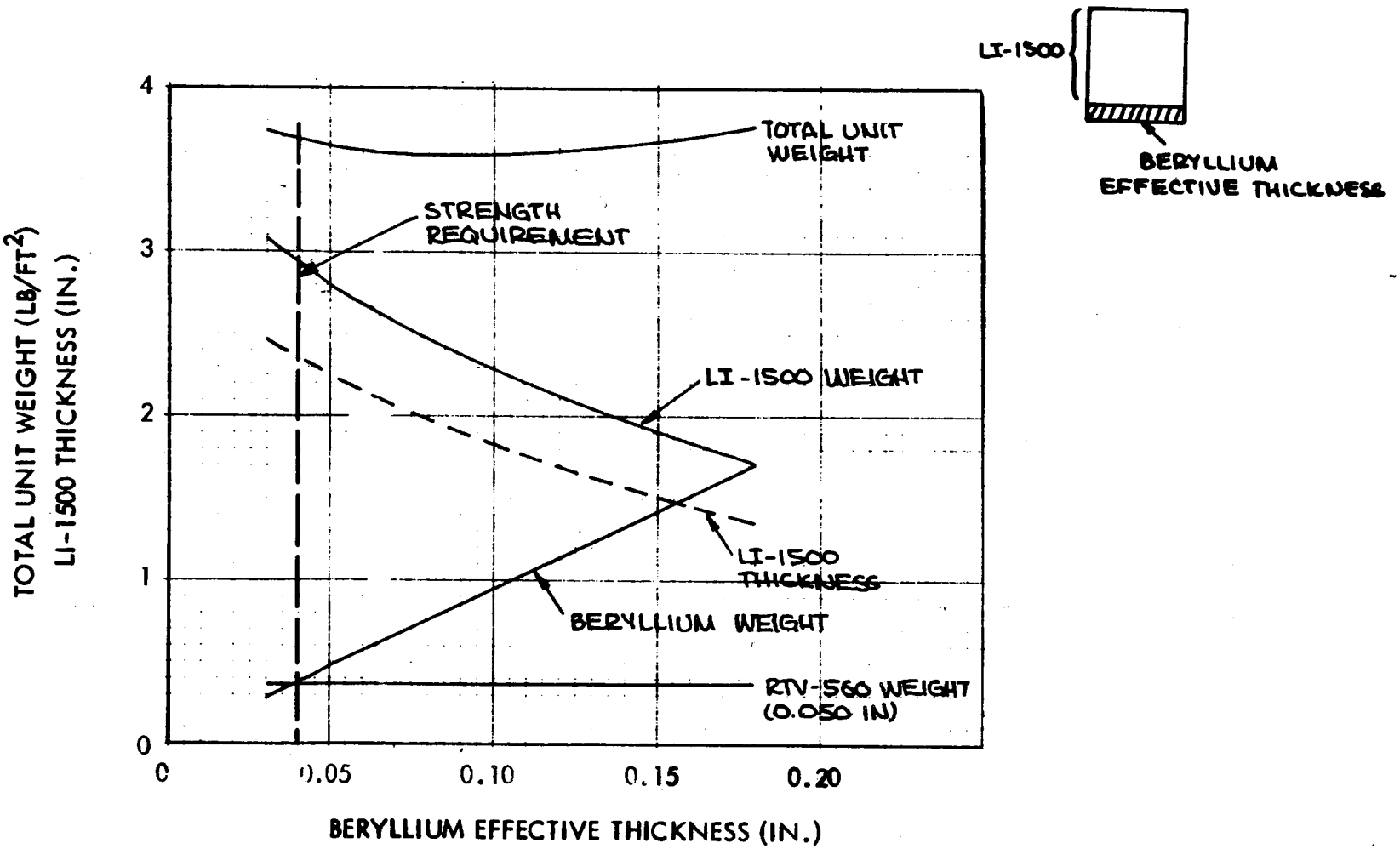


DO6089

Fig. 2.2.2-12

# EFFECT OF BERYLLIUM THICKNESS ON TPS THERMAL-STRUCTURAL OPTIMIZATION

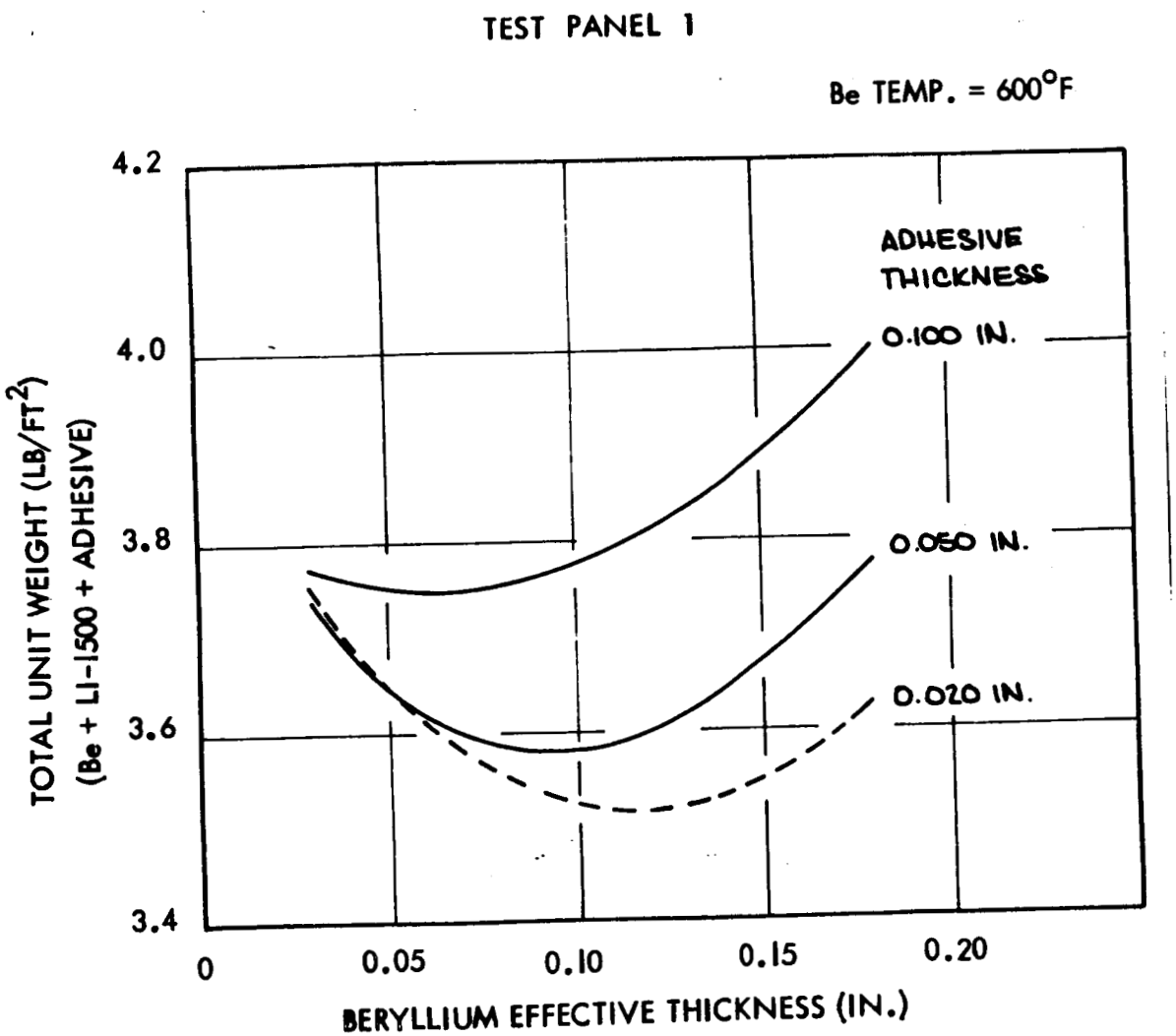


DO6006

Fig. 2.2.2-13

weight to smaller beryllium effective thicknesses. As adhesive thickness was increased from 0.050 in. to 0.100 in., the minimum weight point shifted from 0.090 in. beryllium to 0.060 in. beryllium. There is also an accompanying slight increase in the total unit weight from 3.58 to 3.75 lb/ft$^2$, or a 0.17 lb/ft$^2$ increment upon changing from 0.050 in. to 0.100 in. of RTV 560 adhesive.

Figure 2.2.2-14 shows a thermal-structural optimization for the aluminum test panel No. 2 at a maximum temperature of 300$^\circ$F. Unlike the beryllium panel, the strength requirement also results in the minimum weight system.

Figure 2.2.2-15 shows a thermal/structural optimization for Area 1, aluminum test panel No. 3 at a maximum temperature of 300$^\circ$F. Again the strength requirement corresponds to the minimum weight system.

Figure 2.2.2-16 shows a thermal/structural optimization for the titanium test panel No. 4 at 600$^\circ$F. As in the case of the aluminum panels, the strength requirement for the titanium panel corresponds to the minimum weight system.

Hence, because of the high heat capacity of beryllium, it is the only panel that allows a larger panel thickness than required by strength considerations, while decreasing the total TPS unit weight.

2.2.2.3 Effect of Adiabatic Substrate on Test Conditions. The effect of an adiabatic boundary condition, as specified by NASA, on the maximum attainable backface temperature in a test fixture where the TPS substrate radiates and convects to a 0.375 in. aluminum plate is shown in Fig. 2.2.2-17. A beryllium panel sized adiabatically for a 600$^\circ$F maximum temperature requires 2.3 in. of LI-1500. Allowing the panel to radiate and convect energy to a 0.375 in. test fixture will limit the maximum beryllium temperature to 490$^\circ$F. Hence, to achieve the design temperature on the beryllium panel during the test, the panel should either be sized with a nonadiabatic boundary condition or a piece of low density insulation (i.e., dynaflex, fiberfrax, or LI-1500) should be attached to the bottom of the test fixture to limit the energy loss.

# TPS THERMAL-STRUCTURAL OPTIMIZATION FOR TEST PANEL NO. 2

AREA 2 MAXIMUM AL. TEMP = 300°F, SURFACE TEMP. = 2300°F

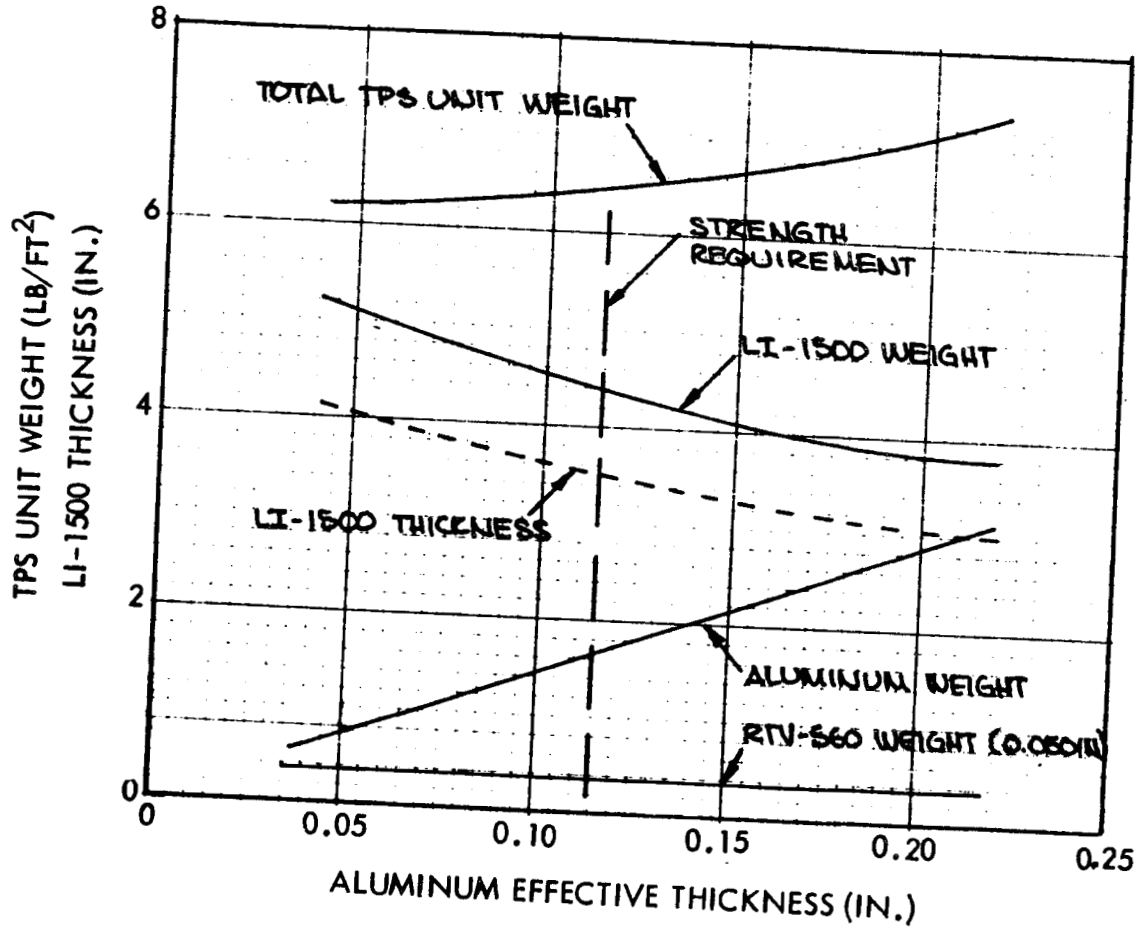


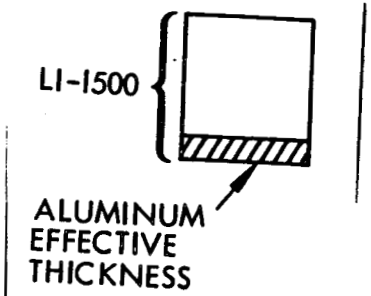


DO6015

Fig. 2.2.2-14

# TPS THERMAL - STRUCTURAL OPTMIZATION FOR TEST PANEL NO. 3

AREA 1 – MAXIMUM Al TEMP = 300°F, SURFACE TEMP = 1480°F

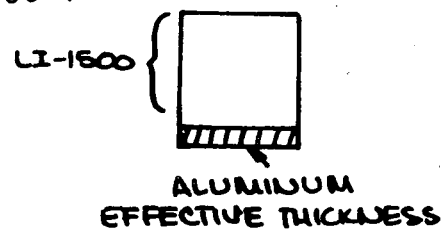


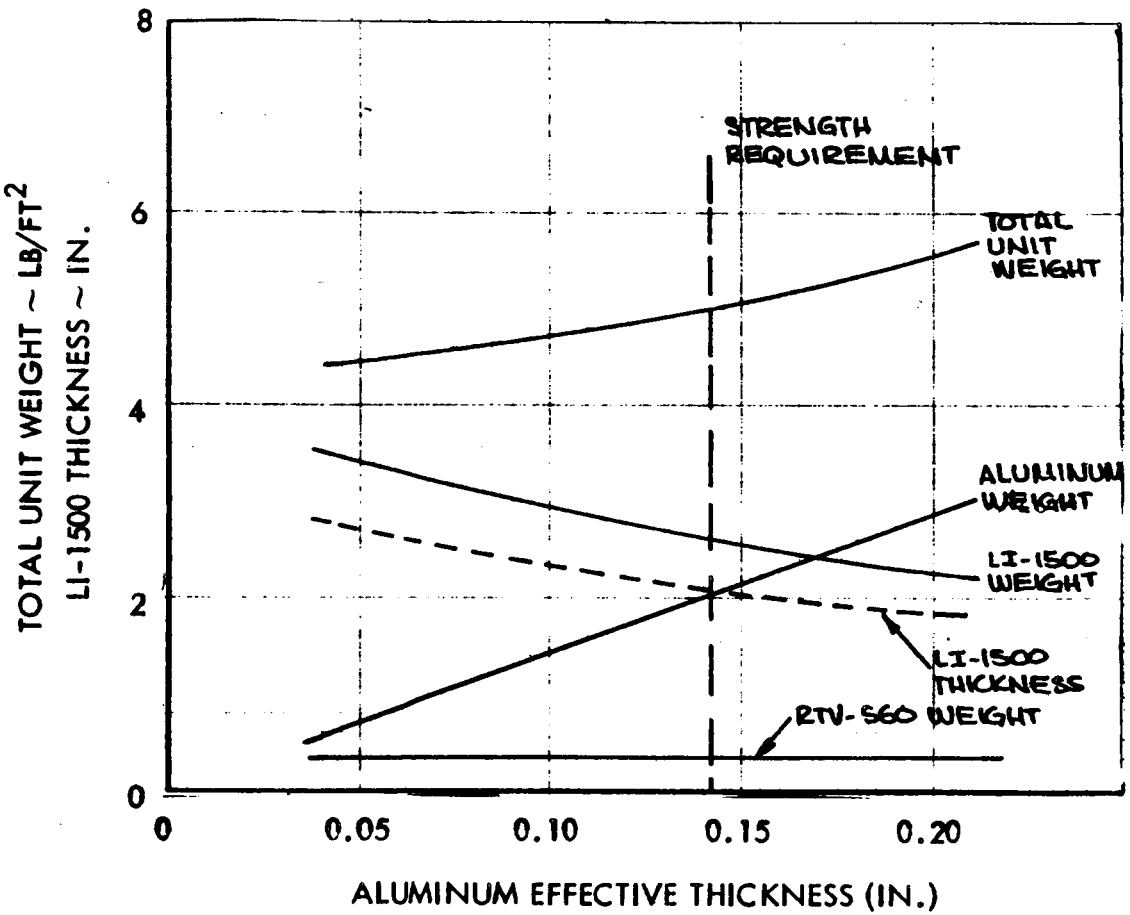


Fig. 2.2.2-15

# TPS THERMAL - STRUCTURAL OPTIMIZATION FOR TEST PANEL NO. 4

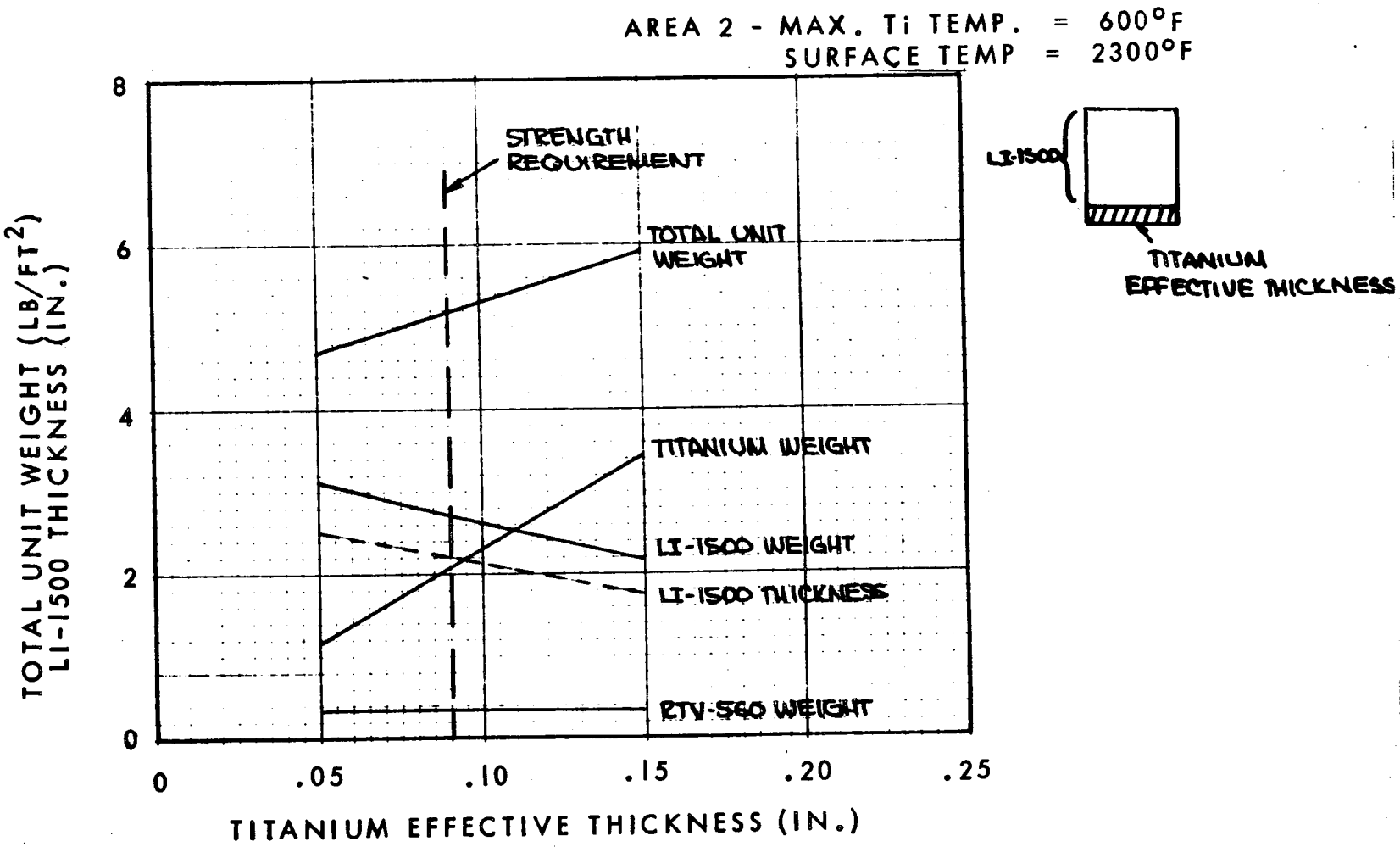


DO6004

Fig. 2.2.2-16

# EFFECT OF SUBSTRATE BOUNDARY CONDITIONS ON MAXIMUM BERYLLIUM TEMPERATURE

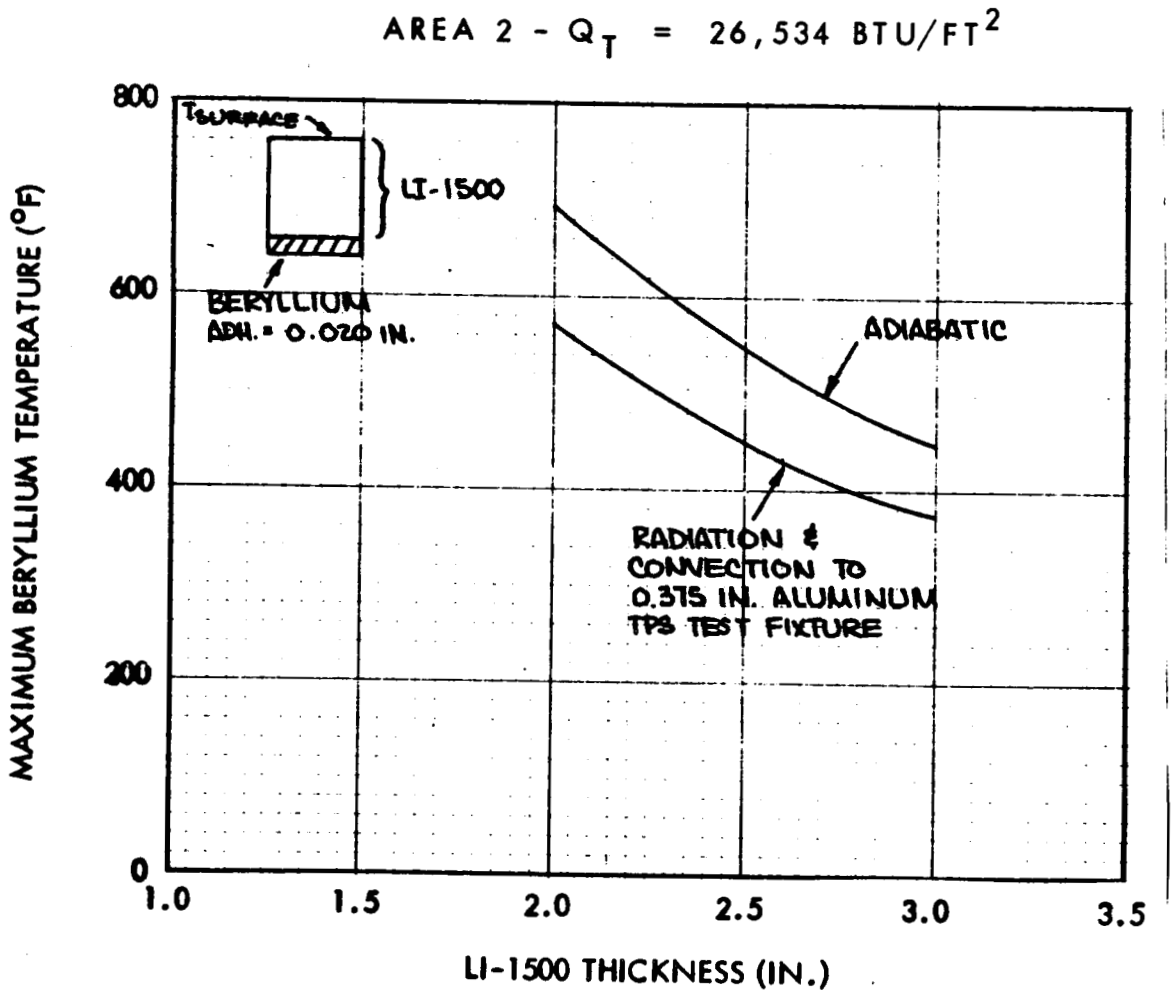


DO6008

Fig. 2.2.2-17

2.2.2.4 Thermal Structural Optimization for Flight Panels. The LI-1500 sizing for flight panels would consider the effect of local static pressure on the thermal conductivity of LI-1500. At 2000°F the vacuum thermal conductivity of LI-1500 is about 45 percent of the 1 ATM value. Hence, the sizing for the flight panels assumes that the pressure within the LI-1500 during entry equals the local static pressure at the edge of the boundary layer (see Figs. 2.2.2-7 and -8 for Areas 1 and 2 on the orbiter). During entry, a pressure lag will probably exist, allowing the actual pressure within the LI-1500 to lag the local static pressure; therefore, use of the local static pressure will result in conservative LI-1500 thickness requirements. Tests to be performed under Task 5 will assist in determining the magnitude of the thickness reduction due to the entry pressure history.

Figure 2.2.2-18 shows a comparison of the LI-1500 thickness requirements for a beryllium flight and test panel. The flight panel results were obtained using the temperature and pressure histories for Area 2 (shown in Fig. 2.2.2-8) to determine the thermal conductivity of LI-1500. The test panel results utilized the 1-ATM thermal conductivity values.

For a 600°F maximum temperature, the LI-1500 requirements are reduced about 31 percent from 2.1 to 1.45 in. of LI-1500. Similar reductions can be obtained for the other three flight panels.

TPS thermal/structural optimizations are shown for flight panels 1, 2, 3, and 4 in Figs. 2.2.2-19, -20 and -21. As indicated previously for the test panel, the beryllium total unit weight curve is rather flat and the minimum weight system occurs at a larger beryllium thickness than that dictated by strength requirements. Minimum weight occurs at about 0.090 in. while the strength requirement is at 0.040 in. beryllium (Fig. 2.2.2-19). For the aluminum and titanium flight panels (Figs. 2.2.2-20 and -21), the strength requirement corresponds to the minimum weight system.

Table 2.2.2-3 shows a comparison of LI-1500 thickness and unit weight between the flight and test panels. In all cases, the flight panels require about 22-33 percent less LI-1500 and are 10-15 percent lighter in unit weight than the test panels.

Table 2.2.2-3

COMPARISON OF PROTOTYPE PANELS FOR TEST AND FLIGHT

| Panel No. | Description | Orbiter Area | Panel Design Temp | LI-1500 Thickness~in. | | Panel Unit Weight~lb/ft$^2$ | |
|---|---|---|---|---|---|---|---|
| | | | | Test[1] Panel | Flight[2] Panel | Test[1] | Flight[2] |
| 1 | Beryllium Subpanel Application $\bar{t}$ = 0.61 in., 0.050 in., RTV-560 Adhesive | 2 | 600°F | 2.10 | 1.45 | 3.6 (5.3)* | 2.8 (4.5)* |
| 2 | Aluminum Primary Structure Application $\bar{t}$ = 0.114 in., 0.050 in., RTV-560 Adhesive | 2 | 300°F | 3.55 | 2.75 | 6.4 | 5.5 |
| 3 | Aluminum Primary Structure Application $\bar{t}$ = 0.143 in., 0.050 in., RTV-560 Adhesive | 1 | 300°F | 2.12 | 1.63 | 5.0 | 4.5 |
| 4 | Titanium Primary Structure Application $\bar{t}$ = 0.090 in., 0.050 in., RTV-560 Adhesive | 2 | 600°F | 2.20 | 1.47 | 5.2 | 4.3 |

[1]LI-1500 thermal conductivity is a function of temperature only (pressure = 1 atm)

[2]LI-1500 thermal conductivity is a function of temperature and pressure

*Value includes the weight of a $\bar{t}$ 1 0.114 in. aluminum primary structure

# COMPARISON OF LI-1500 THICKNESS BETWEEN FLIGHT AND TEST PANEL

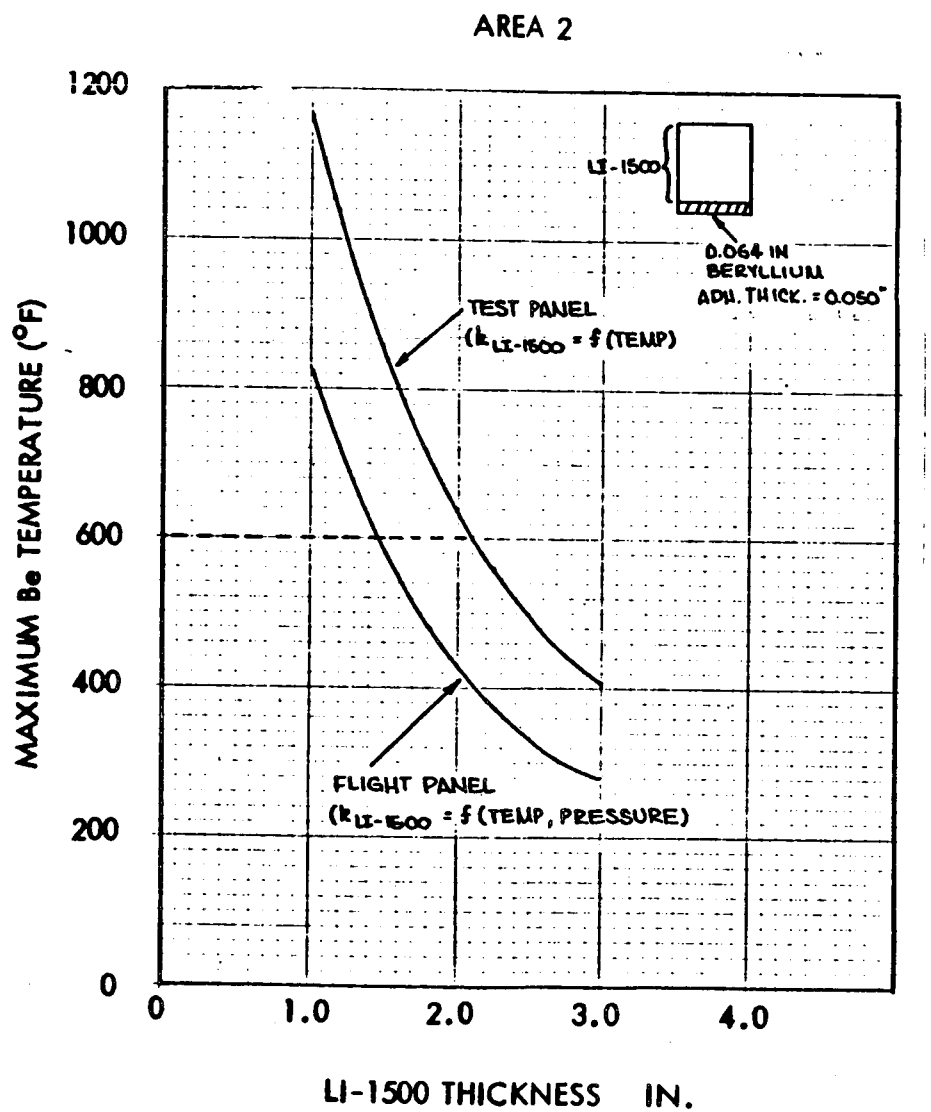


DO6001

Fig. 2.2.2-18

# TPS THERMAL-STRUCTURAL OPTIMIZATION FOR FLIGHT PANEL NO. 1

AREA 2 – Be TEMP = 600°F, SURFACE TEMP = 2300°F

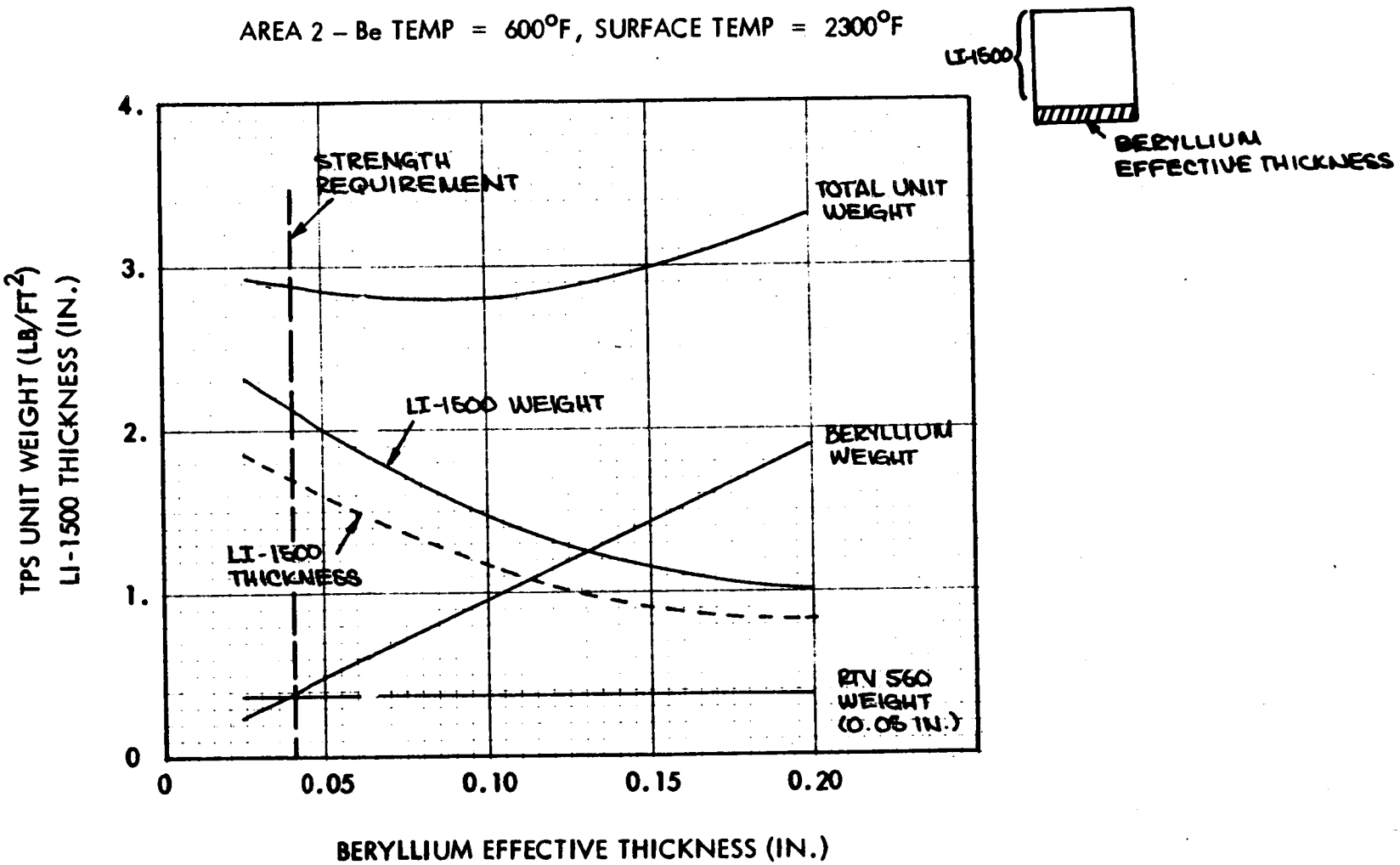


Fig. 2.2.2-19

DO6094

# TPS THERMAL-STRUCTURAL OPTIMIZATION FOR FLIGHT PANEL NO. 3

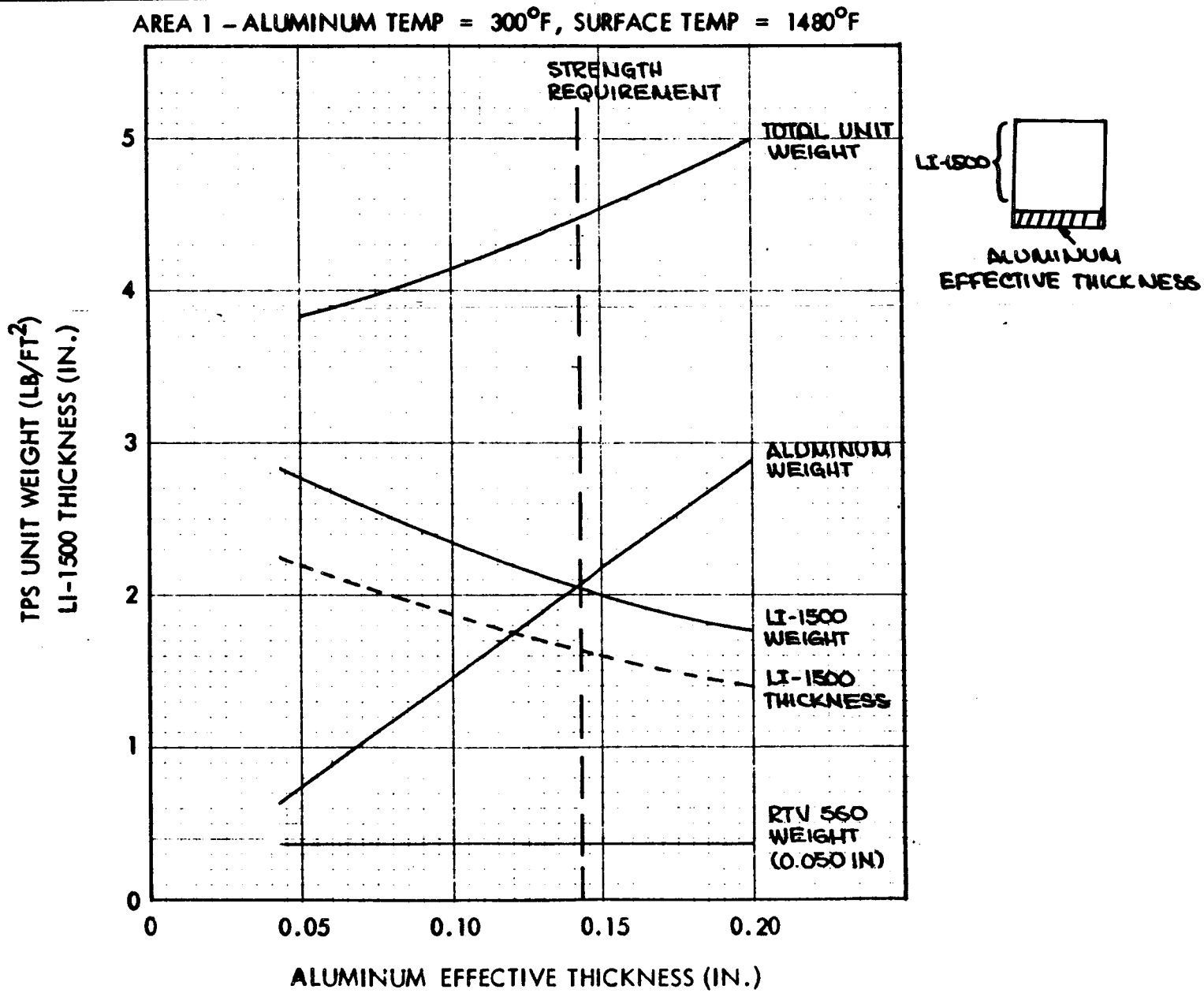


Fig. 2-20

DO6093

# TPS THERMAL-STRUCTURAL OPTIMIZATION FOR FLIGHT PANEL 2 AND 4

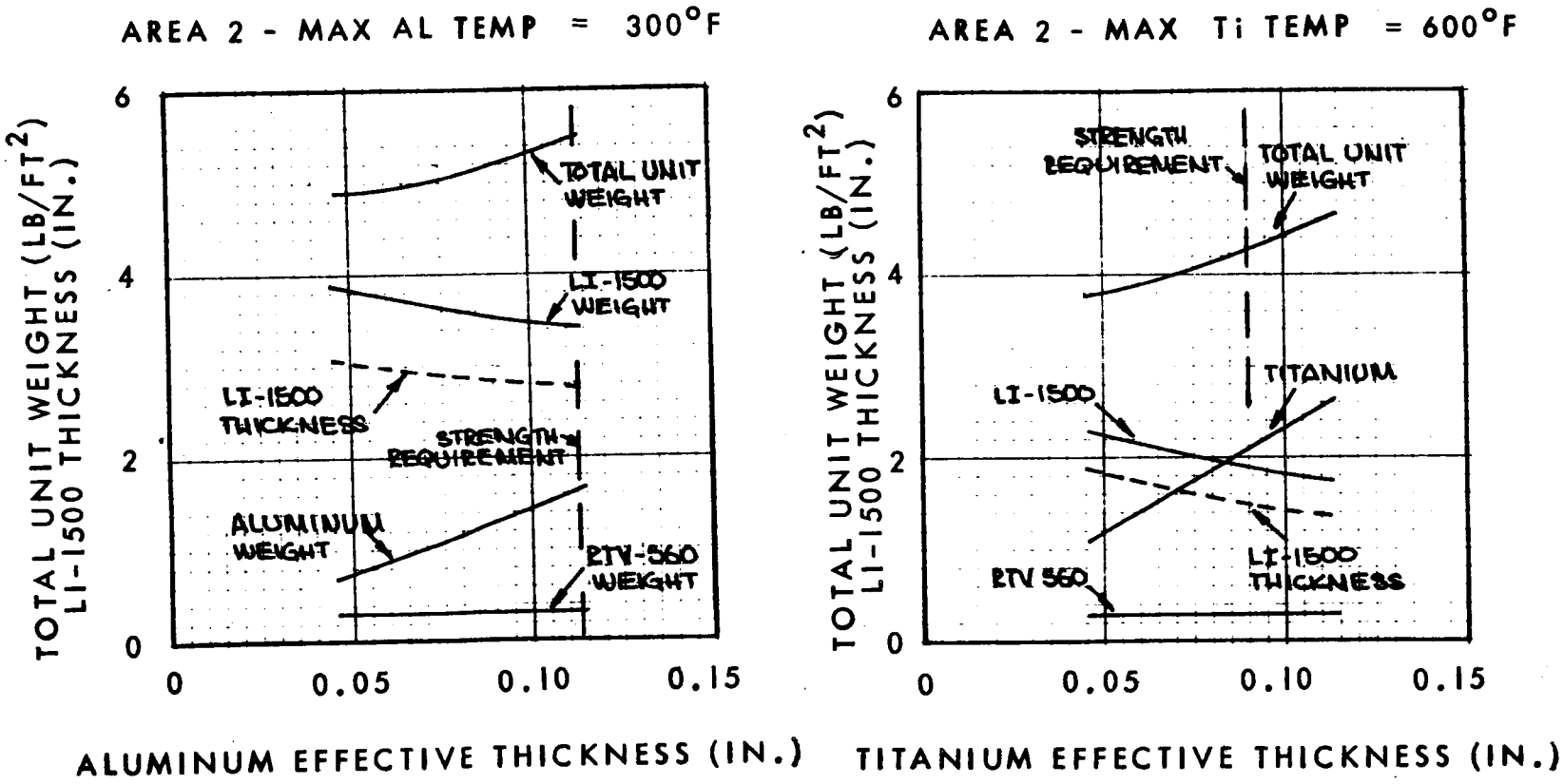


DO6007

Fig. 2.2.2-21

Table 2.2.2-3

COMPARISON OF PROTOTYPE PANELS FOR TEST AND FLIGHT

| Panel No. | Description | Orbiter Area | Panel Design Temp | LI-1500 Thickness~in. | | Panel Unit Weight ~lb/ft$^2$ | |
|---|---|---|---|---|---|---|---|
| | | | | Test[1] Panel | Flight[2] Panel | Test[1] | Flight[2] |
| 1 | Beryllium Subpanel Application $\bar{t}$ = 0.61 in., 0.050 in., RTV-560 Adhesive | 2 | 600°F | 2.10 | 1.45 | 3.6 (5.3)* | 2.8 (4.5)* |
| 2 | Aluminum Primary Structure Application $\bar{t}$ = 0.114 in., 0.050 in., RTV-560 Adhesive | 2 | 300°F | 3.55 | 2.75 | 6.4 | 5.5 |
| 3 | Aluminum Primary Structure Application $\bar{t}$ = 0.143 in., 0.050 in., RTV-560 Adhesive | 1 | 300°F | 2.12 | 1.63 | 5.0 | 4.5 |
| 4 | Titanium Primary Structure Application $\bar{t}$ = 0.090 in., 0.050 in., RTV-560 Adhesive | 2 | 600°F | 2.20 | 1.47 | 5.2 | 4.3 |

[1]LI-1500 thermal conductivity is a function of temperature only (pressure = 1 atm)

[2]LI-1500 thermal conductivity is a function of temperature and pressure

*Value includes the weight of a $\bar{t}$ 1 0.114 in. aluminum primary structure

Typical temperature histories and temperature distributions for test panels No. 1, 2, 3, and 4 are shown in Figs. 2.2.2-22, -23, -24, and -25, respectively. All substrate temperatures reach their maximum values after the assumed touchdown of 3600 sec. For Area 2 where the maximum surface temperature is 2300°F, the beryllium and titanium panels (Nos. 1 and 4) reach 600°F at about 5000 sec. The aluminum test panle (No. 3) reaches 300°F at about 8000 sec. For Area 1, where the maximum surface temperature is 1480°F, the aluminum test panel (No. 2) reaches 300°F at 4500 sec. A nonadiabatic boundary condition for the substrate would result in peak temperatures at earlier times.

Temperature histories and temperature distributions for the flight panels are shown in Figs. 2.2.2-26, -27, -28, and -29, respectively. The beryllium and titanium panels (Nos. 1 and 4) reach their design temperature of 600°F at about touchdown (3600 sec), whereas aluminum panels Nos. 2 and 3 reach their design temperature of 300° at about 6500 sec and 4000 sec, respectively.

The temperature distributions for both flight and test panels indicate that for a 2300°F maximum surface temperature, only about 0.15 in. of the material experiences temperatures greater than 2000°F.

2.2.2.5 Effect of Adhesive Thickness on LI-1500 Thickness. Another tradeoff in the design methodology logic is the variation of adhesive thickness with LI-1500 thickness. As the adhesive thickness is increased to produce allowable stress values within the LI-1500 or on the surface coating, the LI-1500 thickness may be reduced. This effect is shown in Fig. 2.2.2-30 where the variation of adhesive thickness with LI-1500 thickness is plotted for various beryllium effective thickness for a beryllium temperature of 600°F. For the 0.061 in. beryllium (which corresponds to test panel No. 1), an increase in adhesive of 0.075 (from 0.025 to 0.100 in.) allows a reduction in LI-1500 thickness of 0.32 (from 2.25 to 1.93). This amounts to a thickness tradeoff of 4 to 1. For example, an increase of adhesive of 0.010 in. would allow a decrease of 0.040 in. in the LI-1500 thickness.

# TPS TEMPERATURE HISTORIES AND DISTRIBUTIONS
## TEST PANEL NO. 1

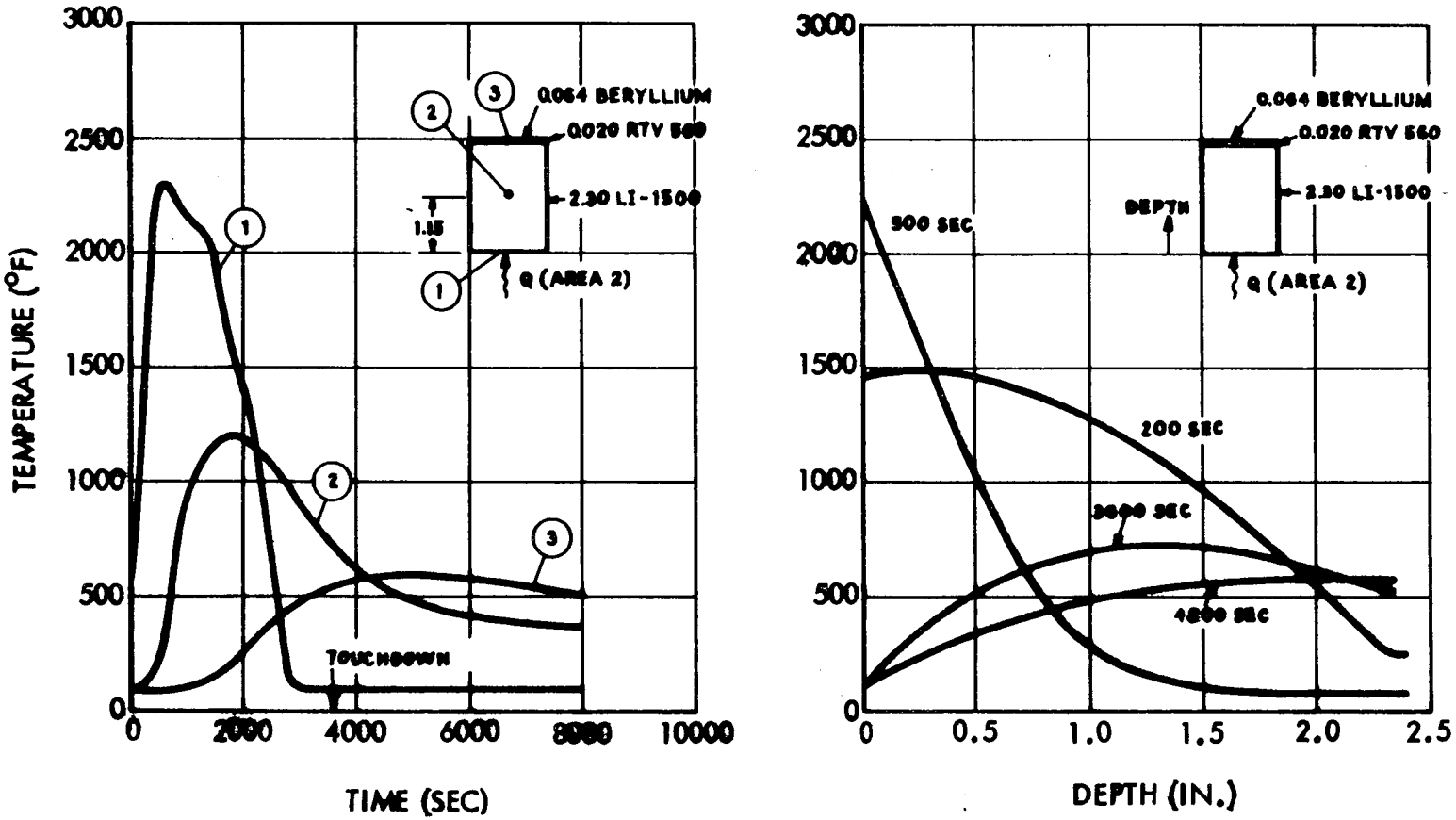


DO6103

Fig. 2.2.2-22

# TPS TEMPERATURE HISTORIES AND DISTRIBUTIONS
## TEST PANEL NO. 2

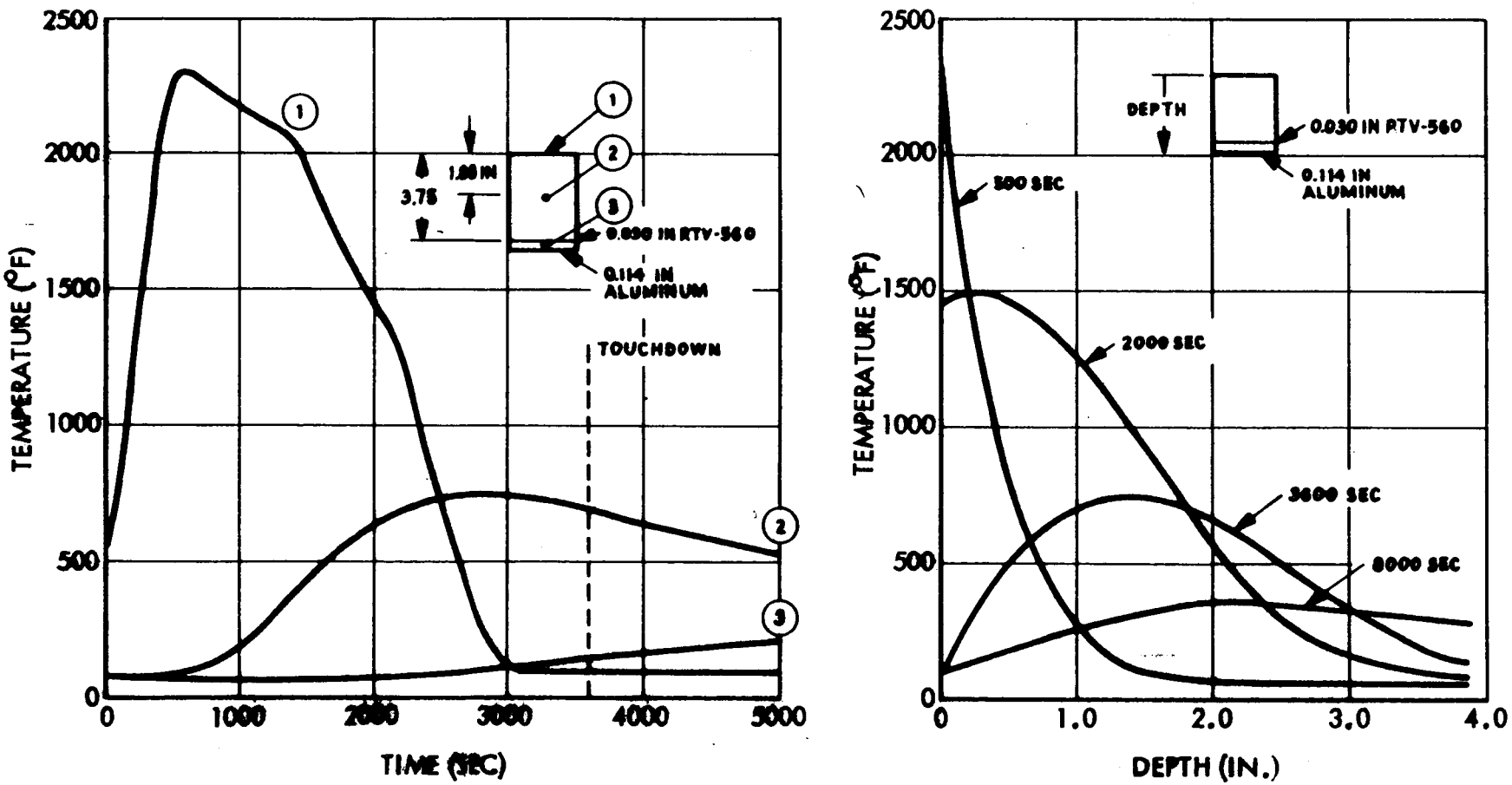


Fig. 2.2.2-23

# TEMPERATURE HISTORIES AND DISTRIBUTIONS FOR TEST PANEL NO. 3

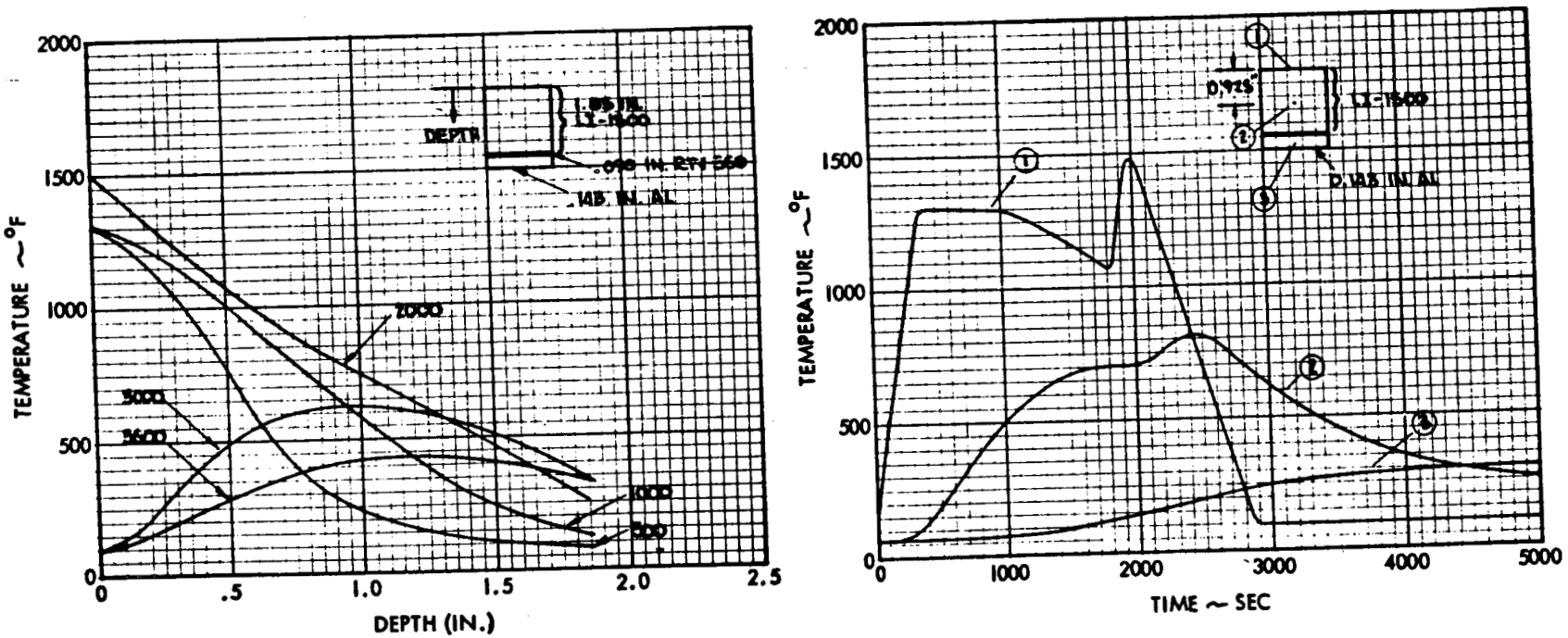


DO6140

Fig. 2.2.2-24

# TPS TEMPERATURE HISTORIES & DISTRIBUTIONS
## TEST PANEL 4

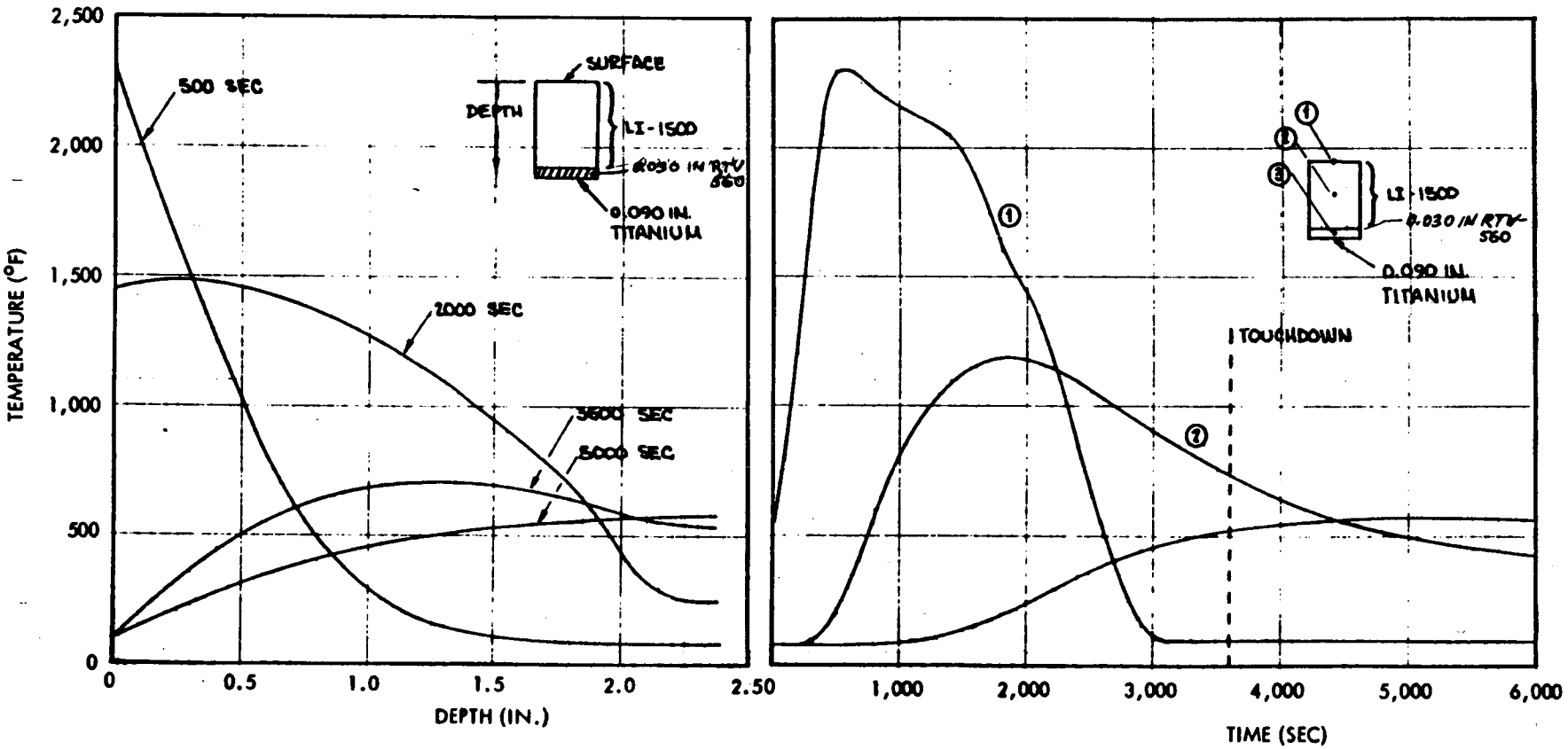


D05111

Fig. 2.2.2-25

# TEMPERATURE HISTORIES AND DISTRIBUTIONS FOR FLIGHT PANEL NO. 1

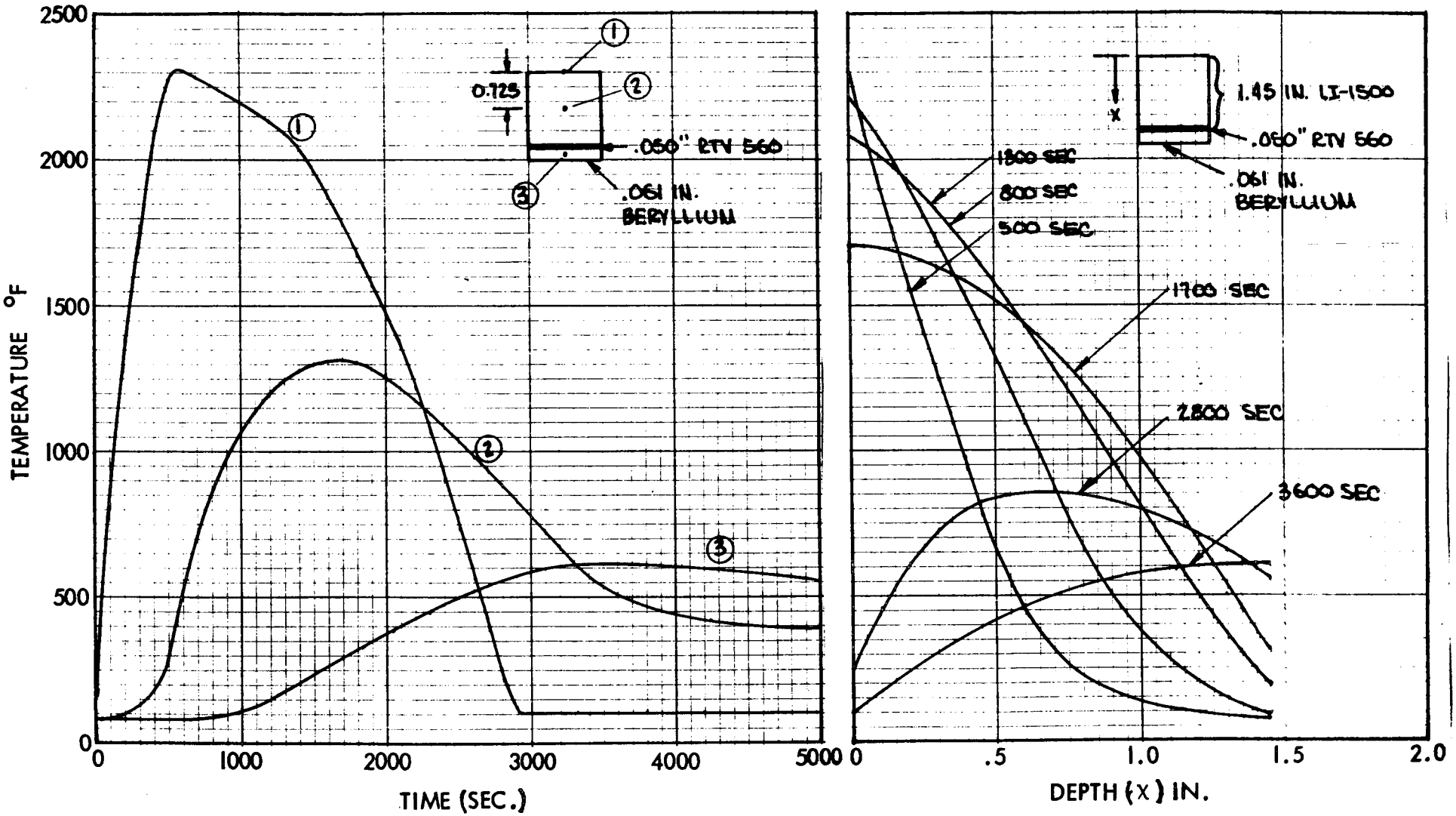


D05998

Fig. 2.2.2-26

# TEMPERATURE HISTORIES AND DISTRIBUTIONS FOR FLIGHT PANEL NO. 2

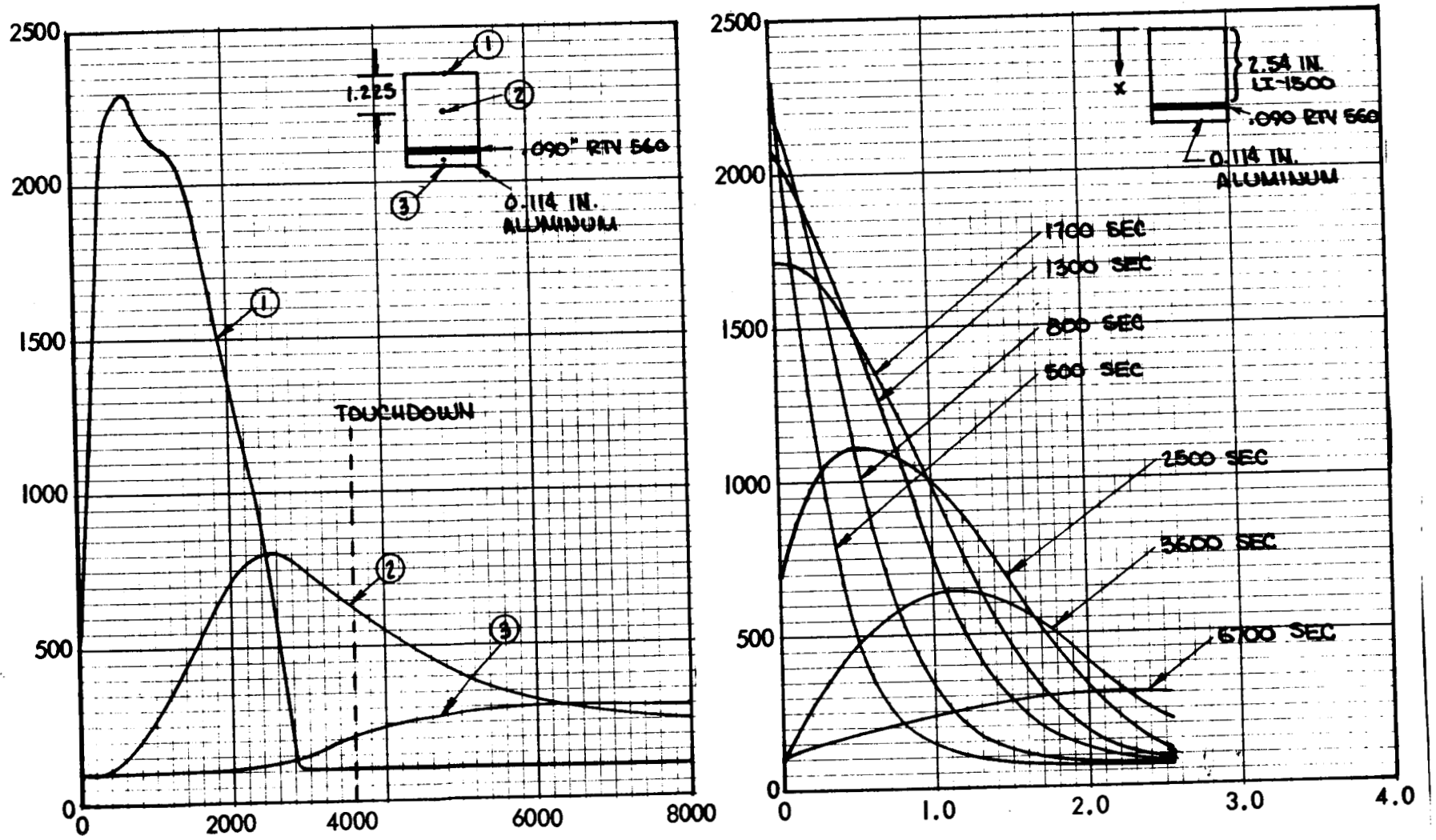


DO6047

Fig. 2.2.2-27

# TPS TEMPERATURE HISTORIES AND DISTRIBUTIONS
## FLIGHT PANEL NO; 3

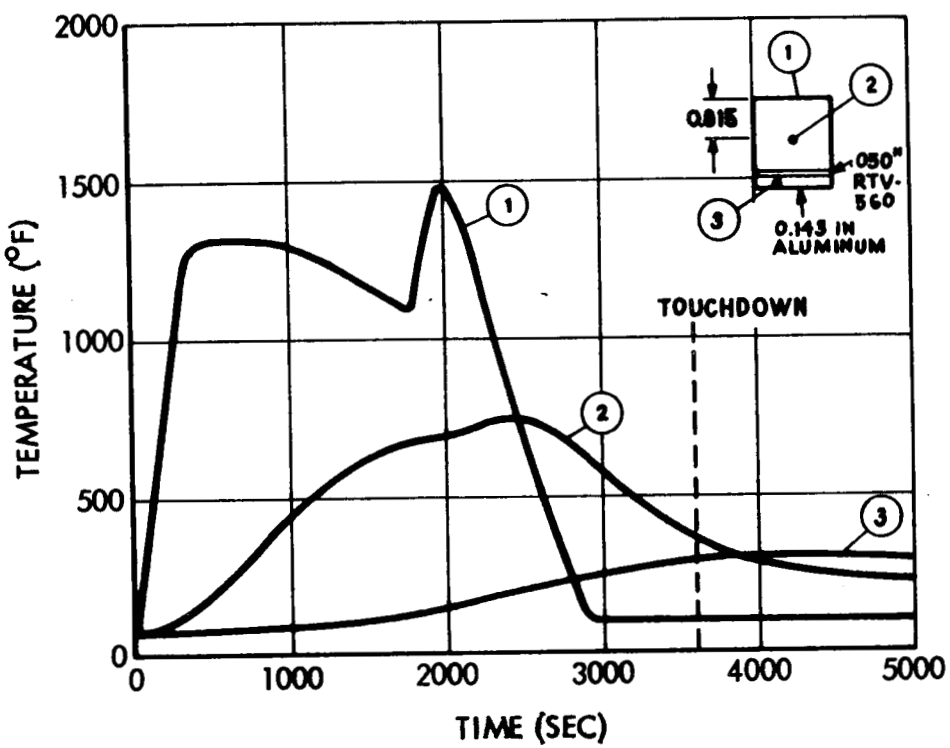


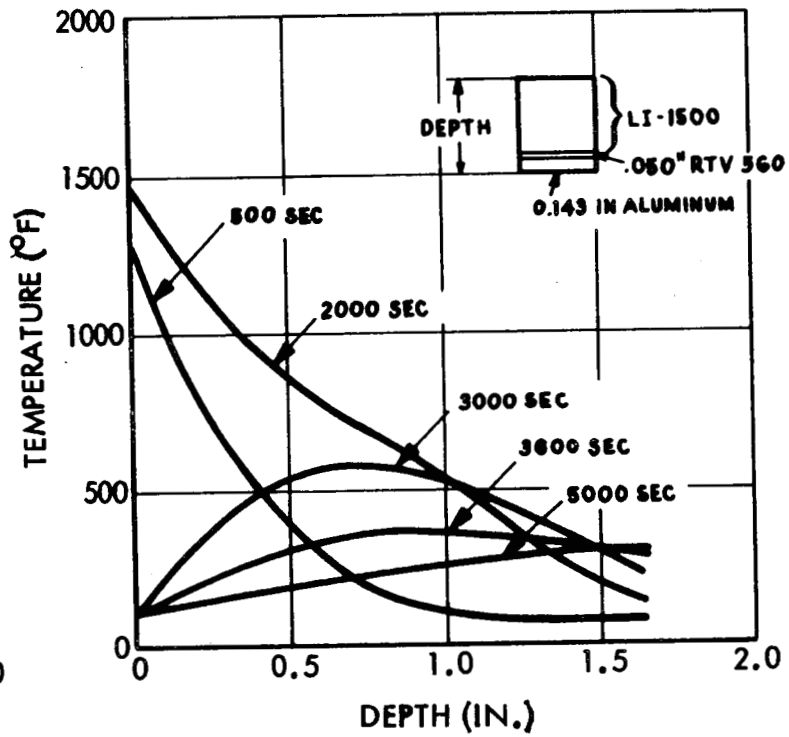


Fig. 2.2.2-28

# TPS TEMPERATURE HISTORIES AND DISTRIBUTIONS

## FLIGHT PANEL NO. 4

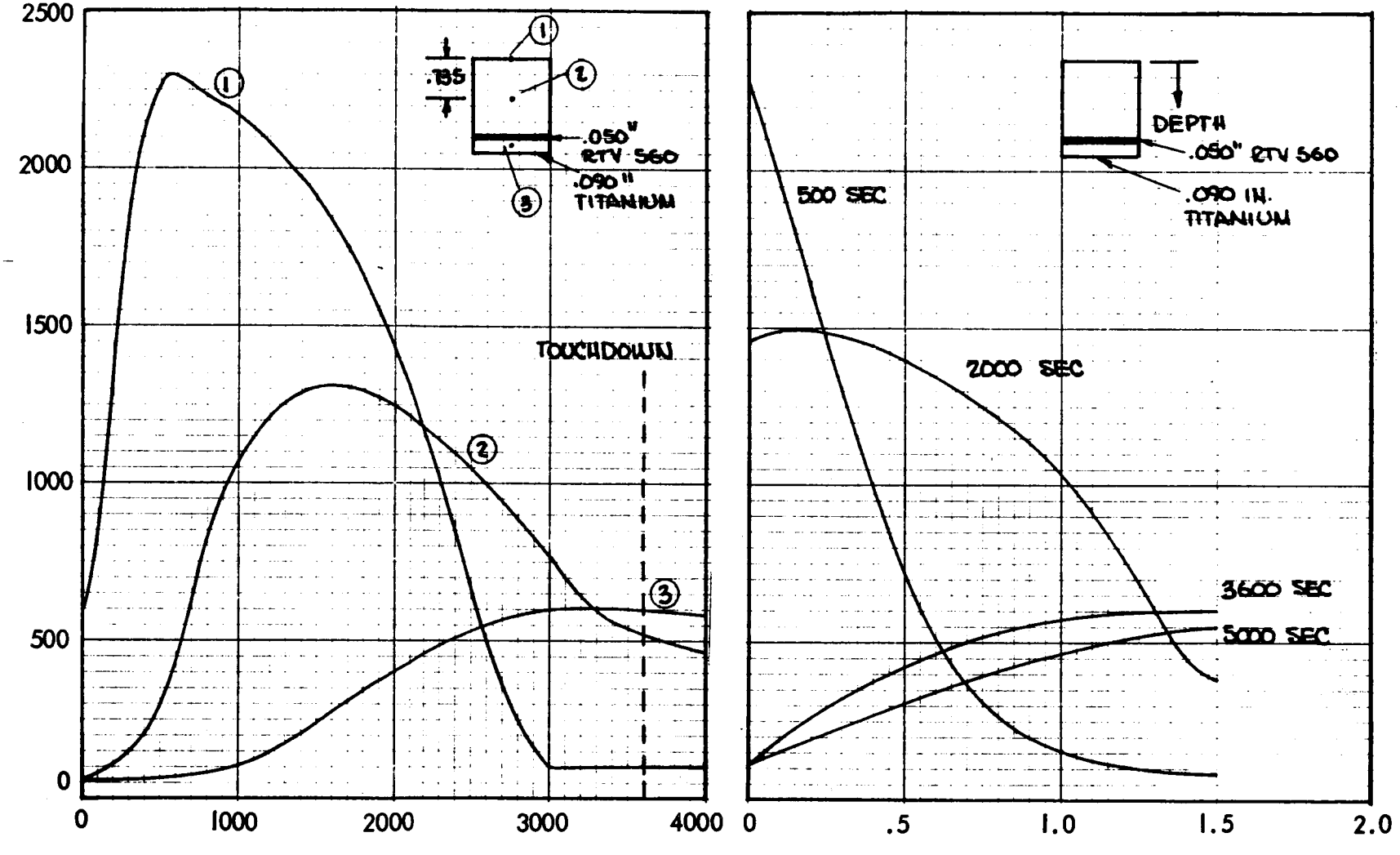


DO5996

Fig. 2.2.2-29

# VARIATION OF ADHESIVE THICKNESS WITH LI-1500 THICKNESS - TEST PANEL 1

MAXIMUM BERYLLIUM TEMPERATURE = 600°F

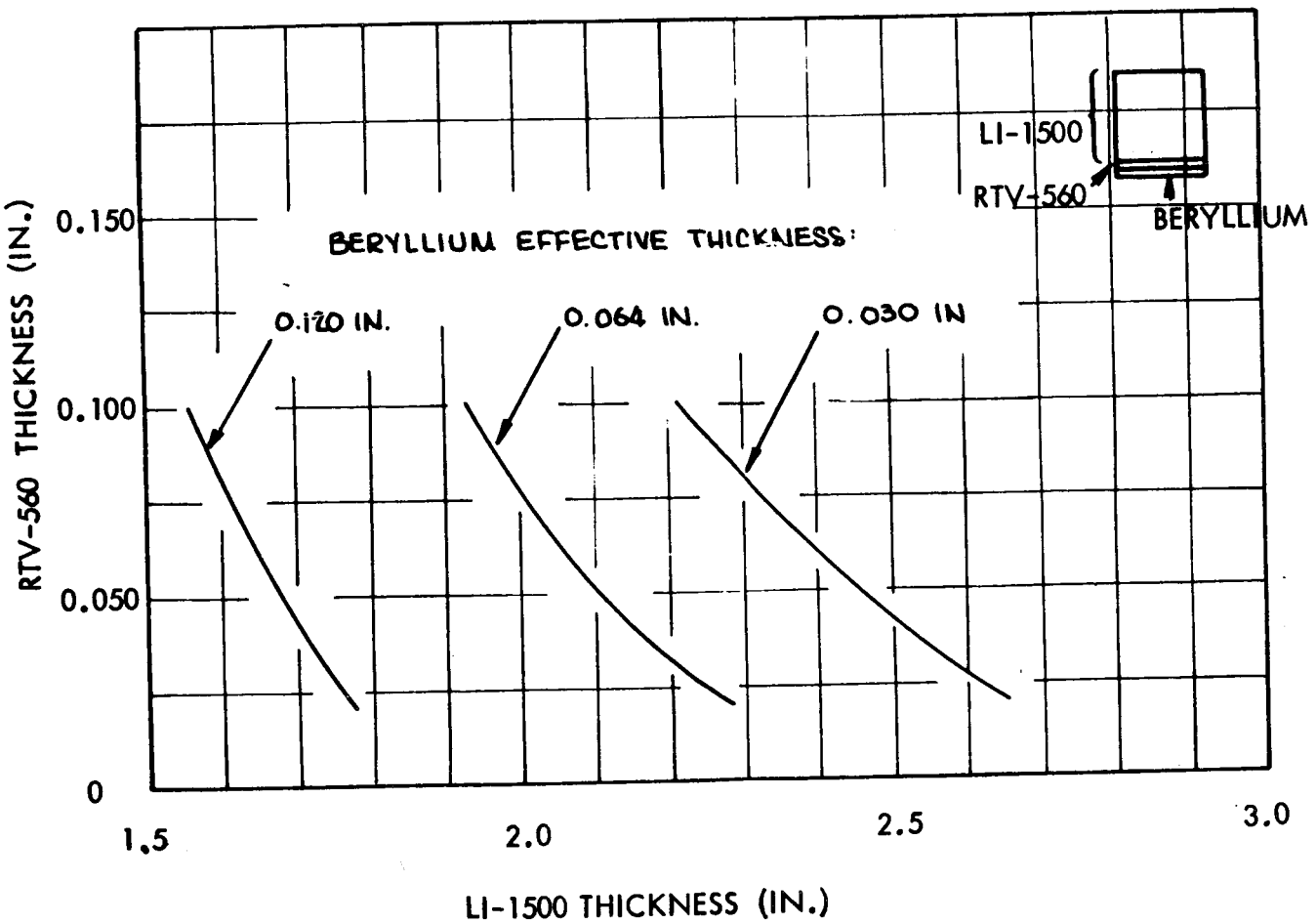


Fig. 2.2.2-30

DO6003

Similar results are shown in Figs. 2.2.2-31, -32, and -33 for test panels Nos. 2, 3, and 4, respectively. Tradeoff factors have been determined from computer runs that considered various adhesive thickness for a constant substrate thickness. The tradeoff factors are dependent on the density-specific heat products of the adhesive, LI-1500 and the substrate material. Approximate tradeoff factors of 4.5, 3.5, and 4.0 were determined for test panels Nos. 2, 3, and 4 from the data of Figs. 2.2.2-31, -32, and -33, respectively. Hence an average tradeoff of about 4.0 could be used for all four test panels.

2.2.2.6 Effect of LI-1500 Sizing With Two-Dimensional Thermal Models. To check the adequacy of the one-dimensional LI-1500 sizing and to obtain transient temperature differences for various elements of the TPS, two-dimensional thermal models were generated and LI-1500 sizing was performed with the THERM computer code.

The thermal model used for test panels Nos. 2 and 4 is shown in Fig. 2.2.2-34. The dimensions shown are for the titanium panel. The thermal model for the beryllium test panel is shown in Fig. 2.2.2-35. The LI-1500 thickness can be easily changed for consecutive computer runs. As in the one dimensional sizing discussed previously, an adiabatic boundary condition was used. An isotropic thermal conductivity for 1 ATM air was used for this model. The thermal conductivity and specific heat values for LI-1500 are given in Section 4.1.

A comparison of the LI-1500 thermal sizing between a one- and two-dimensional thermal model for the titanium test panel is shown in Fig. 2.2.2-36. The results are shown with a plot of maximum titanium face sheet temperature versus LI-1500 thickness. The results indicate a negligible difference in LI-1500 thickness (0.10 in.) at the titanium design temperature of 600$^{\circ}$F. Larger adhesive thickness than that shown will not change the results, since the LI-1500 thickness will be reduced in accordance with the tradeoff factors discussed previously. Temperature histories for the titanium face sheet and stiffener are shown in Fig. 2.2.2-37. Large transient temperature differences are indicated (50-75$^{\circ}$F), but these eventually decrease as the TPS approaches its maximum values. These transient temperatures are used to determine temperature induced bending loads in the panels.

# VARIATION OF ADHESIVE THICKNESS WITH LI-1500 THICKNESS - TEST PANEL NO. 2

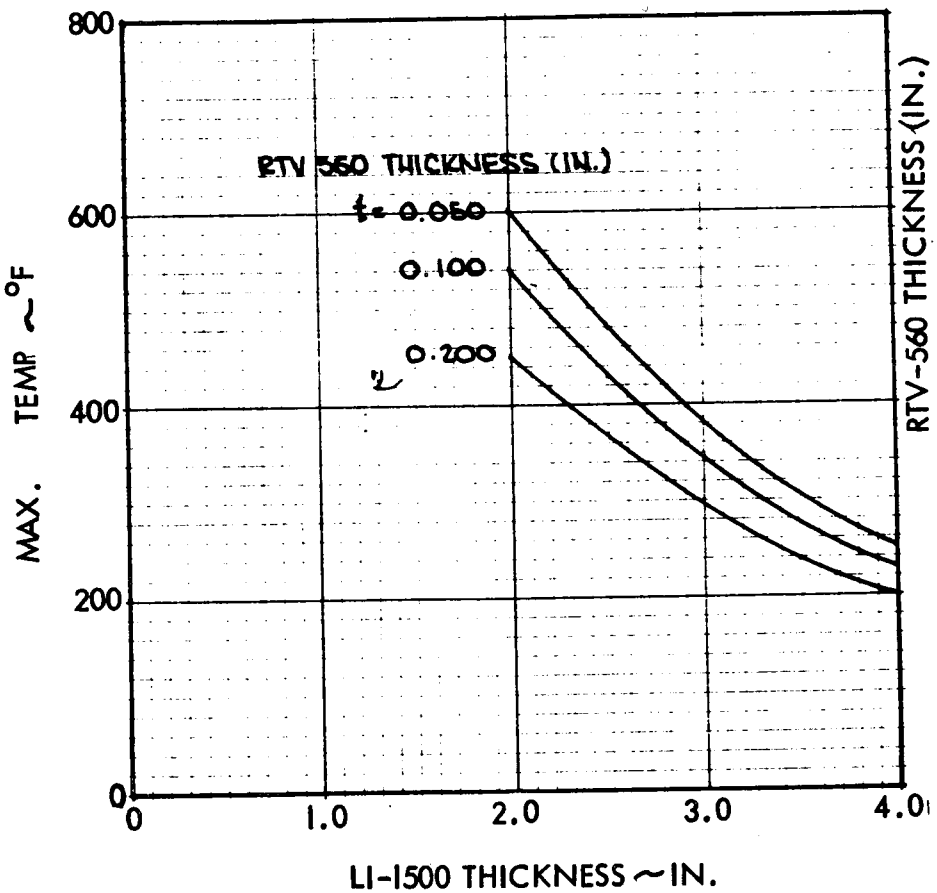


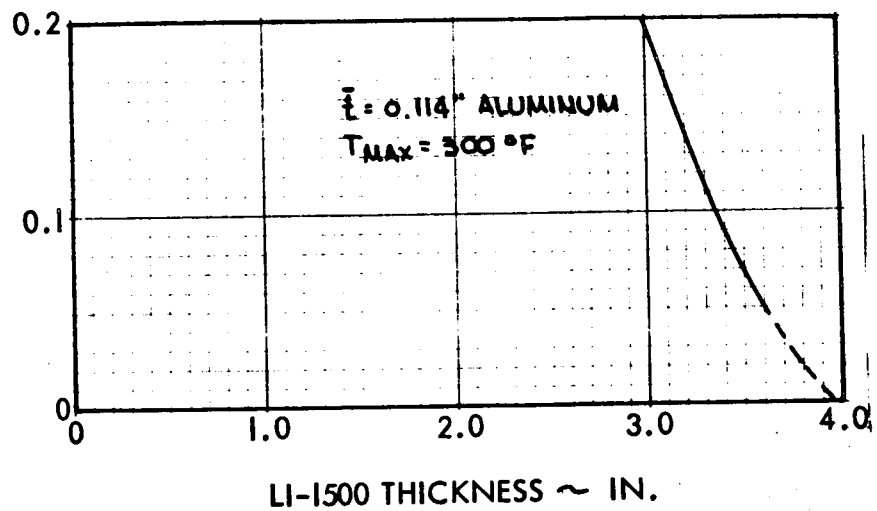


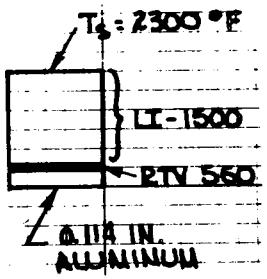


DO6081

Fig. 2.2.2-31

# VARIATION OF ADHESIVE THICKNESS WITH LI-1500 THICKNESS - TEST PANEL NO. 3

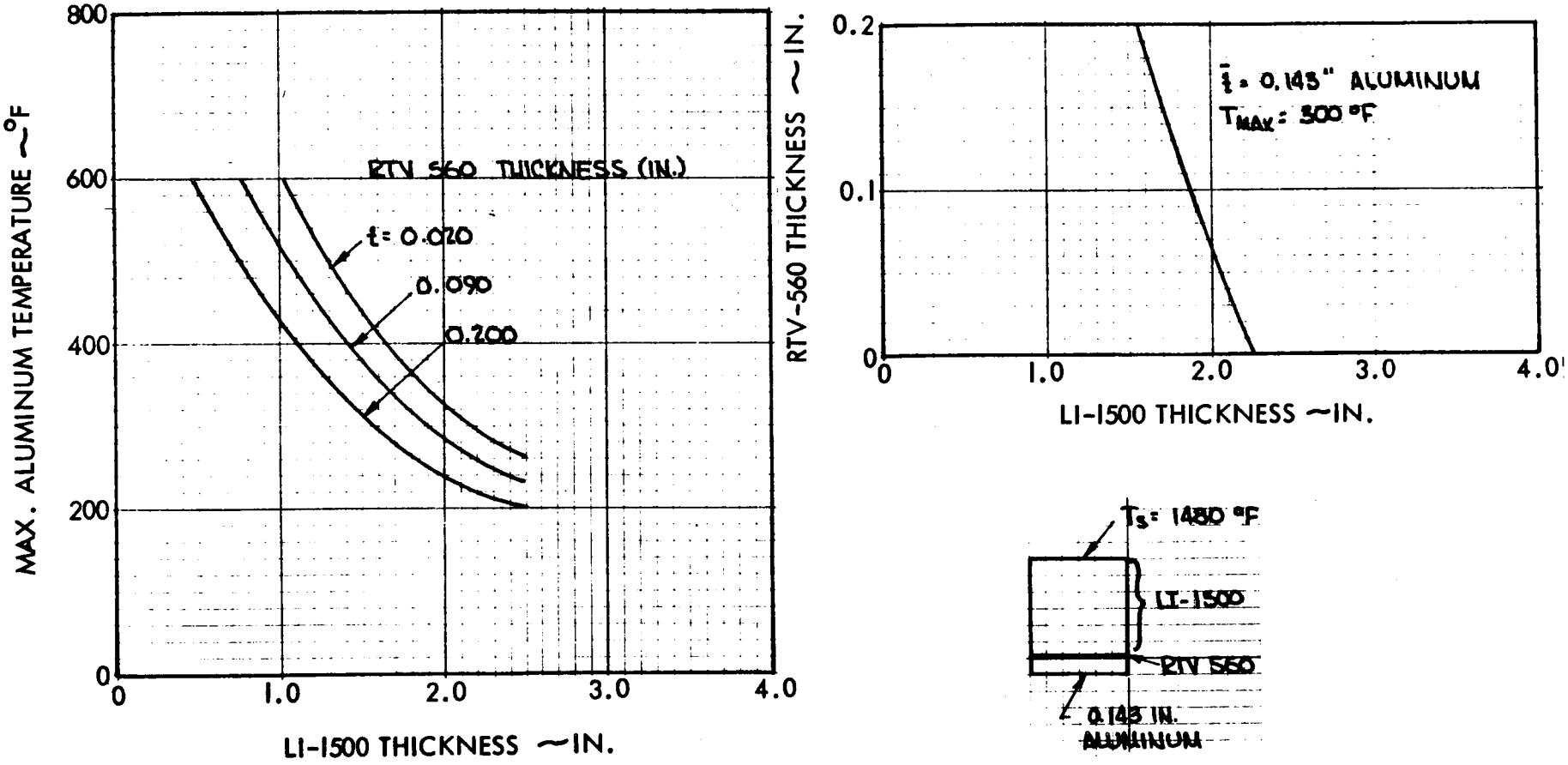


Fig. 2.2.2-32

# VARIATION OF ADHESIVE THICKNESS WITH LI-1500 THICKNESS - TEST PANEL NO. 4

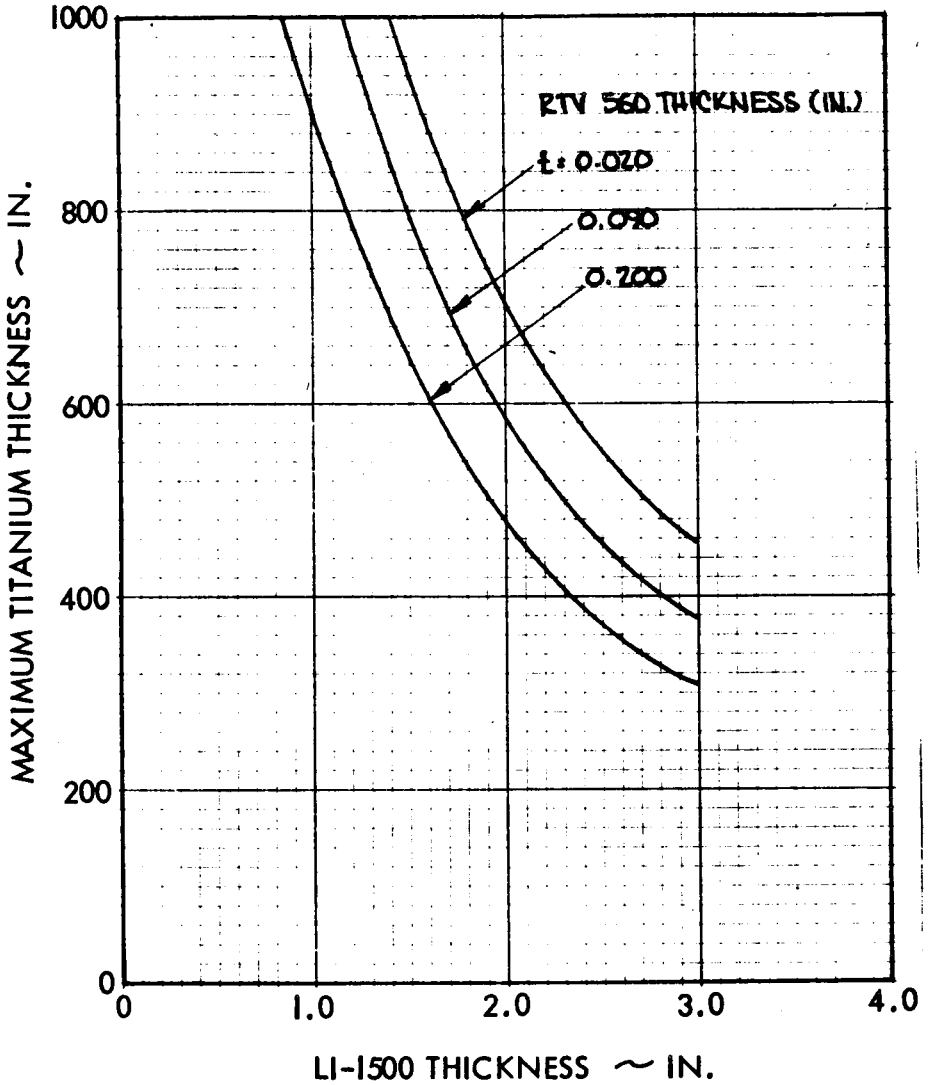


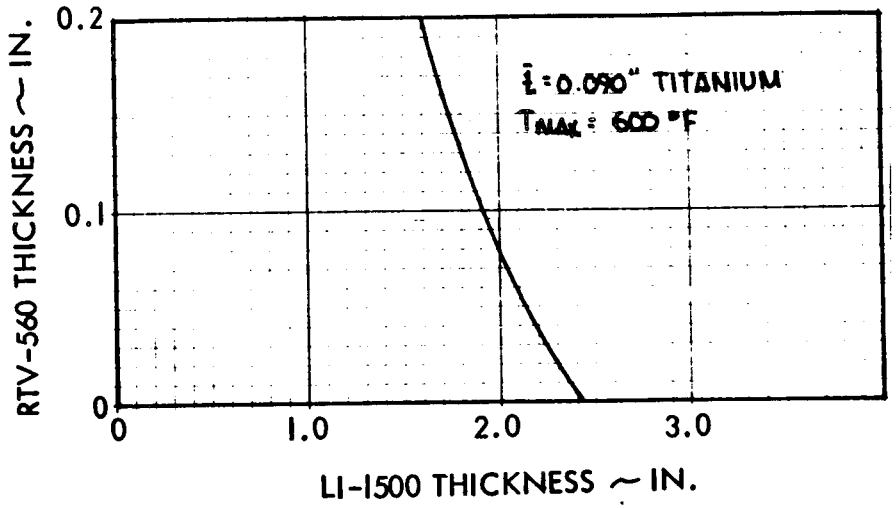


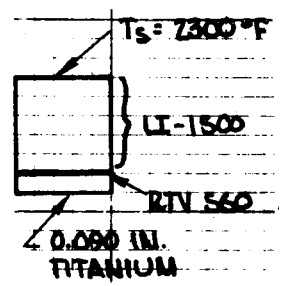


DO6029

Fig. 2.2.2-33

# TWO-DIMENSIONAL THERMAL MODEL FOR TITANIUM AND ALUMINUM PANEL

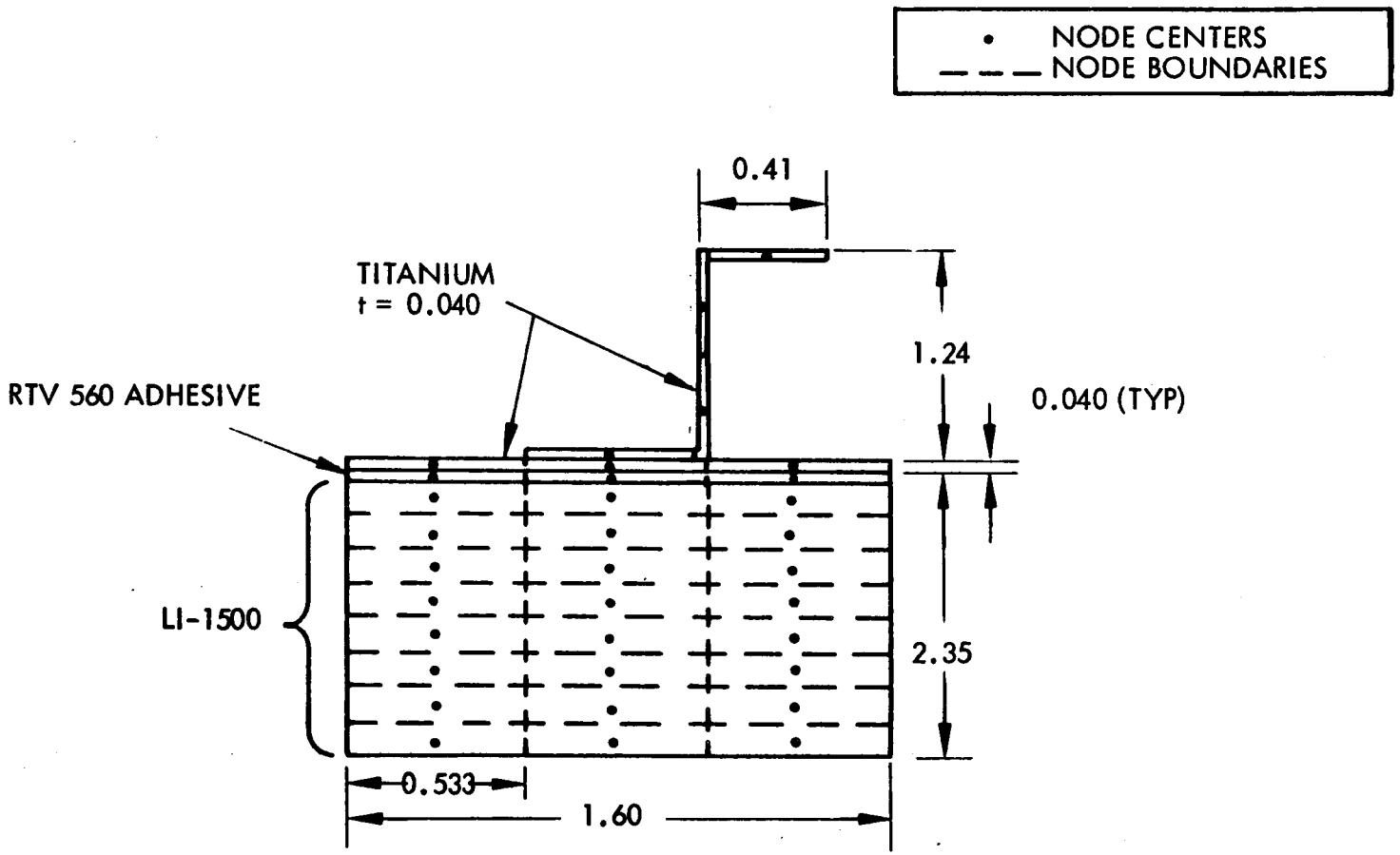


DIMENSIONS SHOWN ARE FOR PANEL 4 TITANIUM

DO6096

Fig. 2.2.2-34

# TWO-DIMENSIONAL THERMAL MODEL FOR BERYLLIUM PANEL

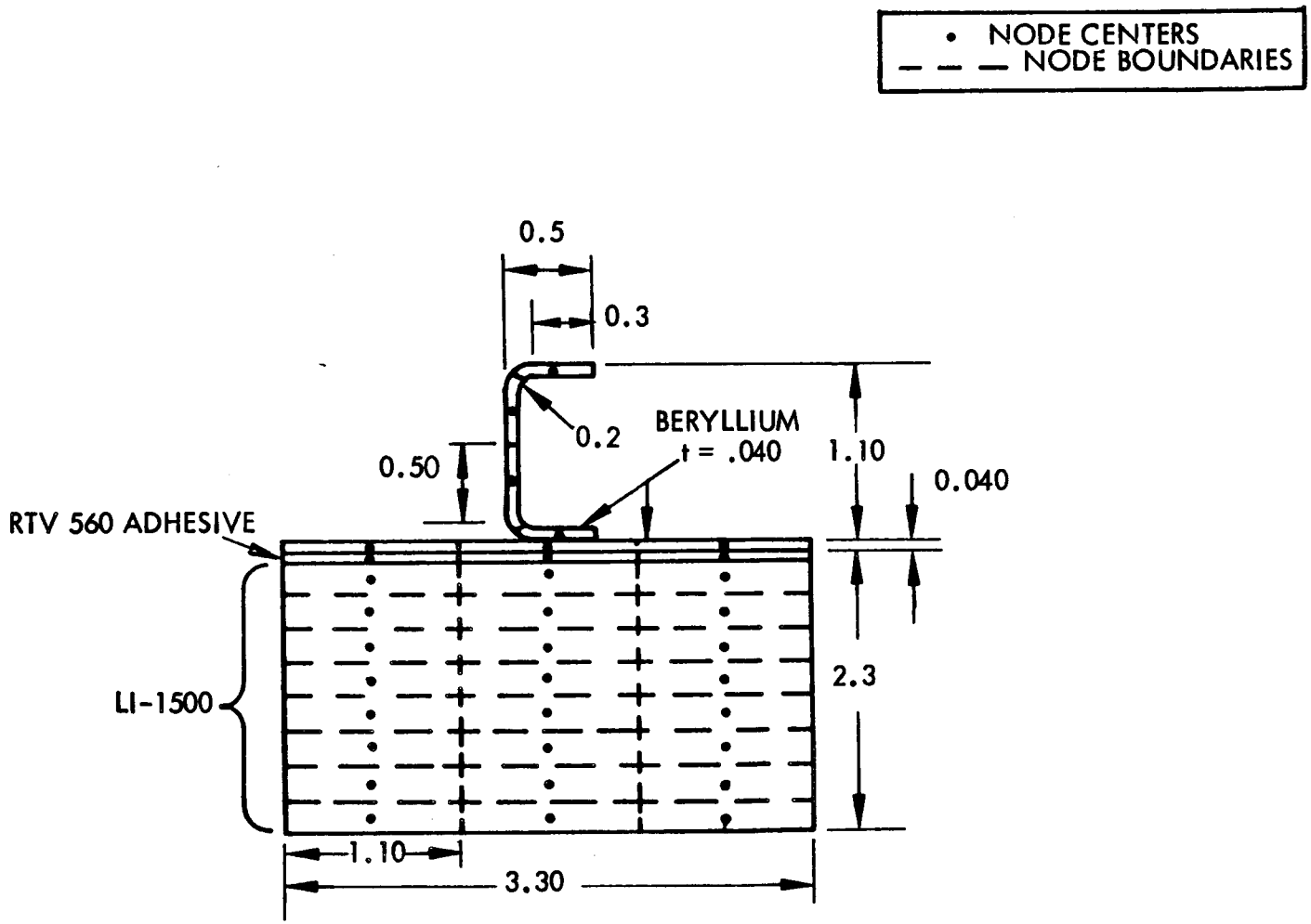


DO6095

Fig. 2.2.2-35

# EFFECTS OF THERMAL MODEL ON TPS SIZING RESULTS

TEST PANEL NO. 4

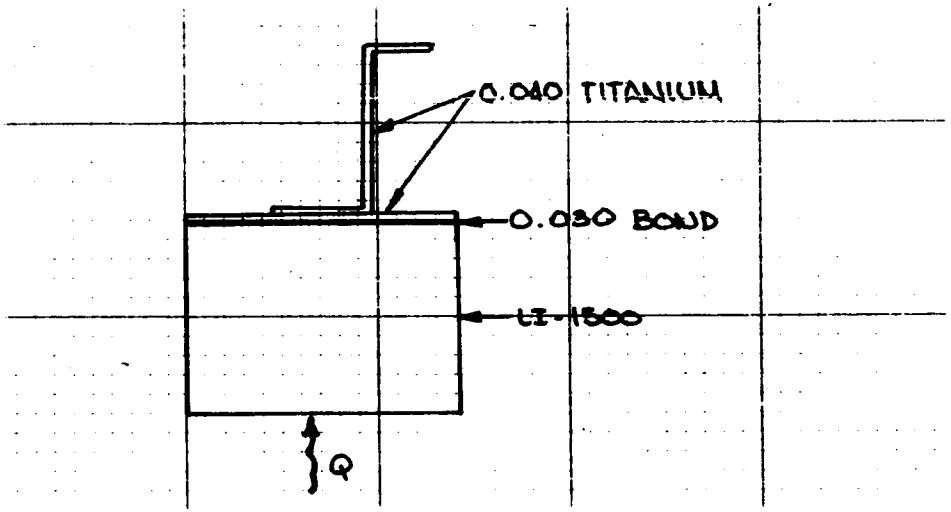


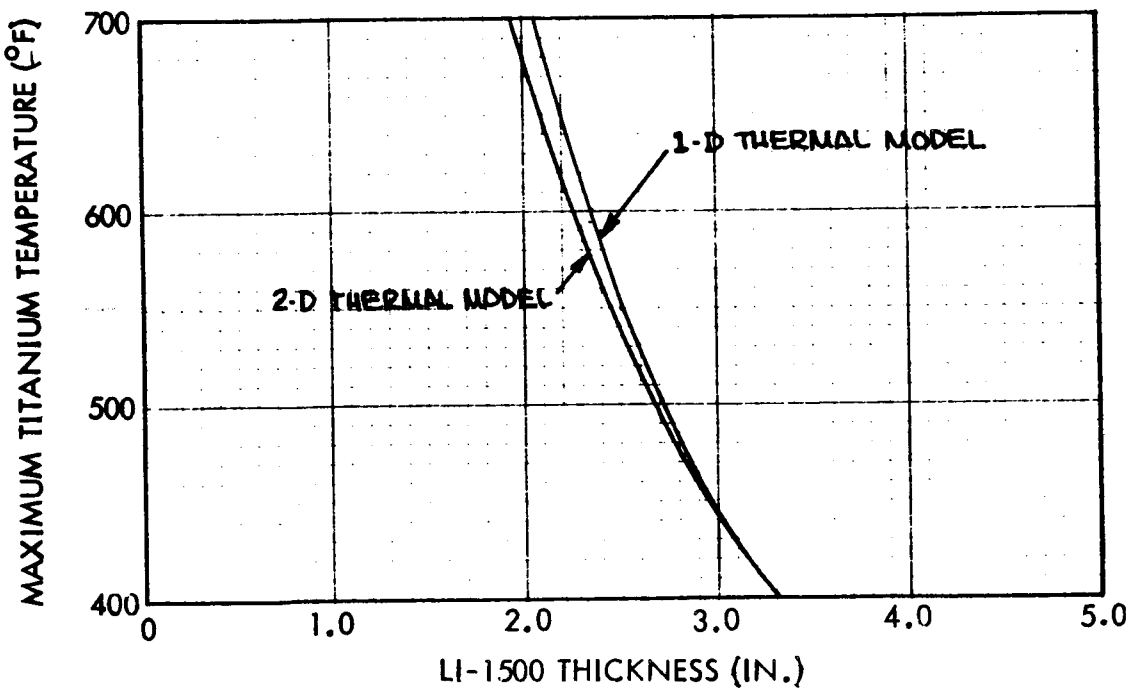


DO6092

Fig. 2.2.2-36

# TEMPERATURE HISTORIES FOR TITANIUM TEST PANEL

## TWO-DIMENSIONAL THERMAL MODEL

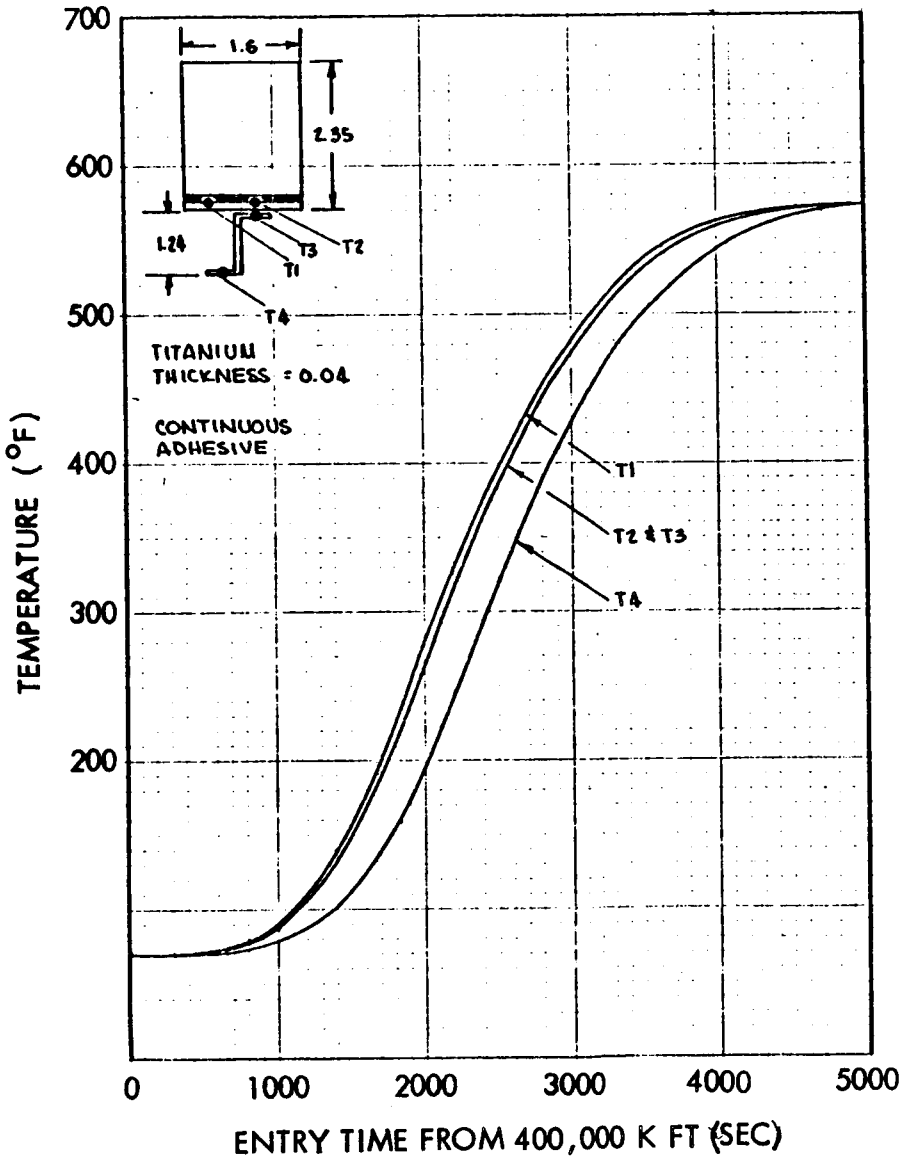


DO6100

Fig. 2.2.2-37

Since the initial fastening method for the titanium and aluminum panels was riveting, the effect of interface contact conductance on the interface between the face sheet and stiffener upon face sheet and stiffener temperatures was calculated and is shown in Fig. 2.2.2-38. The values of conductance used were based on the results of NASA investigations* and were applied to the titanium panel. With the weld bond technique currently selected for fastening the stiffener to the face sheet, values of conductance greater than 1000 $Btu/ft^2 hr^{\circ}F$ are expected.

Since a promising method of attachment appeared to be an interrupted adhesive which could reduce weight and stresses in the LI-1500, the two-dimensional thermal model was used to show the effect of the adhesive void on the substrate temperatures. Figure 2.2.2-39 shows temperature histories for an adhesive void located directly above the location of the stiffener. The results indicate about a $20^{\circ}F$ increase in the maximum titanium temperature as compared to the results of Fig. 2.2.2-37, where a continuous adhesive was used.

The effect of the face sheet temperature distribution at various reentry times is shown in Fig. 2.2.2-40 for the continuous and interrupted adhesive. The maximum face sheet temperature difference occurs at about 4000 sec into the reentry. The effect of the stiffener heat sink is indicated at earlier times (2000 sec) by the lower temperature in the vicinity of the stiffener.

A comparison of results between the one- and two-dimensional thermal models for the aluminum test Panel 2 is shown in Fig. 2.2.2-41. The maximum backface temperatures are nearly identical, which ascertains the adequacy of the one-dimensional thermal model for the TPS sizing studies on the aluminum panel.

Prior to the decision to use a weldbond technique to fasten the aluminum stiffeners to the aluminum face sheet, riveting of these parts was considered. Hence, an analysis

*"Interface Thermal Conductance of 27 Riveted Aircraft Joints," M. E. Barzelay and G. F. Holloway, NASA TN-3991, July 1957

"Range of Interface Thermal Conductance for Aircraft Joints," M. E. Barzelay, NASA TN-D426, May 1960

# EFFECT OF CONTACT CONDUCTANCE ON STIFFENER TEMPERATURES

## TEST PANEL NO. 4

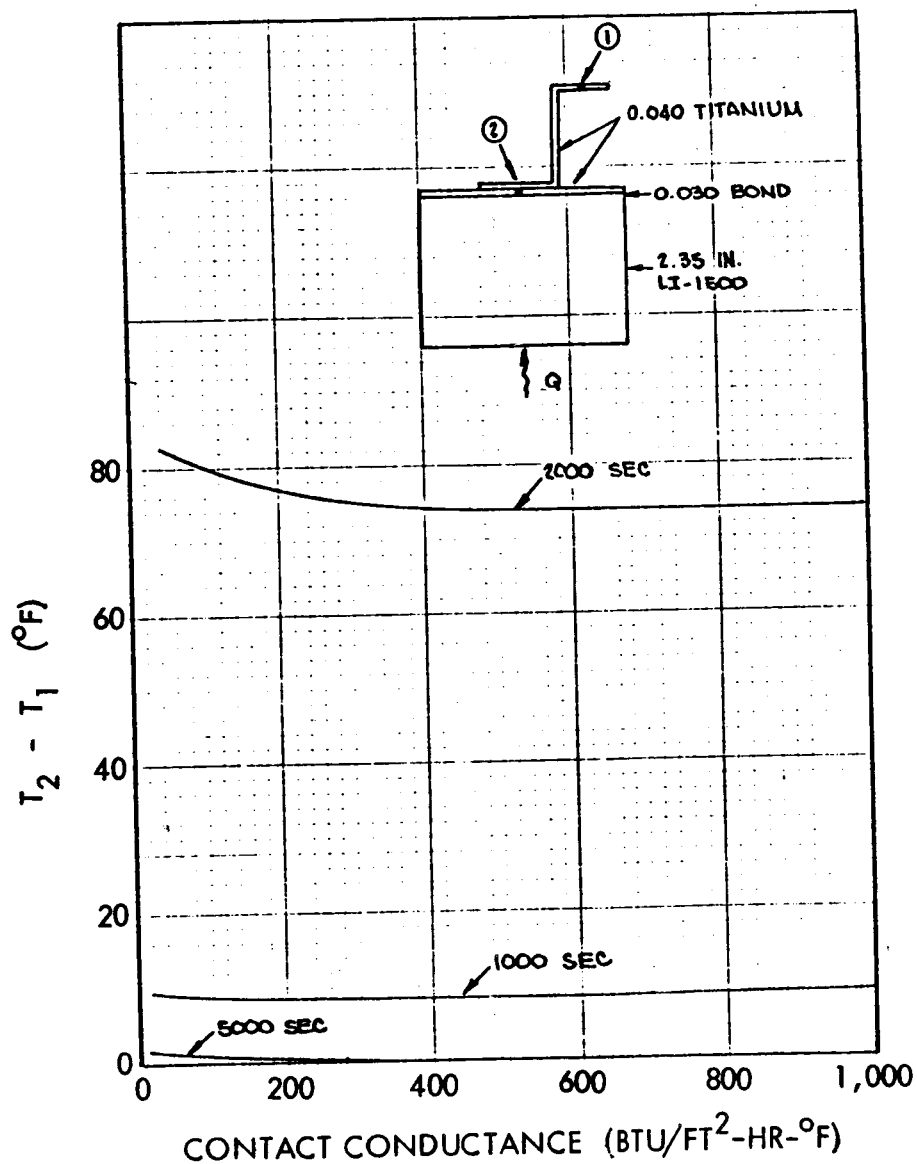


DO6091

Fig. 2.2.2-38

# TEMPERATURE HISTORIES FOR TITANIUM TEST PANEL WITH ADHESIVE VOID

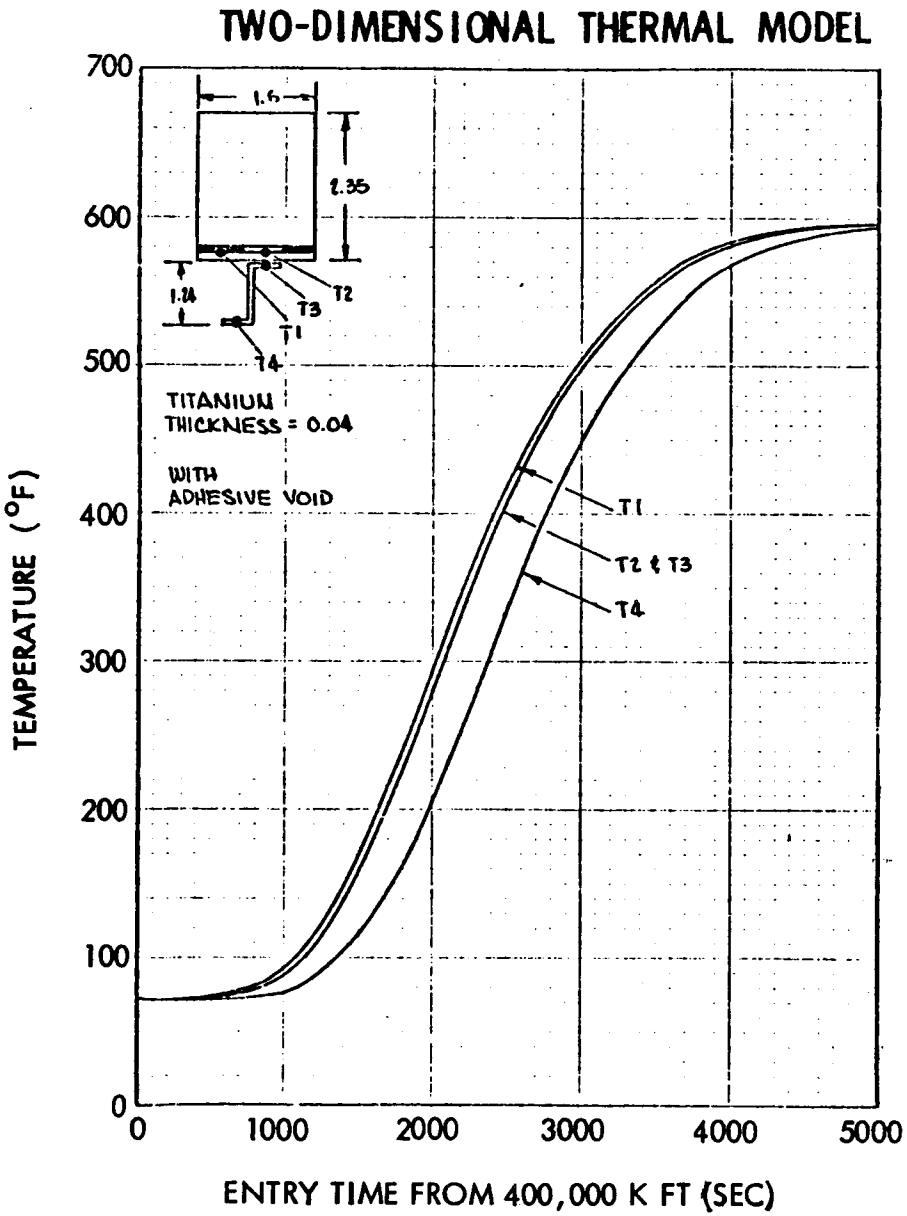


DO6101

Fig. 2.2.2-39

# EFFECT OF ADHESIVE VOID ON TITANIUM FACE SHEET TEMPERATURE DISTRIBUTION

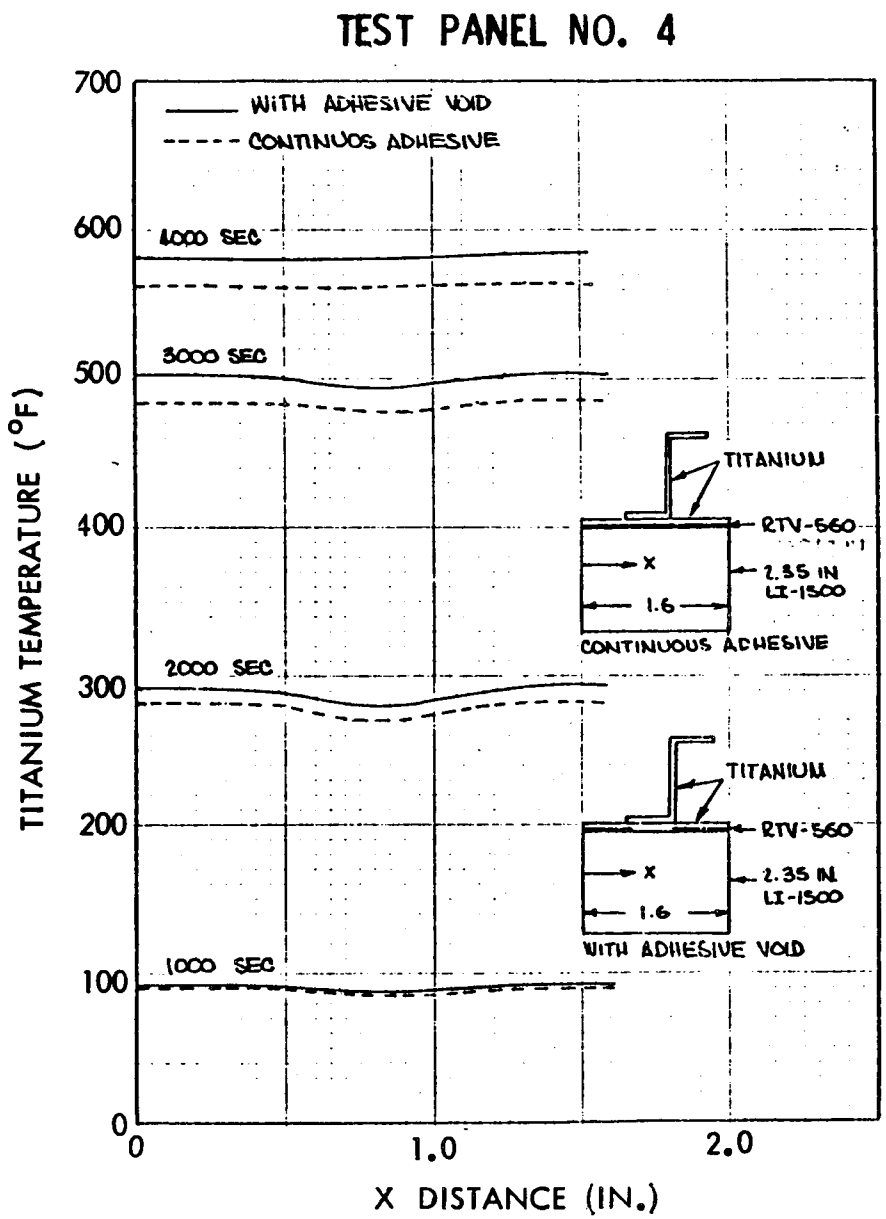


DO6090

Fig. 2.2.2-40

# VARIATION OF MAXIMUM SUBSTRATE TEMPERATURE WITH LI-1500 THICKNESS TEST PANEL NO. 2

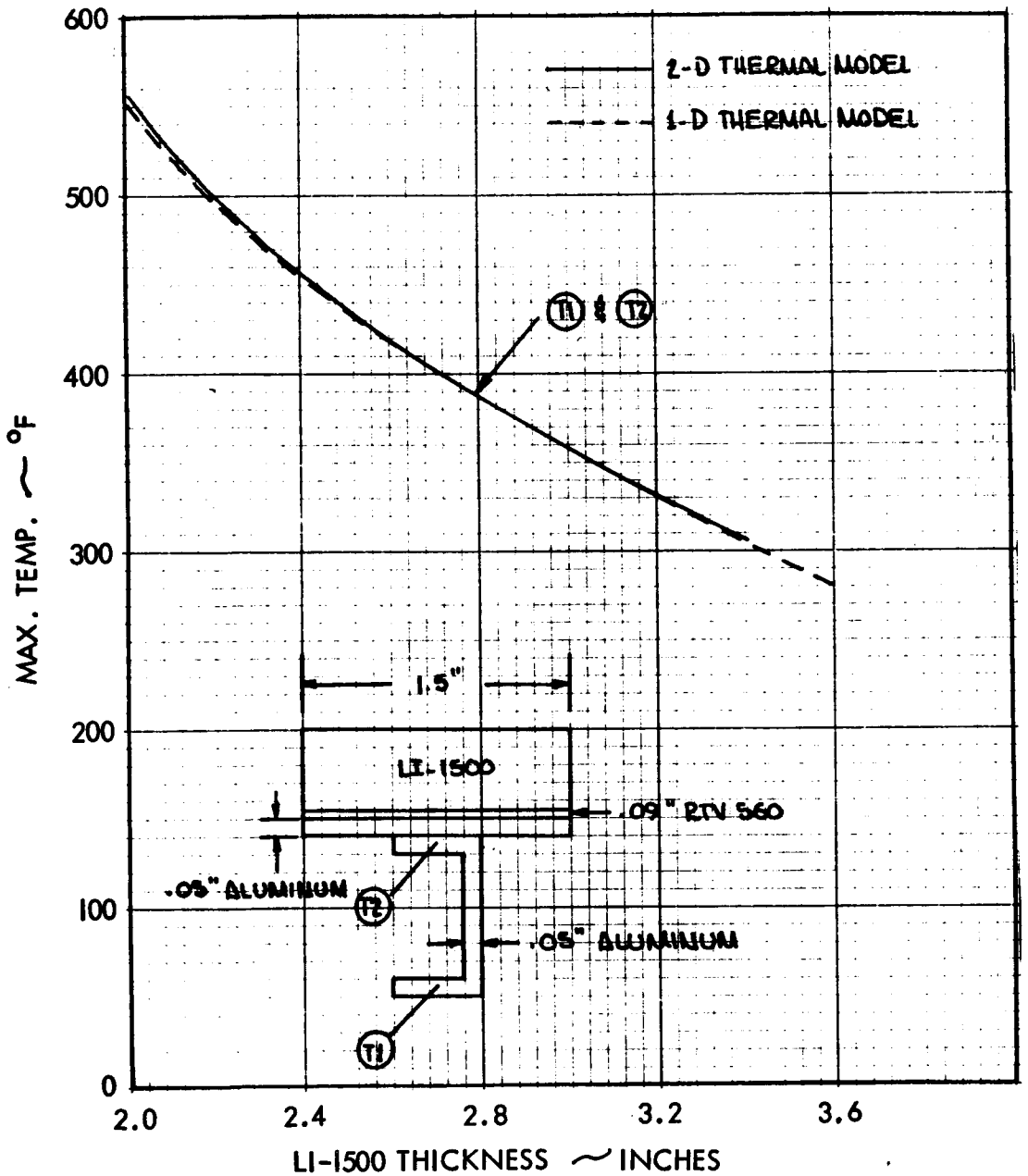


DO6028

Fig. 2.2.2-41

was conducted to determine the effect of contact conductance on the temperature difference between the face sheet and the stiffeners. The results are shown in Fig. 2.2.2-42, where contact conductance from 50 to 1000 Btu/ft$^2$hr$^\circ$F between the face sheet and stiffeners was considered. The maximum temperature difference is about 10$^\circ$F for the values of contact conductance analyzed. Due to the high thermal conductivity of aluminum and the low rate of heat conducted through the LI-1500 into the panel, the temperature difference between the top and bottom of the stiffener is less than 5$^\circ$F.

The effect of the thermal model on the maximum substrate temperature for the beryllium test panel is shown in Fig. 2.2.2-43. The results indicate the one-dimensional thermal model is adequate for insulation sizing.

The results also show the effect of backface boundary conditions on the maximum panel temperature. If the panel is sized with an adiabatic boundary condition for a 600$^\circ$F temperature and tested with a non-adiabatic boundary condition, the maximum temperature will be about 490$^\circ$F. The same result was shown in Fig. 2.2.2-17 for the one-dimensional model. The same comparison between the one- and two-dimensional thermal models would exist for the flight panels with either adiabatic or non-adiabatic assumed boundary conditions.

# EFFECT OF CONTRACT CONDUCTANCE ON TEMPERATURE DIFFERENCE BETWEEN FACE SHEET AND BOTTOM OF STIFFENER

TEST PANEL 2

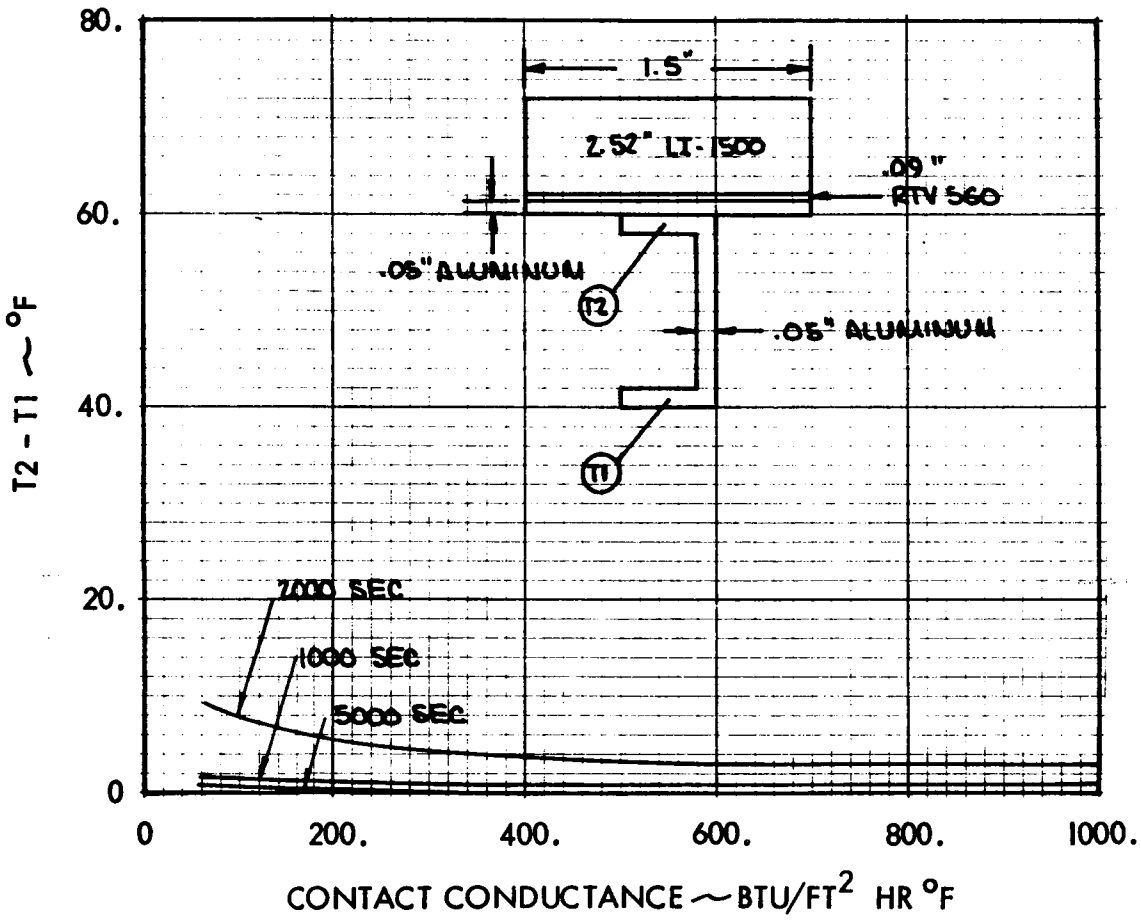


DO6009

Fig. 2.2.2-42

# VARIATION OF MAXIMUM BERYLLIUM TEMPERATURE WITH LI-1500 THICKNESS - TEST PANEL NO. 1

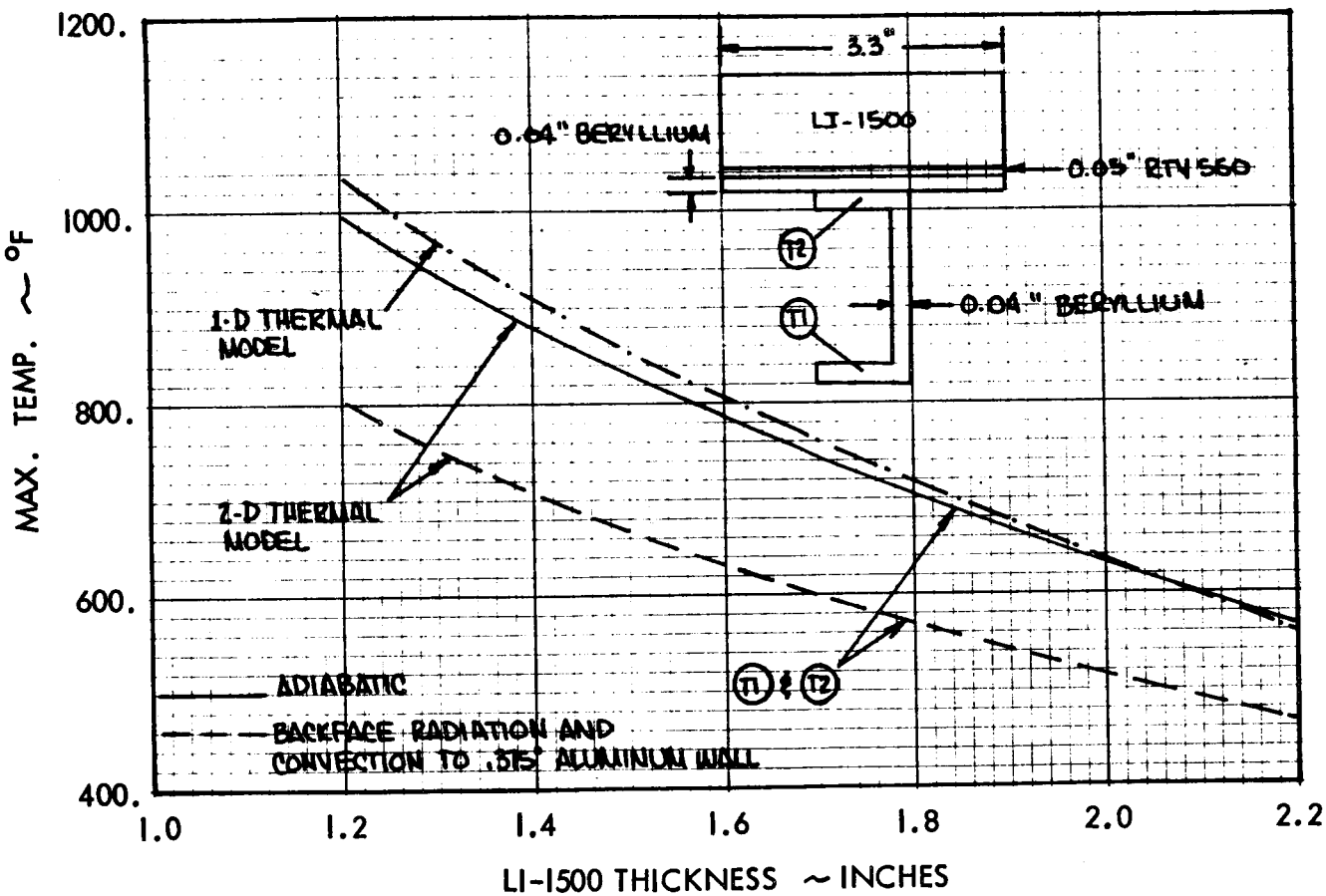


DO5999

Fig. 2.2.2-43

### 2.2.3 RSI Tile Analysis

This section is devoted to the stress analysis of the RSI tile. Included are a discussion of analysis techniques, parametric studies of critical design parameters, and analysis of prototype panels.

2.2.3.1 Methods of Analysis and Modeling. The work described in this subsection is an outline of the development of a linearized two-dimensional model to approximate the behavior of the RSI panel under combined mechanical and thermal loads. Included are a discussion of the two-dimensional (2D) finite element code, WILSON, and its subsequent application to modeling of the panel. This method represents the baseline analytical technique used for the RSI stress analysis. The three-dimensional (3D) program, SAP, which is being used to verify the validity of a 2D analysis, is also briefly discussed and preliminary comparison of the two methods are presented. The manner of temperature profile modeling through the RSI thickness is discussed as well as the effect of using isotropic material properties for LI-1500 early in the program before data were available to show the orthotropic nature of the material.

2-D WILSON Program. This code is a two-dimensional finite element program capable of performing either plane stress or plane strain analyses for orthotropic temperature dependent material properties. The version in use incorporates double precision arithmetic and has a maximum of 1200 nodal points or 2400 degrees of freedom with 1092 elements. The usage of double precision is necessary, due to the wide range of elastic and geometric properties of the materials in the TPS panel design.

2-D RSI System Model. The way in which one half of the TPS panel is modeled for the WILSON code is shown in Fig. 2.2.3.1-1 where it is noted that the panel is assumed to be simply supported. The substrate stiffeners and skin are replaced by an effective substructure material whose elastic properties are those of the substrate but whose thickness is based on the bending stiffness of the actual panel substrate. As seen in the model, two layers of elements are used for the effective substructure – one layer for the bond, eight for the LI-1500, and one layer for the coating. The reason for different size elements in the LI-1500 is that if the coating is lapped over the edges,

# TWO DIMENSIONAL MODELS OF TPS PANELS

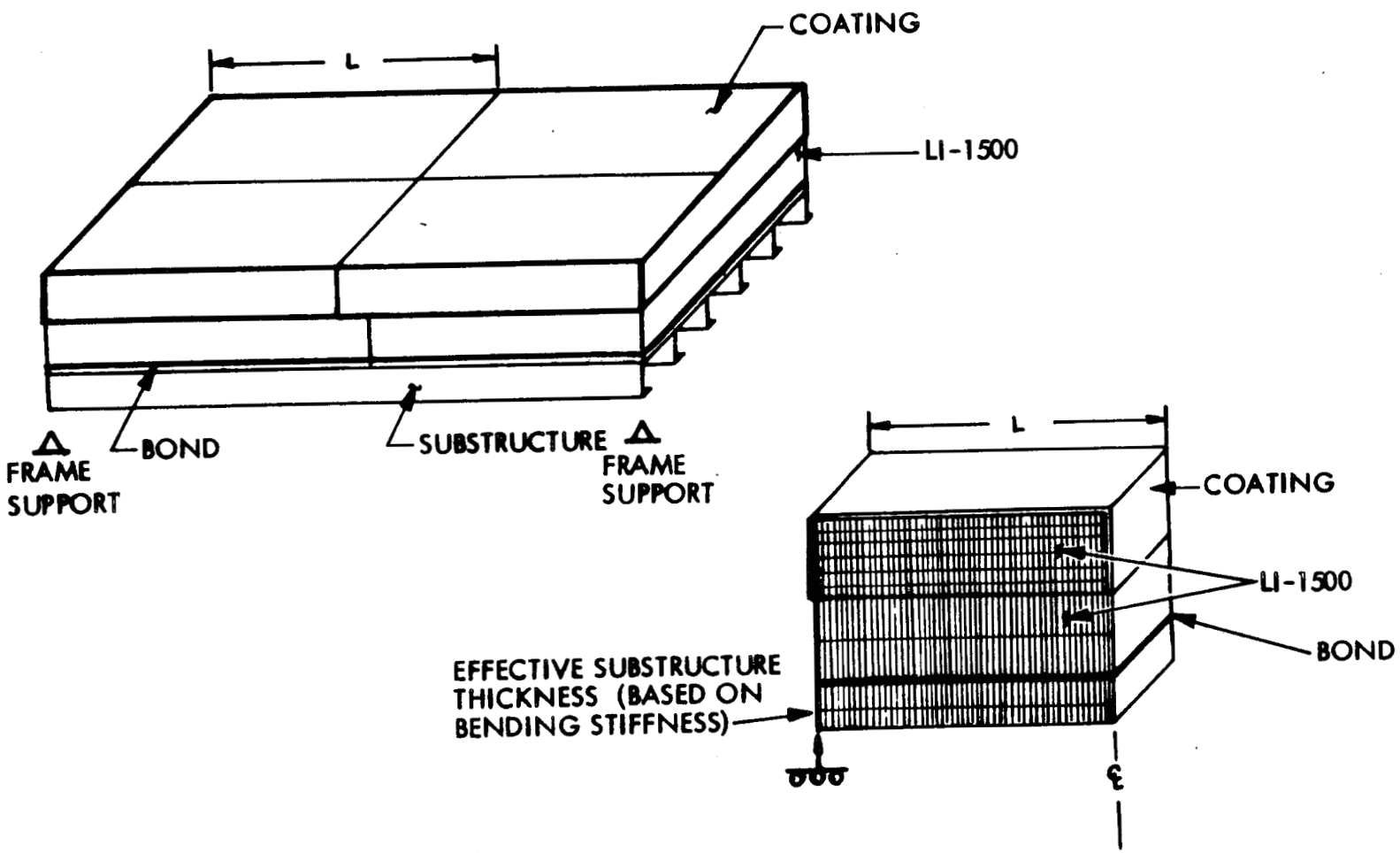


Fig. 2.2.3.1-1

numerical inaccuracies can occur due to elastic and geometric property mismatch. The effect of element aspect ratio has also been studied to minimize these sources of inaccuracy.

Due to mechanical and thermal loads, the panel experiences bending but it is found that the in-plane strain of the substrate is the primary source of RSI stressing. It has been ascertained that the effective thickness model has negligible effects on the location of the neutral axis of the overall RSI system model in the bending mode. In-plane line loads in the primary structure panels are proportioned to the effective thickness so that in-plane substructure stress and strain levels are those of the actual panel. At this time, nonlinear beam-column effects have not been modeled.

Effect of Orthotropic LI-1500 Material Properties. Early in the program, adequate material property data on the anisotropic behavior of LI-1500 were not available, hence, isotropic elastic moduli were assumed for initial parametric studies. After the orthotropic data were obtained, a comparison was drawn to see what effect the use of isotropic data would have on the early parametric studies. The results of this check are shown in Table 2.2.3.1-1, which presents the percent change in RSI system stress levels of interest. Maximum effects are noted in coating stresses that go down markedly, but some LI-1500 stress components do go up somewhat. Although stress magnitudes are dependent upon anisotropic effects, the general conclusions of the initial parametric studies carried out with isotropic data continue to hold; all subsequent studies and prototype panel verification calculations utilize orthotropic property data.

Plane Stress/Plane Strain Comparison. Initial studies in the TPS program were carried out with a version of the WILSON program that was capable of plane stress analyses alone. This usage can be justified, however, the program was modified to incorporate a plane strain solution for direct comparison. The case studied is for a beryllium subpanel with a 600$^{o}$F backface temperature and a 1.14 burst pressure. The analysis assumed isotropic LI-1500 elastic properties with $E = 60,000$ psi, and the expansion coefficients of each material in the third direction have been set to zero. The comparisons are shown in Table 2.2.3.1-2,

# PERCENT CHANGE IN STRESS INTENSITIES USING ORTHOTROPIC MATERIAL PROPERTIES

BERYLLIUM FUSELAGE PANEL (SHORT TRAJECTORY)

$P = 1.14$ PSI BURST

$Be_T = 600^{\circ}F$, $COATING_T = 75^{\circ}F$

| STRESS (PSI) | CHANGE (%) |
|---|---|
| **LI-1500** | |
| MAXIMUM | +17.5 |
| MINIMUM | +23.8 |
| SHEAR | -19.2 |
| LONGITUDINAL | +22.8 |
| NORMAL | -14.1 |
| **RTV-560** | |
| MAXIMUM | -8.8 |
| MINIMUM | -9.2 |
| SHEAR | -19.1 |
| LONGITUDINAL | -8.5 |
| NORMAL (PEEL) | +2.6 |
| **COATING** | |
| MAXIMUM | -55.7 |
| MINIMUM | -55.4 |

ISOTROPIC PROPERTIES

$E = 20{,}000$ PSI

ORTHOTROPIC PROPERTIES

$E_{LONGITUDINAL} = 20{,}000$ PSI

$E_{NORMAL} = 2{,}000$ PSI

\+ INCREASE FROM ISOTROPIC ANALYSIS
\- DECREASE FROM ISOTROPIC ANALYSIS

DO6063

Table 2.2.3.1-2

## PLANE-STRESS/PLANE-STRAIN COMPARISON, ISOTROPIC ANALYSIS

| | PLANE-STRESS SOLUTION | PLANE-STRAIN SOLUTION |
|---|---|---|
| MAX. LI-1500 STRESS (PSI) | | |
| PRINCIPAL TENSILE | 77.3 | 79.1 |
| PRINCIPAL COMPRESSIVE | -89.1 | -92.4 |
| SHEAR | 64.9 | 63.5 |
| LONGITUDINAL | 73.9 | 75.8 |
| NORMAL | 26.8 | 27.8 |
| $\sigma_T$* | 0.0 | 21.9 |
| MAX. RTV-560 STRESS (PSI) | | |
| PRINCIPAL TENSILE | 48.9 | 52.1 |
| PRINCIPAL COMPRESSIVE | -31.6 | -33.3 |
| SHEAR | 37.8 | 38.4 |
| LONGITUDINAL | -19.3 | -22.0 |
| NORMAL | 30.0 | 32.1 |
| COATING (0025) STRESS (PSI) | | |
| MAXIMUM | 1793 | 1759 |
| MINIMUM | -274 | -269 |

*$\sigma_T$ IS PERPENDICULAR TO LONGITUDINAL AND NORMAL STRESSES

where it is noted that there is very little difference in the two solutions except, of course, for the normal stress in the third direction, $\sigma_T$. This stress is due to the restraint of Poisson effects in the third direction and would apply only for a tile infinitely long in that direction. Hence Poisson effects can be bounded by the two solutions, although it is expected that they are of less importance than other three-dimensional effects.

Linear/Nonlinear Temperature Comparison. Temperature distributions through the LI-1500 thickness, during reentry are essentially nonlinear; however, for convenience of computer data input, a linear distribution has been assumed. This decision is based upon the comparisons shown in Table 2.2.3.1-3, where the worst nonlinear case has been approximated by a linear distribution. All stress levels are within 5 percent, with the exception of coating stresses, which are greater in the linear case, although they are not critical. Hence, a linear assumption leads to some conservatism in coating stress levels and does not basically influence other RSI system stresses.

3-D SAP Program. The program used for the three-dimensional analysis of the thermal protection system test panels is a version of SAP, a general finite element program developed by E. Wilson of the University of California at Berkeley.* Two types of elements are available in this version: A four-node numerically integrated plane stress quadrilateral (QM5) and an eight-node isoparametric hexahedral element (BRICK8). The BRICK8 element, originally formulated by Irons, was modified to include a general temperature distribution within the element. Although the program may be run on either the UNIVAC 1108 or the CDC 6600 computer, increased numerical accuracy due to a larger word size makes CDC the first choice.

*SAP, A General Structural Analysis Program, E. L. Wilson, Report to Walla Walla District's U. S. Engineer's Office, Structural Engineering Laboratory, University of California, Berkeley, California, September 1970.

Table 2.3.1-3

# BERYLLIUM SUBPANEL – 6-IN. TILE LINEAR – NONLINEAR TEMPERATURE COMPARISON

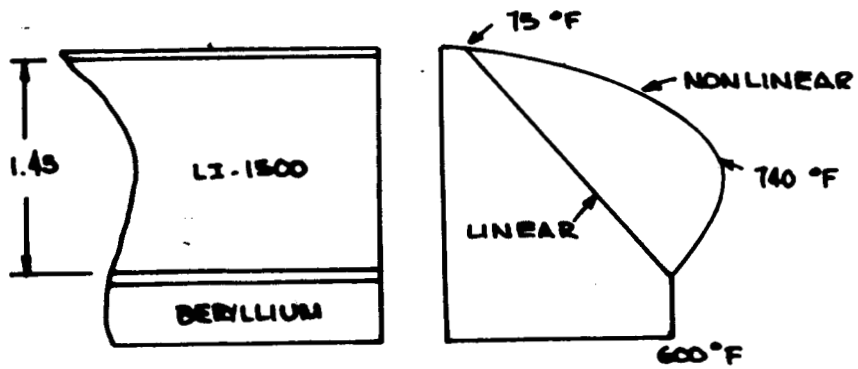


TEMPERATURE DISTRIBUTION

MAXIMUM STRESSES IN PANEL

| QUANTITY | LINEAR | NONLINEAR |
|---|---|---|
| MAXIMUM LI-1500 | 57.7 | 60.4 |
| MINIMUM LI-1500 | -4.3 | -3.8 |
| SHEAR LI-1500 | 17.3 | 17.2 |
| LONG. LI-1500 | 57.7 | 60.4 |
| PEEL LI-1500 | 8.9 | 8.8 |
| MAXIMUM RTV-560 | 20.6 | 20.1 |
| MINIMUM RTV-560 | -23.4 | -23.6 |
| SHEAR RTV-560 | 16.8 | 16.6 |
| LONG. RTV-560 | -18.5 | -19.2 |
| PEEL RTV-560 | 11.7 | 11.5 |
| MAXIMUM COATING | 0.1 | 7.0 |
| MINIMUM COATING | -160.4 | -52.9 |

ORTHOTROPIC ANALYSIS

2-127

D05168
rdb

3-D RSI System Model. Since the TPS panel to be analyzed is symmetrical in two directions about its center, only one quarter of the panel was modeled. Each panel is composed of four LI-1500 tiles, so only the beryllium substructure is assumed continuous across the symmetry planes and the panel is simply supported along its unstiffened edge. Six layers of BRICK8 elements are used in the model – four layers through the LI-1500 insulation, one layer through the bond, and one layer through the beryllium. Along the stiffened edge of the panel an additional layer of BRICK8 elements is used to model the base of the edge stiffener. Plane stress QM5 are used to model the coating on the outside of the LI-1500 and the longitudinal beryllium stiffeners. The completed model is illustrated in Fig. 2.2.3.1-2 with a view looking up under the panel. This quarter panel finite element model has 1638 nodal points, 960 BRICK8 elements, and 204 QM5 elements resulting in problem size of 3968 equations with a maximum half bandwidth of 362. Temperature for the problem was assumed to be 600°F throughout the beryllium and the bond, and decreasing linearly from 600°F to 75°F through the LI-1500 with the stress-free temperature being 75°F. A burst pressure of 1.14 psi was applied to the beryllium panel.

2-D, 3-D Stress Analysis Comparisons. At this time, only preliminary comparisons are available; these indicate a qualitative confirmation of analysis methods. However, some questions do remain concerning the exact magnitudes of some RSI system stresses of interest. For example, comparative results for coating stresses and bond line shear are presented in Figs. 2.2.3.1-3 and 2.2.3.1-4. These stresses and shear are along a line near the edge of the tile where a 2-D plane stress analysis would be most appropriate. The reason for numerical differences in the curves is under investigation; however, it should be stated that other results associated with the 3-D effort do not completely satisfy required conditions on the solution. In contrast, using elementary methods, the 2-D results have satisfied every check condition that has been applied.

# THREE DIMENSIONAL MODEL OF TPS PANELS

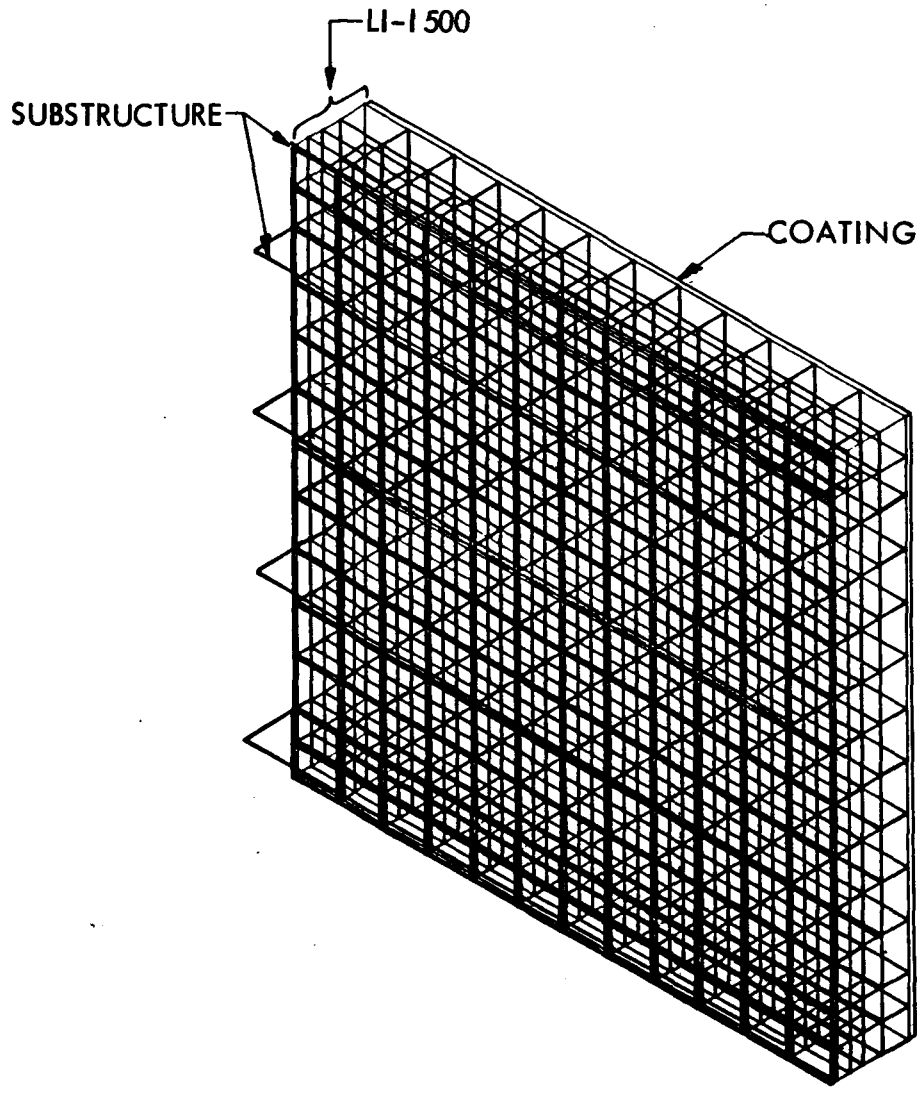


Fig. 2.2.3.1-2

rdb
D04998

# COMPARISON WITH TWO DIMENSIONAL AND THREE DIMENSIONAL ANALYSES

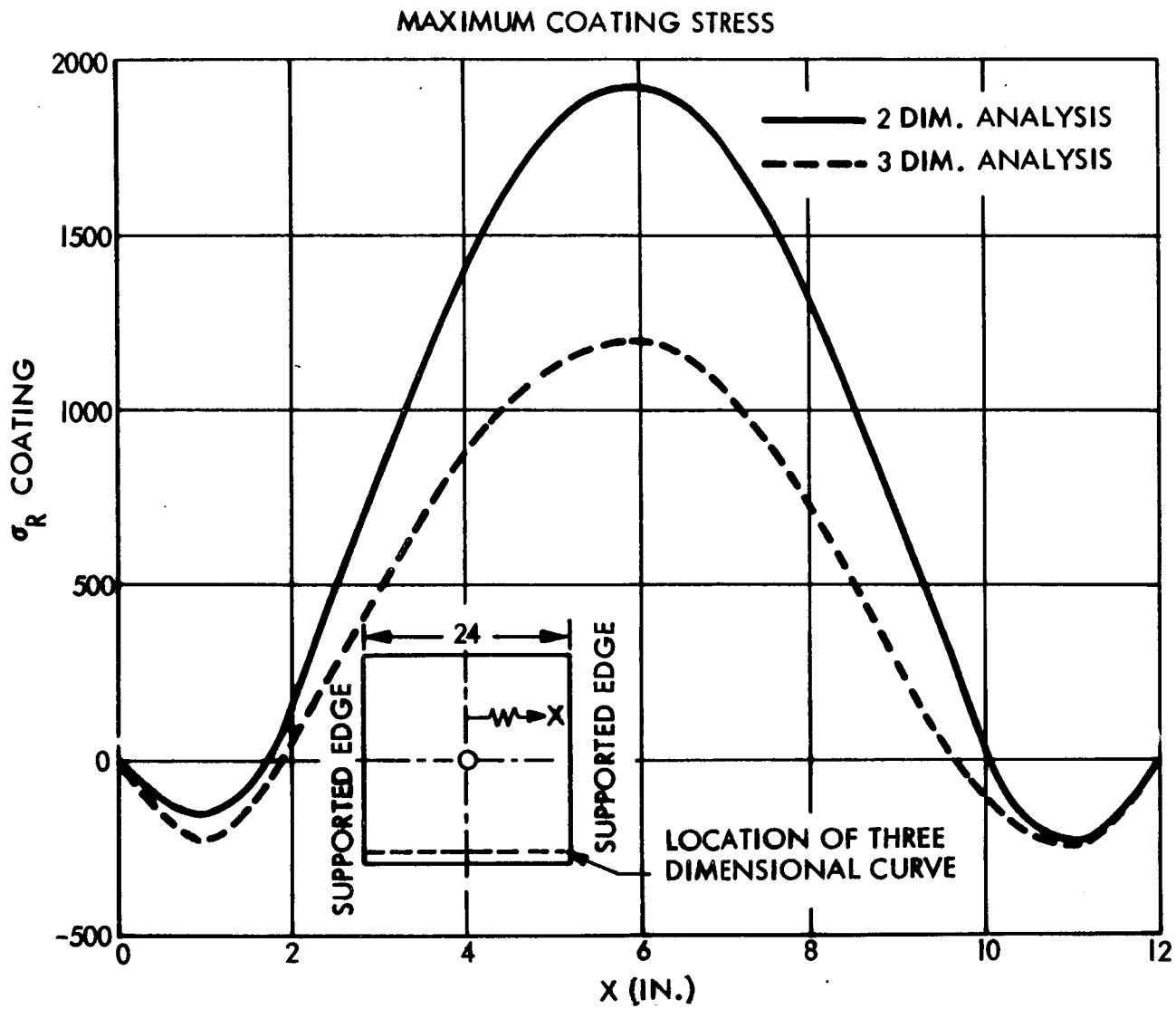


Fig. 2.2.3.1-3



D05175
rdb

# COMPARISON WITH DIMENSIONAL AND THREE DIMENSIONAL ANALYSES

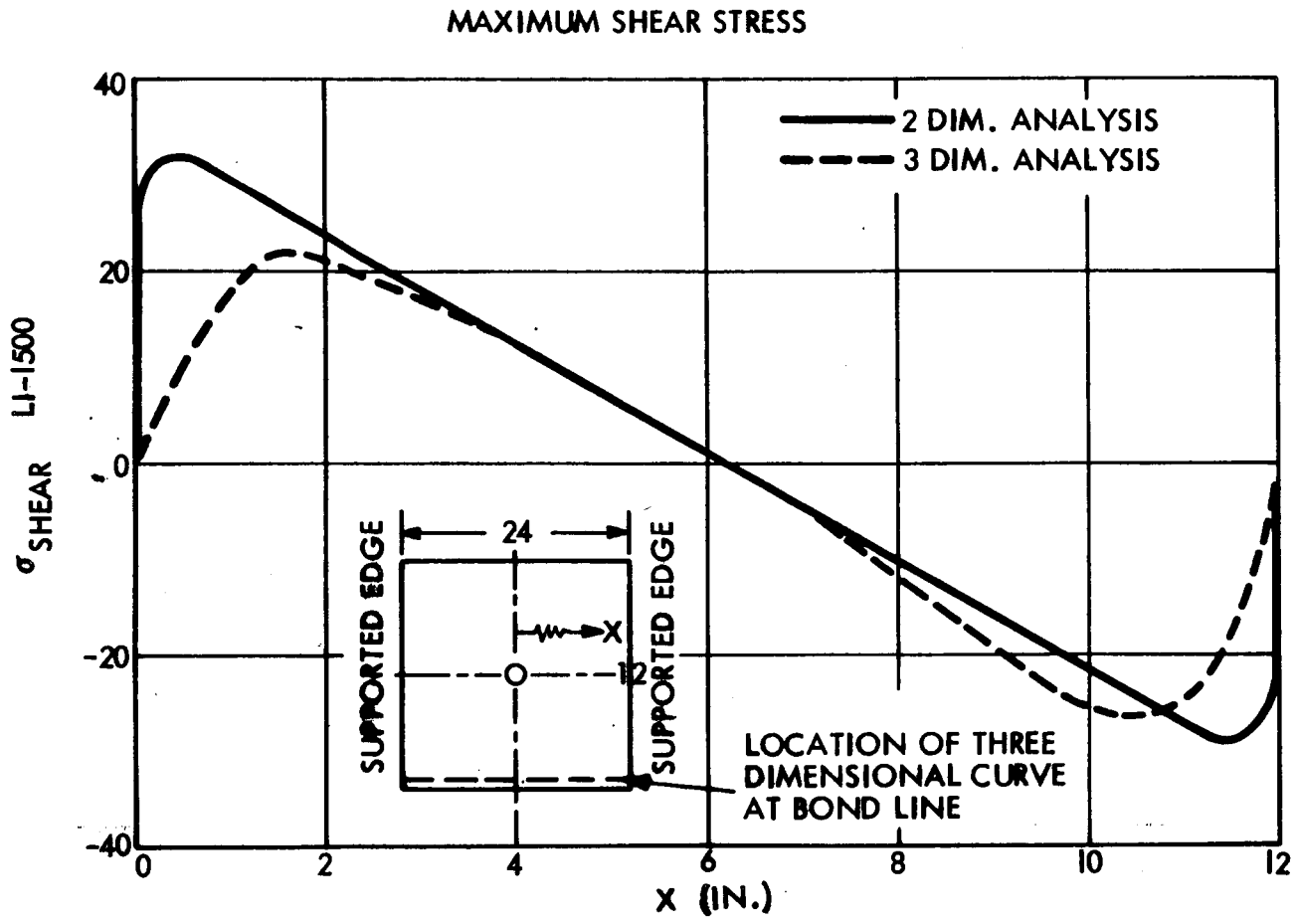


Fig. 2.2.3.1-4

D05176
rdb

2.2.3.2 Parametric Studies. The results of the studies reported in this subsection are broken down into three basic categories:

- Mechanical property variations
- Design details variations
- Environmental variations

Mechanical Property Variations. Of primary concern here is the dependence of coating, LI-1500, and bond stress levels as a function of respective moduli. In addition, the integral coating concept is considered and the effect of thermal cycling of a thin layer of LI-1500 near the coating is investigated.

Coating Modulus Variations. Variations of coating modulus are primarily reflected in coating stress levels. The results of this study are summarized in Fig. 2.2.3.2-1 for a beryllium subpanel, using an isotropic plane stress WILSON analysis. From these curves it is apparent that the "driver" is principally the thermal loading, although the direction of the applied pressure is important. In effect, the temperature rise induces a tensile field in the coating while bending effects due to the pressure field either add or subtract from the thermal effect. These general conclusions are also representative of other panel configurations.

Variation of LI-1500 Modulus. The effect of varying Young's modulus for an assumed isotropic L1-1500 material is summarized in Figs. 2.2.3.2-2 through 2.2.3.2-5. These studies were carried out early in the program before anisotropic data on L1-1500 were available. Some comparisons of isotropic versus anisotropic analysis are presented in subsection 2.2.3.1. The curves show increasing LI-1500 stress with increasing modulus, which is consistent with the substrate strain being the driving variable. On the other hand, the RTV-560 peel stress appears insensitive to LI-1500 modulus. As might be expected, coating stress decreases as the LI-1500 and the coating tend toward each other. Finally, the maximum principal tensile stress and the maximum shear in the RTV are seen to increase with increasing LI-1500 modulus. A beryllium subpanel with a 600$^{o}$F backface temperature and a 1.14 psi burst pressure was chosen for this study.

# VARIATION OF COATING STRESSES WITH COATING MODULUS

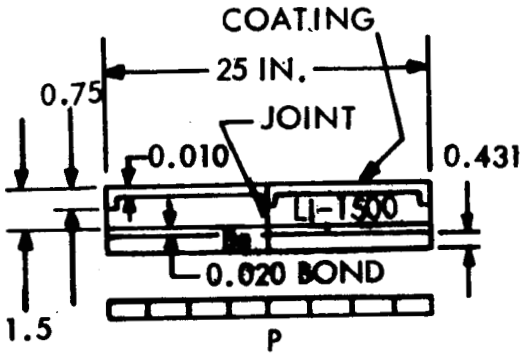


TEMPERATURE PROFILE "A"

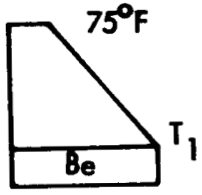


ISOTROPIC ANALYSIS

LI-1500

E = 20,000 psi
G = 8,000 psi

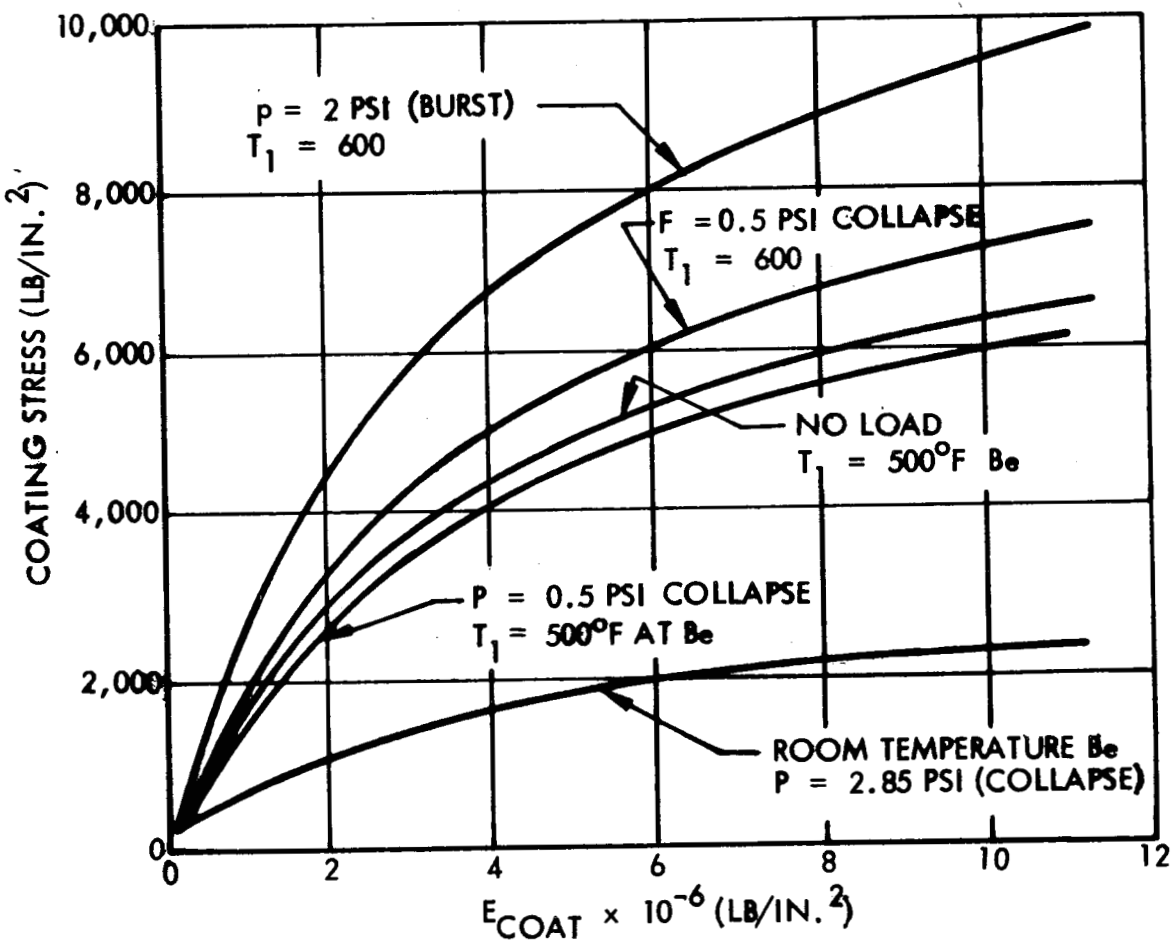


D04956 (1)
RDB

Fig. 2.2.3.2-1

# VARIATION OF LI-1500 STRESSES WITH LI-1500 ELASTIC MODULUS

BERYLLIUM FUSELAGE SUBPANEL (SHORT TRAJECTORY)

TEMPERATURE PROFILE

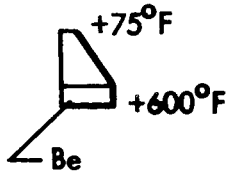


| | | |
|---|---|---|
| $t_{LI-1500}$ | = | 1.6 IN. |
| $t_{RTV-560}$ | = | 0.020 IN. |
| $t_{COATING}$ | = | 0.010 IN. |
| LOADING | p = | 1.14 PSI BURST |
| $E_{RTV-560}$ | = | 300 PSI |
| $E_{COATING}$ | = | $3.5 \times 10^6$ PSI |
| $G_{LI-1500}$ | = | 0.4E |

ISOTROPIC ANALYSIS

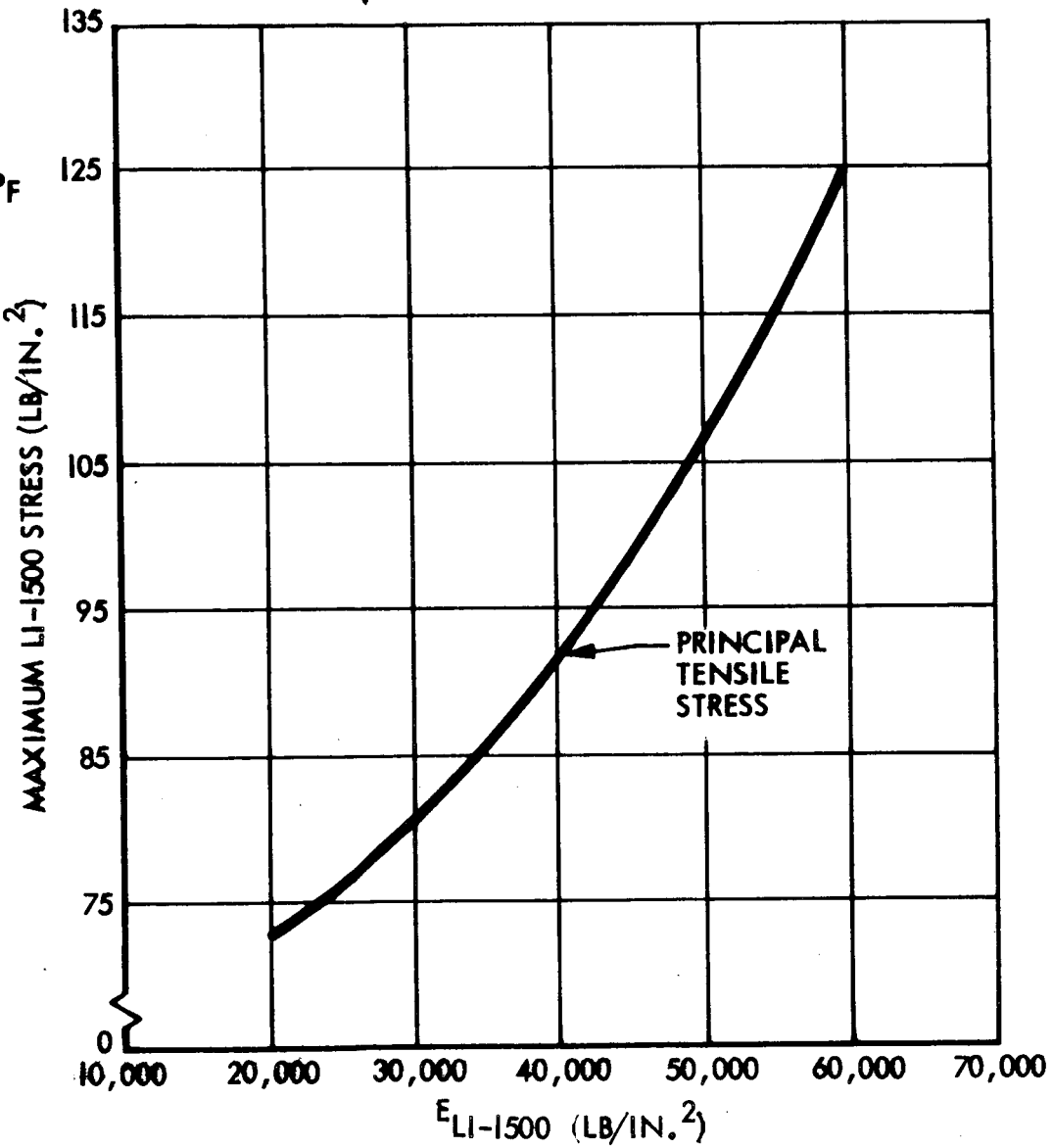


D04969(1)
RDB

Fig. 2.2.3.2-2

# VARIATION OF SHEAR AND PEEL STRESSES WITH LI-1500 ELASTIC MODULUS

BERYLLIUM FUSELAGE SUBPANEL (SHORT TRAJECTORY)

TEMPERATURE PROFILE

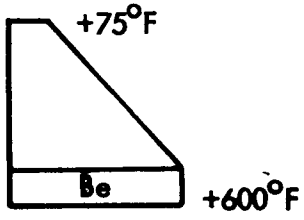


| | | |
|---|---|---|
| $t_{LI-1500}$ | = | 1.6 IN. |
| $t_{RTV-560}$ | = | 0.020 IN. |
| $t_{COATING}$ | = | 0.010 IN. |
| LOADING | p = | 1.14 PSI BURST |
| $E_{RTV-560}$ | = | 300 PSI |
| $E_{COATING}$ | = | $3.5 \times 10^6$ PSI |
| $G_{LI-1500}$ | = | 0.4E |

ISOTROPIC ANALYSIS

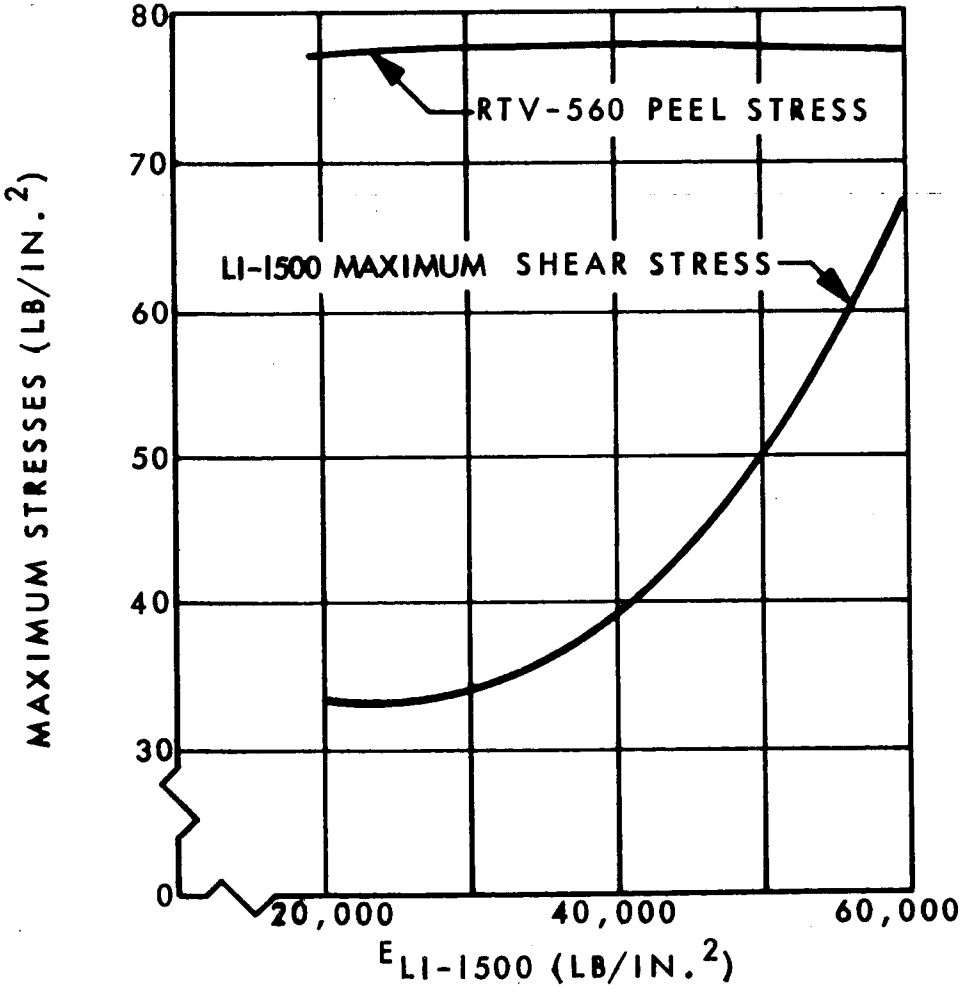


Fig. 2.2.3.2-3

D05009(1)

rdb

# VARIATION OF COATING STRESS WITH LI-1500 ELASTIC MODULUS

$t_{LI-1500}$ = 1.6 IN.

$t_{RTV-560}$ = 0.020 IN.

$t_{COATING}$ = 0.010 IN.

$E_{RTV-560}$ = [redacted]

$E_{COATING}$ = $3.5 \times 10^6$ PSI

$G_{LI-1500}$ = 0.4E

LOADING p = 1.14 PSI BURST

TEMPERATURE PROFILE

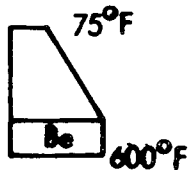


ISOTROPIC ANALYSIS

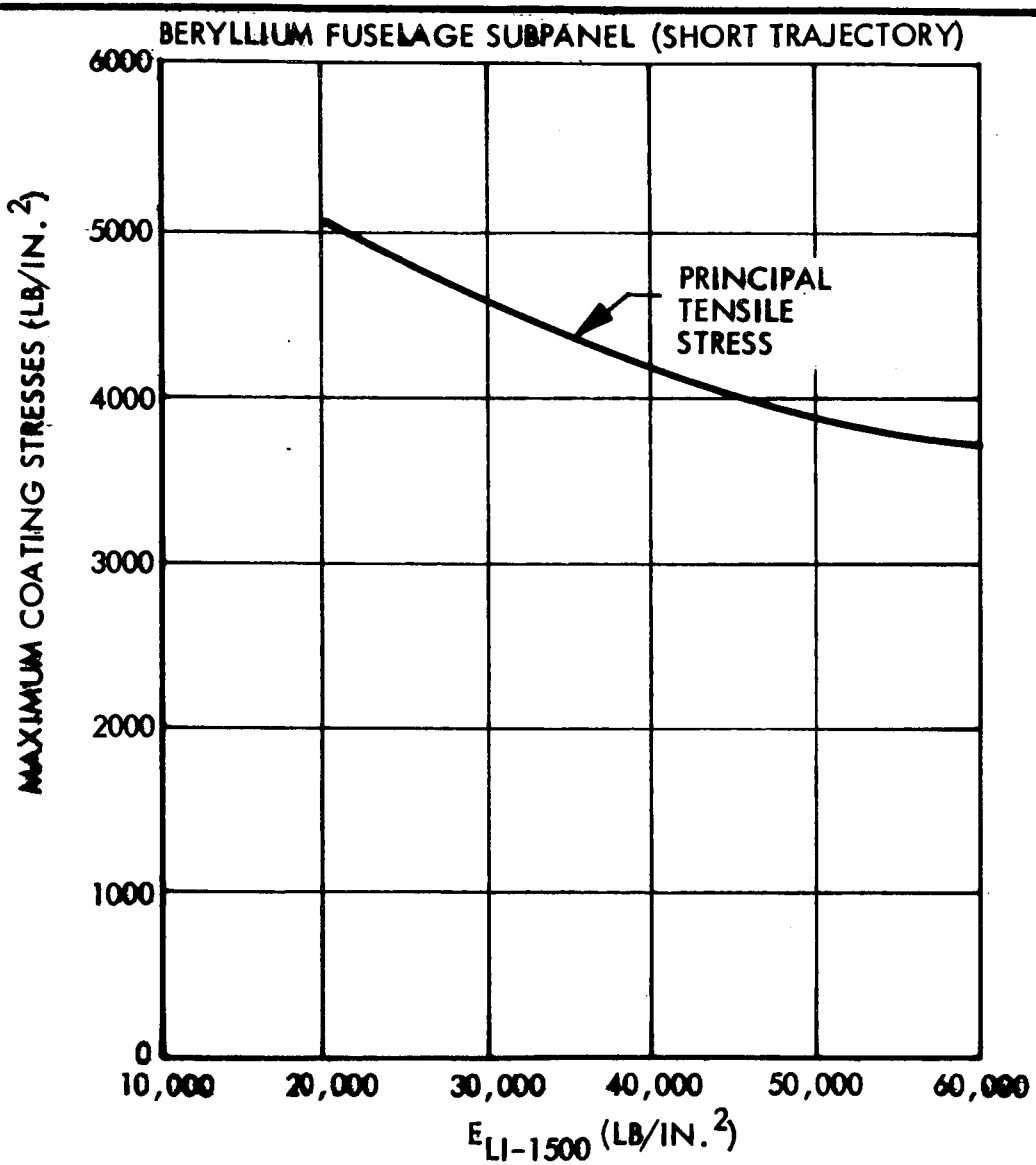


Fig. 2.2.3.2-4

D04970(1)
RDB

# VARIATION OF BOND STRESSES WITH LI-1500 ELASTIC MODULUS

LOCKHEED

BERYLLIUM FUSELAGE SUBPANEL (SHORT TRAJECTORY)

TEMPERATURE PROFILE

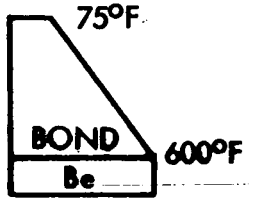


$t_{LI-1500}$ = 1.6 IN.

$t_{RTV-560}$ = 0.020 IN.

$t_{COATING}$ = 0.010 IN.

$G_{LI-1500}$ = 0.4 E

$E_{RTV-560}$ = 300 PSI

$E_{COATING}$ = $3.5 \times 10^6$ PSI

LOADING: p = 1.14 PSI BURST

ISOTROPIC ANALYSIS

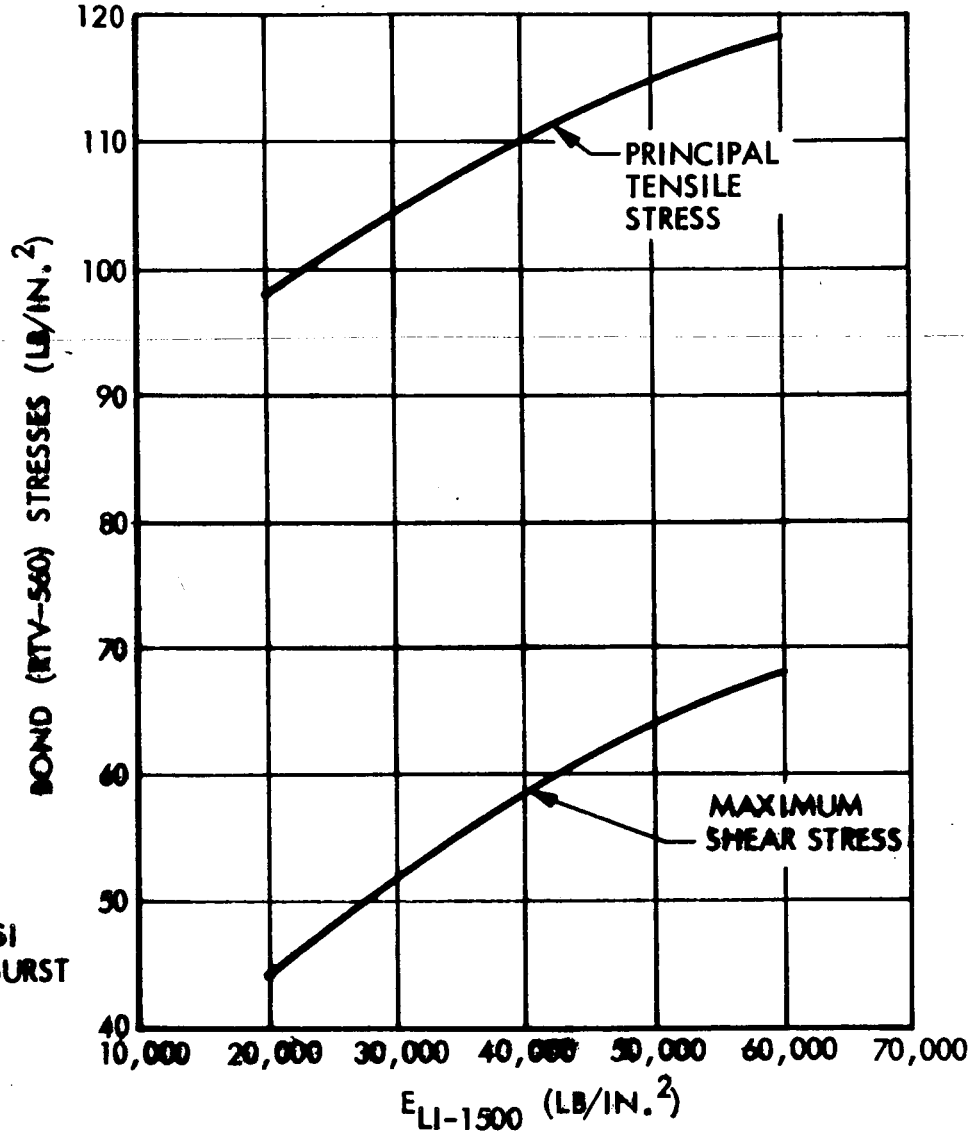


D04949(1)
RDB

Fig. 2.2.3.2-5

Effects of Bond Moduli Variation. The sensitivity of RSI stresses to variations of Young's modulus, $E_{RTV}$, and Poisson's ratio, $\mu_{RTV}$, are summarized in Tables 2.2.3.2-1 and 2.2.3.2-2. As would be expected, lower values of $E_{RTV}$ provide more effective strain isolation as seen in Table 2.2.3.2-1, indicating a factor of approximately 2 in LI-1500 stresses for the values investigated. These changes amount to about 20 percent when Poisson's ratio is varied over the range chosen. It is expected that $\mu_{RTV}$ for RTV-560 is closer to 0.5, which is the theoretical value for an incompressible material. These tables have been constructed with data corresponding to a critical loading case of an aluminum primary structure panel; similar results would be expected under other conditions.

Integral Coating Concept. Since LI-1500 can be locally densified in a surface layer, a study was performed to ascertain what effects this might have on an RSI system design. In Fig. 2.2.3.2-6 are shown typical bounding profiles of density variation; Figs. 2.2.3.2-7 and 2.2.3.2-8 present strong direction elastic modulus and strength of LI-1500 as functions of density. Comparative results for a beryllium subpanel (Table 2.2.3.2-3) show that there is virtually no difference in stress levels for the thin or thick profile, except for the coating (densified layer) stress. It is noted that the integral coating or local densification concept results in lower coating stresses than a system with an add-on coating, in this case, chrome oxide. The large change here is due to the difference in elastic moduli. It can be tentatively concluded that a thin profile integral coating is best under the conditions presented here, offering a weight savings over the thick profile.

Effects of Thermal Cycling on LI-1500. As discussed in Section 4.2, thermal cycling of LI-1500 apparently leads to a higher modulus in LI-1500. The effect of these changes in a thin layer under the coating was investigated for an aluminum fuselage panel and compared with results for virgin LI-1500. These are summarized in Table 2.2.3.2-4, where it is noted that there is little change in stress level and that the cycled LI-1500 experiences little or no stress. From this example, it may be tentatively concluded that the thermal cycling of a thin layer underneath the coating does not degrade the mechanical strength of the RSI system.

Table 2.2.3.2-1

LOCKHEED

# EFFECT OF BOND MODULUS OF ELASTICITY ON STRESS INTENSITY

ALUMINUM PANEL AT AREA 2 – 1.5 PSI BURST,
6,000 PPI TENSION, ALUMINUM PANEL AT 250°F

| STRESS (PSI) | $E_{RTV}$ = 300 PSI | $E_{RTV}$ = 100 PSI |
|---|---|---|
| LI-1500 | | |
| MAXIMUM | 48.9 | 25.0 |
| MINIMUM | - 8.7 | - 4.8 |
| SHEAR | 15.8 | 7.6 |
| LONGITUDINAL | 48.9 | 25.0 |
| NORMAL | 5.6 | 2.8 |
| RTV-560 | | |
| MAXIMUM | 16.9 | 7.6 |
| MINIMUM | -14.6 | - 7.3 |
| SHEAR | 14.8 | 7.3 |
| LONGITUDINAL | - 2.2 | - 2.6 |
| NORMAL | 5.5 | 1.8 |
| COATING | | |
| MAXIMUM | 20.3 | 23.5 |
| MINIMUM | - 1.0 | - 1.7 |



DO5022 (1)
RDB

# EFFECT OF POISSON'S RATIO OF BOND ON TPS STRESS INTENSITY

ALUMINUM PANEL, FUSELAGE AREA NO. 2

| STRESS (PSI) | $\mu_{RTV} = 0.3$ | $\mu_{RTV} = 0.5$ |
|---|---|---|
| **LI-1500** | | |
| MAXIMUM | 58.1 | 48.9 |
| MINIMUM | -10.5 | -8.7 |
| SHEAR | 18.2 | 15.8 |
| LONGITUDINAL | 58.1 | 48.9 |
| NORMAL | 6.1 | 5.6 |
| **RTV-560** | | |
| MAXIMUM | 19.0 | 16.9 |
| MINIMUM | -17.2 | -14.6 |
| SHEAR | 17.4 | 14.8 |
| LONGITUDINAL | -5.4 | -2.2 |
| NORMAL | 5.4 | 5.5 |
| **COATING** | | |
| MAXIMUM | 18.8 | 20.3 |
| MINIMUM | — | -1.0 |

| | |
|---|---|
| PRESSURE | = 1.5 PSI BURST |
| Al TEMPERATURE | = 250°F |
| COATING TEMPERATURE | = 100°F |
| Al THICKNESS | = 0.711 IN. |
| RTV THICKNESS | = 0.090 IN. |
| LI-1500 THICKNESS | = 3.4 IN. |
| COATING THICKNESS | = 0.010 IN. |
| TILE LENGTH | = 4.0 IN. |
| TENSILE LINE LOAD | = 6000 PPI |

D04991 (1)
RDB

# LI-1500 INTEGRAL COATING DENSITY PROFILES

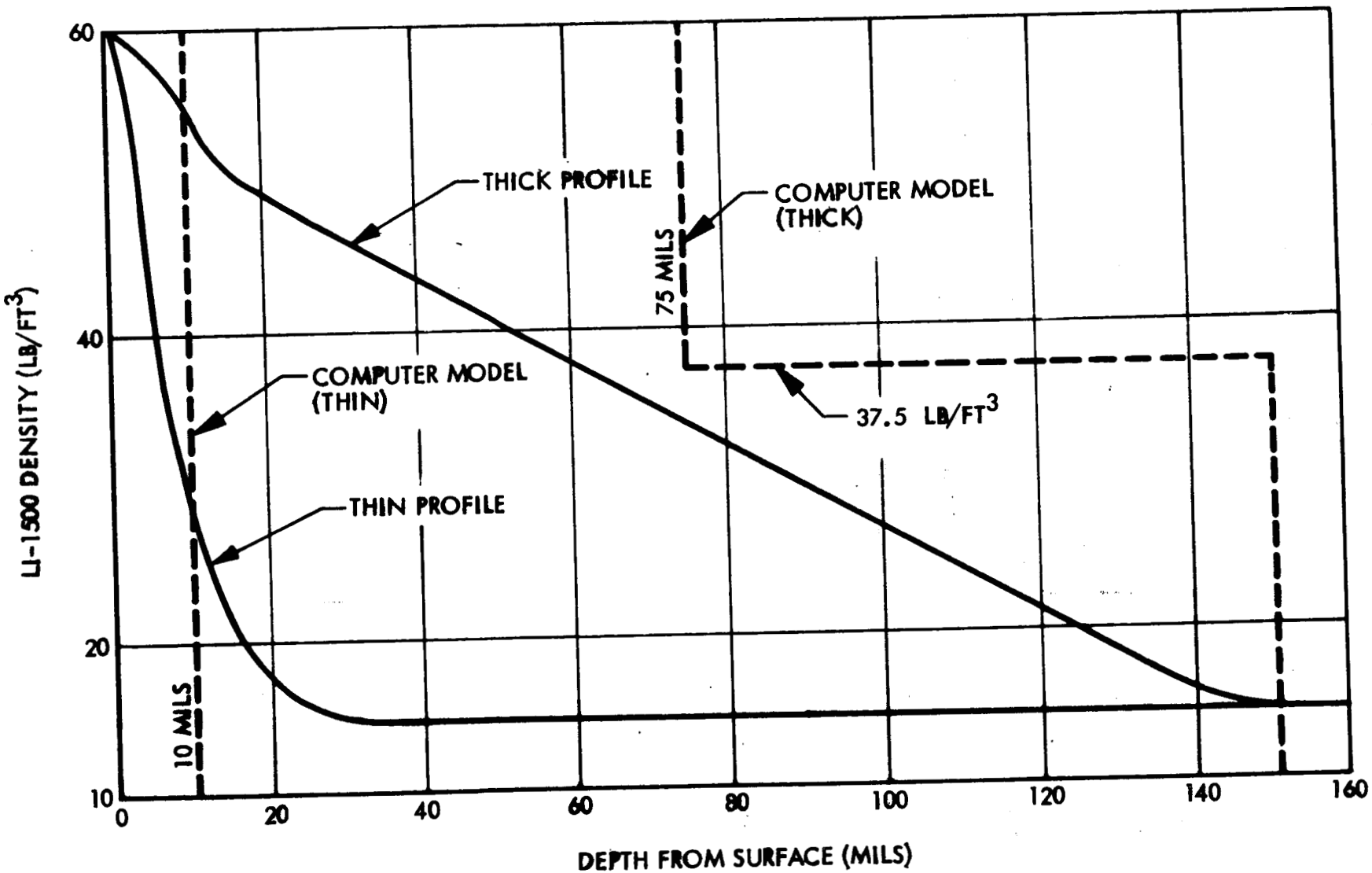


D04984(1)

rdb

Fig. 2.2.3.2-6

# LI-1500 STRONG DIRECTION
# ELASTIC MODULUS VS SPECIMEN DENSITY

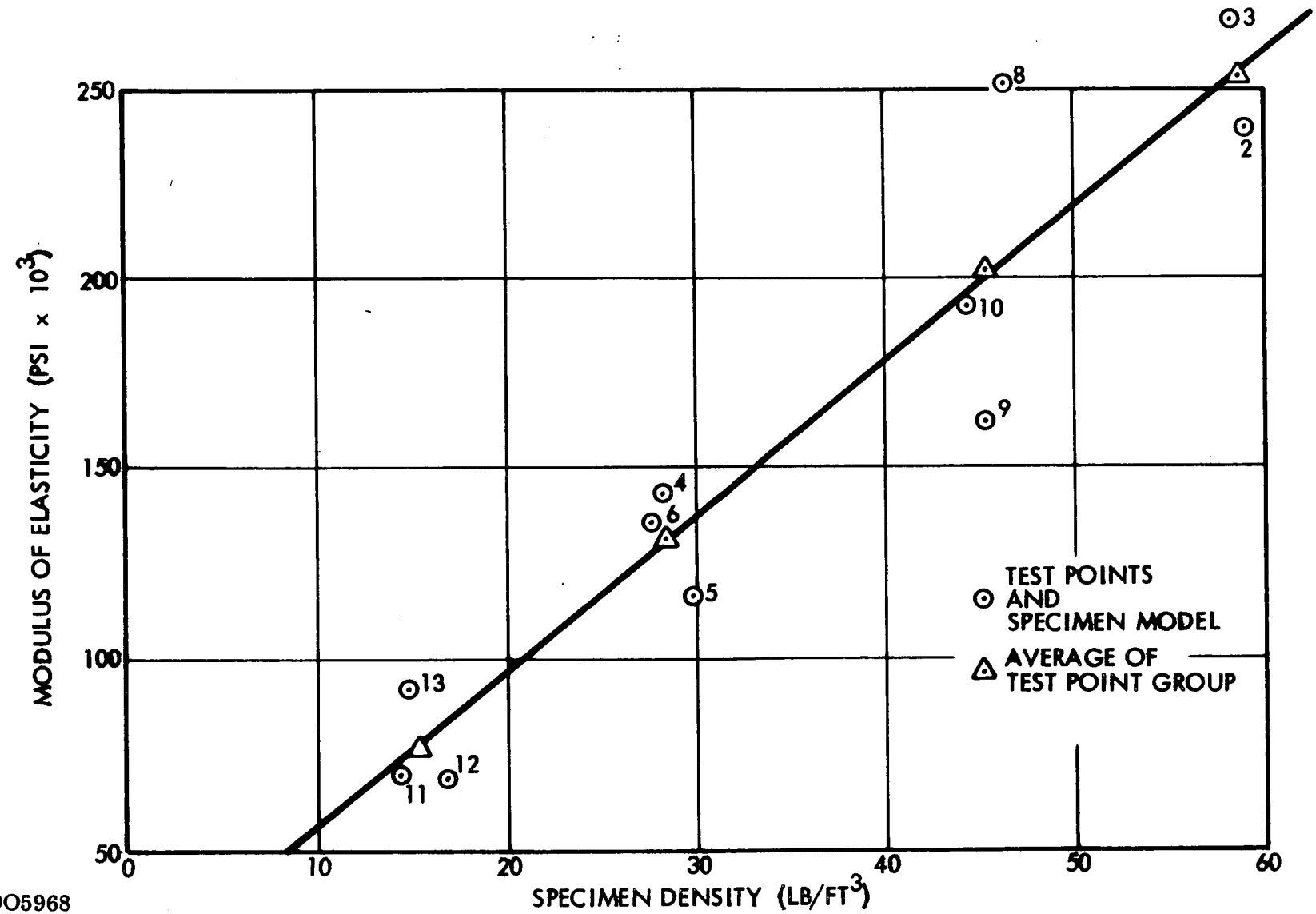


DO5968

Fig. 2.2.3.2-7

# LI-1500 DENSITY - STRENGTH CURVE (TEST RESULTS) STRONG DIRECTION

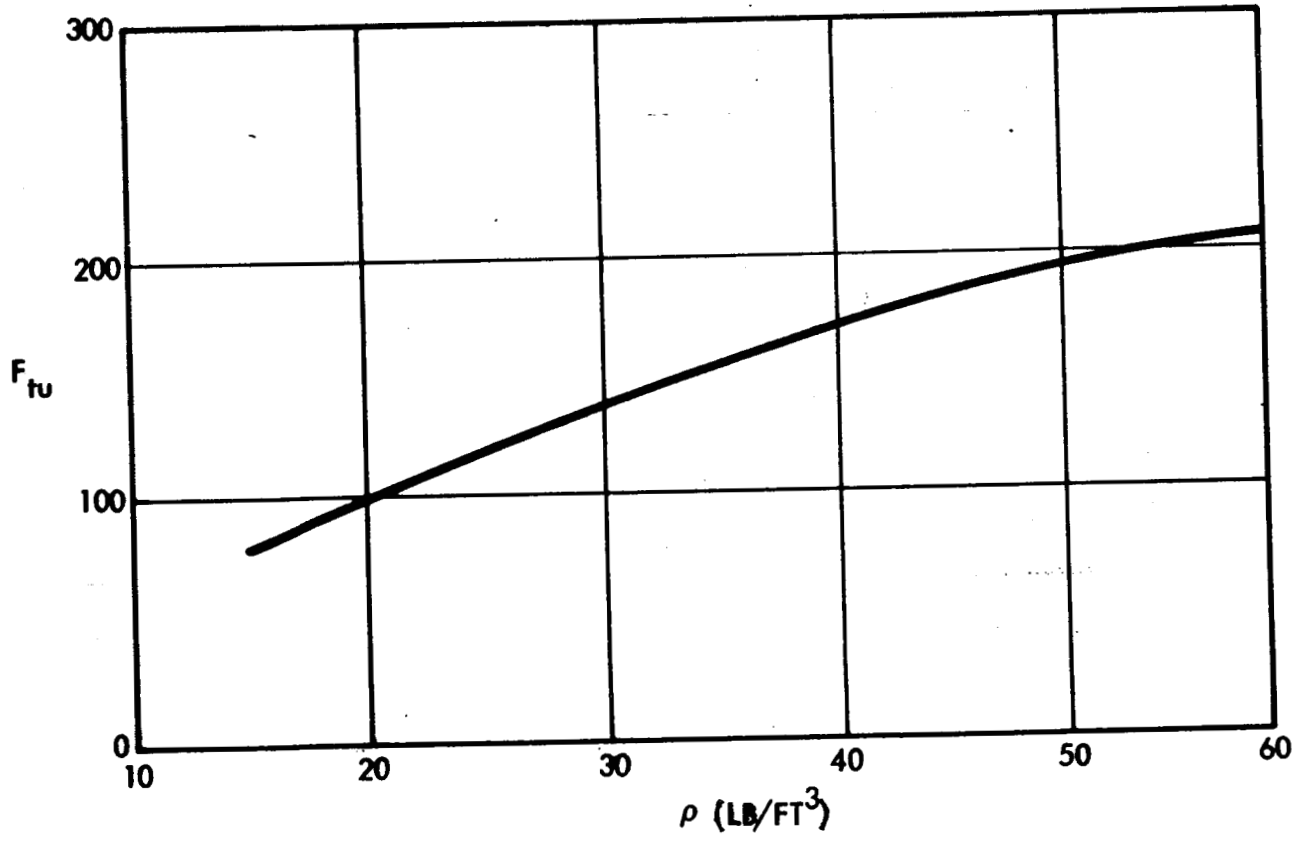


DO5967

Fig. 2.2.3.2-8

Table 2.2.3.2-3

# STRUCTURAL COMPARISON OF COATING CONCEPTS

| | STRESS (PSI) | ADD-ON COATING | INTEGRAL COATING THIN PROFILE | INTEGRAL COATING THICK PROFILE |
|---|---|---|---|---|
| LI-1500 | MAXIMUM | 13.4 | 13.6 | 13.6 |
| | MINIMUM | - 120.4 | -109.1 | -110.2 |
| | SHEAR | 51.5 | - 49.2 | - 49.2 |
| | LONGITUDINAL | - 68.9 | - 69.4 | - 69.5 |
| | PEEL | 11.1 | 10.3 | 10.8 |
| RTV-560 | MAXIMUM | 48.0 | 48.6 | 48.2 |
| | MINIMUM | - 145.5 | -114.6 | -116.0 |
| | SHEAR | 50.8 | - 47.6 | - 47.6 |
| | LONGITUDINAL | 32.5 | 32.3 | 32.4 |
| | PEEL | 11.5 | 10.4 | 10.9 |
| COATING | THICKNESS | t = 0.010 | t = 0.010 | t = 0.150 |
| | MAXIMUM | 11.3 | 14.4 | 6.1 |
| | MINIMUM | -1761.2 | -230.0 | -161.4 |

ALL STRESSES IN LB/IN.$^2$

PRESSURE = 6.75 PSI COLLAPSE

$t_{BERYLLIUM}$ = 0.4312 IN.

$t_{RTV-560}$ = 0.020 IN.

$t_{LI-1500}$ = 2.3 IN.

$t_{COATING}$ = AS SHOWN

LI-1500 TILE LENGTH = 12 IN.

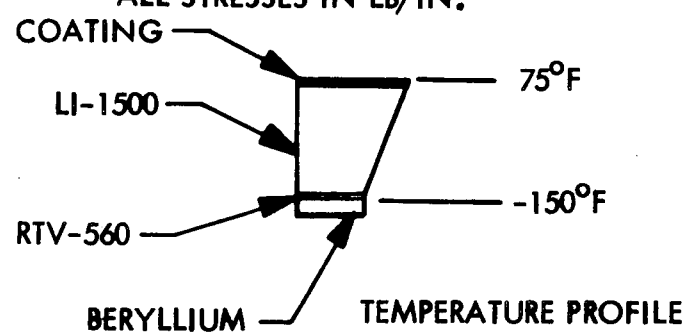


D04979 (1)
RDB

Table 2.2.3.2-4

# AL TEST PANEL NO. 2 ORBITER FUSELAGE AREA 2

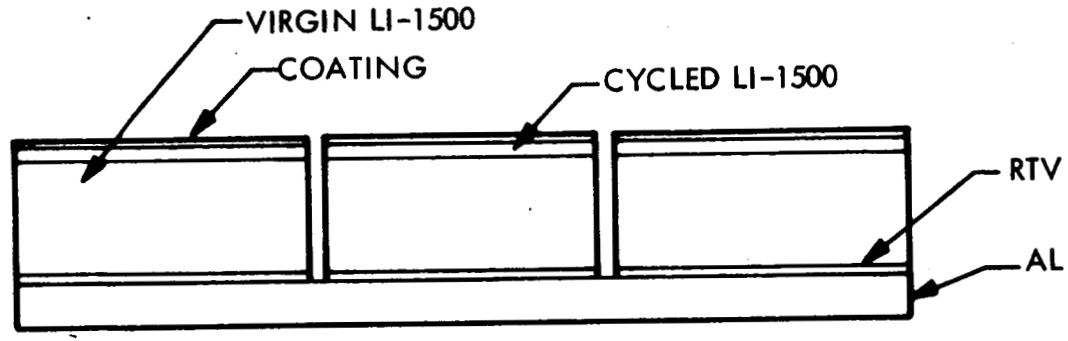


| | COATING | CYCLED LI-1500 | VIRGIN LI-1500 | RTV BOND | WITHOUT CYCLED LI-1500 | | |
|---|---|---|---|---|---|---|---|
| | | | | | COAT | LT-1500 | RTV |
| MAX | 26 | 1 | 50 | 17 | 20 | 49 | 17 |
| MIN | -2 | 0 | -9 | -15 | -1 | -9 | -15 |
| SHEAR | | 0 | 16 | 15 | | 16 | 15 |
| R-Z PRINCP | | 1 | 25 | 17 | | | |
| LONG | | 1 | 50 | -6 | | 49 | -2 |
| PEEL | | 0 | 6 | 6 | | 6 | 6 |

$T_{COAT} = 0.01$

$T_{CY.\ LI-1500} = 0.2$

4-IN. TILES

$E_{COAT} = 3.5 \times 10^6$

$E_{CY.\ LI-1500} = 90{,}000$

| LOADING CONDITION | | 1.5 PSI BURST 6000 LB/IN. TENS |
|---|---|---|
| TEMP | SURFACE | 100°F |
| | ALUMINUM | 250°F |
| THICK | COATING | 0.010 |
| | LI-1500 | 3.396 |
| | RTV-560 | 0.090 |
| | ALUMINUM | 0.711 |

Design Details Variations. The effects of geometric sizing of the coating, LI-1500, and the RTV bond on the stress levels in these RSI components are considered here as well as tile gap sizes, texturing of the coating, and discontinuities in the coating and in the bond line. The effect of a steel fastener insert in the LI-1500 is also considered as well as an all-around local densification of an LI-1500 tile.

Effects of Varying Coating Thickness. The results of this study are presented in Figs. 2.2.3.2-9 through 2.2.3.2-12 for an assumed isotropic LI-1500 material. Inspection of these curves indicate that coating thickness variation does not affect stress levels in the LI-1500 or the RTV-560 bond. However, coating stress decreases with coating thickness, indicating that, although the line load carried by the coating increases with increasing thickness, it does so at a lower rate than the thickness itself. Hence, a lower coating stress. Such results would seem to apply to panel configurations other than those investigated here.

Effects Due to LI-1500 Thickness. These isotropic analytical studies are summarized in Figs. 2.2.3.2-13 through 2.2.3.2-16, where it is seen that bond and LI-1500 stress levels are not affected by LI-1500 thickness. However, coating stresses decrease with LI-1500 thickness for the worst possible case shown here. Essentially, thermal expansion and burst pressure induce tensile loads in the coating. In addition, the thermal load causes the substrate to bend in such a direction so as to cause a compressive stress in the coating. This latter stress is dependent upon the distance of the coating from the location of the neutral axis of bending, which is in the substrate. A thicker layer of LI-1500 thus results in higher compressive bending stresses which have a net effect of subtracting from the dominant tensile load in the coating, due to substrate expansion.

Bond Thickness Variation. Isotropic WILSON analyses were carried out for a beryllium subpanel; the results are shown in Figs. 2.2.3.2-17 through 2.2.3.2-20. It is evident from these curves that bond thickness is a critical variable in RSI design. Effectively, a thicker bond offers more strain isolation from the deformations of the substrate than a thin bond.

# VARIATION OF LI-1500 STRESS WITH COATING THICKNESS

FUSELAGE PANEL PER LMSC-A989337 (SKW 100510)

TEMP PROFILE:

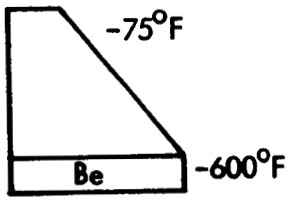


ISOTROPIC ANALYSIS

$T_{LI-1500}$ = 1.60 IN.

$T_{RTV-560}$ = 0.060 IN.

$E_{RTV-560}$ = 300 PSI

$E_{COATING}$ = $3.5 \times 10^6$ PSI

$E_{LI-1500}$ = 60,000 PSI

$G_{LI-1500}$ = 24,000 PSI

LOADING: SUBSONIC CRUISE, =1.14 PSI BURST

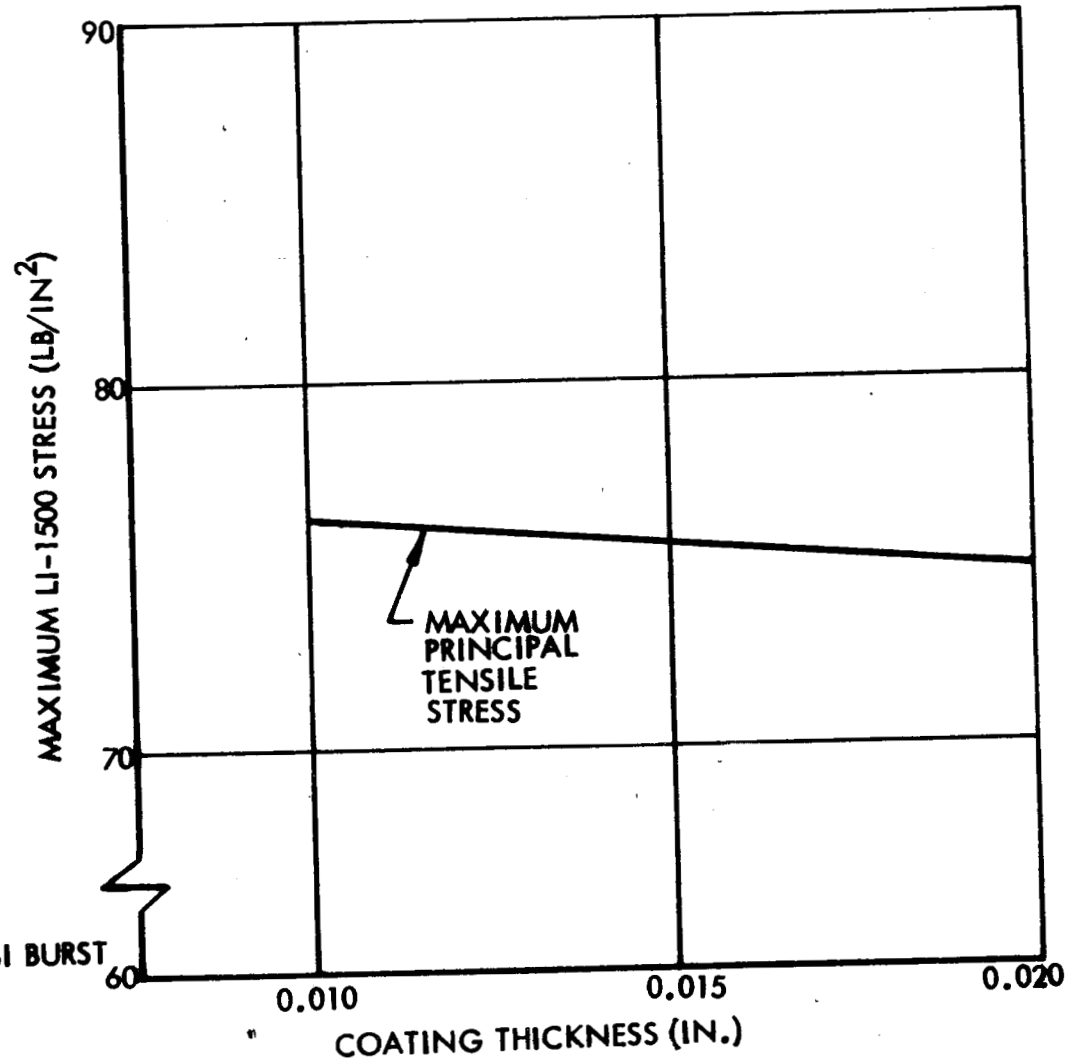


DO5994

Fig. 2.2.3.2-9

# VARIATION OF SHEAR AND PEEL STRESSES WITH COATING THICKNESS

BERYLLIUM FUSELAGE SUBPANEL (SHORT TRAJECTORY)

TEMPERATURE PROFILE

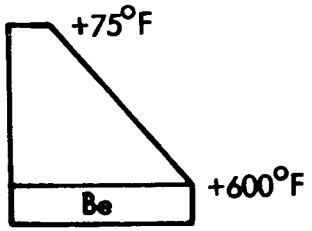


| | | |
|---|---|---|
| $t_{LI-1500}$ | = | 1.60 IN. |
| $E_{RTV-560}$ | = | 300 PSI |
| $G_{LI-1500}$ | = | 24,000 PSI |
| $t_{RTV-560}$ | = | 0.060 IN. |
| $E_{COATING}$ | = | $3.5 \times 10^6$ PSI |
| $E_{LI-1500}$ | = | 60,000 SPI |
| LOADING | p = | 1.14 PSI BURST |

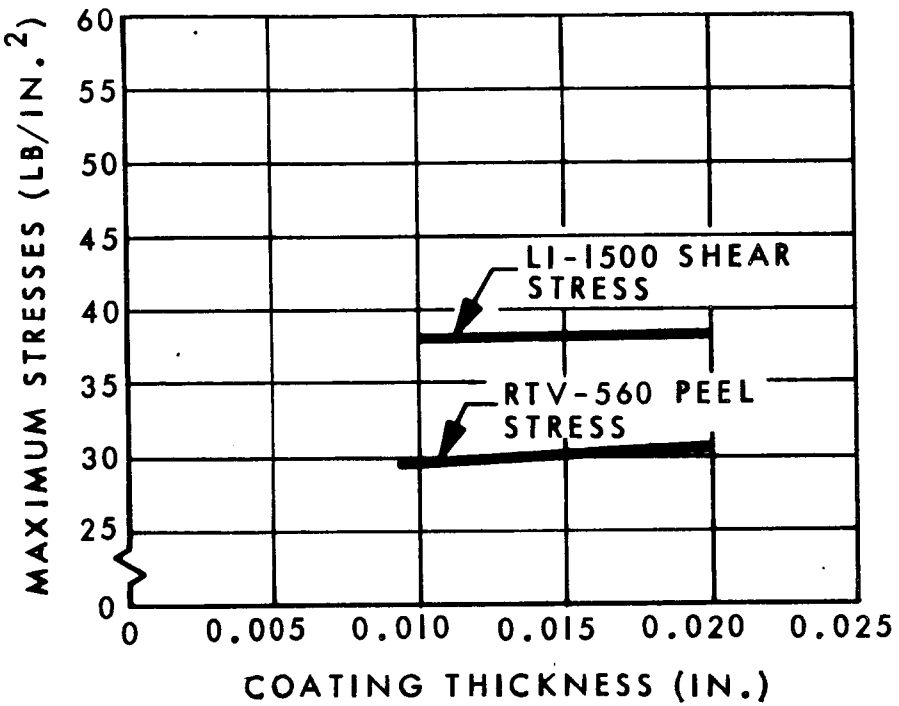


ISOTROPIC ANALYSIS

rdb

D05007(1)

Fig. 2.2.3.2-10

# VARIATION OF BOND STRESSES WITH COATING THICKNESS

BERYLLIUM FUSELAGE SUBPANEL
(SHORT TRAJECTORY)

$t_{LI-1500}$ = 1.60 IN. $E_{RTV-560}$ = 300 PSI,
$G_{LI-1500}$ = 24,000 PSI

$t_{RTV-560}$ = 0.060 IN.
$E_{COATING}$ = $3.5 \times 10^6$ PSI
$E_{LI-1500}$ = 60,000 PSI

LOADING p = 1.14 PSI BURST

TEMPERATURE PROFILE

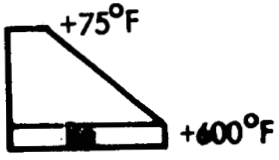


ISOTROPIC ANALYSIS

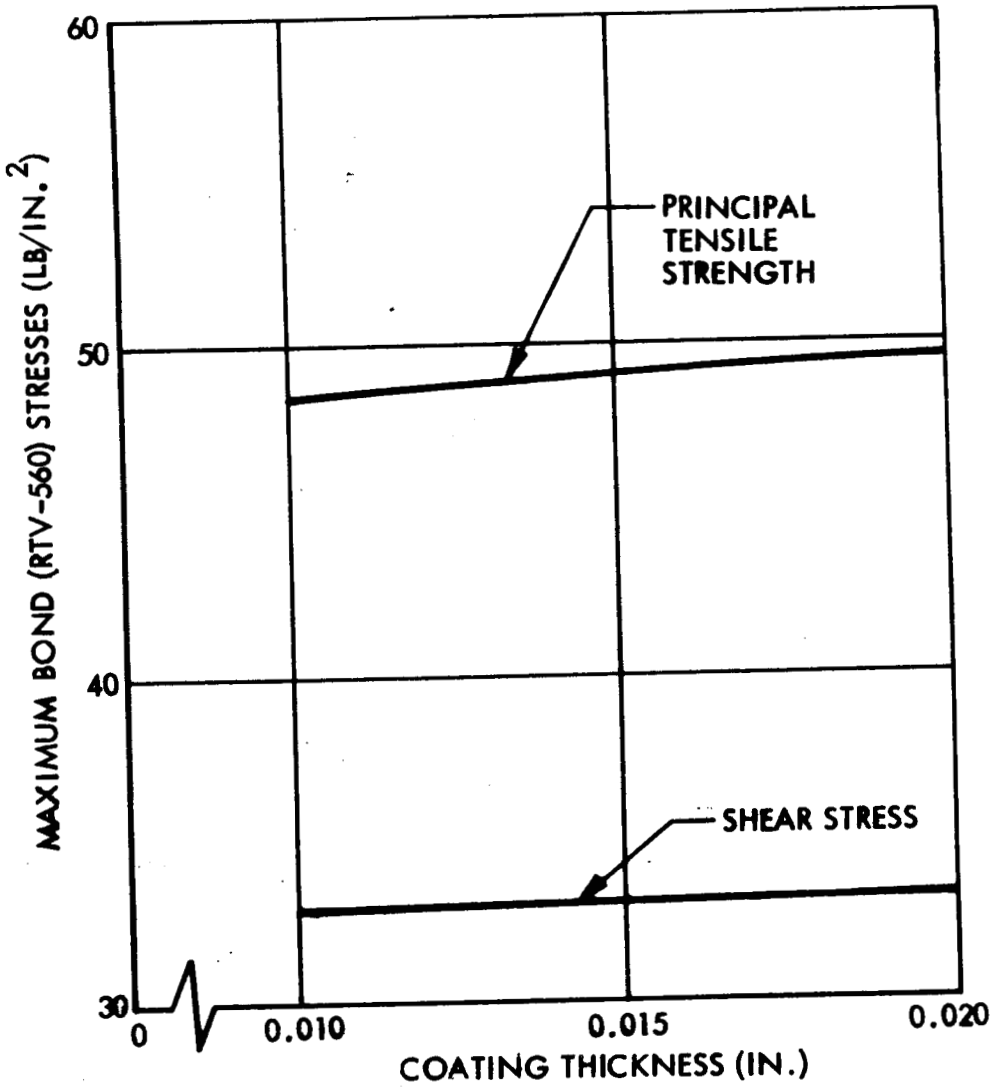


D04965(1)
RDB

Fig. 2.2.3.2-11

# VARIATION OF COATING STRESS WITH COATING THICKNESS

BERYLLIUM FUSELAGE SUBPANEL (SHORT TRAJECTORY)

$t_{LI-1500}$ = 1.60 IN.

$E_{RTV-560}$ = 300 PSI

$G_{LI-1500}$ = 24,000 PSI

$t_{RTV-560}$ = 0.060 IN.

$E_{COATING}$ = $3.5 \times 10^6$ PSI

$E_{LI-1500}$ = 60,000 PSI

LOADING p = 1.14 PSI BURST

TEMPERATURE PROFILE:

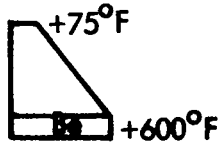


ISOTROPIC ANALYSIS

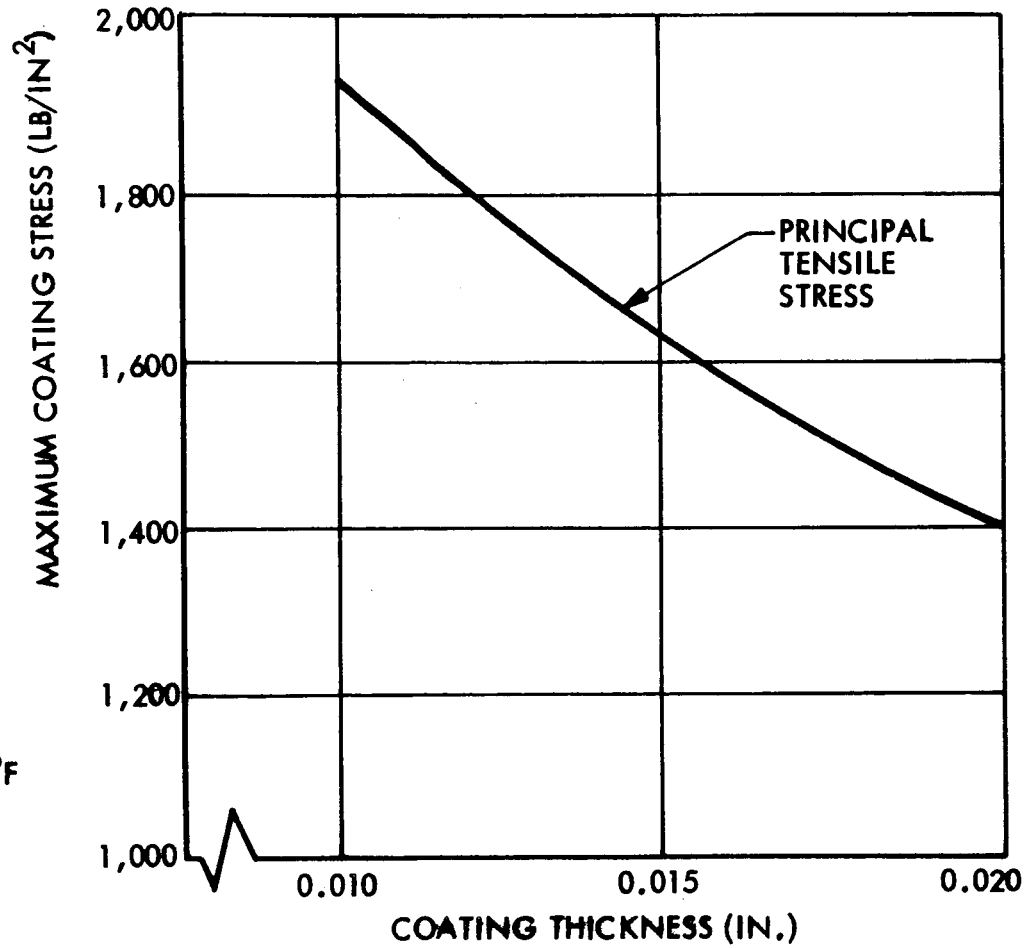


D04963 (1)
RDB

Fig. 2.2.3.2-12

# VARIATION OF SHEAR AND PEEL STRESSES WITH LI-1500 THICKNESS

BERYLLIUM FUSELAGE SUBPANEL (SHORT TRAJECTORY)

| | | |
|---|---|---|
| $t_{COATING}$ | = | 0.010 IN. |
| $t_{RTV-560}$ | = | 0.060 IN. |
| $E_{RTV-560}$ | = | 300 PSI |
| $G_{LI-1500}$ | = | 24,000 PSI |
| $E_{COATING}$ | = | $3.5 \times 10^6$ PSI |
| $E_{LI-1500}$ | = | 60,000 PSI |
| LOADING: | p = | 1.14 PSI BURST |

TEMPERATURE PROFILE

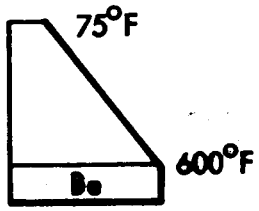


ISOTROPIC ANALYSIS

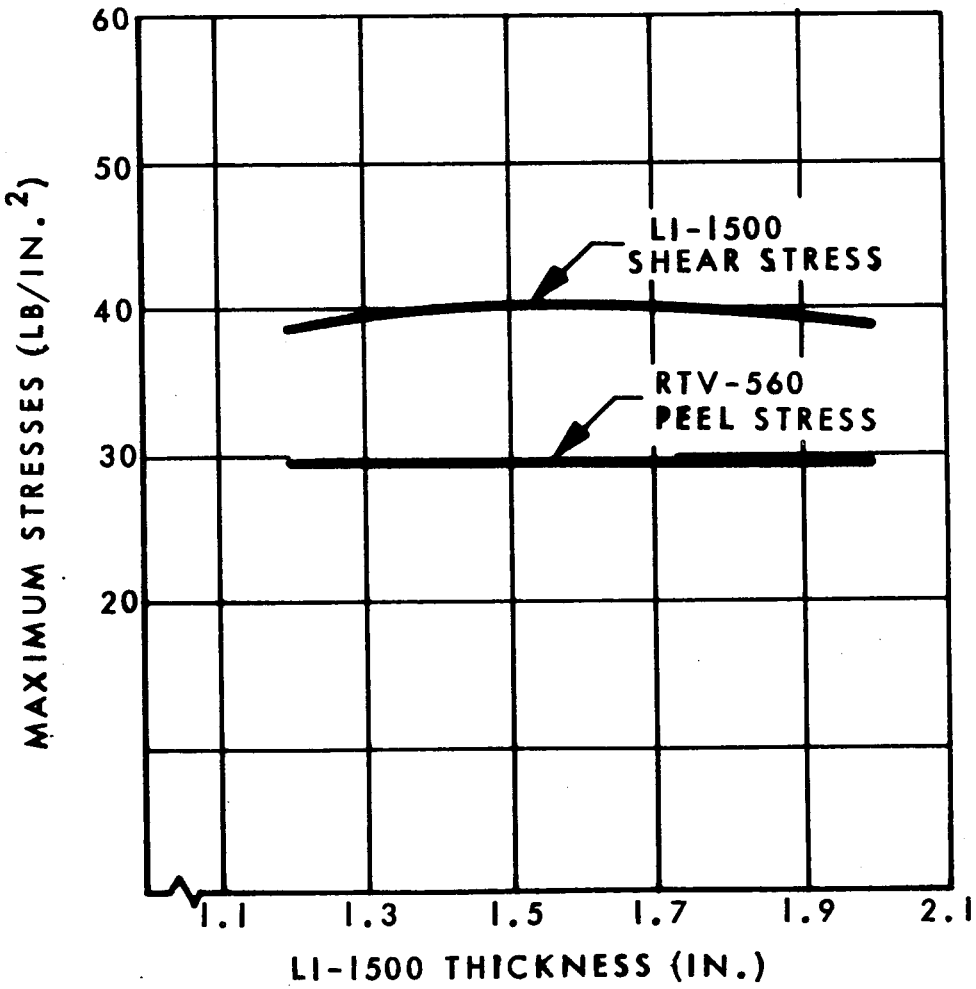


D05010(1)

Fig. 2.2.3.2-13

rdb

# VARIATION OF BOND STRESSES WITH LI-1500 THICKNESS

BERYLLIUM FUSELAGE SUBPANEL (SHORT TRAJECTORY)

$t_{COATING}$ = 0.010 IN.
$t_{RTV-560}$ = 0.060 IN.
$E_{RTV-560}$ = 300 PSI,
$G_{LI-1500}$ = 24,000 PSI
$E_{COATING}$ = $3.5 \times 10^6$ PSI
$E_{LI-1500}$ = 60,000 PSI
LOADING:
p = 1.14 PSI BURST

TEMPERATURE PROFILE

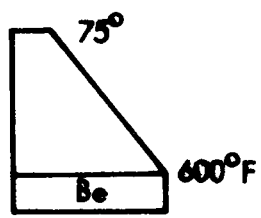


ISOTROPIC ANALYSIS

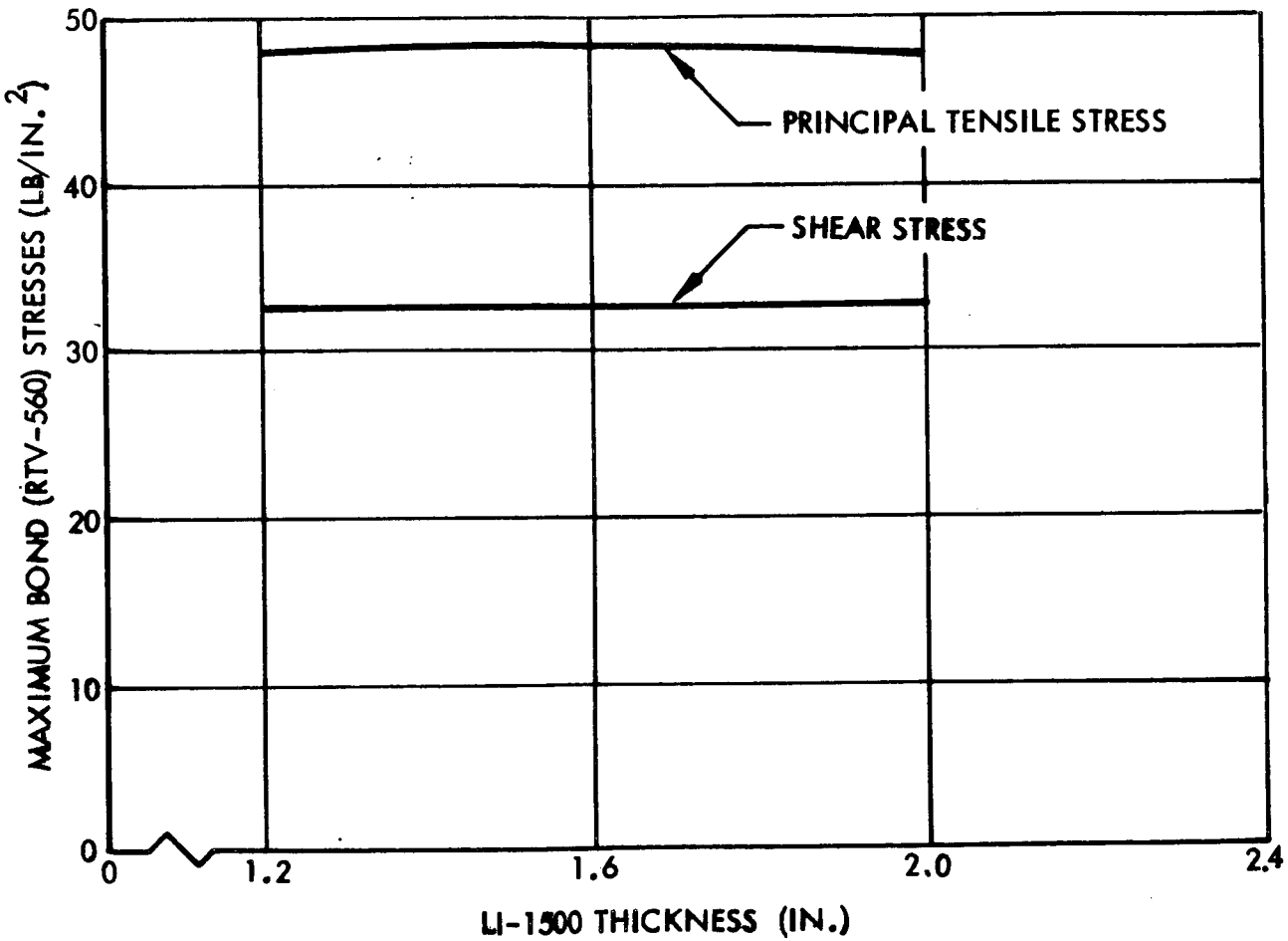


D04960 (1)
RDB

Fig. 2-2.3.2-14

# VARIATION OF LI-1500 STRESS WITH LI-1500 THICKNESS

FUSELAGE PANEL PER LMSC- (SKW 100510)

TEMP. PROFILE:

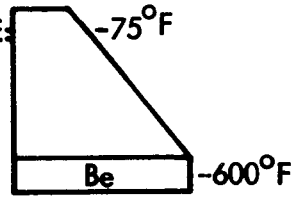


$T_{COATING}$ = 0.010 IN.

$T_{COATING}$ = 0.060 IN.

$E_{RTV-560}$ =

$E_{COATING}$ =

$E_{LI-1500}$ = 60,000 PSI

LOADING: SUBSONIC CRUISE

P - 1.14 PSI

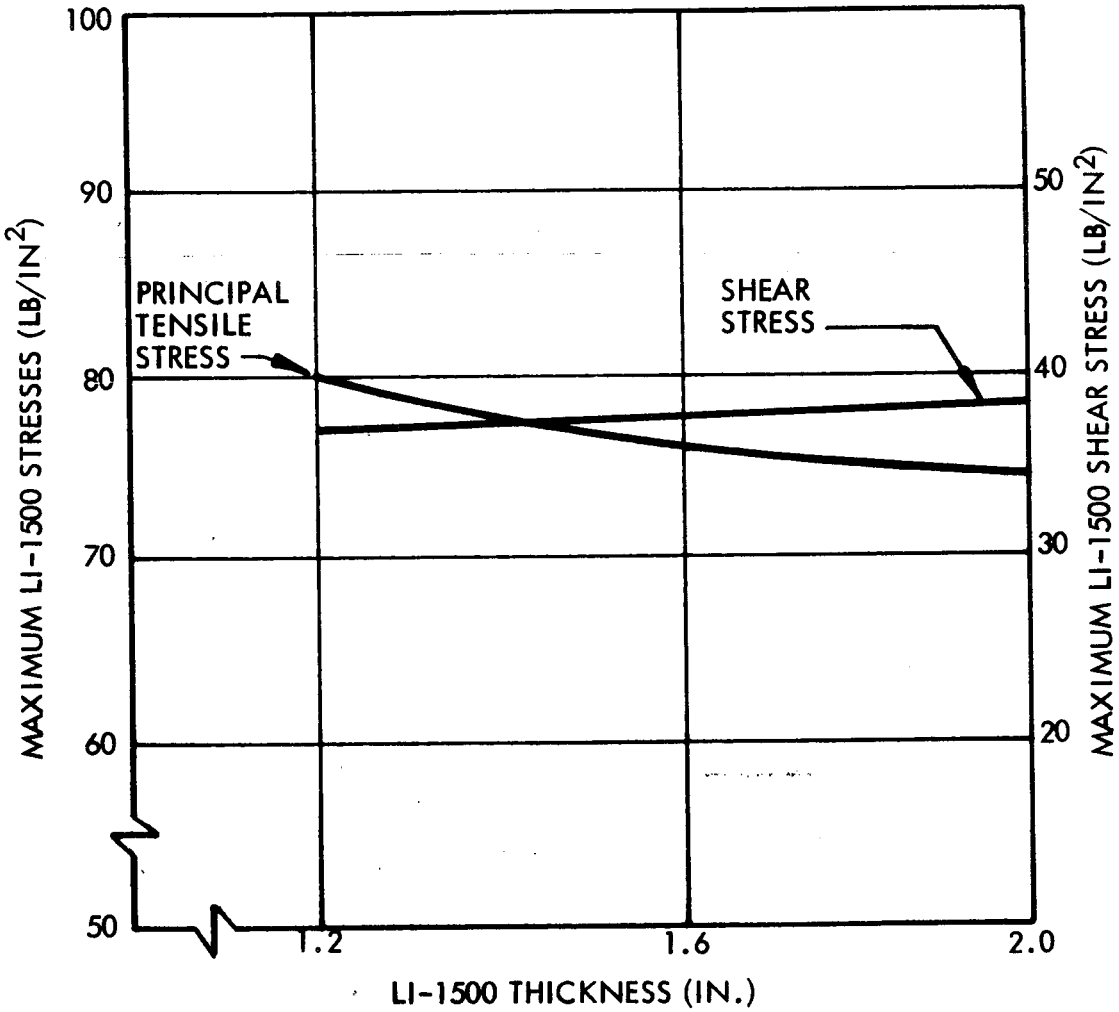


VARIATION OF LI-1500 STRESS WITH LI-1500 THICKNESS

DO5983

Fig. 2.2.3.2-15

# VARIATION OF COATING STRESSES WITH LI-1500 THICKNESS

TEMP PROFILE:

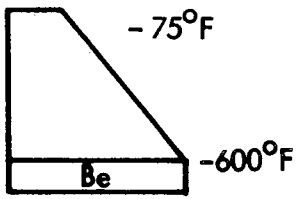


FUSELAGE PANEL PER LMSC-A989337

$T_{COATING}$ = 0.010 IN.

$T_{RTV-560}$ = 0.060 IN.

$E_{RTV-560}$ = 300 PSI

$E_{COATING}$ = $3.5 \times 10^6$ PSI

$E_{LI-1500}$ = 60,000 PSI

LOADING: SUBSONIC CRUISE
P-1.14 PSI BURST

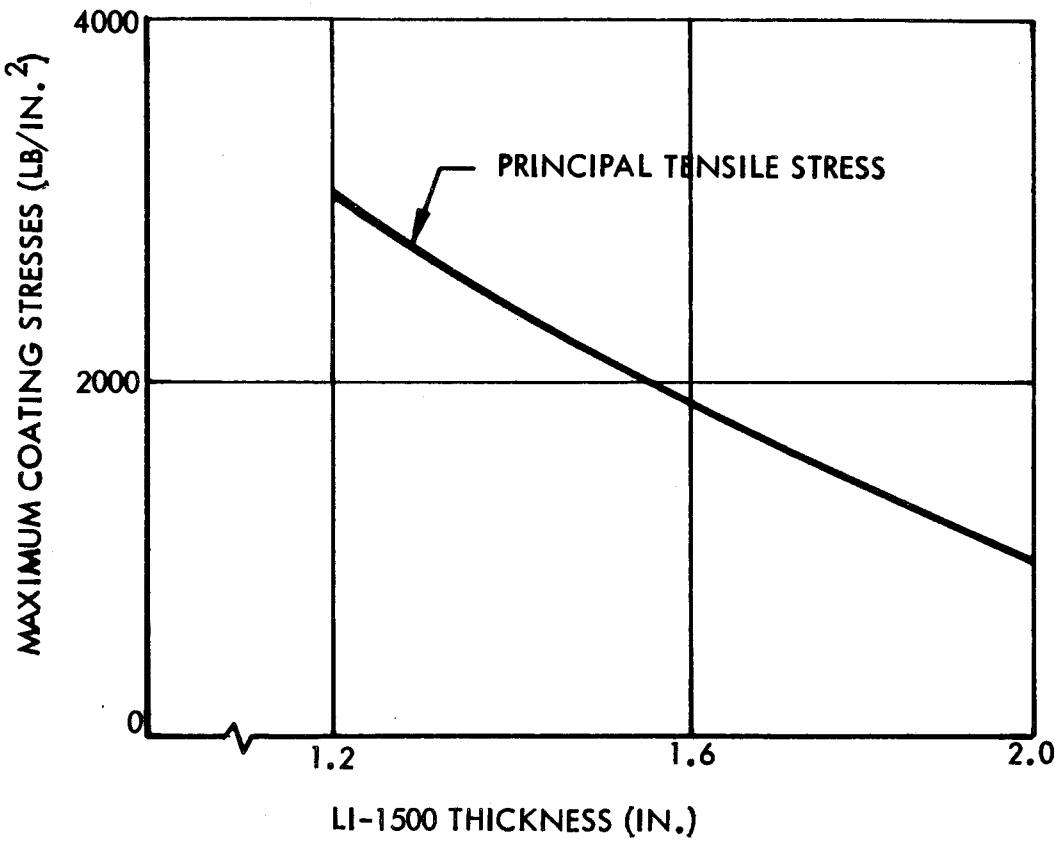


D05972

Fig. 2.2.3.2-16

# VARIATION OF COATING STRESSES WITH BOND THICKNESS

FUSELAGE PANEL PER LMSC-A989337 (SKW 100510)

TEMP. PROFILE:

$T_{COATING}$ = 0.010 IN.

$E_{COATING}$ = $3.5 \times 10^6$ PSI

LOADING: SUBSONIC CRUISE

P = 1.14 PSI BURST

$E_{RTV-560}$ = 300 PSI

$E_{LI-1500}$ = 60,000 PSI

$G_{LI-1500}$ = 24,000 PSI

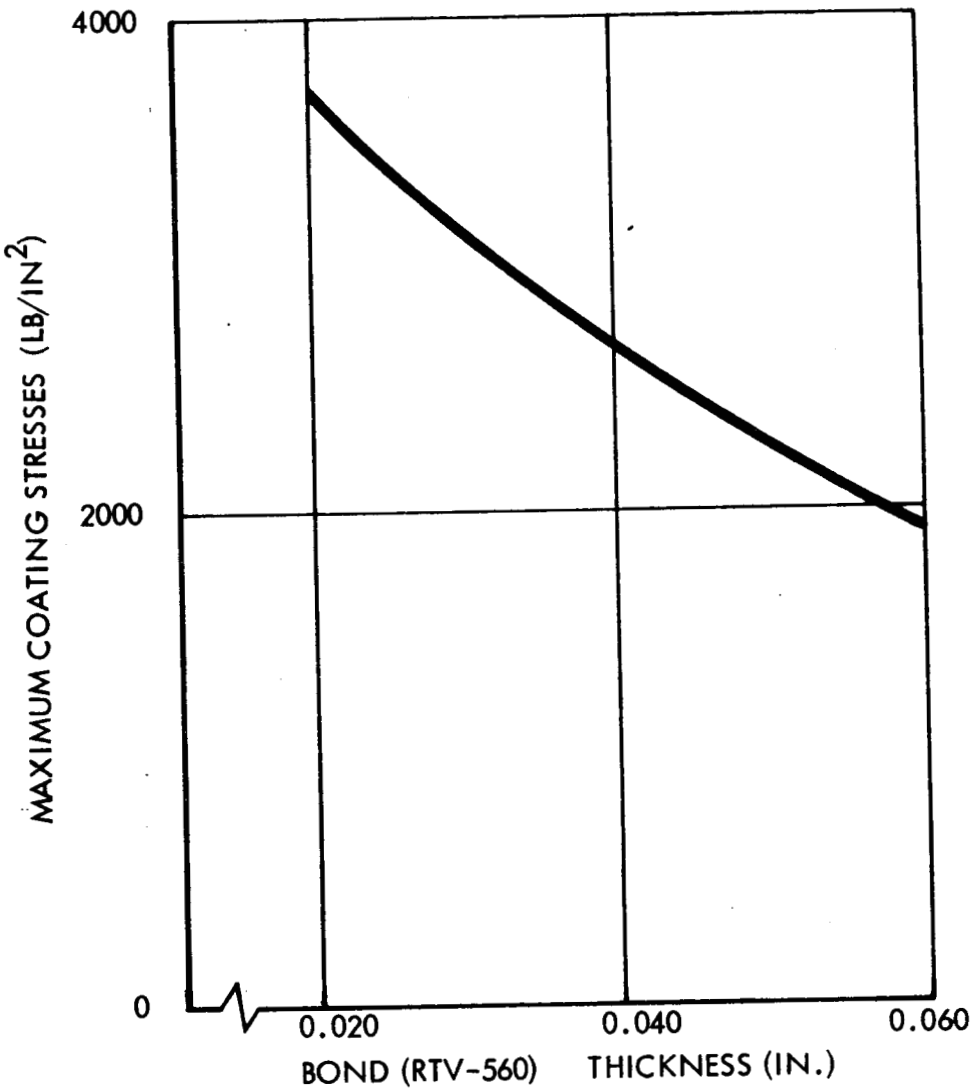


VARIATION OF COATING STRESSES WITH BOND THICKNESS

DO5993

Fig. 2.2.3.2-17

# VARIATION OF LI-1500 STRESSES WITH BOND THICKNESS

BERYLLIUM FUSELAGE SUBPANEL (SHORT TRAJECTORY)

TEMPERATURE PROFILE

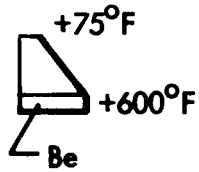


$t_{LI-1500}$ = 1.6 IN.

$t_{COATING}$ = 0.010 IN.

$E_{COATING}$ = $3.5 \times 10^6$ PSI

LOADING: p = 1.14 PSI BURST

$G_{LI-1500}$ = 24,000 PSI

$E_{RTV-560}$ = 300 PSI

$E_{LI-1500}$ = 60,000 PSI

ISOTROPIC ANALYSIS

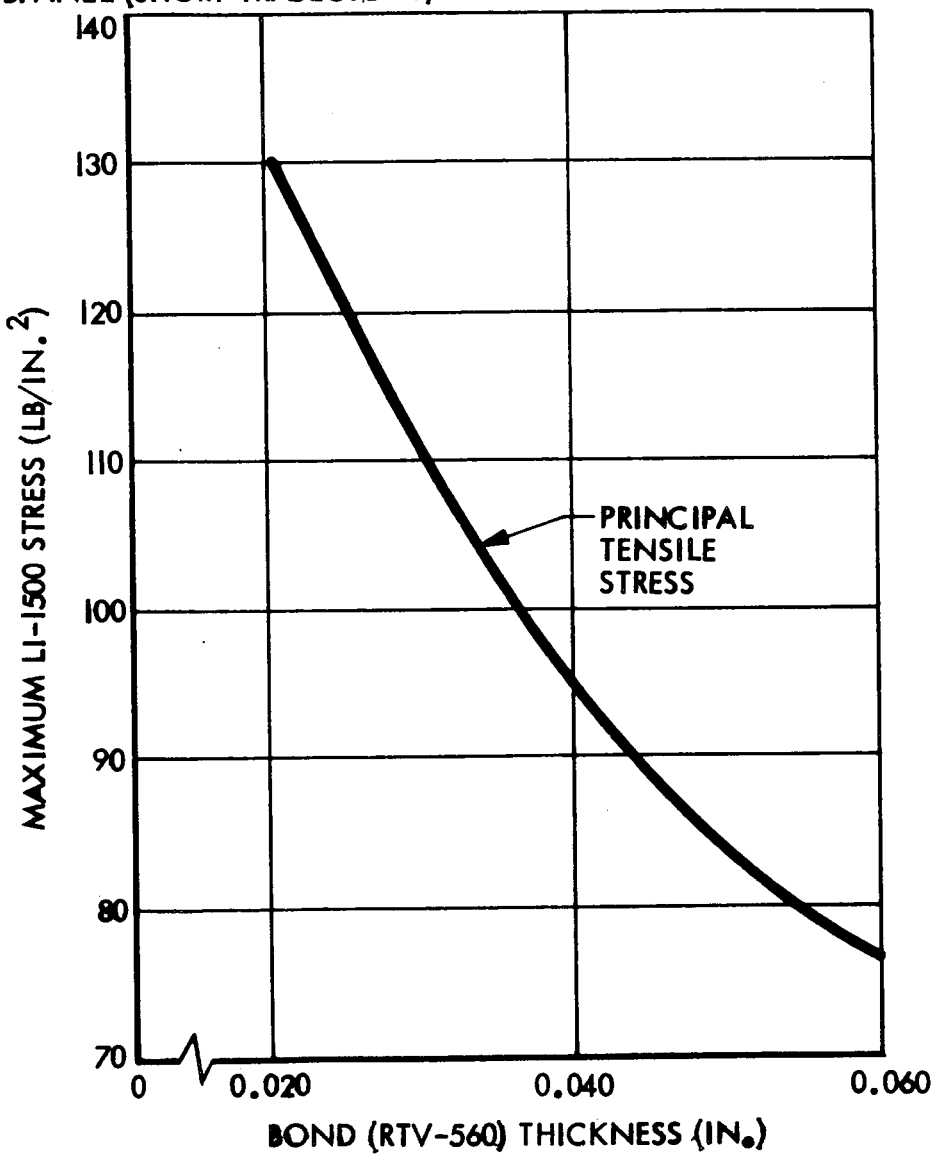


Fig. 2.2.3.2-18

D04982 (1)
RDB

# VARIATION OF SHEAR AND PEEL STRESSES WITH RTV-560 BOND THICKNESS

BERYLLIUM FUSELAGE SUBPANEL (SHORT TRAJECTORY)

TEMPERATURE PROFILE

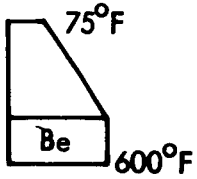


$t_{LI-1500}$ = 1.6 IN.

$t_{COATING}$ = 0.010 IN.

$E_{COATING}$ = $3.5 \times 10^6$ PSI

LOADING $p$ = 1.14 PSI BURST

$G_{LI-1500}$ = 24,000 PSI

$E_{RTV-560}$ = 300 PSI

$E_{LI-1500}$ = 60,000 PSI

ISOTROPIC ANALYSIS

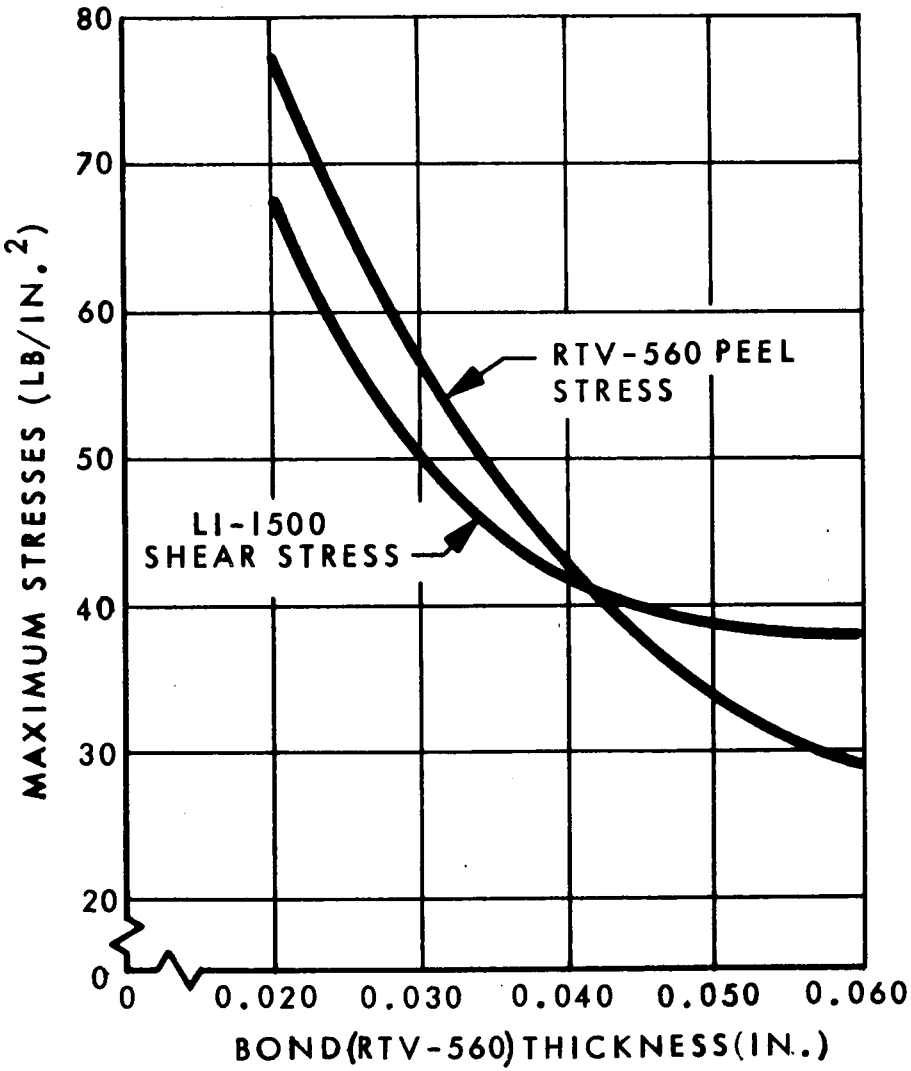


D05008 (1)

Fig. 2.2.3.2-19



rdb

# VARIATION OF BOND STRESSES WITH BOND THICKNESS

BERYLLIUM FUSELAGE SUBPANEL (SHORT TRAJECTORY)

TEMPERATURE PROFILE

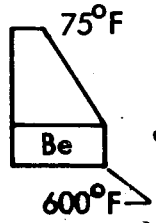


$t_{LI-1500} \doteq 1.6$ IN.

$t_{COATING} = 0.010$ IN.

$E_{COATING} \doteq 3.5 \times 10^6$ PSI

LOADING: p = 1.14 PSI BURST

$E_{RTV-560} = 300$ PSI,

$G_{LI-1500} = 24{,}000$ PSI

$E_{LI-1500} = 60{,}000$ PSI

ISOTROPIC ANALYSIS

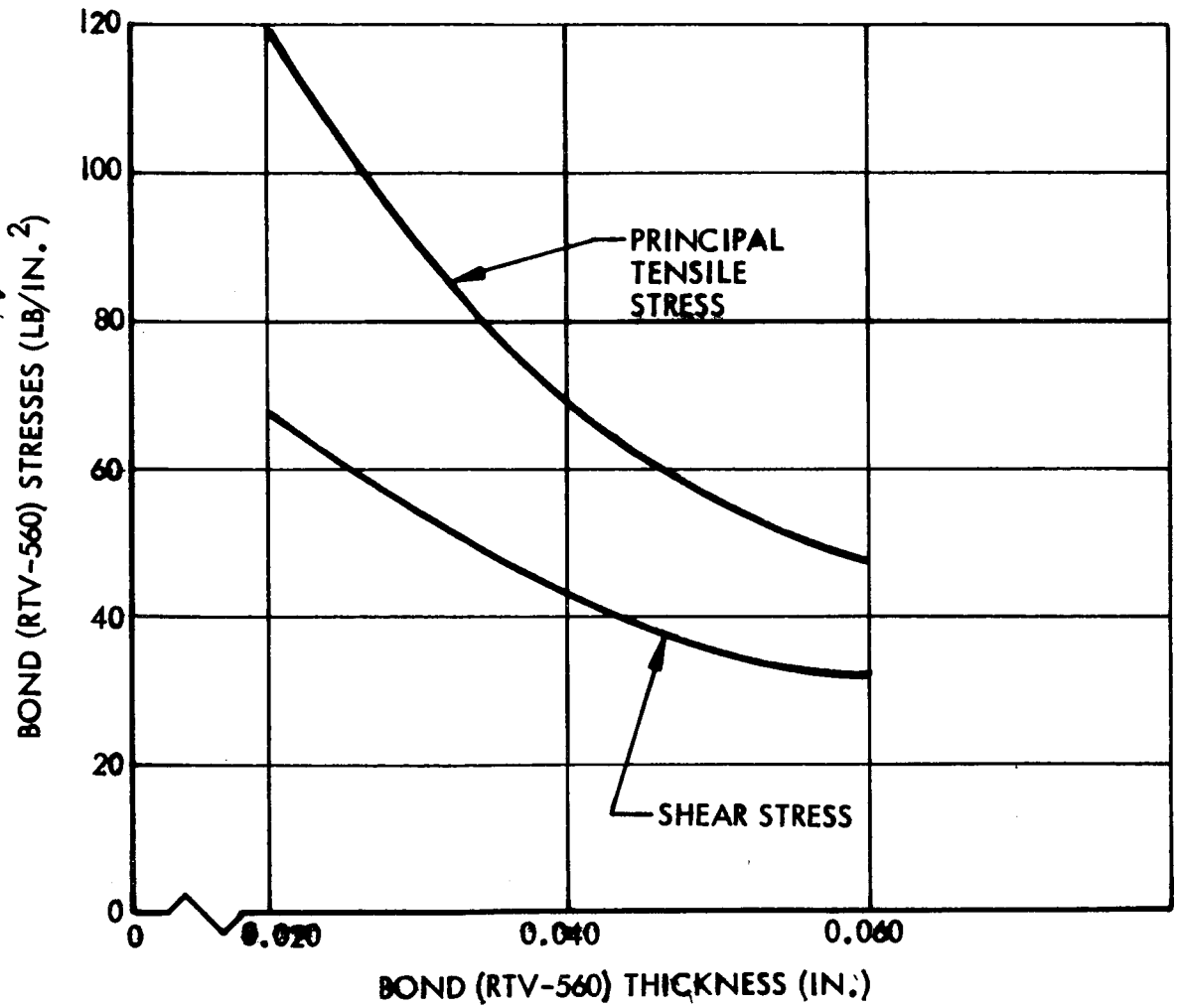


D04973 (1)
RDB

Fig. 2.2.3.2-20

Gap and Joint Studies. The effect of joint design on stress levels and gap dimensions between tiles has been investigated for a beryllium subpanel configuration. Table 2.2.3.2-5 summarizes a number of Wilson analyses for this study, in which the adjacent surfaces in the joint have been modeled in various ways. Case A represents a baseline configuration with surfaces never in bearing contact while Case B assumes that adjacent surfaces are partially continuous, due to bearing forces that lead to stress concentrations. Similar results are experienced in C. Case D represents the joint being filled with a material possessing LI-1500 elastic properties, except that the shear modulus has been assumed to be zero, simulating a frictionless joint. This case effectively behaves as a 12-inch tile, which leads to higher stress levels over the Case A baseline 6-inch tile. Case E is included for comparative purposes only, since it is not a suitable joint for other reasons as well as leading to slightly higher stress levels than the baseline joint. Case A is clearly superior, since the bonded length of tile is less than 6 inches and the stress levels are comparable to a shorter tile length. Similar results are shown in Table 2.2.3.2-6.

Studies of gap motion for an open joint during reentry are presented in Figs. 2.2.3.2-21 and 2.2.3.2-22 for a beryllium subpanel with 6-inch tiles and an aluminum primary structure panel with 4-inch panels. In the former case, high temperature conditions at the surface initially tend to close the gap followed by domination of the substrate expansion. Maximum gap opening occurs at the panel ends, and the 50-mil enlargement (which occurs at touchdown following reentry) shown for the beryllium panel is the total opening due to both panels at the common support as shown in Fig. 2.2.3.2-23. Results for the aluminum panel are qualitatively similar, although the maximum in this case is approximately 65 mils. From these studies, it appears that the baseline joint is most desirable in that large gaps directly open to the bond line are not possible during reentry.

Initial closing of the baseline joint is presented for the beryllium subpanel in Fig. 2.2.3.2-24 where appropriate gap dimensions for zero bearing forces are deduced. Minimum required gaps for other configurations are also summarized in Table 2.2.3.2-7. Since the primary difference in test and flight panels is one of LI-1500 thickness, it is seen that gap size is linearly related to LI-1500 thickness. This is plausible since collapse pressure induces overall panel bending.

Table 2.2.3.2-5

LOCKHEED

# K-18 BLOCK JOINT COMPARISON

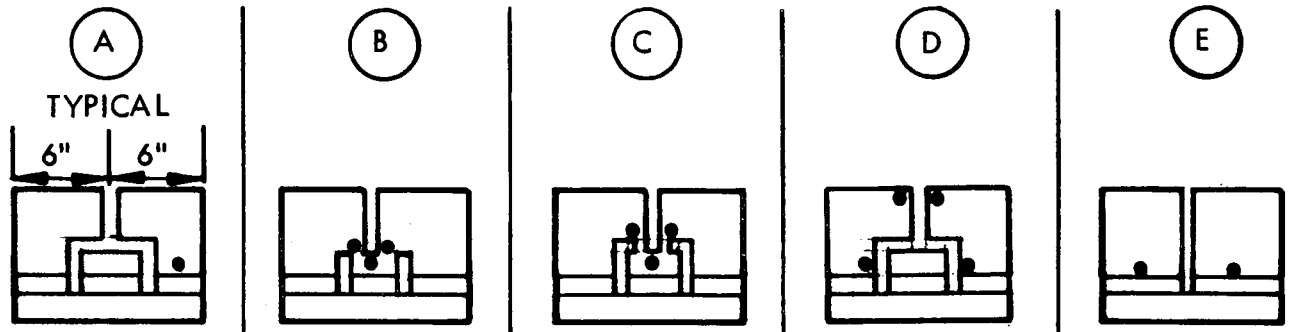


| | A | B | C | D | E |
|---|---|---|---|---|---|
| MAX. LI-1500 | 12.4 | 19.4 | 58.5 | 47.3 | 14.8 |
| MIN. LI-1500 | -8.7 | -221.4 | -227.1 | -32.0 | -10.0 |
| SHEAR (R2) LI-1500 | 3.0 | 41.9 | 82.2 | 10.1 | 3.5 |
| LONG. LI-1500 | 12.4 | -221.4 | -227.0 | 46.6 | 14.8 |
| PEEL LI-1500 | 4.1 | 6.5 | 4.6 | 9.2 | 4.5 |
| MAX. RTV-560 | 4.1 | 6.0 | 5.9 | 5.5 | 4.5 |
| MIN. RTV-560 | -10.0 | -16.0 | -15.7 | -21.0 | -11.4 |
| SHEAR RTV-560 | 1.6 | 4.0 | 3.8 | 4.4 | 1.8 |
| LONG. RTV-560 | -4.8 | -7.1 | -7.0 | -9.6 | -5.4 |
| PEEL RTV-560 | 4.1 | 4.6 | 4.6 | 4.2 | 4.5 |
| MAX. COATING | 0.4 | 25.6 | 25.2 | 9.2 | 0.3 |
| MIN. COATING | -236.1 | -395.4 | -396.7 | -1539.5 | -333.8 |

BERYLLIUM TEST PANEL 6.75 PSI COLLAPSE PRESSURE
LOADING CONDITION: 75°F. UNIFORM

• LOCATION OF MAXIMUM STRESS

DO5970

Table 2.2.3.2-6

# BERYLLIUM FUSELAGE PANEL, AREA 2
## JOINT CONCEPTS

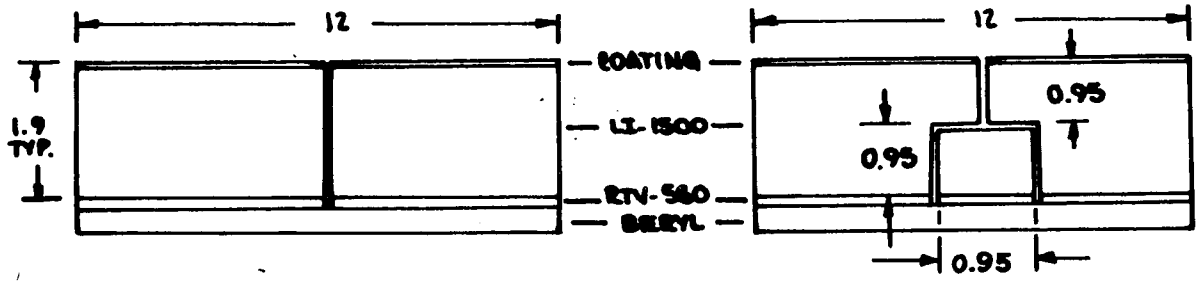


| | MAXIMUM STRESSES | MAXIMUM STRESSES |
|---|---|---|
| MAX LI-1500 | 34.9 | 32.6 |
| MIN LI-1500 | -1.7 | -1.5 |
| SHEAR LI-1500 | 9.0 | 8.4 |
| LONG LI-1500 | 34.8 | 32.5 |
| PEEL LI-1500 | 7.0 | 6.1 |
| MAX RTV-560 | 11.4 | 9.9 |
| MIN RTV-560 | -17.9 | -17.6 |
| SHEAR RTV-560 | 9.3 | 8.6 |
| LONG RTV-560 | -17.0 | -16.9 |
| PEEL RTV-560 | 7.7 | 6.7 |
| MAX COATING | 69.3 | 49.9 |
| MIN COATING | - | - |

LOADING

P = 1.5 PSI BURST

$T_{Be}$ = 550°F

$T_{COAT}$ = 100°F

D05138 (1)
rdb

# GAP ENLARGEMENT BETWEEN TILES ON 24" ALUMINUM FLIGHT PANEL #2 AT VARIOUS TIMES AFTER START OF REENTRY

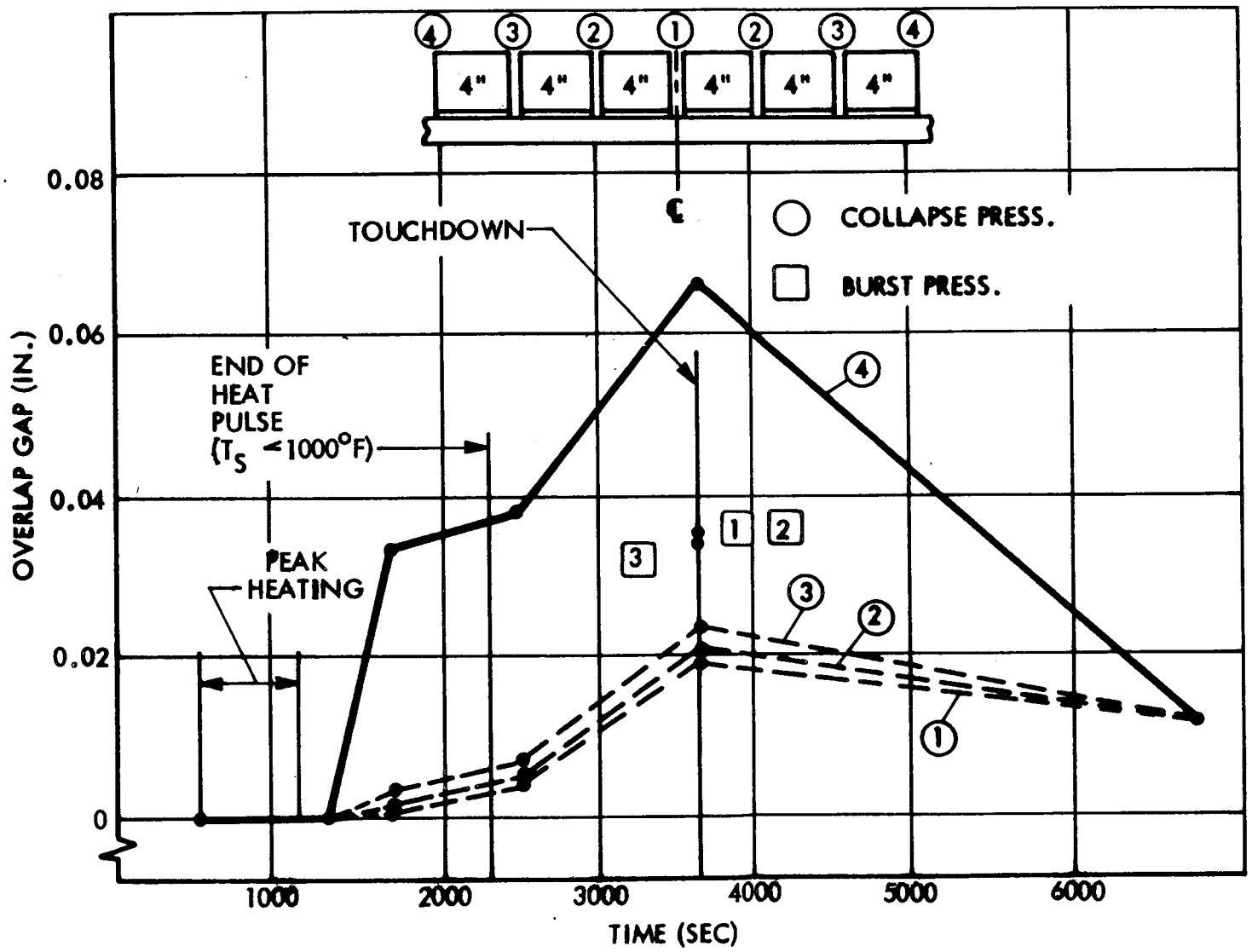


DO5973

Fig. 2.2.3.2-21

# GAP ENLARGEMENT BETWEEN TILES ON 24" BERYLLIUM SUBPANEL #1 AT VARIOUS TIMES AFTER START OF REENTRY

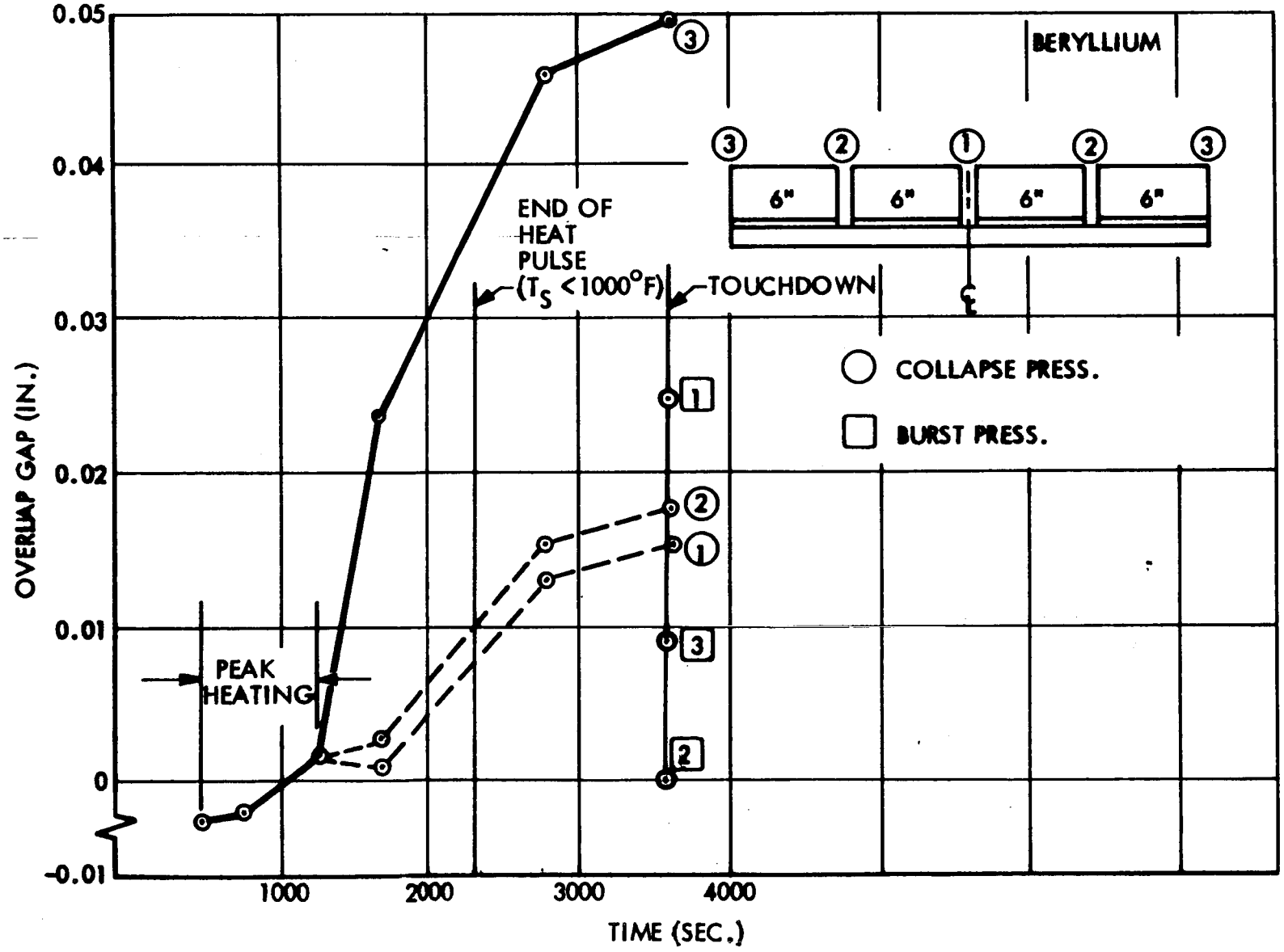


Fig. 2.2.3.2-22



DO5981

# GAP OPENING DUE TO THERMAL EXPANSION

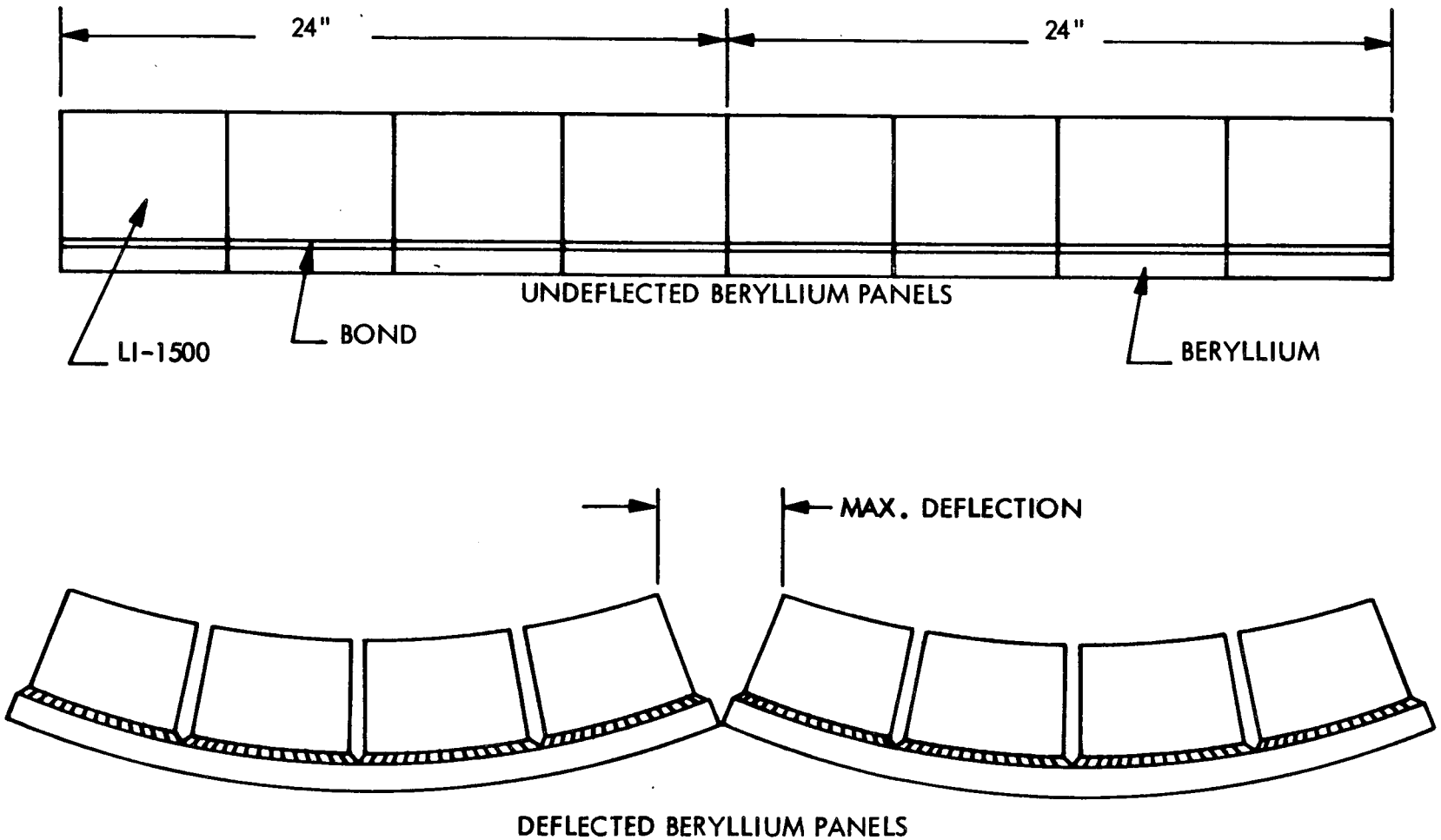


DO6022

Fig. 2.2.3.2-23

# MINIMUM GAPS REQUIRED IN Be PANEL JOINT

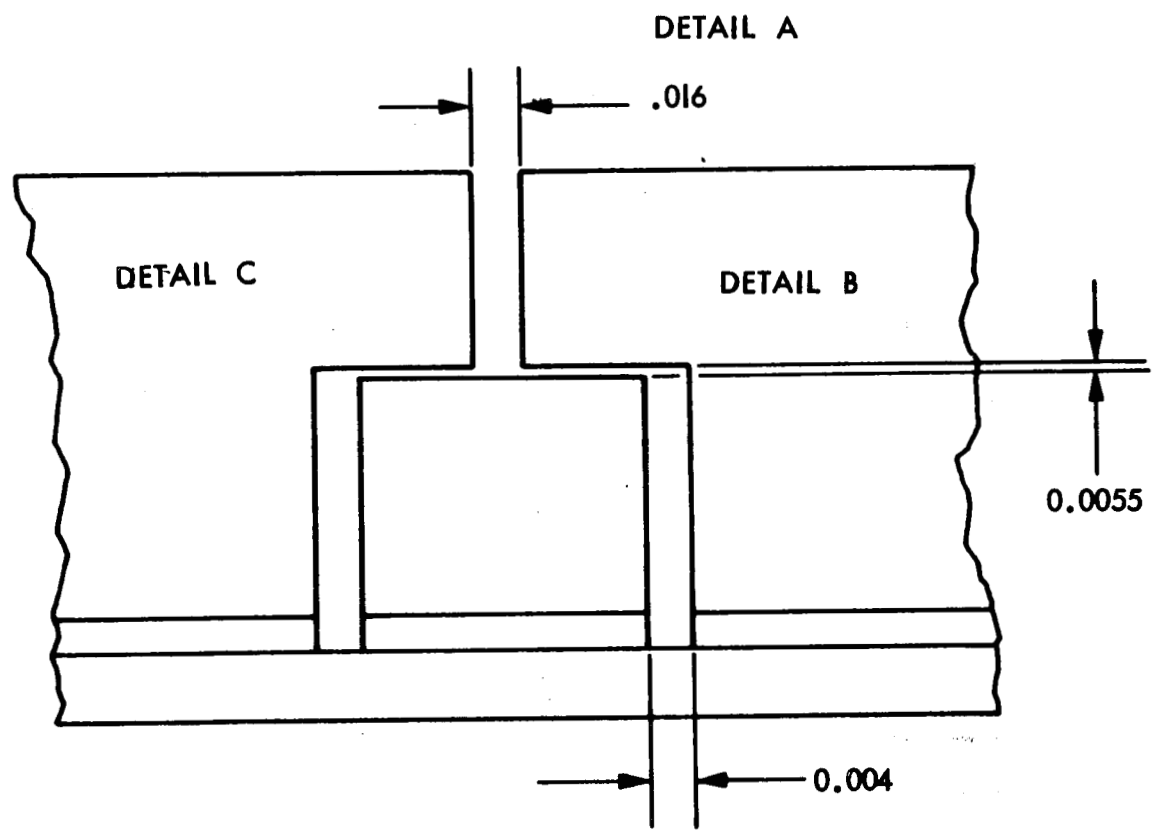


(TILE LENGTH = 6") (6.75 PSI COLLAPSE PRESSURE AT R.T.)

Fig. 2.2.3.2-24

Table 2.2.3.2-7

# MINIMUM GAPS REQUIRED AT THE JOINTS FOR ZERO INTERFERENCE

| PANEL | REQUIRED GAP |
|---|---|
| BERYLLIUM TEST NO. 1 | 0.035 |
| ALUMINUM TEST NO. 2 | 0.045 |
| ALUMINUM TEST NO. 3 | 0.024 |
| TITANIUM TEST NO. 4 | 0.030 |
| BERYLLIUM FLIGHT NO. 1 | 0.023 |
| ALUMINUM FLIGHT NO. 2 | 0.034 |
| ALUMINUM FLIGHT NO. 3 | 0.018 |
| TITANIUM FLIGHT NO. 4 | 0.019 |

Effects of Texturing and Discontinuities in Coating. The desirability of a waved surface coating to reduce stress has been investigated. The results shown in Fig. 2.2.3.2-25 indicate wide fluctuations in coating stress, principally caused by local bending effects due to eccentric load paths through the coating. These fluctuations depend on the wave length of the texturing and, for the case shown, there is approximately a 10-percent decrease in maximum coating stress. In effect, the texturing acts to lower the overall modulus of the coating, hence a lower stress for a given strain.

Studies of discontinuous coatings are presented in Figs. 2.2.3.2-26 through 2.2.3.2-28. The overall effect on coating stress is essentially the same as that due to texturing, although the coating stress must go to zero at the discontinuities. However as noted in Fig. 2.2.3.2-26, the maximum stresses in the LI-1500 at the discontinuity are magnified approximately five times over those corresponding to a continuous coating. This is clearly unacceptable, hence the use of this concept is precluded. These conclusions apply to the general case although these studies were carried out on a specific beryllium subpanel configuration.

Effects of Partial Bonding and Bond Discontinuities. An investigation was made to evaluate the effects of partial and discontinuous bonding. The effects of partial bonding are summarized in Table 2.2.3.2-8; a magnified computer plot of tile and substrate deflection with partial bonding is shown in Fig. 2.2.3.2-29. In general, stress levels decrease as the length of bond goes down, and it is noted that a partially bonded 6-inch tile results in the same state of stress as a fully bonded 4-inch tile for an aluminum panel with the loading conditions considered here. Hence, partial bonding can offer some measure of strain isolation from the substrate material. However, dynamic effects must be empirically evaluated before acceptance as a viable attachment method. Figure 2.2.3.2.-30, shows the results of a study that considers the effects of bond discontinuity at the joints. In essence, a continuous bond allows a considerable in-plane load to develop in the bond; this is transferred into the tiles at the corners, thereby raising stress levels over those for a bond discontinuity at tile joints. Hence, it is concluded that a discontinuity in the bond at tile joints is a desirable design objective.

# TEXTURED COATING STUDY – BERYLLIUM FUSELAGE PANEL

LOCKHEED

P = 1.14 PSI BURST, $T_{Be}$ = 600°F, $T_{COAT}$ = 75°F, TILE LENGTH = 12 IN.

COMPUTER MODEL

NO LOAD

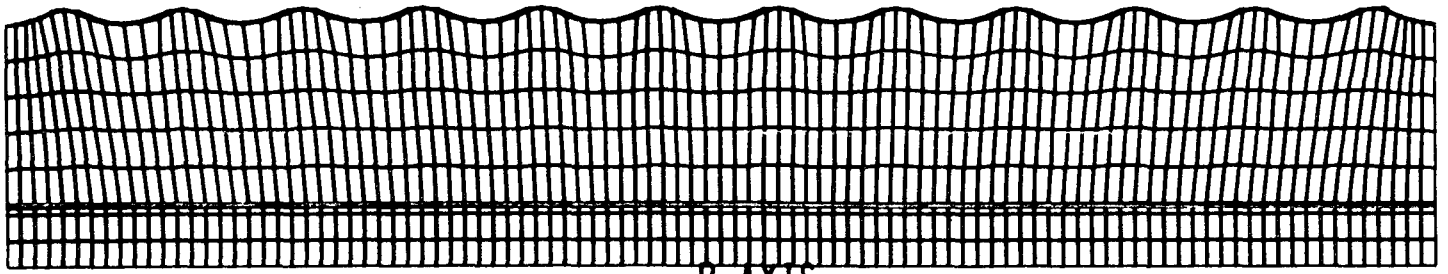


DURING LOADING

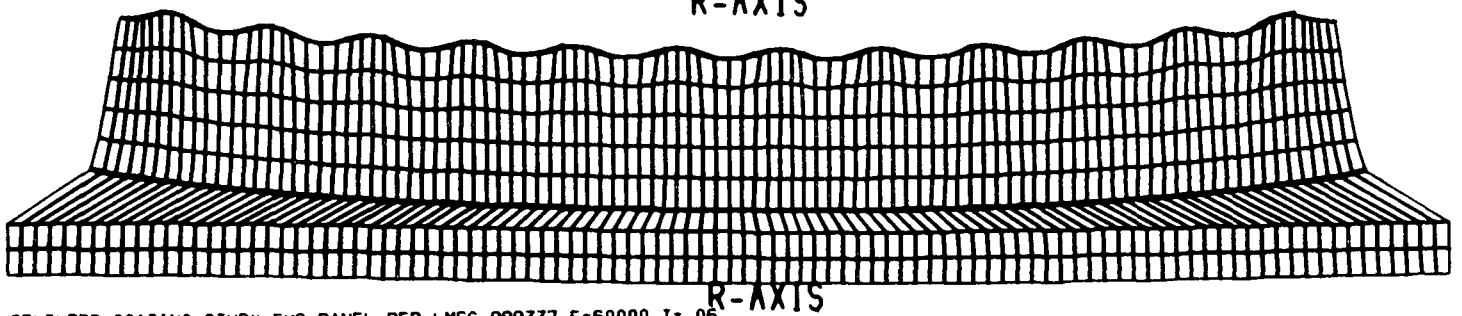


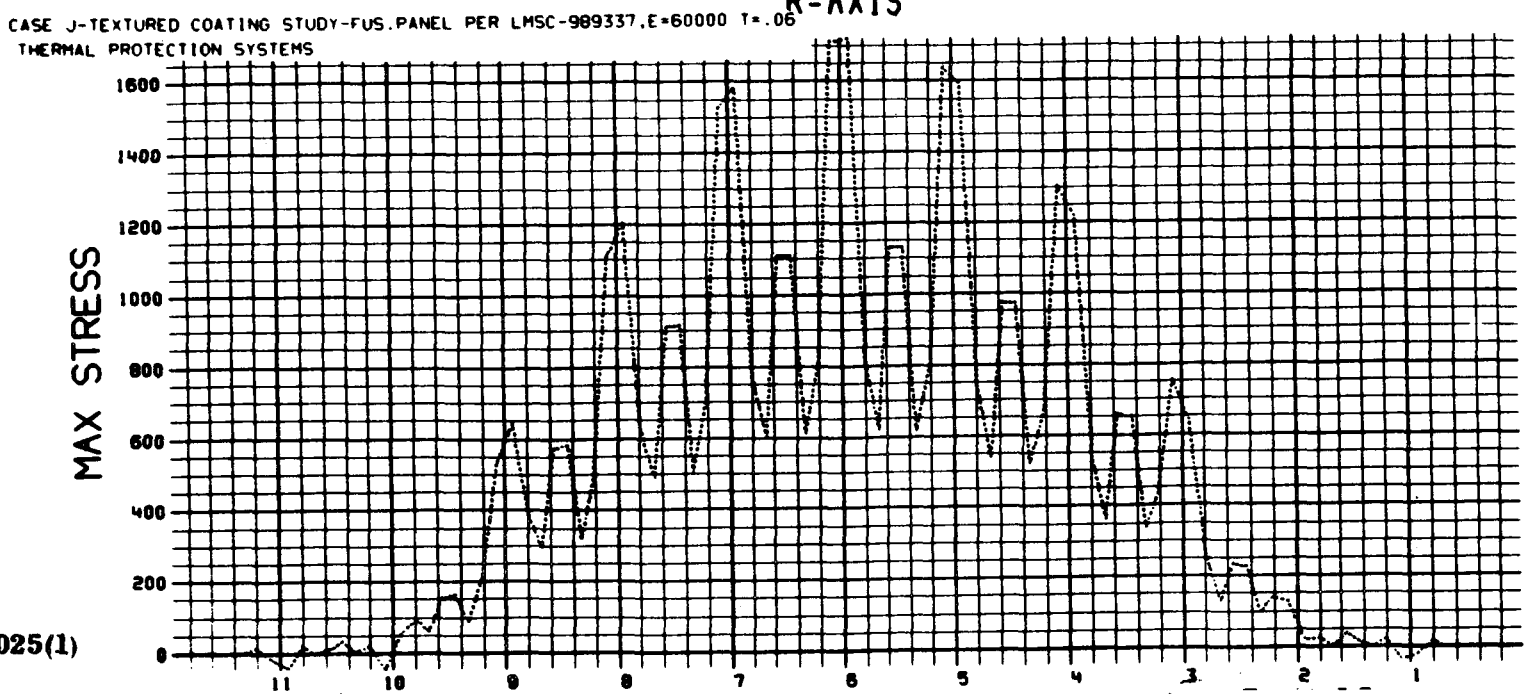


MAX TEXTURED COATING STRESS = 1718 PSI (TENSION)
MAX STRAIGHT COATING STRESS = 1950 PSI (TENSION)

DO5025(1)
RDB

Fig. 2.2.3.2-25

# VARIATION OF COATING STRESS WITH NUMBER OF COATING DISCONTINUITIES

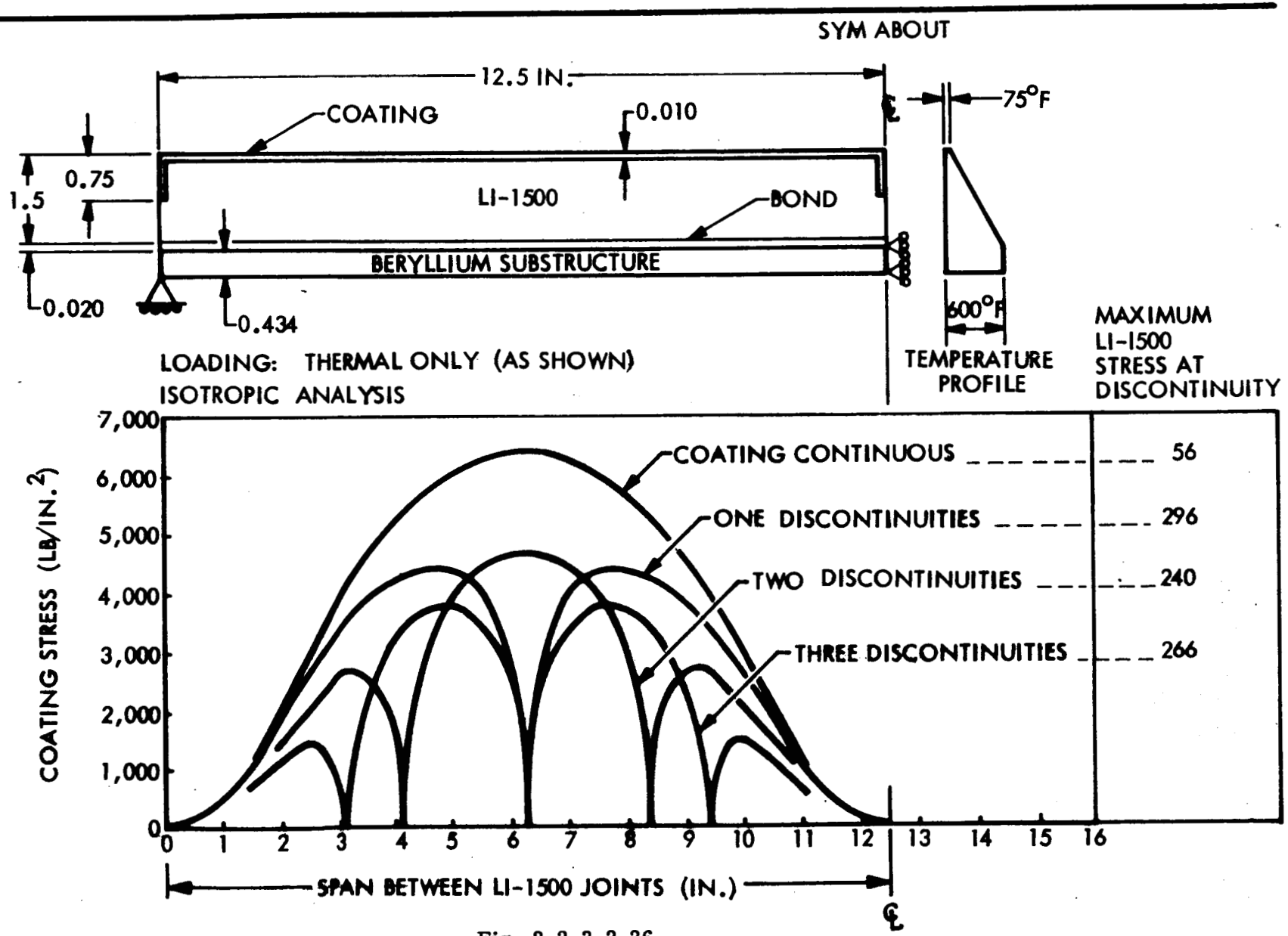


Fig. 2.2.3.2-26

D04950 (1)
RDB

# VARIATION OF COATING STRESS WITH NUMBER OF COATING DISCONTINUITIES

MAXIMUM LI-1500 STRESS = 157 PSI

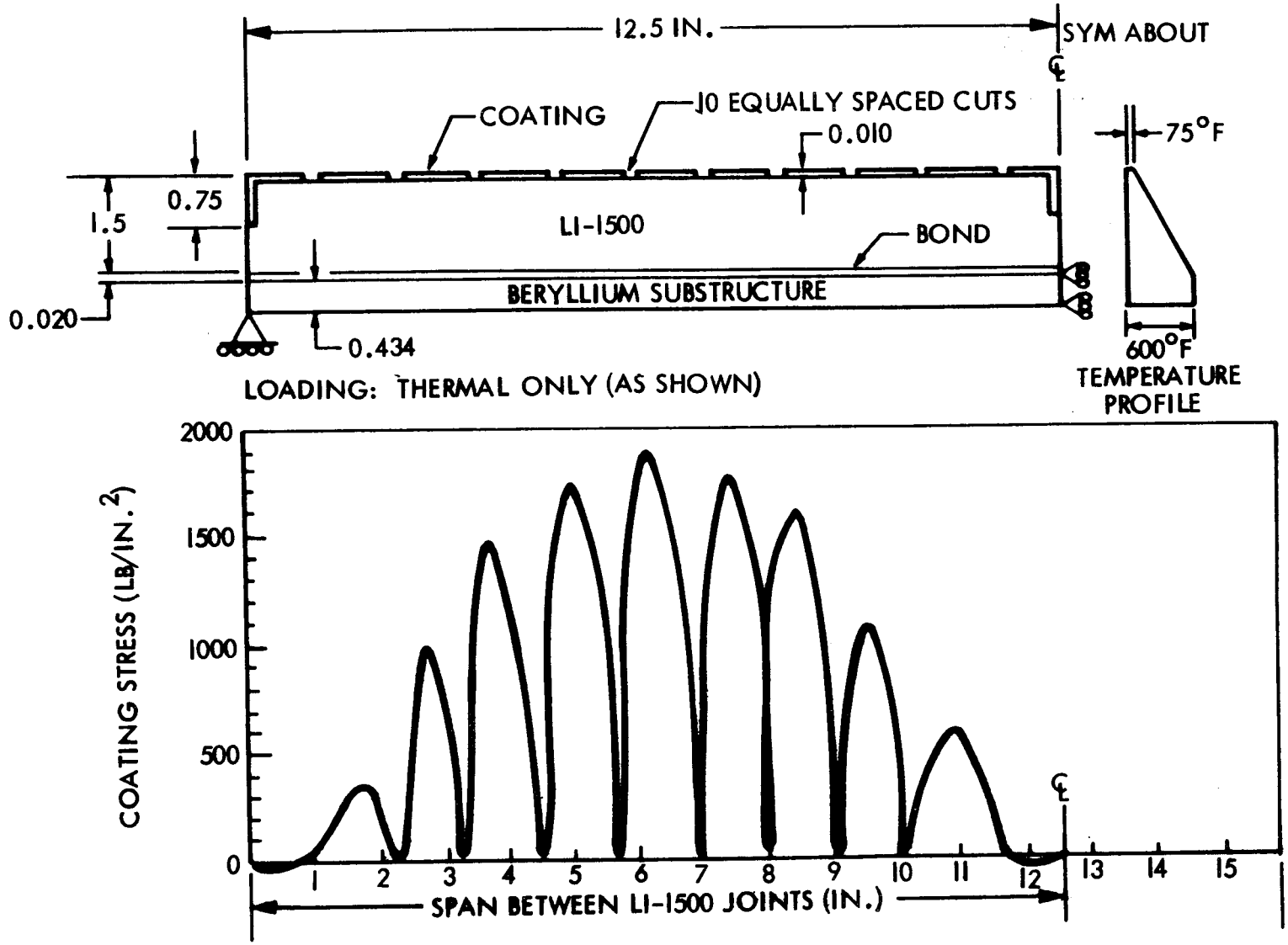


Fig. 2.2.3.2-27

D05161
rdb

# VARIATION OF COATING STRESS WITH NUMBER OF COATING DISCONTINUITIES

MAXIMUM LI-1500 STRESS = -8 PSI

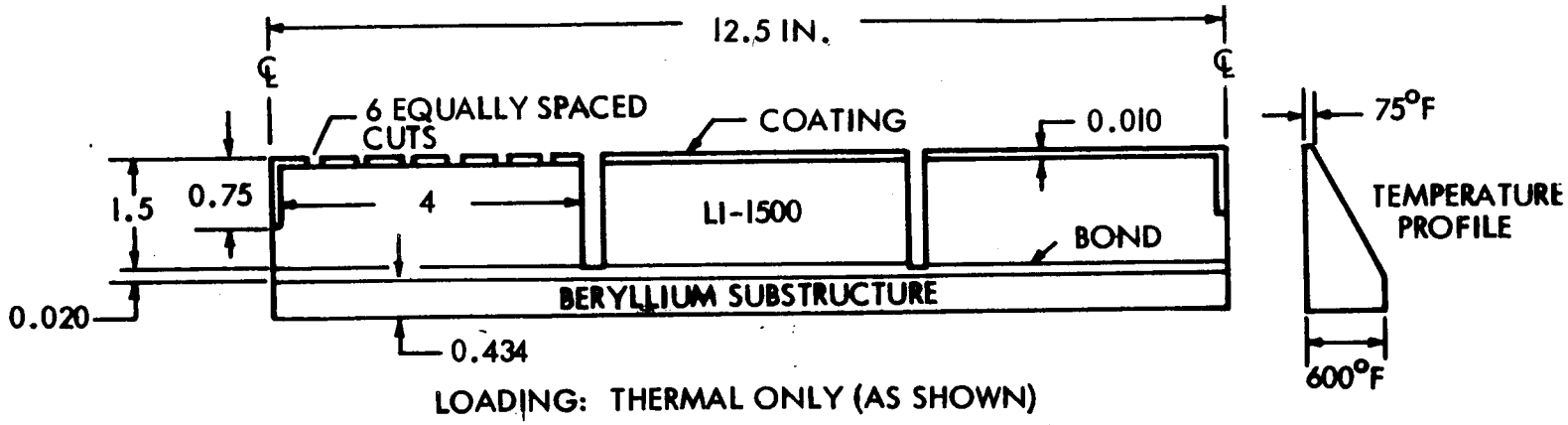


LOADING: THERMAL ONLY (AS SHOWN)

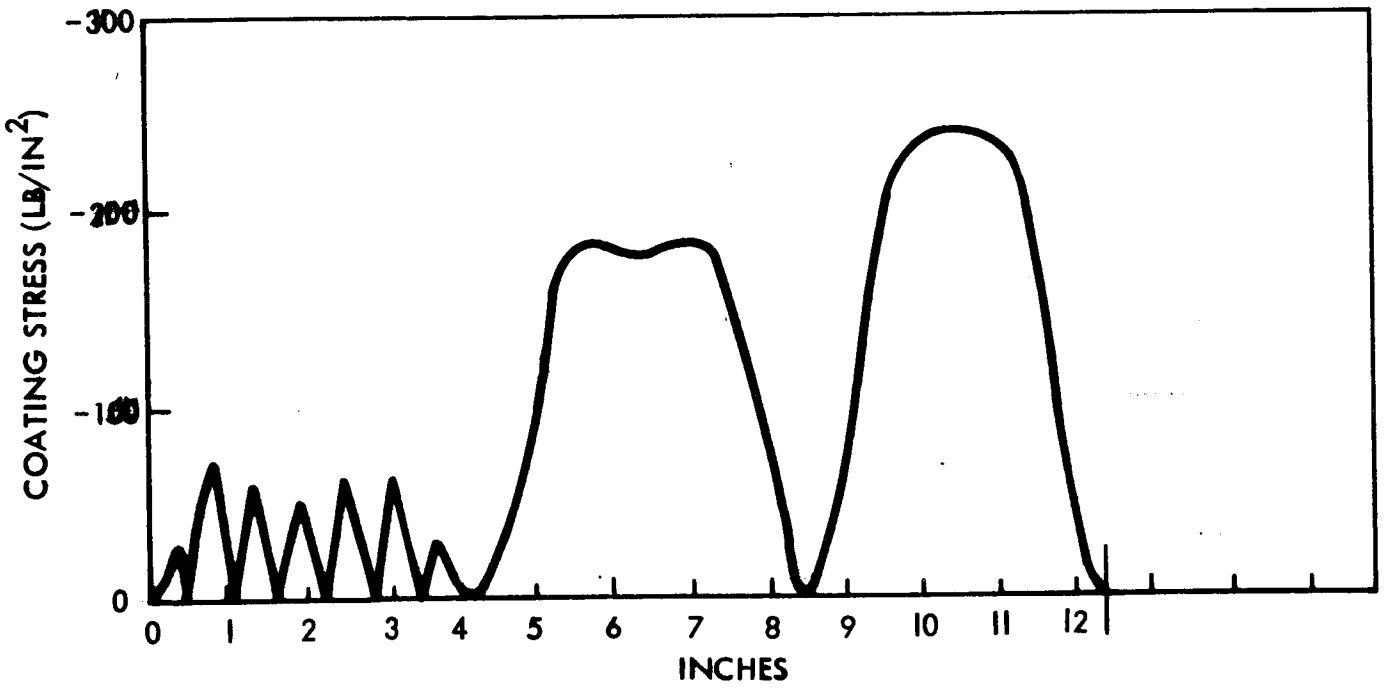


Fig. 2.2.3.2-28

D05160
rdb

Table 2.2.3.2-8

# EFFECT OF TILE SIZE/BOND AREA ON STRESS INTENSITY

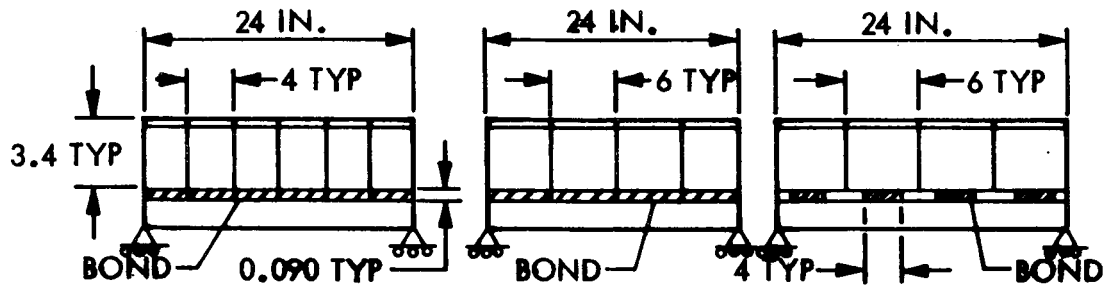


AREA 2 ALUMINUM PANEL ($T_{Al}$ = 250°F , $T_{COAT}$ = 75°F)

AXIAL LOAD = 6,000 LB/IN. PRESSURE = 1.5 PSI BURST

| STRESS (PSI) | FULL BOND 4 IN. TILE | FULL BOND 6 IN. TILE | PARTIAL BOND 6 IN. TILE |
|---|---|---|---|
| LI-1500 | | | |
| MAXIMUM | 48.9 | 71.5 | 44.4 |
| MINIMUM | - 8.7 | -10.5 | -29.0 |
| SHEAR | 15.8 | 23.5 | 15.4 |
| LONGITUDINAL | 48.9 | 71.5 | 44.4 |
| NORMAL | 5.6 | 10.5 | 3.7 |
| RTV-560 | | | |
| MAXIMUM | 16.9 | 27.7 | 15.7 |
| MINIMUM | -14.6 | -19.0 | -16.2 |
| SHEAR | 14.8 | 21.4 | 15.3 |
| LONGITUDINAL | - 2.2 | - 6.4 | - 5.6 |
| NORMAL | - 5.5 | 10.9 | 3.3 |
| COATING | | | |
| MAXIMUM | 20.3 | 11.8 | 16.4 |
| MINIMUM | -- | -32.6 | -- |

D04976
RDB

# COMPUTER MODEL OF THE PARTIALLY BONDED ALUMINUM PRIMARY STRUCTURE

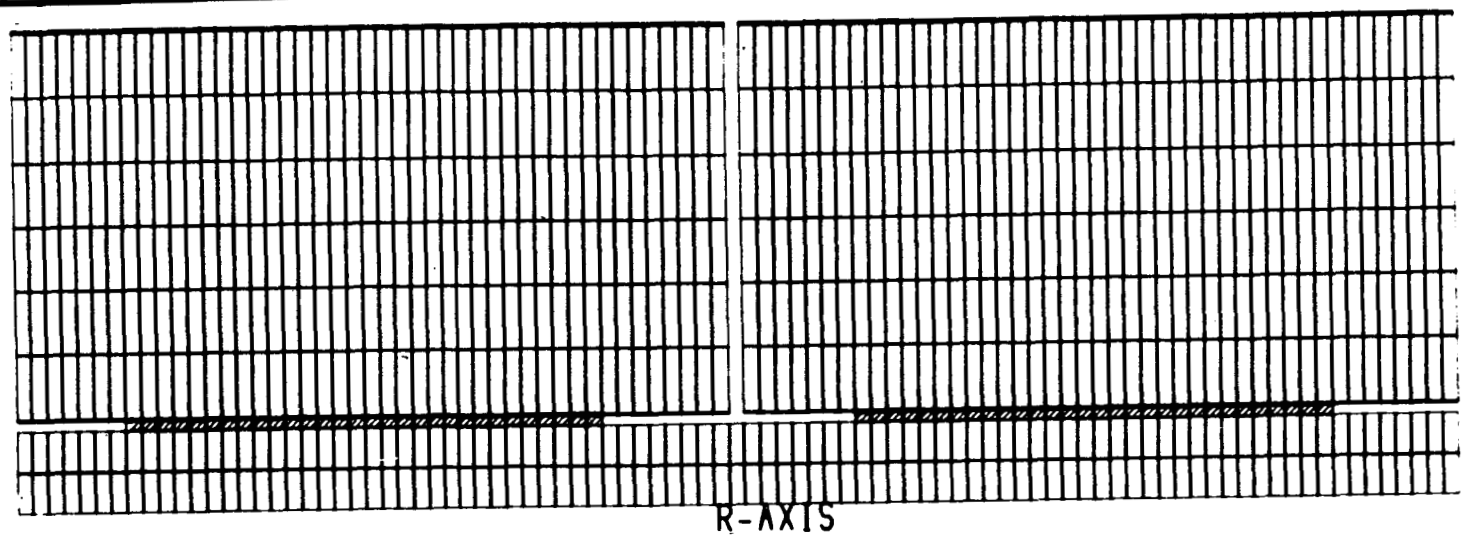

R-AXIS

BEFORE LOADING

DURING LOADING

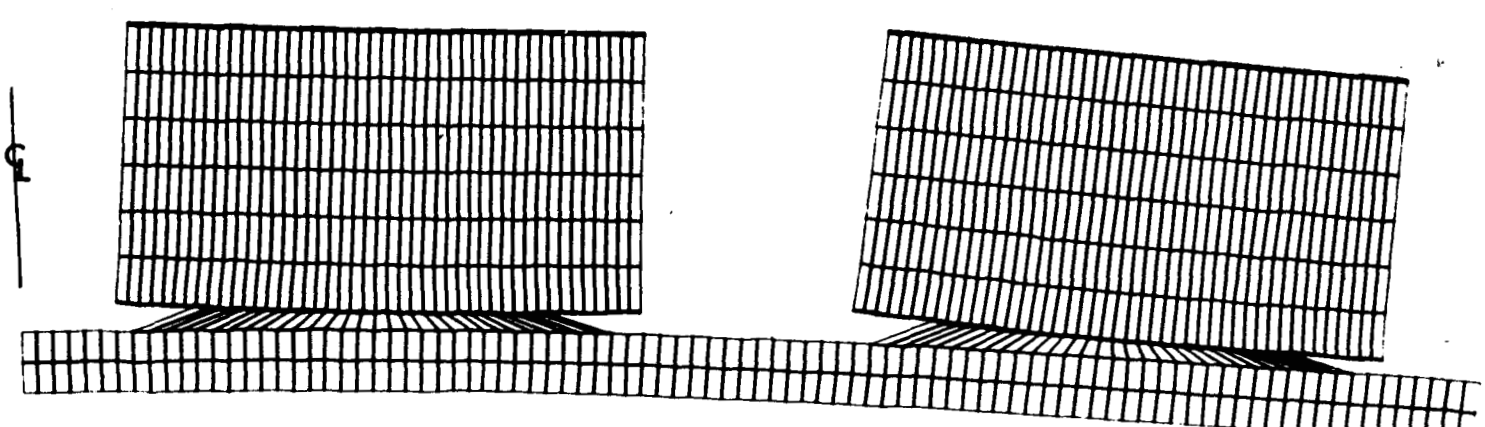

R-AXIS

Fig. 2.2.3.2-29

rdb

DO5020

# EFFECT OF BOND DISCONTINUITY AT TILE JOINTS ON STRESS INTENSITY

COMPUTER MODEL

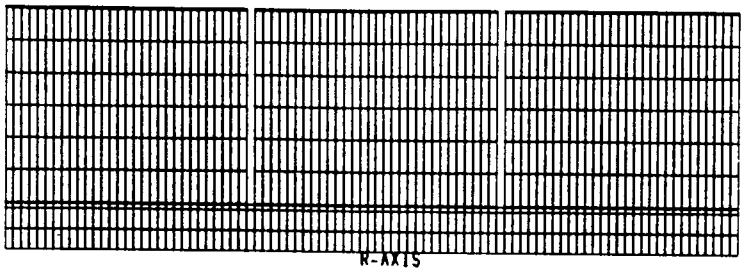


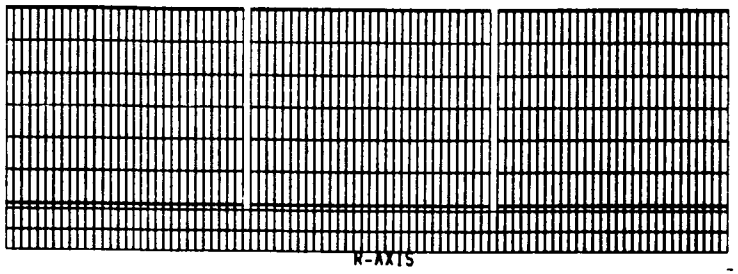


DEFLECTED SHAPE

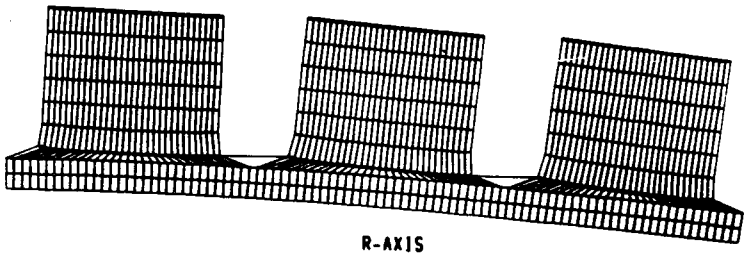


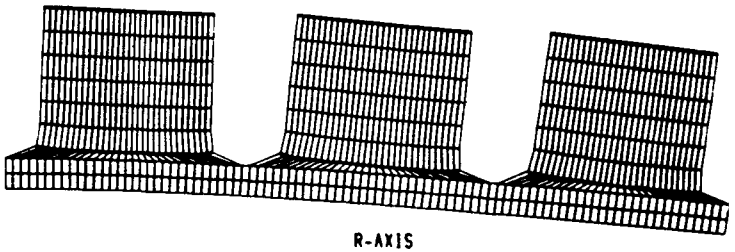


| STRESS PSI | BOND CONTINUOUS AT TILE JOINTS | BOND DELETED AT TILE JOINTS |
|---|---|---|
| **LI-1500** | | |
| MAXIMUM | 93.6 | 58.1 |
| MINIMUM | -10.5 | -10.5 |
| SHEAR | 31.9 | 18.2 |
| LONGITUDINAL | 82.3 | 58.1 |
| NORMAL | 6.5 | 6.1 |

| STRESS PSI | BOND CONTINUOUS AT TILE JOINTS | BOND DELETED AT TILE JOINTS |
|---|---|---|
| **RTV-560** | | |
| MAXIMUM | 31.0 | 19.0 |
| MINIMUM | -17.7 | -17.2 |
| SHEAR STRESS | 17.8 | 17.4 |
| LONGITUDINAL | 31.0 | -5.4 |
| NORMAL | 15.3 | 5.4 |
| **COATING** | | |
| MAXIMUM | 18.8 | 18.8 |
| MINIMUM | -1.6 | -- |

ALUMINUM PANEL AT AREA 2 - p = 1.5 PSI, 6000 PPI TENSION

DO5046(1)

rdb

Fig. 2.2.3.2-30

Mechanical Fastener Study. Two WILSON analyses were conducted to ascertain the influence of a steel screw insert on the stress levels in LI-1500 subjected to the design temperature profile. This profile and related results are shown in Table 2.2.3.2-9. It is noted that high stresses are experienced in the LI-1500 due to the large mismatch in thermal expansion properties of steel and LI-1500. These results seem to preclude the usage of this method of attachment, at least for common metal inserts. Further discussion of this concept is to be found in Section 3.3.

Tile Size Variation. The general trend of RSI stress levels versus tile length can easily be seen from Table 2.2.3.2-10. Essentially a longer tile allows the substrate strain to influence the LI-1500 more severely, due to the longer length throughout which shear transfer can take place. In a short tile, load is transferred in from one edge and then out again as another free edge is approached (thus holding down the net load transferred to the RSI) and hence producing lower stress levels. It is interesting to note that no relief to maximum LI-1500 stresses results by partially cutting through the tiles, although coating stresses are reduced.

Quantitative relationships for both aluminum and titanium primary structure panels are established in Figs. 2.2.3.2-31 through 2.2.3.2-39 for critical RSI system stress levels as a function of tile length. It is seen that all these curves display a monotonically increasing stress with increasing tile length.

Table 2.2.3.2-9

# THREADED FASTENER STUDY - THERMAL STRESSES

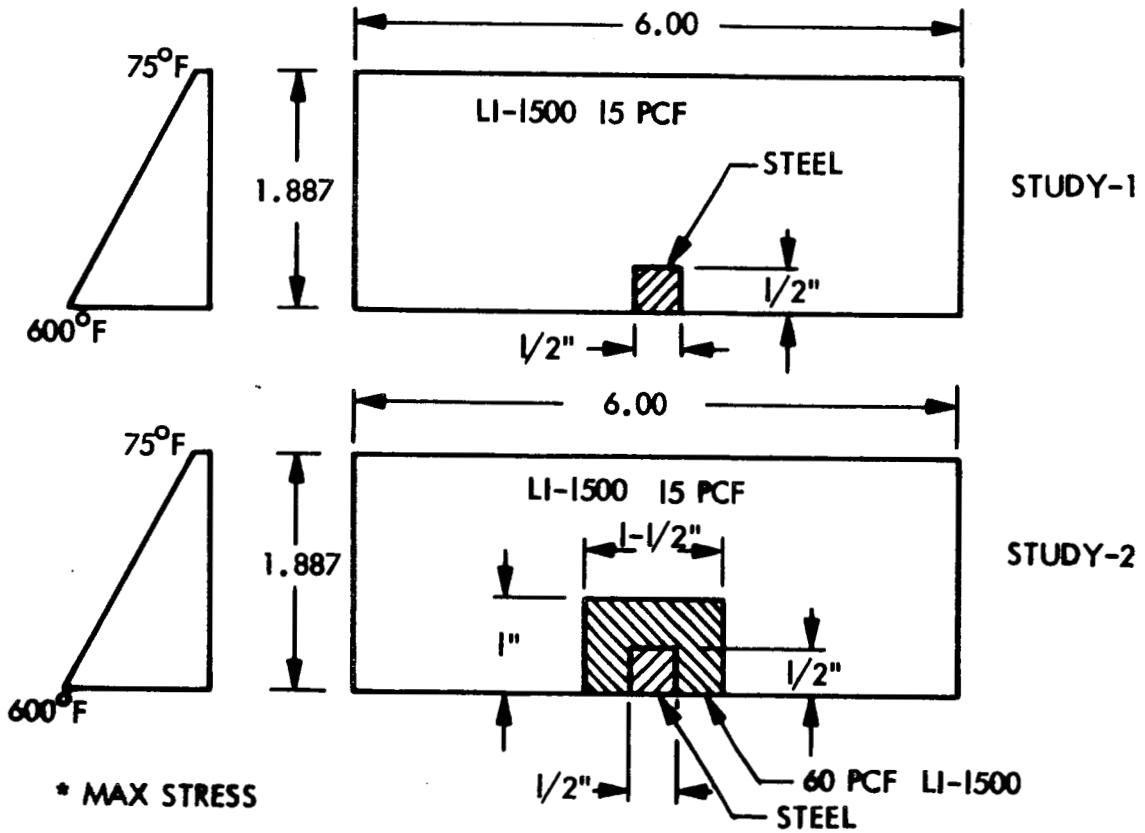


| | STUDY 1 | STUDY 2 | |
|---|---|---|---|
| | | 15 PCF | 60 PCF |
| MAX LI-1500 | 91 | 14 | 395 |
| MIN LI-1500 | -36 | -9 | -162 |
| SHEAR LI-1500 | 17 | 5 | 74 |
| RZ PRNCD LI-1500 | 47 | 8 | 205 |
| LONG LI-1500 | 91 | 14 | 395 |
| PEEL LI-1500 | 15 | 3 | 65 |

Table 2.2.3[illegible]10

# ALUMINUM TEST PANEL NO. 2
# ORBITER FUSELAGE AREA 2
## COMPARISON OF STRESSES IN PANELS CUT TO VARIOUS DEPTHS

LOADING:
P = 1.5 PSI BURST
6000 LB/IN. TENSION
THICKNESSES:
LI-1500 = 3.396 IN.
RTV-560 = 0.090 IN.
COATING = 0.010 IN.
ALUMINUM = 0.711 IN.

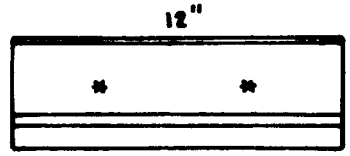


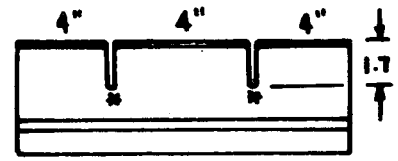


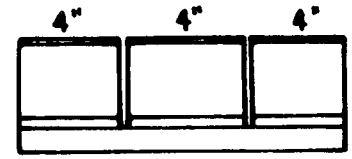


| STRESSES | AT BOND-LINE | * | AT BOND-LINE | * | AT BOND-LINE |
|---|---|---|---|---|---|
| MAXIMUM LI-1500 | 131.5 | 27.1 | 132.9 | 25.0 | 48.9 |
| MINIMUM LI-1500 | -12.7 | 0.5 | -11.2 | -2.6 | -8.7 |
| SHEAR LI-1500 | 43.6 | 2.7 | 43.4 | 4.7 | 15.8 |
| LONG LI-1500 | 131.5 | 26.9 | 132.9 | 24.3 | 48.9 |
| PEEL LI-1500 | 26.9 | 0.8 | 28.9 | -1.7 | 5.6 |
| MAXIMUM RTV-560 | 59.0 | | 60.4 | | 16.9 |
| MINIMUM RTV-560 | -30.5 | | -29.3 | | -14.6 |
| SHEAR RTV-560 | 38.4 | | 38.3 | | 14.8 |
| LONG RTV-560 | 9.6 | | 10.6 | | -2.2 |
| PEEL RTV-560 | 29.0 | | 31.0 | | 5.5 |
| MAXIMUM COATING | 6.1 | | 11.2 | | 20.3 |
| MINIMUM COATING | -530.4 | | -26.0 | | -1.0 |



D05151
rdb

# VARIATION OF LI-1500 MINIMUM PRINCIPAL COMPRESSION STRESS AND NORMAL COMPRESSION STRESS WITH LI-1500 TILE LENGTH

ALUMINUM PRIMARY STRUCTURE PANEL NO. 2
(FUSELAGE AREA NO. 2)
ORTHOTROPIC ANALYSIS

$T_{COATING}$ = 0.010 IN
$T_{LI-1500}$ = 3.396 IN
$T_{RTV-560}$ 0.090 IN
$T_{ALUMINUM}$ = 0.711 IN
$E_{COATING}$ = $10.6 \times 10^6$ PSI

LOADING:
p = 1.5 PSI BURST
6,000 LB/IN AXIAL TENSION

$E_{LI-1500}$ = 60,000 PSI (L)
6,000 PSI (T)

$G_{LI-1500}$ = 4,150 PSI
$E_{RTV-560}$ = 300 PSI
SURFACE T = 100°F
ALUMINUM T = 250°F

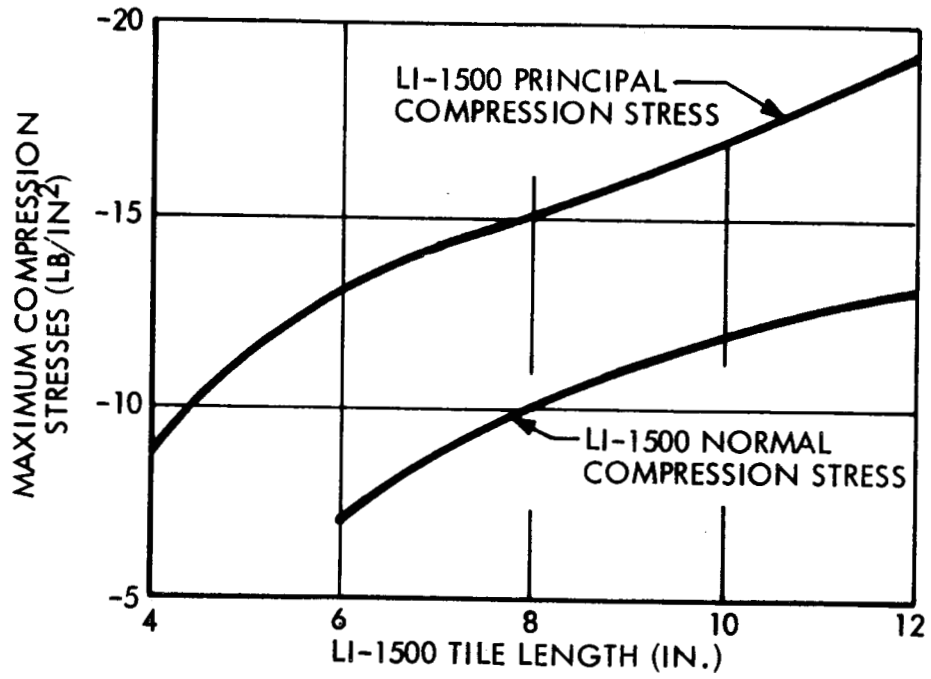


Fig. 2.2.3.2-31

D05978

# VARIATION OF LI-1500 MAXIMUM SHEAR STRESS AND MAXIMUM PEEL STRESS WITH LI-1500 TILE LENGTH

ALUMINUM PRIMARY STRUCTURE PANEL NO. 2
(FUSELAGE AREA NO. 2)
ORTHOTROPIC ANALYSIS

$T_{COATING} = 0.010$ IN.
$T_{LI-1500} = 3.396$ IN.
$T_{RTV-560} = 0.090$ IN.
$T_{ALUMINUM} = 0.711$ IN.
$E_{COATING} = 10.6 \times 10^6$ PSI
$E_{LI-1500} = 60{,}000$ PSI (L)
$= 6{,}000$ PSI (T)
$G_{LI-1500} = 4{,}150$ PSI
$E_{RTV-560} = 300$ PSI
LOADING:
P = 1.5 PSI BURST
6000 LB/IN AXIAL TENSION
SURFACE T = 100°F
ALUMINUM T = 250°F

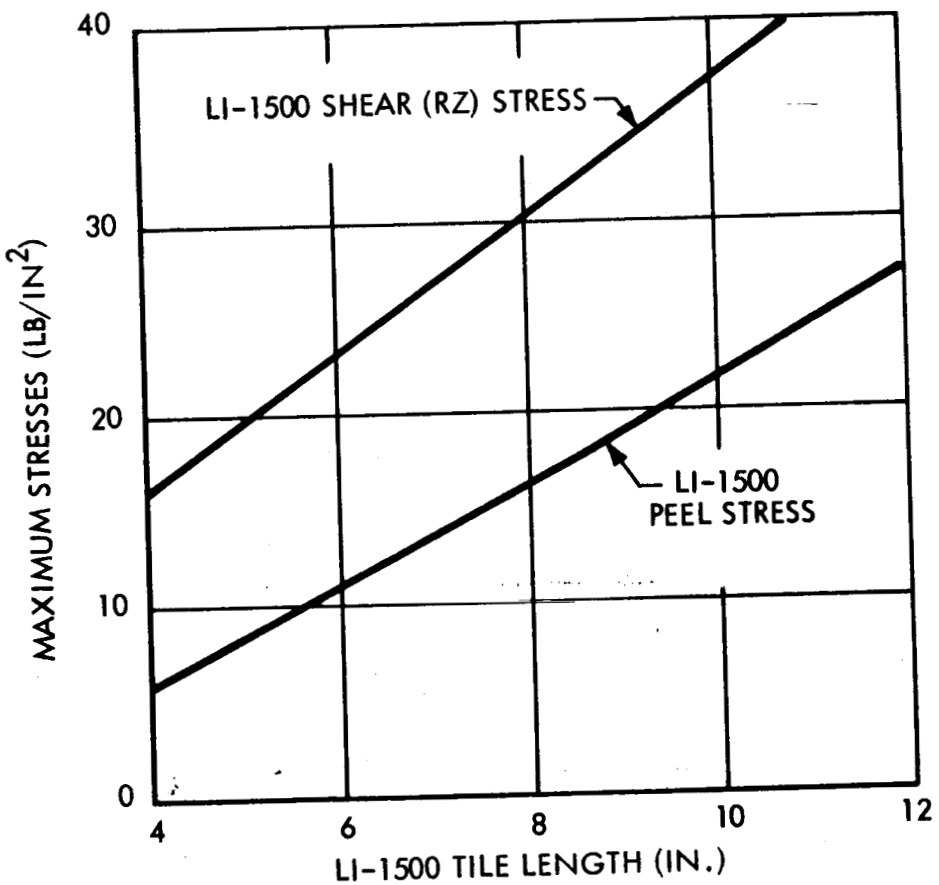


Fig. 2.2.3.2-32

# VARIATION OF RTV-560 MAXIMUM PRINCIPAL TENSION STRESS, SHEAR STRESS, AND PEEL STRESS WITH LI-1500 TILE LENGTH

STRESS, SHEAR STRESS, AND PEEL STRESS WITH LI-1500 TILE LENGTH

ALUMINUM PRIMARY STRUCTURE PANEL NO. 2 (FUSELAGE AREA NO. 2)

ORTHOTROPIC ANALYSIS

| | | |
|---|---|---|
| $T_{COATING}$ | = | 0.010 IN |
| $T_{LI-1500}$ | = | 3.396 IN |
| $T_{RTV-560}$ | = | 0.090 IN |
| $T_{ALUMINUM}$ | = | 0.711 IN |
| $E_{COATING}$ | = | $10.6 \times 10^6$ PSI |
| $E_{LI-1500}$ | = | 60,000 PSI (L) |
| | = | 6,000 PSI (T) |
| $G_{LI-1500}$ | = | 4,150 PSI |
| $E_{RTV-560}$ | = | 300 PSI |

LOADING:
p = 1.5 PSI BURST
6,000 LB/IN AXIAL TENSION

SURFACE T = 100°F
ALUMINUM T = 250°F

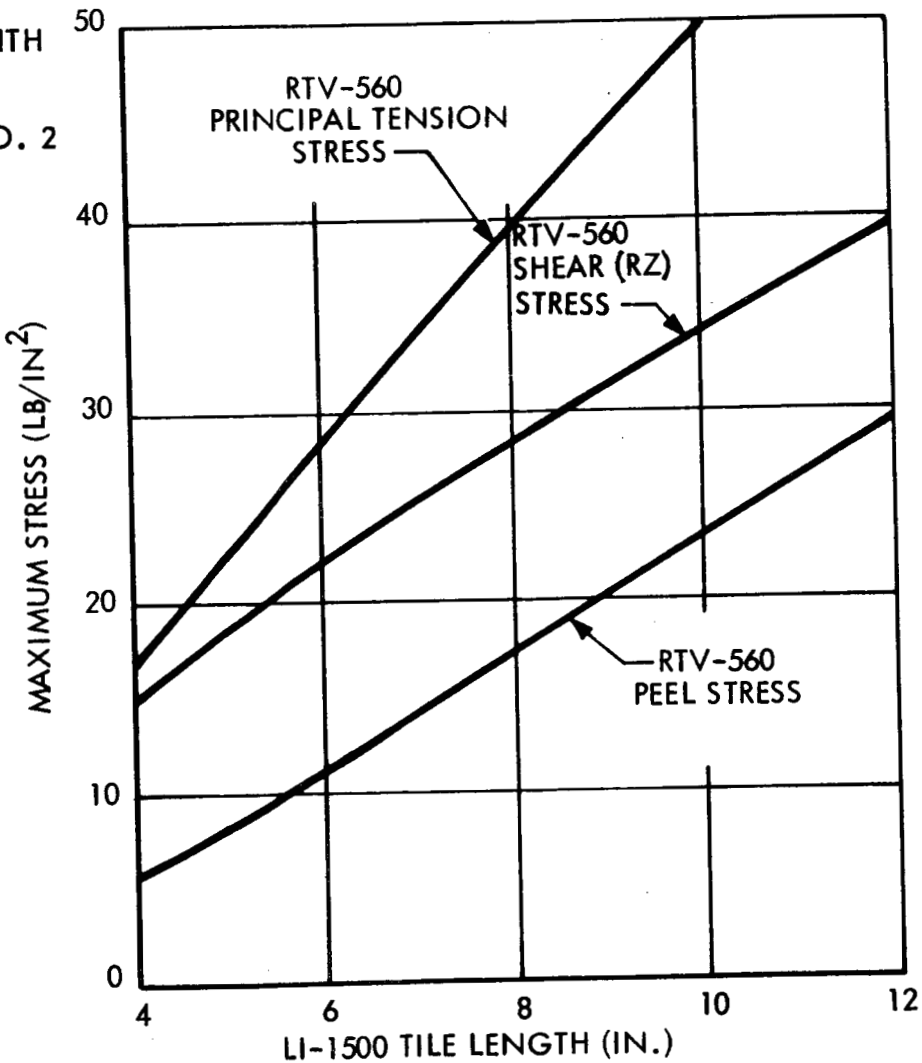


DO5976

Fig. 2.2.3.2-33

# VARIATION OF RTV-560 MINIMUM PRINCIPAL COMPRESSIVE STRESS WITH LI-1500 TILE LENGTH

ALUMINUM PRIMARY STRUCTURE PANEL NO. 2
(FUSELAGE AREA NO. 2)

ORTHOTROPIC ANALYSIS

| | | |
|---|---|---|
| $T_{COATING}$ | = | 0.010 IN |
| $T_{LI-1500}$ | = | 3.396 IN |
| $T_{RTV-560}$ | = | 0.090 IN |
| $T_{ALUMINUM}$ | = | 0.711 IN |
| $E_{COATING}$ | = | $10.6 \times 10^6$ PSI |
| $E_{LI-1500}$ | = | 60,000 PSI<br>6,000 PSI |
| $G_{LI-1500}$ | = | 4,150 PSI |
| $E_{RTV-560}$ | = | 300 PSI |

LOADING:
p = 1.5 PSI BURST
6000 LB/IN AXIAL TENSION

| | |
|---|---|
| SURFACE | T = 100°F |
| ALUMINUM | T = 250°F |

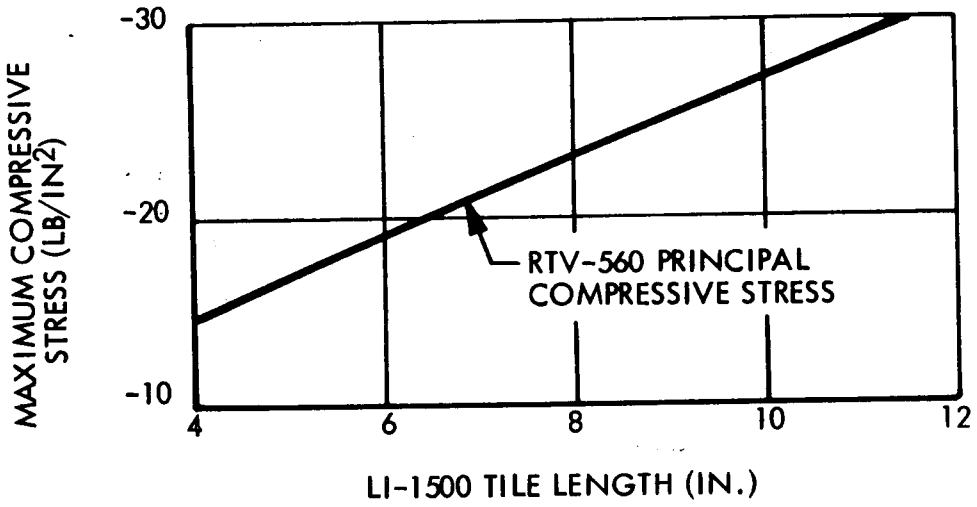


Fig. 2.2.3.2-34

# VARIATION OF MAXIMUM COATING COMPRESSION STRESS WITH LI-1500 TILE LENGTH

ALUMINUM PRIMARY STRUCTURE PANEL NO. 2
(FUSELAGE AREA NO. 2)
ORTHOTROPIC ANALYSIS

| | | |
|---|---|---|
| $T_{COATING}$ | = | 0.010 IN |
| $T_{LI-1500}$ | = | 3.396 IN |
| $T_{RTV-560}$ | = | 0.090 IN |
| $T_{ALUMINUM}$ | = | 0.711 IN |
| $E_{COATING}$ | = | $10.6 \times 10^6$ PSI |
| $E_{LI-1500}$ | = | 60,000 PSI (L)<br>6,000 PSI (T) |
| $G_{LI-1500}$ | = | 4,150 PSI |
| $E_{RTV-560}$ | = | 300 PSI |

LOADING:
p = 1.5 PSI BURST
6000 LB/IN AXIAL TENSION

SURFACE T = 100°F
ALUMINUM T = 250°F

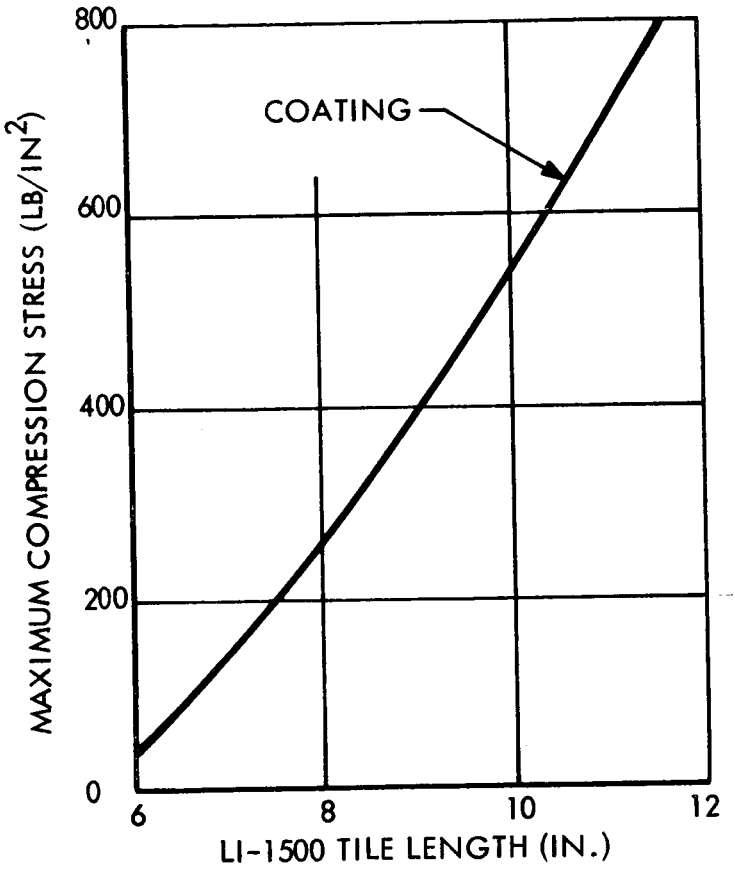


DO5977

Fig. 2.2.3.2-35

# VARIATION OF LI-1500 MAXIMUM PRINCIPAL TENSILE STRESS WITH LI-1500 TILE LENGTH

TITANIUM PRIMARY STRUCTURE PANEL NO. 4
(FUSELAGE AREA NO. 2)

ORTHOTROPIC ANALYSIS

$T_{COATING}$ = 0.010 IN
$T_{LI-1500}$ = 2.00 IN
$T_{RTV-560}$ = 0.090 IN
$T_{TITANIUM}$ = 0.628 IN
$E_{COATING}$ = $10.6 \times 10^6$ PSI
$E_{LI-1500}$ = 60,000 PSI (L)
6,000 PSI (T)
$G_{LI-1500}$ = 4,150 PSI
$E_{RTV-560}$ = 300 PSI

LOADING:
P = 1.5 PSI BURST
6000 LB/IN AXIAL TENSION

SURFACE T = 100°F
TITANIUM T = 550°F

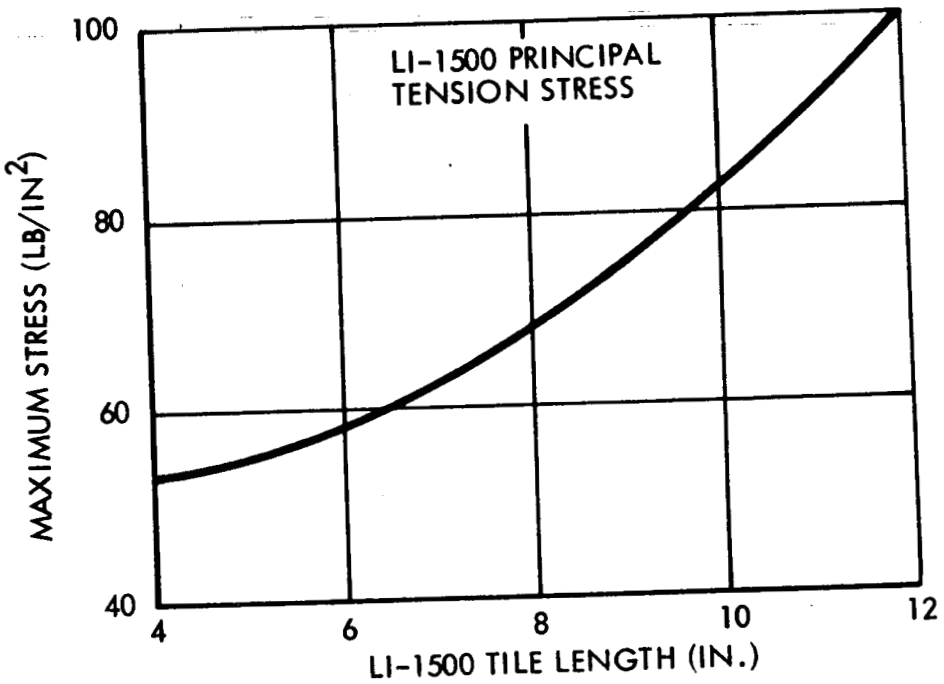


Fig. 2.2.3.2-36

DO5971

# VARIATION OF LI-1500 STRESSES WITH LI-1500 TILE LENGTH

TITANIUM PRIMARY STRUCTURE PANEL NO.4
(FUSELAGE AREA NO.2)

ORTHOTROPIC ANALYSIS

$T_{COATING}$ = 0.010 IN.
$T_{LI-1500}$ = 2.00 IN
$T_{RTV-560}$ = 0.090 IN
$T_{TITANIUM}$ = 0.628 IN
$E_{COATING}$ = $10.6 \times 10^6$ PSI
$E_{LI-1500}$ = 60,000 PSI (L)
= 6,000 PSI (T)
$G_{LI-1500}$ = 4,150 PSI
$E_{RTV-560}$ = 300 PSI

LOADING:
P = 1.5 PSI BURST
6000 LB/IN AXIAL TENSION

SURFACE T = 100°F
TITANIUM T = 550°F

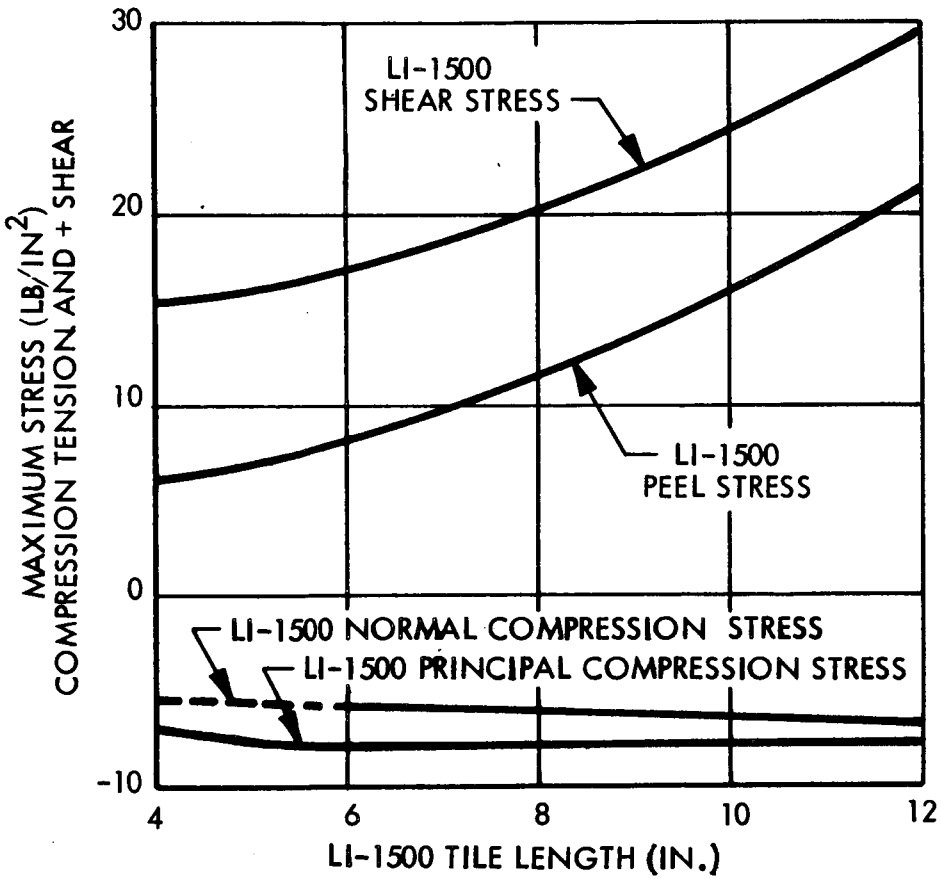


Fig. 2.2.3.2-37

# VARIATION OF RTV-560 STRESSES WITH LI-1500 TILE LENGTH

TITANIUM PRIMARY STRUCTURE PANEL NO. 4
(FUSELAGE AREA NO. 2)

ORTHOTROPIC ANALYSIS

| | | |
|---|---|---|
| $T_{COATING}$ | = | 0.010 IN |
| $T_{LI-1500}$ | = | 2.00 IN |
| $T_{RTV-560}$ | = | 0.090 IN |
| $T_{TITANIUM}$ | = | 0.628 IN |
| $E_{COATING}$ | = | $10.6 \times 10^6$ PSI |
| $E_{LI-1500}$ | = | 60,000 PSI (L)<br>6,000 PSI (T) |
| $G_{LI-1500}$ | = | 4,150 PSI |
| $E_{RTV-560}$ | = | 300 PSI |

LOADING:
p = 1.5 PSI BURST
6000 LB/IN AXIAL TENSION

SURFACE T=100°F
TITANIUM T=550°F

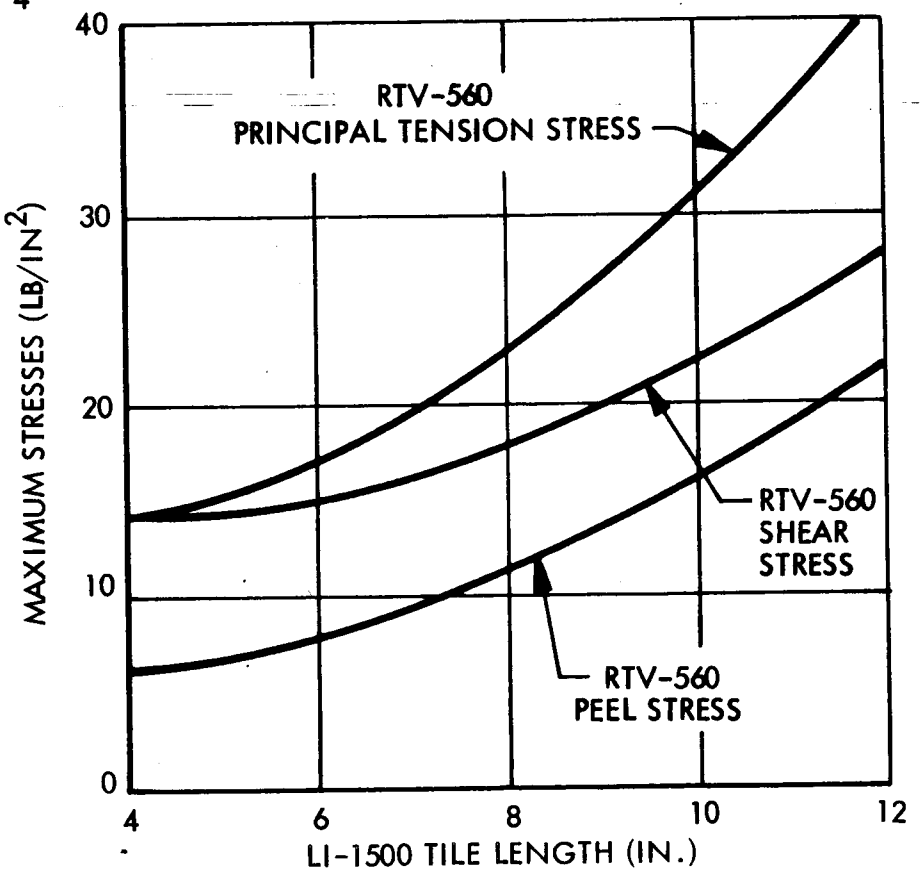


Fig. 2.2.3.2-38

# VARIATION OF LI-1500 MAXIMUM PRINCIPAL TENSION STRESS WITH LI-1500 TILE LENGTH

ALUMINUM PRIMARY STRUCTURE PANEL NO. 2
(FUSELAGE AREA NO. 2)

ORTHOTROPIC ANALYSIS

| | | |
|---|---|---|
| $T_{COATING}$ | = | 0.010 IN |
| $T_{LI-1500}$ | = | 3.396 IN |
| $T_{RTV-560}$ | = | 0.080 IN |
| $T_{ALUMINUM}$ | = | 0.711 IN |
| $E_{COATING}$ | = | $10.6 \times 10^6$ PSI |
| $E_{LI-1500}$ | = | 60,000 PSI (L)<br>6,000 PSI (T) |
| $G_{LI-1500}$ | = | 4,150 PSI |
| $E_{RTV-560}$ | = | 300 PSI |

LOADING:
p = 1.5 PSI BURST
6,000 LB/IN AXIAL TENSION

| | |
|---|---|
| SURFACE | T = 100°F |
| ALUMINUM | T = 250°F |

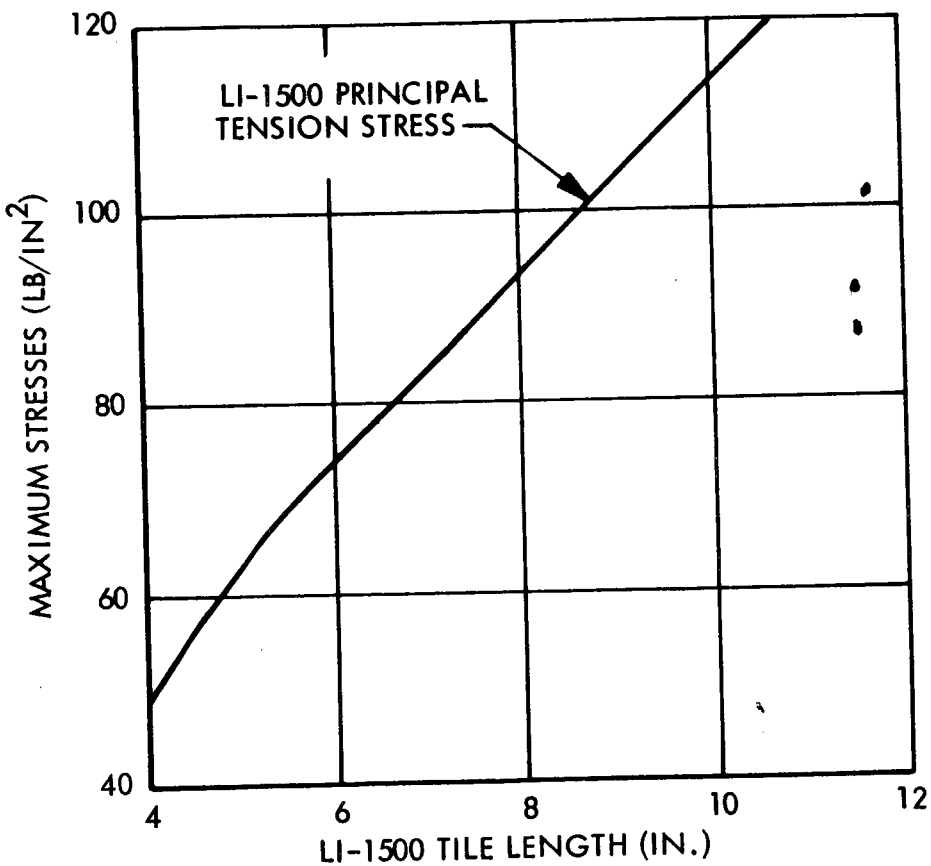


Fig. 2.2.3.2-39

Effects of Different Coating Configurations on RSI Stress Levels. A series of coating studies is summarized in the following figures, which consider the two basic cases of (1) local densification of LI-1500 to 60 pcf, and (2) an add-on coating, alone or in combination with densification. In the studies, the effects of two different add-on coatings were modeled: A 0.010-in. thick chrome oxide coating used along and a 0.004-in. thick silicon carbide coating used alone or with a 0.010-in. thick 60 pcf LI-1500 densified layer. Typical beryllium subpanel configurations studied are presented in Fig. 2.2.3.2-40. In Fig. 2.2.3.2-41 is shown the shear stress variation through the panel at the location of the critical shear stress in the LI-1500, for a chrome oxide coating alone. As might be expected, the shear stress is maximum at the bond line and rapidly decays with distance from the bond. In Figs. 2.2.3.2-42 and 2.2.3.2-43 are shown, qualitatively, the same type of behavior for an all-around 60 pcf densified layer of LI-1500 with a 15 pcf core. However, as noted, the maximum stress in the LI-1500 has dropped about 30 percent. These two figures can be compared with Figs. 2.2.3-2-44 and 2.2.3.2-45, in which the core density was reduced to 10 pcf. From these curves it appears that core density in this range does not have any significant influence on shear stress in the LI-1500. From Table 2.2.3.2-11, it is noted that this lack of core density influence is also carried over to other stresses of interest; however, LI-1500 allowable stresses would be proportionately lower for a 10 pcf material.

Another series of similar curves is presented in Figs. 2.2.3.2-46 and 2.2.3.2-47, which also summarize maximum core and coating shear stresses for a silicon carbide add-on coating in conjunction with a 10-mil layer of all-around densified LI-1500. Again, maximum stresses occur in the treated regions while core stresses are small. These results are also summarized in Table 2.2.3.2-11.

Another set of similar curves is presented for an aluminum primary structure panel configuration with a 15 pcf LI-1500 core in Figures 2.2.3.2-48 and 2.2.3.2-49. Table 2.2.3.2-12 is a brief summary of selected results. This study indicates a qualitative similarity with the previous beryllium subpanel results but quantitatively the effect of the surface densification in this case offers only about a 10-percent reduction in LI-1500 stress levels as compared with the baseline configuration of the chrome oxide coating alone. Local densification is less effective here, due to the fact that the substructure strain is increased. Aluminum at 250°F experiences nearly as much

# SHEAR STRESS PROFILE CONFIGURATIONS

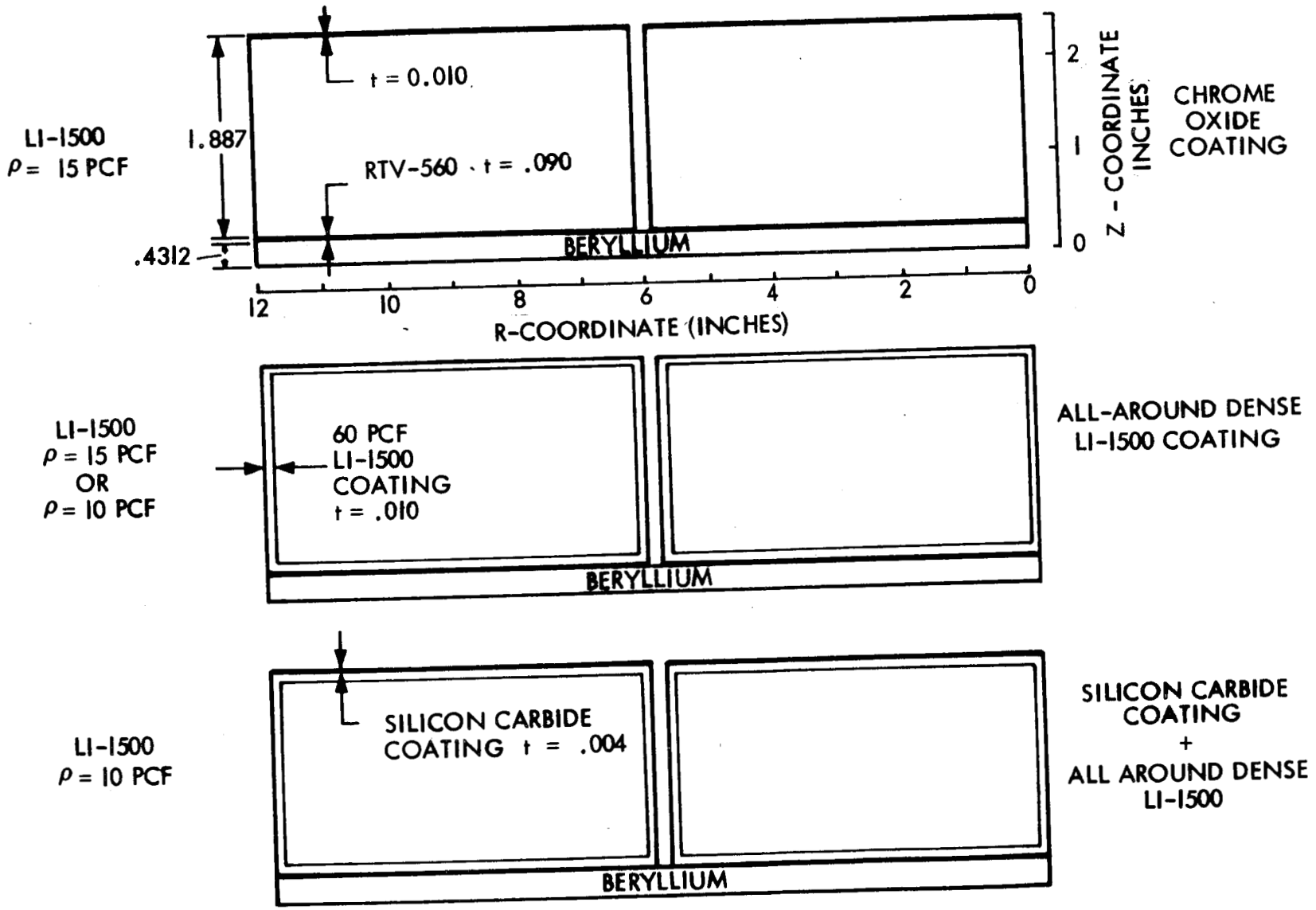


Fig. 2.2.3.2-40

DO6018

# STRESS PROFILE AT MAXIMUM LI-1500 SHEAR STRESS
## ($\rho$ LI-1500 = 15 PCF)

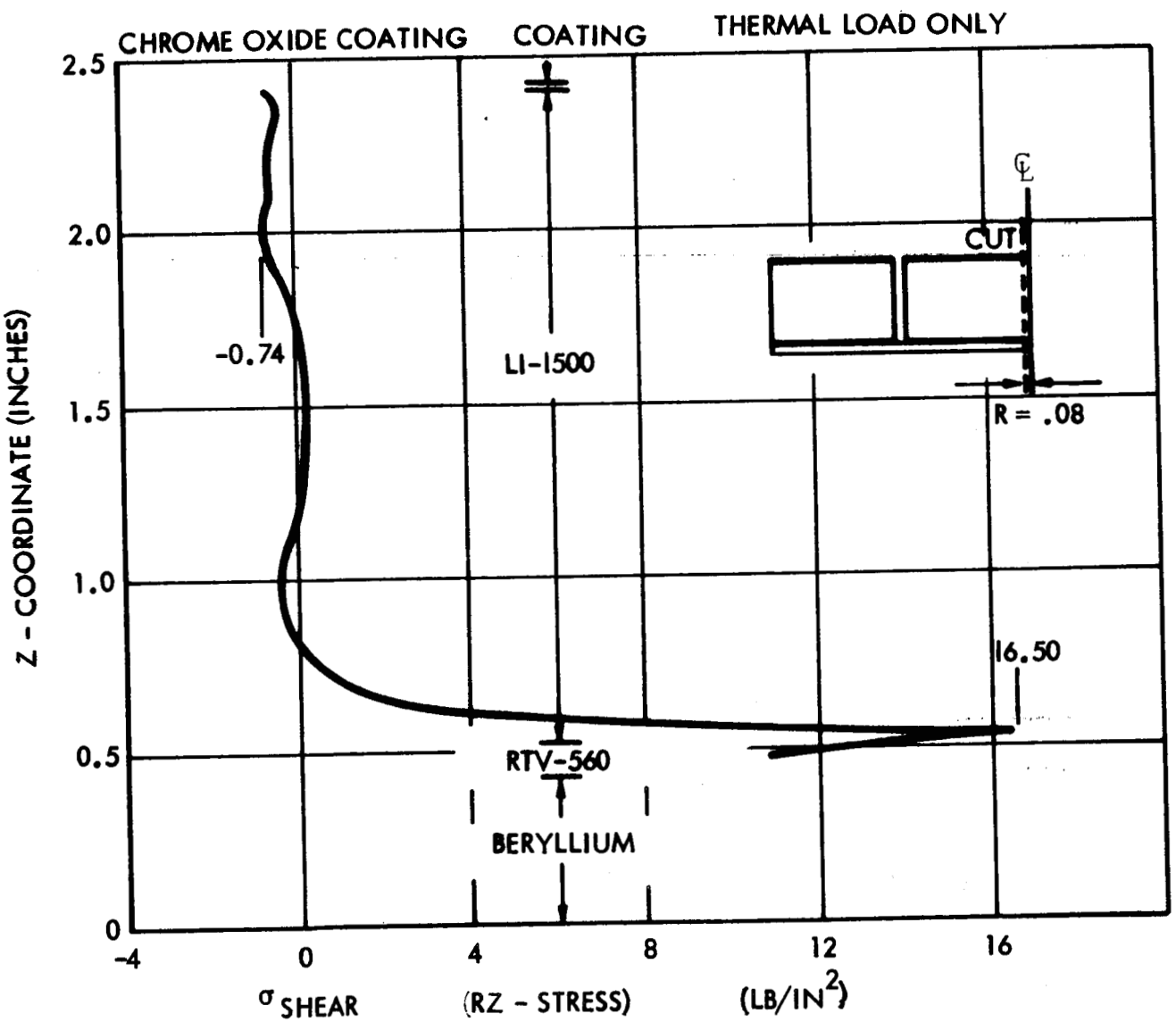


Fig. 2.2.3.2-41

# STRESS PROFILE AT MAX SHEAR STRESS

($\rho$ CORE = 15 PCF, $\rho$ COATING = 60 PCF)

MAX CORE SHEAR STRESS

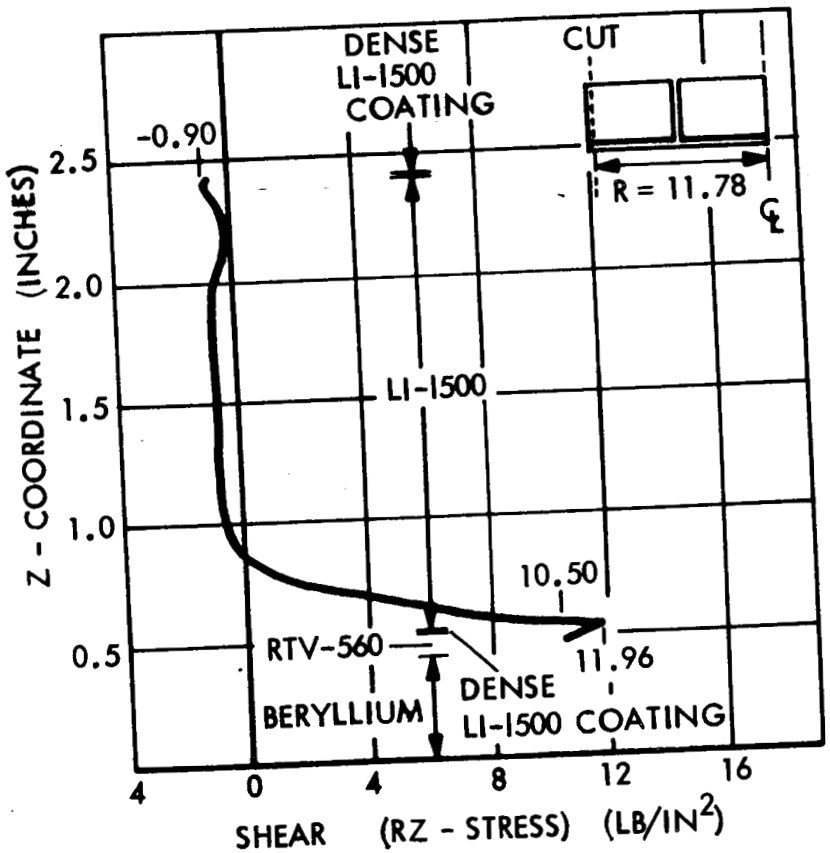


Fig. 2.2.3.2-42

MAX COATING SHEAR

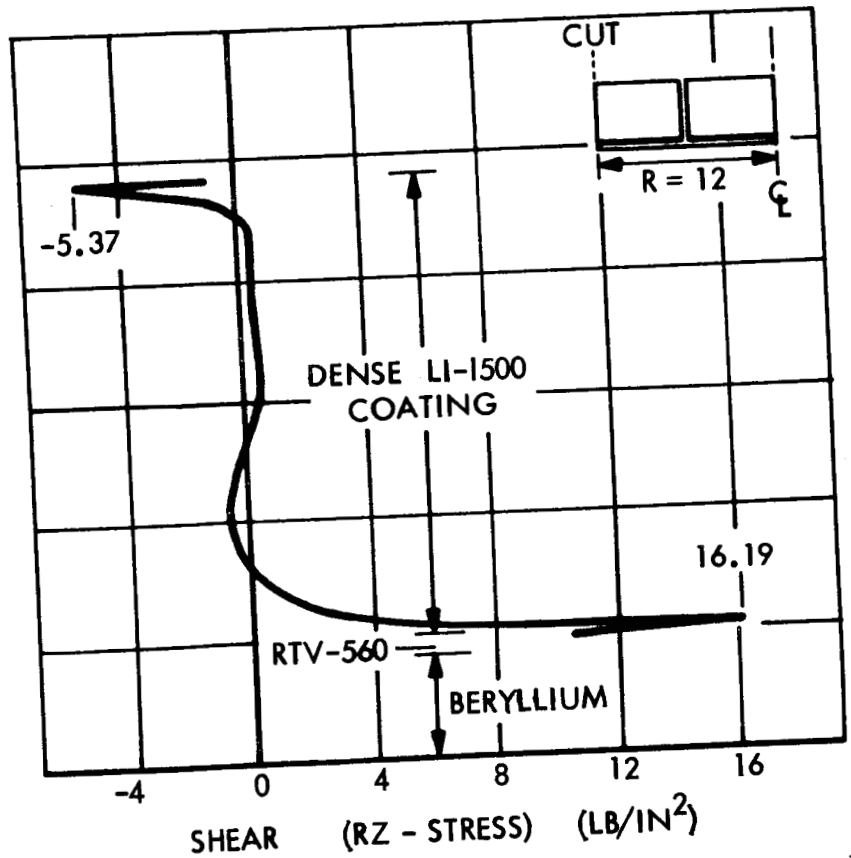


Fig. 2.2.3.2-43

DO6153

# STRESS PROFILE AT MAX SHEAR STRESS

($\rho$ CORE = 10 PCF, $\rho$ COATING = 60 PCF)

MAX CORE SHEAR

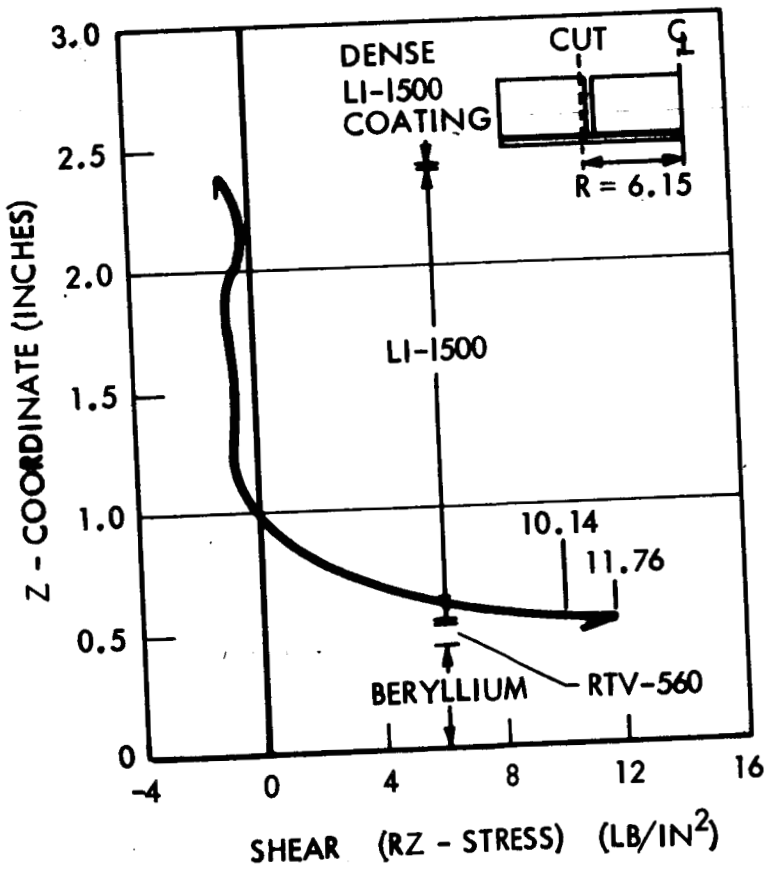


Fig. 2.2.3.2-44

MAX COATING SHEAR

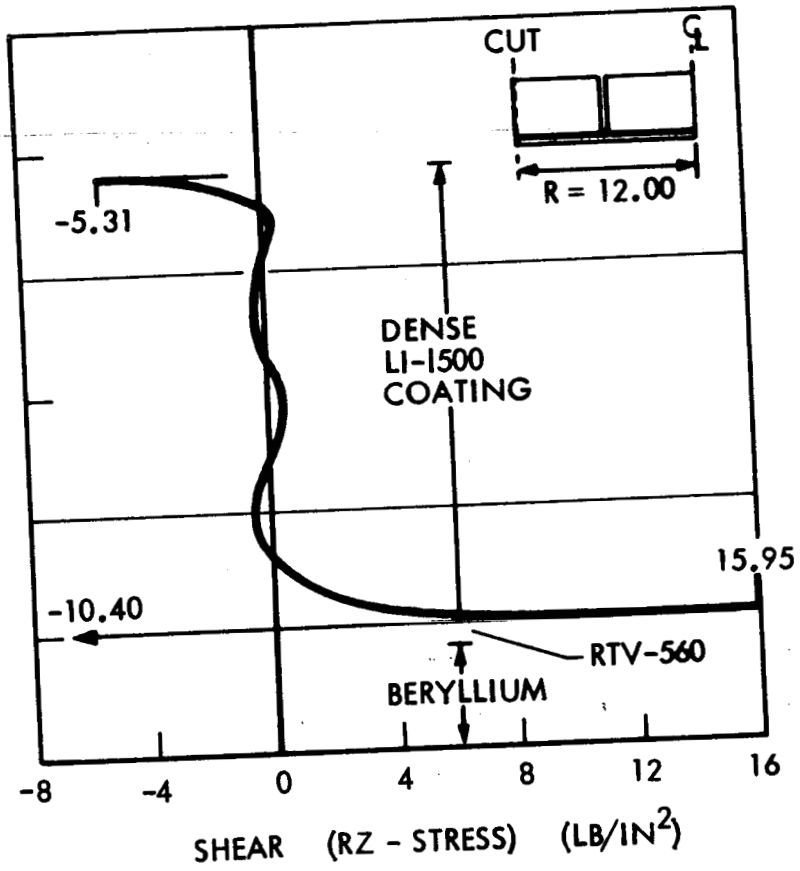


Fig. 2.2.3.2-45

DO6152

Table 2.2.3.2-11

# MAXIMUM STRESS SUMMARY - DENSIFICATION STUDY

BERYLLIUM PANEL - GROUND CONDITION
(75°F SURFACE TEMP., 600°F SUBSTRATE TEMP)

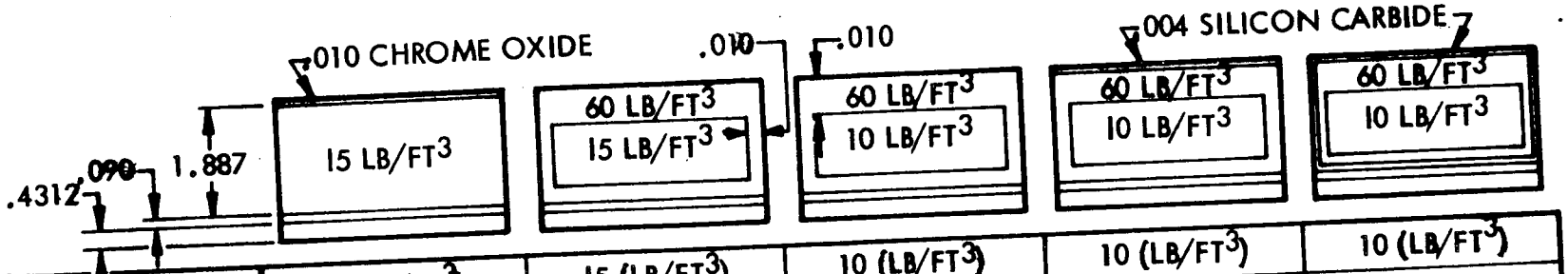


| DENSITY | 15 (LB/FT$^3$) | 15 (LB/FT$^3$) | 10 (LB/FT$^3$) | 10 (LB/FT$^3$) | 10 (LB/FT$^3$) |
|---|---|---|---|---|---|
| MAX. LI-1500 | 54 | 36 | 35 | 35 | 13 |
| MIN. LI-1500 | -39 | -6 | -6 | -4 | -2 |
| SHEAR LI-1500 | 17 | 12 | 12 | 12 | 3 |
| LONG. LI-1500 | 52 | 36 | 35 | 35 | 13 |
| PEEL LI-1500 | 5 | 5 | 5 | 4 | 2 |
| DENSITY | — | 60 (LB/FT$^3$) | 60 (LB/FT$^3$) | 60 (LB/FT$^3$) | 60 (LB/FT$^3$) |
| MAX. LI-1500 | — | 160 | 169 | 167 | 64 |
| MIN. LI-1500 | — | -54 | -53 | -54 | -12 |
| SHEAR LI-1500 | — | 16 | 16 | 16 | 7 |
| LONG. LI-1500 | — | 160 | 169 | 167 | 64 |
| PEEL LI-1500 | — | -52 | -52 | -52 | 2 |
| MAX. RTV-560 | 11 | 11 | 11 | 11 | 8 |
| MIN. RTV-560 | -20 | -20 | -20 | -20 | -22 |
| SHEAR RTV-560 | 11 | 11 | 11 | 11 | 12 |
| LONG. RTV-560 | -18 | -18 | -18 | -18 | -17 |
| PEEL RTV-560 | 7 | 6 | 7 | 7 | 2 |
| MAX. COATING | 9 | — | — | 15 | 3137 |
| MIN. COATING | -156 | — | — | -381 | -242 |

# STRESS PROFILE AT MAX SHEAR STRESS

LOCKHEED

($\rho$ CORE = 10 PCF, $\rho$ DENSE LI-1500 = 60 PCF)

MAX CORE SHEAR STRESS

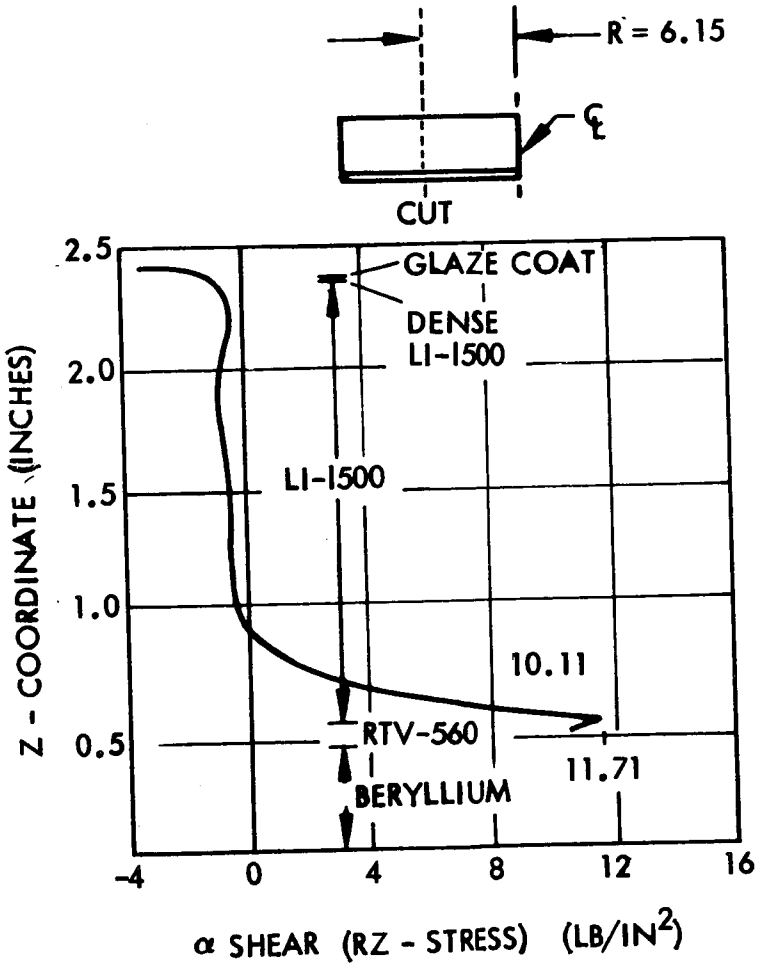


Fig. 2.2.3.2-46

MAX DENSE LI-1500 SHEAR STRESS

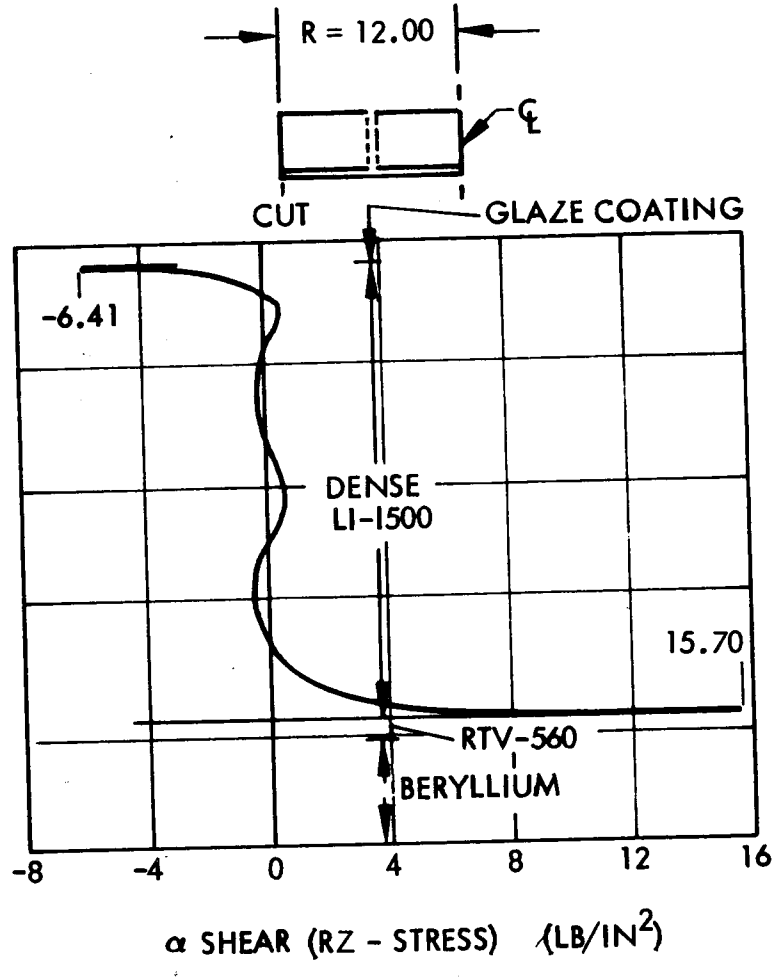


Fig. 2.2.3.2-47



DO6151

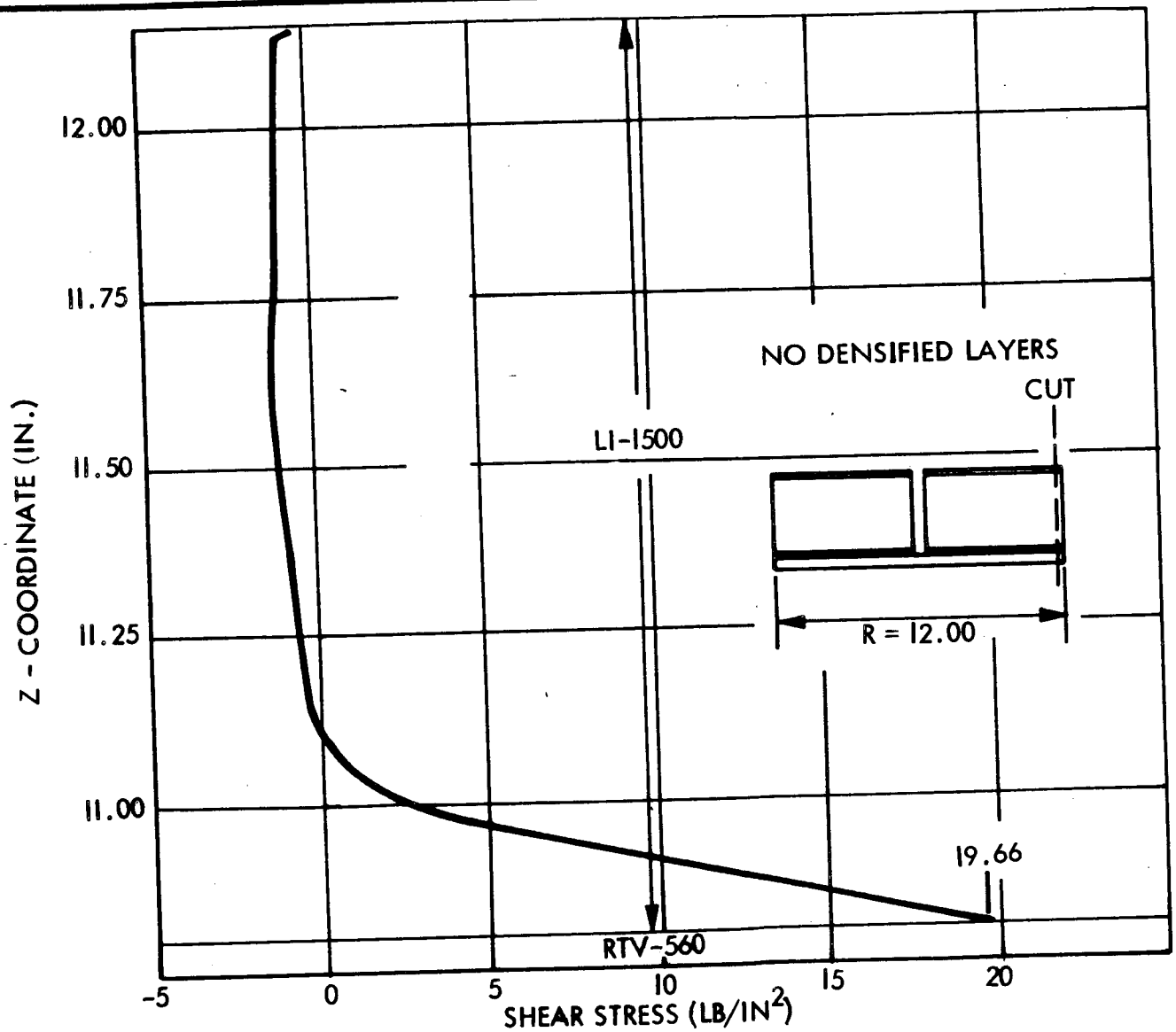
12.00
11.75
11.50
11.25
11.00
Z - COORDINATE (IN.)
-5
0
5
10
15
20
SHEAR STRESS (LB/IN$^2$)
NO DENSIFIED LAYERS
CUT
LI-1500
R = 12.00
19.66
RTV-560

Fig. 2.2.3.2-48

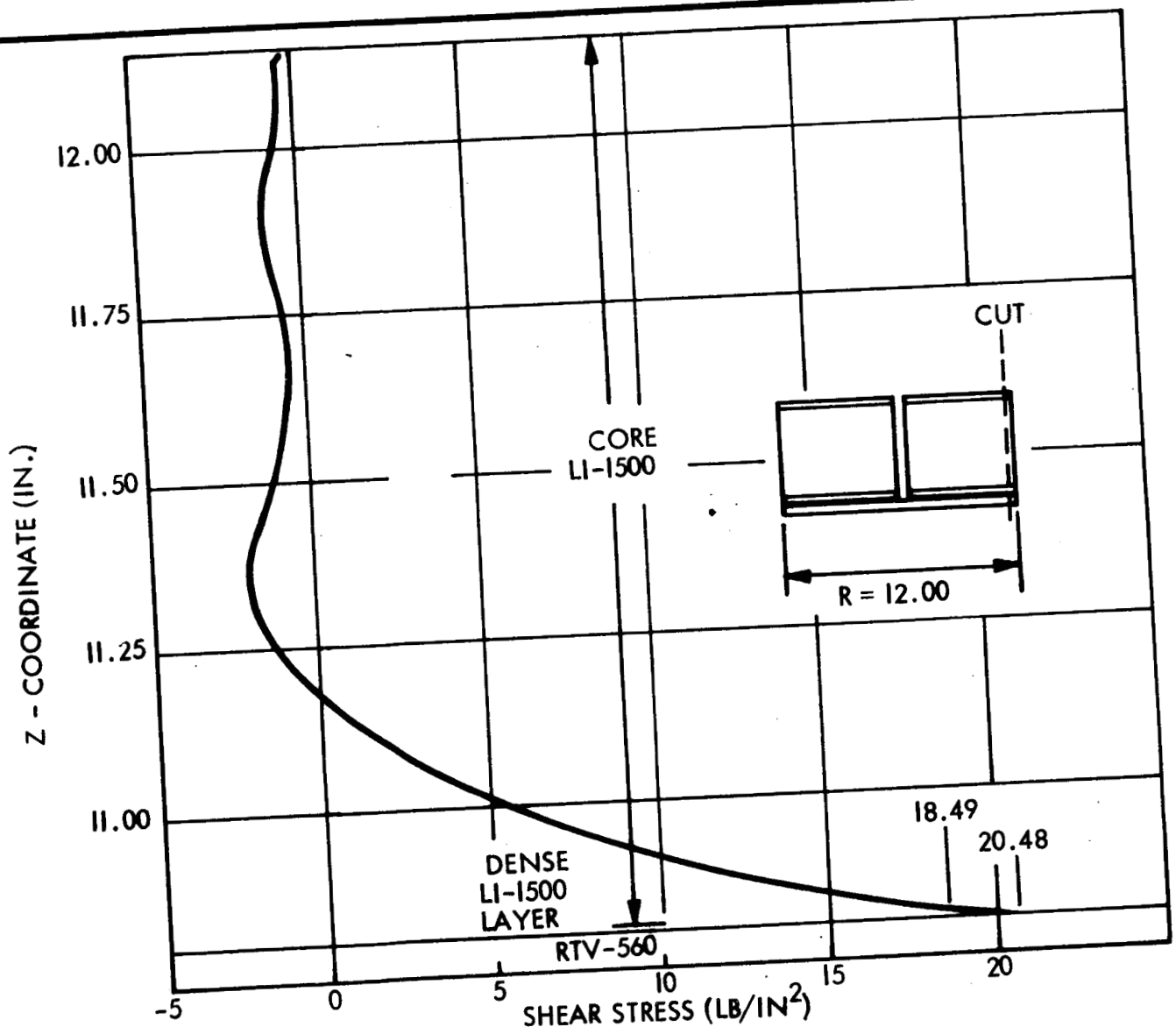
12.00
11.75
11.50
11.25
11.00
Z - COORDINATE (IN.)
CORE
LI-1500
CUT
R = 12.00
18.49
20.48
DENSE
LI-1500
LAYER
RTV-560
-5
0
5
10
15
20
SHEAR STRESS (LB/IN$^2$)

Fig. 2.2.3.2-49

Table 2.2.3.2-12

# MAXIMUM STRESS SUMMARY - DENSIFICATION STUDY

## ALUMINUM PANEL

1.5 PSI BURST PRESSURE

6000 PPI LINE LOAD

100°F SURFACE TEMP., 250°F SUBSTRATE TEMP.

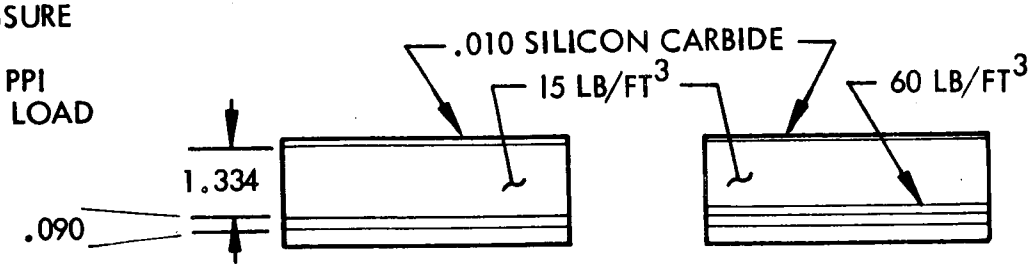


| DENSITY | 15 LB/FT$^3$ | 15 LB/FT$^3$ |
|---|---|---|
| MAX. LI-1500 | 68 | 63 |
| MIN. LI-1500 | -6 | -6 |
| SHEAR LI-1500 | 20 | 18 |
| LONG. LI-1500 | 68 | 63 |
| PEEL LI-1500 | 11 | 10 |
| **DENSITY** | | **60 LB/FT$^3$** |
| MAX. LI-1500 | — | 280 |
| MIN. LI-1500 | | -3 |
| SHEAR LI-1500 | | 20 |
| LONG. LI-1500 | | 280 |
| PEEL LI-1500 | | 10 |
| MAX. RTV-560 | 25 | 25 |
| MIN. RTV-560 | -15 | -16 |
| SHEAR RTV-560 | 18 | 18 |
| LONG. RTV-560 | -7 | -7 |
| PEEL RTV-560 | 12 | 11 |
| MAX. COATING | 0 | 0 |
| MIN. COATING | -191 | -176 |

thermal strain as beryllium does at 600°F. In addition, the aluminum substructure must also carry an in-plane line load which accounts for mechanical strain of the same order as the thermal strain. Hence, the aluminum panel results correspond to a substrate strain state roughly double that for the beryllium subpanel case.

The conclusion to be drawn from these studies is that all-around densification may be desirable for other reasons such as handling, but it will generally not offer significant stress reduction. In addition, the total system weight will be increased.

Environmental Variations. RSI component stresses have been investigated as a function of reentry time, using design flight loadings and temperatures. Results of this study are presented in Tables 2.2.3.2-13 and 2.2.3.2-14 and their companion Figs. 2.2.3.2-50 and 2.2.3.2-51, where coating stress is plotted as a function of reentry time for a beryllium flight panel and an aluminum flight panel. Maximum loads and surface temperatures used are shown in Figs. 2.2.3.2-52 and 2.2.3.2-53. In addition, the elastic modulus of fused silica, $E = 10.6 \times 10^6$ psi, has been used to simulate the worst possible case of coating modulus. Qualitatively, the coating first experiences compressive stresses, since only the coating is first heated and is restrained from expanding by the LI-1500. Later, as the LI-1500 begins to heat, the coating goes into tension due to the expansion of the LI-1500 being greater than that of the coating. Finally, as the substrate heats up with the surface cooling, the panel bows, again developing compressive coating stresses. The net effect of this thermal sequence in combination with applied loads results in a final net coating compression for the beryllium panel at 3600 sec. The aluminum panel experiences a relatively low net tensile stress in the coating at this time, due to high in-plane axial loads. Variations of other stresses in the RSI system are shown in the tables also as a function of time where it is noted that the ground condition, t = 3600 sec, is critical for the LI-1500.

Additional comparative data for 6- and 12-inch tiles with 0025 coating under thermal load only are shown in Table 2.2.3.2-15.

Conclusions – Parametric Studies. Parametric relationships have been established between mechanical properties, design details, and environmental conditions with their consequent effects on RSI system stress levels. These relationships can be summarized as follows:

Table 2.2.3.2-13

LOCKHEED

# BERYLLIUM FLIGHT PANEL #1

| TIME (SEC) | 500 | 800 | 1300 | 1700 | 2800 | 3600 |
|---|---|---|---|---|---|---|
| PRESSURE (PSI) | 0.0 | 0.0 | 0.0 | 2.25 | 3.0 | 3.0 |
| MAX. COAT | 104 | 172 | 206 | 133 | 47 | 24 |
| MIN. COAT | -134 | -175 | -172 | -141 | -386 | -560 |
| MAX. LI-1500 | 5 | 6 | 17 | 35 | 65 | 68 |
| MIN. LI-1500 | -14 | -13 | -12 | -10 | -8 | -8 |
| SHEAR LI-1500 | 2 | 3 | 3 | 6 | 15 | 17 |
| LONG. LI-1500 | -14 | -13 | 17 | 35 | 65 | 68 |
| PEEL LI-1500 | 1 | 1 | 1 | 1 | 6 | 6 |
| MAX. RTV-560 | 1 | 1 | 0 | 3 | 15 | 18 |
| MIN. RTV-560 | -2 | -2 | -5 | -11 | -23 | -25 |
| SHEAR RTV-560 | 0 | 0 | 2 | 5 | 15 | 17 |
| LONG. RTV-560 | -1 | -2 | -4 | -9 | -17 | -18 |
| PEEL RTV-560 | 1 | 1 | 0 | 1 | 8 | 9 |

$t_{COATING} = 0.010$

$t_{LI-1500} = 1.45$

$t_{RTV-560} = 0.050$

$t_{Be} = 0.4312$

$E_{COATING} = 10.6 \times 10^6$ PSI

DO5966

Table 2.2.3.2-14

LOCKHEED

# ALUMINUM FLIGHT PANEL #2

| TIME (SEC) | 500 | 800 | 1300 | 1700 | 2500 | 3600 | 6700 |
|---|---|---|---|---|---|---|---|
| COLLAPSE PRESSURE (PSI) | 0 | 0 | 0 | 2.25 | 2.25 | 3.00 | 0 |
| TENS LOAD | 450 | 450 | 450 | 2400 | 2400 | 6000 | 0 |
| MAX. COAT | 2701 | 162 | 285 | 300 | 245 | 94 | 18 |
| MIN. COAT | 3641 | -200 | -195 | -195 | -148 | -57 | -9 |
| MAX. LI-1500 | 5 | 3 | 3 | 15 | 21 | 50 | 20 |
| MIN. LI-1500 | -13 | -13 | -13 | -10 | -5 | -9 | -3 |
| SHEAR LI-1500 | 1 | 4 | 5 | 4 | 5 | 13 | 7 |
| LONG LI-1500 | -13 | -12 | -11 | 15 | 21 | 50 | 20 |
| PEEL LI-1500 | 1 | 2 | 2 | 2 | 2 | 3 | 18 |
| MAX RTV | 1 | 1 | 1 | 4 | 5 | 13 | 4 |
| MIN RTV | -1 | -1 | -1 | -4 | -6 | -14 | -9 |
| SHEAR RTV | 1 | 1 | 1 | 4 | 5 | 13 | 5 |
| LONG RTV | 0 | 0 | 0 | 1 | -2 | -4 | 8 |
| PEEL RTV | 0 | 0 | 0 | 1 | 1 | 3 | 2 |

$t_{COATING} = 0.010$

$t_{LI-1500} = 2.524$

$t_{RTV-560} = 0.090$

$t_{AL} = 0.711$

$E_{COATING} = 10.6 \times 10^6$ PSI

DO5965

# COATING STRESS AT VARIOUS TEMPERATURE PROFILES AND LOADS

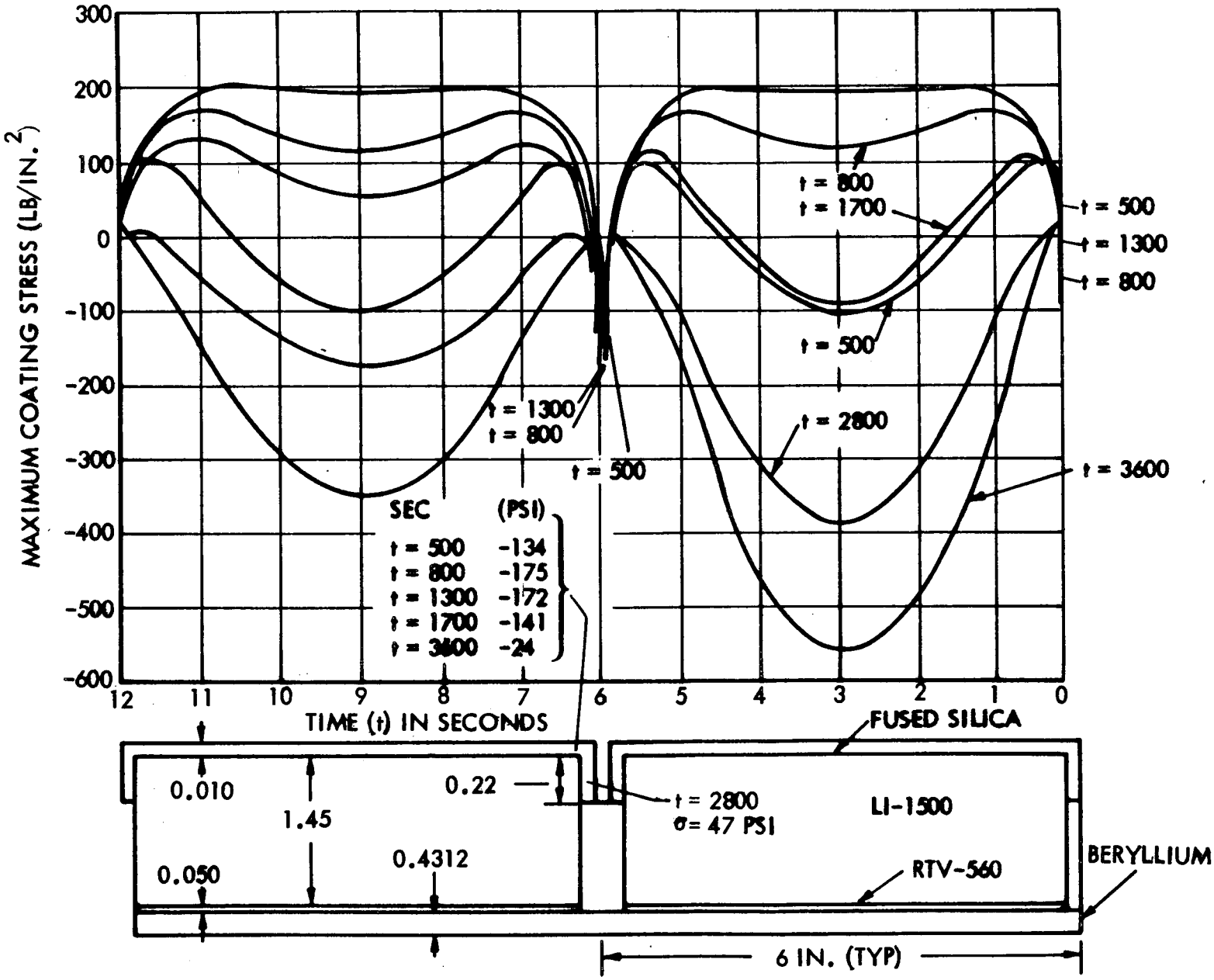


Fig. 2.2.3.2-50

# COATING STRESS AT VARIOUS TEMPERATURE PROFILES AND LOADS

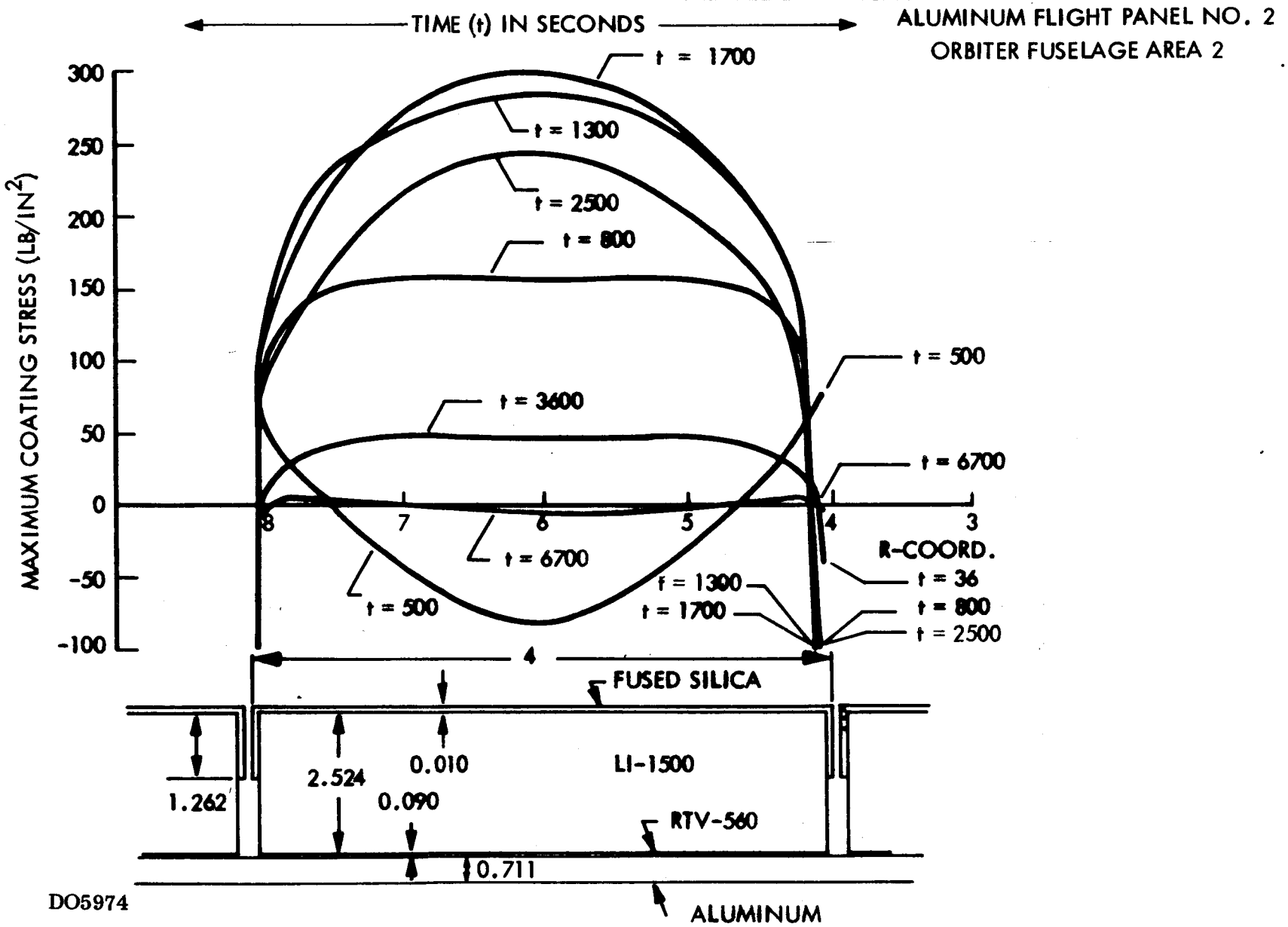


Fig. 2.2.3.2-51

# LI-1500 TEMPERATURE DISTRIBUTION FLIGHT

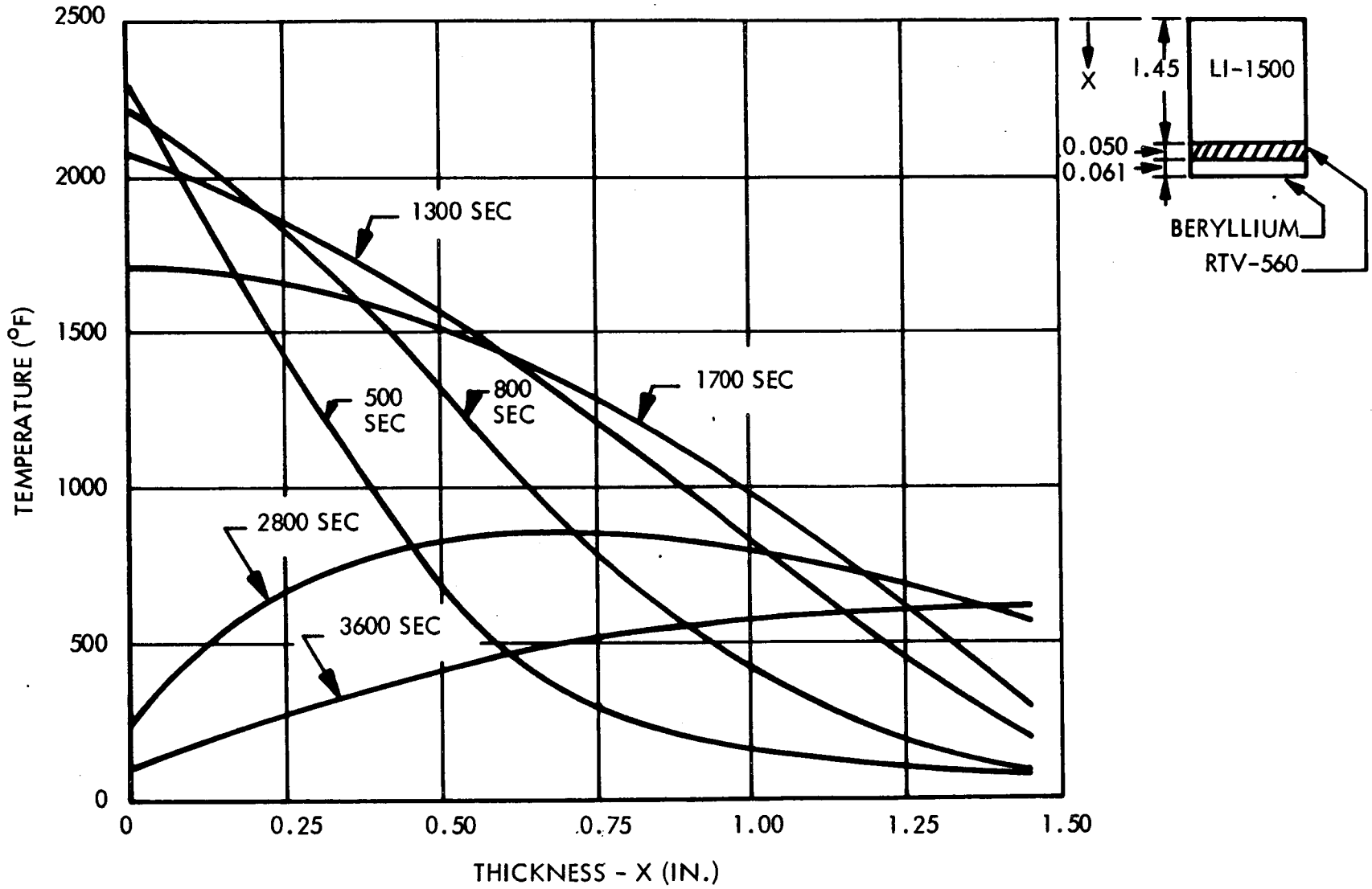


Fig. 2.2.3.2-52

# LI-1500 TEMPERATURE DISTRIBUTION
# ALUMINUM FLIGHT PANEL NO. 2

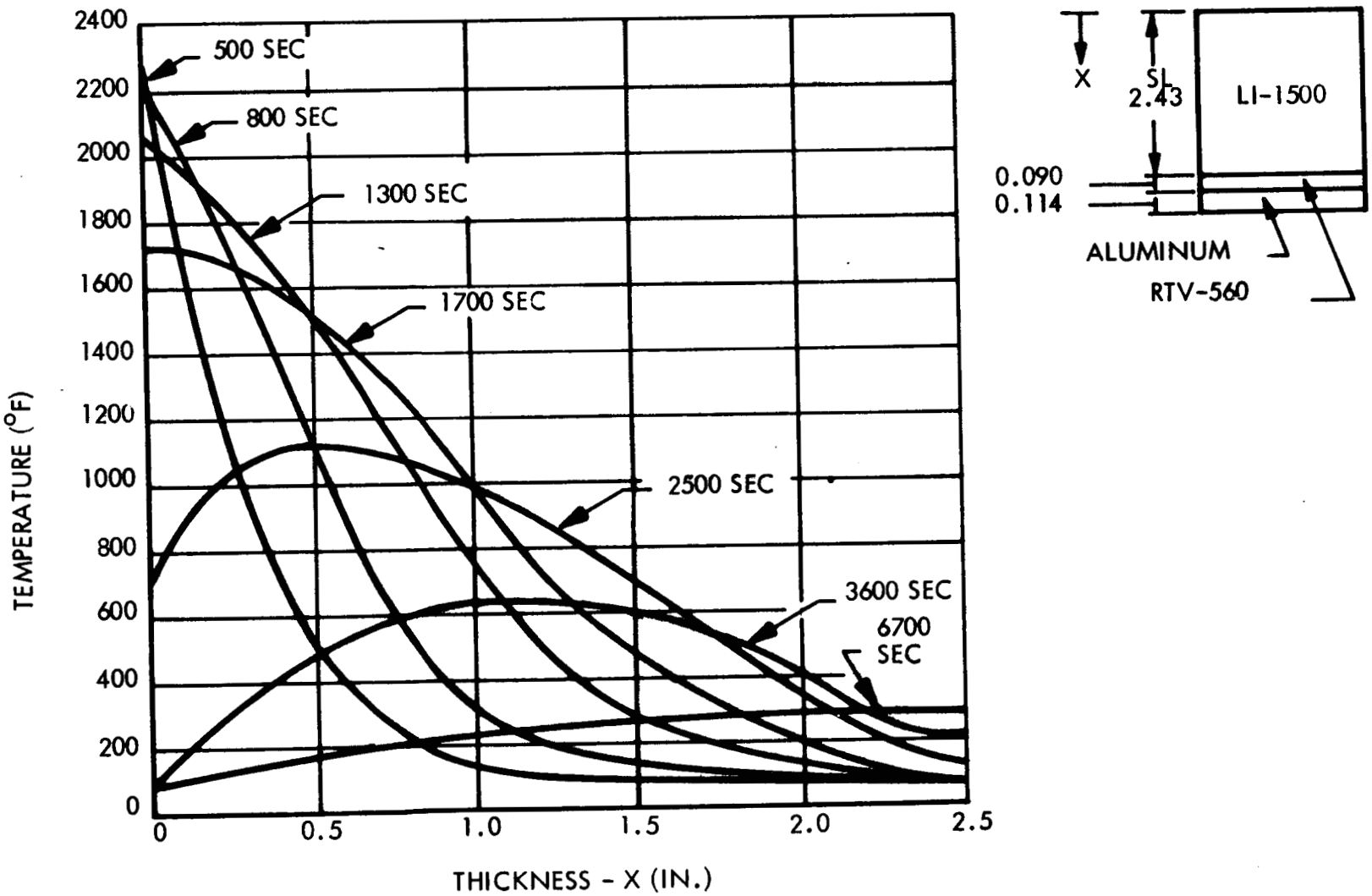


Fig. 2.2.3.2-53

Table 2.2.3.2-15

# FUSELAGE BERYLLIUM PANEL COATING STRESSES AT MAXIMUM HEAT IMPULSE – NO MECHANICAL LOAD

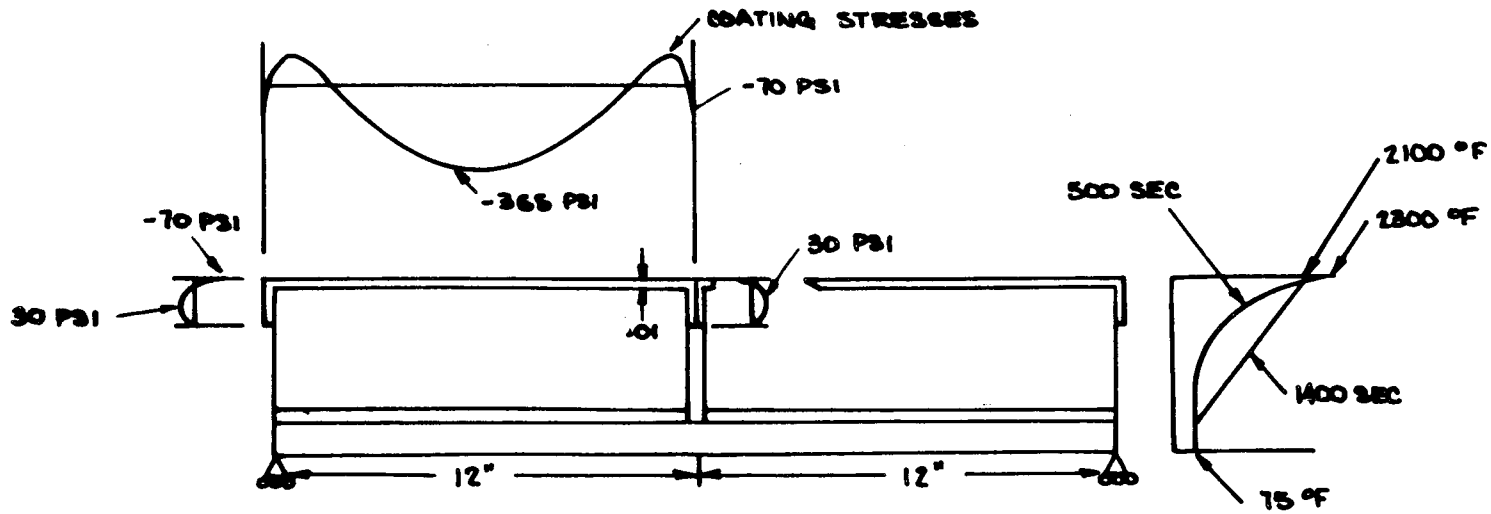


MAXIMUM STRESSES IN PANELS (PSI)

| QUANTITY | 12-IN. TILE TEST PANEL (t = 500 SEC) | 6-IN. TILE FLIGHT PANEL (t = 500 SEC) | 6-IN. TILE FLIGHT PANEL (t = 1400 SEC) |
|---|---|---|---|
| MAXIMUM COATING | 110 | 80 | 155 |
| MINIMUM COATING | -365 | -140 | - 75 |
| MAXIMUM LI-1500 | 7 | 6 | 7 |
| MIMUMUM LI-1500 | -19 | -15 | -11 |
| SHEAR LI-1500 | 2 | 3 | 3 |
| LONG. LI-1500 | -19 | -15 | -11 |
| PEEL LI-1500 | 1 | 1 | 2 |
| MAXIMUM RTV-560 | 1 | 1 | 1 |
| MINIMUM RTV-560 | -4 | -2 | -3 |
| SHEAR RTV-560 | 0 | 0 | 0 |
| LONG. RTV-560 | -2 | -1 | -1 |
| PEEL RTV-560 | 1 | 1 | 1 |

$E_{COATING} = 3.5 \times 10^6$ PSI

D05152 (1)
rdb

- RSI system stresses vary directly with tile length.
- RSI system stresses vary inversely with bond thickness.
- RSI stresses vary directly with modulus of elasticity of the material.
- Coating stresses vary inversely with RSI modulus of elasticity.
- Thickness of RSI material does not appreciably alter RSI stresses. However, coating stresses vary inversely with RSI thickness.
- Coating stresses vary inversely with coating thickness. Other stresses in the RSI are not affected.
- Coating stresses vary directly with coating modulus of elasticity.
- Integral coating (densified insulation material) is structurally feasible.
- Reduction in bond modulus of elasticity reduces RSI system stresses.
- Bond discontinuity at tile joints reduces RSI stresses appreciably.
- Partial bond strain isolation technique is sound from a structural point of view.
- Textured coatings do not appreciably lower coating stresses.
- Intentional cracks (discontinuities) in the coating decrease coating stresses. However, RSI stresses are increased considerably due to stress concentration effects. Both stresses approach zero as the number of discontinuities in the coating is increased.
- Stresses in the RSI system are mainly due to inplane deformation of the substrate (mechanical and/or thermal loading).
- Common metal mechanical fasteners inserted in LI-1500 induce large stresses due to difference in thermal expansion properties.
- Ground condition is the worst case for LI-1500 stresses.

For convenience, some of the more important relationships are presented in Table 2.2.3.2-16.

Table 2.2.3.2-16

# PARAMETRICALLY ESTABLISHED RELATIONSHIPS

| | |
|---|---|
| LI-1500 MODULUS ↑ | ↑ LI-1500 SHEAR STRESS<br>↔ RTV-560 PEEL STRESS<br>↑ LI-1500 MAX STRESS<br>↓ COATING STRESS<br>↑ RTV-560 SHEAR STRESS |
| LI-1500 THICKNESS ↑ | ↔ LI-1500 SHEAR STRESS<br>↔ LI-1500 MAX STRESS<br>↔ RTV-560 PEEL STRESS<br>↔ RTV-560 SHEAR STRESS |
| RTV-560 THICKNESS ↑ | ↓ LI-1500 STRESSES<br>↓ RTV-560 STRESSES<br>↓ COATING STRESS |
| COATING THICKNESS ↑ | COATING STRESS<br>↔ RTV-560 STRESSES<br>↔ LI-1500 SHEAR |
| COATING MODULUS ↑ | ↑ COATING STRESS |
| TILE SIZE ↑ | ↑ LI-1500 SHEAR STRESS<br>↑ LI-1500 MAX STRESS<br>↑ LI-1500 PEEL STRESS<br>↑ RTV-560 PEEL STRESS<br>↑ RTV-560 SHEAR STRESS |

2.2.3.3 Prototype Panel Design. This section summarizes the final design of tile size and bond thickness for the deliverable prototype panels. As discussed in the introduction to Section 2.2 and elaborated upon in Task 4, LI-1500 conductivity is a function of environmental pressure. Different LI-1500 thicknesses are therefore required for a "flight" panel as opposed to a "test" panel, so eight panel designs are to be discussed here.

At this point in the design the metallic substrate has already been determined according to Section 2.2.1 and LI-1500 thickness/bond thickness requirements have been determined in the form of the heat sink tradeoff factor discussed in Section 2.2.2. The final step in the design process then consists of choosing a balanced set of LI-1500 and bond thicknesses in conjunction with a tile length which also satisfies stress allowables.

LI-1500 design properties are summarized in Table 2.2.3.3-1 and final analysis results for the eight prototype panels are given in Tables 2.2.3.3-2 through 2.2.3.3-9. Table 2.2.3.3-10 summarizes required RSI system thicknesses and lists weight comparisons between flight and test prototype panels.

As compared with preliminary designs presented in LMSC-A995708, tile length has been increased for all panels. For the beryllium and titanium panels, bond modulus at elevated temperature ($500^{\circ}$) is now used, which is in contrast to the room temperature properties temporarily assumed previously. Test data given in Table 3.3-1 show reduced moduli at temperature, hence strain isolation of the RSI tile is improved. Consistency of the $600^{\circ}$ data in the table is in question, so use of the $500^{\circ}$ modulus lends some conservatism to the results. For the aluminum panels room temperature properties of RTV-560 were used as before due to lack of data at $250^{\circ}$ and $300^{\circ}$, again leading to a degree of conservatism. Increase in tile length for these panels was permissible since the LI-1500 weak direction shear allowable is actually larger than previously reported in LMSC-A995708. Of course this increase in a critical design parameter also contributes to the longer tile lengths selected for the beryllium and titanium panels.

Table 2.2.3.3-1

# LI-1500 INSULATION SYSTEM DESIGN PROPERTIES

(ROOM TEMPERATURE UNLESS OTHERWISE NOTED)

| PROPERTY (ULTIMATE) | | LI-1500 STRONG DIRECTION | LI-1500 WEAK DIRECTION | RTV-560 BOND | LI-0042 COATING | LI-0025 COATING |
|---|---|---|---|---|---|---|
| TENSION (PSI | | 70 | 15 | 800 | > 2000 | 600 |
| TENSILE MODULUS (PSI) | | 60,000 | 6,000 | 300 | $<9.2 \times 10^6$ | $3.5 \times 10^6$ |
| COMPRESSION (PSI) | | 150 | 40 | - | > 2000 | >>600 |
| COMPRESSION MODULUS (PSI) | | 50,000 | 5,000 | - | $<9.2 \times 10^6$ | $3.5 \times 10^6$ |
| SHEAR (PSI) | | 40 | 25 | 400 | - | |
| SHEAR MODULUS (PSI) | | 20,000 | 4,000 | 100 | $<3.7 \times 10^6$ | $1.4 \times 10^6$ |
| | | PARALLEL TO FIBER | PERPENDICULAR TO FIBER | | | |
| THERMAL EXPANSION (IN./IN./°F) | | $3.0 \times 10^{-7}$ | $3.0 \times 10^{-7}$ | $1.14 \times 10^{-4}$ | $2.0 \times 10^{-7}$ | $2 \times 10^{-7}$ |
| HEAT CAPACITY (BTU/LB-°F) | (RT) | 0.15 | 0.15 | 0.30 | - | |
| | (2000°F) | 0.32 | 0.32 | - | | |
| THERMAL CONDUCTIVITY (BTU-IN./FT²-HR-°F) ~1 ATMOSPHERE | (RT) | 0.35 | - | 2.16 | - | |
| | (2000°F) | 1.56 | - | - | | |
| THERMAL CONDUCTIVITY (BTU-IN./FT² HR-°F) ~VACUUM | (RT) | 0.17 | - | - | - | |
| | (2000°F) | 0.67 | | | | |
| EMITTANCE | (RT) | - | - | - | 0.85 | 0.85 |
| | (2000°F) | - | - | - | 0.93 | 0.63 |

D05165
rdb

Table 2.2.3.3-2

LOCKHEED

# BERYLLIUM TEST PANEL NO. 1
# ORBITER FUSELAGE AREA 2

COATING THICK = 0.010 IN. LI-1500 THICK = 1.887 IN. RTV-560 THICK = 0.090 IN. TILE LENGTH = 12

| LOADING CONDITIONS | | | 6.75 COLLAPSE | 3 COLLAPSE | 1.5 BURST | |
|---|---|---|---|---|---|---|
| | | PRESSURE (PSI) | 0 | 0 | 0 | 0 |
| | | AXIAL LOAD (PPI) | 0 | 0 | 0 | 0 |
| TEMPERATURE | | SURFACE (°F) | 75 | 100 | 100 | 75 |
| | | BACKFACE (°F) | 75 | 550 | 550 | 600 |
| MAXIMUM STRESSES (PSI) | LI-1500 | PRIN. TEN. | 31 | 61 | 39 | |
| | | PRIN. COMP. | - 21 | - 28 | - 25 | |
| | | SHEAR | 8 | 14 | 13 | |
| | | LONG. | 31 | 61 | 38 | |
| | | NORMAL TEN. | 5 | 1 | 11 | |
| | | NORMAL COMP. | - 17 | - 9 | - 3 | |
| | RTV-560 | PRIN. TEN. | 6 | 7 | 17 | |
| | | PRIN. COMP. | - 20 | - 17 | - 15 | |
| | | SHEAR | 4 | 10 | 12 | |
| | | LONG. | - 9 | - 12 | - 13 | |
| | | PEEL | 5 | 1 | 11 | |
| | COATING | PRIN. TEN. | 1 | 17 | 569 | |
| | | PRIN. COMP. | -2012 | -791 | 0 | |

| MATERIAL PROPERTIES | E (PSI) | G (PSI) | $\mu$ | $\alpha$ (IN./IN./F°) |
|---|---|---|---|---|
| COATING | $9.1 \times 10^6$ | $3.9 \times 10^6$ | 0.17 | $0.2 \times 10^{-6}$ |
| LI-1500 | 60,000 (L), 6,000 (T) | 4150 | 0.3 | $0.3 \times 10^{-6}$ |
| RTV-560 | 300 (RT) - 200 (500°F-600°F) | 100 (RT) - 67 (500°F-600°F) | 0.5 | $115.0 \times 10^{-6}$ |
| SUBSTRATE | $42 \times 10^6$ (RT) - $37.2 \times 10^6$ (600°F) | $20 \times 10^6$ (RT) - $18.8 \times 10^6$ (600°F) | 0.1 | $5.75 \times 10^{-6}$ (RT) - $7.7 \times 10^{-6}$ (600°F) |

Table 2.2.3.3-3

# ALUMINUM TEST PANEL NO. 2
# ORBITER FUSELAGE AREA 2

COATING THICK = 0.010 IN. LI-1500 THICK = 3.396 IN. RTV-560 THICK = 0.090 IN. TILE LENGTH = 6

| LOADING CONDITIONS | | PRESSURE (PSI)<br>AXIAL LOAD (PPI) | 6.75 COLLAPSE<br>2250<br>COMPRESSION | 3 COLLAPSE<br>3000<br>COMPRESSION | 1.5 BURST<br>6000<br>TENSION | 0<br>0 |
|---|---|---|---|---|---|---|
| TEMPERATURE | | SURFACE (°F)<br>BACKFACE (°F) | 75<br>75 | 100<br>250 | 100<br>250 | 75<br>300 |
| MAXIMUM STRESSES (PSI) | LI-1500 | PRIN. TEN. | 5 | 15 | 61 | 24 |
| | | PRIN. COMP. | - 18 | - 10 | - 27 | - 16 |
| | | SHEAR | 8 | 4 | 19 | 9 |
| | | LONG. | - 12 | 14 | 61 | 24 |
| | | NORMAL TEN. | 4 | 2 | 8 | 2 |
| | | NORMAL COMP. | - 8 | - 4 | - 5 | - 2 |
| | RTV-560 | PRIN. TEN. | 4 | 2 | 22 | 6 |
| | | PRIN. COMP. | - 13 | - 9 | - 17 | - 10 |
| | | SHEAR | 6 | 2 | 18 | 7 |
| | | LONG. | - 5 | - 8 | - 6 | - 7 |
| | | PEEL | 4 | 2 | 8 | 3 |
| | COATING | PRIN. TEN. | 0 | 58 | 32 | 6 |
| | | PRIN. COMP. | - 14 | 0 | - 1 | - 5 |

| MATERIAL PROPERTIES | E (PSI) | G (PSI) | $\mu$ | $\alpha$ (IN./IN./F°) |
|---|---|---|---|---|
| COATING | $9.1 \times 10^6$ | $3.9 \times 10^6$ | 0.17 | $0.2 \times 10^{-6}$ |
| LI-1500 | 60,000 (L), 6,000 (T) | 4150 | 0.3 | $0.3 \times 10^{-6}$ |
| RTV-560 | 300 (RT – 300°F) | 100 (RT – 300°F) | 0.5 | $115.0 \times 10^{-6}$ |
| SUBSTRATE | $10.5 \times 10^6$ (RT) - $9.15 \times 10^6$ (300°F) | $4.2 \times 10^6$ (RT) - $3.66 \times 10^6$ (300°F) | 0.3 | $13.1 \times 10^{-6}$ (RT) - $13.5 \times 10^{-6}$ (300°F) |

Table 2.2.3.3-4

# ALUMINUM TEST PANEL NO. 3
# ORBITER FUSELAGE AREA 1

COATING THICK = 0.010 IN. LI-1500 THICK = 1.846 IN. RTV-560 THICK = 0.090 IN. TILE LENGTH = 6

| LOADING CONDITIONS | | PRESSURE (PSI)<br>AXIAL LOAD (PPI) | 3.75 COLLAPSE<br>3150<br>COMPRESSION | 3 COLLAPSE<br>3000<br>COMPRESSION | 1.5 BURST<br>6000<br>TENSION | 0<br>0 |
|---|---|---|---|---|---|---|
| TEMPERATURE | | SURFACE (°F)<br>BACKFACE (°F) | 75<br>75 | 100<br>250 | 100<br>250 | 75<br>300 |
| MAXIMUM STRESSES (PSI) | LI-1500 | PRIN. TEN. | 7 | 16 | 56 | 25 |
| | | PRIN. COMP. | - 17 | - 6 | - 27 | - 17 |
| | | SHEAR | 7 | 3 | 16 | 9 |
| | | LONG. | - 14 | 16 | 56 | 25 |
| | | NORMAL TEN. | 2 | 1 | 7 | 3 |
| | | NORMAL COMP. | - 5 | - 3 | - 6 | - 3 |
| | RTV-560 | PRIN. TEN. | 3 | 1 | 20 | 7 |
| | | PRIN. COMP. | - 10 | - 8 | - 14 | - 10 |
| | | SHEAR | 6 | 1 | 16 | 7 |
| | | LONG. | - 3 | - 8 | - 6 | - 7 |
| | | PEEL | 2 | 1 | 8 | 3 |
| | COATING | PRIN. TEN. | 27 | 49 | 12 | 1 |
| | | PRIN. COMP. | - 21 | 0 | -103 | -101 |

| MATERIAL PROPERTIES | E (PSI) | G (PSI) | $\mu$ | $\alpha$ (IN./IN./F°) |
|---|---|---|---|---|
| COATING | $9.1 \times 10^6$ | $3.9 \times 10^6$ | 0.17 | $0.2 \times 10^{-6}$ |
| LI-1500 | 60,000 (L), 6,000 (T) | 4150 | 0.3 | $0.3 \times 10^{-6}$ |
| RTV-560 | 300 (RT – 300°F) | 100 (RT – 300°F) | 0.5 | $115.0 \times 10^{-6}$ |
| SUBSTRATE | $10.5 \times 10^6$ (RT) – $9.15 \times 10^6$ (300°F) | $4.2 \times 10^6$ (RT) – $3.66 \times 10^6$ (300°F) | 0.3 | $13.1 \times 10^{-6}$ (RT) – $13.5 \times 10^{-6}$ (300°F) |

Table 2.2.3.3-5

# TITANIUM TEST PANEL NO. 4
# ORBITER FUSELAGE AREA 2

COATING THICK = 0.010 IN. LI-1500 THICK = 2.000 IN. RTV-560 THICK = 0.090 IN. TILE LENGTH = 6

| LOADING CONDITIONS | | PRESSURE (PSI)<br>AXIAL LOAD (PPI) | 6.75 COLLAPSE<br>2250<br>COMPRESSION | 3 COLLAPSE<br>3000<br>COMPRESSION | 1.5 BURST<br>6000<br>TENSION | 0<br>0 |
|---|---|---|---|---|---|---|
| TEMPERATURE | | SURFACE (°F)<br>BACKFACE (°F) | 75<br>75 | 100<br>550 | 100<br>550 | 75<br>600 |
| MAXIMUM STRESSES (PSI) | LI-1500 | PRIN. TEN.<br>PRIN. COMP.<br>SHEAR<br>LONG.<br>NORMAL TEN.<br>NORMAL COMP. | 5<br>- 16<br>6<br>- 12<br>3<br>- 7 | 27<br>- 11<br>6<br>26<br>1<br>- 2 | 48<br>- 28<br>15<br>48<br>6<br>- 5 | 30<br>- 18<br>9<br>27<br>2<br>- 2 |
| | RTV-560 | PRIN. TEN.<br>PRIN. COMP.<br>SHEAR<br>LONG.<br>PEEL | 4<br>- 12<br>5<br>- 4<br>3 | 1<br>- 13<br>0<br>- 13<br>1 | 13<br>- 16<br>13<br>- 11<br>5 | 3<br>- 13<br>5<br>- 12<br>2 |
| | COATING | PRIN. TEN.<br>PRIN. COMP. | 1<br>- 93 | 95<br>0 | 37<br>- 15 | 3<br>- 63 |

| MATERIAL PROPERTIES | E (PSI) | G (PSI) | $\mu$ | $\alpha$ (IN./IN./F°) |
|---|---|---|---|---|
| COATING | $9.1 \times 10^6$ | $3.9 \times 10^6$ | 0.17 | $0.2 \times 10^{-6}$ |
| LI-1500 | 60,000 (L), 6,000 (T) | 4150 | 0.3 | $0.3 \times 10^{-6}$ |
| RTV-560 | 300 (RT) - 200 (500°-600°F) | 100 (RT) - 67 (500°-600°F) | 0.5 | $115.0 \times 10^6$ |
| SUBSTRATE | $16.0 \times 10^6$ (RT) - $13.1 \times 10^6$ (600°F) | $6.4 \times 10^6$ (RT) - $5.2 \times 10^6$ (600°F) | 0.3 | $5.8 \times 10^{-6}$ (RT – 600°F) |

Table 2.2.3.3-6

# BERYLLIUM FLIGHT PANEL NO. 1
# ORBITER FUSELAGE AREA 2

COATING THICK = 0.010 IN. LI-1500 THICK = 1.224 IN. RTV-560 THICK = 0.090 IN. TILE LENGTH = 12

| LOADING CONDITIONS | | PRESSURE (PSI)<br>AXIAL LOAD | 6.75 COLLAPSE<br>0 | 3 COLLAPSE<br>0 | 1.5 BURST<br>0 | 0<br>0 |
|---|---|---|---|---|---|---|
| TEMPERATURE | | SURFACE (°F)<br>BACKFACE (°F) | 75<br>75 | 100<br>550 | 100<br>550 | 75<br>600 |
| MAXIMUM STRESSES (PSI) | LI-1500 | PRIN. TEN. | 35 | 59 | 41 | 43 |
| | | PRIN. COMP. | - 17 | - 20 | - 20 | - 26 |
| | | SHEAR | 8 | 12 | 13 | 14 |
| | | LONG. | 35 | 59 | 38 | 43 |
| | | NORMAL TEN. | 3 | 5 | 12 | 9 |
| | | NORMAL COMP. | - 13 | - 6 | - 3 | - 4 |
| | RTV-560 | PRIN. TEN. | 5 | 10 | 18 | 16 |
| | | PRIN. COMP. | - 17 | - 15 | - 15 | - 16 |
| | | SHEAR | 4 | 10 | 12 | 12 |
| | | LONG. | - 7 | - 12 | - 13 | - 13 |
| | | PEEL | 3 | 5 | 12 | 9 |
| | COATING | PRIN. TEN. | 0 | 6 | 1283 | 598 |
| | | PRIN. COMP. | -2207 | -310 | 0 | - 86 |

| MATERIAL PROPERTIES | E (PSI) | G (PSI) | $\mu$ | $\alpha$ (IN./IN./F°) |
|---|---|---|---|---|
| COATING | $9.1 \times 10^6$ | $3.9 \times 10^6$ | 0.17 | $0.2 \times 10^{-6}$ |
| LI-1500 | 60,000 (L), 6,000 (T) | 4150 | 0.3 | $0.3 \times 10^{-6}$ |
| RTV-506 | 300 (RT) - 200 (500°-600°F) | 100 (RT) - 67 (500°-600°F) | 0.5 | $115.0 \times 10^{-6}$ |
| SUBSTRATE | $42 \times 10^6$ (RT) - $37.2 \times 10^6$ (600°F) | $20 \times 10^6$ (RT) - $18.8 \times 10^6$ (600°F) | 0.1 | $5.15 \times 10^{-6}$ (RT)<br>$7.7 \times 10^{-6}$ (600°F) |

Table 2.2.3.3-7

# ALUMINUM FLIGHT PANEL NO. 2
# ORBITER FUSELAGE AREA 2

COATING THICK = 0.010 IN. LI-1500 THICK = 2.524 IN. RTV-560 THICK = 0.090 IN. TILE LENGTH = 6

| LOADING CONDITIONS | | PRESSURE (PSI)<br>AXIAL LOAD (PPI) | 6.75 COLLAPSE<br>2250<br>COMPRESSION | 3 COLLAPSE<br>3000<br>COMPRESSION | 1.5 BURST<br>6000<br>TENSION | 0<br>0 |
|---|---|---|---|---|---|---|
| TEMPERATURE | | SURFACE (°F)<br>BACKFACE (°F) | 75<br>75 | 100<br>250 | 100<br>250 | 75<br>300 |
| MAXIMUM STRESSES (PSI) | LI-1500 | PRIN. TEN.<br>PRIN. COMP.<br>SHEAR<br>LONG.<br>NORMAL TEN.<br>NORMAL COMP. | 6<br>- 17<br>7<br>- 12<br>4<br>- 8 | 13<br>- 7<br>3<br>13<br>2<br>- 3 | 61<br>- 32<br>19<br>61<br>8<br>- 6 | 23<br>- 16<br>8<br>23<br>3<br>- 3 |
| | RTV-560 | PRIN. TEN.<br>PRIN. COMP.<br>SHEAR<br>LONG.<br>PEEL | 4<br>- 13<br>6<br>- 5<br>4 | 2<br>- 9<br>2<br>- 8<br>2 | 22<br>- 17<br>18<br>- 6<br>8 | 6<br>- 10<br>7<br>- 7<br>3 |
| | COATING | PRIN. TEN.<br>PRIN. COMP. | 1<br>- 45 | 56<br>0 | 16<br>- 44 | 2<br>- 50 |

| MATERIAL PROPERTIES | E (PSI) | G (PSI) | $\mu$ | $\alpha$ (IN./IN./F°) |
|---|---|---|---|---|
| COATING | $9.1 \times 10^6$ | $3.9 \times 10^6$ | 0.17 | $0.2 \times 10^{-6}$ |
| LI-1500 | 60,000 (L), 6,000 (T) | 4150 | 0.3 | $0.3 \times 10^{-6}$ |
| RTV-560 | 300 (RT – 300°F) | 100 (RT – 300°F) | 0.5 | $115.0 \times 10^{-6}$ |
| SUBSTRATE | $10.5 \times 10^6$ (RT) – $9.5 \times 10^6$ (300°F) | $4.2 \times 10^6$ (RT) – $3.66 \times 10^6$ (300°F) | 0.3 | $13.1 \times 10^{-6}$ (RT) – $13.5 \times 10^{-6}$ (300°F) |

Table 2.2.3.3-8

# ALUMINUM FLIGHT PANEL NO. 3
# ORBITER FUSELAGE AREA 1

COATING THICK = 0.010 IN. LI-1500 THICK = 1.334 IN. RTV-560 THICK = 0.090 IN. TILE LENGTH = 6

| LOADING CONDITIONS | | PRESSURE (PSI)<br>AXIAL LOAD (PPI) | 3.75 COLLAPSE<br>3150<br>COMPRESSION | 3.0 COLLAPSE<br>3000<br>COMPRESSION | 1.5 BURST<br>6000<br>TENSION | 0<br>0 |
|---|---|---|---|---|---|---|
| TEMPERATURE | | SURFACE (°F)<br>BACKFACE (°F) | 75<br>75 | 100<br>250 | 100<br>250 | 75<br>300 |
| MAXIMUM STRESSES (PSI) | LI-1500 | PRIN. TEN. | 8 | 18 | 57 | 26 |
| | | PRIN. COMP. | - 18 | - 5 | - 30 | - 20 |
| | | SHEAR | 7 | 3 | 17 | 8 |
| | | LONG. | - 14 | 17 | 57 | 24 |
| | | NORMAL TEN. | 2 | 1 | 8 | 3 |
| | | NORMAL COMP. | - 5 | - 3 | - 4 | - 2 |
| | RTV-560 | PRIN. TEN. | 3 | 1 | 19 | 6 |
| | | PRIN. COMP. | - 10 | - 8 | - 14 | - 10 |
| | | SHEAR | 6 | 1 | 15 | 6 |
| | | LONG. | - 3 | - 7 | - 6 | - 8 |
| | | PEEL | 2 | 1 | 8 | 3 |
| | COATING | PRIN. TEN. | 34 | 34 | 8 | 2 |
| | | PRIN. COMP. | - 66 | - 51 | -171 | -127 |

| MATERIAL PROPERTIES | E (PSI) | G (PSI) | $\mu$ | $\alpha$ (IN./IN./F°) |
|---|---|---|---|---|
| COATING | $9.1 \times 10^6$ | $3.9 \times 10^6$ | 0.17 | $0.2 \times 10^{-6}$ |
| LI-1500 | 60,000 (L), 6,000 (T) | 4150 | 0.3 | $0.3 \times 10^{-6}$ |
| RTV-560 | 300 (RT – 300°F) | 100 (RT – 300°F) | 0.5 | $115.0 \times 10^{-6}$ |
| SUBSTRATE | $10.5 \times 10^6$ (RT) - $9.15 \times 10^6$ (600°F) | $4.2 \times 10^6$ (RT) - $3.16 \times 10^6$ (300°F) | 0.3 | $13.1 \times 10^{-6}$ (RT) - $13.5 \times 10^{-6}$ (300°F) |

Table 2.2.3.3-9

LOCKHEED

# TITANIUM FLIGHT PANEL NO. 4
# ORBITER FUSELAGE AREA 2

COATING THICK = 0.010 IN. LI-1500 THICK = 1.234 IN. RTV-560 THICK = 0.090 IN. TILE LENGTH = 6

| LOADING CONDITIONS | | PRESSURE (PSI)<br>AXIAL LOAD (PPI) | 6.75 COLLAPSE<br>2250<br>COMPRESSION | 3 COLLAPSE<br>3000<br>COMPRESSION | 1.5 BURST<br>6000<br>TENSION | 0<br>0 |
|---|---|---|---|---|---|---|
| TEMPERATURE | | SURFACE (°F)<br>BACKFACE (°F) | 75<br>75 | 100<br>550 | 100<br>550 | 75<br>600 |
| MAXIMUM STRESSES (PSI) | LI-1500 | PRIN. TEN. | 4 | 21 | 49 | 24 |
| | | PRIN. COMP. | - 14 | - 8 | - 22 | - 14 |
| | | SHEAR | 6 | 4 | 13 | 7 |
| | | LONG. | - 10 | 20 | 49 | 22 |
| | | NORMAL TEN. | 3 | 1 | 6 | 2 |
| | | NORMAL COMP. | - 7 | - 2 | - 3 | - 1 |
| | RTV-560 | PRIN. TEN. | 4 | 1 | 13 | 4 |
| | | PRIN. COMP. | - 12 | - 12 | - 16 | - 12 |
| | | SHEAR | 5 | 0 | 13 | 5 |
| | | LONG. | - 4 | - 12 | - 12 | - 12 |
| | | PEEL | 3 | 1 | 6 | 2 |
| | COATING | PRIN. TEN. | 2 | 105 | 21 | 2 |
| | | PRIN. COMP. | -248 | 0 | - 85 | - 81 |

| MATERIAL PROPERTIES | E (PSI) | G (PSI) | $\mu$ | $\alpha$ (IN./IN./F°) |
|---|---|---|---|---|
| COATING | $9.1 \times 10^6$ | $3.9 \times 10^6$ | 0.17 | $0.2 \times 10^{-6}$ |
| LI-1500 | 60,000 (L), 6,000 (T) | 4150 | 0.3 | $0.3 \times 10^{-6}$ |
| RTV-560 | 300 (RT) - 200 (500°-600°F) | 100 (RT) - 67 (500°-600°F) | 0.5 | $115.0 \times 10^{-6}$ |
| SUBSTRATE | $16 \times 10^6$ (RT) - $13.1 \times 10^6$ (600°F) | $6.4 \times 10^6$ (RT) - $5.2 \times 10^6$ (600°F) | 0.3 | $5.8 \times 10^{-6}$ (RT – 600°F) |

# TILE-BOND-COATING SUMMARY CHART

| | PANEL | | | | | | | |
|---|---|---|---|---|---|---|---|---|
| | BERYLLIUM | | ALUMINUM | | | | TITANIUM | |
| | NO. 1 TEST | NO. 1 FLT | NO. 2 TEST | NO. 2 FLT | NO. 3 TEST | NO.3 FLT | NO.4 TEST | NO.4 FLT |
| SUBSTRATE $t_e$ | 0.064 | 0.064 | 0.114 | 0.114 | 0.143 | 0.143 | 0.090 | 0.090 |
| RTV-560 t | 0.090 | 0.090 | 0.090 | 0.090 | 0.090 | 0.090 | 0.090 | 0.090 |
| LI-1500 t | 1.89 | 1.22 | 3.34 | 2.52 | 1.85 | 1.33 | 2.00 | 1.23 |
| COATING t | 0.010 | 0.010 | 0.010 | 0.010 | 0.010 | 0.010 | 0.010 | 0.010 |
| LI-1500 TILE L | 12 | 12 | 6 | 6 | 6 | 6 | 6 | 6 |
| WEIGHT (LB/FT$^2$) | 5.2* | 4.4* | 6.4 | 5.5 | 5.0 | 4.5 | 5.2 | 4.3 |
| Δ WEIGHT (PSF) | +0.84 | - | +1.09 | - | +0.59 | - | + 0.96 | - |

ALL DIMENSIONS IN INCHES

ADIABATIC BACKFACE FOR ALL PANELS

ADDITIONAL OPTIMIZATION CYCLES PLANNED TO IMPROVE DESIGNS

* WT. OF Be PANEL INCLUDES 1.6 LB/FT$^2$ FOR PRIMARY STRUCTURE

TEST VS FLIGHT CONDITIONS

- SIMPLE SUPT IN TEST
- CONTINUOUS SPAN IN FLIGHT
- LOAD FITTINGS UNIQUE TO TEST

DO6144

Table 2.2.3.3-10

### 2.2.4 Attachment Methods

Three attachment methods have been evaluated for the LI-1500 application to the shuttle: direct bonding, mechanical strain isolation techniques, and partial support of tile on external vehicle stringers have been evaluated. These methods are discussed in more detail below. One of the best strain isolation techniques is that used on prototype panel No. 1. The use of the beryllium subpanel isolates the LI-1500 from the high in-plane loadings in the primary structure and results in a lower TPS weight. Both this concept and the partial support concept discussed in section 2.2.4.3 would result in an easy conversion of TPS from the Mark I to the Mark II version.

2.2.4.1 Bonding Attachment (Baseline). LMSC's baseline attachment method is direct bonding with RTV-560. The bond agent acts as a strain isolation layer between the tile and substrate. Trade studies on the prototype panel designs have shown that as bond thickness increases, only a small portion of its weight is additive to the TPS weights due to the heat sink effect. Bonded LI-1500 material has been tested both by LMSC and NASA, resulting in confidence in this proven system.

LMSC has considered a number of commercially available adhesives for attaching LI-1500 to substrate materials. The systems considered are shown in Table 2.2.4-1. RTV-560 has been selected as the baseline adhesive due to these unique characteristics:

- Relatively low stiffness with high strength
- Temperature range, $-150^{\circ}$ to $600^{\circ}$F
- Excellent adhesion to LI-1500 and metals
- Thermal stability and oxidation resistance

2.2.4.2 Mechanical Attachment. LMSC has considered many strain relief attachment methods that utilize mechanical fasteners. These methods can be considered in two general categories: (1) carrier plates the size of each tile which are mechanically fastened to the structure and (2) fasteners that are tapped into the LI-1500 and attached directly to the structure.

Table 2.2.4-1

BOND SYSTEMS EVALUATED

| System | Evaluation |
|---|---|
| HT-424 | Not room curable; high stiffness |
| DC 96-052 | Poor cure under tiles; inconsistent |
| RTV-30 | Low temperature limited (-90°F) |
| RTV-511 | Limited to 500°F |
| RTV-560 (Sheet) | Lower shear strength than liquid; same stiffness and weight |
| RTV-560 (Liquid) | Selected as baseline |

Various attachments have been designed; weight of selected configurations are compared in Fig. 2.2.4-1. Designs 1, 2, 3, 6, and 7 are the threaded type (2); 4, 5, 8, and 9 utilize the bonding to carrier plates type (1). Figure 2.2.4-2 shows a concept with a carrier plate that is attached to primary structure by stainless velcro. Figure 2.2.4-3 shows a hybrid concept with rails in LI-1500 which, in turn, are mechanically attached to the structure with quarter-turn fasteners. These last two concepts have been weighed and are compared to the baseline bonded system in Table 2.2.4-2.

Table 2.2.4-2

WEIGHT OF VARIOUS ATTACHMENT METHODS

| Method | Weight ($lb/ft^2$) | | |
|---|---|---|---|
| | Attachment | LI-1500 + Coating | Total |
| Velcro | 0.48 | 3.90 | 4.38 |
| Rail Support | 0.41 | 3.90 | 4.31 |
| Bonding | 0.66 | 3.53 | 4.19 |

The values displayed in Table 2.2.4-2 show that LI-1500 is lighter for the direct bonding system as the result of the bond heat sink effect previously noted. These various

# WEIGHT COMPARISON OF MECHANICAL FASTENERS FOR LI-1500

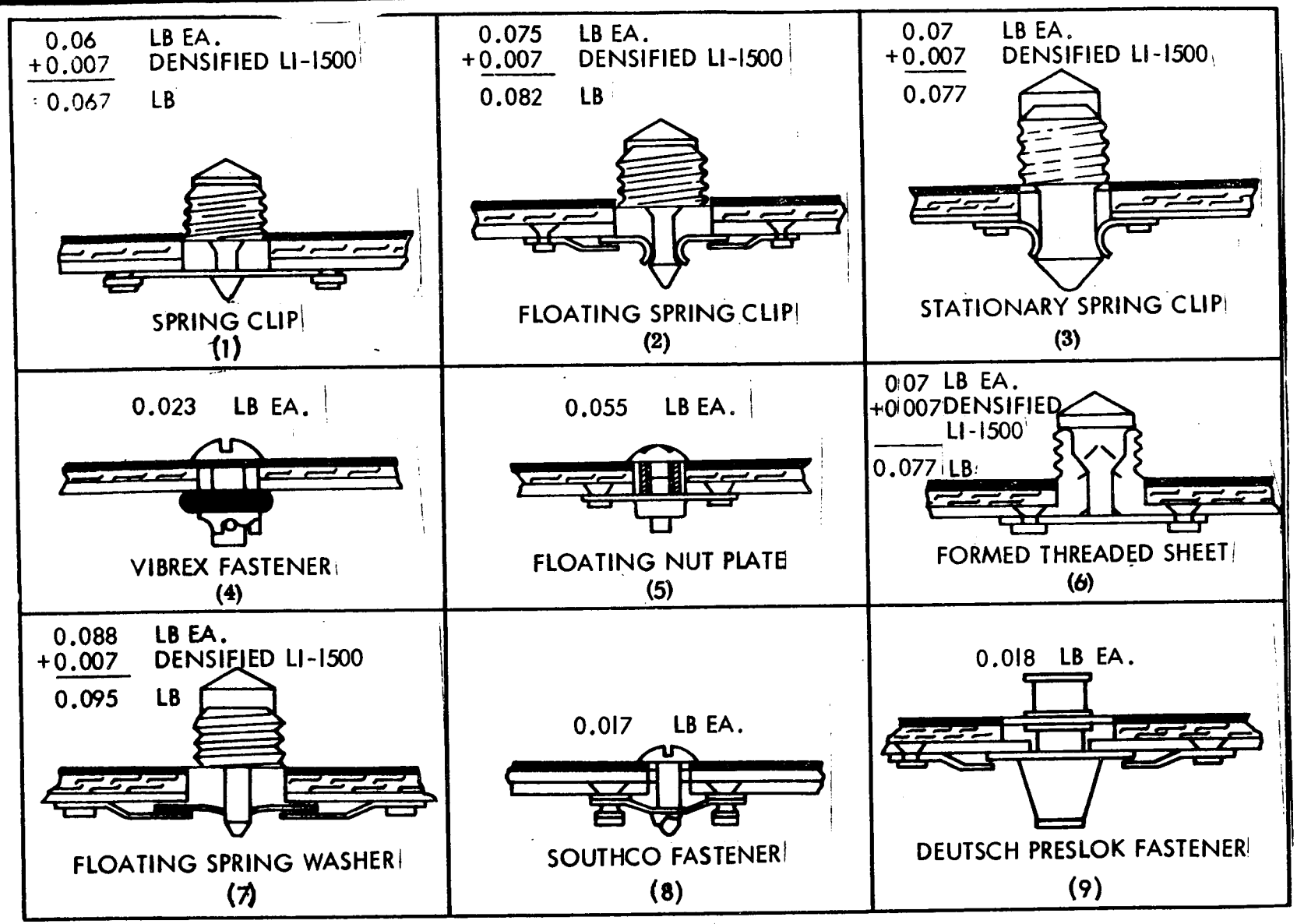


Fig. 2.2.4-1

# VELCRO ATTACHMENT WITH CARRIER PLATE

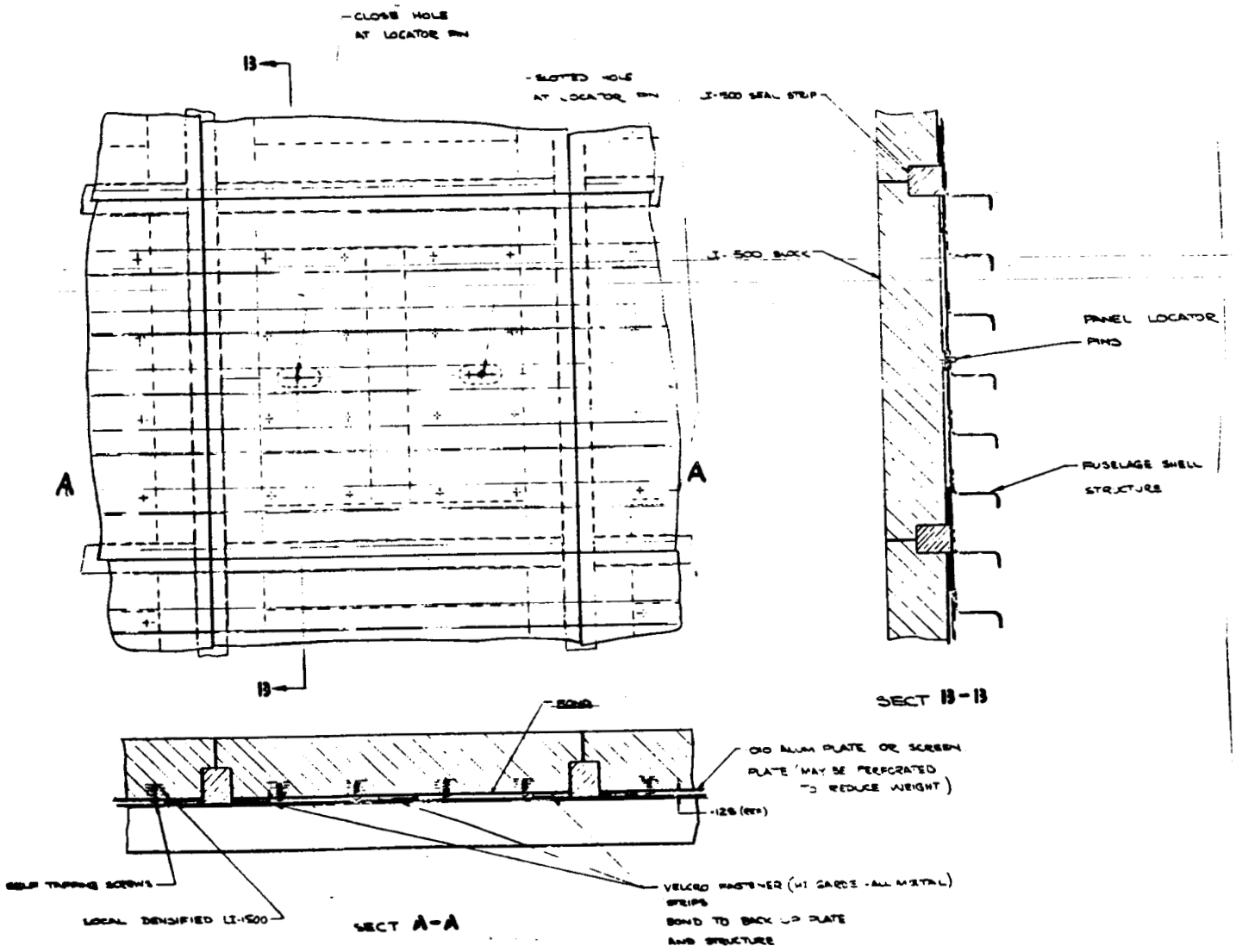


Fig. 2.2.4-2

# RAIL ATTACHMENT SCHEME

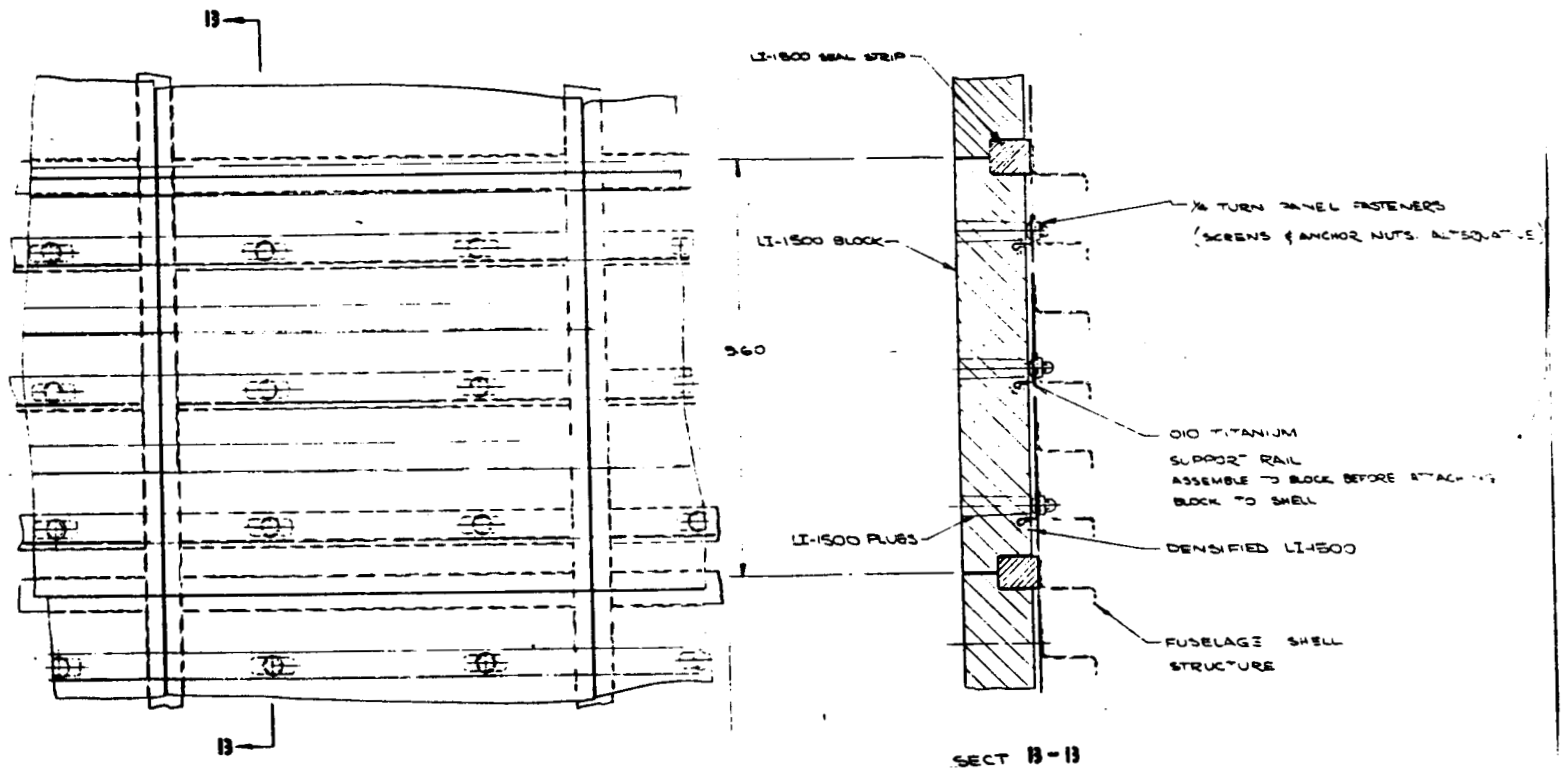


Fig. 2.2.4-3

# DESIGN CONCEPT UTILIZING VENTING ACROSS LI-1500

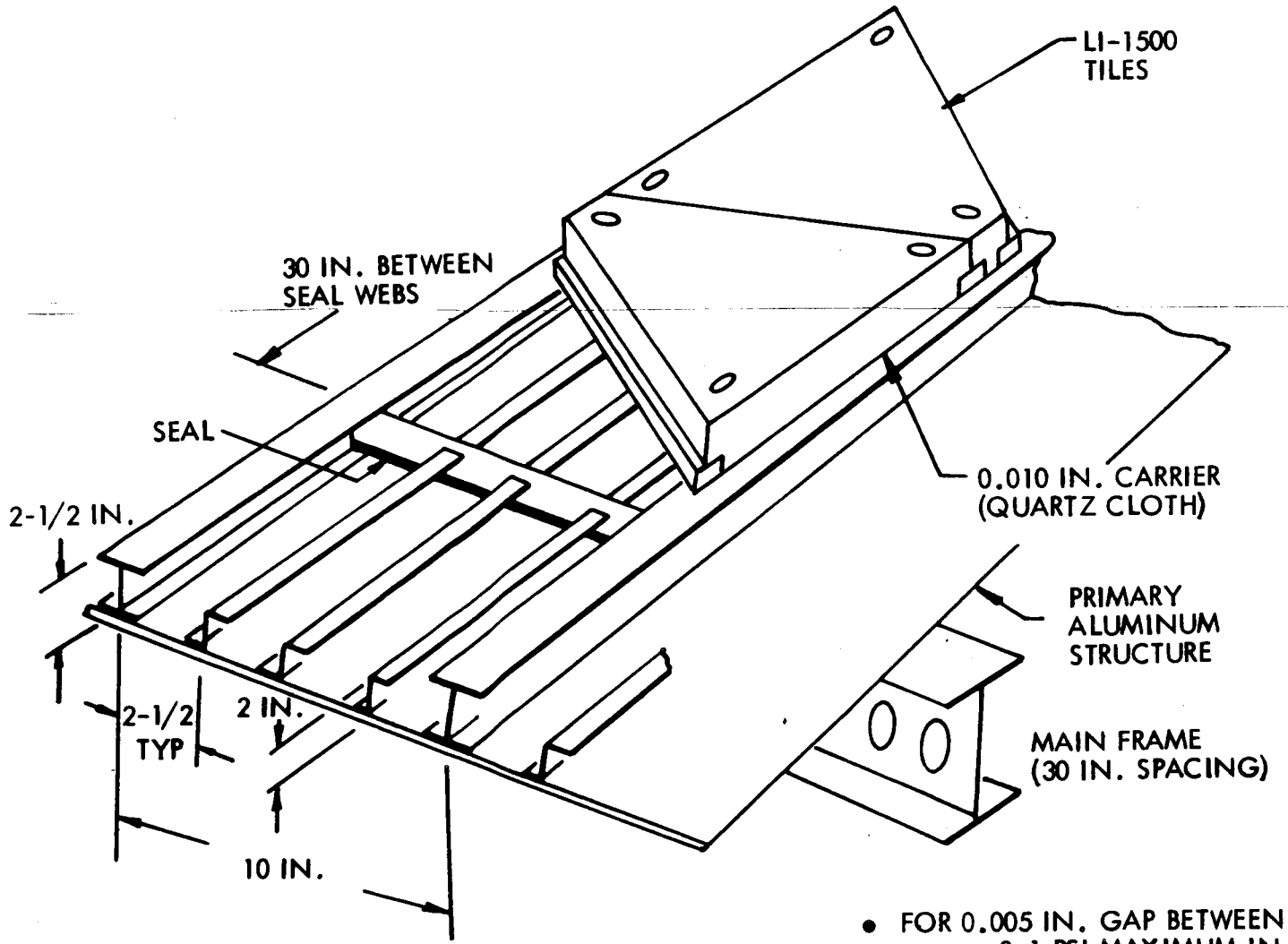


- FOR 0.005 IN. GAP BETWEEN TILES
  $\Delta p$ = 0.1 PSI MAXIMUM IN REENTRY
- FOR 30 IN. X 10 IN. X 2-1/2 IN. CHAMBER
  $\Delta T$ < 1°F ON ALUMINUM PRIMARY STRUCTURE
  FROM 0-TO-2 PSI (ASSUMING NO MASS FLOW)

D05166
rdb

Fig. 2.2.4-4

systems show promise as an effective method of reducing LI-1500 stress levels. However, a considerable test effort is required to evaluate the environmental effects. This is discussed in more detail in section 3.3.

2.2.4.3 Partial Tile Support. The third method of strain isolation considered is that of supporting tiles on external vehicle stringers. Figure 2.2.4-4 shows such a concept with 10-in. tiles. This concept can also allow venting across the tiles into the chamber below to reduce design pressures. LMSC has performed such a venting analysis, assuming a sealed chamber with a 0.52 cu ft volume.

Various gaps widths were considered with a 10-in. gap length through which all air is vented. For the NASA ascent pressure envelope shown in section 2.1.6 and using gap widths of 0.005 and 0.0025 in., the maximum differential pressures are 0.1 and 0.25 psi, respectively. An analysis of rapid external pressure changes was also performed. The resulting differential pressures are quite low. For example, for the recommended design condition with a pressure rate change of 2 psi/sec for 4 sec, a gap of 0.020 in. would vent sufficiently to realize only a 0.175 psi differential pressure. This study has been documented and is included as Appendix E in this report.

### 2.2.5 TPS Cost Study

Unit costs (dollars per pound and dollars per square foot) have been projected for the first orbiter vehicle. These costs are based on extrapolations of present manufacturing experience. During the first few months of 1971, LMSC brought the pilot plant manufacturing facility into full operational status. While the material produced in the first 4 months of 1971 has performed well in arcjet and radiant heat tests, production scale-up problems, combined with variability in raw fiber material, led to relatively expensive processed tiles (approximately $840/pound). During the past 6 months, the production problems have been resolved and raw material consistency from lot to lot has improved, reducing costs by more than one-third. Furthermore, changing from the pilot plant operation to full-scale production will result in automation of various time-consuming hand operations that are now required and will reduce processing time by more than a factor of 2. Projected manufacturing costs for processed LI-1500 range from $50 per pound to $100 per pound. Machining the LI-1500 tiles to size and attaching (bonding) to the vehicle will result in a total installed cost of $80 to $135 per pound. Fabrication and installation data are shown in Table 2.2.5-1. Costs per pound and costs per square foot are shown as a function of tile size and thickness.* The range shown indicates the expected cost bounds; the upper bound is used in all the following cost studies.

Cost estimates for a metallic thermal protection system are generated, using the standard cost complexity factors (C.F.) in Tables 2.2.5-2 and 2.2.5-3, which relate the fabricated costs of each metal to that for a stiffened aluminum structure. The metallic heat shield weights for the 040A delta wing orbiter (using a 2800-second reentry trajectory with peak temperature of 2050°F) are shown in Table 2.2.5-2.

Cost Estimating Relationships (CERs) have been used to project the total TPS first unit costs. These data are summarized in Table 2.2.5-3 for three TPSs: LI-1500, the SLA-561 ablator, and the metallic heat shield. As can be seen, the metallic system is far heavier and more costly than the LI-1500.

* See Figs. 2.2.5-1 and -2

Table 2.2.5-1

LI-1500 TPS UNIT COST VERSUS TILE SIZE

| Labor Cost Element | Number and Size of Tiles | | |
|---|---|---|---|
| | 4 (12 x 12 in.) | 16 (6 x 6 in.) | 36 (4 x 4 in.) |
| Saw Cut Tiles to Size | 0 | 0.4 | 0.8 |
| Grind-Rout Edges | 0.8 | 2.4 | 4.0 |
| Cut Seal Strips | 0.5 | 1.5 | 2.5 |
| Bond Tiles to Structure | 4.0 | 6.0 | 12.0 |
| Labor Hours per Panel | 5.3 | 10.3 | 19.3 |
| Labor Cost ($/ft$^2$) | 21.2 | 41.2 | 77.2 |
| Total Cost ($/ft$^2$) | 340 | 358 | 390 |
| Total Cost ($/lb) | 135 | 143 | 156 |

NOTES:

1. Estimate is based upon bonding material to primary structure, over an area 2 ft x 2 ft in size, with the LI-1500 material delivered in 12 x 12 x 2 in. tiles shaped and ready for bonding.

$$W/A = 0.24 + 1.25\ (t) = 2.74\ \text{lb/ft}^2$$

2. Tile size and assembly is illustrated below.

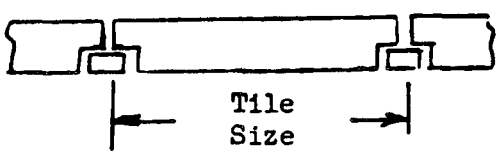


3. Total costs include basic LI-1500 tile and raw material as well as manufacturing and installation labor.

# PROJECTED FIRST UNIT COSTS

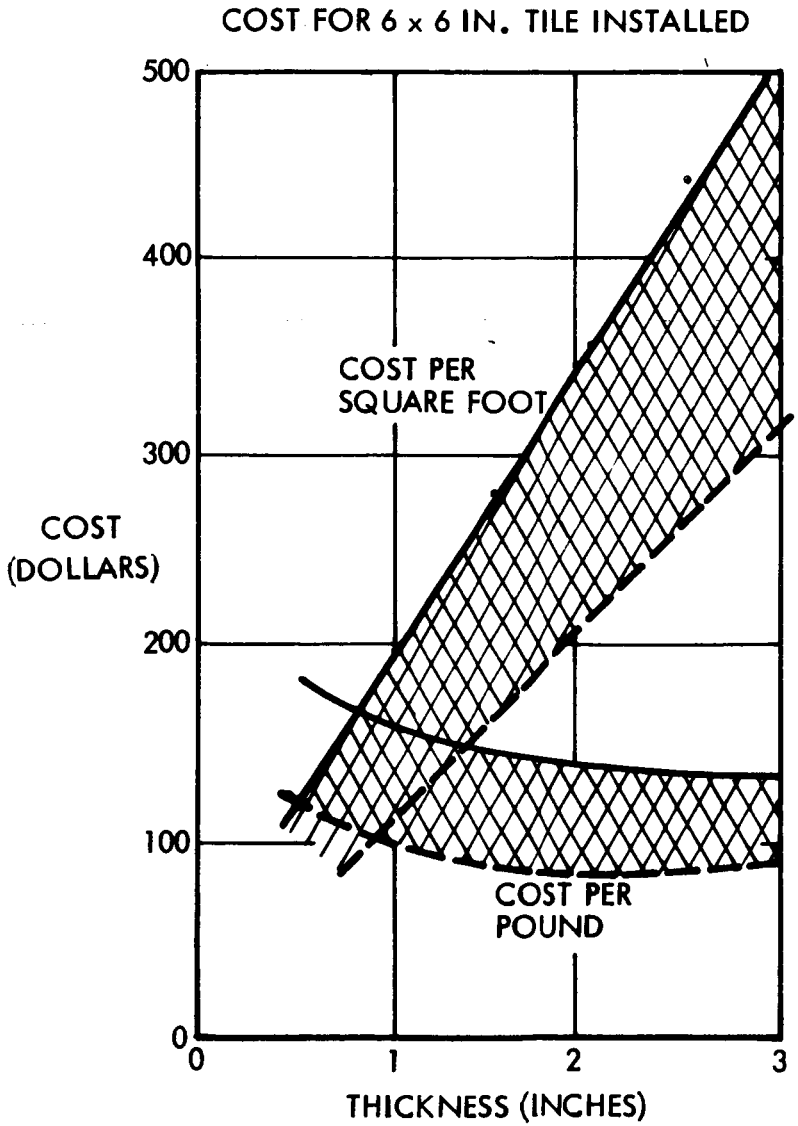


Fig. 2.2.5-1

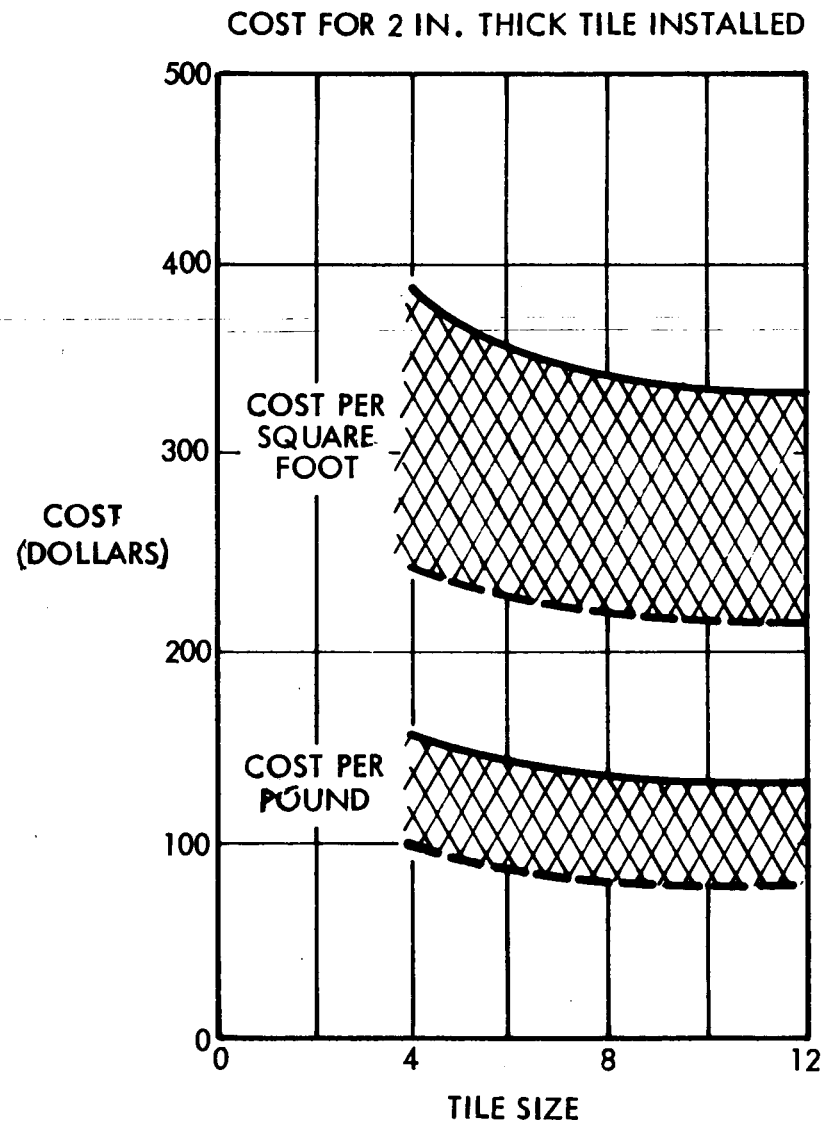


Fig. 2.2.5-2

DO6098

Table 2.2.5-2

040A DELTA WING ORBITER – METALLIC TPS SYSTEM – AVERAGE COMPLEXITY FACTOR

| Surface Panel Material | Surface Area ($ft^2$) | Unit Weight ($lb/ft^2$) | Weight (lb) | C. F. | Weight x C. F. |
|---|---|---|---|---|---|
| Cb | 90 | 5.11 | 460 | 7.49 | 3,450 |
| TDNiCrAl | 3,513 | 4.16 | 14,630 | 3.37 | 49,600 |
| Rene 41 | 722 | 2.69 | 1,942 | 2.75 | 5,340 |
| Ti | 6,713 | 1.42 | 9,510 | 3.25 | 30,900 |
| Carbon/Carbon | 177 | 3.50 | 620 | 7.50 | 4,150 |
| $\Sigma$ = | 11,215 | (2.42) | 27,162 | (3.44) | 93,440 |

Table 2.2.5-3

040A DELTA WING ORBITER – TPS COST SUMMARY

| TPS | Total System Weight (lb) | System C. F. | First Unit Cost(1) ($M) | Cost Per Pound ($/lb) | Cost Per Sq Ft ($/$ft^2$) |
|---|---|---|---|---|---|
| LI-1500 | 21,870 | 0.8 | 3.5 | 144 | 312 |
| SLA-561 | 21,650 | 0.7 | 3.1 | 127 | 276 |
| Metallic | 27,162 | 3.5 | 16.2 | 596 | 1,445 |

(1) Manufacturing cost of total TPS for first orbiter:

$$c = 2.8\,(10^{-2})\,(W)^{.5}\,(C.F.) = \$\text{ Million}$$

A detailed comparison of the ablator and LI-1500 weights and thicknesses is presented in Table 2.2.5-4 and forms the basis for the system costs projected in Fig. 2.2.5-3. The DDT&E (Design, Development, Test, and Engineering) and first unit costs are shown on the figure. The total program costs are highly sensitive to the refurbishment rates assumed and, hence, a range is shown. The present design guidelines call for 100-percent replacement of the ablator after every flight (upper bound). It is possible that the ablator can be reused in regions where the maximum temperature is below 600°F. Hence, the lower bound shown in Fig. 2.2.5-3 is based on replacement over 70 percent of the surface area after every flight.

The LI-1500 rigid surface installation has a demonstrated reuse capability of 100 cycles for trajectories having a peak temperature of 2500°F. In order to project realistic program costs, however, a reasonable refurbishment rate must be estimated. A refurbishment rate of 5 percent of the surface of each flight is shown as the upper bound; a 2 percent refurbishment rate is assumed for the lower bound in Fig. 2.2.5-3.

One remaining question to be answered is what method of attachment will result in the least cost space shuttle system. The answer to this requires a detailed analysis of the combined orbiter structure and TPS. Such a study has been completed and will be documented in the final report. Five primary structural materials have been considered for the orbiter (7075-T6 aluminum, 2024-T81 aluminum, magnesium, titanium, and beryllium) in combination with three TPSs: direct bond of LI-1500 to primary structure, LI-1500 bonded to subpanels, and metallic heat shield (titanium or beryllium) for upper surfaces. The all aluminum structure with direct-bond LI-1500 TPS was selected as baseline.

It is interesting that the lightest system (beryllium skin over titanium frames with direct bond of LI-1500 results in 18,000 lb reduction in system weight) is far more expensive than the baseline ($178 million increase in the total program costs). The least-cost system is obtained by using LI-1500 directly bonded to beryllium subpanels attached to an all aluminum airframe. The system weight is reduced by 7000 lb and total program cost is reduced by $250 million.

Table 2.2.5-4

040A ORBITER TPS WEIGHTS

| Location | Surface Area ($ft^2$) | SLA-561 Ablator | | LI-1500 | |
|---|---|---|---|---|---|
| | | Thickness (in.) | Weight (lb) | Thickness (in.) | Weight (lb) |
| Body Lower Surface | 1,647 | 2.05 | 4,674 | 2.20 | 5,528 |
| Body Upper Surface | 4,757 | 1.05 | 7,257 | 0.65 | 6,293 |
| Wing Lower Surface | 1,956 | 2.05 | 5,550 | 2.10 | 6,308 |
| Wing Upper Surface | 1,956 | 0.60 | 1,829 | 0.45 | 2,074 |
| Tail (Sides) | 722 | 1.20 | 1,244 | 0.75 | 1,050 |
| Nose Cap | 27 | 2.40 | 174 | – | 95 |
| Wing Leading Edge | 126 | 2.40 | 812 | – | 441 |
| Tail Leading Edge | 24 | 1.75 | 114 | – | 84 |
| Total | 11,215 | | 21,654 | | 21,873 |

Ablator for nose cap and leading edge is 30 $lb/ft^3$, ESA 3560; for other areas it is 15 $lb/ft^3$.

Ablator weight loss during entry is 1515 lb.

All thicknesses are averages for the surface areas indicated.

Weights include 5 percent non-optimum factor.

Thermal environment is based on LMSC high-crossrange trajectory, RE-230 (2000 sec reentry) (040A delta wing design trajectory).

# TPS COST COMPARISON

040A DELTA WING ORBITER

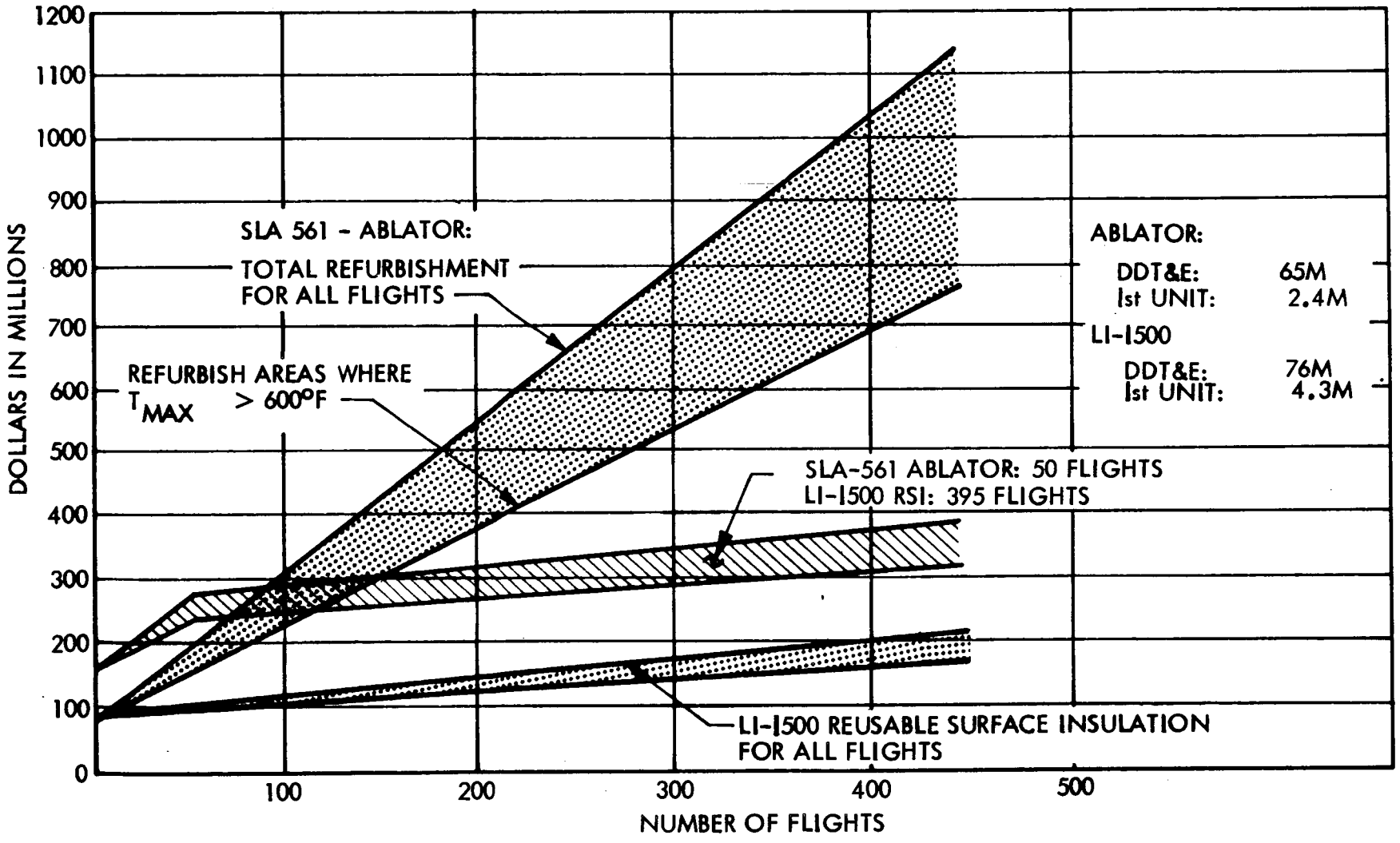


Fig. 2.2.5-3

DO6079

These studies emphasize the fact that the lightest system is not necessarily the cheapest, and one must consider the entire vehicle in reaching a decision as to which approach to adopt for attaching the TPS to the structure.

# Section 3
# MATERIALS OPTIMIZATION

The production of acceptable LI-1500 has been demonstrated by fabrication of a total of 40 12 in. x 12 in. x 2 in. tiles under this contract to date. These tiles have been used in the various tasks as test specimens or NASA deliverable items. The remaining efforts under this task are discussed under the appropriate subtask. The costing effort required to accumulate all incurred costs in material and panel fabrication has not been started. Following prototype panel design approval and start of fabrication, this task will be initiated.

## 3.1 COATING EVALUATION

The contract baseline coating is the 0025 $Cr_2O_3$ system used on tile No. TT-14B (delivered under Contract NAS 9-11222) which was tested by Battelle Memorial Institute. This interim coating system exhibits many undesirable qualities including apparent low emissivity, degradation with time, porosity, and cracking tendencies. Under NASA Contract NAS 9-12137, LMSC is developing an improved coating system. The most promising coating systems developed to date have been subjected to an accelerated 100-cycle test program to evaluate possible usage on this contract.

### 3.1.1 Specimen Description

A 100-cycle test program was performed at LMSC to demonstrate the reusability and integrity of three improved surface coatings. Six specimens, two of each surface coating, were tested. The specimens were nominally 4 x 4 x 2.45 in. and were coated on the top (heated) surface. The coatings were identified as follows: (1) an improved 0025 consisting of a borosilicate coating with a chrome oxide emittance agent and overglaze applied to specimens TT 42-1 and TT 42-2, (2) 0042 consisting of a borosilicate coating with a silicon carbide emittance agent and overglaze applied to specimens TT 42-5 and TT 42-6, and (3) an integral coating with a silicon carbide emittance agent applied to specimens TT 42-3 and TT 42-4.

### 3.1.2 Instrumentation

One specimen with each coating was instrumented with five thermocouples (one surface, three in-depth, and one substrate) and bonded with RTV 560 to a 0.125 in. aluminum substrate. Instrumentation locations are shown in Fig. 3.1-1. A pretest photograph of the test specimens is shown in Fig. 3.1-2.

### 3.1.3 Test Pulse

The testing was performed in LMSC's 1 ATM pressure radiant facility (HIRAD) shown in Fig. 3.1-3. This radiant facility can impose radiant heat rates up to 50 Btu/ft$^2$ sec on an area of 15 x 15 in.

The test environment imposed on the specimens is shown by the surface temperature history in Fig. 3.1-6. The test pulse simulates the surface temperature for Area 2, shown in Fig. 2.2.2-8, with a 200$^\circ$F temperature overshoot to 2500$^\circ$F. This corresponds to an 1100 nm crossrange trajectory. The duration is 50 minutes with 2.5 minutes at 2500$^\circ$F.

The peak surface temperature was intentionally perturbed to 2500$^\circ$F to evaluate the overshoot capability of the coatings and the LI-1500. The 0042 surface coating was designed to remain waterproof at peak temperatures up to 2300$^\circ$F, and this capability will be tested prior to the end of the contract.

The test pulse was controlled by the surface thermocouple and monitored by a calorimeter during the entire 100 cycles. To reduce the cool down time between cycles (2-1/2 hours initially) a water-cooled copper plate was placed under the specimens. The water was turned on at about 55 minutes into the run or 5 minutes after the end of a cycle.

# THERMOCOUPLE LOCATION FOR LI-1500 TEST SPECIMENS

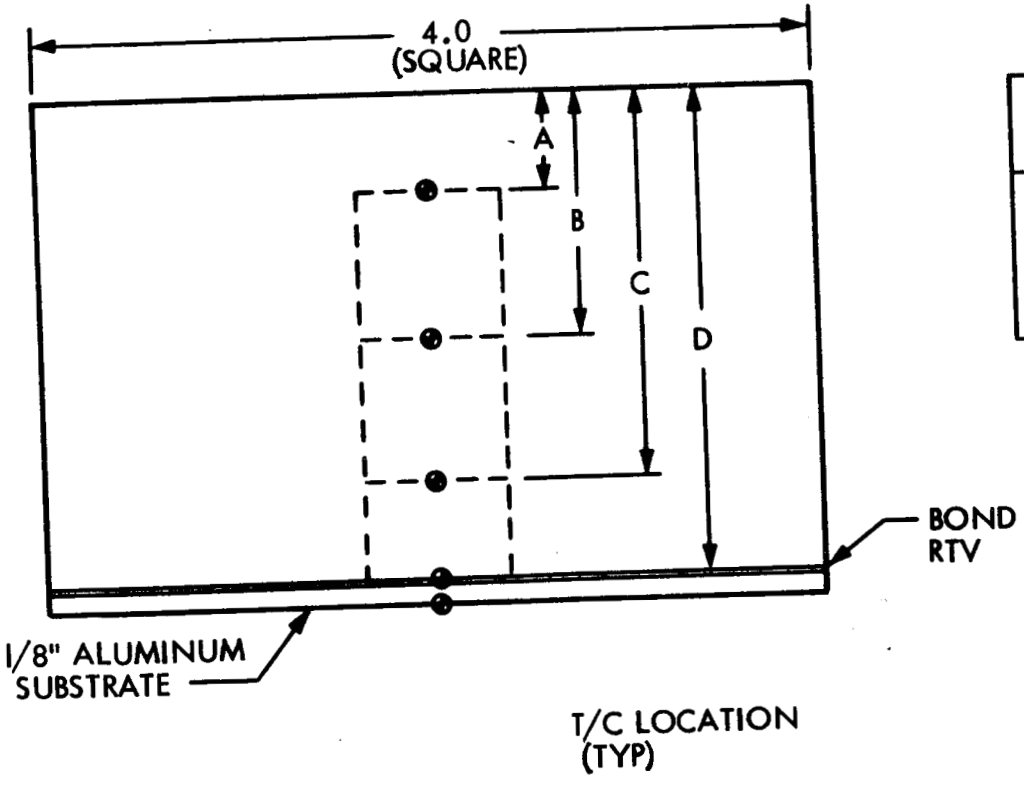


| PANEL NO. | A IN. | B IN. | C IN. | D IN. |
|---|---|---|---|---|
| 42-2 | .56 | 1.32 | 2.07 | 2.42 |
| 42-4 | .51 | 1.25 | 1.98 | 2.26 |
| 42-6 | .59 | 1.32 | 2.09 | 2.45 |

Fig. 3.1-1

# PRETEST PHOTO OF 100 CYCLE LI-1500 TEST SPECIMENS

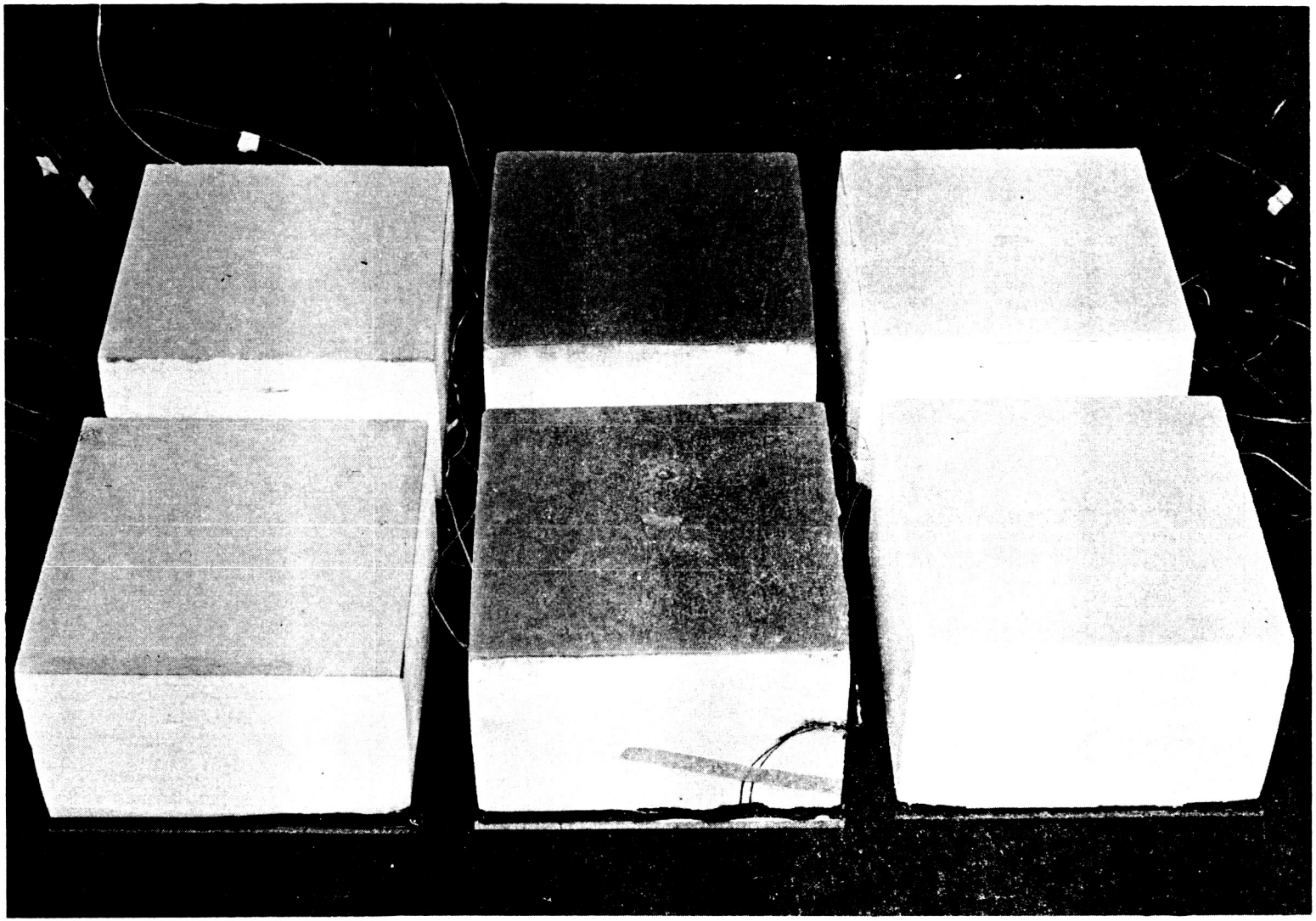

DO6145

Fig. 3.1-2

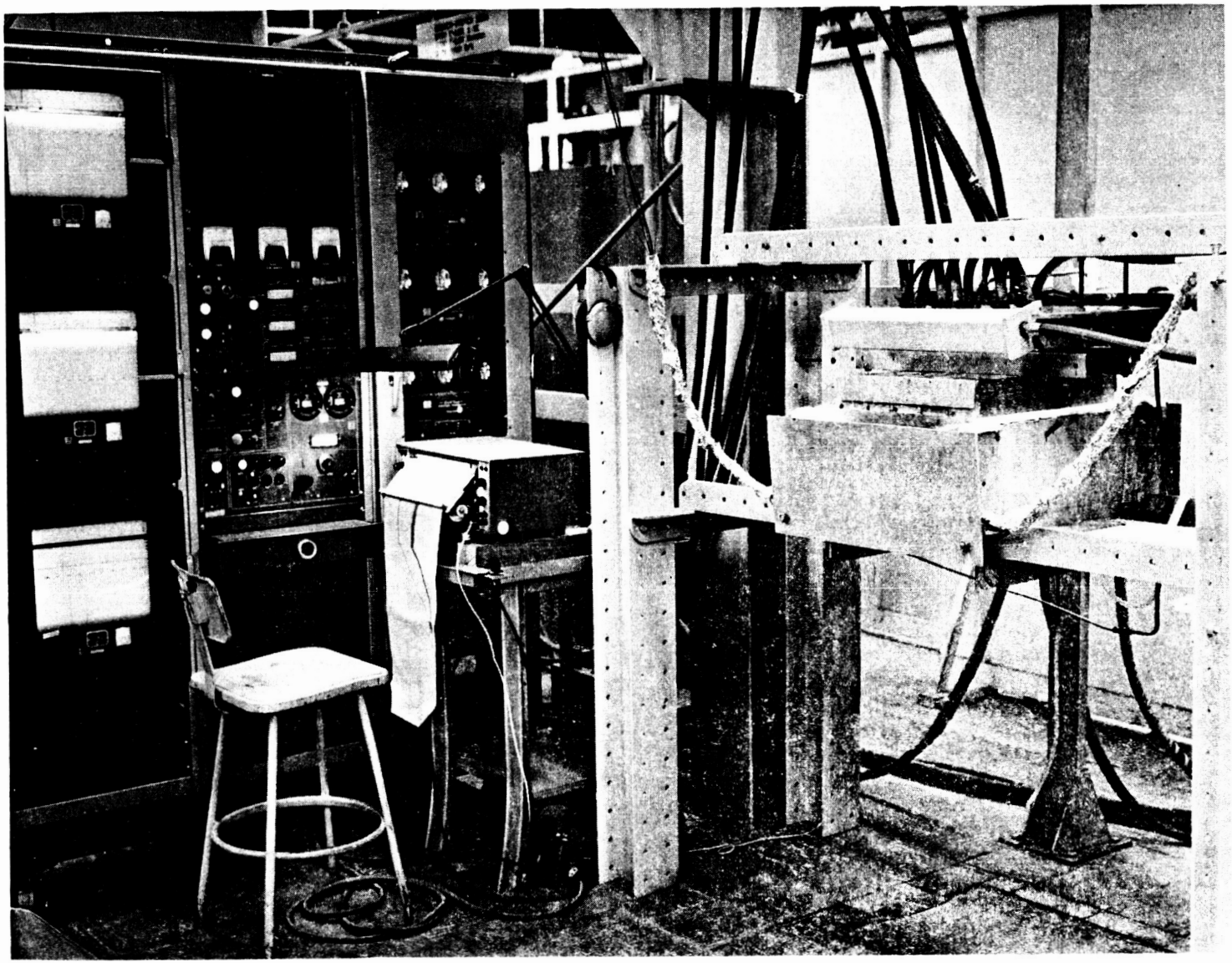

DO6146

Fig. 3.1-3

### 3.1.4 Qualitative Results

Visible inspection of the specimens during and after the 100 cycles at 2500°F indicated the following:

a. The uninstrumented 0042 coating sustained no damage after 100 cycles.

b. The instrumented 0042 coating had hairline cracks in the surface; these emanated from the position where the surface thermocouple was installed below the coating. These cracks appeared to close during the high temperature portions of the test pulse.

c. The integral coating specimens with a silicon carbide emittance agent had hairline cracks.

d. The 0025 coating developed cracks in the surface early in the test program and was removed after the forty-second cycle.

Post-test photos of the specimens after 100 cycles are shown in Figs. 3.1-4 and 3.1-5. The 0025 coated specimens are not shown. The 0042 coated specimens are shown on the right side of the figures. The specimens on the left are the integral coating with a silicon carbide emittance agent.

### 3.1.5 Quantitative Results

Temperature predictions were performed for the 100 cycle LI-1500 tests, using the following ground rules and assumptions:

a. THERM computer code

b. One-dimensional thermal model

c. Variation of thermal conductives and specific heat from Tables 4.1-6 and -7, density = 15 $lb/ft^3$

d. Input measured surface temperature as boundary condition

e. Adiabatic substrate

f. 0.030 in. RTV 560 adhesive between LI-1500 and aluminum substrate

The measured temperature histories are shown in Figs. 3.1-6a, b, c, and d for the instrumented LI-1500 specimen with the 0042 coating (TT 42-6). Data are plotted for for the 4th, 47th, 75th and 100th thermal cycles.

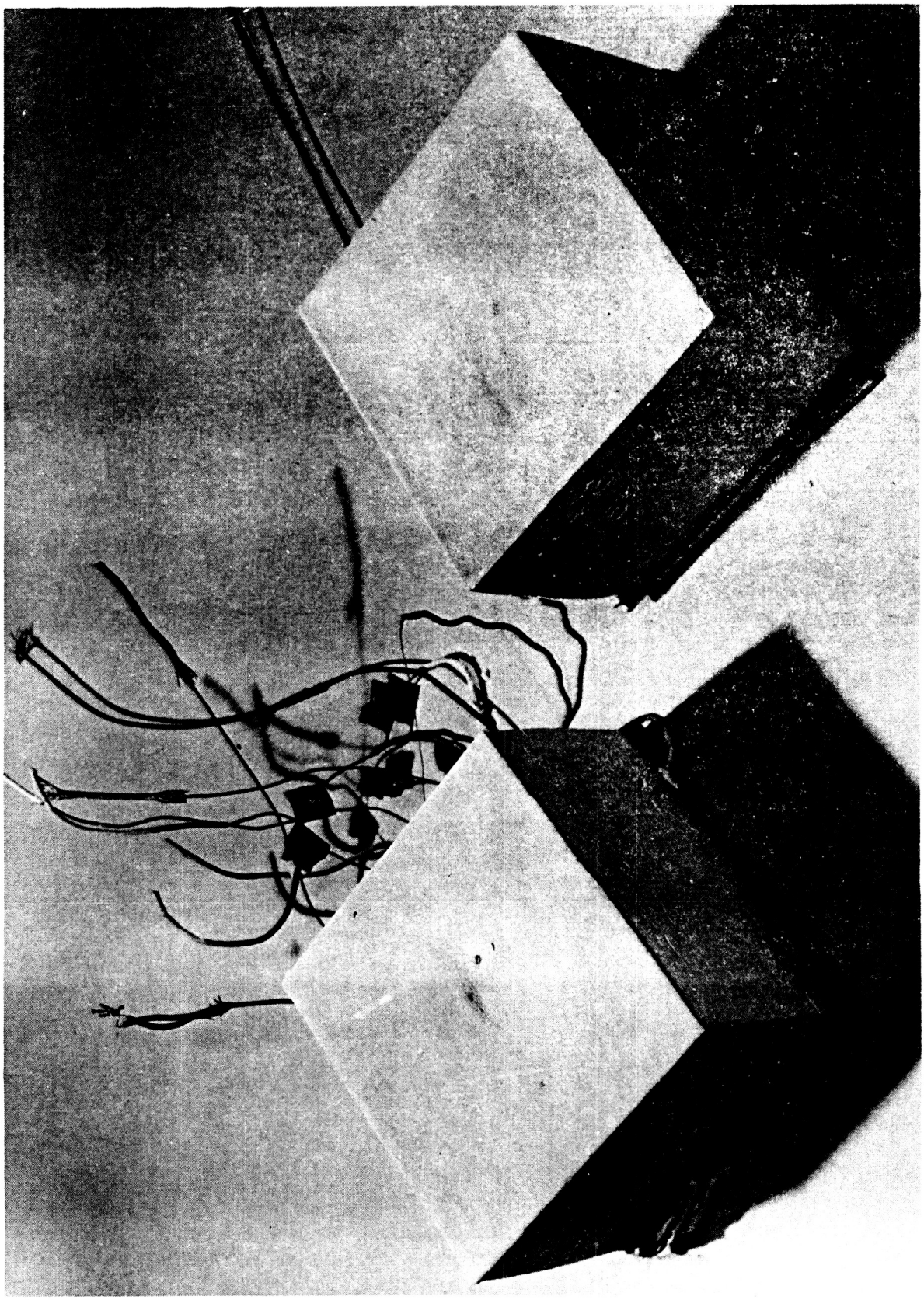

Fig. 3.1-4 LI-1500 Specimens With 0042 Coating After 100 Thermal Cycles

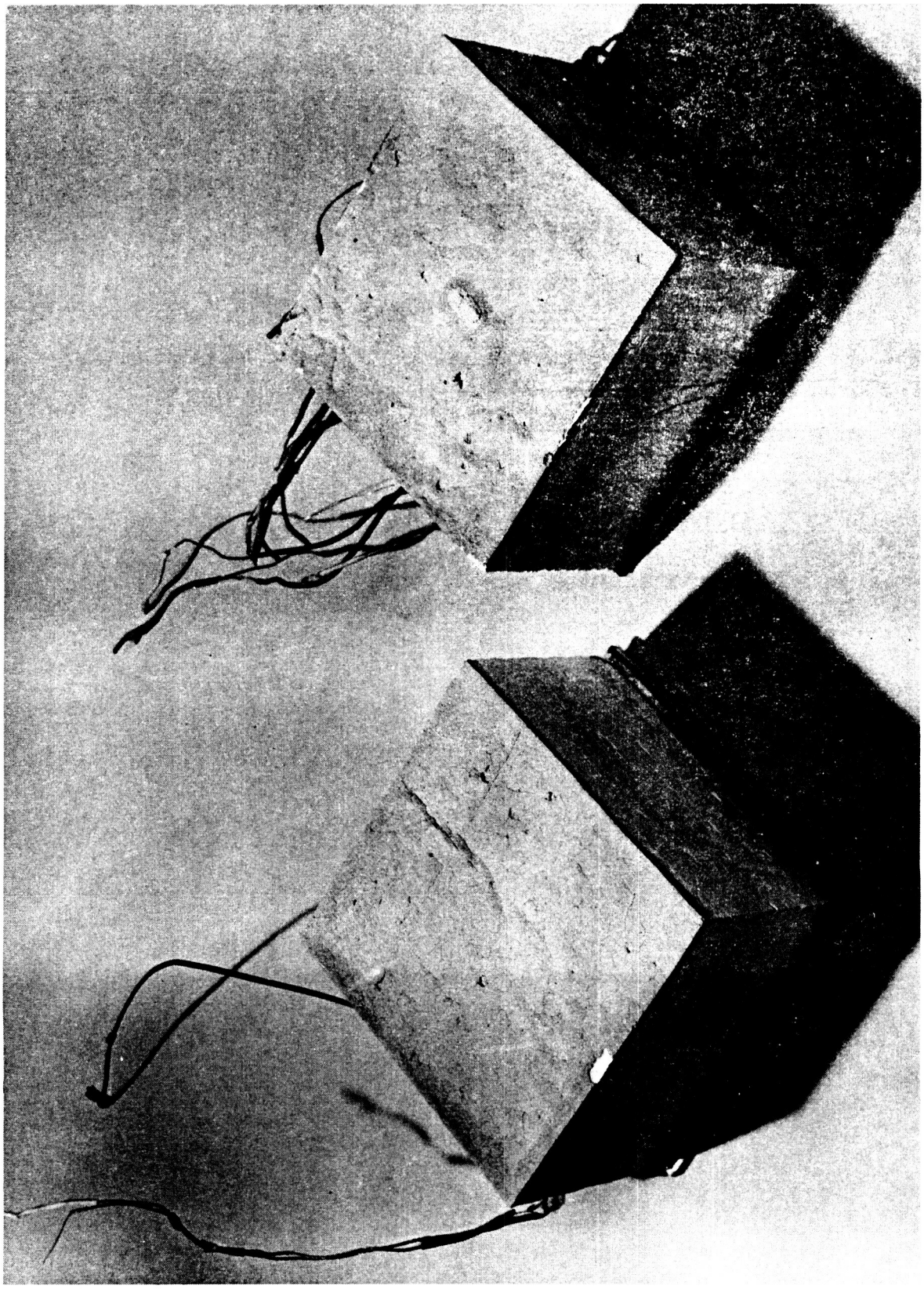

Fig. 3.1-5 LI-1500 Specimens With Integral/Silicon Carbide Coating After 100 Thermal Cycles

# TEMPERATURE HISTORIES FOR SPECIMEN TT 42-6 DURING 100 CYCLE TESTS

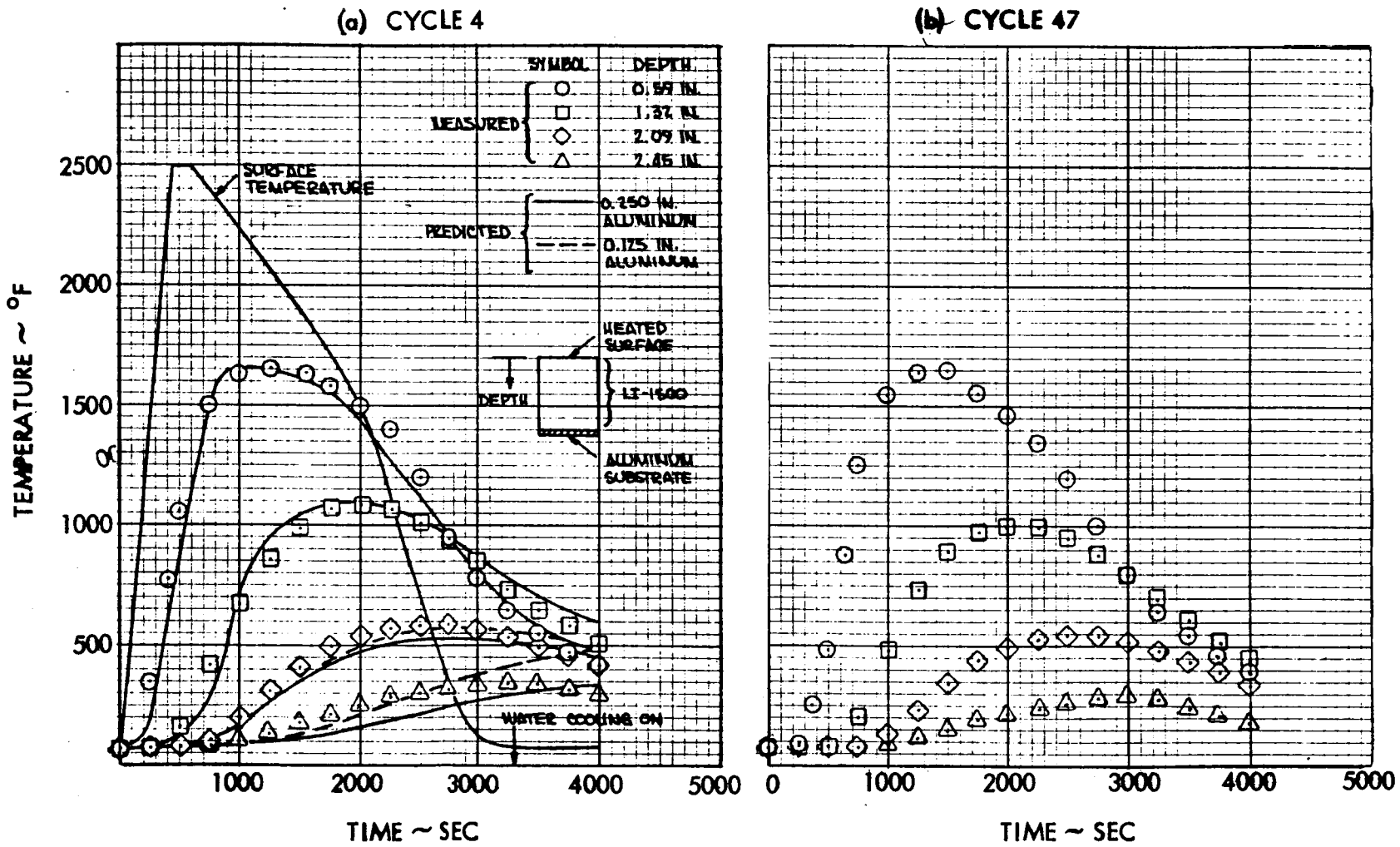


DO6156

Fig 3.1-6

# TEMPERATURE HISTORIES FOR SPECIMEN TT 42-6 DURING 100 CYCLE TESTS

(c) CYCLE 75

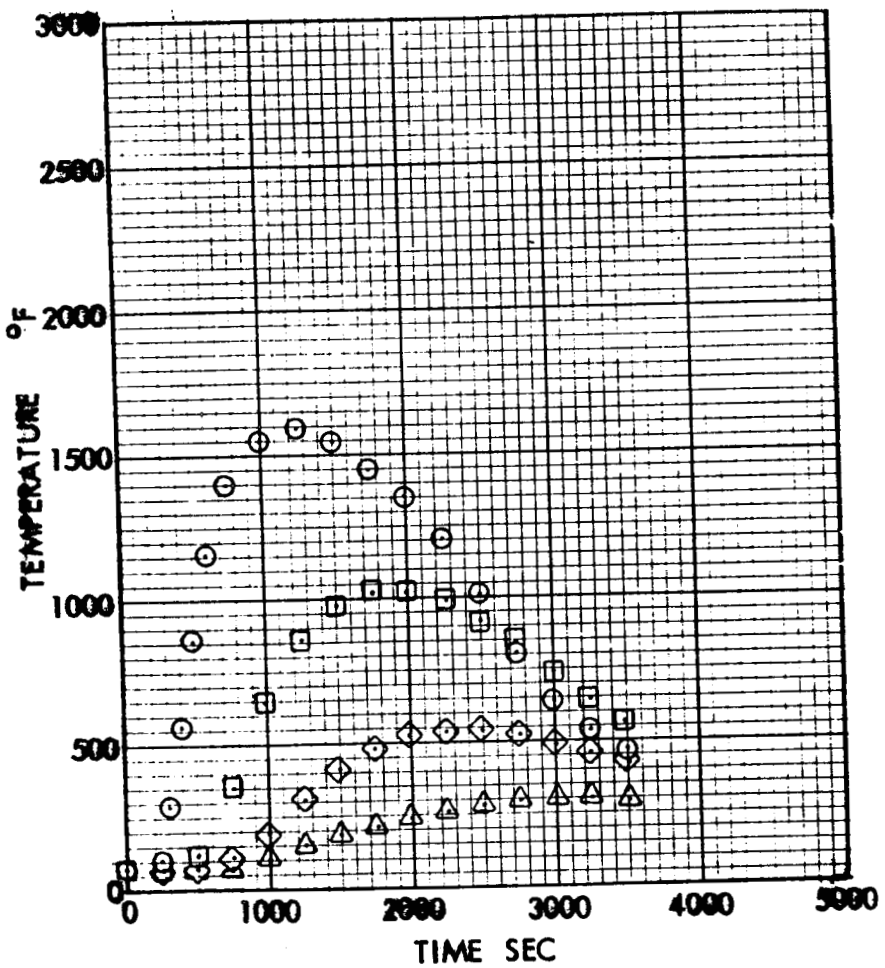


(d) CYCLE 100

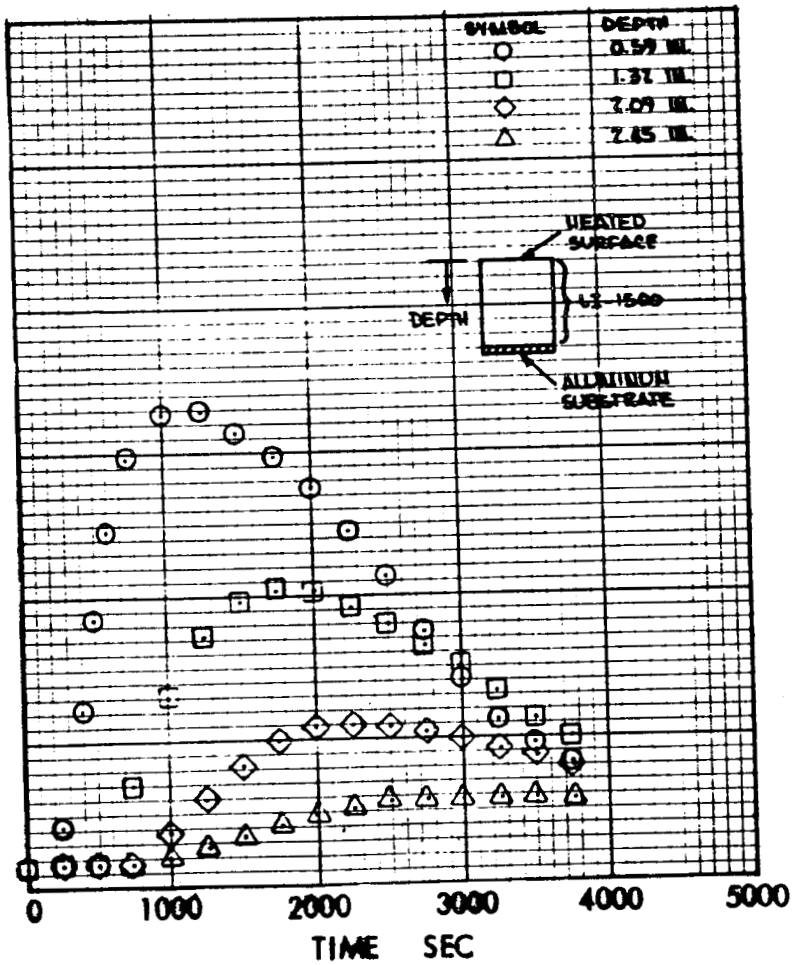


DO6160

Fig. 3.1-6 (Cont)

The consistency and repeatability of the measured temperature data are shown in Fig. 3.1-6. The repeatability demonstrates the thermal stability of the LI-1500.

Figure 3.1-6a shows a comparison of measured and predicted temperatures at various locations within the LI-1500. Since the specimens were bonded to 0.125 in. aluminum substrates which were placed on a second piece of 0.125 in. aluminum, the predictions were made for two substrate thicknesses. As shown, the effect of the substrate upon the predicted temperature becomes negligible at depths between 1.3 and 2.09 in. The effect is small at a depth of 2.09 in. The predictions were also complicated by the fact that the contact resistance between the two 0.125 in. aluminum plates was not known and also, the adiabatic boundary condition was not met.

A summary of the peak predicted and measured temperatures for the 4th, 47th, 75th, and 100th cycles is shown in Fig. 3.1-7.

Figure 3.1-8 shows measured temperature histories for specimens TT 42-4, the integral silicon carbide coated specimen, for the 4th, 47th, 75th, and 100th cycles. The first thermocouple failed sometime after the 47th cycle, and no data are shown for the 75th and 100th cycles.

The excellent repeatability of the measured data is also shown in Fig. 3.1-9, where the peak measured temperatures for the 4th, 47th, 75th, and 100th cycles are compared to the predicted values.

Hence even after 83.3 hr of accumulated thermal exposure with about 4.17 hr at the peak temperature of 2500°F and 14 hr above 2300°F, the use of the as-fabricated thermal conductivity values results in good agreement between the measured and predicted temperatures for both instrumented specimens TT 42-4 and TT 42-6.

Specimen pre-test and post-test dimensional weight data are shown in Table 3.1-1. The dimensional change of the specimens varied from 1.4 to 3 percent. A 3-percent thickness change is considered minimal for a specimen that has experienced 100 thermal cycles corresponding to 100 entries on a 1100 nm crossrange trajectory.

# COMPARISON OF MEASURED AND PREDICTED PEAK TEMPERATURES FOR 100 CYCLE TESTS - SPECIMEN TT 42-6

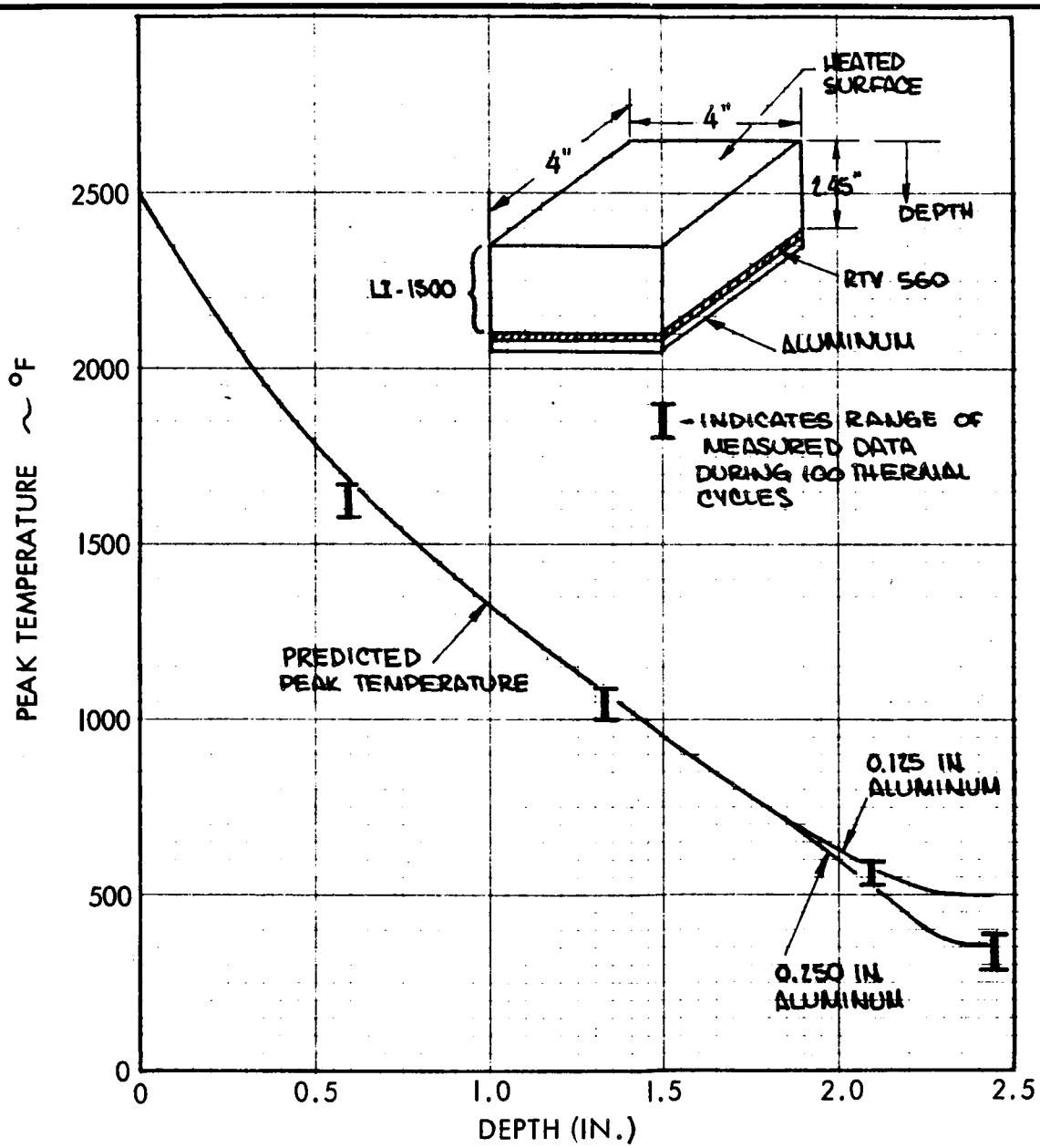


Fig. 3.1-7

DO6066

# TEMPERATURE HISTORIES FOR SPECIMEN TT 42-4 DURING 100 CYCLE TESTS

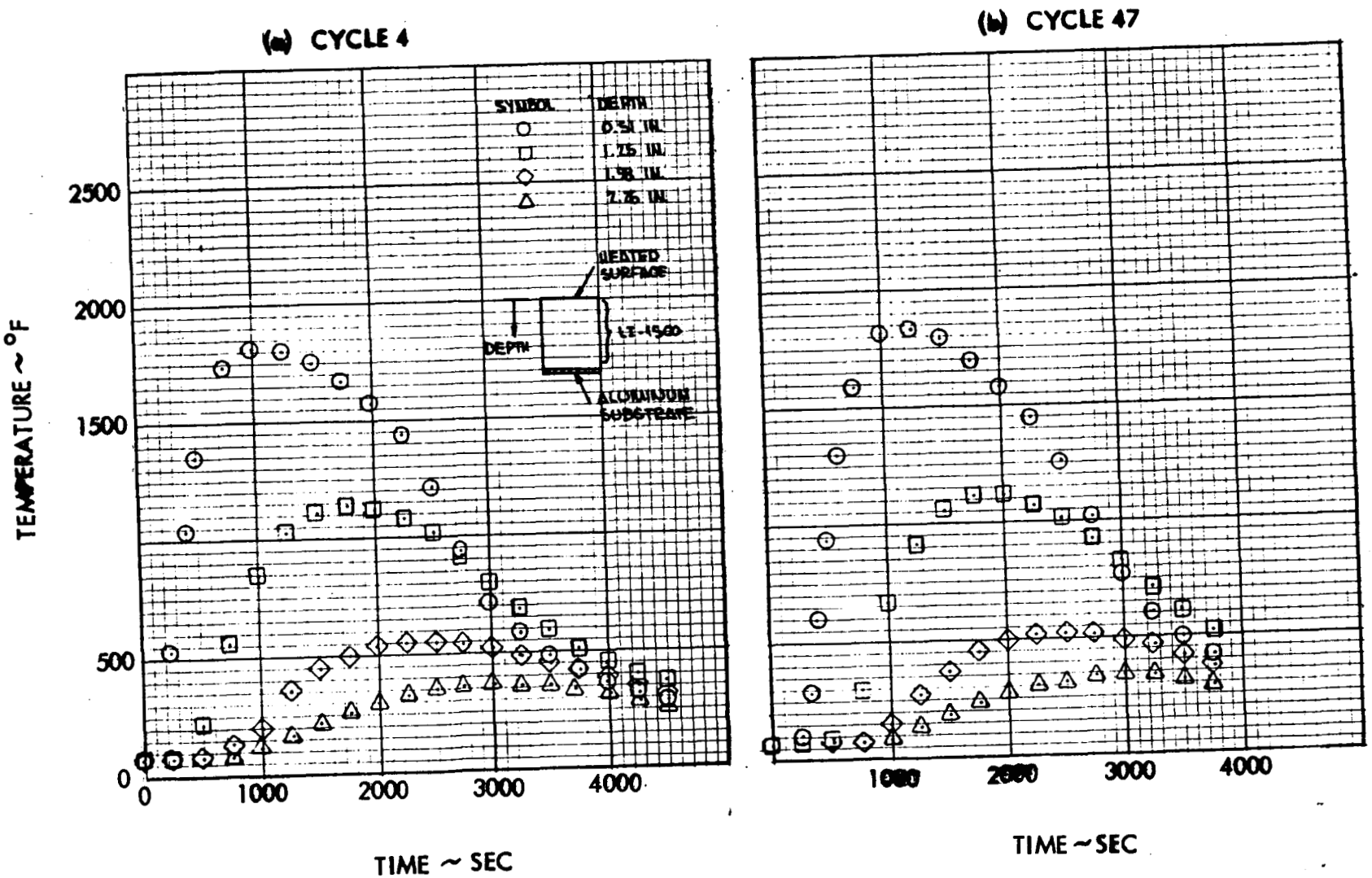


DO6154

Fig. 3.1-8

# TEMPERATURE HISTORIES FOR SPECIMEN TT 42-4 DURING 100 CYCLE TESTS (CONTINUED)

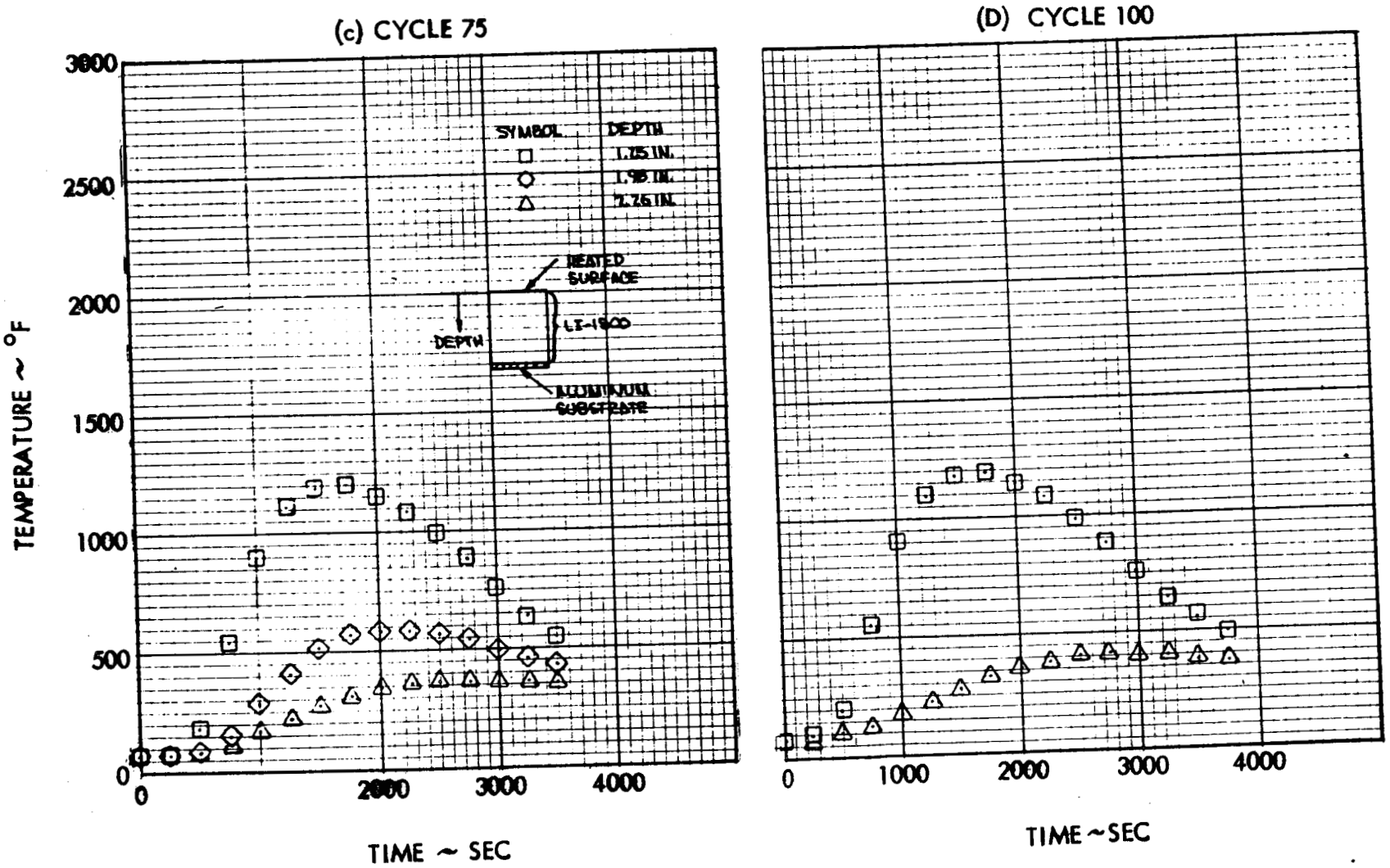


DO6155

Fig. 3.1-8 (Cont)

# COMPARISON OF MEASURED AND PREDICTED PEAK TEMPERATURES FOR 100 CYCLE TESTS - SPECIMEN TT42-4

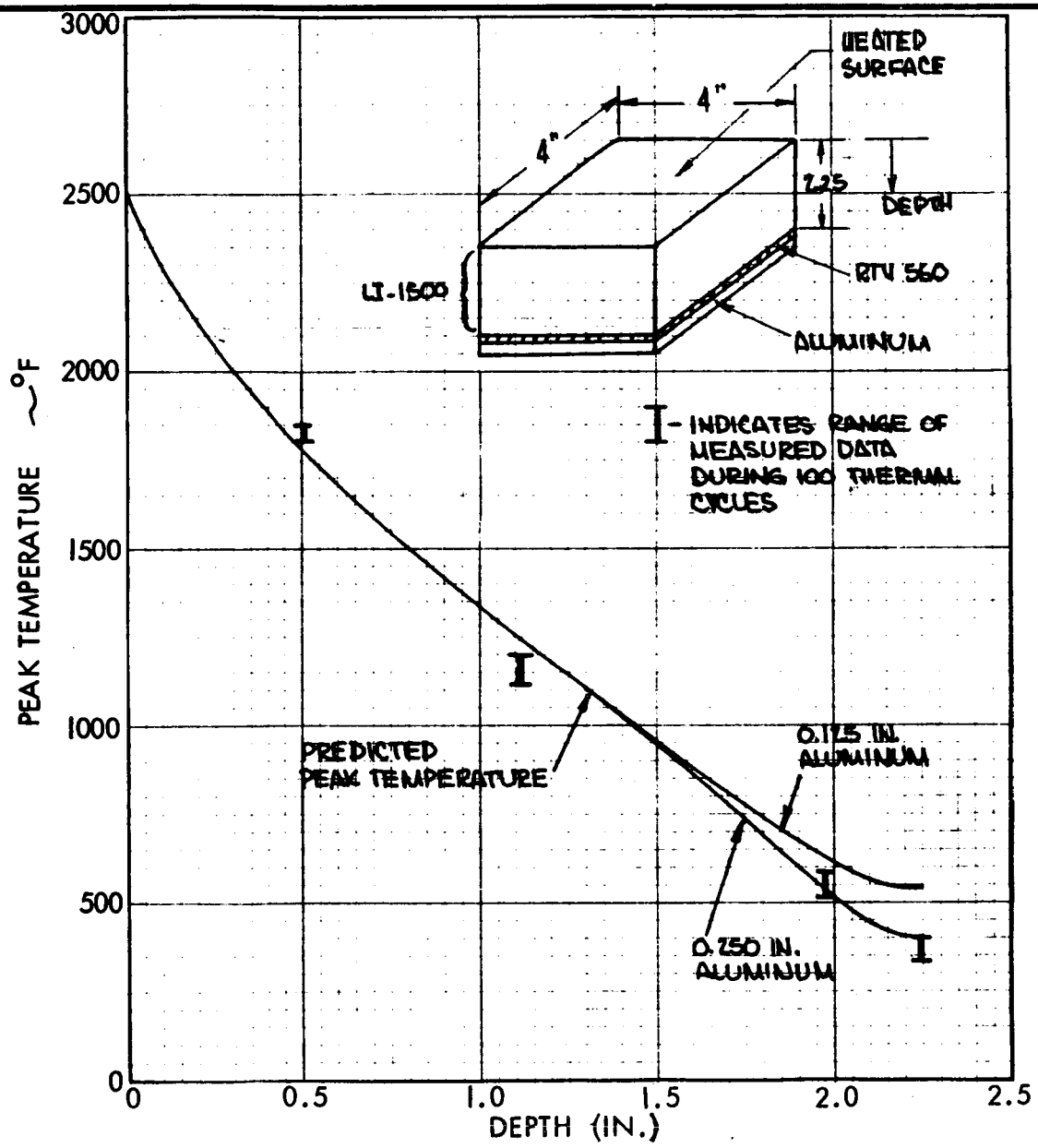


Fig. 3.1-9

DO6097

Table 3.1-1

# DIMENSIONAL DATA FOR 100 CYCLE TEST PROGRAM

| SPECIMEN NO. | SURFACE COATING | LENGTH (IN.) | | WIDTH (IN.) | | THICKNESS (IN.) | |
|---|---|---|---|---|---|---|---|
| | | PRE-TEST | POST-TEST | PRE-TEST | POST-TEST | PRE-TEST | POST-TEST |
| TT42-3 | INTEGRAL BOROSILICATE WITH SILICON CARBIDE EMITTANCE AGENT | 3.933 | 3.930 | 3.930 | 3.917 | 2.270 | 2.164 |
| TT42-4 | INTEGRAL BOROSILICATE WITH SILICON CARBIDE EMITTANCE AGENT | 3.957 | 3.946 | 3.940 | 3.922 | 2.407 | 2.150 |
| TT42-5 | OO42 – BOROSILICATE WITH SILICON CARBIDE EMITTANCE AGENT | 3.932 | 3.932 | 3.914 | 3.914 | 2.450 | 2.376 |
| TT42-6 | OO42 – BOROSILICATE WITH SILICON CARBIDE EMITTANCE AGENT | 3.924 | 3.924 | 3.920 | 3.918 | 2.445 | 2.411 |

Future plans for these cycled specimens include:

a. Thermal exposure to a simulated pressure and temperature environment
b. Sectioning and morphology study to determine any in-depth phase changes
c. Exposure to an acoustic environment
d. Waterproofing and cycling to 2300°F to establish life of the waterproof coating

In summary, the Material Improvement Program NAS 9-12137 has produced a surface coating capable of withstanding 83.3 hr of accumulated thermal exposure with 14 hr at temperatures greater than 2300°F (2500°F). This environment corresponds to 100 consecutive overshoot reentries representative of a 1100 nm crossrange mission.

## 3.2 POTENTIAL FAILURE MODES

The potential failure mode characteristics of the LI-1500 coating and attachments are to be identified through both testing efforts and analytical investigations. The efforts performed under Task 2.0 have concentrated on the overstress mechanical and thermal loading of the composite TPS as a primary failure mode. Testing under Tasks 4.0 and 5.0 is not complete, and conclusions as to failure modes will be made as data become available.

A primary problem with RSI materials is the difficulty involved in establishing mechanical properties. This problem is discussed in more detail in Section 4.2. A primary potential failure mode to be considered is in overstress conditions and the ability of analytical techniques to ensure design adequacy becomes of primary importance. To demonstrate this failure mode and verify analytical techniques, a test specimen has been fabricated and is currently in test. Fig. 3.2-1 shows the test specimen, which consists of two small LI-1500 tiles (with the 0042 coating) bonded to an aluminum substrate. The bonding agent is RTV-560 and was sized to 0.020-in. thickness to ensure LI-1500 overstress conditions at loads below the aluminum yield.

A stress analysis has been performed, using the methods discussed in Section 2.2 for tensile loads in the aluminum plate. The specimen will be pulled to a load sufficient to severely damage the LI-1500. Following this failure test, additional testing is planned for this specimen in a radiant heat and acoustic environment. These tests will establish the significance of failures such as this on TPS performance.

LMSC recognizes the fact that under actual flight conditions the LI-1500 will be subjected to combined stresses and the value of uniaxial allowable results are somewhat questionable for the actual use conditions. To become fully acquainted with a new material's capabilities, it is necessary to first establish its uniaxial properties. Once these properties are established, combined stress states must be investigated. Although LMSC is not completely satisfied with the uniaxial results and realizes more data points are required, a series of combined shear and tension tests have been performed in an effort to determine the allowables in the weak shear tension

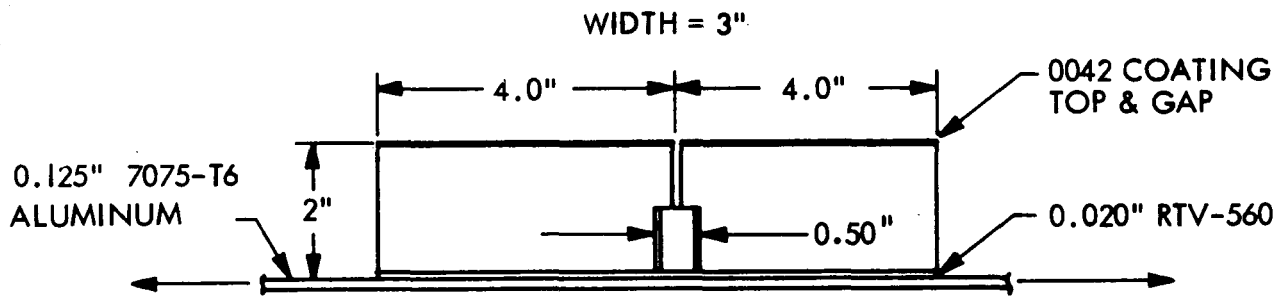


Fig. 3.2-1 Analytical Verification Model

directions (i.e., shear parallel to the fiber orientation direction and tension normal to the fiber orientation direction). This particular combination of stress components appears to be one critical design condition and occurs at the ends of a tile. Room temperature tests were performed in the torsion tester (described in Section 4.2) through a modification of the test fixture that allowed a predetermined tension load to be put on the shear specimens prior to application of the torque load. Of course the results of these tests suffer from the same conditions of nonuniformity of the state of stress as discussed in Section 4.2. However, the results provide lower bounds on the failure envelope and offer preliminary guidelines for future work.

Ideally such tests should be carried out on thin walled cylinders in a combined tension-torsion mode; however, due to basic LI-1500 characteristics, such cylinders would have to be at least 4-in. long with a 3 to 4 in. outer diameter and a 3/8-in. wall thickness, minimum. Such dimensions would require vast quantities of LI-1500 (beyond those available) and the close tolerance machining required for meaningfull data might not be practical.

The results of preliminary testing are summarized in Fig. 3.2-2 and Table 3.2-1. These apply to LI-1500 of various densities for a restricted range of weak direction tension $\sigma$, which was dictated by test apparatus limitations for the denser materials. The data appear to correspond to a linear failure criterion, which is not precluded by any theoretical considerations but seems to indicate a large degree of interaction between these stress components. By way of contrast, no interaction would be characterized by a rectangular profile joining the uniaxial allowables.

No definitive conclusions can be drawn from the above tests, particularly, since the results are in direct conflict with data concerning a titanium wing panel designed under the preceding contract. This panel withstood an axial line load equivalent to 60,000 psi with a backface temperature of 320$^{\circ}$F without experiencing the failure mode discussed here.* Stress levels computed for this test are summarized in Table 3.2-2 and the state of combined stress under consideration here is shown as the point not only outside the linear interaction curve but the no-interaction curve as well. Results from the analytical verification testing will also be compared with these data. Material variability could conceivably account for some discrepancy, however, it is believed that part of the effect could be due to the fact that LI-1500 is brittle at room temperature but seems to become more ductile with increasing temperature. In addition, statistical theories of brittle materials can allow such apparent discrepancies, although not to the extent seen here. This is due to testing material samples with nearly uniform stress states over a relatively large volume of material and then applying the results to a critical stress state that occurs in a very small volume of material. In other words, average stress measurements can be very misleading. Brittle materials experience size effects connected with the fact that they fail at the weakest or most critical flow without allowing stress distribution to occur as in ductile metals. Hence, the probability of having a critical flow in the material goes up as the stressed volume increases, which leads to lower strength levels.

*Data according to NASA document ES65-9/2/71-099 supplied by ES6/Chief, Structural Test Branch, G. E. Griffith

# PRELIMINARY INTERACTION DATA

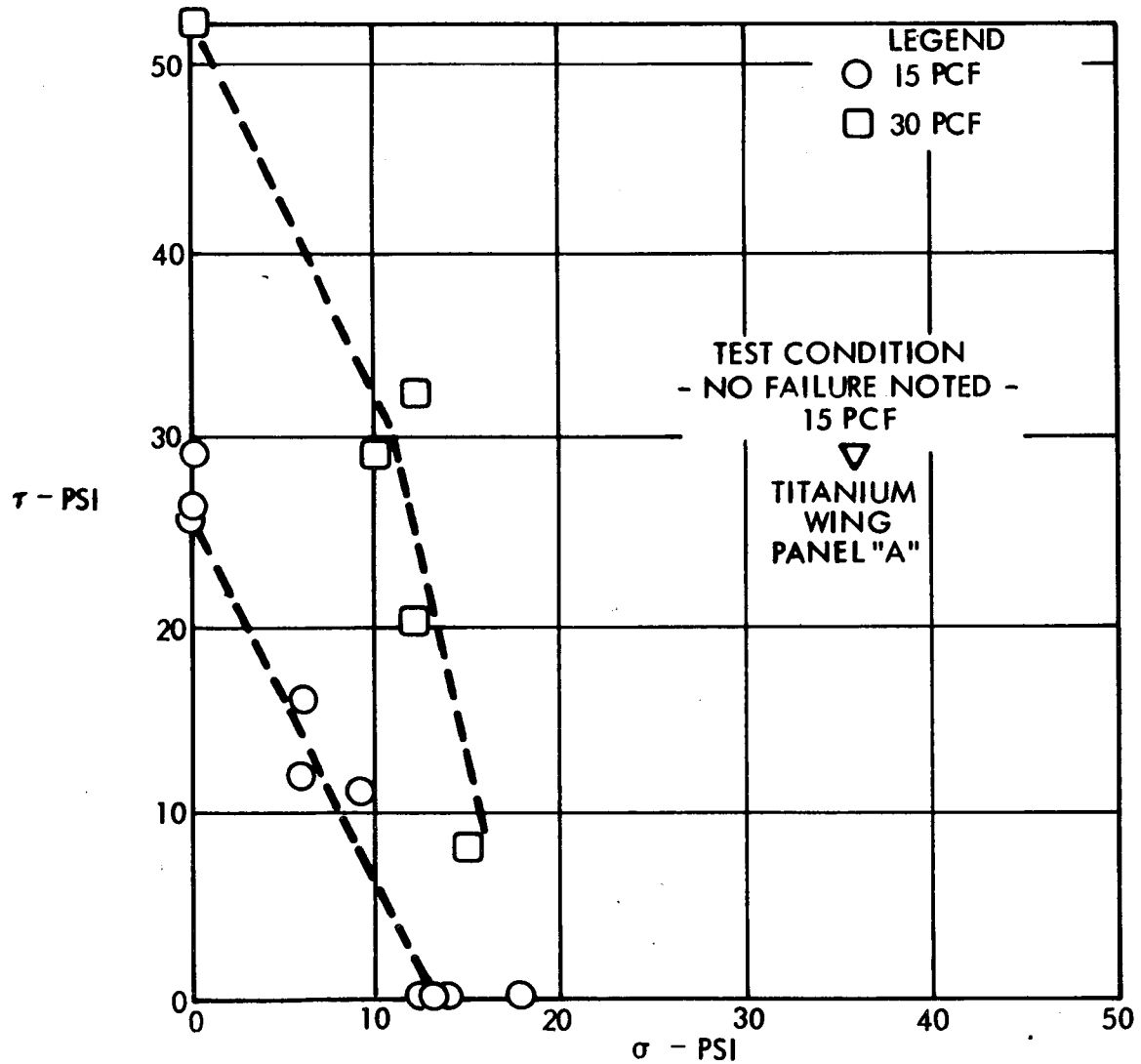


DO6024

Fig. 3.2-2

Table 3.2-1

RESULTS OF LIMITED BIAXIAL TESTING

| LI-1500 Density | $\sigma_{ult}$ (psi) | $\tau_{ult}$ (psi) |
|---|---|---|
| 15 pcf | 0 | 25 |
| | 0 | 26 |
| | 0 | 29 |
| | 6 | 16 |
| | 6 | 12 |
| | 9 | 11 |
| | 13 | 0 |
| | 14 | 0 |
| | 14 | 0 |
| | 18 | 0 |
| 30 pcf | 0 | 52 |
| | 10 | 29 |
| | 12 | 32 |
| | 12 | 20 |
| | 15 | 8 |
| 55 pcf | 10 | 100 |
| | 15 | 80 |
| | 20 | 76 |
| | 20 | 96 |
| | 20 | 92 |
| 60 pcf | 15 | 58 |

Table 3.2-2

CALCULATED STRESS LEVELS IN TITANIUM WING PANEL

| | | |
|---|---|---|
| Tile Size | 6 in. | 12 in. |
| Temp Surface | $75^{o}F$ | $75^{o}F$ |
| Temp TI | $320^{o}F$ | $320^{o}F$ |
| Axial Load | 60,000 (T) | 0 |
| Pressure | 0 | 0 |
| $E_{coat} = 35 \times 10^{6}$ psi | | |
| $T_{RTV} = 0.035$ | | |
| $T_{TI} = 0.19$ | | |
| Max LI-1500 | 102 | 38 |
| Min LI-1500 | -6 | -3 |
| RZ LI-1500 | 36(28) | 13(10) |
| RZ PRINCP | 54 | 19 |
| Long | 102 | 37 |
| Z + | 28 | 11 |
| Z - | -6 | -2 |
| Max RTV | 54 | 22 |
| Min RTV | -27 | -15 |
| RZ RTV | 32 | 13 |
| RZ PRINCP | 34 | 15 |
| Long | -10 | -9 |
| Peel | 31 | 15 |
| Max Coat | 770 | 1460 |
| Min Coat | -47 | -2 |

## 3.3 ATTACHMENT METHODS

The various bonding agents and mechanical fastener schemes considered by LMSC are presented in Section 2.2.4. The present LMSC baseline utilizes bonding of LI-1500 to the various vehicle metallic surfaces. As noted, RVT-560 has been selected as the adhesive system offering the best condition of characteristics of the commercially available adhesives.

Properties of adhesives for the various shuttle environmental conditions are not available in the literature. Therefore, LMSC has conducted some limited testing to establish critical design properties. The major design driver in establishing minimum bond thickness is shear modulus. To establish this property, shear tests were run at temperatures up to 600$^{o}$F, using a double shear fixture shown in Fig. 3.3-1.

In this fixture, a bond area of 3.00-in. length by 0.50-in. width is tested on both sides of a rod having a half-inch square cross-section. To create double shear, a bar cut in the shape of a tuning fork served as the other bonding face. The stem of the tuning fork and the square rod are colinear and coincide with the axis of applied force. This is illustrated in Fig. 3.3-2. The "jaw" of the tuning fork is machined to a specific width so that when the rod is correctly centered in the jaw, the gap between the fork and the rod (to be filled with elastomer) has a carefully controlled width. The alignment and centering during bond application is maintained by a template which has pins that pass through the stems of both the fork and the rod.

For test at high temperature, holes are drilled in the fork and rod, and thermocouples are embedded in the holes to monitor the temperature at the rod or fork mid-thickness and very near the bond (0.050 to 0.060 in. away). To prevent excessive heat from the heat lamps from burning the outermost layer of bond (while attempting to heat the center), the outer (exposed) bond area is covered with heavy foil that serves to shield the bond material from the direct radiation of the lamps. The surface of the fork and rod are coated with a black paint of high absorptivity so that the heat penetrates the

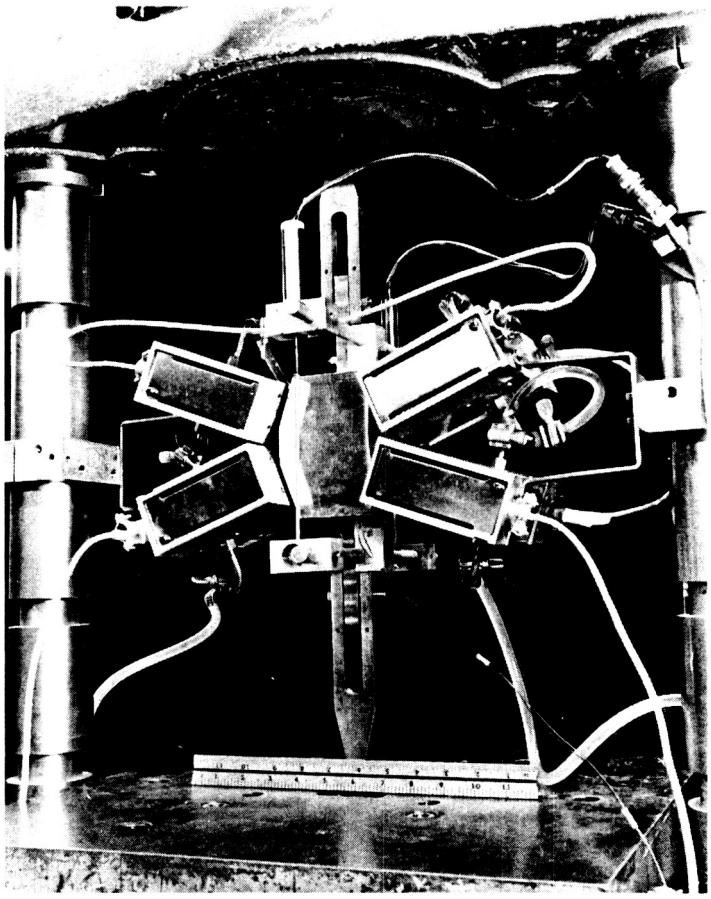

Fig. 3.3-1 High Temperature Bond Test Fixture

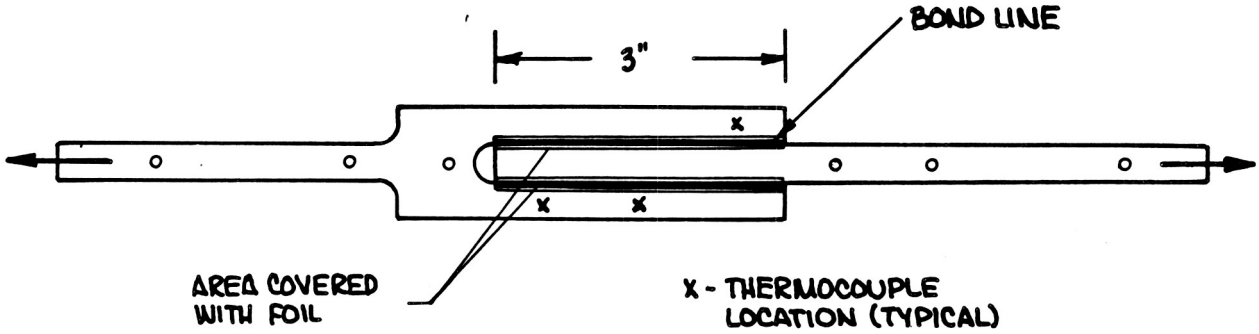


Fig. 3.3-2 Bond Shear Test Specimen

fork and rod and reaches the bond through conduction. The three thermocouples indicated that at 500°F the temperature spread on the three thermocouples is within a range of 10°F during the test.

The strain was measured by two averaging deflectometers placed outside the heated zone and connected to the rod and fork by two pairs of brackets. The brackets were attached to the fork and rod (respectively) at points only 1 in. from the termination of the bond line, so that deformation of the rod and fork (especially at the low failure loads involved) is minimal. Load versus the averaged deflection was recorded on X-Y plotter. Table 3.3-1 shows the results of the shear tests performed at 500°F and 600°F. As a result of these tests, LMSC is currently using a reduced shear modulus of 67 psi for 500°F and 600°F.

The techniques of controlling bond line thickness and application techniques are under investigation and will be continued for ultimate use on the prototype pack.

Various mechanical attachment designs are presented in Section 2.2.4. Preliminary tests performed under NAS 9-12137 have shown that LI-1500 can be locally densified by either silica or resin impregnation to increase strength. Figure 3.3-3 summarizes the results of eight pull-out tests on fasteners tapped into LI-1500 with local resin reinforcement. The strength of this type fastener system was not truly demonstrated, due to the failure in the weak tensile direction of the specimen (this would not occur on larger specimens in more controlled testing). Additional controlled testing will be accomplished in the near future.

Some analysis effort has been conducted on this type mechanical system as related in subsection 2.2.3.2. These investigations showed that such fastener concepts are not practical with the required close tolerance when made from common metals. One metal, Invar, is suited for this type application, however. Invar is 35 percent nickel and 65 percent iron with a coefficient of thermal expansion of approximately $1.2 \times 10^{-6}$ in./in./°F. An analysis has been made for a half inch diameter Invar insert in undensified LI-1500 at 600°F with negligible resulting stresses.

# TEST RESULTS – MECHANICAL FASTENER WITH LOCAL REINFORCEMENT

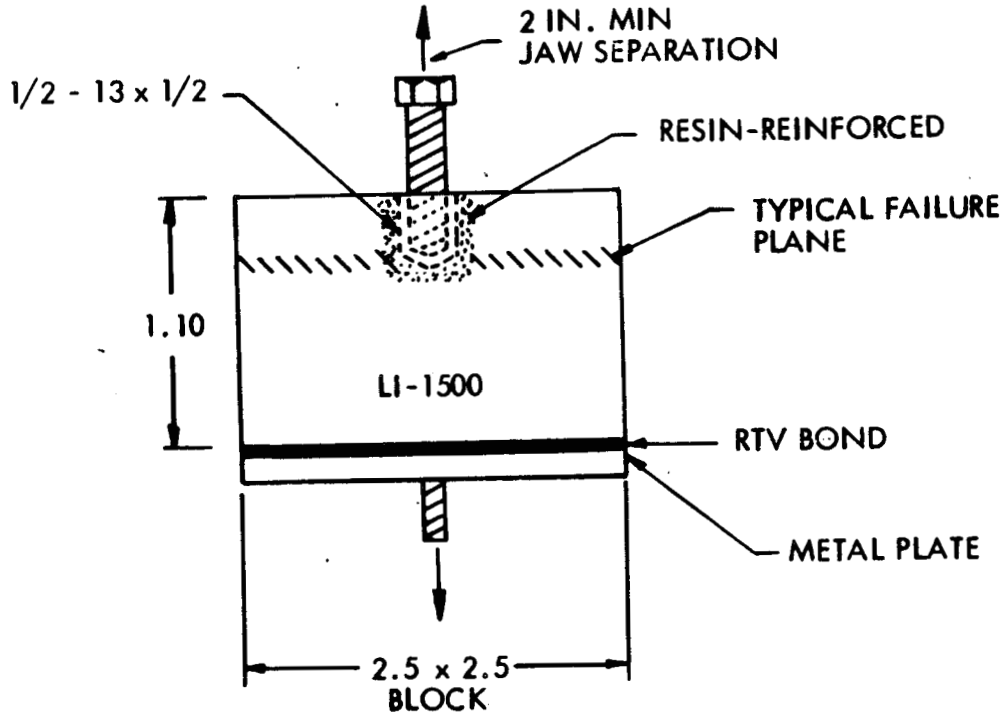


| | GRAMS |
|---|---|
| WEIGHT RESIN REINFORCEMENT ADDED | ~0.5 |
| WEIGHT OF LI-1500 MATERIAL REMOVED | ~0.5 |
| NET WEIGHT GAIN | 0 |

| | LB |
|---|---|
| 8 SPECIMEN – FAILURE LOAD: | |
| AVERAGE | 31 |
| MAXIMUM | 40 |
| MINIMUM | 29 |

Fig. 3.3-3

D05162
rdb

Table 3.3-1

RTV-560 BOND SHEAR TESTS

| Bond Thickness (in.) | Specimen Number | Maximum Load at 600°F (lb) | Maximum Shear Stress at 600°F (psi) | Shear Modulus at 600°F (psi) | Shear Modulus at 500°F (psi) |
|---|---|---|---|---|---|
| 0.020 | A1 | 52 | 17.3 | 28.1 | 78.5 |
| 0.020 | A2 | 38 | 12.7 | 23.8 | 59.4 |
| 0.030 | B1 | 18 | 6.0 | 11.8 | 53.3 |
| 0.030 | B2 | 33 | 11.0 | 17.9 | 84.0 |
| 0.040 | C1 | 18 | 6.0 | 19.6 | 54.4 |
| 0.040 | C2 | 34 | 11.3 | 25.8 | 70.0 |

Figure 3.3-4 shows two Invar fastening device configurations that have been fabricated. The first device (a) snaps into position on the shuttle by installation pressure. The second device (b) requires a small access hole through the tile for installation with a half turn lock device. Installation, dynamic and pull out tests of these devices have not been completed.

## 3.4 NON-DESTRUCTIVE EVALUATION (NDE) METHODS

As delineated in the contract, LMSC has has a continuing in-house Independent Development effort concerned with establishing NDE inspection techniques for LI-1500. The results to date of the effort are reported in Appendix G.

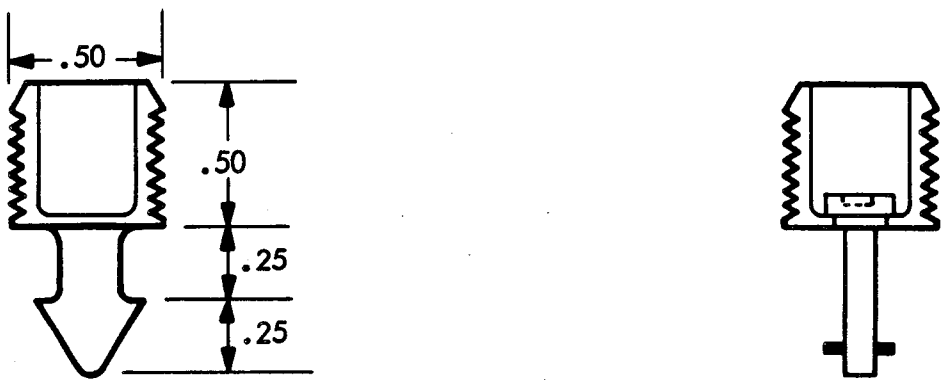


Fig. 3.3-4 Invar Fastening Devices

# Section 4
# PROPERTY CHARACTERIZATION

The objective of this task is to obtain detailed physical, mechanical, and thermophysical properties of LI-1500. The testing program has followed the Property Test Plan (NAS 9-11222) approved by NASA/MSC during the second month of the contract. This mid-term document reports on the results to date and compares them with existing data.

## 4.1 THERMOPHYSICAL PROPERTIES

### 4.1.1 Specific Heat

A flooded-ice mantle drop type calorimeter was used to measure the enthalpy of the LI-1500 material, referenced to 273°K, over the temperature range from 200°F to 1800°F. The specimen was contained in an oxidized Type 316 stainless steel capsule for temperatures up to 1800°F. In past tests, the specimen was in a graphite capsule for the temperatures above 1800° F. The specimens were heated in an air atmosphere in an alumina furnace for the measurements to 1800°F.

Enthalpy measurements were made on 12-gram specimens of the material, pulverized to obtain maximum mass for the capsule. Specimens were taken from as-fabricated LI-1500 and from LI-1500 which was thermally cycled in a 1 atmosphere air furnace for a total of 20 half hour cycles at 2300°F. Preliminary calculations of specific heat were made, using a graphical fit of the enthalpy-temperature data. These results are shown in Fig. 4.1-1. The data are in agreement with those reported earlier (NAS 9-11222) and no significant differences were observed between the as-fabricated and the thermally cycled specimens.

### 4.1.2 Thermal Expansion

Measurements of linear thermal expansion were performed in an air atmosphere over the temperature range from 70°F to 2350°F. Measurement directions were parallel

# VARIATION OF LI-1500 SPECIFIC HEAT WITH TEMPERATURE

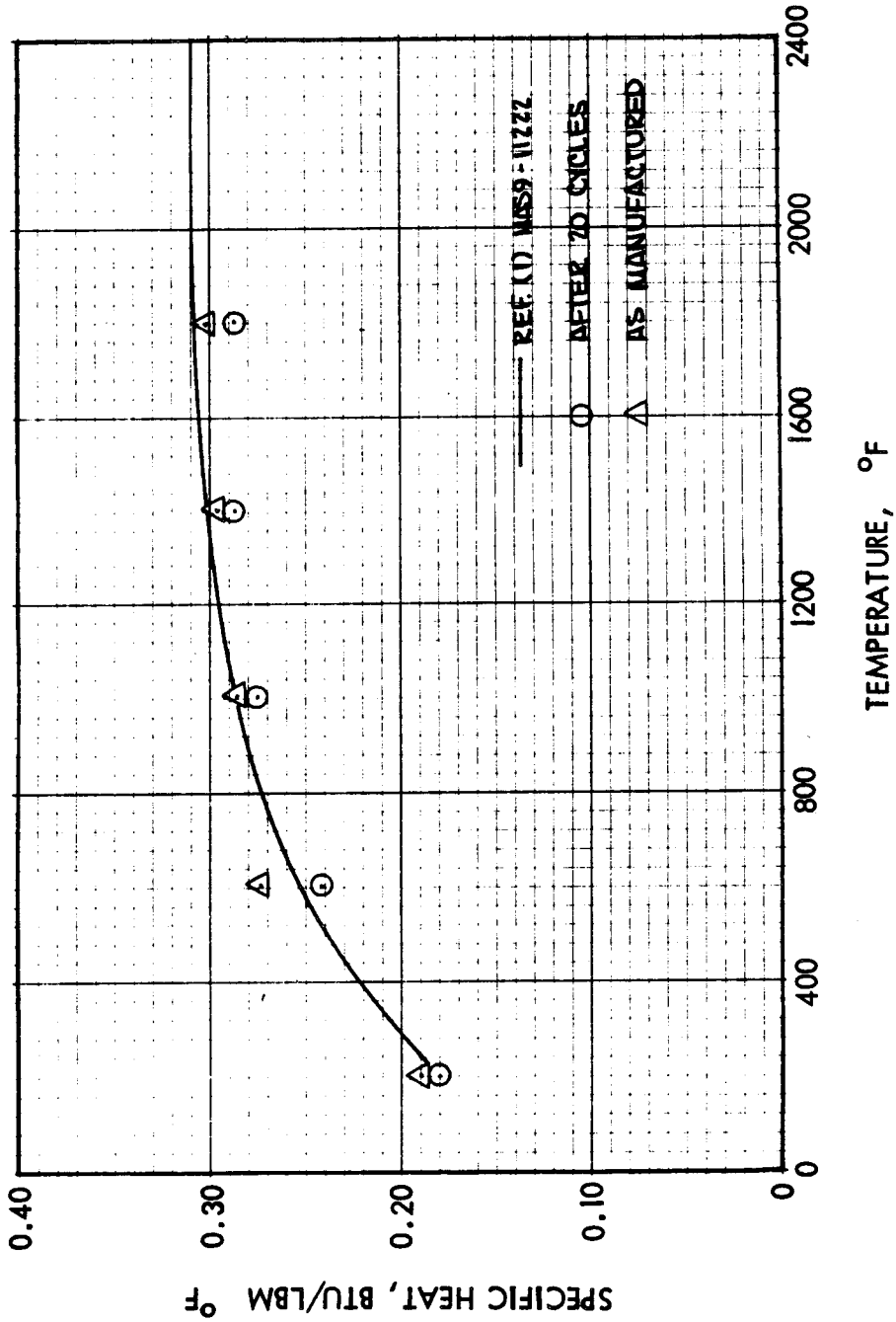


Fig. 4.1-1

DO6002

and normal to the thickness direction of the as-fabricated material and material that was exposed to 20 thermal cycles of half hour exposure to 2300°F in a 1-atmpshere air furnace. Push-rod dilatometers of two materials were used for the measurements. A fused silica dilatometer was employed up to 1650°F. This apparatus was initially calibrated against an NBS Fused Silica Standard, SRM 739, to within 5 percent over this temperature range. The specimens were heated in a furnace with a programmed temperature rate of 1.5 to 2°F/min over this temperature range. After cooling to room temperature the specimens were then placed in an alumina tube dilatometer for the temperatures above 1700°F. Dimensional changes were recorded at steady state temperatures using a calibrated dial gauge having a least count of $2 \times 10^{-5}$ in. Exposure time from 1700° to 2300°F varied from 1-1/2 to 2 hours.

Three specimens were measured for both directions from the as-fabricated material. For the normal-to-thickness direction (parallel to the fiber orientation) the specimen size was 3 in. x 3/8 in. diameter rods. The specimen for the parallel-to-thickness direction (normal to the fiber orientation) was composed of two 1-1/2 in. x 3/8 in. diameter rods stacked to give an overall length of 3 in. This length was chosen to increase the measurement accuracy for low expansion material.

Specimen dimensions and pre-test exposure conditions together with post-test length and weight change data are given in Table 4.1-1. All specimens showed a negligible weight loss and a shrinkage of 0.9 to 1.4 percent. Exposure time at the highest temperature varied, and this undoubtedly has an effect on the recorded dimensional change. Also, pre-and-post test X-ray diffraction patterns were obtained to determine if the test exposure resulted in a change in crystallography of the material. Results have not been completed for Specimens 1-20 and 4-20, but for Specimens 1 and 4 both pre-and-post-test results did not reveal the presence of crystobalite or $\alpha$ quartz.

Thermal expansion data for Specimens 1 through 6 (pre-cycling) are shown in Fig. 4.1-2 and 4.1-3. Data for the material after exposure to 20 thermal cycles is shown in Fig. 4.1-4. In all cases, the as-manufactured material started to shrink in the temperature range of 2100° to 2200°F. The post-20 cycle material showed the start of shrinkage in the 2000° to 2050°F range.

Table 4.1-1

THERMAL EXPANSION SPECIMEN DESCRIPTIONS

| Direction | Exposure Prior to Expansion Measurement | Specimen Number | Define Test Bulk | | Post Test | |
|---|---|---|---|---|---|---|
| | | | Length (In.) | Density ($Lb/Ft^3$) | Length Change (%) | Weight Change (%) [a] |
| Perpendicular-to-Block Thickness | As Manufactured | 1 | 3.001 | 14.6 | -0.9 | <0.3 |
| | As Manufactured | 2 | 2.999 | 12.8 | -1.0 | <0.3 |
| | As Manufactured | 3 | 2.958 | 14.6 | -1.0 | <0.3 |
| | After 20 thermal cycles | 1 - 20 | 3.092 | 15.6 | -0.9 | <0.3 |
| Parallel-to-Block Thickness | As Manufactured | 4 | 2.992 [b] | 14.3 [b] | -1.3 | <0.3 |
| | As Manufactured | 5 | 2.990 [b] | 13.7 [b] | -1.4 | <0.4 |
| | As Manufactured | 6 | 2.988 [b] | 13.9 [b] | — | <0.4 |
| | After 20 thermal cycles | 4 - 20 | | — | | |

(a) Weight change may be due in part to abrasion of specimen during handling.

(b) Two specimens stacked end-to-end, density is average of two specimens.

# THERMAL EXPANSION IN DIRECTION PARALLEL TO FIBER ORIENTATION

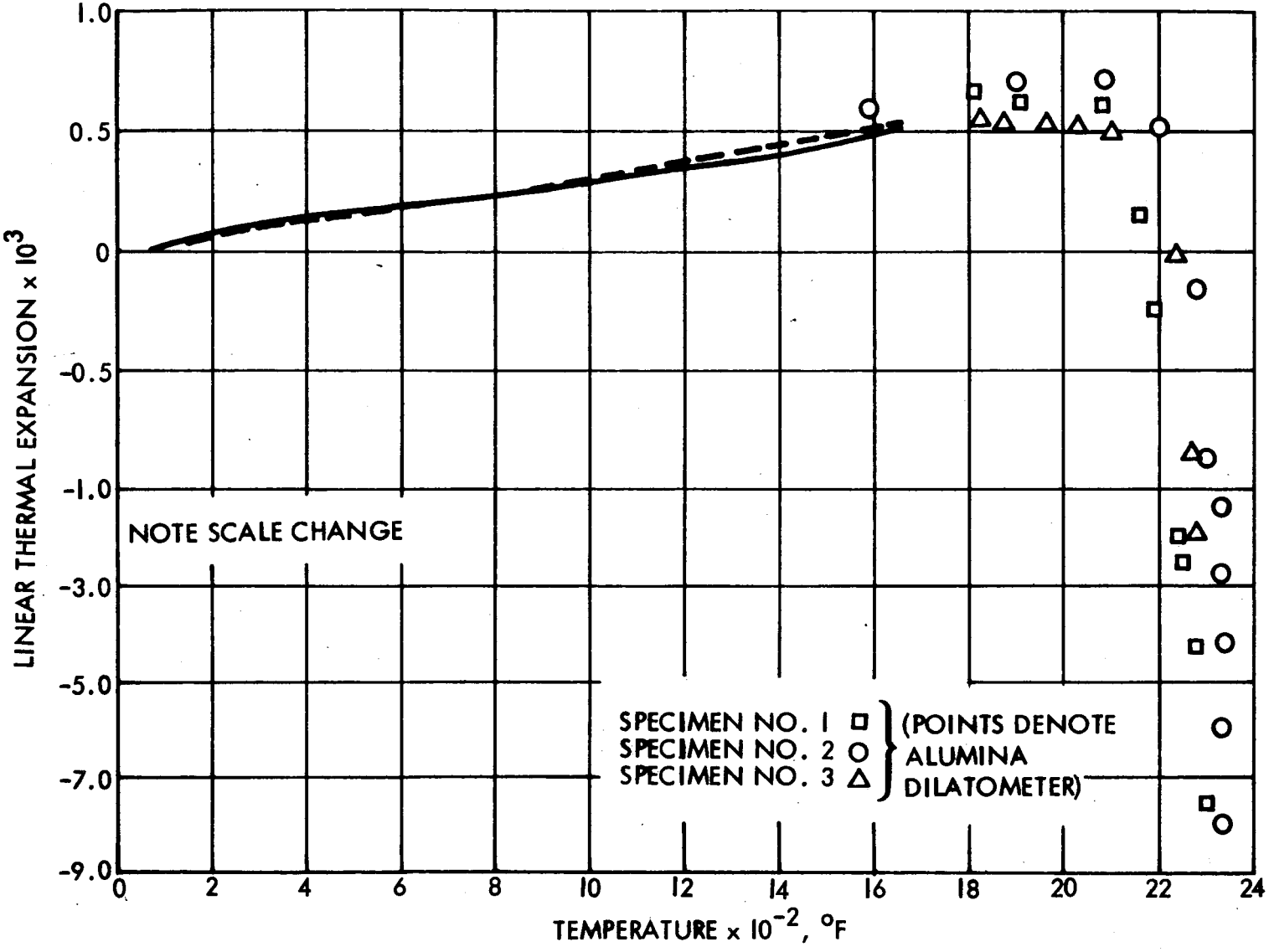


DO6118

Fig. 4.1-3

# THERMAL EXPANSION IN DIRECTION NORMAL TO FIBER ORIENTATION

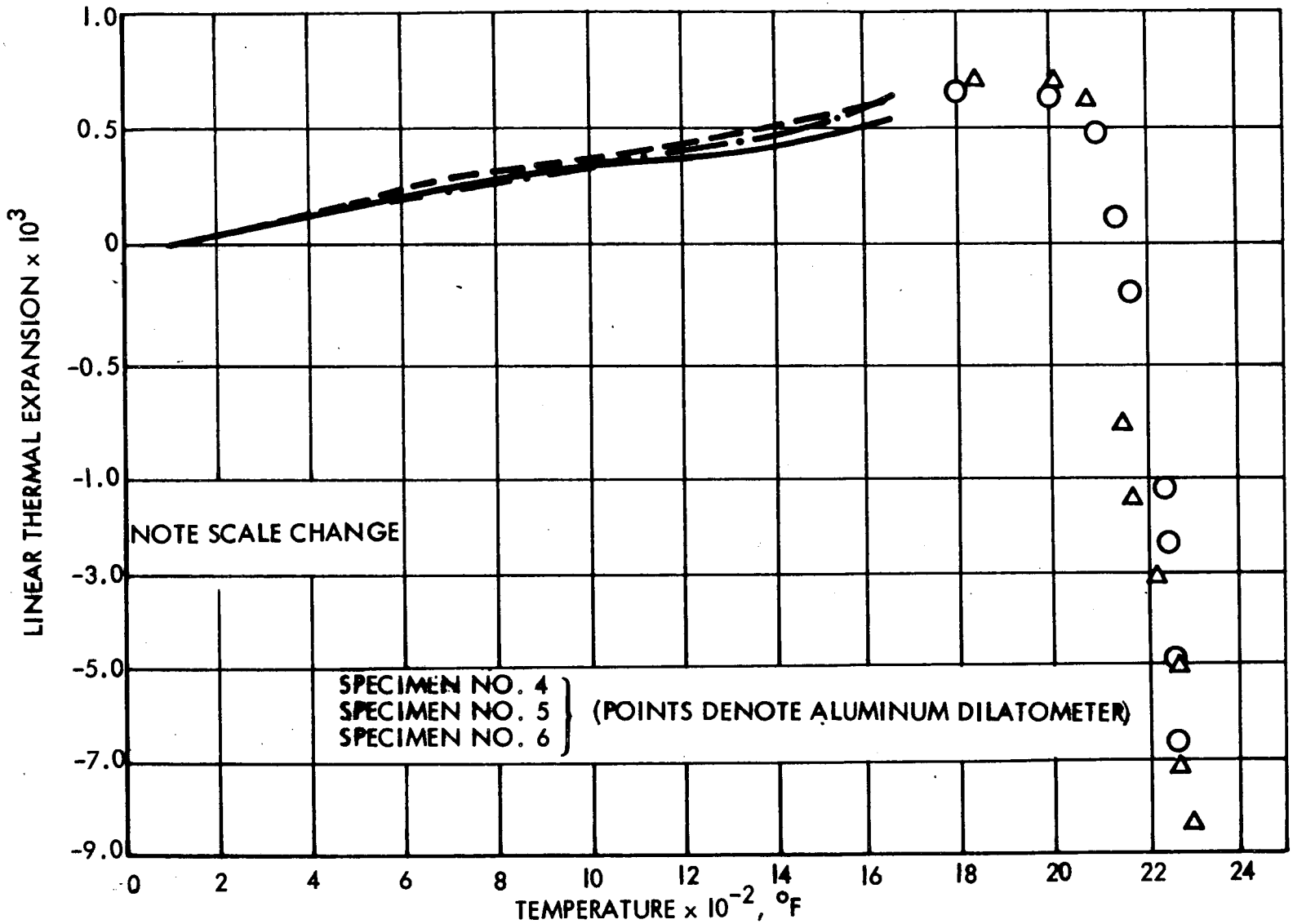


DO6119

Fig. 4.1-3

# THERMAL EXPANSION FOR THERMALLY CYCLED SPECIMENS

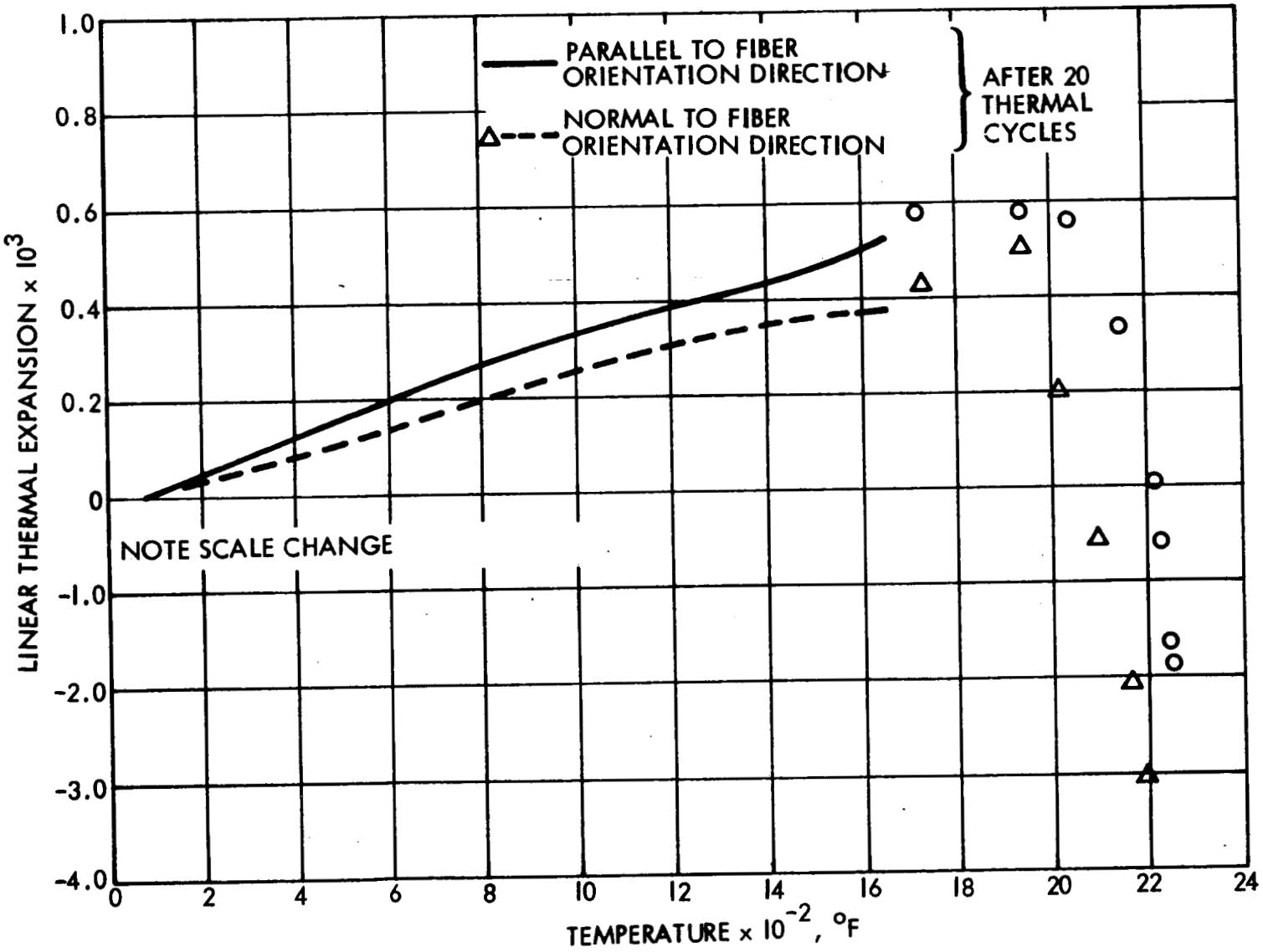


Fig. 4.1-4

DO6124

Table 4.1-2 gives a comparison of expansion at several temperatures for all of the specimens tested. The exposure to 20 thermal cycles did not have a significant effect on the expansion behavior of the material. Thermal expansion coefficients between $70^{\circ}$ and $2000^{\circ}F$ ranged from 3.3 to 3.6 x $10^{-7}$ in./in. $^{\circ}F$ for Specimens 5 and 6, and 2.8 to 3.8 x $10^{-7}$ in./in. $^{\circ}F$ for Specimens 1 through 3. For the post-thermal cycling specimens, expansion coefficients were 2.7 to 3.0 x $10^{-7}$ in./in. $^{\circ}F$ for normal and parallel to fiber orientation directions, respectively.

Comparison of the as-fabricated thermal expansion coefficients over past contracts is shown in Table 4.1-3. The thermal expansion coefficient in the fiber orientation direction has remained fairly constant for the various batches shown. The high value of expansion coefficient reported under NAS 9-11222 in the normal to fiber orientation direction is attributed to impurities in the raw fiber used to manufacture LI-1500. This situation has been remedied as evidenced by the current low values of thermal expansion coefficient.

### 4.1.3 Thermal Conductivity

To provide NASA with an independent evaluation of thermal conductivity of LI-1500, a subcontract was let to the Southern Research Institute (So.R.I.) of Birmingham, Alabama, for measurement of thermal conductivity data. So.R.I. had previous experience measuring thermal conductivity of LI-1500 Mallite and Alumina-Silica-Chromia under a contract from NASA/LaRC.

A description of the apparatus follows.

The ASTM C-177 guarded hot plate apparatus was used for thermal conductivity measurements from -150 to $500^{\circ}F$. The apparatus was installed in a vacuum bell jar to provide environmental control. Liquid nitrogen was used in the cold plates to provide the cryogenic temperatures. Gaseous nitrogen was used as the environmental gas for the system. The uncertainty in measurements with the guarded hot plate was ±5 percent.

Table 4.1-2

COMPARISON OF LINEAR THERMAL EXPANSION BEFORE AND AFTER CYCLIC EXPOSURE TESTING IN PARALLEL AND NORMAL TO FIBER ORIENTATION DIRECTION

| Temperature (°F) | Before Cycling[a] (inch/inch) | | After Cycling[b] (inch/inch) | |
|---|---|---|---|---|
| | Normal | Parallel | Normal | Parallel |
| 400 | 9.7 to 13.5x10$^{-5}$ | 10.3 to 13.6x10$^{-5}$ | 8.6x10$^{-5}$ | 12.4x10$^{-5}$ |
| 650 | 20.1 to 25.1x10$^{-5}$ | 10.3 to 19.6x10$^{-5}$ | 15.1x10$^{-5}$ | 21.2x10$^{-5}$ |
| 900 | 30.3 to 33.8x10$^{-5}$ | 22.3 to 25.9x10$^{-5}$ | 22.5x10$^{-5}$ | 30.2x10$^{-5}$ |
| 1300 | 39.4 to 47.0x10$^{-5}$ | 37.7 to 42.3x10$^{-5}$ | 33.3x10$^{-5}$ | 41.0x10$^{-5}$ |
| 1650 | 54.6 to 62.7x10$^{-5}$ | 50.4 to 56.0x10$^{-5}$ | 37.6x10$^{-5}$ | 53.6x10$^{-5}$ |
| 2000 | 64.0 to 69.8x10$^{-5}$ | 53.0 to 73.0x10$^{-5}$ | | 58x10$^{-5}$ |
| 2200 | -40.0 to 200x10$^{-5}$ | +52.0 to -25.0x10$^{-5}$ | | 5x10$^{-5}$ |

Table 4.1-3

COMPARISON OF PAST LI-1500 THERMAL EXPANSION RESULTS

| Source/Date → | LMSC 1967 | SO R.I. 12-70 | NAS 9-11222 2-16-71 | Battelle 3-1-71 | Battelle 7-1-71 (TT 14B) | NAS 9-12083 10-71 |
|---|---|---|---|---|---|---|
| $\alpha$ Fiber Orientation Direction (in./in.-°F) 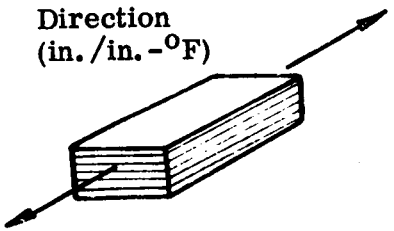 | $3 \times 10^{-7}$ | $5.1 \times 10^{-7}$ | $4.3 \times 10^{-7}$ | $5\text{-}10 \times 10^{-7}$ | $3\text{-}7 \times 10^{-7}$ | $2.8\text{-}3.8 \times 10^{-7}$ |
| $\alpha$ Normal to Fiber Orientation Direction (in./in.-°F) 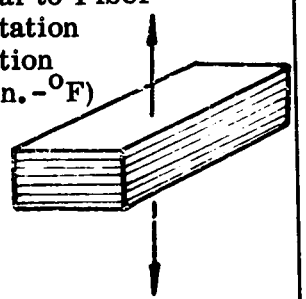 | – | $5.7 \times 10^{-7}$ | $2.7 \times 10^{-6}$ | – | – | $3.4 \times 10^{-7}$ |
| Temperature Range (°F) | 80-1700 | 80-2050 | 80-1700 | 80-1400 | 80-1700 | 80-2000 |

A radial inflow apparatus (RIA) was used for the measurements of thermal conductivity from 800 to 2000°F. Basically, the apparatus consists of a graphite heater tube that surrounds a specimen mounted on a water flow calorimeter centered axially through the specimen. Heat flows inwardly through the specimen into the calorimeter.

The basic random uncertainty with the radial inflow apparatus on "well-behaved" materials is ±7 percent. For the particular measurements in this program, with the strip specimens, random uncertainty is estimated to be ±10 percent. In addition to the random uncertainty, there is a systematic uncertainty due to the heat flow that tends to bypass the specimen through the thermatomic carbon in the corners and gives an erroneously high value. For the thermal conductivity level of the LI-1500, the uncertainty due to heat bypass is estimated to be no more than +10 percent. Hence, the total uncertainty is estimated to be -10 percent to +20 percent. A more detailed description of the RIA apparatus will be provided in the final report.

The results of the first batch of specimens (as-fabricated LI-1500) are contained herein. The final report will contain thermal conductivity data on specimens that have been exposed to 10 and 20 thermal cycles of 1/2 hour duration at 2300°F in a 1 atmosphere air oven.

Figure 4.1-5 shows a comparison of as-fabricated thermal conductivity data with the design curves used for NAS 9-11222. The low pressure data ($10^{-3}$ mm Hg) compares well with the design curve, while the average value of the atmospheric pressure data is about 5 to 8 percent higher than the design curve at 2000°F. Predictions of measured in-depth thermocouple data from the LI-1500 specimens exposed to 100 reentry cycles (see Task 3, Fig. 3.1-7) resulted in very good agreement with the measured data. Hence the current design curves (NAS 9-11222) are considered adequate for LI-1500 sizing.

The large difference in thermal conductivity at 2000°F between the 0.1 mm and the 760 mm Hg curve, about a factor of 2, is the primary reason for the large decrease in LI-1500 thickness (~30 percent) for the flight panels discussed in Section 2.2.2.

# COMPARISON OF RECENT LI-1500 THERMAL CONDUCTIVITY DATA WITH DESIGN CURVES

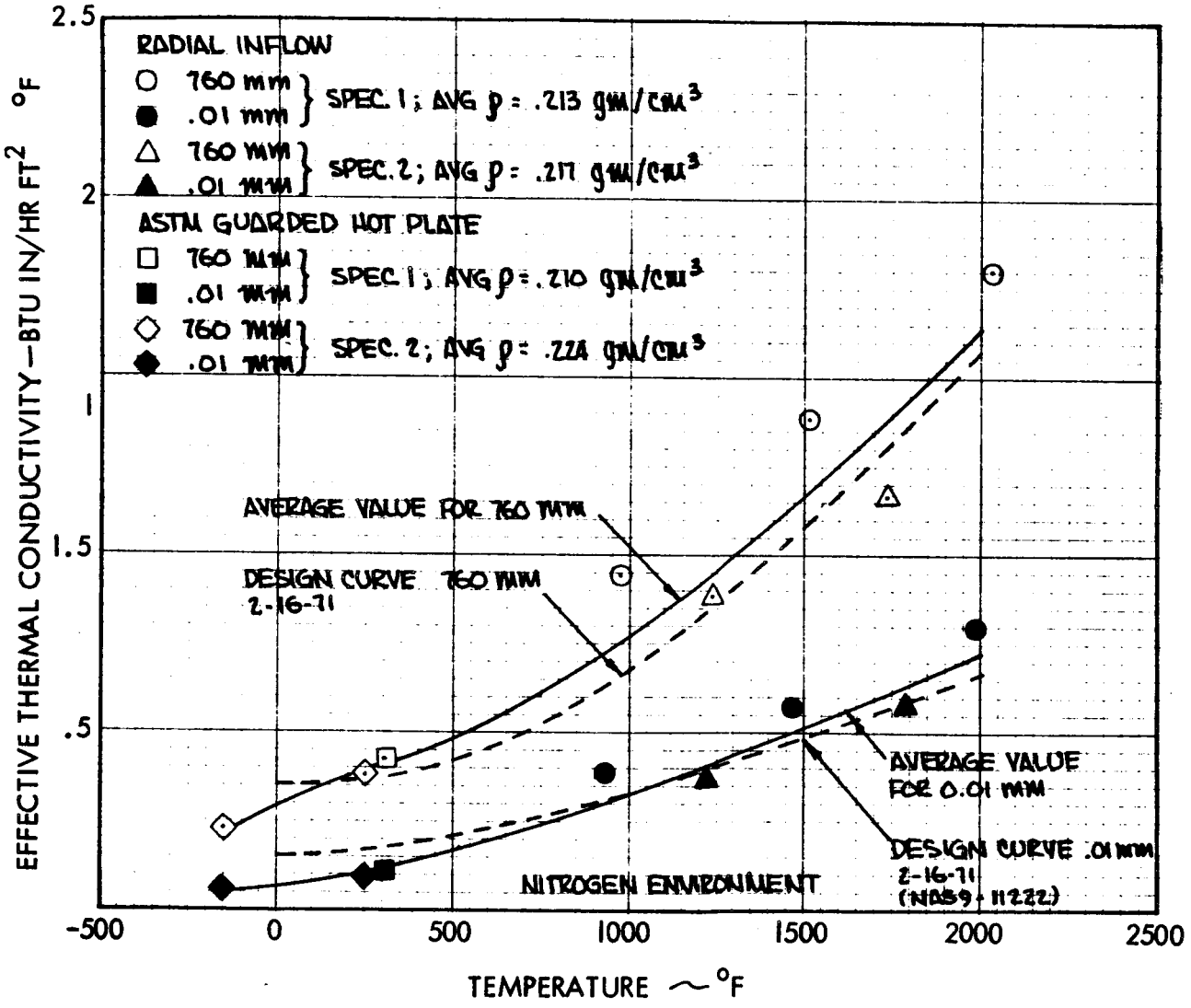


Fig. 4.1-5

DO6062

Data were also obtained at 5 mm and 50 mm Hg to allow verification of the variation of thermal conductivity with pressure data currently being used for design purposes. These data are shown in Tables 4.1-4 and 4.1-5.

Future testing in LMSC's vacuum radiant facility should verify the low pressure design curves and the variation of LI-1500 thermal conductivity with pressure. Correlation of arc-jet data obtained at NASA/ARC is presently underway to verify the low pressure design curve. Since arc-jet data are more representative of the reentry convective environment, they will be more significant in establishing the low pressure conductivity curve.

The current variation of LI-1500 thermal conductivity with temperature and pressure used for flight panel designs is shown in Fig. 4.1-6. Tabulated design values of specific heat and thermal conductivity are listed in Table 4.1-6 and 4.1-7. A comparison of LI-1500 apparent thermal conductivity data from various sources, on various specimens and different apparatus is shown in Fig. 4.1-7. The maximum spread in the data (about ±12 percent) is considered within the measuring uncertainty of the apparatus and the data reduction methods. An indication of the repeatability of LI-1500 thermal conductivity during 100 cycles of thermal exposure is illustrated in Figs. 3.1-8 and 3.1-10 where the measured data were within 7 percent of the predicted value.

### 4.1.4 Thermal Degradation

The thermal degradation tests were performed on the LI-1500 material that was eventually used for the 10 and 20 thermal cycle mechanical property tests. The material (fiber lot 2085) was cycled in a 1-atmosphere air furnace with heating on five sides, according to the oven cycle shown in Fig. 4.1-8. The procedure consisted of putting the material in an oven preheated to 2300°F. The material was left in the oven for 30 min, then removed and allowed to cool in 70°F air. The time at temperature for one cycle is equivalent to three 1100 nm trajectories when following a 2300°F heating boundary as per LMSC Alternate Concept Study trajectories. The total heat (Btu/ft$^2$) in the oven cycle is also approximately equal to three 1100 nm trajectories.

Table 4.1-4

SUMMARY OF THERMAL CONDUCTIVITY DATA FOR LI-1500 (AS-FABRICATED) OBTAINED IN ASTM GUARDED HOT PLATE

| Specimen Number | Pressure (mm Hg) | Mean Temp ($^oF$) | Temp Difference ($^oF$) | Thermal Conductivity $\left(\frac{Btu/in.}{hr\text{-}ft^2\text{-}^oF}\right)$ |
|---|---|---|---|---|
| LI-1500, Specimen 1<br>Discs 1 and 2<br>Density: 13 $lb/ft^3$<br>1.31 $lb/ft^3$<br>Initial Thickness = 0.296 in.<br>Gage Length = 0.196 in. | 0.004 | 292 | 248 | 0.100 |
| | 5 | 293 | 240 | 0.197 |
| | 50 | 299 | 230 | 0.34 |
| | 760 | 304 | 223 | 0.42 |
| LI-1500, Specimen 2<br>Density: 13.8 $lb/ft^3$<br>13.5 $lb/ft^3$<br>Initial Thickness = 0.252 in.<br>Gage Length = 0.150 in. | 0.004 | -160 | 148 | 0.055 |
| | 5 | -159 | 154 | 0.148 |
| | 50 | -151 | 153 | 0.20 |
| | 760 | -149 | 153 | 0.22 |
| | 0.004 | 251 | 182 | 0.093 |
| | 5 | 247 | 172 | 0.173 |
| | 50 | 251 | 160 | 0.310 |
| | 760 | 250 | 150 | 0.38 |
| | 0.005 | 612 | 296 | 0.141 |
| | 5 | 598 | 246 | 0.21 |
| | 50 | 602 | 203 | 0.37 |
| | 760 | | | |

Note: Nitrogen was environmental gas.

Table 4.1-5

SUMMARY OF THERMAL CONDUCTIVITY DATA FOR LI-1500 (AS-FABRICATED) RADIAL INFLOW APPARATUS – STRIP SPECIMENS

| Specimen Number | Pressure (mm Hg) | Mean Temp (°F) | Temp Difference (°F) | Thermal Conductivity $\left(\frac{\text{Btu/in.}}{\text{hr-ft}^2\text{-}^\circ\text{F}}\right)$ |
|---|---|---|---|---|
| LI-1500, Specimen 1<br>Strips 1, 2, 3 and 4<br>Initial Thickness = 0.101 in.<br>Final Thickness = 0.090 in.<br>Average Density = 13.3 lb/ft$^3$ | 0.004 | 928 | 752 | 0.38 |
| | 5 | 964 | 675 | 0.49 |
| | 50 | 1002 | 591 | 0.74 |
| | 760 | 983 | 575 | 0.94 |
| | 0.008 | 1463 | 972 | 0.56 |
| | 5 | 1499 | 889 | 0.75 |
| | 50 | 1488 | 757 | 1.06 |
| | 760 | 1508 | 744 | 1.39 |
| | 0.003 | 2017 | 546 | 0.80 |
| | 5 | 2055 | 568 | 0.95 |
| | 48 | 2032 | 569 | 1.32 |
| | 760 | 2065 | 651 | 1.81 |
| LI-1500, Specimen 2<br>Strips 5, 6, 7 and 8<br>Initial Thickness = 0.100 in.<br>Final Thickness = 0.036 in.<br>Average Density = 13.5 lb/ft | 0.005 | 1218 | 663 | 0.36 |
| | 5 | 1206 | 604 | 0.40 |
| | 50 | 1242 | 542 | 0.61 |
| | 760 | 1245 | 548 | 0.88 |
| | 0.004 | 1779 | 721 | 0.57 |
| | 5 | 1782 | 662 | 0.71 |
| | 50 | 1772 | 605 | 0.91 |
| | 760 | 1739 | 614 | 1.16 |

Notes: 1. Specimen thicknesses were 0.100 in.
2. Nitrogen was environmental gas.

# VARIATION OF LI-1500 THERMAL CONDUCTIVITY WITH TEMPERATURE AND PRESSURE

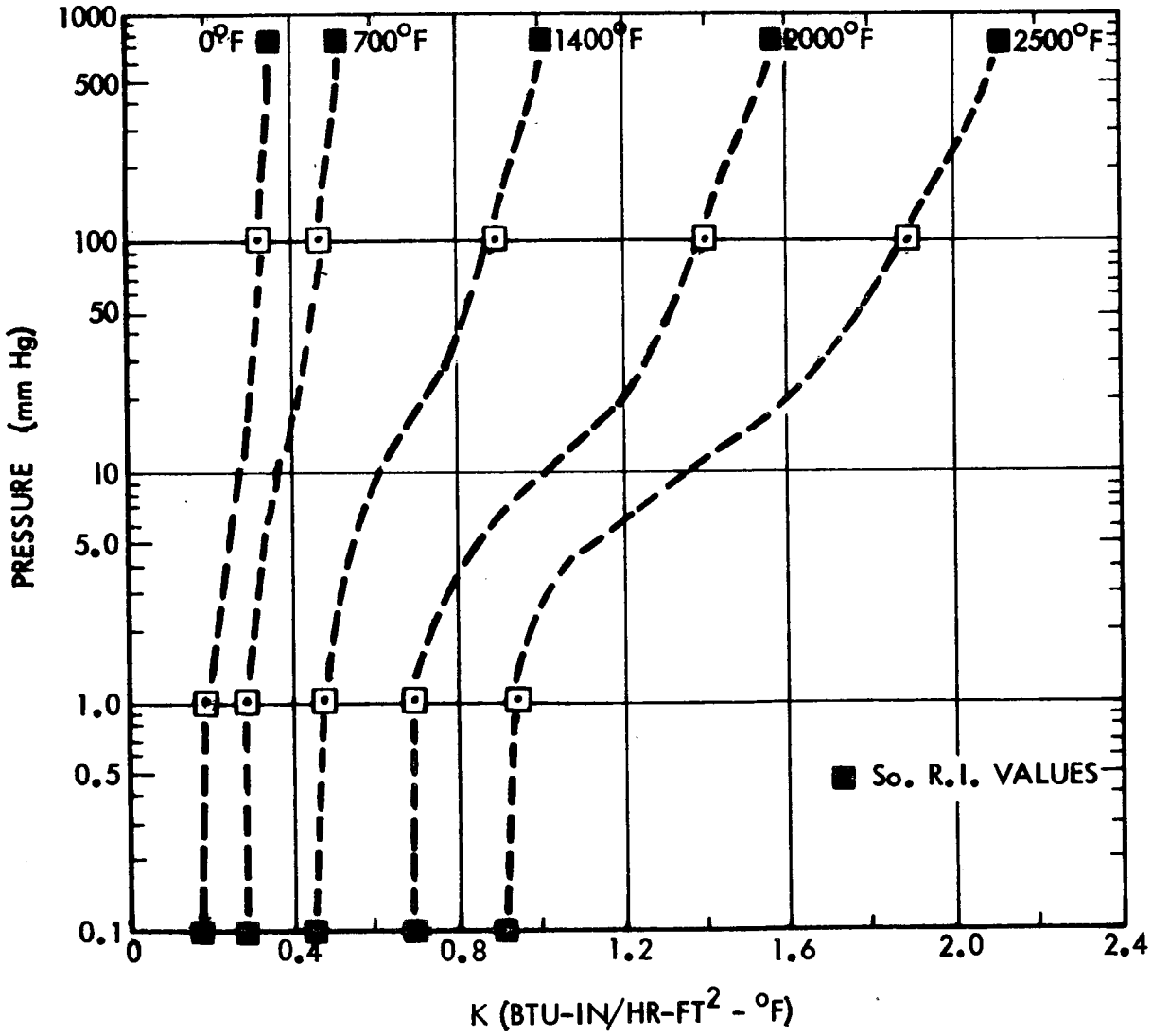


Fig 4.1-6

DO6083

Table 4.1-6

INTERIM DESIGN VALUES – THERMAL CONDUCTIVITY
(Btu-in./ft$^2$-hr-$^o$R)

| Temp ($^o$R) \ Pressure (mm Hg) | 0.1 | 1.0 | 10.0 | 100.0 | 760.0 |
|---|---|---|---|---|---|
| 460 | 0.17 | 0.19 | 0.28 | 0.32 | 0.35 |
| 760 | 0.21 | 0.23 | 0.31 | 0.34 | 0.37 |
| 1160 | 0.27 | 0.29 | 0.35 | 0.47 | 0.52 |
| 1860 | 0.45 | 0.47 | 0.60 | 0.90 | 1.00 |
| 2460 | 0.67 | 0.69 | 1.02 | 1.40 | 1.56 |
| 2960 | 0.92 | 0.94 | 1.35 | 1.88 | 2.09 |

Table 4.1-7

INTERIM DESIGN VALUES –SPECIFIC HEAT
(Btu/lb-$^o$R)

| Temperature ($^o$R) | $C_p$ (Btu/lb-$^o$R) |
|---|---|
| 360 | 0.0716 |
| 540 | 0.151 |
| 720 | 0.198 |
| 900 | 0.234 |
| 1080 | 0.263 |
| 1260 | 0.280 |
| 1440 | 0.287 |
| 1800 | 0.294 |
| 2160 | 0.306 |
| 2520 | 0.316 |
| 2890 | 0.320 |

# COMPARISON OF LI-1500 THERMAL CONDUCTIVITY DATA FROM VARIOUS SOURCES

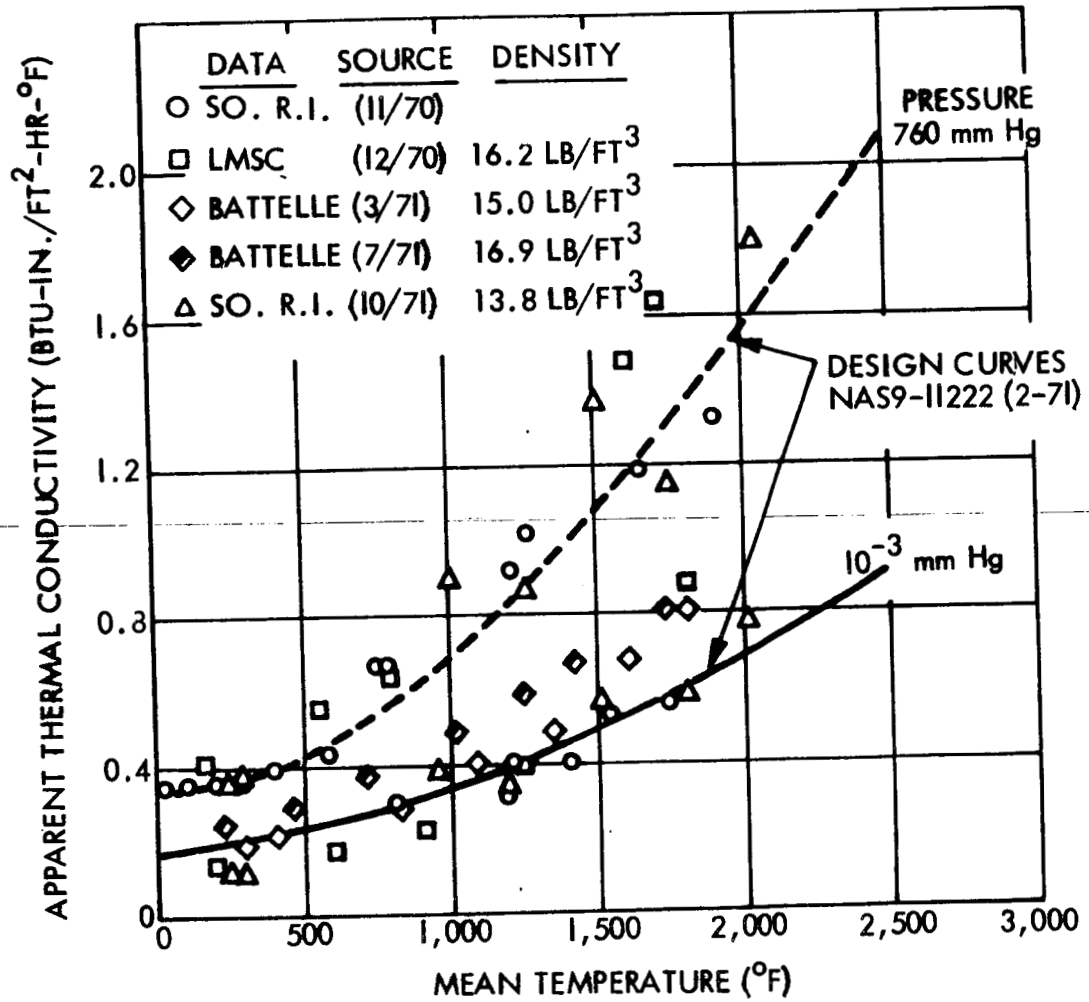


Fig. 1-7

DO5060 (1)

# OVEN THERMAL CYCLE FOR THERMAL DEGRADATION TESTS

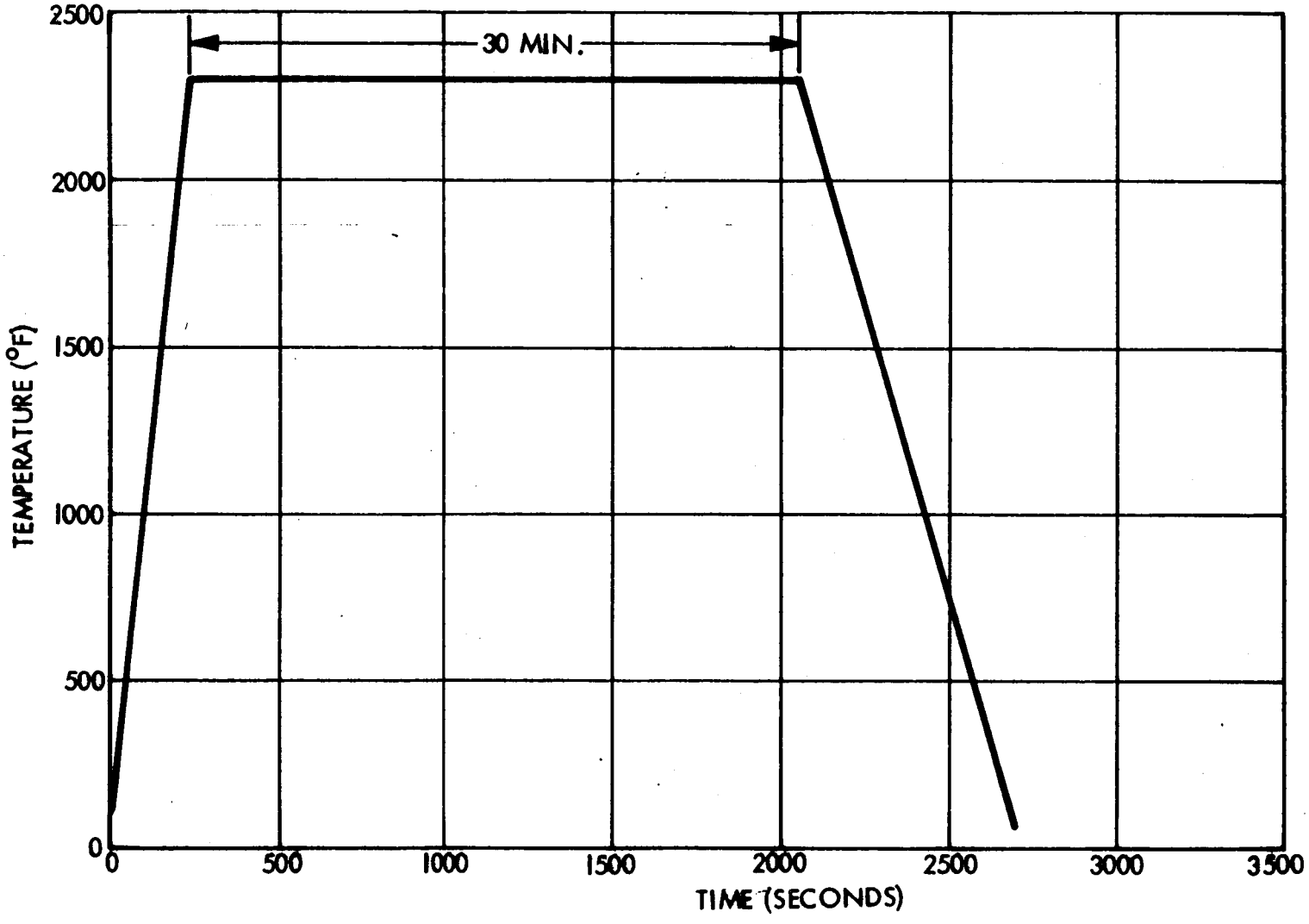


DO6129

Fig. 4.1-8

For the NASA reentry surface temperature history shown in Fig. 2.2.2-8, which sustains 2300°F for about 150 sec, the one 30 min (1800 sec) oven cycle is equal to about 11 flights in terms of time at temperature.

The density and dimensional change for the cycled material after 5 and 10 hours accumulated exposure to 2300°F is shown in the lower part of Table 4.1-8.

The acoustic environment to which the mechanical property test specimens were exposed is shown in Fig. 4.1-9. The environment is based on the design conditions outlined in Task 2.1.6. During each shuttle mission, the specified design areas of the TPS would be exposed to 20 sec of an overall SPL of 159.4 db.

All test specimens listed for acoustic exposure successfully passed the acoustic test. Two additional specimens were exposed to 35 and 45 min, respectively, with no apparent degradation.

### 4.1.5 Coating Emittance

The total normal emittance values for three coating formulations were computed from spectral reflectance measurements performed by the Thermophysics Section of TRW Systems, Redondo Beach, California, using a paraboloid reflectometer. Measurements were made in air at atmospheric pressure at temperatures of 240, 900, 1400, and 1800°F. The spectral region covered was 0.9 to 25.0 μm. For these measurements, the specimens were backed with a platinum black (very low reflectance) surface. After the measurements, a polished platinum strip (high reflectance) was substituted for this backing to determine if the specimens were transparent by comparing the data at several wavelengths for the two backing materials. The data at 1.2, 2.4, 3.4, and 5.0 μm showed no difference in measured reflectance at 240° and 1800°F for the SiC and SiC + $Cr_2O_3$ specimens. The two coatings measured are not transparent in the 20/30 mil thicknesses to temperatures of 1800°F.

The spectral reflectance data for the three coatings at several temperatures are shown in Figs. 4.1-10, 4.1-11, and 4.1-12. With the exception of the 7 to 10 μm regions, the spectral reflectance is essentially independent of temperature. In the 7 to 10 μm region, the absorption band decreased in amplitude with increasing temperature.

Table 4.1-8

THERMAL DEGRADATION OF CYCLED SPECIMENS

| Type of Test Specimens | Specimen I. D. No. | No. of Thermal Cycles | No. of Acoustic Cycles | Total Time (thermal) | Total Time (acoustic) |
|---|---|---|---|---|---|
| Tension | 1-1 to 1-6<br>2-1 to 2-6 | 10<br>20 | 10<br>20 | 5 hours<br>10 hours | 10 min.(1)<br>20 min. |
| Compression | 3-1 to 3-5 | 10 | 10 | 5 hours | 10 min.(2) |
| Shear | 4-1 to 4-10 | 10 | – | – | – |
| Bending | 2085-1 to -4 | 10 | 10 | 5 hours | 10 min. |
| Thermal Expansion | | 20 | – | 10 hours | – |
| Specific Heat | – | 20 | – | 10 hours | – |
| Infrared Transmission | – | 10 and 20 | – | 5 & 10 hours | – |
| Hard Vacuum | – | 10 and 20 | – | 5 & 10 hours | – |

All material came from fiber lot 2085

(1) One specimen exposed to 45 min. total time
(2) One specimen exposed to 35 min. total time

RESULTS AFTER THERMAL CYCLING

| No. of Cycles | Density ~ Lb/Ft$^3$ | | Dimensional Change | | |
|---|---|---|---|---|---|
| | Before | After | Length | Width | Thickness |
| 10* | 15.0 | 16.1 | 2.0% | 2.2% | 2.9% |
| 20** | 15.0 | 16.5 | 3.7% | 4.1% | 4.3% |

No weight loss was detected

*Average value for nine blocks
**Average value for four blocks

# COMPARISON OF APPLIED ACOUSTIC TEST ENVIRONMENT WITH REQUIREMENT

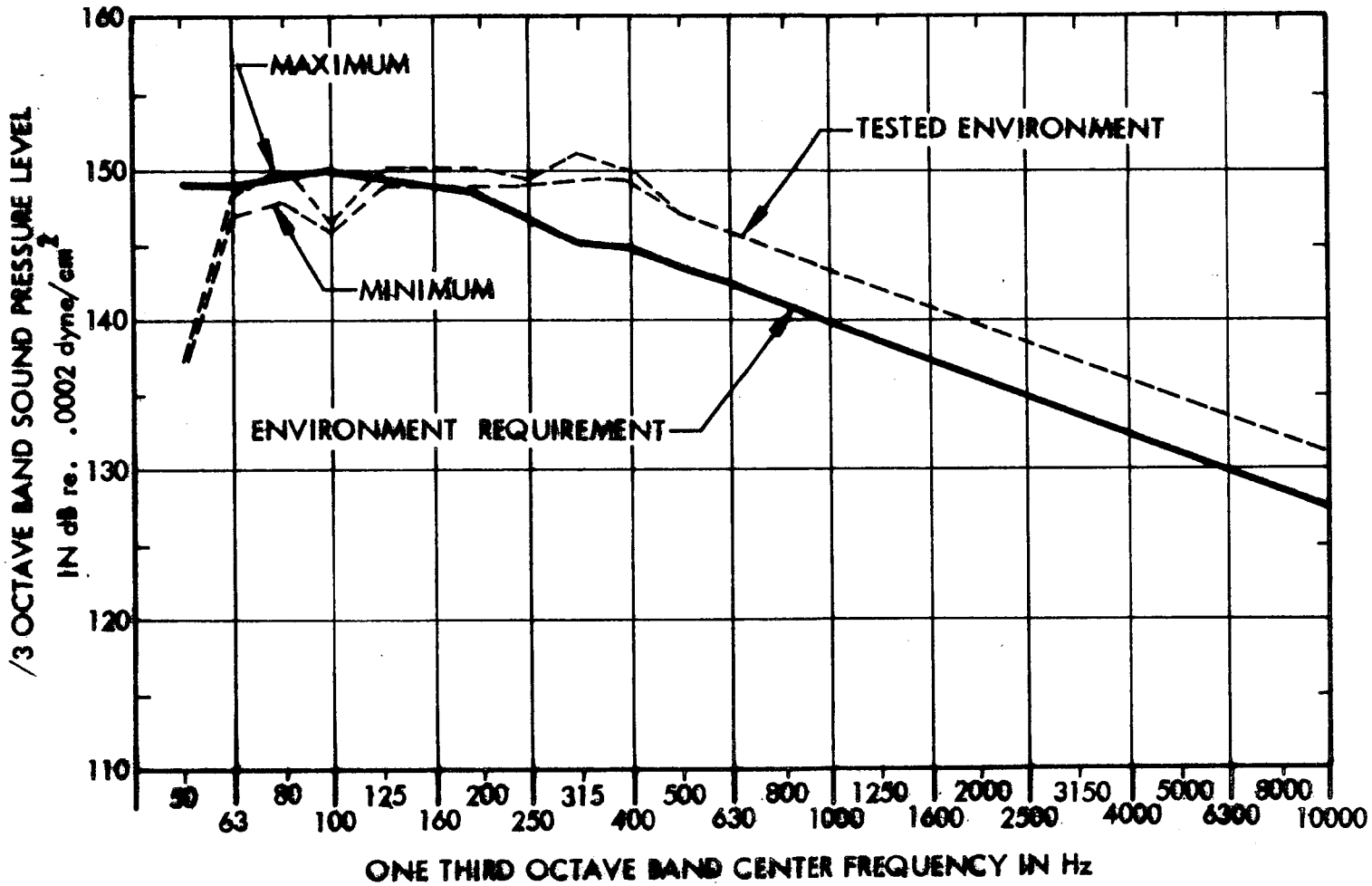


DO6128

Fig. 4.1-9

# SPECTRAL REFLECTANCE FOR A BOROSILICATE COATING WITH A SILICON CARBIDE EMITTANCE AGENT

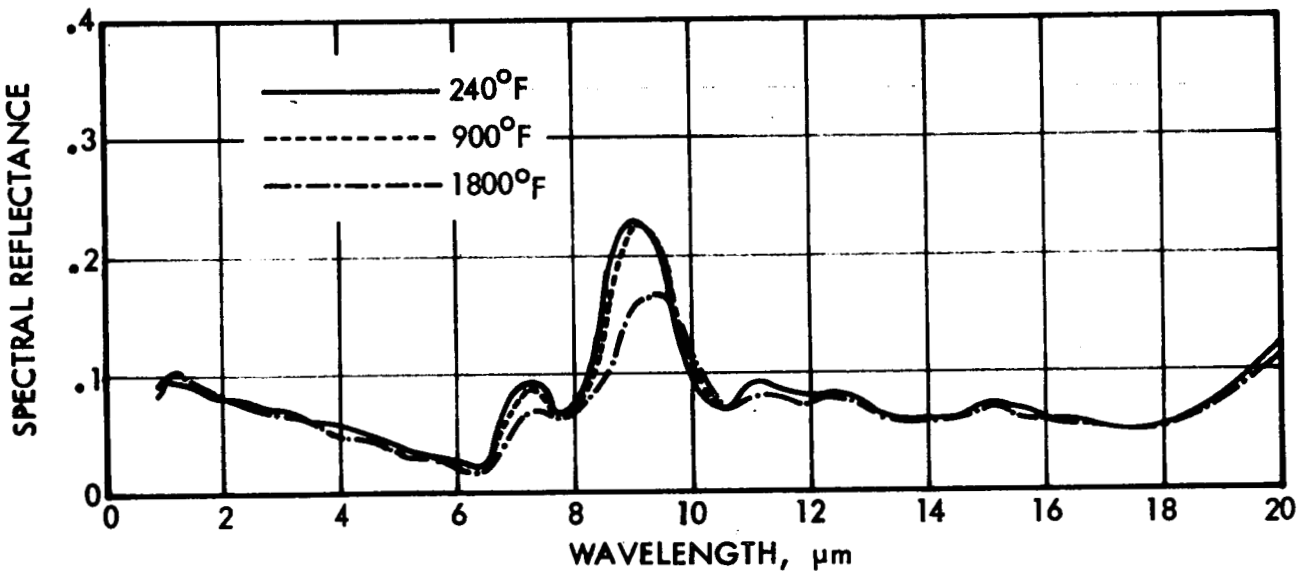


Fig. 4.1-10

# SPECTRAL REFLECTANCE FOR A BOROSILICATE COATING WITH A COBALT OXIDE EMITTANCE COATING

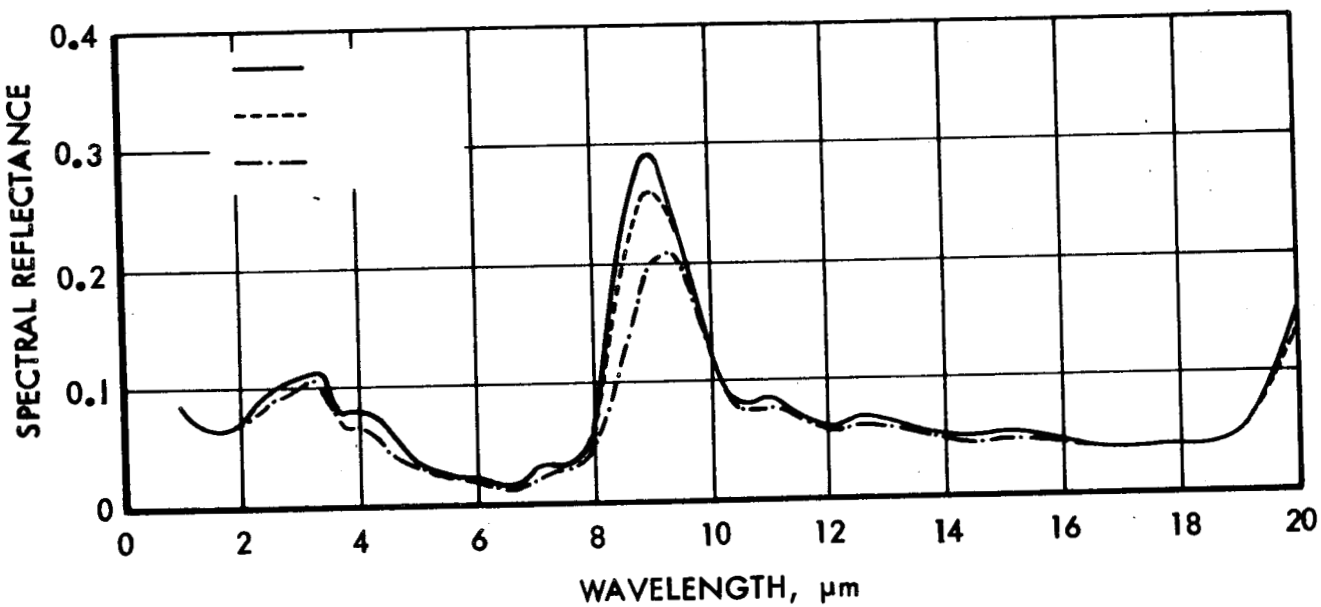


Fig. 4.1-11

DO6121

# SPECTRAL REFLECTANCE FOR BOROSILICATE COATING WITH SILICON CARBIDE AND CHROME OXIDE EMITTANCE AGENTS

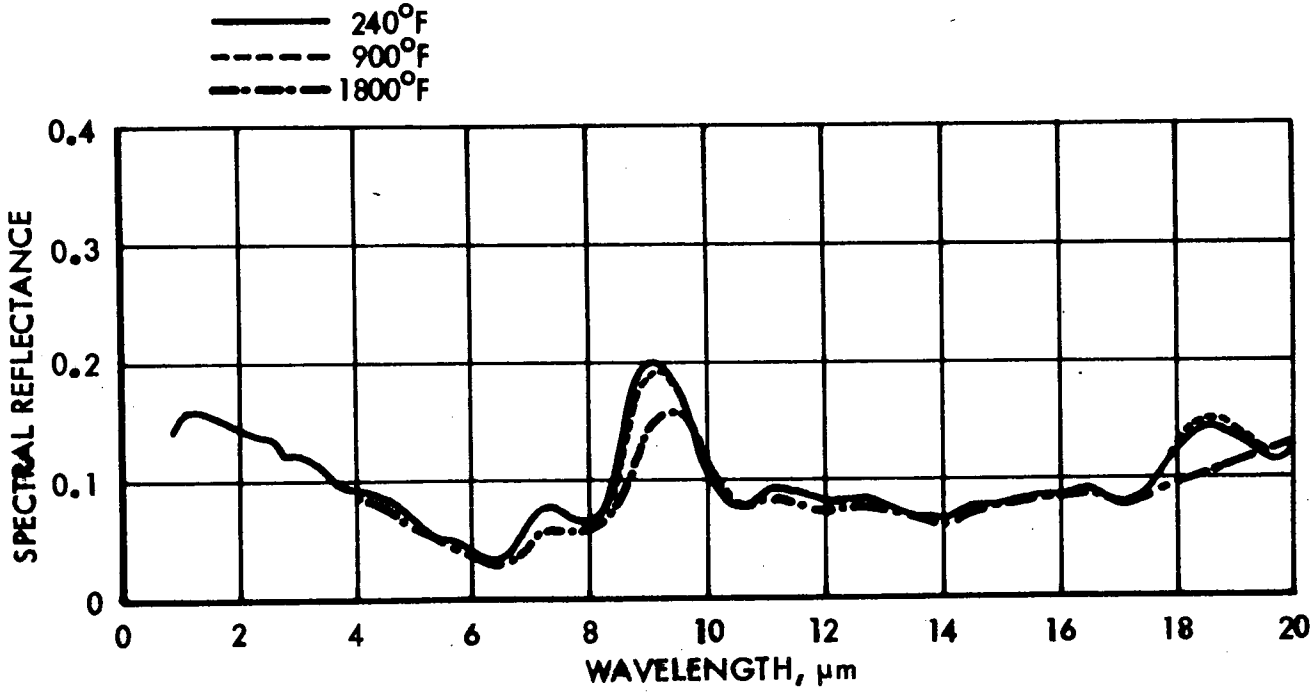


DO6127

Fig. 4.1-12

Total normal emittance values were computed at three temperatures, using the reflectance data and interpolating over the black body energy spectrum for these temperatures. The computed emittance values are given in Table 4.1-9.

Based on Jakob's curve, the total hemispherical emittance is 96 percent of the total normal emittances shown in Table 4.1-9. Hence, the total hemispherical emittance of all three coating formulations approaches 0.90 at temperatures up to 2000°F. The values at 2500°F are expected to be similar to those shown in Table 4.1-9.

Table 4.1-9

TOTAL NORMAL EMITTANCE

| Coating Description \ Temp | 70°F | 1000°F | 2000°F |
|---|---|---|---|
| Borosilicate coating with silicon carbide (SiC) - 0042 | 0.89 | 0.93 | 0.93 |
| Borosilicate coating with cobalt oxide (CoO) | 0.92 | 0.93 | 0.93 |
| Borosilicate coating with mixture of silicon carbide and chrome oxide ($SiC + Cr_2O_3$) | 0.88 | 0.91 | 0.89 |

## 4.2 MECHANICAL PROPERTIES

LMSC recognizes that a major area of uncertainty in RSI technology is that of correct testing methods. Hence, the property test methods and results are constantly being reviewed and new tests are being run as additional information becomes available on the behavior of LI-1500. LMSC believes that the only way to truly characterize the material is to constantly scrutinize the data in conjunction with analytical design application studies and perform any additional tests necessary.

The major effort to date has been to perform the mechanical property tests detailed in the Property Test Plan (LMSC-A991210, 30 July 1971) approved by NASA/MSC. The test matrix is shown in Table 4.2-1 along with average values of strength and modulus for the completed tests. The anisotropic properties of LI-1500, as indicated in the table, are due to preferred biaxial orientation of the fibers. The material supports higher stresses to fracture in the fiber orientation direction than in a direction normal to the fibers. The tensile fracture values are about 78 psi and 14 psi for the parallel and normal to fiber orientation directions, respectively. This variation in properties is accounted for in the anisotropic structural analysis performed in Task 2.

The remaining parts of this section contain a detailed discussion of the test techniques and results from which the average values were obtained for each type of test.

### 4.2.1 Room Temperature Tension Tests

Room temperature (75$^{\circ}$F) tensile tests were run on 2-in. cubes, using the fixture shown in Fig. 4.2-2. The specimen is bonded to two blocks (B), using Hysol 150 epoxy. A pair of deflectometers (D) are attached to the blocks (B) by the brackets (A). Blocks are attached to the testing machine through universal joints (U) at each end. The testing machine is a 50,000 SR-4 screw-driven universal testing machine.

Since the specimen fails at considerably less than full-scale of the most sensitive range on this testing machine, a more sensitive load cell is introduced between the universal joint and crosshead of the machine. With this load cell, load resolution of 0.5 percent of typical failure loads is possible.

# SKETCH OF MECHANICAL PROPERTY TEST SPECIMENS

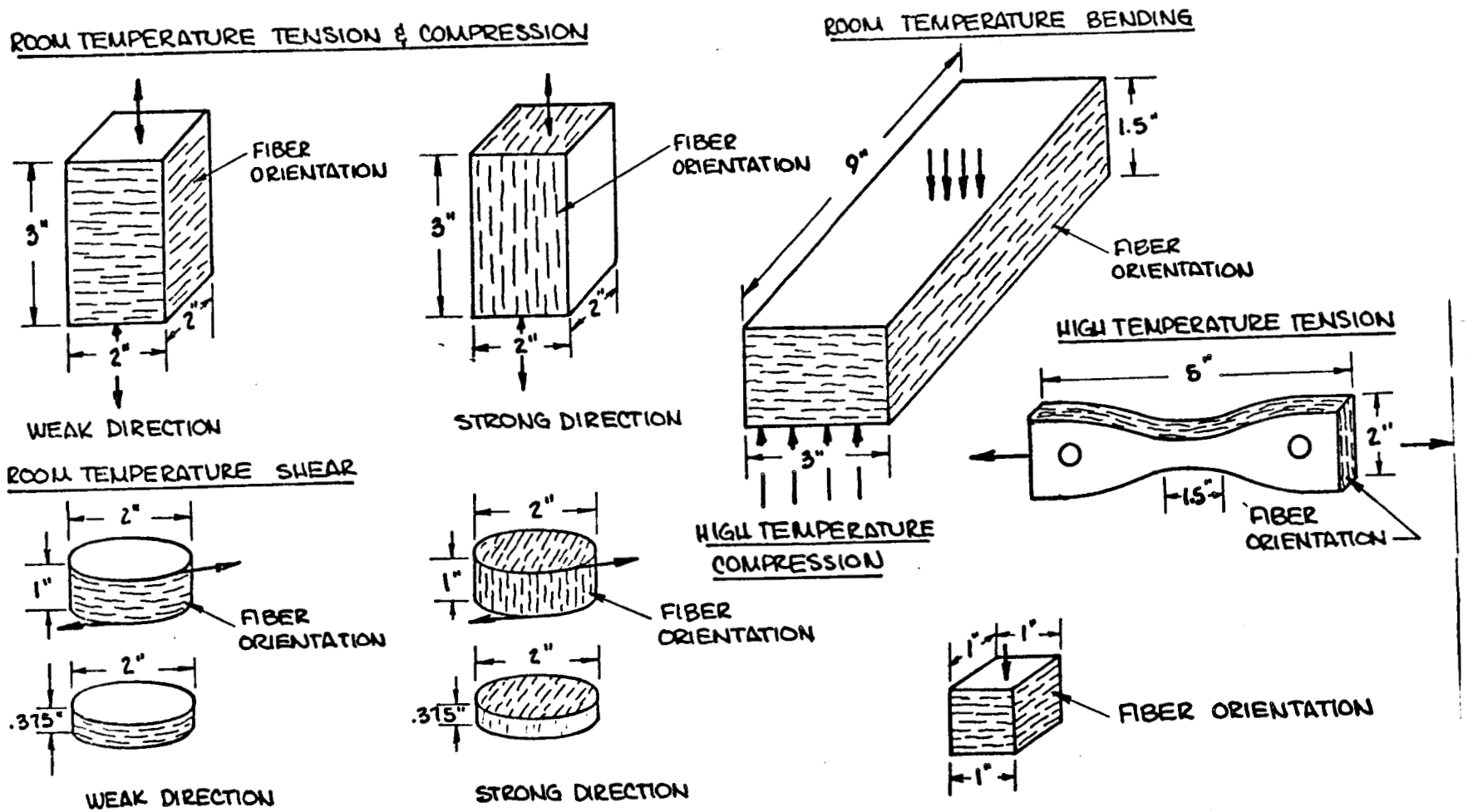


Fig. 4.2-1

Table 4.2-1

SUMMARY OF LI-1500 MECHANICAL PROPERTY TEST RESULTS

| Type of Test | Test Direction | Location in Block | Temp (°F) | Cycles | Equivalent Flights | No. of Specimens | Average Strength (lb/in.$^2$) | Average Modulus (lb/in.$^2$) |
|---|---|---|---|---|---|---|---|---|
| Tension | Parallel(1) | #1 | RT | 0 | | 4 | 78 | 56,400 |
| | Parallel | #2 | RT | 0 | | 4 | 70 | 57,450 |
| | Normal (2) | #1 | RT | 0 | | 4 | 14.5 | 5,780 |
| | Normal | #2 | RT | 0 | | 4 | 14 | 9,518 |
| | Parallel | #1 | -150 | 0 | | 4 | 91 | 40,575 |
| | Parallel | #1 | 1500 | 0 | | 4 | 101 | 46,700 |
| | Parallel | #1 | 2000 | 0 | | 4 | 165 | 16,000 |
| | Parallel | #1 | 2500 | 0 | | 4 | TBD | TBD |
| | Parallel | #1 | RT (3) | 0 | | 3 | 77 | 60,850 |
| | Parallel | #1 | RT | 10 | 30 | 4 | 47 | 91,300 |
| | Parallel | #1 | RT | 20 | 60 | 4 | 56 | 89,500 |
| Compression | Parallel | #1 | RT | 0 | | 6 | 174 | 39,700 |
| | Normal | #1 | RT | 0 | | 4 | 42 | 4,070 |
| | Normal | #1 | 2200 | 0 | | 3 | TBD | TBD |
| | Parallel | #1 | 2200 | 0 | | 3 | TBD | TBD |
| | Parallel | #1 | RT | 10 | 30 | 3 | 234 | 84,700 |
| | Parallel (Coated) | #1 | RT | 0 | | 4 | 167 | 60,300 |
| Shear | Parallel | #1 | RT | 0 | | 2 | 27.5 | 6,605 |
| | Normal | #1 | RT | 0 | | 4 | 75 | 31,900 |
| | Parallel | #1 | RT | 10 | 30 | 4 | 39 | TBD |
| Bending | Parallel | #1 | RT | 0 | | 5 | 115 | 53,780 |
| | Parallel | #1 | RT | 10 | 30 | 4 | TBD | TBD |
| Coating (0025) | Parallel | #1 | RT | 0 | | 7 | 480 | 960,000 |

(1) Parallel to the fiber orientation direction
(2) Normal to the fiber orientation direction
(3) Control specimens for tests in elevated temperature fixture

TBD - To be determined

# TEST FIXTURE FOR TENSILE TESTS OF LI-1500 (ROOM TEMPERATURE AND -150°F)

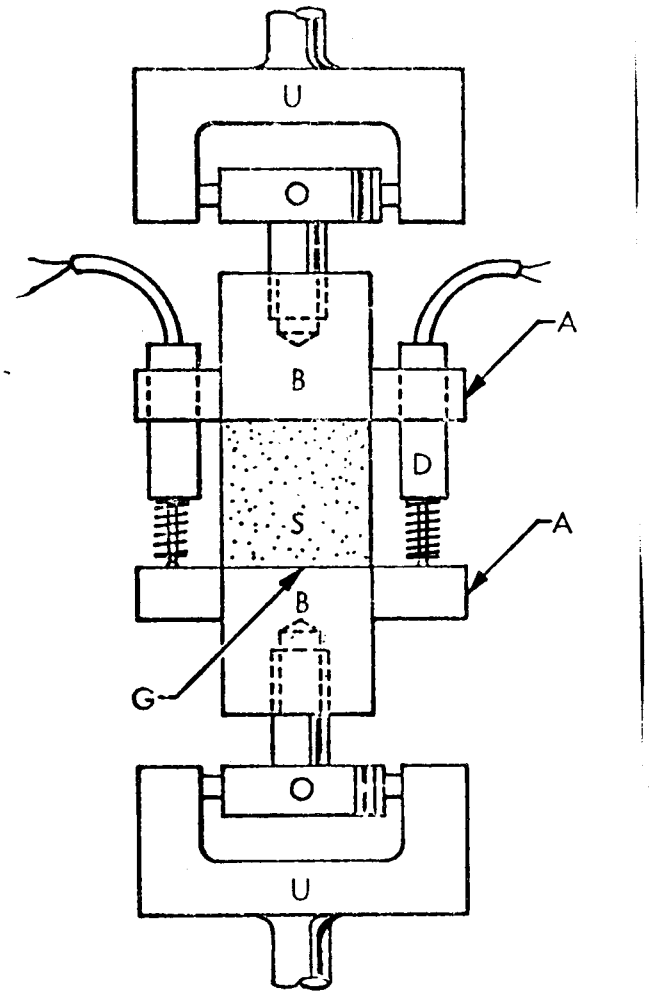


Fig. 4.2-2

DO6032

Load and strain are recorded continuously on an X-Y plotter. System measurement accuracy is within ±1.5 percent on either the X or Y scale.

Crosshead motion of the machine is set for an approximate strain rate of 0.25 percent per minute. (It takes approximately 1 minute to load the specimens to failure.)

Universal joints are essential to ensure uniform loading, and a pair of averaging deflectometers eliminate the gross strain-measurement errors that would result from a specimen having nonuniform properties across its width.

Specimen dimensions are measured to 0.020 in. accuracy. An average of five readings is taken on each dimension.

The room temperature tension results for specimens taken from the top of a 16 x 16 x 6 in. LI-1500 block are shown in Table 4.2-2. Also shown in the table is the average value obtained during the last contract, NAS 9-11222. The average values are essentially the same, considering that the test technique was a dog bone specimen and a universal test machine was used for NAS 9-11222 testing.

Room temperature tension results for specimens taken from the botton of a 16 x 16 x 6 in. LI-1500 block are shown in Table 4.2-3. Tension results for specimens exposed to thermal and acoustic cycles are shown in Table 4.2-4. The specimens were exposed to 2300°F for a total of 5 hours in two 1/2 hour intervals. A more detailed description of the thermal and acoustic exposures is given under thermal degradation, Section 4.1.

The effect of the increased tension modulus, representative of that obtained on the thermal and acoustically cycled tension specimens (89,500 lb/in.$^2$), was analyzed in subsection 2.2.3.2 for the aluminum test Panel No. 2. The design condition analyzed was a line load of 6000 lb/in. with a 1.5 lb/in.$^2$ burst pressure. These results are shown in Table 2.2.3.2-4.

The higher tension modulus allowed the cycled layer of LI-1500 to have a modulus more compatible with the coating modulus. Hence, the calculated stresses within the cycled LI-1500 were less than those for the as-fabricated material.

Table 4.2-2

LI-1500 TENSION TESTS (UNCOATED SPECIMENS), LOCATION 1

| Direction Test Temp | Specimen Number | Total Length (in.) | Test Section Width (in.) | Thickness (in.) | Weight (gm) | Test Section Area (in.$^2$) | Load (lb) | Stress (psi) | Modulus (psi) |
|---|---|---|---|---|---|---|---|---|---|
| Parallel | | | | | | | | | |
| R. T. | TT 28-1 | 3.00 | 2.00 | 2.00 | 44.3 | 4.00 | 354 | 88.5 | 61,100 |
| R. T. | TT 28-2 | 3.00 | 2.00 | 2.00 | 44.0 | 4.00 | 260 | 65.0 | 50,500 |
| R. T. | TT 28-3 | 3.00 | 2.00 | 2.00 | 44.2 | 4.00 | 286 | 71.5 | 60,000 |
| R. T. | TT 28-4 | 3.00 | 2.00 | 2.00 | 44.0 | 4.00 | 342 | 85.5 | 54.000 |
| | | | | | | Average | | 78.0 | 56,400 |
| | | | | | | NAS 9-11222 avg | | 74.0 | 59,650 |
| -150°F | TT 28-5 | 3.00 | 2.00 | 2.00 | 44.0 | 4.00 | 358 | 89.5 | 56,300 |
| -150°F | TT 28-6 | 3.00 | 2.00 | 2.00 | 43.5 | 4.00 | 370 | 92.5 | 54,000 |
| -150°F | TT 28-7 | 3.00 | 2.00 | 2.00 | 42.0 | 4.00 | 350 | 87.5 | 48,800 |
| -150°F | TT 28-8 | 3.00 | 2.00 | 2.00 | 43.0 | 4.00 | 376 | 94.0 | 39,200 |
| | | | | | | Average | | 91.0 | 40,575 |
| Normal | | | | | | | | | |
| R. T. | TT 28-41 | 2.00 | 2.00 | 2.00 | 29.0 | 4.00 | 72 | 18.0 | 5,660 |
| R. T. | TT 28-42 | 2.00 | 2.00 | 2.00 | 29.5 | 4.00 | 55 | 13.8 | 6,130 |
| R. T. | TT 28-43 | 2.00 | 2.00 | 2.00 | 29.0 | 4.00 | 54 | 13.5 | 6,450 |
| R. T. | TT 28-44 | 2.00 | 2.00 | 2.00 | 29.3 | 4.00 | 51 | 12.8 | 4,890 |
| | | | | | | Average | | 14.5 | 5,780 |

Table 4.2-3

LI-1500 TENSION TEST (R.T.), LOCATION 2

| Test Direction | Specimen Number | Length (in.) | Width (in.) | Thick-ness (in.) | Test Section Area (in.$^2$) | Load (lb) | Stress (psi) | Modulus (psi) |
|---|---|---|---|---|---|---|---|---|
| Normal | TT 39-1 | 3.00 | 2.00 | 2.00 | 4.00 | 59 | 14.8 | 9,400 |
| | TT 39-2 | 3.00 | 2.00 | 2.00 | 4.00 | 50 | 12.5 | 9,150 |
| | TT 39-3 | 3.00 | 2.00 | 4.00 | 4.00 | 65 | 16.2 | 9,650 |
| | TT 39-4 | 3.00 | 2.00 | 2.00 | 4.00 | 50 | 12.5 | 9,870 |
| | | | | | Average | | 14.0 | 9,518 |
| Parallel | TT 39-6 | 3.00 | 2.00 | 2.00 | 4.00 | 225 | 56.2 | 67,300 |
| | TT 39-7 | 3.00 | 2.00 | 2.00 | 4.00 | 363 | 90.8 | 27,600 |
| | TT 39-8 | 3.00 | 2.00 | 2.00 | 4.00 | 245 | 61.2 | 66,900 |
| | TT 39-9 | 3.00 | 2.00 | 2.00 | 4.00 | 286 | 71.5 | 68,000 |
| | | | | | Average | | 69.9 | 57,450 |



LOCKHEED MISSILES & SPACE COMPANY

Table 4.2-4

LI-1500 TENSION TESTS
(Post Thermal and Acoustical Cycling)

| Number of Thermal and Acoustical Cycles | Specimen Number | Maximum Load (lb) | Maximum Stress (psi) | Modulus (psi) |
|---|---|---|---|---|
| 10 | 1-1 | 230 | 57.5 | 94,300 |
| | 1-2 | 218 | 54.5 | 85,400 |
| | 1-3 | 165 | 41.2 | 101,400 |
| | 1-4 | 136 | 34.0 | 84,000 |
| | | Average | 46.8 | 91,300 |
| 20 | 2-1 | 274 | 68.5 | 102,000 |
| | 2-2 | 460 | 115. | 61,000 |
| | 2-3 | 114 | 28.5 | 86,000 |
| | 2-4 | 48 | 12.0 | 109,000 |
| | | Average | 56.0 | 89,500 |

Tested parallel to fiber orientation direction

All specimens 2 x 2 x 3 in.

Test section area = 4.00 in.$^2$

### 4.2.2 High Temperature Tension Tests

The tensile properties at 1500, 2000, and 2500°F were evaluated under both static and dynamic loading conditions. Tests under static loads were conducted to establish stress-strain relationships at elevated temperatures. Dynamic tests at low strain rates, which is the normal loading tests used for determining tensile properties, were made to establish the stress for fracture.

A detailed sketch of the test specimen is shown in Fig. 4.2-3. The 2 in. long reduced section had a cross-section of 0.37 x 0.75 in. for tests at room temperature and 1500°F and a 0.27 x 0.75 in. cross-section for tests at 2000°F.

The specimens were heated to test temperature with a platinum wound tube furnace having a 3-in. diameter by 15 in. long hot zone. Temperature within the gage section was within ±15°F of the stated test temperature. Specimens were held by pin and clevices machined from HS-25 alloy bar for tests at 1500 and 2000°F. The load train was assembled above the hot furnace as shown in Figs. 4.2-4A and 4.2-5A, and the furnace was then lifted into position with the specimen in the center of the hot zone (Figs. 4.2-4B and 4.2-5B). About 30 min. was required to stabilize at the test temperature. The specimens were soaked for an additional 30 and 20 min. at 1500 and 2000°F, respectively, prior to loading. Temperature measurement from thermocouples imbedded in the interior of the gage section indicated the gage section reached the test temperature within 5 min. after immersion into a furnace at 2000°F.

The dynamic tensile tests were made with an Instron Model TM tensile test machine.

Static tests were conducted in an arc-weld creep frame with the sample fixed at the upper end. Loads were applied in 2 lb increments to a pan suspended from the lower clevice (Fig. 4.2-5B). Strain within the gage section was measured optically with a platinum strip extensometer fixed to each end of the gage section. After establishing a stress-strain curve, the specimens were loaded to fracture.

# PIN END LOADED TENSILE SPECIMEN

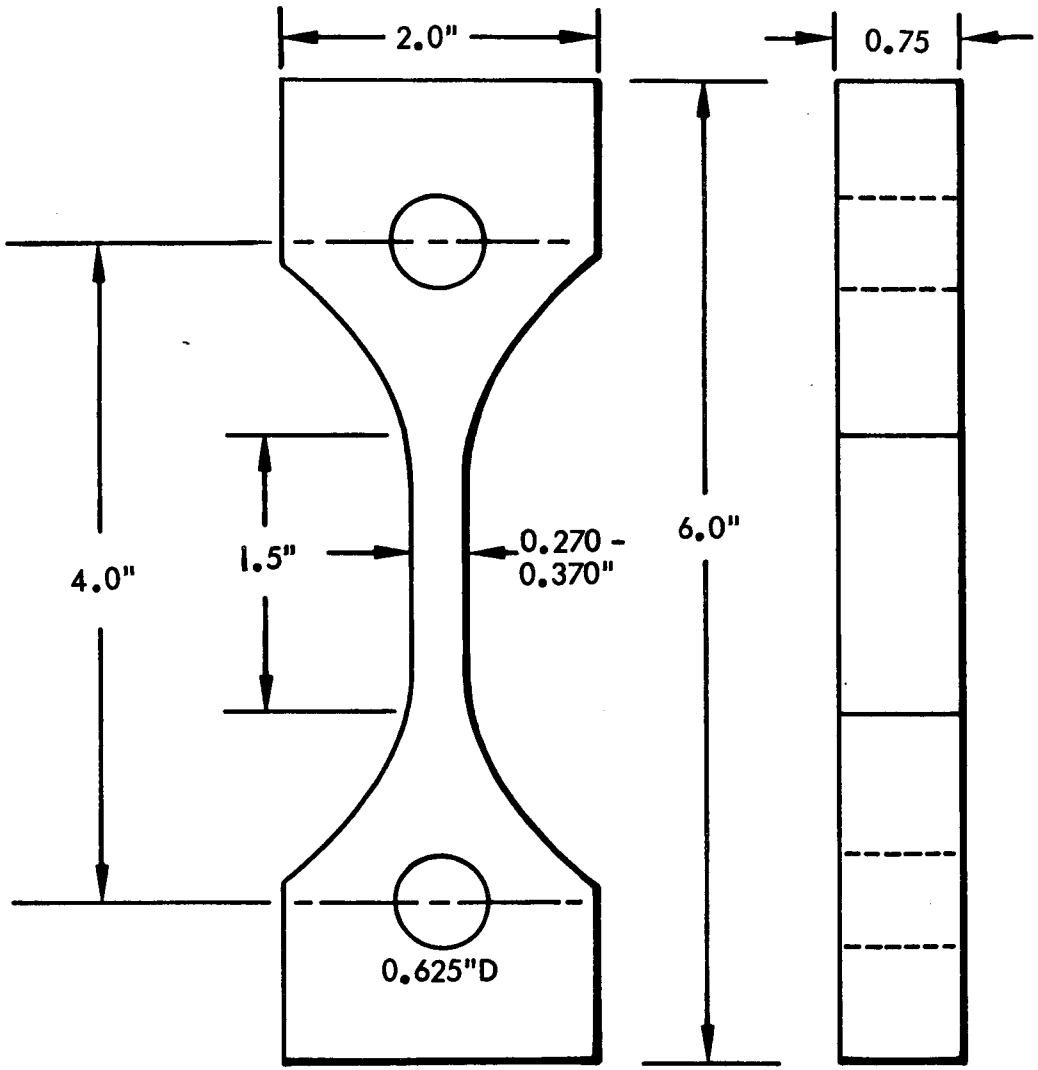


DO6087

Fig. 4.2-3

# SETUP FOR HIGH TEMPERATURE DYNAMIC TENSILE TEST

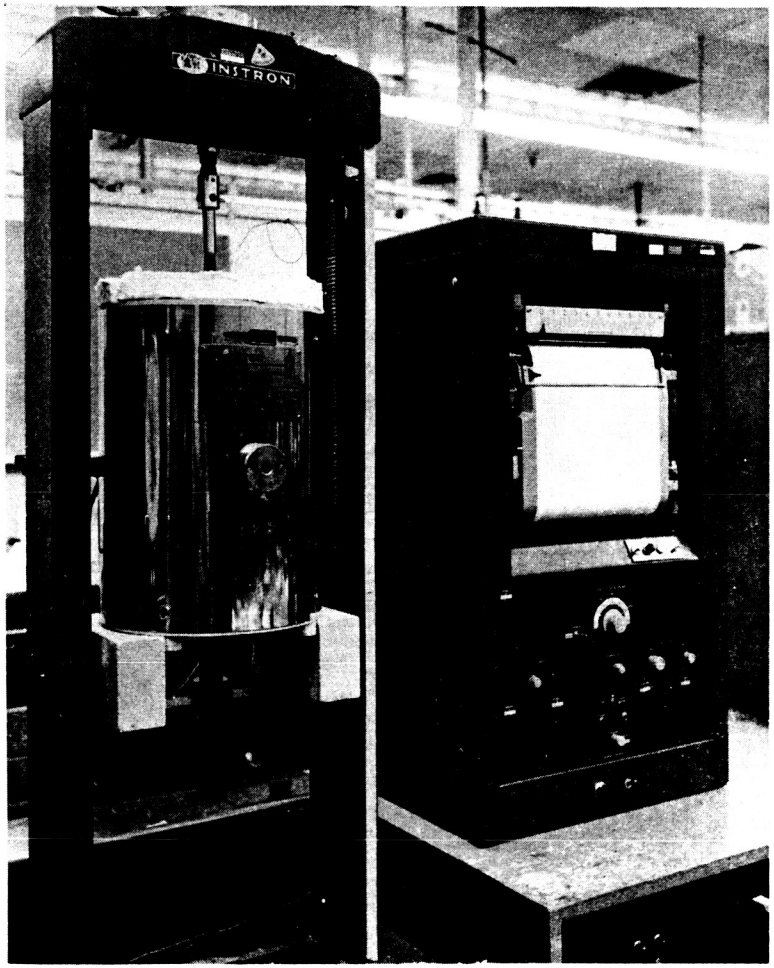


A. LOAD TRAIN ASSEMBLY

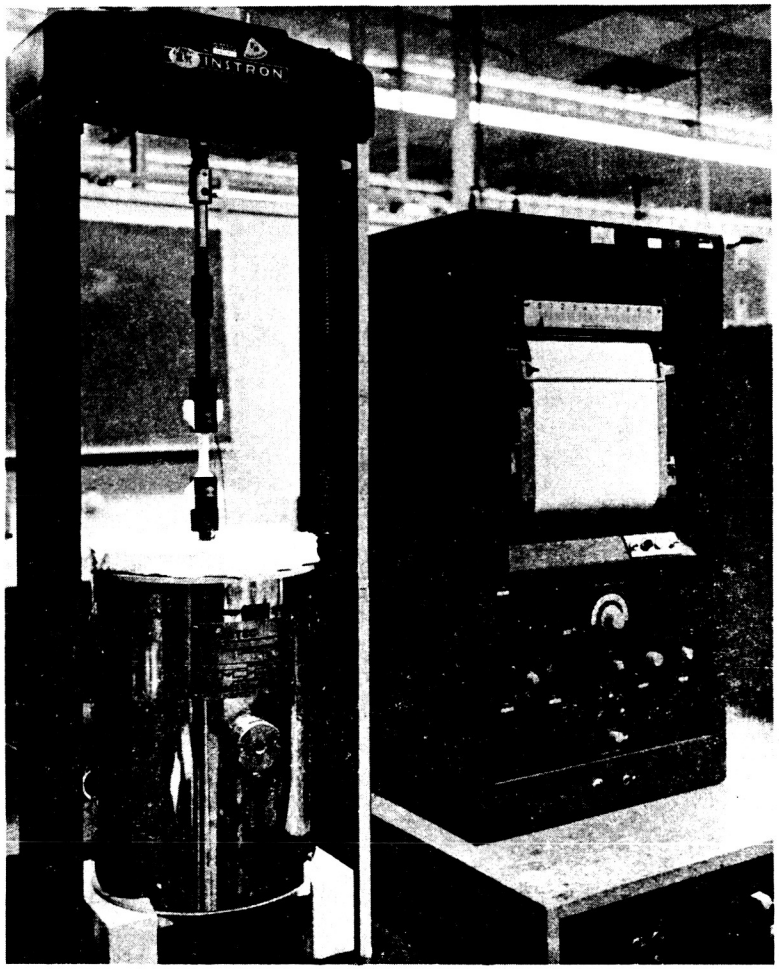


B. FURNACE IN TEST POSITION

Fig. 4.2-4

# SETUP FOR HIGH TEMPERATURE STATIC LOAD TENSILE TESTS

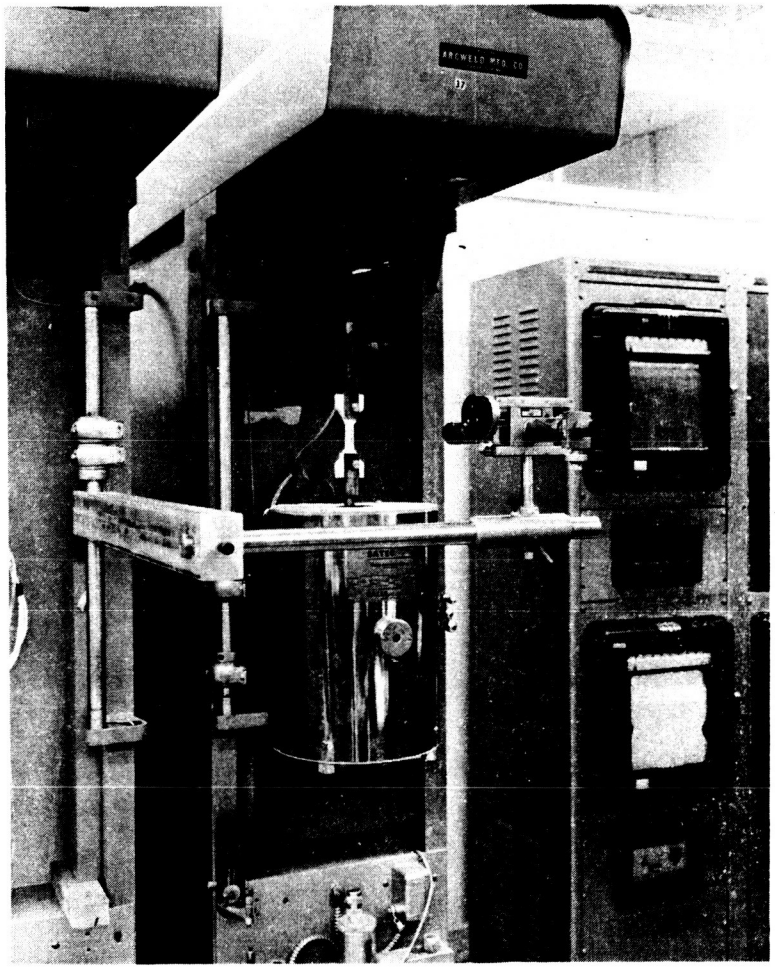


A. LOAD TRAIN ASSEMBLY

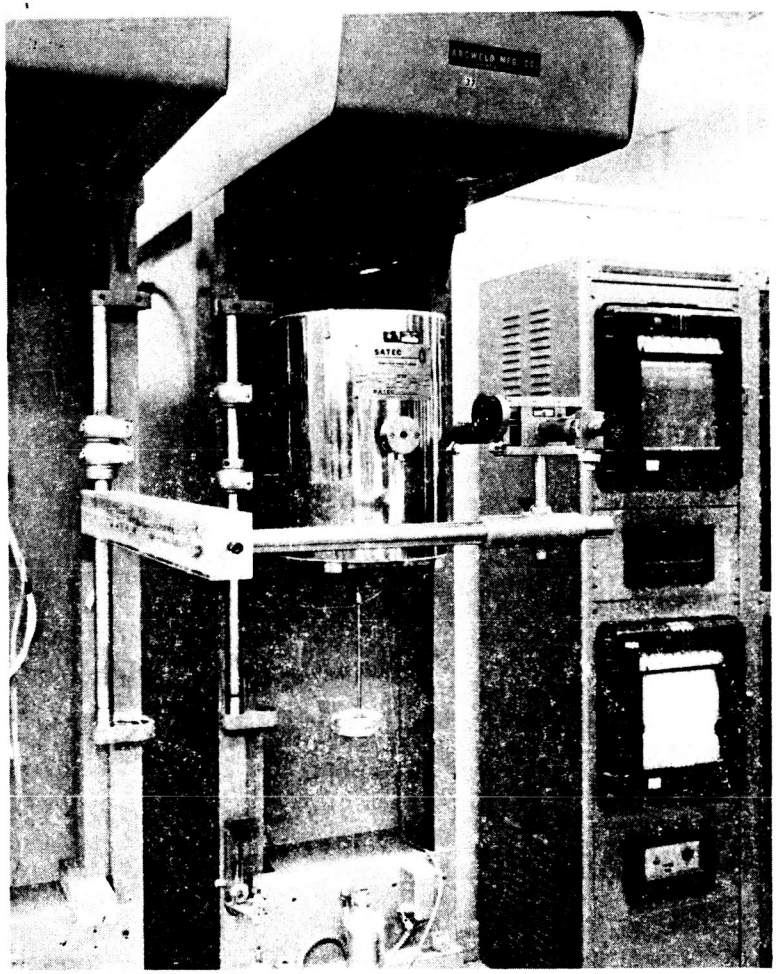


B. FURNACE IN TEST POSITION

Fig. 4.2-5

The results for the room temperature, 1500°F, and 2000°F tests are shown in Table 4.2-5. The room temperature results agree well with the room temperature results on the 3 x 2 x 2 in. specimens shown in Tables 4.2-1 and 4.2-2.

The results at 1500°F reveal about a 33 percent increase in average tensile strength and about an 18 percent decrease in modulus. At 2000°F, the average tensile strength increases to 165 lb/in.$^2$, while the modulus decreases to 16,000 lb/in.$^2$ from the room temperature value of 56,000 lb/in.$^2$. Hence, at elevated temperatures, the material apparently becomes more ductile and has higher tensile strength. One explanation for this trend is that at high temperatures small flaws in a brittle material have less of an effect. This is due to ductile redistribution of the stress field in the neighborhood of the flaw; i.e., alternate load paths of less intensity are created around the flaw. Hence, the load carrying capability is increased compared to that when the flaw behaves in a brittle manner.

This trend of increased tensile strength with temperature will exist until the viscosity of the material decreases to the point where the material flows easily at high temperature. At this point, the tensile strength will decrease sharply. Future tests at 2500°F will be performed prior to the end of this contract.

A preliminary stress-strain curve, obtained on the static setup for test results at 1500°F and 2000°F is shown in Fig. 4.2-6. The increased ductility is indicated by the decrease in modulus from 46,700 lb/in.$^2$ at 1500°F to 16,000 lb/in.$^2$ at 2000°F.

### 4.2.3 Room Temperature Compression Test

The compression test setup is shown in Fig. 4.2-7. All details are similar in concept to those of the tensile test, except that a spherical universal joint is used at only one end of the specimen. Accuracies, measurement procedures, and test rates are the same as for the tensile test. The test results are shown in Table 4.2-6.

Table 4.2-5

HIGH TEMPERATURE LI-1500 TENSION TESTS
(Uncoated Specimens)

| Test Temp (°F) | Specimen Number | Test Section Width (in.) | Test Section Thickness (in.) | Test Section Area (in.$^2$) | Load (lb) | Stress (psi) | Modulus (psi) |
|---|---|---|---|---|---|---|---|
| R.T. | TT 441 | .450 | .75 | .364 | 27.2 | 74.7 | 75,500 |
| R.T. | TT 442 | .369 | .75 | .2765 | 15.0 | 54.2 | 46,200 |
| R.T. | TT 443 | .364 | .75 | .2655 | 27.0 | 101.6 | * |
| R.T. | | | | | | | |
| | | | | | Average | 76.8 | 60,850 |
| 1500 | TT 445 | .365 | .75 | .274 | 25.8 | 94.2 | * |
| 1500 | TT 446 | .368 | .75 | .276 | 27.7 | 100.4 | * |
| 1500 | TT 447 | .365 | .75 | .274 | 30.35 | 110.7 | |
| 1500 | TT 448 | .371 | .75 | .278 | 27.35 | 98.3 | 46,700 |
| | | | | | Average | 100.9 | 46,700 |
| 2000 | TT 4410 | .365 | .75 | .274 | 42.5 | 155 | * |
| 2000 | TT 4412 | .365 | .75 | .274 | 42.9 | 156.5 | * |
| 2000 | TT 4409 | .27 | .75 | .203 | 33.35 | 164 | (See Fig. 4) |
| 2000 | TT 4413 | .27 | .75 | .203 | 37.35 | 185 | |
| | | | | | Average | 165 | 16,000 |
| 2500 | To Be Determined | | | | | | |
| 2500 | | | | | | | |
| 2500 | | | | | | | |
| 2500 | | | | | | | |

*Dog Bone Specimen Strength Test Only With Dynamic Setup (Other Results Performed With Static Setup)



LOCKHEED MISSILES & SPACE COMPANY

# HIGH TEMPERATURE STRESS - STRAIN CURVES

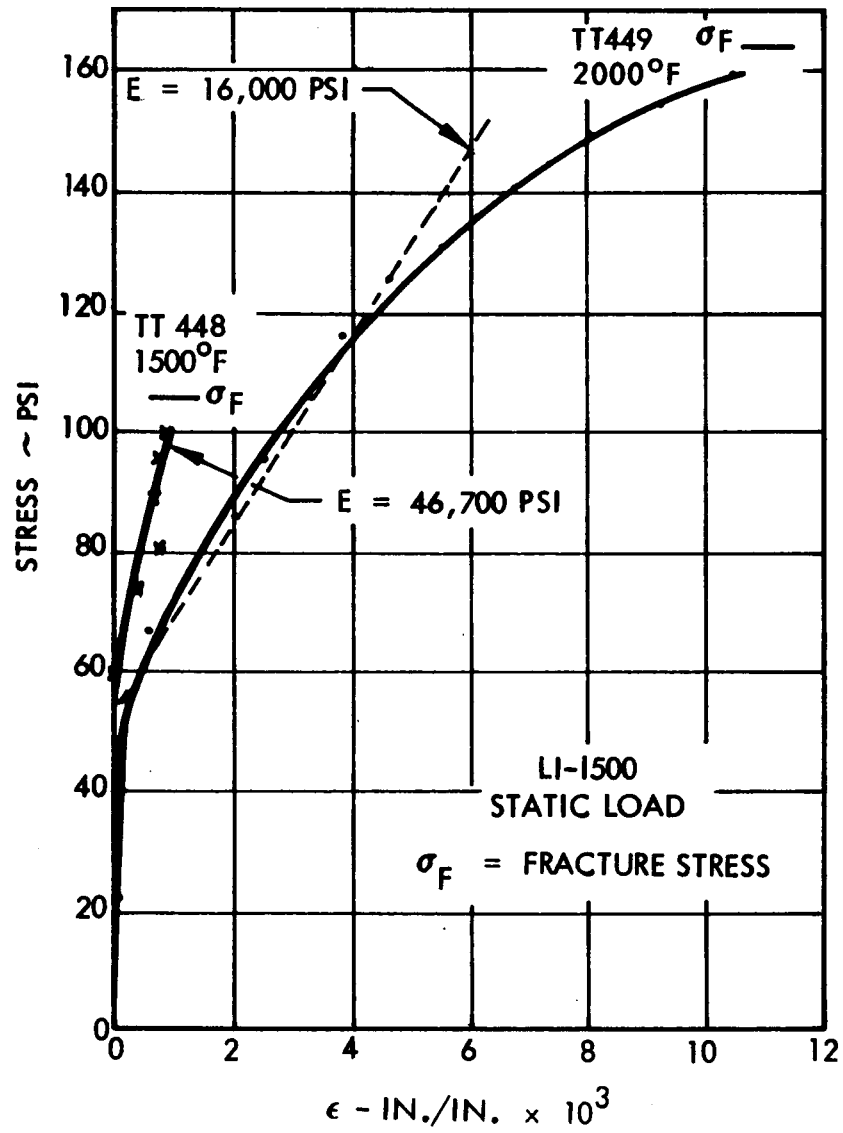


Fig. 4.2-6

# TEST FIXTURE FOR COMPRESSION TESTS OF LI-1500

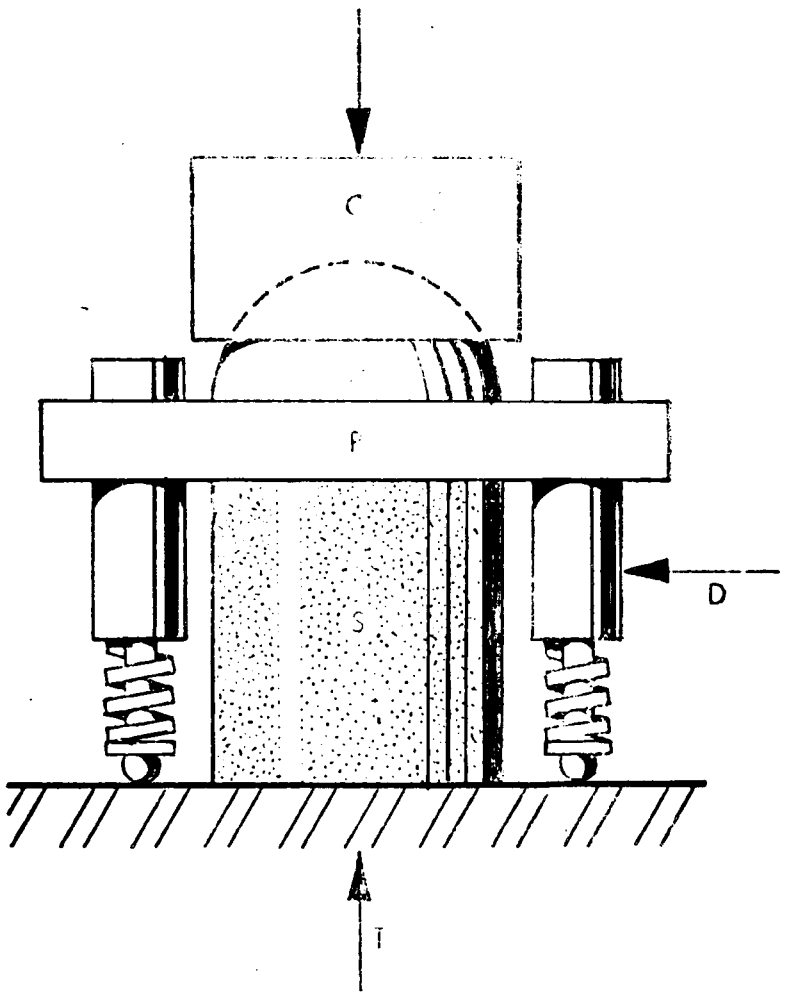


Fig. 4.2-7

Table 4.2-6

LI-1500 ROOM TEMPERATURE COMPRESSION TESTS
(Uncoated Specimens)

| Direction | Specimen Number | Total Length (in.) | Test Section Width (in.) | Thick-ness (in.) | Weight (gm) | Test Section Area (in.) | Load (lb) | Stress (psi) | Modulus (psi) |
|---|---|---|---|---|---|---|---|---|---|
| Parallel | TT 29-1 | 3.00 | 2.00 | 2.00 | 43.5 | 4.00 | 720 | 180 | 37,800 |
| | TT 29-2 | 3.05 | 2.05 | 2.08 | 46.0 | 4.26 | 810 | 190 | 40,000 |
| | TT 29-3 | 3.00 | 2.00 | 2.05 | 46.0 | 4.10 | 698 | 170 | 47,000 |
| | TT 29-4 | 3.05 | 2.05 | 2.05 | 46.0 | 4.20 | 755 | 180 | 46,500 |
| | TT 29-19 | 3.00 | 2.05 | 2.05 | 44.5 | 4.20 | 742 | 177 | 36,100 |
| | TT 29-20 | 2.00 | 2.05 | 3.00 | 44.0 | 6.15 | 906 | 148 | 30,800 |
| | | | | | Average | | | 174 | 39,700 |
| | | | | | NAS 9-11222 Average | | | 156 | 42,560 |
| Normal | TT 29-5 | 2.05 | 3.00 | 2.00 | 44.0 | 6.00 | 253 | 42.2 | 5,120 |
| | TT 29-6 | 2.05 | 3.05 | 2.05 | 44.0 | 6.25 | 268 | 42.9 | 3,620 |
| | TT 29-7 | 2.05 | 3.00 | 2.00 | 44.0 | 6.00 | 257 | 44.2 | 4,070 |
| | TT 29-8 | 2.05 | 3.00 | 2.05 | 44.0 | 6.15 | 242 | 39.4 | 3,470 |
| | | | | | Average | | | 42 | 4,070 |
| | | | | | NAS 9-11222 Average | | | 41 | 4,574 |



LOCKHEED MISSILES & SPACE COMPANY

Table 4.2-7

LI-1500 COMPRESSION TESTS
(Post-Thermal and Acoustical Cycling)

| Number of Thermal and Acoustical Cycles | Specimen Number | Maximum Load (lb) | Maximum Stress (psi) | Modulus (psi) |
|---|---|---|---|---|
| 10 | 3-1 | 948 | 237 | 82,900 |
| | 3-2 | 988 | 247 | 83,600 |
| | 3-3 | 868 | 217 | 87,700 |
| | | Average | 234 | 84,700 |

All specimens 2 x 2 x 3 in.

Test section area = 4.00 in.$^2$

Tested in parallel to fiber orientation direction

Table 4.2-8

LI-1500 ROOM TEMPERATURE COMPRESSION TEST
(Coated Specimens*)

| Direction | Specimen Number | Total Length (in.) | Test Section Width (in.) | Thick-ness (in.) | Weight (gm) | Test Section Area (in.$^2$) | Load (lb) | Stress (psi) | Modulus (psi) |
|---|---|---|---|---|---|---|---|---|---|
| Parallel | TT 29-10 | 3.00 | 2.00 | 2.00 | 47.5 | 4.00 | 730 | 182 | 58,900 |
| | TT 29-11 | 3.00 | 2.00 | 2.00 | 46.0 | 4.00 | 612 | 153 | 52,100 |
| | TT 29-12 | 3.00 | 2.00 | 2.00 | 46.5 | 4.00 | 662 | 164 | 69,300 |
| | TT 29-14 | 3.00 | 2.00 | 2.00 | 46.0 | 4.00 | 680 | 170 | 61,000 |
| | | | | | | Average | | 167 | 60,300 |

*Coating on one 3 in. x 2 in. face



LOCKHEED MISSILES & SPACE COMPANY

The test results for the thermally and acoustically cycled specimens are shown in Table 4.2-7.

The results of the compression tests on specimens that were coated with LI-1500 on one 3 in. x 2 in. side are tabulated in Table 4.2-8. The average strength values are essentially the same as those obtained from the uncoated specimens, whereas the modulus is 50 percent higher.

4.2.3.1 Bend Tests. In the bend tests, a four-point loading fixture was used. The four-point loading is indicated, because it reduces the damage at the loading points by a factor of two.

The two lower rollers were placed 8 in. apart, with the two center loading rollers 2 in. apart and symmetrically located. A third roller was placed above the center to ensure load equality at these two points. One-eighth inch shims were bonded to the specimen with double-faced tape to reduce local indentation due to the rollers.

These tests were performed on an SR-4 universal screw-driven testing machine. A high-sensitivity load cell is placed between the upper-most roller and the test machine crosshead to measure failure loads that are very low compared to the machine's capacity. The loading rate is adjusted so that the specimen fails in about 1 min. of loading. This produces a loading rate of about 0.25 percent per min.

Deflection was measured by a linearly variable differential transformer placed at the specimen midspan. A small disc of 0.005 in. shim was bonded to the specimen with double-faced tape so as to present a smooth, flat, and rigid point for the deflectometer probe. Deflection is recorded continuously versus load on an X-Y plotter. System accuracy is ±1.5 percent of the maximum values being recorded.

The specimen is measured to a 0.020 in. accuracy before testing, and an average of five readings is taken for each dimension. The material is assumed to be isotropic and to have the same properties in tension as in compression when computing the failure stress and modulus of elasticity in bending, so that values are for an average or composite beam. The bending results are shown in Table 4.2-9.

Table 4.2-9

LI-1500 BENDING TESTS
(R.T., Four-Point Loading)

| Specimen Number | Width (in.) | Thick-ness* (in.) | Length (in.) | Weight (gm) | Density ($lb/ft^3$) | Load (lb) | Deflection (in.) | Stress ($lb/in.^2$) | Modulus ($lb/in.^2$) |
|---|---|---|---|---|---|---|---|---|---|
| 1 | 3.0 | 1.5 | 9.0 | 150.0 | 14.1 | 70 | 0.0272 | 93.3 | 29,600 |
| 2 | 3.0 | 1.5 | 9.0 | 151.5 | 14.2 | 87 | 0.0172 | 116. | 58,300 |
| 3 | 3.0 | 1.5 | 9.0 | 155.0 | 14.6 | 90 | 0.0167 | 120. | 62,400 |
| 4 | 3.0 | 1.5 | 9.0 | 151.0 | 14.2 | 100 | 0.0186 | 133. | 62,600 |
| 5 | 3.0 | 1.5 | 9.0 | 143.5 | 13.5 | 84 | 0.0176 | 112. | 56,000 |
| Average | | | | | | | | 114.9 | 53,780 |

*Normal to fiber orientation direction

4.2.3.2 Disc Shear Tests. The anisotropic properties of LI-1500 are due to a layering effect known to exist in the fibers that make up the material. Although randomly oriented within these layers or planes, the fibers do not, to any appreciable extent, cross the boundaries between the layers and tie the layers together. The result is a material that tends to behave like a stack of boards or sheets that (1) can easily be deformed (pushed out of plumb) if loaded horizontally (assuming the boards are lying in a horizontal plane), but (2) is harder to deform if load is applied across the plane of boards so that a shearing force is applied to the stack. To do this, the stack of boards would have to be overhanging a loading dock. A fork lift applying upward force or a man standing on the overhanging end would be more likely to displace the whole stack rather than disrupt their relative position.

This effect is illustrated more specifically in Figs. 3.2-8a, b, and c. In each figure, the shear force is in the X-direction, and the diagonal tension (maximum tension arising out of the shear force) force lies at 45-deg to the X-axis in the X-Z plane. Referring to Fig. 3.2-8a, note that the layers are such that the fibers lie in the X-Y plane and none come closer than 45 deg to resisting the maximum diagonal tension. Note in Fig. 3.2-8b that although the layers are now such that the fibers fall in the Y-Z plane, none come closer than 45-deg to resisting the maximum diagonal tension, which is still at 45-deg to the X-axis in the X-Z plane. In Fig. 3.2-8c, the layers are so arranged that all the fibers lie in the X-Z plane and, since they are randomly oriented in this plane, it is evident that many must be in the 45-deg direction of maximum tension, or at least close to it. This is also illustrated in Fig. 4.2-8c, where both component vectors $T_Z$ and $T_X$ lie in the fiber orientation plane. The result is that when specimens are tested as shown in Fig. 3.2-8c, they will show a greater shear strength and modulus.

For the most recent series of tests, a new fixture was designed that made it easier to display this significant difference between the weak and strong directions of the material. The fixture used in earlier test series (see Fig. 4.2-11) was capable of showing this variation in properties, but the specimens had to be cut from a slab at least 6 in. thick, which was impractical because of excessive cost.

# ORIENTATION FOR SHEAR TEST

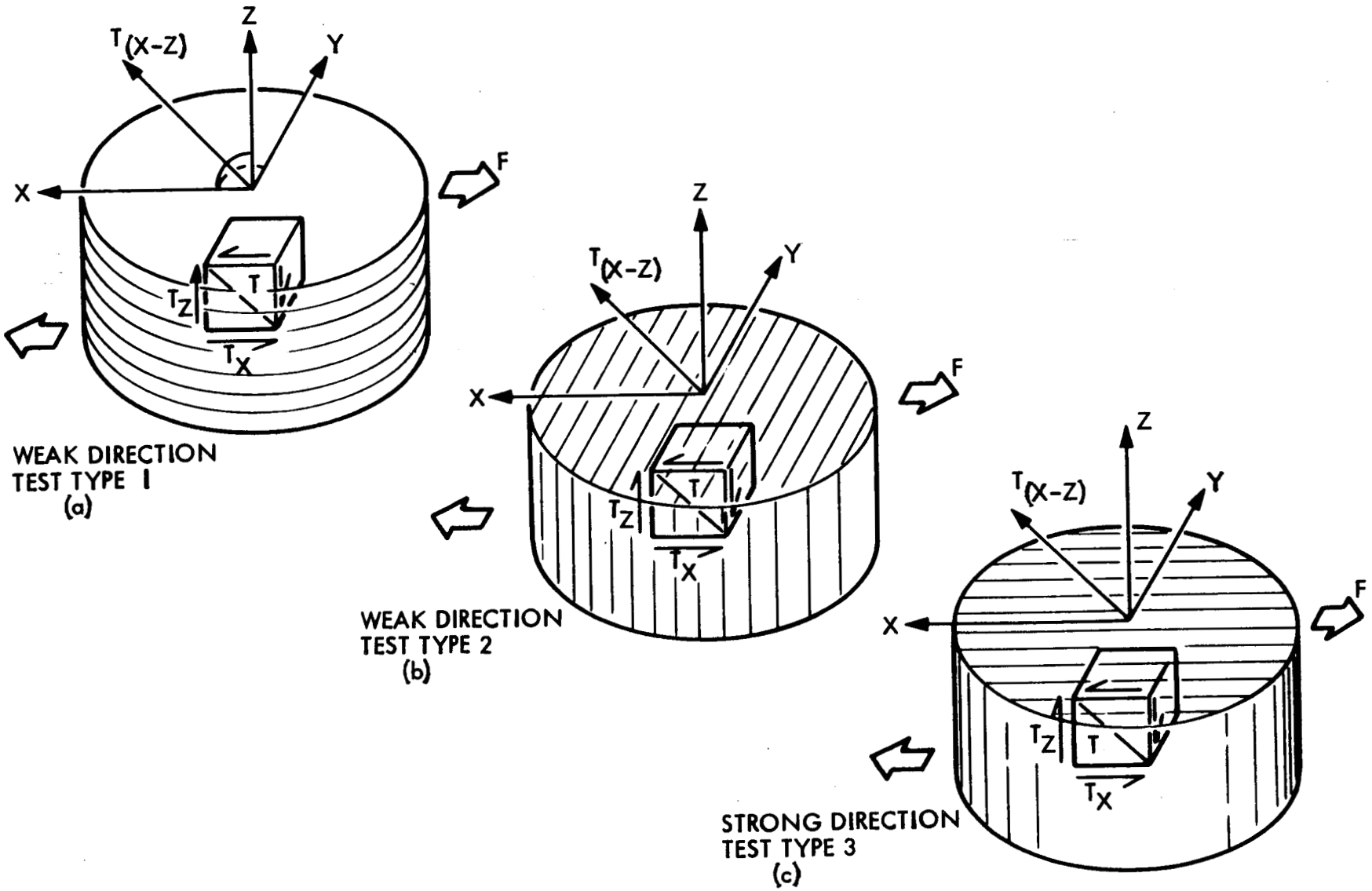


DO6078

Fig. 4.2-8

The present fixture applies a shearing motion to two specimens bonded to two bars, as shown in Fig. 4.2-9. This fixture is of a unique design, which makes it possible to apply only torsion to the assembly. At the base of the frame is a torque generator consisting of a cable wound around a drum and pulled by a hydraulic ram. A load cell is inserted into the cable between the ram and the drum so that the applied force is accurately measured. The drum is supported on high-quality bearings so that the friction is negligible. The lower plate of the specimen assembly (Fig. 4.2-9) is bolted to this drum.

The upper plate (Fig. 4.2-9) is connected to a torque-resisting head. This head has five degrees-of-freedom; i.e., it is free to rotate or translate about either horizontal axis by virtue of linear ball bushings mounted in gimbal configuration. In addition, the head can translate in a vertical direction (by virtue of linear ball bushings), but rotation about the vertical axis is impossible. The high-quality bearings make the five-degrees-of-freedom motion very free. In addition, the weight of the torque resisting head is "eliminated" from the specimen by suspending the head by a very soft spring and turnbuckle. The latter is adjusted until a very fine air gap exists between the upper specimen plate and the attachment plate. The spring rate of the suspension system is about 0.5 lb/in. so that gap closure induces only 0.005 lb of force to the specimen assembly, which is less than the weight of one of the plates bonded onto the LI-1500.

Deflectometers measure the relative movement of the two plates, and load (torque) is recorded versus this movement on an X-Y plotter.

Specimens required for one test are a pair of discs, each 2 in. in diameter by 1 in. in height. An additional test series is planned with specimens only 3/8-in. high. The height of the specimen is the chief shortcoming of the test method. The higher the specimen, the greater the overturning moment (see Fig. 4.2-10) and, consequently, the greater the normal forces on the end faces of the specimen. (The normal forces are only shown on the base face in Fig. 4.2-10, but obviously they exist on the top and bottom face and in a distribution pattern that is unknown but self-balancing in the vertical direction.

# SHEAR TEST SPECIMENS AND MOUNTING PLATES

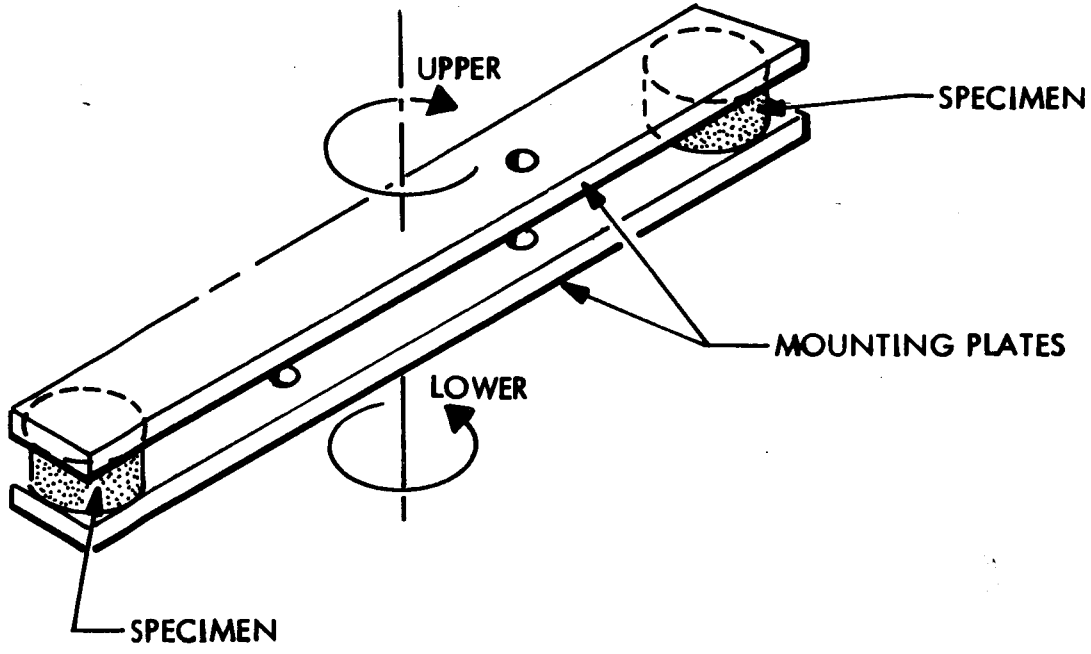


Fig. 4.2-9

# SHEAR TEST SPECIMEN

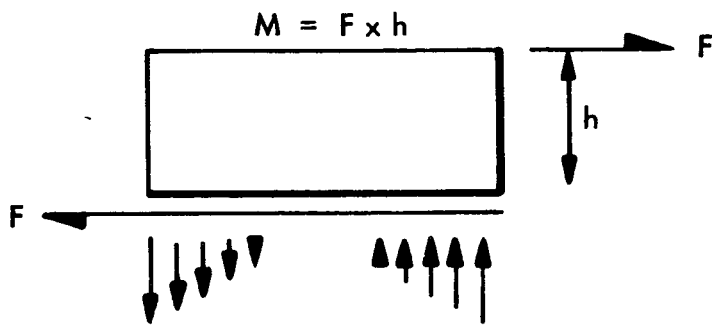


Fig. 4.2-10

There is no doubt that these normal forces, superimposed on the maximum diagonal tension produced by the shear, influence the results of the shear test – probably unfavorably. The only method of testing that would theoretically remove normal forces is a test on a cylindrical specimen having a relatively thin wall. Such a test would be expensive because the specimen must be large to make possible a relatively thin wall to obtain an unbiased shear test. Manufacture of a consistent specimen would be difficult.

Note that a test fixture used on an earlier series of tests, NAS 9-11222, produced somewhat stronger shear test results on a batch of material that generally showed lower strength values in all other mechanical tests. Figure 4.2-11a shows the test fixture conforming to requirements set forth by the ASTM for testing honeycomb sandwich in shear. One refinement added to the fixture is believed to cause higher shear test values; this refinement is the addition of a rim to the bonding plate, shown in Fig. 4.2-11b. This rim consists of three plates (one end plate and two triangular edge end plates) bolted to the main plates to which the specimen is bonded. Thus, the specimen is partially boxed in. In addition, bonding is used on all surfaces of the rim in contact with the specimen.

It is believed that the fixture with the rim produced higher test results because it resulted in a favorable superimposed compression field that partially cancelled the maximum diagonal tension. The effect is easier to visualize by the use of a diagram, in which the box is slightly distorted (see Fig. 4.2-12). In this diagram, a tensile force applied to the fixture results in a compressive force on the specimen. If it is remembered that the specimen is weak (i.e., has a low modulus) in shear, it is not difficult to see why an alternate load path (in this case that of a strut in compression) should carry such a disproportionately large share of the load. (Some values in the previous shear test series (NAS 9-11222) ran as much as twice the values of one weak direction in the present test series, and on the average about 25-to-30 percent higher.) The shear modulus values in the earlier test series are about 25 percent of the values reported in the present (weak-direction) series. The modulus on the early series test was obtained by measuring table motion, which explains the lower values. The present system using deflectometers placed very near the specimen is obviously much more accurate.

# SCHEMATIC OF NAS9-11222 SHEAR TEST FIXTURE

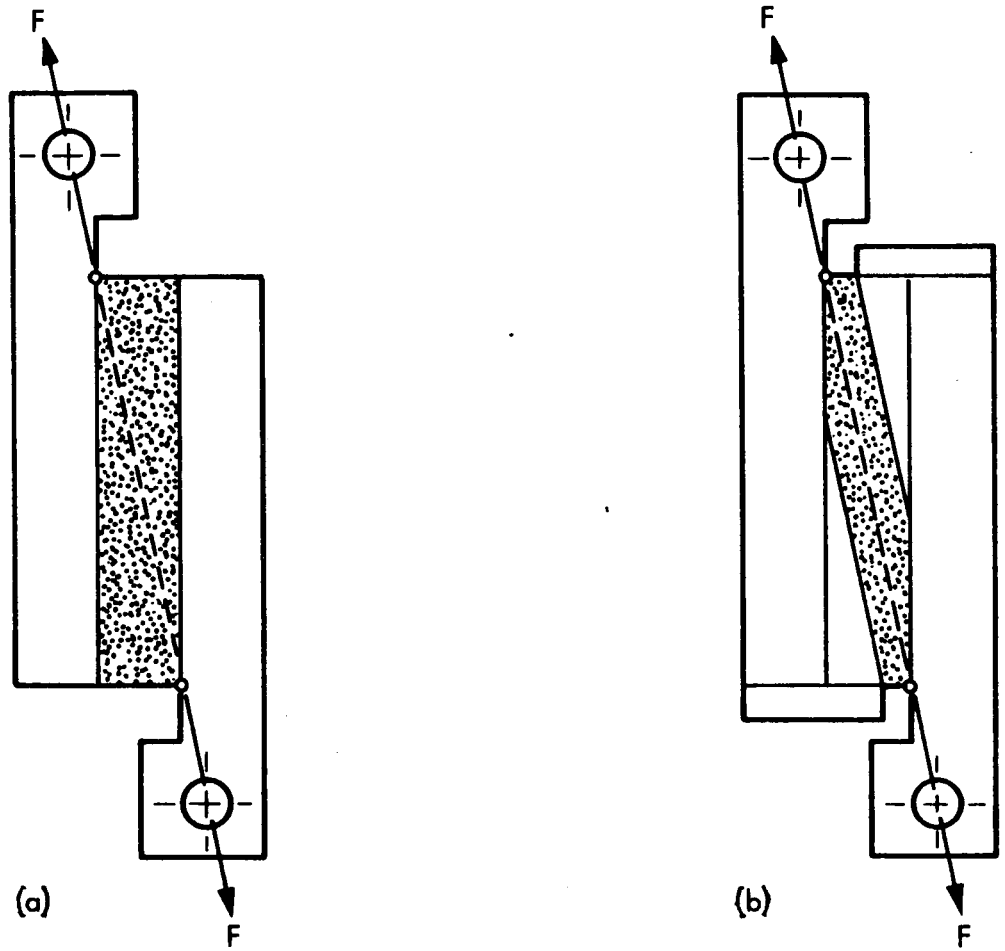


ASTM FIXTURE
(NO RIM)

RIM ADDED TO
ASTM FIXTURE

DO6077

Fig. 4.2-11

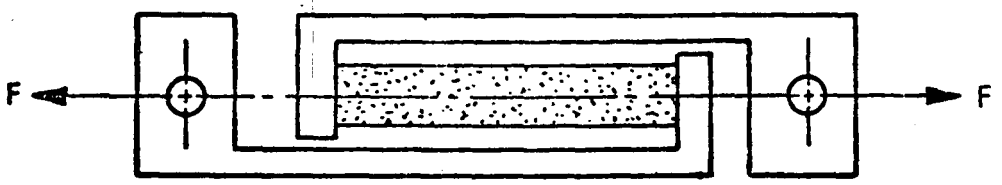


Fig. 4.2-12 Schematic of Compression Load Path

In the present test method, the maximum shear is calculated by multiplying the average stress by the ratio of the maximum radius to the average radius. That is, the shear force is assumed to act at the center of the 2-in. diameter specimens, but since the stress distribution varies as the distance to the center of rotation (in the case of torsion), the stress is obviously higher at the outermost point on the specimen. The shear modulus is calculated by dividing the average stress by the average strain, i.e., no prorating is performed here, since the strain must also be prorated by the same ratio.

The LI-1500 shear test results for the 2-in.-diameter x 1-in.-thick specimens are shown in Table 4.2-10. Since these values were lower than those measured during the past contract, NAS 9-11222, additional tests were performed on 2-in.-diameter x 0.375-in.-thick specimens. As discussed previously and illustrated in Fig. 4.2-5, thinner specimens tend to reduce the normal forces acting on the end faces of the specimen and tend to put the specimen in a purer state of shear. The results of the 0.375-in.-thick specimens shown in Table 4.2-11 indicate about 145 percent increase in the weak direction (parallel to fiber orientation) shear values over the values obtained from the 1-in.-thick specimens. A 75 percent increase in the strong (normal to fiber orientation direction) direction shear results occurred for the 0.375-in.-thick specimens. LMSC plans to perform more shear tests in the weak direction, since the parallel shear allowable is current a major design driver and more data points are required.

### 4.2.4 Tension Tests on Higher Density LI-1500

Preliminary screening tests to determine the tensile strength and tensile modulus of higher density LI-1500 were performed for the Material Improvement Contract, NAS 9-12137. These results are included here to indicate the trend in strength and modulus. Figure 4.2-13 shows the variation of tensile strength with specimen density. The average tensile strength varies from 75 to 210 lb/in.$^2$ as the density increases from 15 to 59 lb/ft$^3$.

Table 4.2-10

ROOM TEMPERATURE DISC SHEAR TESTS

| Direction | Specimen Numbers | Maximum Load (lb) | Maximum Shear Stress (psi) | Maximum Shear Strain (%) | Shear Modulus (psi) |
|---|---|---|---|---|---|
| Parallel | 1 and 2 | 118 | 10.0 | 0.391 | 3,970 |
| | 3 and 4 | 144 | 12.2 | 0.289 | 5,000 |
| | 5 and 6 | 149 | 12.6 | 0.238 | 6,530 |
| | 7 and 8 | 120 | 10.2 | 0.238 | 5,240 |
| | 9 and 10 | 130 | 11.0 | 0.306 | 3,690 |
| | | Average | 11.0 | | 4,890 |
| | | NAS 9-11222 | 16.0 | | 1,174 |
| Normal | 14 and 15 | 580 | 49.1 | 0.211 | 28,200 |
| | 16 and 17 | 465 | 39.4 | 0.331 | 14,500 |
| | 18 and 19 | 493 | 41.8 | 0.216 | 20,600 |
| | | Average | 43.0 | - | 21,100 |

All specimens - 2.00 in. diameter x 1.00 in. thick.

Table 4.2-11

ROOM TEMPERATURE SHEAR TEST RESULTS
(Torsion Tester)

| Direction | Specimen Numbers | Diameter (in.) | Height (in.) | Density ($lb/ft^3$) | Load (lb) | Shear Stress Max ($lb/in.^2$) | Shear Modulus ($lb/in.^2$) |
|---|---|---|---|---|---|---|---|
| Parallel | 111 | 2.00 | 0.375 | | 350 | 29.6 | 6,370 |
| | 113/113 | 2.00 | 0.375 | | 300 | 25.4 | 6,840 |
| | | | | Average | | 27.5 | 6,605 |
| Normal | TI 30/D113 | 2.00 | 0.375 | | 715 | 60.6 | 32,900 |
| | TT 38-1/-2 | 2.00 | 0.375 | | 1,010 | 85.6 | 25,600 |
| | TT 38-3/-4 | 2.00 | 0.375 | | 662 | 56.1 | 25,900 |
| | TT 38-5/-6 | 2.00 | 0.375 | | 1,155 | 97.8 | 43,100 |
| | | | | Average | | 75.0 | 31,900 |



LOCKHEED MISSILES & SPACE COMPANY

# VARIATION OF TENSILE STRENGTH WITH LI-1500 DENSITY

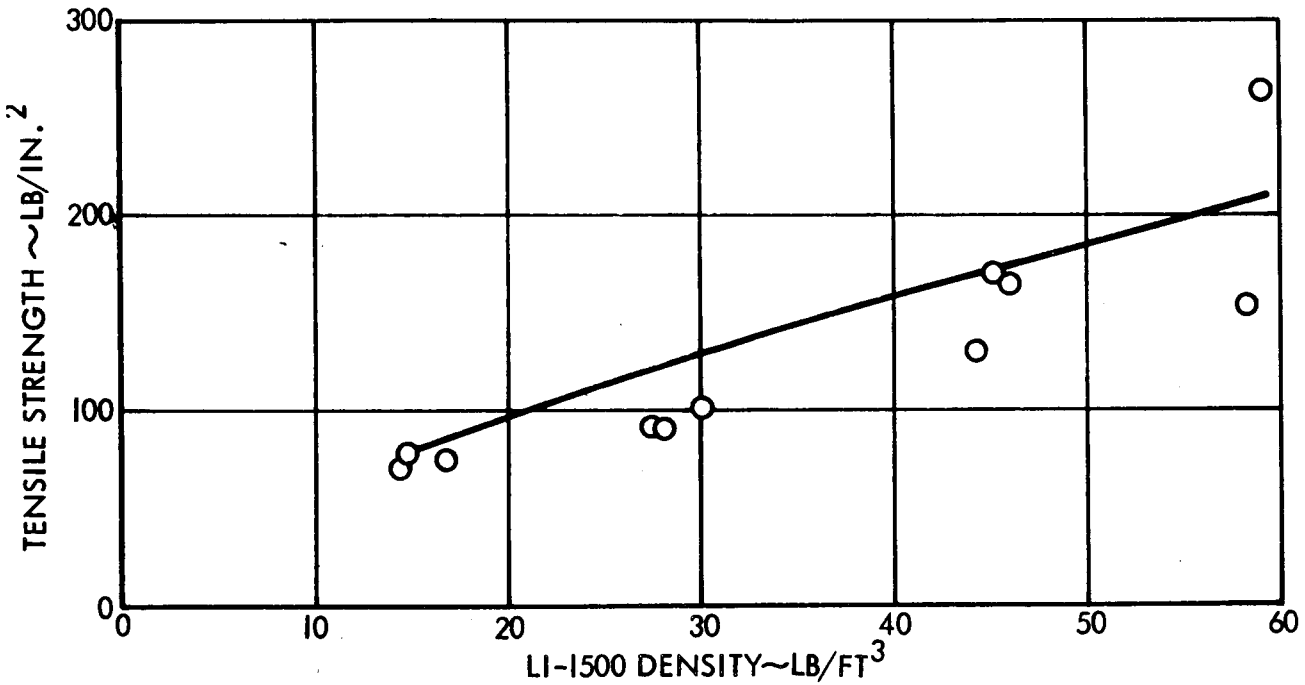


Fig. 4.2-13

# VARIATION OF ELASTIC MODULUS WITH LI-1500 DENSITY

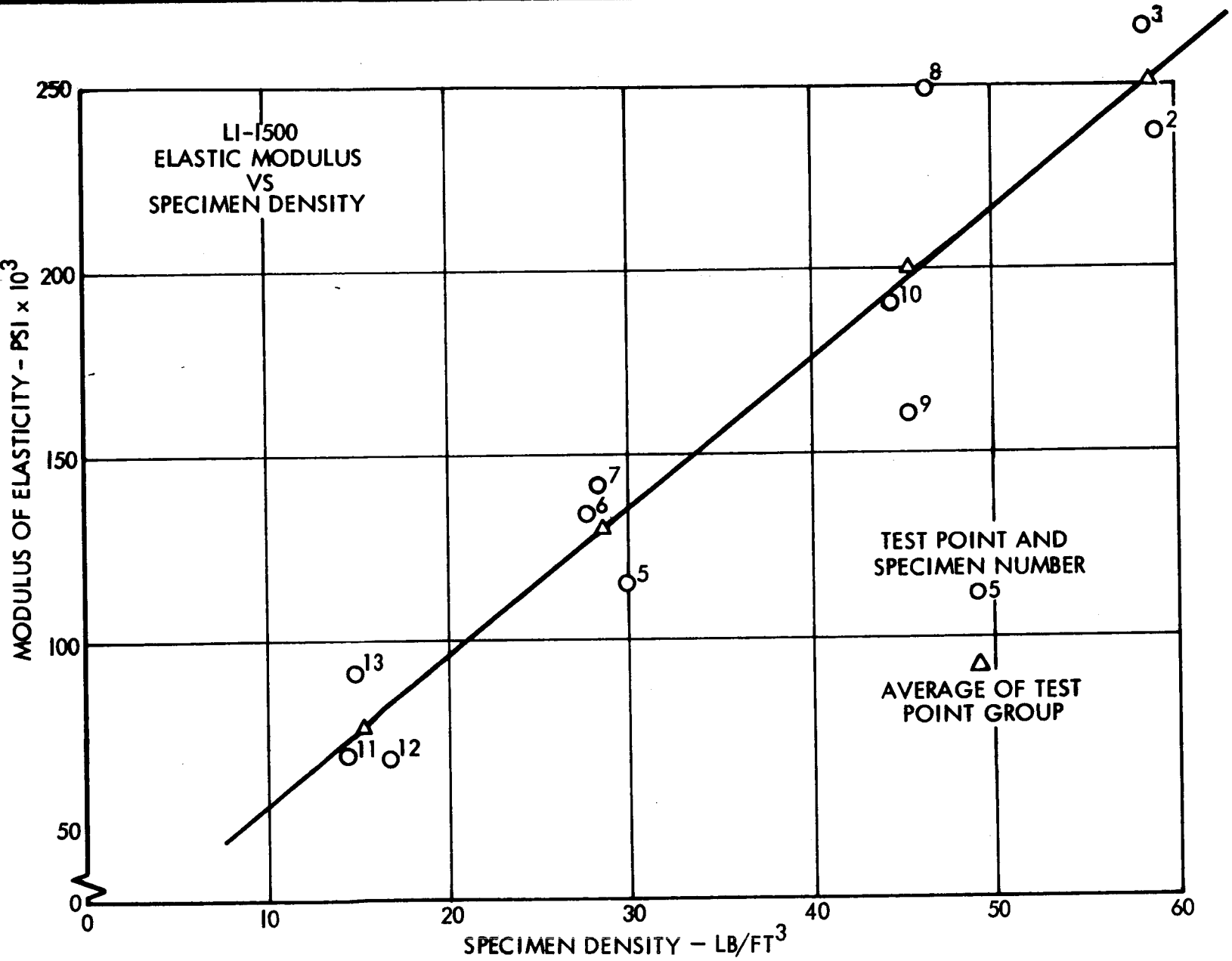


DO6035

Fig. 4.2-14

The variation of elastic modulus with specimen density is shown in Fig. 4.2-14. The overage modulus varies from about 60,000 lb/in.$^2$ to 250,000 lb/in.$^2$. Tabulated data from these tests are shown in Table 4.2-12.

4.2.5 Coating Cantilever Test

The purpose of this test is to obtain the mechanical properties of the LI-1500 surface coating alone, by applying a cantilever bending moment to a small rectangular plate specimen of the coating. From the simple relations of statics, it is possible to determine the stress and strain in the cantilever from the applied load and measured tip deflection.

As in all tests on the coating, the greatest source of error and uncertainty in the test results stems from the thickness characteristics of the coating. The coating is applied to the porous substrate in liquid form; therefore, it permeates the latter to varying degrees. In attempting to obtain a specimen of coating alone, the difficulty arises in deciding just where the coating boundary is located. The tendency is to have a thin layer of LI-1500 attached to the coating, since its contribution to the coating's ability to sustain load will be minor. The LI-1500 is removed by careful scraping with an Exacto knife. The final scraping is done after the specimen is bonded to an anchor block, which provides fixity in the test.

The specimen thickness is measured after the test, because the risk of specimen breakage during measurement is very high. A micrometer is used to measure the thickness to ±0.001 in. resolution, and the average of twelve readings is taken.

The LI-1500 tends to crush under the micrometer pressure, a fact that tends to make the reading (as a measure of the coatings actual thickness) somewhat more accurate than if it (the LI-1500) remained intact. The scatter in thickness readings is usually within ±0.005 in. When scatter falls outside of this range, extra readings on either side (one micrometer anvil diameter) of the high reading are taken, since high readings tend to be caused by lumps on the backface of the coating. The lumps are from intrusion of the coating into a larger than average void in the LI-1500 base mater. If either of the

Table 4.2-12

DENSIFIED LI-1500 TENSION AND MODULUS RESULTS
(Room Temperature Tests)

| Specimen Number | LI-1500 Density ($lb/ft^3$) | Gage Length (in.) | Test Section Width (in.) | Thick-ness (in.) | Weight (gm) | Test Section Area ($in.^2$) | Load (lb) | Stress (psi) | Modulus (psi) |
|---|---|---|---|---|---|---|---|---|---|
| 2 | 58.9 | 4.00 | 1.51 | 0.24 | 29.5 | 0.362 | 96.0 | 265 | 238,000 |
| 3 | 58.3 | 4.00 | 1.50 | 0.27 | 29.0 | 0.405 | 62.8 | 155 | 267,000 |
| 8 | 46.3 | 4.03 | 1.50 | 0.20 | 22.0 | 0.300 | 50.4 | 168 | 250,000 |
| 9 | 45.2 | 4.00 | 1.49 | 0.20 | 21.0 | 0.298 | 51.0 | 171 | 161,000 |
| 10 | 44.4 | 4.05 | 1.50 | 0.20 | 21.0 | 0.294 | 38.4 | 131 | 192,000 |
| 5 | 29.8 | 4.00 | 1.50 | 0.20 | 17.0 | 0.300 | 30.4 | 101.0 | 116,000 |
| 4 | 28.1 | 4.00 | 1.50 | 0.24 | 16.5 | 0.360 | 32.0 | 88.9 | 142,000 |
| 6 | 27.6 | 4.00 | 1.58 | 0.24 | 16.0 | 0.380 | 34.8 | 91.6 | 135,500 |
| 12 | 16.6 | 4.00 | 1.50 | 0.25 | 8.0 | 0.375 | 28.8 | 74.7 | 68,200 |
| 13 | 14.7 | 4.00 | 1.50 | 0.20 | 7.0 | 0.300 | 23.2 | 77.3 | 91,900 |
| 11 | 14.5 | 4.00 | 1.50 | 0.24 | 7.0 | 0.360 | 26.0 | 72.2 | 69,500 |

extra readings falls outside the ±0.005 in. range, the initial high reading is retained as valid. If both of the extra readings fall inside the ±0.005 in. range, the average of the extra readings is reported as a single value replacing the one that originally fell outside the ±0.005 in. range. The need for extra readings is fairly rare.

Despite these precautions, it is recognized that uncertainty remains as to the true coating thickness. Indeed, whether a true thickness does, in fact, exist is questionable, since there is probably a region (as the thickness of the specimen is traversed) where the material encountered is part coating and part base material; the thickness of this "no-man's land" probably varies from one location on the specimen to another.

This uncertainty affects the results considerably, since it has a large leverage effect in the data reduction. First, there is the physical reality that a thick layer of diluted coating represents a layer of reduced strength, which is counted as if it had full strength. Second, is the fact that in calculating the stress as a function of the applied load, the measured thickness, t , appears as a quantity squared in the denominator of the expression for stress:

$$\sigma = \frac{6 \times P \times L}{w \times t^2}$$

where

P = applied load

L = length of the cantilever

w = width of the cantilever

t = thickness of the cantilever

Thus, P is lowered (by the diluted coating) and t is increased, resulting in a value of $\sigma$ (the calculated stress) substantially reduced from its true value.

The apparatus used for the cantilever coating tests is shown schematically in Fig. 4.2-15. Photographs of the apparatus and the test specimen are shown in Figs. 4.2-16 and 4.2-17.

# SCHEMATIC OF COATING TEST APPARATUS

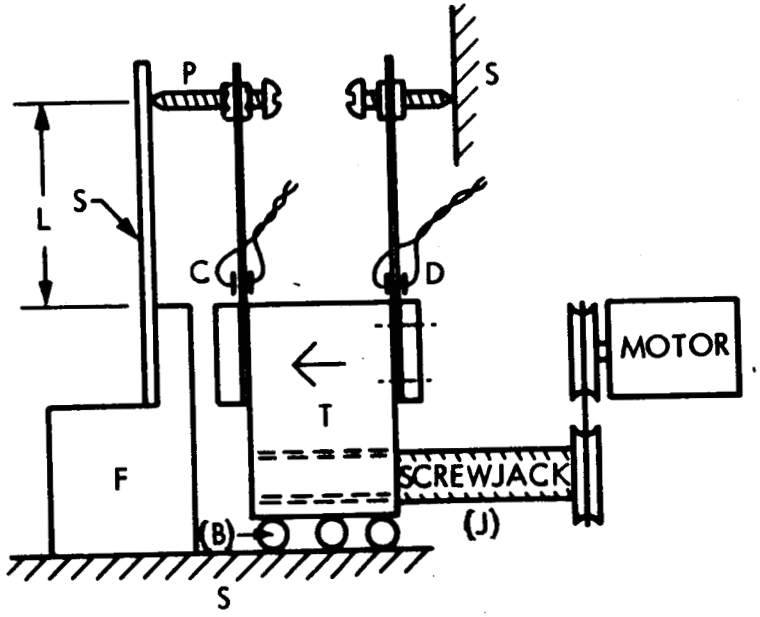


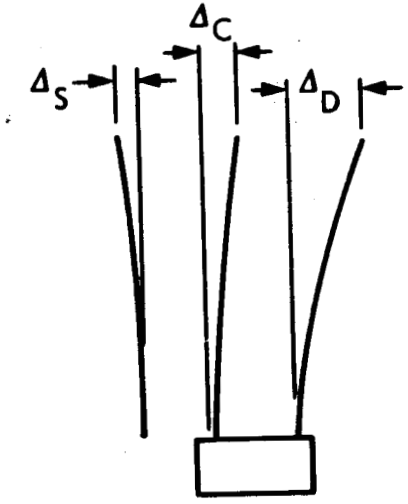


$$\Delta_S = \Delta_D - \Delta_C$$

$$M_{(SPECIMEN)} = PL \qquad \sigma = \frac{Mc}{I} \quad \therefore \quad \sigma = \frac{PLt}{IZ} = \frac{6PL}{bt^2}$$

$$\Delta_S = \frac{PL^3}{3EI} = \frac{ML^2}{3EI} = \frac{\sigma \times I \times L^2}{3EI \times C} = \frac{\varepsilon EL^2}{3EC} = \frac{\varepsilon L^2}{3C}$$

$$\varepsilon = \frac{3\,\Delta\, t}{2\,L^2} \qquad \varepsilon = 3.14 \times 10^{-5} \times \Delta \quad (\Delta \text{ IN MILS}, \ \varepsilon \text{ IN } \mu\varepsilon, \ t = 0.022 \text{ IN.} \ \ L = 1.05 \text{ IN.})$$

$$\sigma = 64P \qquad \sigma \text{ IN PSI}, \quad P \text{ IN GRAM}, \quad b = 0.45 \text{ IN.}, \quad t = 0.022 \text{ IN.}, \quad L = 1.05 \text{ IN.}$$

Fig. 4.2-15

DO6069

# PRESENT COATING CANTILEVER TEST FIXTURE

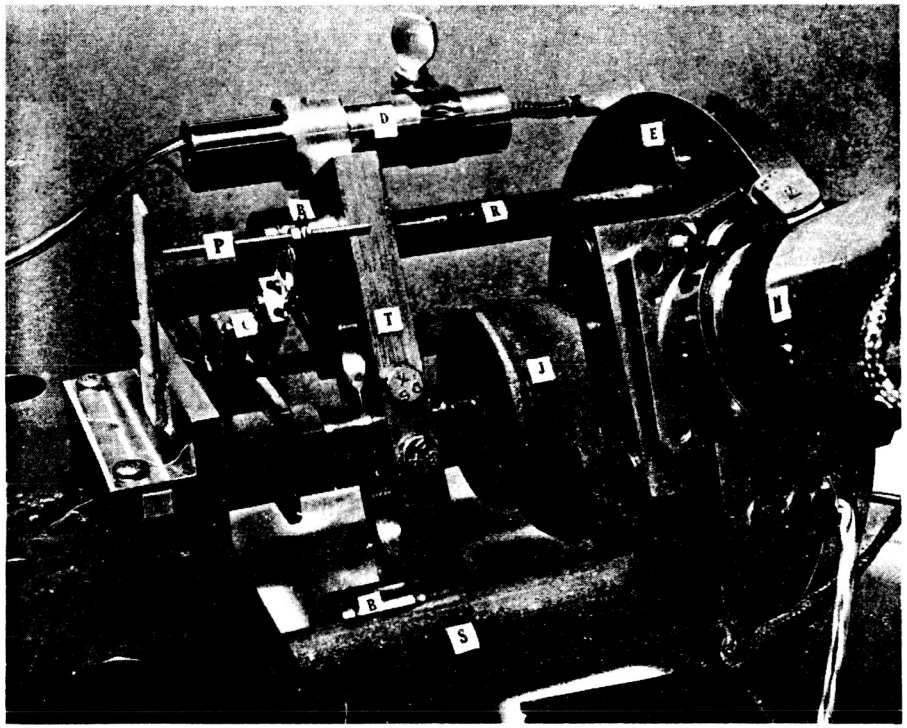


Fig. 4.2-16

DO6079

# COATING CANTILEVER TEST SPECIMEN

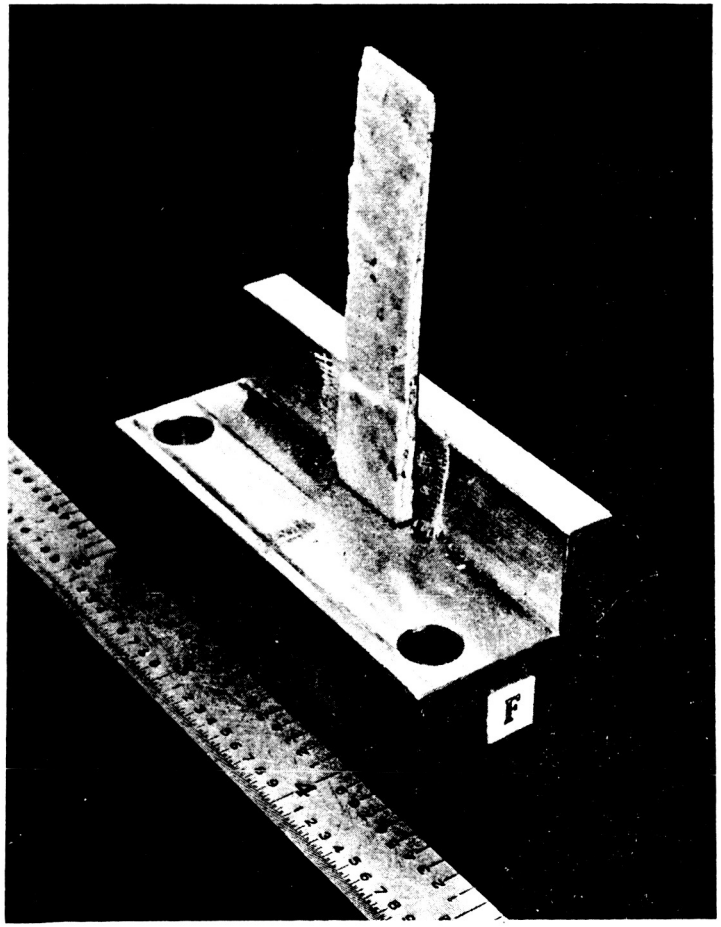


Fig. 4.2-17

The specimen is attached to a fixed block (F), which is rigidly connected to the main structural frame by bolting. In the diagram, the endplate (E) is connected by the columns (labeled S) to fixed block (F). The screwjack (J) and motor are attached to an endplate as are two rods that serve to guide the linear ball bushings (B). The endplate and rods are not shown on the schematic.

The screwjack causes an assembly (T) to translate on the rods. Two transducers are attached to the translating assembly (T); one of these is a linearly variable differential transformer (D) whose probe bears against the fixed endplate, so that this transducer measures the motion of T with respect to the fixed frame. The second transducer is a thin-steel cantilever blade (C) strain gaged near its base and calibrated so that both the applied load at its tip and the deflection of its tip can be related to its electrical output. The movement of the cantilever specimen tip is then the movement of T, less the movement of the cantilever tip relative to T; or the specimen tip deflection.

$$\Delta_S = \Delta_D - \Delta_C$$

In the schematic, the deflectometer (D) is represented as a second cantilever, which would, in fact, work just as well, but a linearly variable differential transformer was used instead because it was more convenient. The motor is set to drive T at a uniform speed of 0.0002 in./sec, and the two deflectometers are recorded continuously. The data are reduced by a Tymshare computer, using the following relationships:

$$\epsilon = \frac{3 \times \Delta_S \times t}{2 L^2}$$

and,

$$\sigma = \frac{6 \times P \times L}{w \times t^2}$$

where $\epsilon$ is the strain at the cantilever root, and $\sigma$ the stress. All other terms were defined in the previous discussion.

The specimen is bonded to the block (F) using Duco cement and a cotton gauze scrim cloth (to improve the cement drying). A 24-hr drying time is required for the Duco cement.

Test results for seven tests on the 0025 coating are given in Table 4.2-13. Specimens for Tests 1 and 6 were cut from visibly undamaged portions of a slab that had been used in a different and unsuccessful coating test. For all other tests listed in the table, the coatings were obtained from a different specimen.

It is felt that the explanation for the extremely high modulus value for Specimen 1 is due to the fact that the coating may experience some pretest cracking due to handling or shrinkage, and that Test Specimen 1 escaped this fate. There have been other less reliable test attempts in which this higher modulus value seemed to be evident. Although these tests had to be discarded for other reasons, they indicated that the modulus was in the range from 3-to-7 million lb/in.$^2$, rather than the range well below 1 million indicated by Table 4.2-13. It is fairly safe to say that Test Specimen 4 was either damaged or had some serious but invisible manufacturing flaw, since both its strength and modulus are very low compared to the other values in the table.

It should be emphasized that the accuracy of the load and deflection measurements in the cantilever device are at least one-order-of-magnitude more refined than they need to be (relative to the accuracy with which the specimen thickness can be defined). The deflection is measured to 5 $\mu$in. precision and the load is measured to $10^{-2}$ gram precision. The accuracy is probably only 5-to-10 times the above quoted figures, but this is still quite acceptable when it is realized that in a typical test the tip deflects 10,000 $\mu$in. and the tip load reaches 5-to-10 grams.

Preliminary results from tests on the 0042 coating (borosilicate coating with a silicon carbide emittance agent) indicate a tensile strength greater than 2000 lb/in.$^2$ and a modulus of $9.1 \times 10^6$ lb/in.$^2$.

Table 4.2-13

LI-1500 COATING (0025) FLEXURE TEST

| Test | Thickness (in.) | Width (in.) | Span (in.) | Maximum Stress (psi) | Average Modulus (psi x $10^6$) |
|---|---|---|---|---|---|
| 1 | 0.022 | 0.45 | 1.05 | 749 | 4.47 at $\sigma$ = 498 |
| 3 | 0.036 | 0.51 | 1.12 | 720 | 0.397 at $\sigma$ = 701 |
| 4 | 0.040 | 0.52 | 1.16 | 421 | 0.236 at $\sigma$ = 60.5 |
| 5 | 0.038 | 0.51 | 1.19 | 134 | 0.077 at $\sigma$ = 125 |
| 6 | 0.043 | 0.52 | 1.19 | 439 | 0.209 at $\sigma$ = 439 |
| 7 | 0.035 | 0.47 | 0.78 | 427 | 0.342 at $\sigma$ = 374 |
| Average | | | | 480 | 0.96 |

# Section 5
# ENVIRONMENTAL RESPONSE BEHAVIOR

The objective of this task is to demonstrate the capability of the LI-1500 RSI System to withstand various critical environmental conditions to be encountered in shuttle operations. As noted earlier, LMSC is conducting an intensive coating evaluation effort to incorporate an improved coating system into this program. As related in par 3.1, a new coating has been baselined, the 0042 coating system. The majority of tests under Task 5.0 is currently in the process of being initiated with completion rescheduled by 1 December. Since the coating system is an integral part of the LI-1500 TPS, LMSC considered that it was desirable to incorporate the most improved coating available for these tests. The test specimens have been fabricated and testing initiated. Detail test results will be reported in the November Monthly Progress Report.

## 5.1 MATERIAL/SUBSTRATE EVALUATION

The insulation material/coating system must be incorporated into a design that is compatible with the vehicle structure it protects. In addition to withstanding ambient environment conditions throughout its 100-mission operational life, the TPS design must withstand the heating, acoustic, pressure, pressure loading, and structurally induced loading during ascent, entry, and subsonic cruise environmental conditions. Representative structural panels and insulation tile assemblies with realistic joints and attachment methods are needed for evaluation tests. The tests are intended to demonstrate the feasibility of the LI-1500 TPS design for an equivalent 100 Space Shuttle Orbiter missions.

The test specimen consists of a 6 x 24-inch aluminum Z-stiffened panel (one-fourth of a regular vehicle panel) with one 6 x 12 x 2.45 and two 6 x 6 x 2.45 inch LI-1500 tiles bonded to the panel with a 0.090-inch thickness of RTV 560.

Although the aluminum primary structure for the Shuttle orbiter will be subjected to both pressure and axial structural loads, only pressure loads will be simulated in the tests. The test panels will be subjected to 20 simulated missions, enough to determine whether repeated cycling is detrimental to the assemblies. The panels will be subjected to simultaneous heating, pressure, and pressure-loading conditions and interim acoustic excitations. Vibration testing will not be performed, because LMSC considers the acoustically induced vibrations during liftoff to represent the critical environment. The dominant acoustic environment occurs for approximately a 10-second period at liftoff because of first-stage engine acoustic excitation. Test durations duplicate this excitation as a function of temperature/pressure cycles performed between acoustic tests. The acoustic environment for these tests is shown in Fig. 4.1-9. The temperature/pressure histories used to simulate ascent and entry conditions are shown in Figs. 2.2.2-5 and 2.2.2-8.

The initial test series will consist of separate pressure and temperature tests to establish the effects of these conditions independently prior to combined testing. The test sequence is as follows:

a. Maximum positive differential pressure at room temperature
b. Temperature cycle at reduced pressure level with no pressure differential loading
c. One simulated mission cycle
d. One simulated mission cycle with negative pressure loading
e. Eight simulated mission cycles
f. Acoustic exposure at room temperature
g. Ten simulated mission cycles
h. Acoustic exposure at room temperature

These tests will be performed in the Shuttle Transient Ascent/Reentry Simulator (STARS). This unique facility was developed by LMSC to provide simulation of the combined temperature and pressure histories experienced by the Space Shuttle orbiter during ascent and entry phases of its mission. The tests are scheduled for 22 November 1971.

## 5.2 DESIGN DETAILS EVALUATION

As described in the last progress report, the joint gap and joint mismatch model designs were modified to incorporate double-lap joints with a secondary block instead of the originally planned rectangular lap joints. In addition, the specimens have a 0.25-inch layer of LI-1500 attached to the substrate backface to minimize heat leak. This is justified because of the present design criteria of an adiabatic backface assumption in sizing the LI-1500 thickness. The specimens have been completed and delivered to NASA/MSC for testing. The recently baselined 0042 SiC coating system has been used on these models.

## 5.3 SPECIALIZED ENVIRONMENTAL TESTS

The effects of adverse environmental conditions on the basic RSI and surface coating must be established to allow the system service life to be predicted. The tests being conducted under this subtask are intended to establish the effects of the various environmental conditions on the material and coating. In addition to the tests described in the Program Plan, another test is included as par. 5.3.7. Although these tests were not originally included in this description, they are necessary to help fully characterize the material behavior for the expected environmental conditions. Therefore, it is included as a test in this series.

The specialized environmental tests were expected to be completed by the time of this report. Demands on the test facilities and personnel to perform the 100-cycle coating evaluation tests described in par. 3.1. made this impossible. However, the tests are either currently in progress or will be soon. It is expected that the tests will all be completed by 30 November 1971. A brief description of the tests, an outline of the test conditions, and some preliminary test results follow.

### 5.3.1 Infrared Transmission

Spectral transmittance of LI-1500, and also the coating material, will be determined over a range of temperature conditions and wavelengths. Two methods used at LMSC to measure the spectral transmittance of materials are briefly described in the following paragraphs.

5.3.1.1 Method 1 - Total Spectral Transmittance. Measurements by this method determine the total, i.e., normal-plus-scattered, radiation transmitted through a specimen into the $2\pi$-steradian hemispherical space at the back face of the specimen. The incident radiation is monochromatic and is directed onto the specimen at a near-normal angle of incidence, i.e., perpendicular to the front face of the specimen. The irradiated area of the specimen is determined by the slit size of the monochromator and is approximately 8 mm high by 0.10 to 2.0 mm wide. The radiation source is a high-intensity, 54 watt tungsten strip lamp. The source radiation is directed into a Perkin-Elmer Model 98 Monochromator with an $SiO_2$ prism. Monochromatic radiation of the desired wavelength between $0.35\mu$ and $2.5\mu$ is selected and directed from the monochromator exit slits to a Gier-Dunkle Model SP-210 Integrating Sphere. The integrating sphere is equipped with a transmittance-measuring attachment that permits the placement or removal of a specimen in front of the entrance port to the integrating sphere. Incident energy levels are measured with the sample removed, and transmitted energy levels are measured with the sample in front of the entrance port. Two detectors are mounted at the rear surface of the integrating sphere – a Type 1P28 photomultiplier, for measurements at wavelengths between $0.35\mu$ and $0.75\mu$, and a lead sulfide cell, for measurements between $0.70\mu$ and $2.5\mu$. Both detectors collect energy from the walls of the integrating sphere, but they are shielded so they do not directly view the incident or transmitted radiation through the entrance port.

5.3.1.2 Method 2. Spectral Normal Transmittance. Measurements by this method determine only the normal component of radiation transmitted through a specimen. For the spectral region between $0.35\mu$ and $2.5\mu$ the same equipment described above is used; however, the sample is placed in front of the entrance slits to the monochromator instead of in front of the integrating sphere. In this case, the total white-light output of the tungsten lamp is incident on the sample at a near-normal angle of incidence. The viewing angle for the monochromator is approximately 30 milliradians; consequently the normal transmittance of scattering samples such as LI-1500 is much lower (e.g., by a factor of 200 to 300) than the total transmittance values obtained by Method 1. For the longer wavelength IR spectral region, a $1400^{\circ}F$ heated cavity is used as the energy source instead of the tungsten lamp, and the vacuum thermocouple detector located inside the monochromator is used instead of the detectors associated with the integrating sphere.

The tests are currently in progress and are expected to be completed by 19 November 1971. Figure 5.3.1-1 shows some of the room temperature data for a range of LI-1500 material thicknesses over a range of wavelengths from 0.35 to 2.5$\mu$. Additional data are being obtained to extend the range to 15.0$\mu$. The complete test matrix is shown in Table 5.3.1-1.

Table 5.3.1-1
INFRARED TRANSMISSION TEST CONDITIONS

| Specimen Type | Thermal Cycles | Test Temperature ($^{o}$F) | Measurement Range ($\mu$) |
|---|---|---|---|
| LI-1500 | 0 | Ambient | 1.0 to 15.0 |
| | 0 | 1000 | |
| | 0 | 2000 | |
| | 30 | Ambient | |
| | 30 | 1000 | |
| | 30 | 2000 | |
| | 60 | Ambient | |
| | 60 | 1000 | |
| LI-1500 | 60 | 2000 | |
| Coating | 0 | | |
| Coating | 30 | | |
| Coating | 60 | 2000 | 1.0 to 15.0 |

5.3.2 Hard Vacuum Test

A 30-day vacuum exposure test is presently in progress to evaluate any long-term vacuum-induced effects on the dimensional stability of LI-1500 material. For this test the specimens are suspended in a vacuum chamber operated at a pressure of $1 \times 10^{-6}$ torr and at room temperature (75 $\pm 5^{o}$F). The effect of this environment will be assessed by pre- and post-exposure dimensional and weight measurements. Duplicate specimens are being exposed for the before thermal cycling condition and after exposure to 10 and 20 thermal cycles; completion of this test is scheduled for 20 November 1971. Measurement comparison of the specimens prior to and after 18 days of vacuum exposure are shown in Table 5.3.2-1.

# TOTAL SPECTRAL TRANSMITTANCE DATA FOR THREE THICKNESSES OF LI-1500

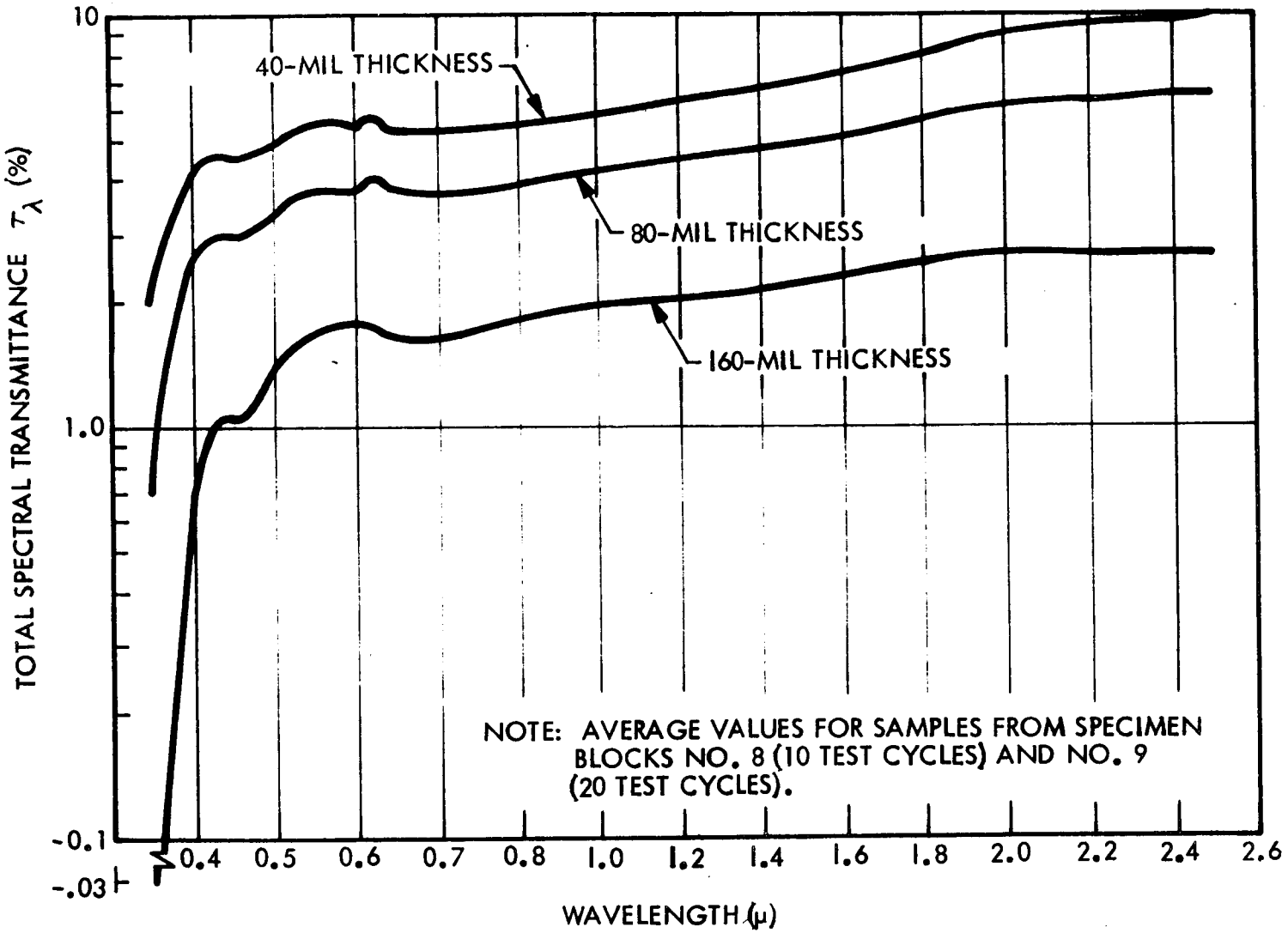


Fig. 5.3.1-1

DO6076

Table 5.3.2-1
VACUUM EXPOSURE TESTS

| No. of Specimens | Thermal Cycles | Percentage Weight Change after 18-day Vacuum Exposure | Percentage Dimensional Change after 18-day Vacuum Exposure |
|---|---|---|---|
| 2 | 0 | No Measurable Change | No Measurable Change |
| 4 | 30 | | |
| 4 | 60 | | |

### 5.3.3 Solar Radiation Tests

Long-term exposure of the RSI to solar radiation may result in surface coating degradation with corresponding changes in the coating solar absorptance. The degree of degradation may also be a function of previous effects caused by reentry heating exposures. The following tests will be performed to determine coating degradation as a function of ultraviolet exposure duration and number of reentry heating exposures.

Coating specimens will be subjected to a 10-sun intensity ultraviolet source for a total 2000 equivalent sun hours of exposure. Solar absorptance values will be obtained from spectral reflectance measurements as a function of exposure time to solar radiation. The spectral reflectance measurement range will be from 0.28 to 25.0$\mu$. Specimens that have been exposed to 0, 30, and 60 simulated reentry heat cycles will be tested. These tests will begin 22 November 1971.

### 5.3.4 Freeze Thaw Tests

Exposure of the Space Shuttle TPS to cyclic temperature conditions that would cause alternate freezing and thawing of the RSI may cause degradation of the basic material and/or coating. The material moisture content prior to freezing determines the level of internal force generated upon freezing of the moisture. High material moisture contents could occur if the TPS were exposed to conditions of high relative humidity or rainfall prior to application of a waterproof overspray. In addition to the moisture content, the rates of freezing and thawing have an effect on the stress patterns

generated within the RSI. The following tests will determine the RSI behavior when subjected to a range of environmental conditions simulating those that may be experienced by the Space Shuttle booster. The tests are scheduled to begin 17 November 1971.

A worst-case approach will be taken in exposing the test specimens to the various temperature conditions. Actual ambient temperature changes occur gradually instead of abruptly as in the tests. However, this represents a most severe test condition and it is felt that acceptable behavior for these conditions will assure integrity for any less severe conditions. In addition, a range of thaw temperatures was chosen to determine thaw temperature level effects that may be encountered for both prelaunch and ascent conditions.

The specimens are 1x4x4-inch LI-1500 tiles coated on one 4x4-inch surface with the 0042 coating. Four of the specimens will be oversprayed with a waterproof treatment before being exposed to the moisture environment conditions and four will not. Each of eight specimens will be subjected to a series of freeze/thaw cycles to determine the amount of LI-1500 material degradation occurring for these environmental conditions. Each specimen will first be subjected to a specific relative humidity environment and then frozen. Thawing at ambient or elevated temperature will then be accomplished. The specific test conditions are shown in Table 5.3.4-1.

Table 5.3.4-1

FREEZE/THAW TEST CONDITIONS

| Specimen | Moisture Environment | Freeze Temperature (°F) | Thaw Temperature (°F) | | |
|---|---|---|---|---|---|
| | | | Cycle 1 | Cycle 2 | Cycle 3 |
| A(2)* | 50% R.H. | 0 | Ambient | 500 | 1,000 |
| B(2)* | 75% R.H. | 0 | Ambient | 500 | 1,000 |
| C(2)* | 95% R.H. | 0 | Ambient | 500 | 1,000 |
| D(2)* | Rain | 0 | Ambient | 500 | 1,000 |

*One specimen with overspray and one without.

The following test procedure will be followed:

a. Exposure to indicated moisture environment for a minimum 2-hour period

b. Exposure to indicated freeze temperature for a minimum 8-hour period

c. Exposure to Cycle 1 thaw temperature for a minimum 8-hour period. (The specimen dimensions and weights were taken and visual inspection was performed prior to a., and after b. and c.)

d. Repetition of a., b., and c. except with Cycle 2 thaw temperature conditions

e. Repetition of a., b., and c. except with Cycle 3 thaw temperature conditions

5.3.5.1 Rain Erosion Tests. Rain conditions may be encountered by the Space Shuttle orbiter during cruise. The erosion resistance of the TPS must be determined to enable establishment of system constraints for these environmental conditions. Since the vehicle design, and therefore its flight characteristics, has not been finalized, it was assumed that the optimum cruise velocity is 350 miles per hour and that 200 miles per hour is the minimum velocity possible to maintain altitude. The velocities, angles of attack, rain intensity, and test durations are those suggested by A. J. Meyer.* The objective of the following test program was to test coated LI-1500 material to demonstrate its ability to survive anticipated rain environmental conditions during flight.

The tests were performed in the Edler Industries, Inc., High Speed Rain Erosion Test Facility located in Newport Beach, California. It is a rotary-arm type tester that subjects specimens mounted on the rotary blade to rainfall conditions of known intensity and mean volumetric drop size, while traveling at a constant velocity for a specified period of time. The following are facility specifications:

| | |
|---|---|
| Rotor Tip Velocity | 566 ±3 mph (RPM measured by Strobotac) |
| Rotor Blade Diameter | 54 inches |
| Rain Nozzle Configuration | Sierracin-designed spray head |
| Rainfall Rate | 0.7 to 1.4 in./hr |
| Droplet Size | 1.2 to 2.0 mm (mean volumetric) |

The water delivery system is unique in its high degree of accuracy of droplet size and rainfall rate. Standard methods of measurement are used, employing a sectioned water-gathering device across the specimen test area, to obtain rainfall rate and distribution in the test area, and to capture representative droplets in a two-level oil-filled tray that allows for the photographing of the actual droplets superimposed upon a millimeter grid screen. These droplets are counted by category, determined by size range, and the percentage of each category is used to calculate the mean volumetric drop size. Twelve samples of droplets are taken at specific stations of the specimen traversing area.

*Meyer, Andre J., "Definition of Erosion Environment for TPS Systems, Tasks A-1 and A-25," July 9, 1971.

Specimen velocity is determined by radial location on the rotary arm. All rainfall and drop size measurements are taken in the specimen test area in a static condition, i.e., without the arm being in motion. The effect of the blade motion upon these static conditions has not been specifically measured, but experimentation has indicated that blade turbulence has only slight influence on the rain conditions.

The specimen test assembly including the LI-1500 specimens, specimen holders, and rotor blade is shown in Fig. 5.3.5-1. The specimens are contained on all sides, except the test surface, with RTV 560 to seal the surfaces and provide a "soft" mounting to prevent high local loads on the specimen sides due to forces generated during the tests. The test conditions are shown in Table 5.3.5-1.

The initial test in the series was performed with Specimens 1 through 4 at 10 deg angle of attack. The test actually consisted of two 1-minute runs to assure mechanical integrity of the setup and to allow calibration of the specimen velocity by measurement of the rotor RPM with a stroboscope. This was necessary because changes in RPM due to drag created by the specimens had to be determined. It was found that at 200 mph the effect was negligible. The specimens sustained no degradation during this first test.

A 5-minute exposure to rain at an intensity of 1.3 in./hr was then performed (Test Number 2). Weight and thickness measurements before and after this test indicated no significant change. Visually the specimens showed no change.

The specimens were then moved to the 350 mph location and a dry run was made to obtain a stroboscope measurement of rotor RPM, which was found to be acceptable (Test Number 3). After completion of the run, it was observed that Specimen 3 had developed a surface crack and Specimen 2 had a surface crack and a chip with coating and material removal. Specimens 1 and 4 showed no change. The failures are attributed to the high mechanical loads at this test condition (~ 6000 g radial acceleration).

Table 5.3.5-1

RAIN EROSION TEST CONDITIONS

| Test No. | Specimen No. | Specimen Angle of Attack (deg) | Velocity (mph) | Rain Intensity (in./hr) | Test Duration (min) | Results |
|---|---|---|---|---|---|---|
| 1 | 1 | 10 | 200 | 0 | 2 | No change |
| | 2 | | | 0 | 2 | No change |
| | 3 | | | 0 | 2 | No change |
| | 4 | | | 0 | 2 | No change |
| 2 | 1 | | | 1.3 | 5 | No change |
| | 2 | | | 1.3 | 5 | No change |
| | 3 | | | 1.3 | 5 | No change |
| | 4 | | 200 | 1.3 | 5 | No change |
| 3 | 1 | | 350 | 0 | 2 | No change |
| | 2 | | | 0 | 2 | Coating cracked and chipped |
| | 3 | | | 0 | 2 | Coating cracked |
| | 4 | | | 0 | 2 | No change |
| 4 | 1 | | | 1.05 | 5 | No change |
| | 2 | | | 1.05 | 5 | No change |
| | 3 | | | 1.05 | 5 | Coating and material loss |
| | 4 | 10 | | 1.05 | 5 | No change |
| 5 | 5 | 20 | | 0 | 2 | No change |
| | 6* | 20 | | 0 | 2 | Lost specimen |
| | 7 | 20 | | 0 | 2 | No change |
| | 8 | 20 | 350 | 0 | 2 | No change |

*Specimen 6 had cracked coating prior to testing.

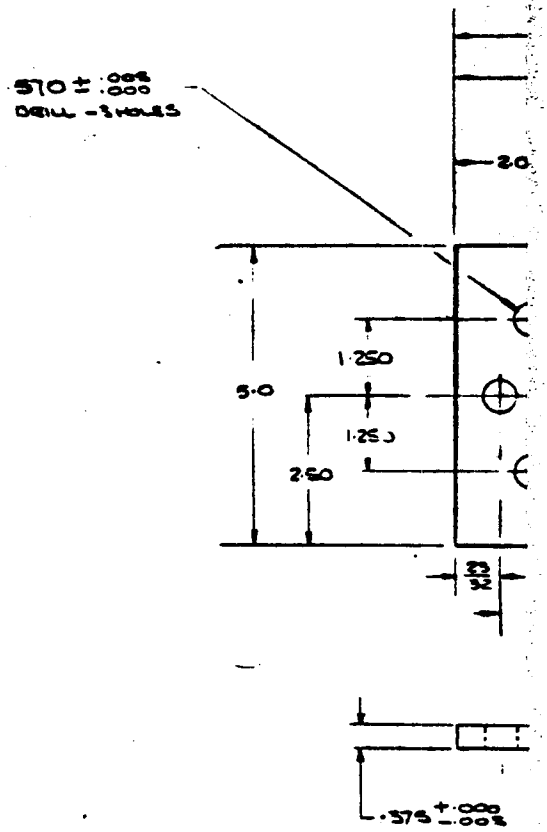
.570 ± .005 .000
DRILL -3 HOLES
2.0
1.250
5.0
1.250
2.50
23/32
.375 +.000 -.005

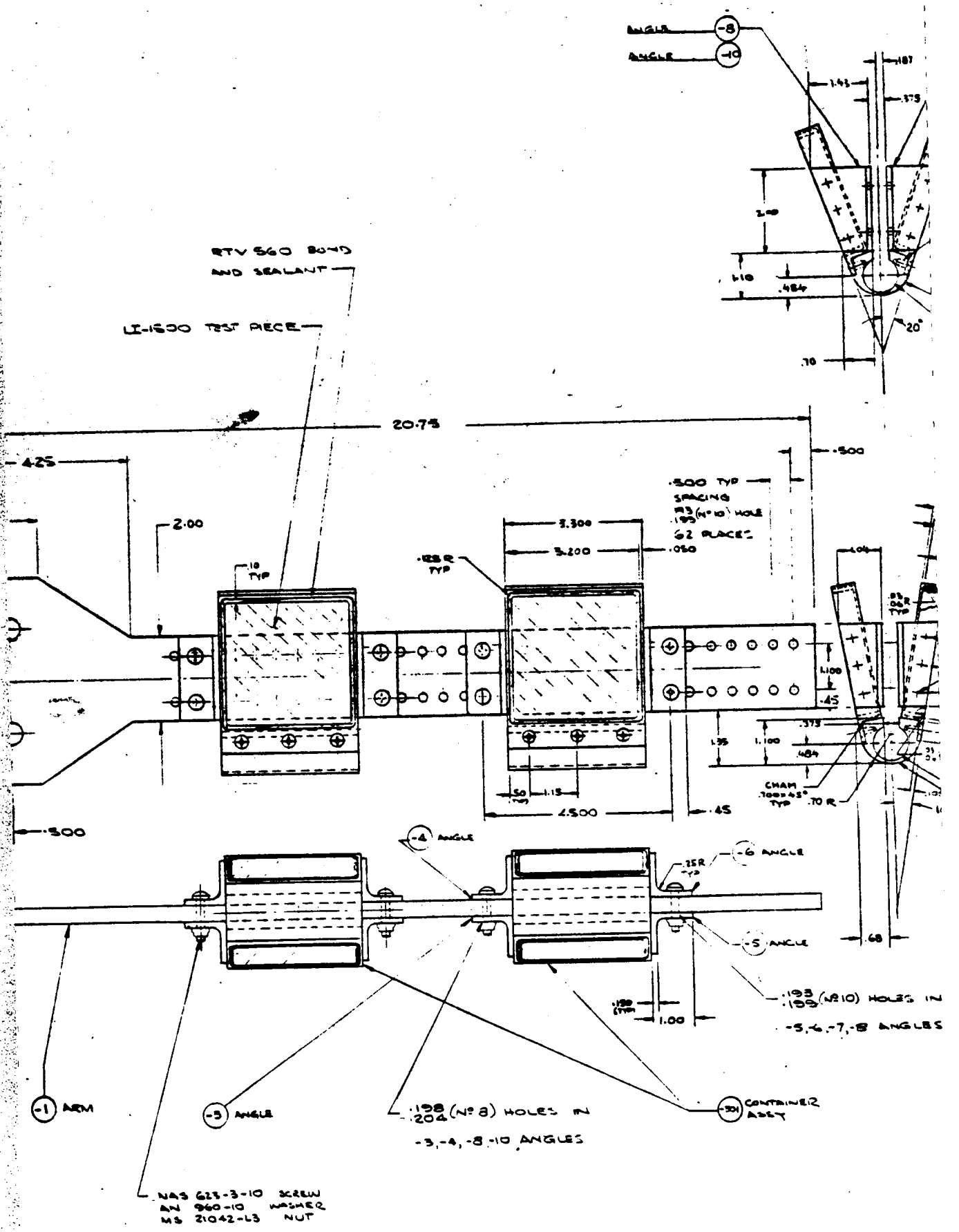
ANGLE -8
ANGLE -10
RTV 560 BOND AND SEALANT
LI-1500 TEST PIECE
20.75
.425
2.00
.500
.500 TYP SPACING
#3 (No 10) HOLE .193 .199
62 PLACES
3.300
3.200
.050
.125 R TYP
.10 TYP
1.100
.45
.375
.484
1.35
.50 TYP
1.15
2.500
CHAM .100 x 45° TYP
.70 R
-4 ANGLE
-6 ANGLE
.25 R TYP
-5 ANGLE
.68
.150 TYP
1.00
.193 .199 (No 10) HOLES IN -5,-6,-7,-8 ANGLES
-1 ARM
-3 ANGLE
.198 .204 (No 8) HOLES IN -3,-4,-8,-10 ANGLES
-301 CONTAINER ASSY
NAS 623-3-10 SCREW
AN 960-10 WASHER
MS 21042-L3 NUT

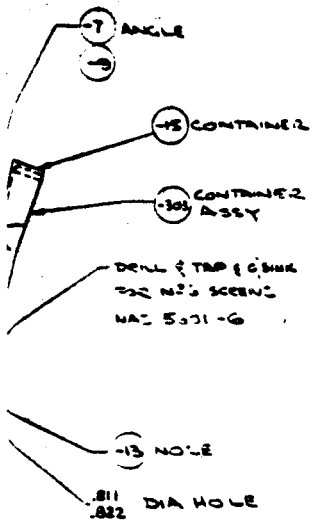


FIG. 5.3.5-1

PAGE 5-13/14

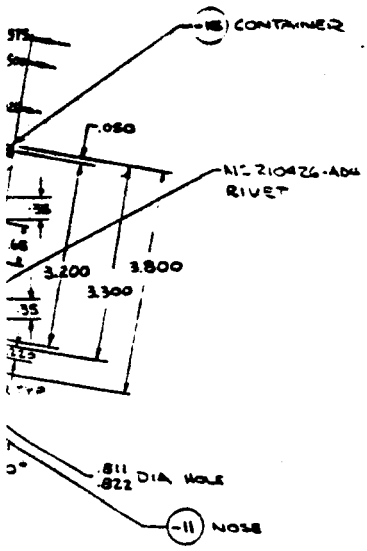


| | | | | | | | | | |
|---|---|---|---|---|---|---|---|---|---|
| 12 | 12 | | | MS20426-AD4 | RIVET | | | | |
| | | 8 | | MS21042-L3 | NUT | | | | |
| | | 8 | | AN 960-10 | WASHER | | | | |
| 8 | 8 | | | NAS 5001-6 | SCREW | | | | |
| | | 8 | | NAS 623-3-10 | SCREW | | | | |
| 1 | 1 | | | | TEST PIECE | LI-1500 | | | |
| 1 | | | | -7 | ANGLE | ALUM EXTRUSION | 2014-T6 | | |
| | | | | -15 | CONTAINER | ALUM PLATE | 2024-T4 | | |
| | | | | -13 | NOSE | ALUM BAR | " | " | |
| | | | | -11 | NOSE | ALUM BAR | " | " | |
| 1 | | | | -10 | ANGLE | ALUM EXTRUSION | 2014-T6 | | |
| 1 | | | | -9 | ANGLE | " | " | | |
| 1 | | | | -8 | ANGLE | | | | |
| | 1 | | | -6 | ANGLE | | | | |
| | 1 | | | -5 | ANGLE | | | | |
| | 1 | | | -4 | ANGLE | | | | |
| | 1 | | | -3 | ANGLE | ALUM EXTRUSION | 2014-T6 | | |
| | | | | -1 | ARM | [illegible] STEEL | [illegible] | | |
| | | QTY REQD | CODE IDENT | PART OR IDENTIFYING NO. | NOMENCLATURE OR DESCRIPTION | MATERIAL DESCRIPTION OR NOTE | MATERIAL SPECIFICATION | ZONE | ITEM NO. |

-301 -301 PARTS LIST

| | | | |
|---|---|---|---|
| INTERPRET DWG PER | UNLESS OTHERWISE SPECIFIED DIMS ARE IN INCHES. TOLERANCES ON FRACTIONS = ± 1/16 DECIMALS: .X = ± .1 .XX = ± .03 .XXX = ± .010 ANGLES = ± 2 DEG | DATE 10-6-71 | LOCKHEED MISSILES & SPACE COMPANY A GROUP DIVISION OF LOCKHEED AIRCRAFT CORPORATION SUNNYVALE, CALIFORNIA |
| | | OR A.M. [illegible] | |
| | | APPD | BLADE ASSY RAIN EROSION TEST RIG (LI-500) |
| | | APPD | |
| | | ENGRG | |
| | | CHK | |
| | | APPD | SIZE / CODE IDENT / DRAWING NO. SKW205015 / REV |
| NEXT ASSY / USED ON | CONTR | | |
| APPLICATION | CCA/CB | APPD | SCALE / SHEET |

A 5-minute test with a rain intensity of 1.05 in./hr was then performed on these specimens. The coating and material on the downstream side of the crack in Specimen 3 was lost. No changes were observed in Specimens 1, 2, and 4. It is apparent from the above tests that degradation due to rain erosion at these conditions is insignificant. However, the severe mechanical loads can cause extensive degradation.

The last test in the series was a dry run performed with Specimens 5, 6, 7, and 8 mounted at 20 deg angle of attack. The specimens were located at the estimated 350 mph position on the rotor. Specimen 6 was lost during the test. This resulted in a rotor imbalance which caused excessive heating of the shaft bearing. As a result, the testing was terminated. Specimen 6 was cracked prior to this test. It was installed in the specimen holder in a cracked condition to determine the effect of rain erosion on a cracked coating. However, it is apparent that degraded specimens have difficulty surviving the mechanical loads imposed by the test facility. Therefore, this type of information will have to be obtained under less severe load conditions.

5.3.5.2 Dust Erosion Tests. Dust erosion tests can be performed in the facility described above for rain erosion testing. A review of the necessary facility modifications and model design is in progress.

### 5.3.6 Moisture Absorption Tests

The Space Shuttle TPS may be subjected to a range of relative humidity and rain conditions either prior to or at the end of a mission. It is necessary to determine the extent to which exposure of the TPS to these conditions may influence the thermal performance and mechanical integrity of the system. Moisture present in the material during ascent or entry may increase the thermal conductivity of the material or cause internal stresses resulting in physical degradation. Since the effectiveness of the overspray in limiting the material moisture content is of primary concern, it is necessary to determine the material behavior after exposure to moisture environments prior to and after application of an overspray. The following tests will be performed to determine the RSI behavior during ascent and entry after exposure to simulated launch pad moisture environment conditions. These tests are scheduled to begin 17 November 1971.

Seven specimens, each 4x4x2.45 inches, were bonded to a 0.125-inch thick aluminum plate with RTV 560. One of the specimens contains a typical joint, while the others are tiles. The outer 4x4-inch surface was coated with the 0042 coating system. Each specimen will be subjected to a specific moisture environment followed by a simulated ascent/entry combined heating and pressure environmental cycle. Some specimens will be oversprayed before moisture environment exposure and some after. Each specimen was instrumented with two chromel alumel thermocouples; one was bonded to the LI-1500 backface and the other to the aluminum baseplate backface. The specimen conditions prior to exposure to ascent/entry environmental conditions are shown in Table 5.3.6-1.

Table 5.3.6-1

SPECIMEN PRETEST CONDITIONS

| Specimen | Configuration | Moisture Environment | Previous Thermal Cycles | Overspray |
|---|---|---|---|---|
| A-1 | Tile | 50% R.H. | 0 | Before M. E.* |
| A-2 | Tile | 50% R.H. | 0 | After M. E. |
| B | Tile | 75% R.H. | 0 | After M. E. |
| C | Tile | 95% R.H. | 0 | After M. E. |
| D-1 | Tile | Rain | 5 | Before M. E. |
| D-2 | Tile | Rain | 5 | After M. E. |
| E | Joint | Rain | 0 | Before M. E. |

*Moisture Environment.

The following test procedure will be followed:

a. Exposure to specified moisture environment for a minimum 2-hour period

b. Exposure to ascent/entry combined heating and pressure environmental cycle

c. Repeat a., and b. two times.

Specimens A-1, D-1, and E will be oversprayed prior to a. Specimens A-2, B, C and D-2 will be oversprayed after b. Dimensions and weights will be recorded prior to a., and after a. and b. Visual inspection will be performed prior to a., and after b.

### 5.3.7 Cold Soak Tests

Regions of the TPS may reach temperatures of -150°F while the Space Shuttle is in orbit. It must be determined whether RSI degradation will occur when the TPS experiences an entry temperature history following an initial -150°F temperature condition. The thermally induced stresses from severe temperature gradients within the LI-1500 will be greatest for these conditions. The following tests are to be performed to determine degradation effects due to repeated temperature cycling between minimum orbit temperature and entry temperatures. The tests are scheduled to begin 15 November 1971.

Two specimens, each 4 x 4 x 2.45 inches, were bonded to aluminum baseplates with RTV 560. The outer 4 x 4-inch surface of each specimen is coated with the 0042 coating system.

Two specimens will be subjected to a series of cold soak tests followed by a simulated reentry heat rate history. Each specimen was instrumented with two thermocouples. One was bonded to the LI-1500 backface and the other to the aluminum baseplate backface. The specimens will be shrouded and enclosed in an evacuated plastic bag during the cold soak tests to prevent water condensation on the specimens. The bag will be retained during handling and installation of the specimens in the radiant heat facility and then removed prior to exposing the specimens to the heating environment. The following test procedure will be followed:

a. Vacuum bagging of specimens ($10^{-3}$ torr)

b. Exposure of vacuum bagged specimens to low-temperature environment until they reach -150°F

c. Exposure of unbagged specimens to simulated entry heating environment (All thermocouple data are recorded during this test.)

d. Repeat of a., b., and c. two times

The specimen dimensions and weights will be taken and visual inspection will be performed prior to a. and after c.

# Section 6
# PROTOTYPE PANELS AND MATERIAL SPECIMENS

## 6.1 PROTOTYPE PANELS

LMSC has designed four prototype panels in accordance with contract requirements to point design conditions specified by NASA/MSC. The design effort was accomplished under Task 2.0 as negotiated and reviewed in this report in Section 2. The panels consist of a metallic structure with coated LI-1500 bonded to one side with the RTV-560 adhesive system. The original panel critical design review was scheduled for 4 October but was extended to 12 November. During the interim, LMSC has conducted sufficient testing on advanced coating systems to change the LI-1500 baseline coating from 0025 to 0042. Accordingly, the prototype panels utilize the 0042 coating system. The testing and resulting coating system are discussed in detail in Section 3.1.

Details of the prototype panels are shown in Figs. 6.1-1 through 6.1-4. The materials/applications/design areas for each panel are reviewed in Table 6.1-1. For vehicle application, the beryllium subpanel bolts directly to external vehicle frames. The primary structural panels will attach to frame, but will be continuous over many spans. Figure 6.1-5 shows how these units are used on the shuttle. The section to be tested is removed from a large panel, and end fixtures are provided for testing.

As pointed out in previous contract documentation, the beryllium material is a pacing delivery item. With NASA/MSC approval, this material was ordered early in the contract and has been delivered to LMSC.

A preliminary panel test plan was provided to NASA/MSC in the 4 October Monthly Status Report. This test plan has been finalized and is included in this report as Appendix F.

Table 6.1-1

PROTOTYPE PANEL CHARACTERISTICS

| Panel No. | Shown in Fig. No. | Substrate Material | Application | Vehicle Area |
|---|---|---|---|---|
| 1 | 6.1-1 | Beryllium | Subpanel | 2 |
| 2 | 6.1-2 | Aluminum | Primary | 2 |
| 3 | 6.1-3 | Aluminum | Primary | 1 |
| 4 | 6.1-4 | Titanium | Primary | 2 |

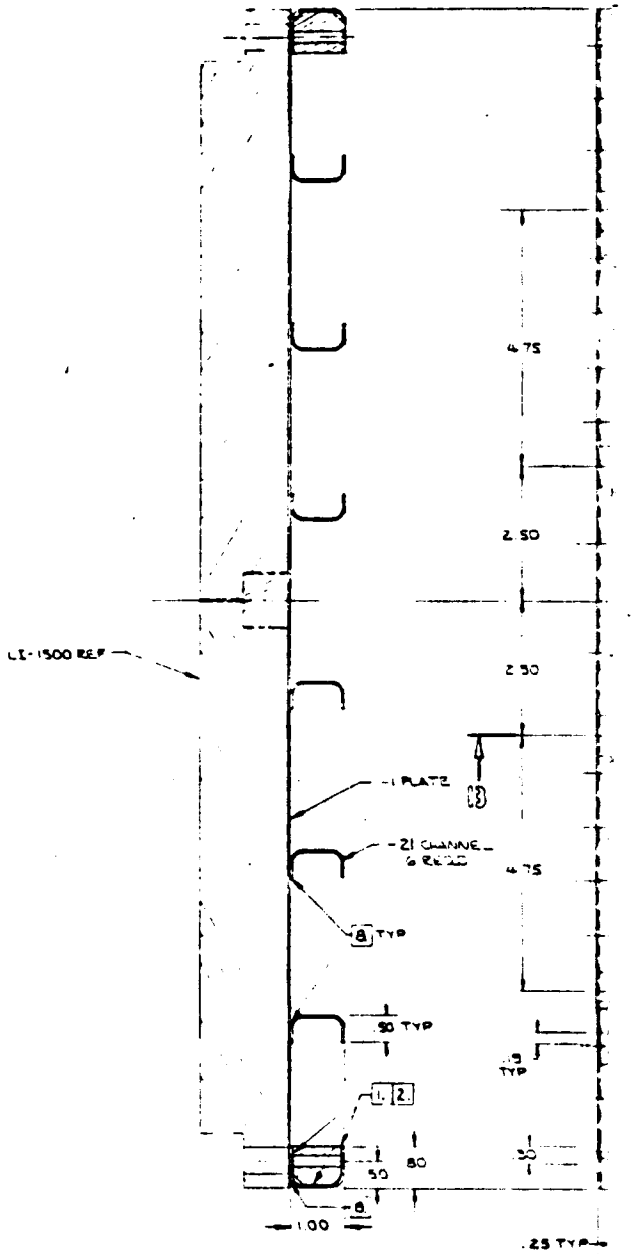


SECTION A-A

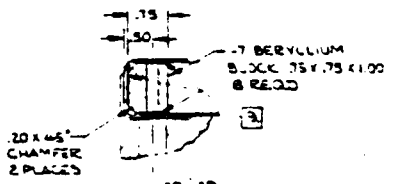


SECTION B-B
8 PLACES

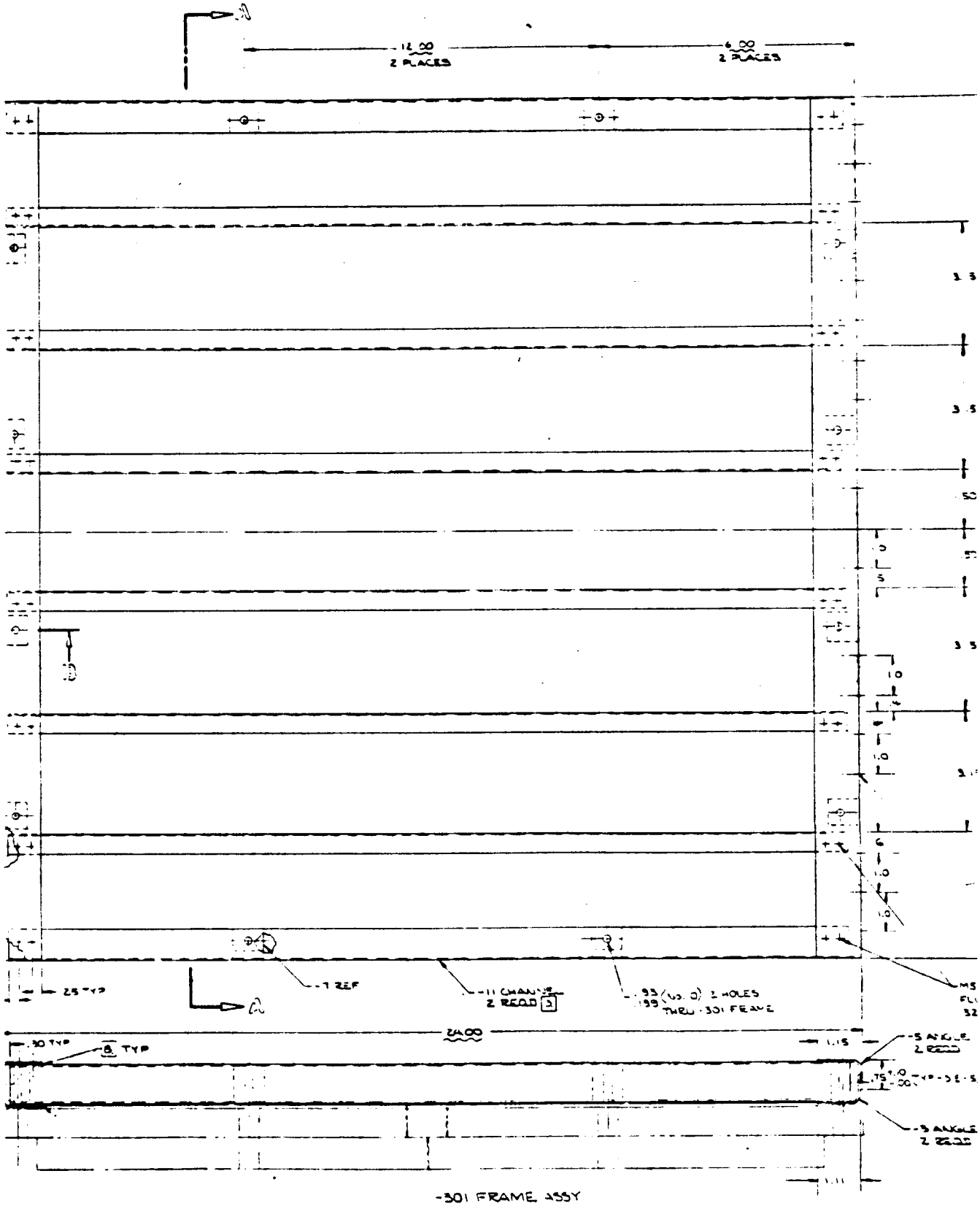


-301 FRAME ASSY

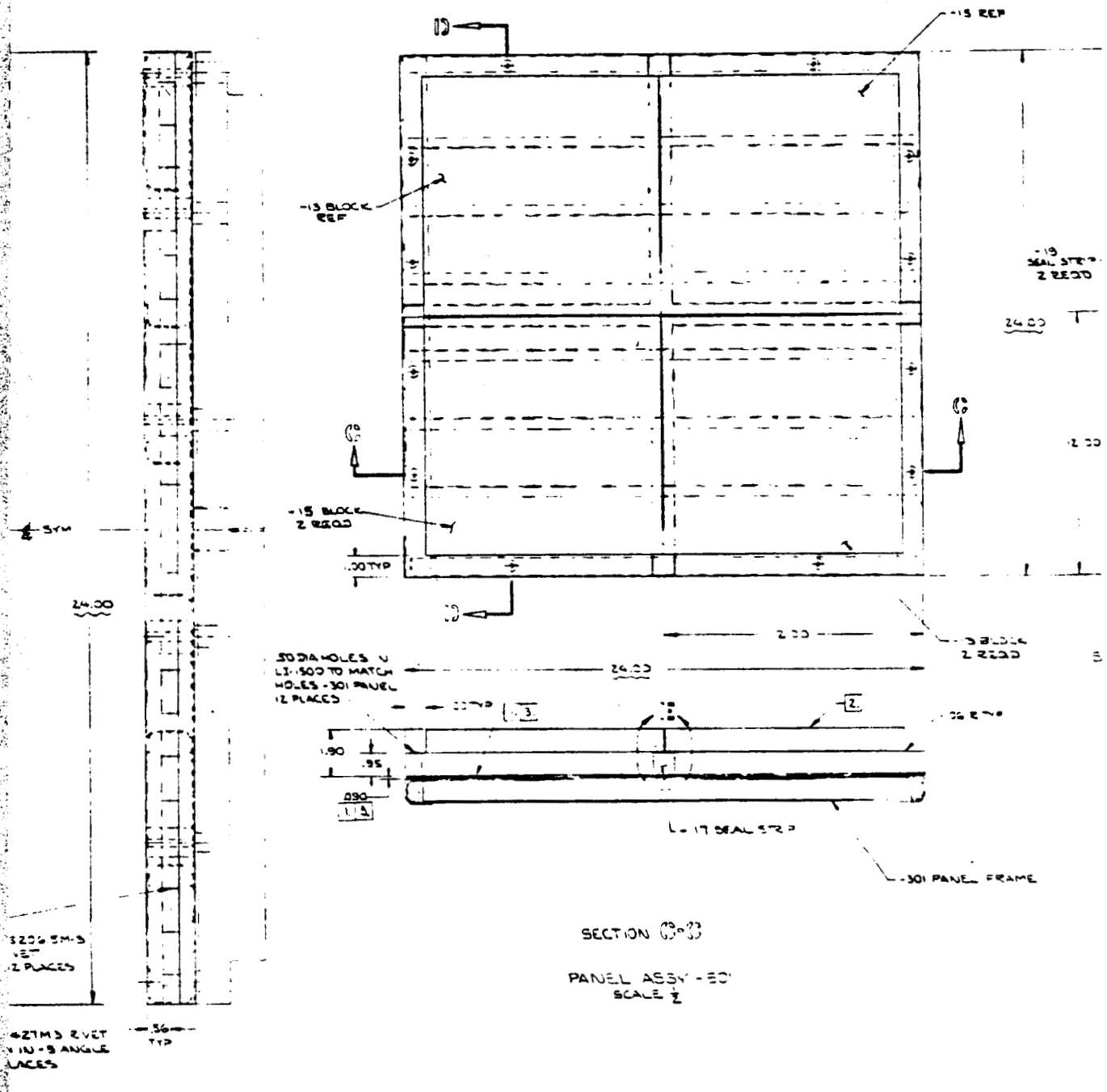


9. BO
8. FU
7. AL
6. CU
5. PR
4. FA
3. HO
2. SU
1. BO PE
NOTE

| LTR | CHANGE | DATE APPD |
|---|---|---|
| A | LI-1500 THICKNESS WAS 2 X TILE SIZE WAS 6"x6", REVISED NOTE 2, ADDED DETAIL "E". | |

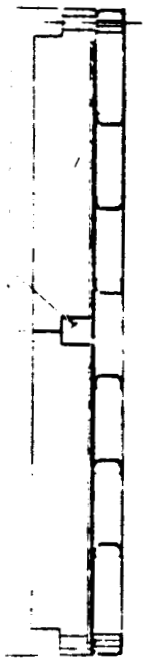

SECTION D-D

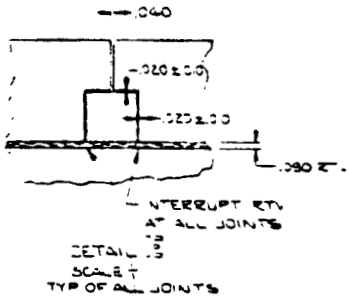


FIG. 6.1-1
PAGE 6-3/4

| QTY REQD | QTY REQD | CODE IDENT | PART OR IDENTIFYING NO | NOMENCLATURE OR DESCRIPTION | MATERIAL DESCRIPTION OR NOTE | MATERIAL SPECIFICATION | ZONE | ITEM NO |
|---|---|---|---|---|---|---|---|---|
| 6 | | | -21 | CHANNEL | 2024 SHEET BERYLLIUM | | | |
| | 2 | | -19 | SEAL STRIP | LI-500 | | | |
| | 1 | | -17 | SEAL STRIP | LI-500 | | | |
| 42 | | | | MS 20427M3 | 2 FLUTE SOLID FLUSH HEAD | MONEL | | |
| | | | -15 | BLOCK | LI-500 | | | |
| | 2 | | -13 | BLOCK | LI-500 | | | |
| 2 | | | -11 | CHANNEL | 2024 SHEET BERYLLIUM | | | |
| 6 | | | -9 | SPACER | 15-7 SS SHEET BERYLLIUM | | | |
| 8 | | | -7 | SPACER | 15-7 SS SHEET BERYLLIUM | | | |
| 2 | | | -5 | ANGLE | 2024 SHEET BERYLLIUM | | | |
| 2 | | | -3 | ANGLE | 2024 SHEET BERYLLIUM | | | |
| 1 | | | -1 | PLATE | 2024 SHEET BERYLLIUM | | | |
| | 1 | | -301 | FRONT ASSY | | | | |

PARTS LIST

ND WITH RTV-560 PER SPEC LAC 30-4455.
ZINCE BRAZE WITH .003 BRAZE ALLOY BAg-18.
L BEAD RADII 5t MIN
CAN PER SPEC LAC 0170.
STECT PER SPEC LAC 1001.
SRICATE PER LAC PB-92.
D GAP BETWEEN PANELS & -301 FRAME TO .030.
RFACE COATING .010 THICK ON LI-1500 PER 0042 COATING SYSTEM.
ND LI-1500 TO -301 FRAME USING RTV 560
R SPEC LAC 30-4455.
S:

| | | | | |
|---|---|---|---|---|
| INTERPRET DWG PER | UNLESS OTHERWISE SPECIFIED DIMS ARE IN INCHES TOLERANCES ON FRACTIONS = ± 1/16 DECIMALS .X = ± .1 .XX = ± .03 .XXX = ± .010 ANGLES = ± 2 DEG | DATE | LOCKHEED MISSILES & SPACE COMPANY A GROUP DIVISION OF LOCKHEED AIRCRAFT CORPORATION SUNNYVALE, CALIFORNIA | |
| | | DR | THERMAL TEST PANEL No. 1 | |
| | | APPD | | |
| | | APPD | | |
| | | ENGRG | | |
| | | CHK | | |
| NEXT ASSY | USED ON | APPD | SIZE | CODE IDENT | DRAWING NO SKJ205008 | REV |
| APPLICATION | | CONTR | SCALE | SHEET |
| | | CCA/CB | | |

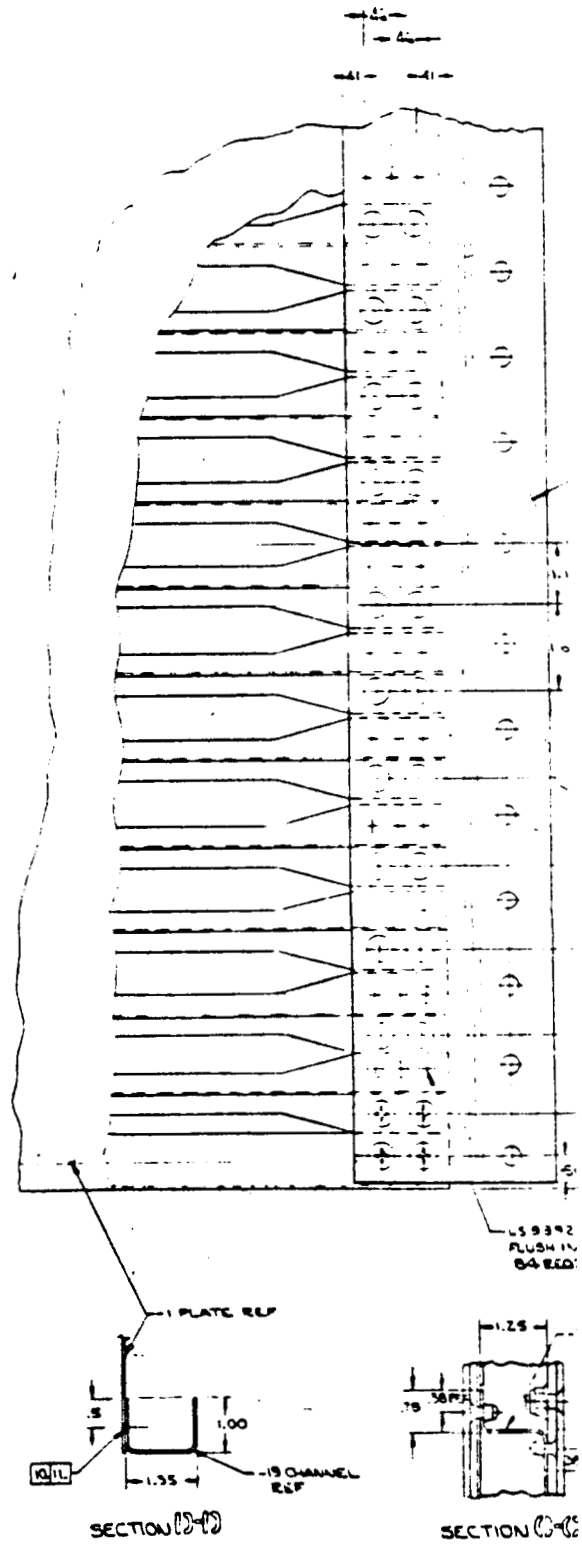
1 PLATE REF
1.00
1.35
19 CHANNEL REF
SECTION
1.25

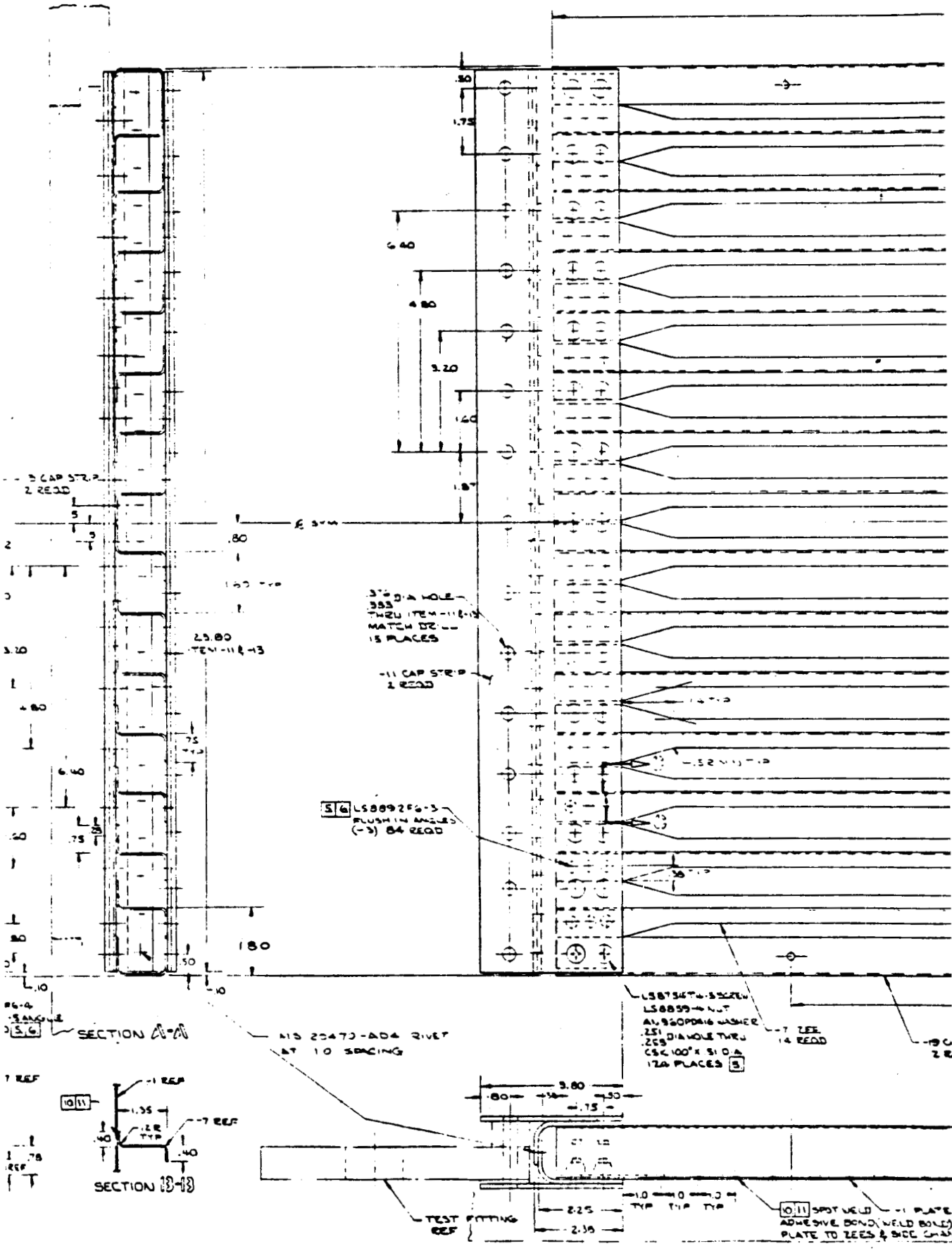

SECTION A-A
SECTION B-B
-3 CAP STRIP 2 REQD
-11 CAP STRIP 2 REQD
LS8892F6-3 FLUSH IN ANGLES (-3) 84 REQD
AN 25470-AD4 RIVET AT 1.0 SPACING
TEST FITTING REF
SPOT WELD
ADHESIVE BOND (WELD BOND)
PLATE TO ZEES & SIDE CHAN

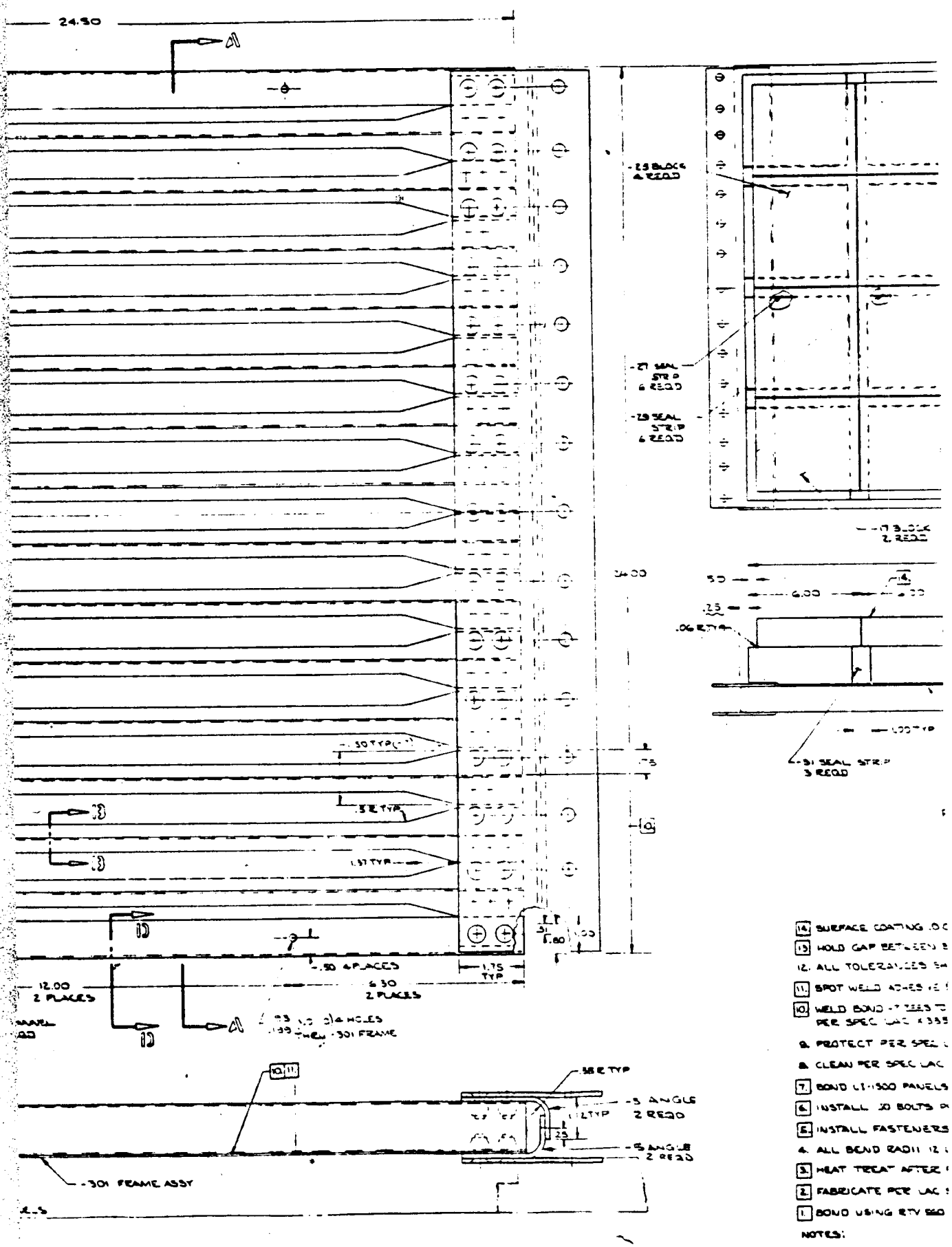
24.50
-25 BLOCK 4 REQD
-27 SEAL STRIP 6 REQD
-29 SEAL STRIP 6 REQD
-17 BLOCK 2 REQD
-31 SEAL STRIP 3 REQD
.50 TYP
.58 TYP
1.37 TYP
.50 4 PLACES
1.75 TYP
12.00 2 PLACES
6.30 2 PLACES
-301 FRAME
.58 TYP
-5 ANGLE 2 REQD
-5 ANGLE 2 REQD
-301 FRAME ASSY
14. SURFACE COATING
13. HOLD GAP BETWEEN
12. ALL TOLERANCES
11. SPOT WELD
10. WELD BOND
PER SPEC
9. PROTECT PER SPEC
8. CLEAN PER SPEC
7. BOND
6. INSTALL
5. INSTALL FASTENERS
4. ALL BEND RADII
3. HEAT TREAT AFTER
2. FABRICATE PER
1. BOND USING RTV
NOTES:

| LTR | CHANGE | DATE | APPD |
|---|---|---|---|
| A | TILE SIZE WAS [illegible] ADDED NOTE [illegible] ADDED DETAIL 2. | | |

FIG. 6.1-2
PAGE 6-5/6

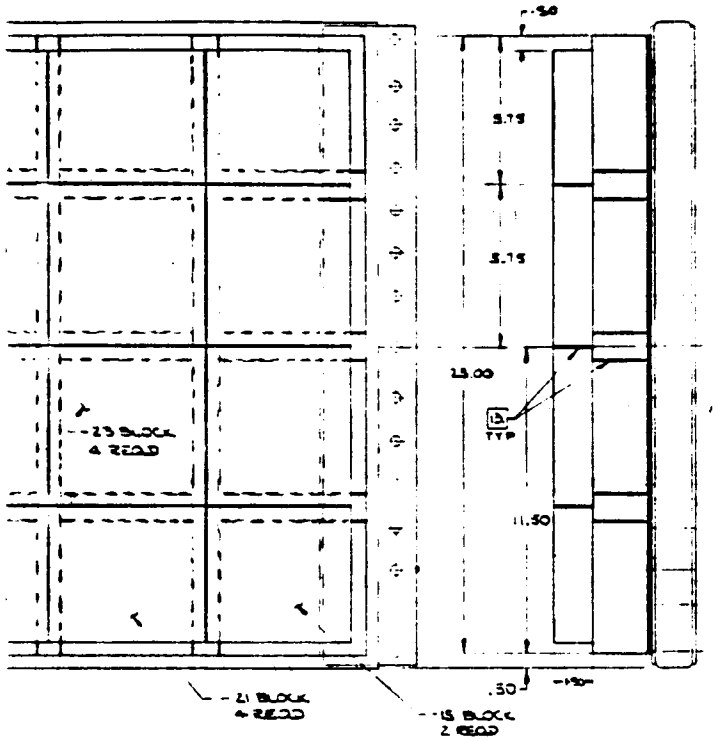


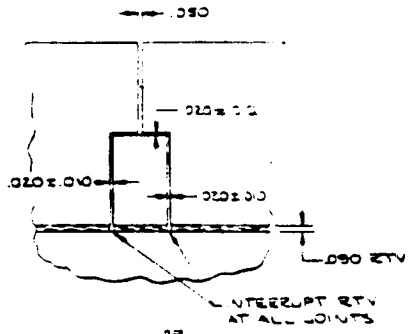


DETAIL 13
TYP OF ALL JOINTS
SCALE 1/1

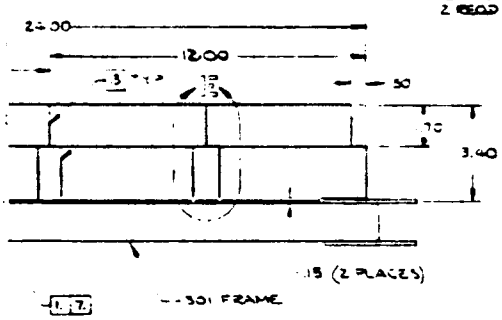


PANEL ASSY -301
SCALE 1/2

| QTY REQD | QTY REQD | CODE IDENT | PART OR IDENTIFYING NO | NOMENCLATURE OR DESCRIPTION | MATERIAL DESCRIPTION OR NOTE | MATERIAL SPECIFICATION | ZONE | ITEM NO |
|---|---|---|---|---|---|---|---|---|
| | 3 | | -21 | SEAL STRIP | LI-1500 | | | |
| | 6 | | -23 | SEAL STRIP | | | | |
| | 6 | | -27 | SEAL STRIP | | | | |
| | 4 | | -25 | BLOCK | | | | |
| | 4 | | -23 | BLOCK | | | | |
| | 4 | | -21 | BLOCK | LI-1500 | | | |
| 124 | | | LS8734-T4-5 | SCREW | | | | |
| 124 | | | LS8853-4 | NUT | | | | |
| 124 | | | AN960PD4-6 | WASHER | | | | |
| 2 | | | -19 | CHANNEL | .050 SHT AL 7075-0 | 3 | | |
| AR | | | M3204T0AD4 | RIVET | | | | |
| 84 | | | LS8892F6-5 | JO-BOLT | | | | |
| 84 | | | LS8892F6-4 | JO-BOLT | | | | |
| | 2 | | -17 | BLOCK | LI-1500 | | | |
| | 2 | | -15 | BLOCK | LI-1500 | | | |
| 2 | | | -13 | CAP STRIP | .125 SHT AL 7075-T6 | | | |
| 2 | | | -11 | CAP STRIP | .125 SHT AL 7075-T6 | | | |
| 28 | | | -9 | CLIP | .050 SHT AL 7075-0 | 3 | | |
| 14 | | | -7 | ZEE | .050 SHT AL 7075-0 | 3 | | |
| 2 | | | -5 | ANGLE | .125 SHT AL 7075-0 | 3 | | |
| 2 | | | -3 | ANGLE | .125 SHT AL 7075-0 | 3 | | |
| 1 | | | -1 | PLATE | .050 SHT AL 7075-T6 | | | |
| | 1 | | -301 | FRAME ASSY | | | | |
| -301 | -301 | | | | | | | |

PARTS LIST

) THICK ON LI-1500 PER 0042 COATING SYSTEM.
LOCKS & SEAL STRIPS TO.
ALL BE NON ACCUMULATIVE.
BONDING (WELD BOND) ON 1.0 CENTERS.
PLATE. WELD BOND -1 PLATE TO -13 CHANNELS
AC 1001.
0170.
TO -301 FRAME PER SPEC LAC 50-4436.
ER DESIGN STD DS 40007.
PER SPEC LAC 0581.
UNLESS OTHERWISE SPECIFIED.
FORMING TO TEMPER T6 PER SPEC LAC 521.
SPEC 1241.
HOLD GAP BETWEEN LI 1500 & -301 FRAME TO .050

INTERPRET DWG PER

NEXT ASSY | USED ON
APPLICATION

UNLESS OTHERWISE SPECIFIED DIM ARE IN INCHES TOLERANCES ON FRACTIONS = ± 1/16 DECIMALS .X = ± .1 .XX = ± .03 .XXX = ± .010 ANGLES = ± 2 DEG

CONTR
CCA/CEI

DATE
DR
APPD
APPD
ENGRG
CHK
APPD
APPD

LOCKHEED MISSILES & SPACE COMPANY
SUNNYVALE, CALIFORNIA

SIZE | CODE IDENT | DRAWING NO | REV
SCALE | SHEET

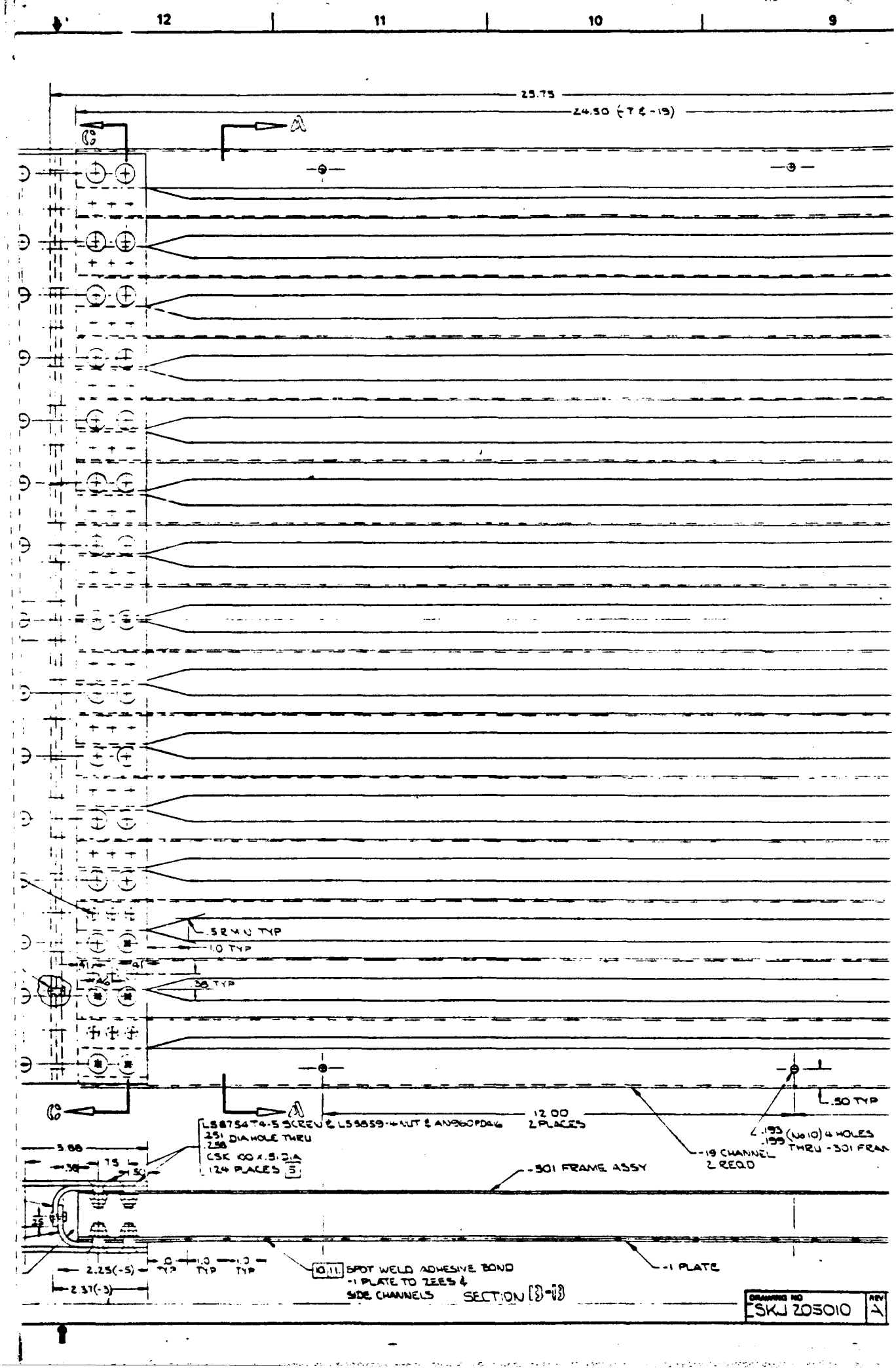

12
11
10
9
25.75
24.50 (-7 & -19)
.5 R MIN TYP
1.0 TYP
.38 TYP
.50 TYP
12.00
2 PLACES
LS8754T4-5 SCREW & LS5859-4 NUT & AN960PD4-6
.251 .258 DIA HOLE THRU
CSK 100 x .5 DIA
124 PLACES 5
3.88
.38
.75
.50
.25
-19 CHANNEL
2 REQD
.193 .199 (No 10) 4 HOLES THRU -301 FRAM
-301 FRAME ASSY
2.25(-5)
2.37(-3)
.0 TYP
1.0 TYP
1.0 TYP
10.11 SPOT WELD ADHESIVE BOND
-1 PLATE TO ZEES &
SIDE CHANNELS
-1 PLATE
SECTION B-B
DRAWING NO
SKJ 205010
REV
A

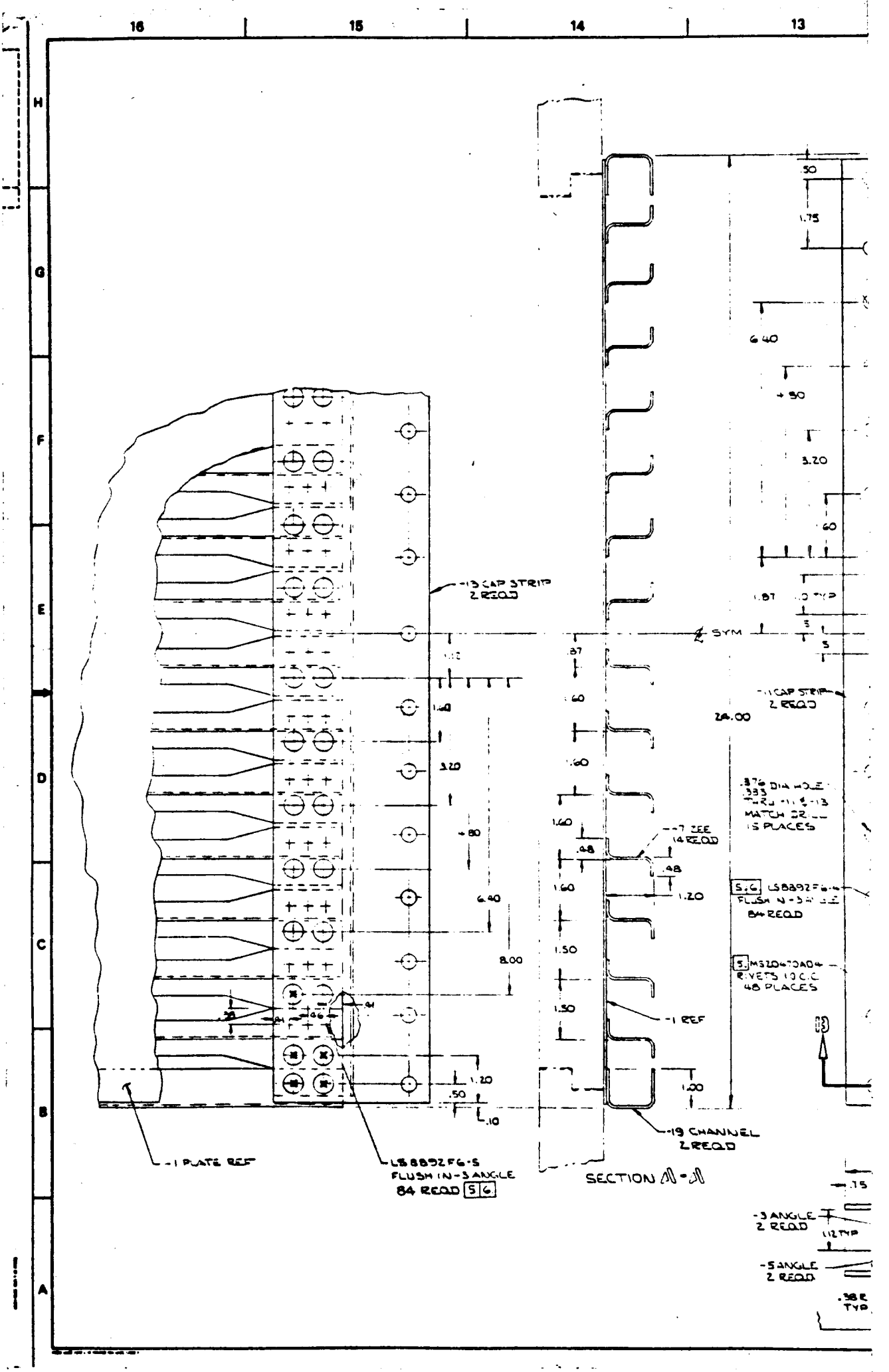
16
15
14
13
H
G
F
E
D
C
B
A
-13 CAP STRIP
2 REQD
SYM
-11 CAP STRIP
2 REQD
24.00
.876 DIA HOLE
.383
THRU -11 & -13
MATCH DRILL
15 PLACES
-7 ZEE
14 REQD
5,6 LS8892F6-5
FLUSH IN-3 ANGLE
84 REQD
5 MS20470AD4
RIVETS 10 C.C.
48 PLACES
-1 REF
-19 CHANNEL
2 REQD
-1 PLATE REF
LS8892F6-5
FLUSH IN-3 ANGLE
84 REQD 5 6
SECTION A-A
-3 ANGLE
2 REQD
-5 ANGLE
2 REQD
.38 R
TYP

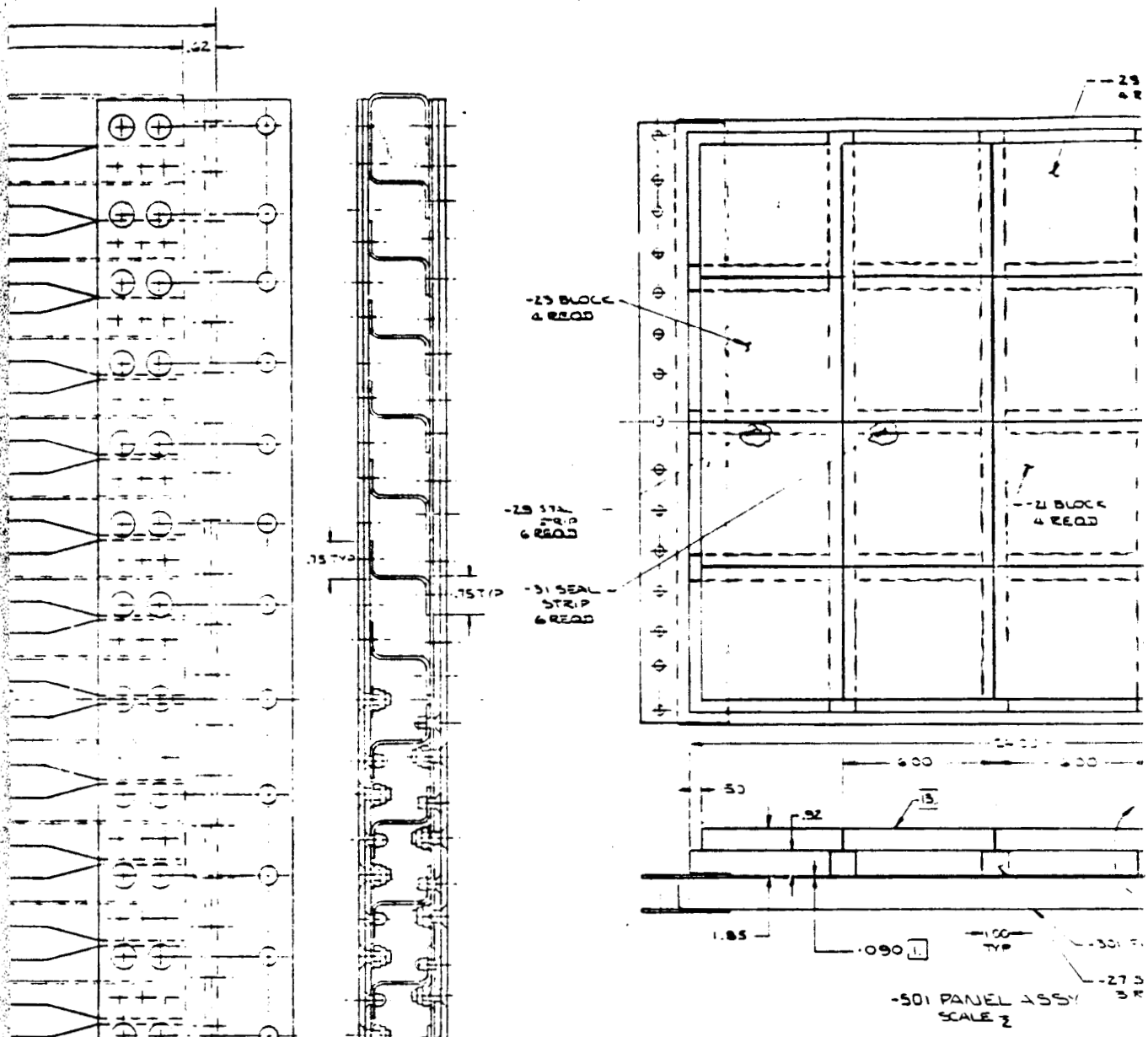


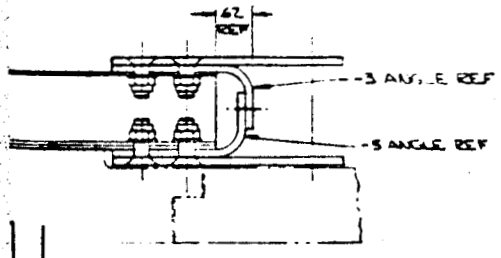


13 SURFACE COATING .010 THICK ON LI-1500 PER 0042 COATING

12. ALL TOLERANCES SHALL BE NON ACCUMULATIVE.

11 SPOT WELD ADHESIVE BONDING (WELD BOND) ON 1.0 CENTERS.

10 WELD BOND -7 ZEES TO -1 PLATE. WELD BOND -1 PLATE TO -19 CHANNELS PER SPEC LAC A 3857.

9 PROTECT PER SPEC LAC 1001.

8. CLEAN PER SPEC LAC 0170.

7 BOND LI-1500 PANELS TO -301 FRAME PER SPEC LAC 30-443

6 INSTALL JO-BOLTS PER DESIGN STD DS 40007.

5 INSTALL FASTENERS PER SPEC LAC 0581.

4. ALL BOND RADII .16 UNLESS OTHERWISE NOTED

3 HEAT TREAT AFTER FORMING TO TEMPER T6 PER SPEC LAC 5

2 FABRICATE PER SPEC LAC 1241.

1 BOND USING RTV 560. HOLD GAP TO BETWEEN PARTS TO .090

NOTES.

| ZONE | LTR | REVISIONS DESCRIPTION | DATE | APVD |
|---|---|---|---|---|
| | A | [illegible] ADDED NOTE [illegible] ADDED DETAIL [illegible] | | |

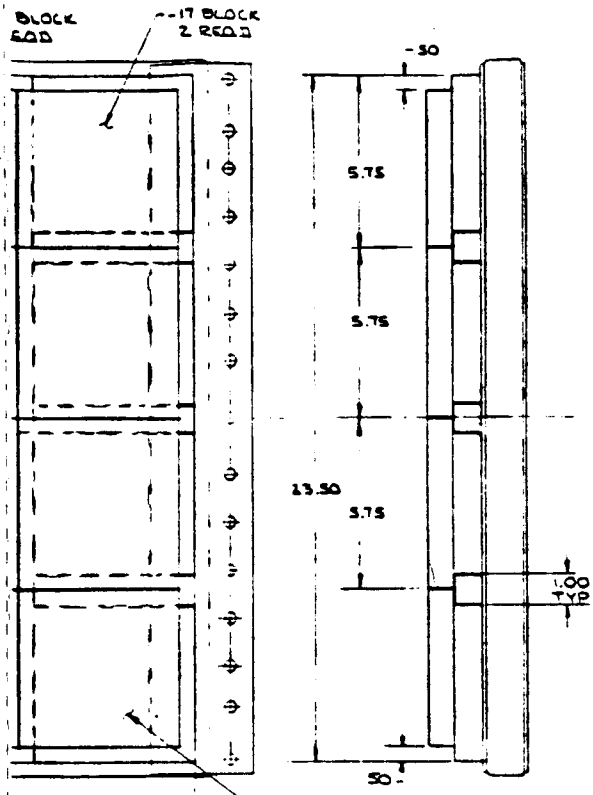


FIG. 6.1-3
PAGE 6-7/8

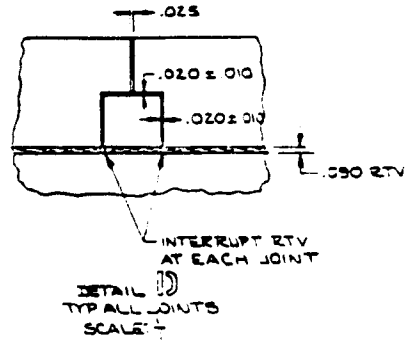


| QTY REQD | QTY REQD | CODE IDENT | PART OR IDENTIFYING NO | NOMENCLATURE OR DESCRIPTION | MATERIAL DESCRIPTION OR NOTE | MATERIAL SPECIFICATION | ZONE | ITEM NO |
|---|---|---|---|---|---|---|---|---|
| | 6 | | -31 | SEAL STRIP | LT-1500 | | | |
| | 6 | | -33 | SEAL STRIP | | | | |
| | 3 | | -35 | SEAL STRIP | | | | |
| | 4 | | -25 | BLOCK | | | | |
| | 4 | | -23 | BLOCK | | | | |
| | 4 | | -21 | BLOCK | LT-1500 | 2 | | |
| 2 | | | -19 | CHANNEL | .062 SHT AL 7075-0 | 3 | | |
| 124 | | | LS8734T4-5 | SCREW | | | | |
| 124 | | | LS8859-4 | NUT | | | | |
| 124 | | | AN960C416 | WASHER | | | | |
| AR | | | MS20470AD4 | RIVET | | | | |
| 84 | | | LS8892F6-5 | JO-BOLT | | | | |
| 84 | | | LS8892F6-4 | JO-BOLT | | | | |
| | 2 | | -17 | BLOCK | LT-1500 | 7 | | |
| | 2 | | -15 | BLOCK | LT-1500 | 7 | | |
| 2 | | | -13 | CAP STRIP | .125 SHT AL 7075-T6 | | | |
| 2 | | | -11 | CAP STRIP | .125 SHT AL 7075-T6 | | | |
| 28 | | | -9 | CLIP | .062 SHT AL 7075-0 | 3 | | |
| 14 | | | -7 | ZEE | .062 SHT AL 7075-0 | | | |
| 2 | | | -5 | ANGLE | .125 SHT AL 7075-0 | | | |
| 2 | | | -3 | ANGLE | .125 SHT AL 7075-0 | 3 | | |
| 1 | | | -1 | PLATE | .062 SHT AL 7075-T6 | | | |
| | 1 | | -301 | FRAME ASSY | | | | |

-301 -501 PARTS LIST

| | | | |
|---|---|---|---|
| INTERPRET DWG PER | UNLESS OTHERWISE SPECIFIED DIM ARE IN INCHES TOLERANCES ON FRACTIONS = ± 1/16 DECIMALS: X = ± 1 .XX = ± .03 .XXX = ± .010 ANGLES = ± 2 DEG | DATE / DWN / APVD / APVD / ENGRG / CHKR / APVD / APVD | LOCKHEED MISSILES & SPACE COMPANY A GROUP DIVISION OF LOCKHEED AIRCRAFT CORPORATION SUNNYVALE CALIFORNIA |
| NEXT ASSY / USED ON | CONTR | | THERMAL TEST PANEL NO 3 |
| APPLICATION | CCA/CI/PD | | SIZE J / CODE IDENT / DRAWING NO SKJ205010 / REV A |
| | | | SCALE / SHEET |

SKJ205010 A

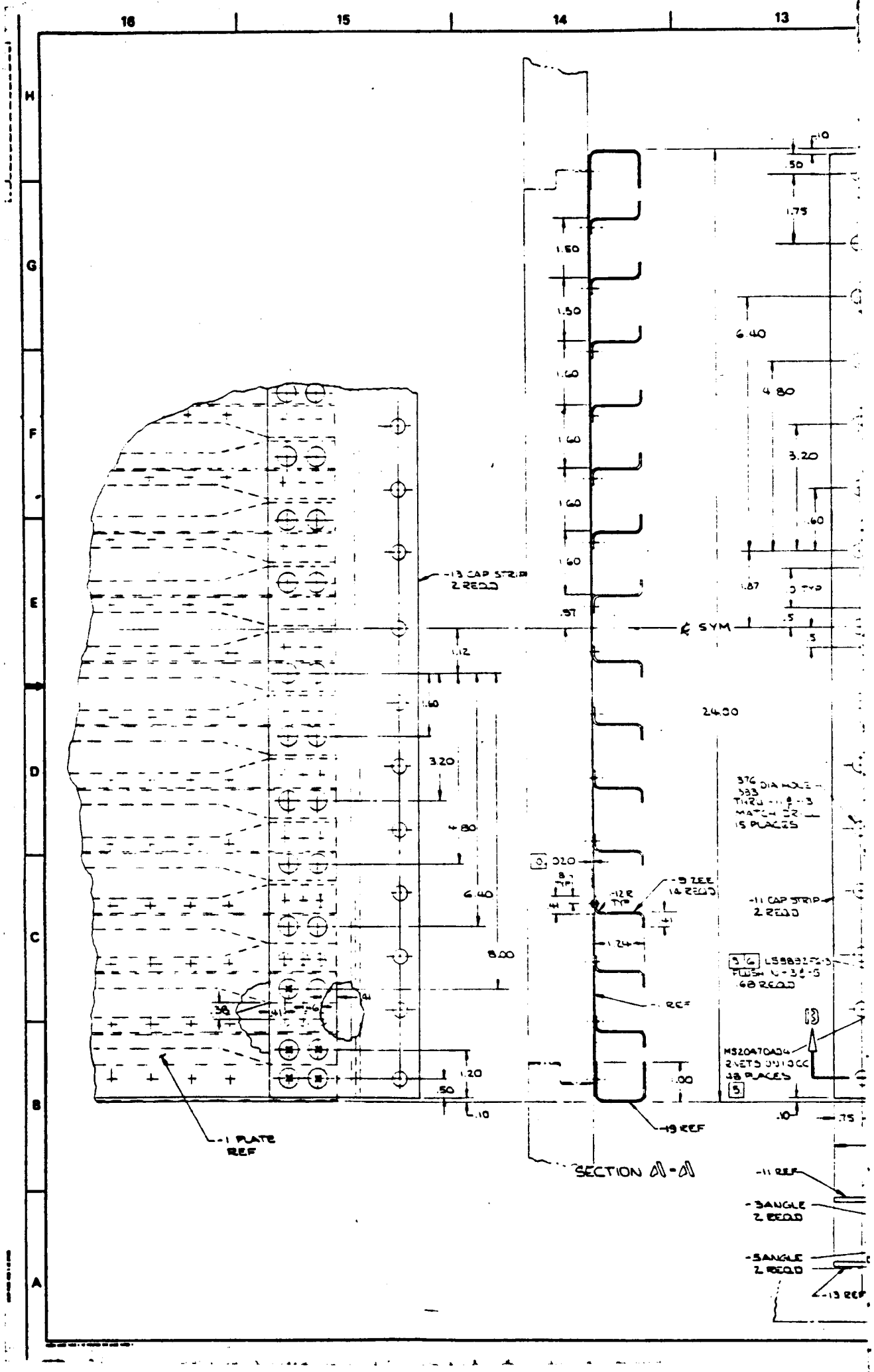

16
15
14
13
H
G
F
E
D
C
B
A
-13 CAP STRIP 2 REQD
℄ SYM
24.00
-11 CAP STRIP 2 REQD
-1 PLATE REF
-19 REF
SECTION A-A
-11 REF
-3 ANGLE 2 REQD
-5 ANGLE 2 REQD
-13 REF

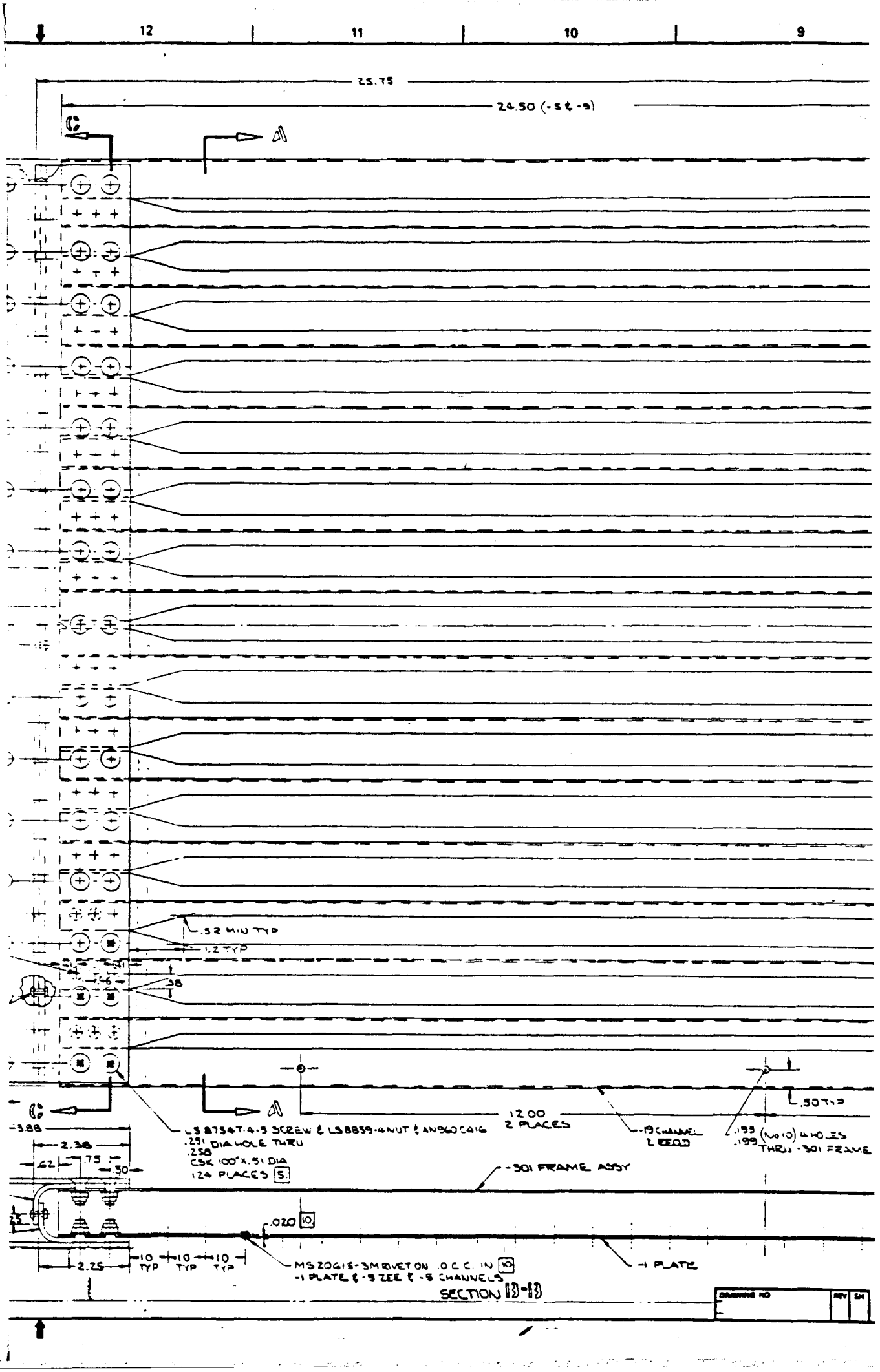
12
11
10
9
25.75
24.50 (-5 & -9)
.52 MIN TYP
1.2 TYP
.46
.38
12.00
2 PLACES
.50 TYP
LS8754T-4-5 SCREW & LS8859-4 NUT & AN960C416
.251 DIA HOLE THRU
.238
CSK 100° X .51 DIA
124 PLACES 5
-19 CHANNEL
2 REQD
.195 (No 10) 4 HOLES
.199 THRU -301 FRAME
-301 FRAME ASSY
.020 10
MS20615-3M RIVET ON .0 C.C. IN 10
-1 PLATE & -9 ZEE & -5 CHANNELS
-1 PLATE
SECTION B-B
3.88
2.38
.62
.75
.50
2.25
.10 TYP
.10 TYP
.10 TYP
DRAWING NO
REV
SH

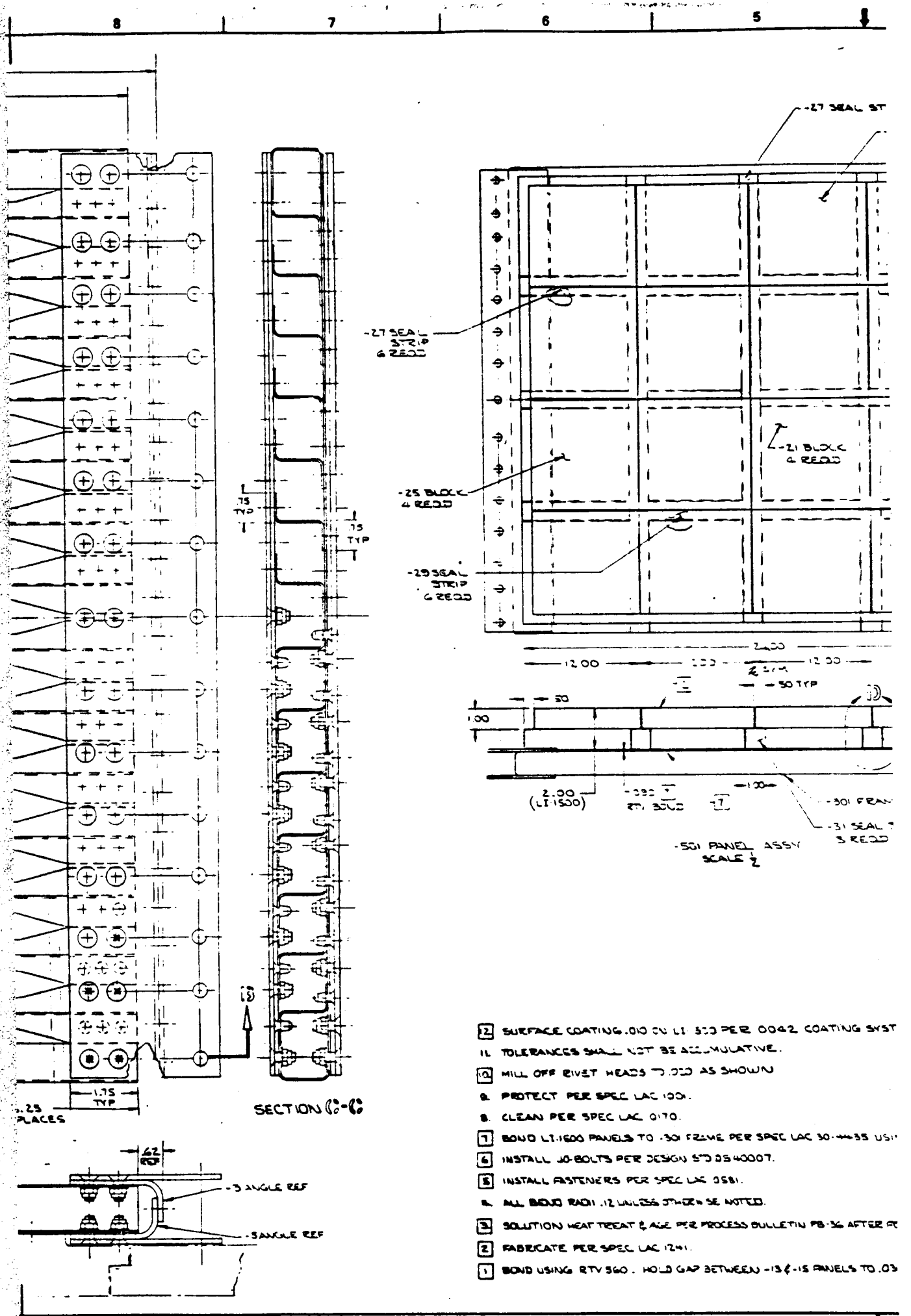
8
7
6
5
-27 SEAL ST
-27 SEAL STRIP 6 REQD
-21 BLOCK 4 REQD
-25 BLOCK 4 REQD
-29 SEAL STRIP 6 REQD
.75 TYP
.75 TYP
12.00
12.00
50 TYP
1.00
2.00 (LI-1500)
-301 FRAM
-31 SEAL 3 REQD
-501 PANEL ASSY SCALE 1/2
1.75 TYP
.25 PLACES
SECTION C-C
.62 REF
-3 ANGLE REF
-5 ANGLE REF
12 SURFACE COATING .010 ON LI-1500 PER 0042 COATING SYST
11 TOLERANCES SHALL NOT BE ACCUMULATIVE.
10 MILL OFF RIVET HEADS TO .020 AS SHOWN
9 PROTECT PER SPEC LAC 1001.
8 CLEAN PER SPEC LAC 0170.
7 BOND LI-1600 PANELS TO -301 FRAME PER SPEC LAC 30-4435 USI
6 INSTALL JO-BOLTS PER DESIGN STD DS 40007.
5 INSTALL FASTENERS PER SPEC LAC 0581.
4 ALL BEND RADII .12 UNLESS OTHERWISE NOTED.
3 SOLUTION HEAT TREAT & AGE PER PROCESS BULLETIN PB-36 AFTER FO
2 FABRICATE PER SPEC LAC 1241.
1 BOND USING RTV 560. HOLD GAP BETWEEN -13 & -15 PANELS TO .03

| ZONE | LTR | REVISIONS DESCRIPTION | DATE | APVD |
|---|---|---|---|---|
| | A | BLOCK SIZE WAS 4 [illegible] 2.20 THICK; ADDED NOTE 12 & 13 | 9 NOV 7 | |

FIG 6.1-4
PAGE 6-9/10

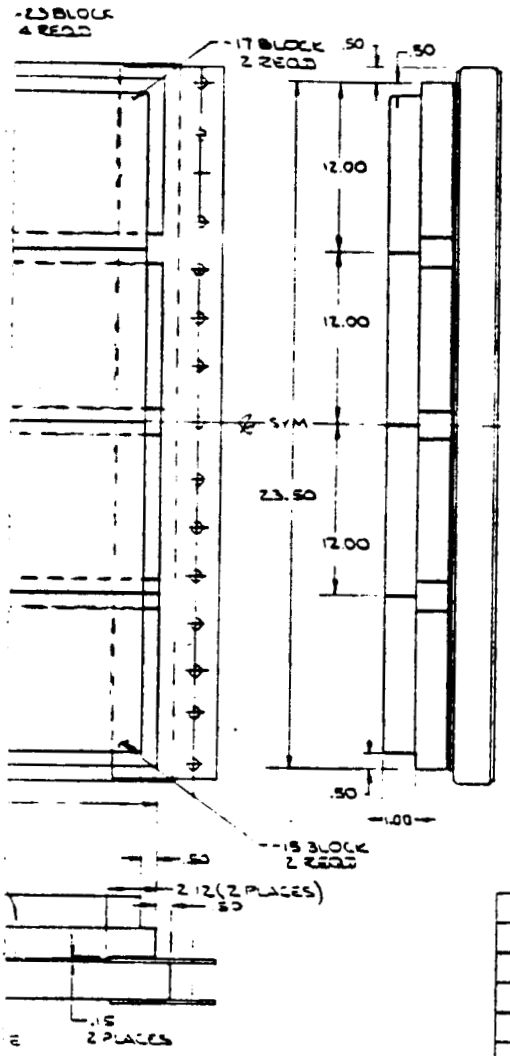


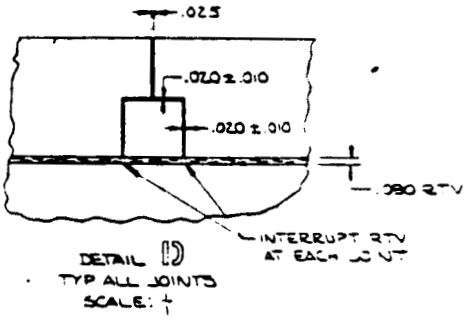


| QTY REQ -301 | QTY REQD -501 | CODE IDENT | PART OR IDENTIFYING NO | NOMENCLATURE OR DESCRIPTION | MATERIAL DESCRIPTION OR NOTE | MATERIAL SPECIFICATION | ZONE | ITEM NO |
|---|---|---|---|---|---|---|---|---|
| | 3 | | -31 | SEAL STRIP | LI-1500 7 | | | |
| | 6 | | -29 | SEAL STRIP | | | | |
| | 6 | | -27 | SEAL STRIP | | | | |
| | 4 | | -25 | BLOCK | | | | |
| | 4 | | -23 | BLOCK | | | | |
| | 4 | | -21 | BLOCK | LI-1500 7 | | | |
| AR | | | MS 20615-3M | RIVET | | | | |
| AR | | | MS 20470AD4 | RIVET | | | | |
| 168 | | | LS8392F6-3 | JO-BOLT | | | | |
| 124 | | | LS8754T4-5 | SCREW | | | | |
| 124 | | | LS8353-4 | NUT | | | | |
| 124 | | | AN960C416 | WASHER | | | | |
| 2 | | | -19 | CHANNEL | .040 SHT GAL-4V | TITANIUM ANNEALED 3 | | |
| | 2 | | -17 | BLOCK | LI-1500 7 | | | |
| | 2 | | -15 | BLOCK | LI-1500 7 | | | |
| 2 | | | -13 | CAP STRIP | .125 SHT GAL-4V | | | |
| 2 | | | -11 | CAP STRIP | .125 SHT GAL-4V | | | |
| 28 | | | -9 | CLIP | .040 SHT GAL-4V | TITANIUM ANNEALED 3 | | |
| 14 | | | -7 | ZEE | .040 SHT GAL-4V | | | |
| 2 | | | -5 | CHANNEL | .125 SHT GAL-4V | | | |
| 2 | | | -3 | CHANNEL | .125 SHT GAL-4V | | | |
| 1 | | | -1 | PLATE | .040 SHT GAL-4V | TITANIUM ANNEALED 3 | | |
| | 1 | | -301 | FRAME ASSY | | | | |

PARTS LIST

EM.

NG RTV 560 & .090 THICKNESS.

RMING.

O TO .035.

INTERPRET DWG PER

NEXT ASSY | USED ON
APPLICATION

UNLESS OTHERWISE SPECIFIED DIM ARE IN INCHES. TOLERANCES ON FRACTIONS = ± 1/16
DECIMALS .X = ± .1
.XX = ± .05
.XXX = ± .010
ANGLES = ± 2 DEG

CONTR
CCA/CI/FD

DATE
DWN
APVD
APVD
ENGRG
CHKR
APVD
APVD

LOCKHEED MISSILES & SPACE COMPANY
A GROUP DIVISION OF LOCKHEED AIRCRAFT CORPORATION
SUNNYVALE, CALIFORNIA

THERMAL TEST PANEL
(1 - Dwg 4)

SIZE J | CODE IDENT | DRAWING NO SKJ205011 | REV A
SCALE | SHEET

SKJ205011

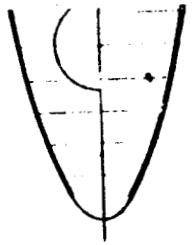

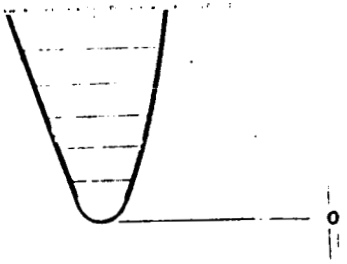

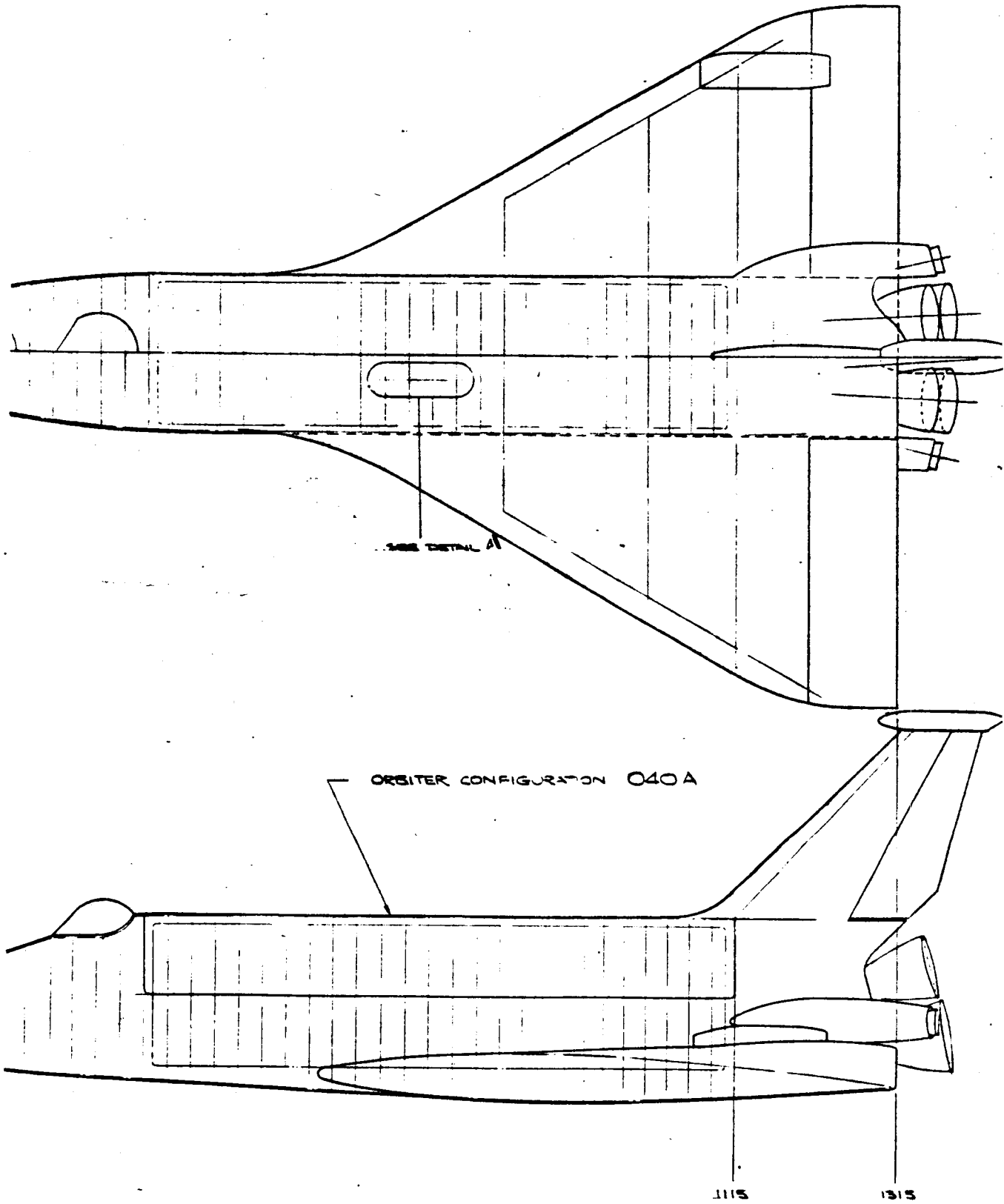
SEE DETAIL A
ORBITER CONFIGURATION 040 A
1115
1315

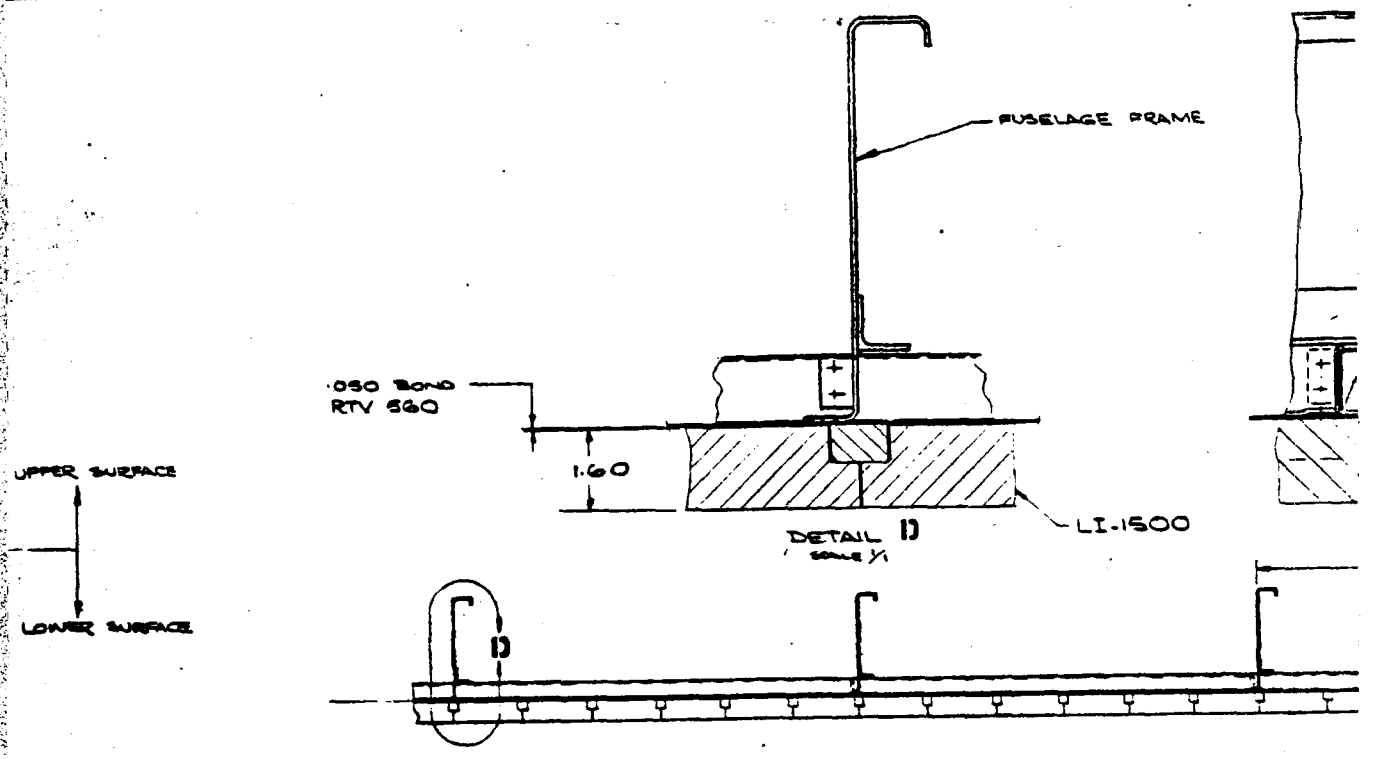


VIEW ON C - C

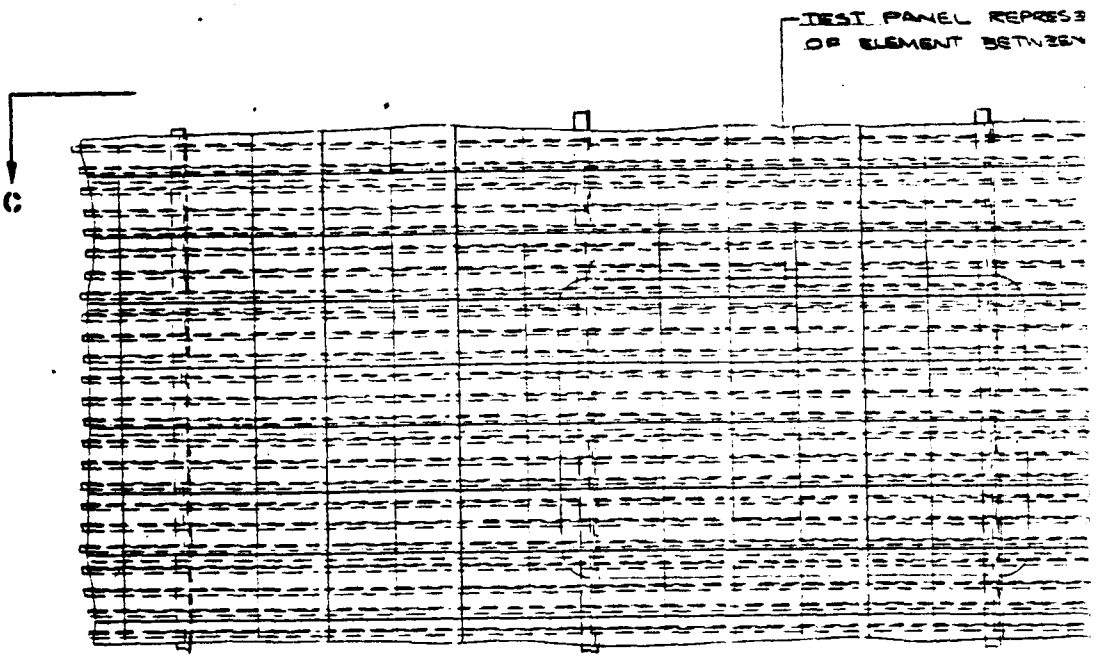


DETAIL A

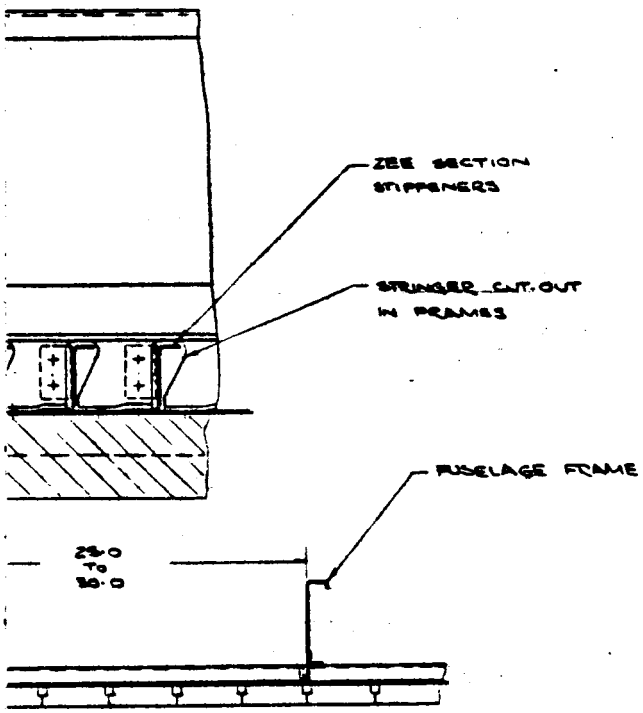


FIG. 6.1-5
PAGE 6 - 11/12

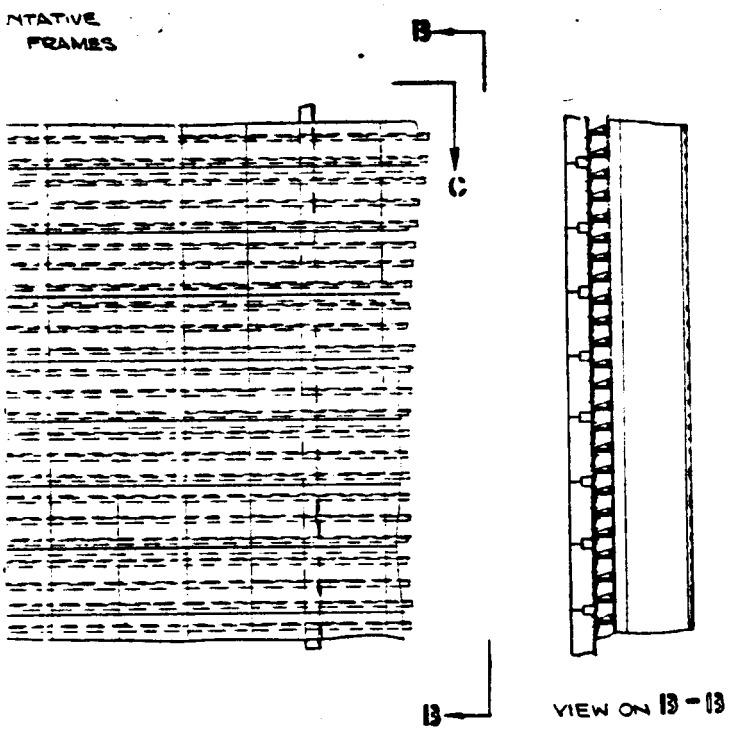

## 6.2 MATERIAL SPECIMENS

LMSC has fabricated and stored for NASA use four 12 by 12 by 2 in. tiles each month of the contract for a total of 16 tiles to date. In compliance with NASA TWX received 8 October, five tiles have been removed from storage, coated on one 12 by 12 in. side (0042 coating), and shipped to the designated recipients.

A TWX requesting 24 material samples for use in exposure testing at KSC was received on 3 November. These samples will be delivered to NASA/MSC before 3 December as directed.

Material fabrication is continuing under this task to provide the four tiles/month for November and December.

# APPENDIX A

## DESIGN AND ANALYSIS OF CANDIDATE PRIMARY STRUCTURE CONFIGURATIONS

## INTRODUCTION

Three primary structure concepts have been optimized (approximately) and analyzed for Area 2 loads to provide weight ($\bar{t}$) comparisons for Prototype Panel Configuration No. 2 ($\bar{t}$ = 0.1144 in.). The three alternate concepts and their $\bar{t}$'s are:

| | | |
|---|---|---|
| a. | Corrugation + Skin | $\bar{t}$ = 0.1341 in. |
| b. | Honeycomb | $\bar{t}$ = 0.1472 in. |
| c. | Integrally Stiffened | $\bar{t}$ = 0.1329 in. |

## MOMENT AMPLIFICATION FACTOR — $2f(u)$

$$M_{MAX} = \frac{w l^2}{8} \cdot 2f(u)$$

$$u = \frac{l}{2}\left(\frac{N x_c}{E_c \bar{I}_o}\right)^{1/2}$$

$$f(u) = \frac{1-\cos u}{u^2 \cos u}$$

REF. TIMOSHENKO & GERE, THEORY of ELASTIC STABILITY, 2ND ED., ARTICLE 1.5

## CORR. + SKIN PANELS

$$u_I = \frac{24}{2}\left(\frac{2250}{10.5(22{,}310)}\right)^{1/2} = 1.176 \;;\; u_I^2 = 1.383 \;;\; u_I\,(\text{DEG}) = 67°23'$$

$$u_{II} = \frac{24}{2}\left(\frac{3000}{10.5(22{,}310)}\right)^{1/2} = 1.358 \;;\; u_{II}^2 = 1.844 \;;\; u_{II}\,(\text{DEG}) = 77°48'$$

$$u_{III} = \frac{24}{2}\left(\frac{3000}{9.66(22{,}310)}\right)^{1/2} = 1.416 \;;\; u_{III}^2 = 2.005 \;;\; u_{III}\,(\text{DEG}) = 81°08'$$

| COND. | $\cos u$ | $1-\cos u$ | $u^2\cos u$ | $f(u)$ | $2f(u)$ |
|---|---|---|---|---|---|
| I | .3846 | .6154 | .5319 | 1.157 | 2.314 |
| II | .2113 | .7887 | .3896 | 2.024 | 4.049 |
| III | .1541 | .8459 | .3090 | 2.738 | 5.475 |

## HONEYCOMB PANELS

$$u_I = \frac{24}{2}\left(\frac{2250}{10.5(25{,}500)}\right)^{1/2} = 1.100 \;;\; u_I^2 = 1.210 \;;\; u_I\,(\text{DEG}) = 63°02'$$

$$u_{II} = \frac{24}{2}\left(\frac{3000}{10.5(25{,}500)}\right)^{1/2} = 1.270 \;;\; u_{II}^2 = 1.613 \;;\; u_{II}\,(\text{DEG}) = 72°46'$$

$$u_{III} = \frac{24}{2}\left(\frac{3000}{9.66(25{,}500)}\right)^{1/2} = 1.324 \;;\; u_{III}^2 = 1.753 \;;\; u_{III}\,(\text{DEG}) = 75°52'$$

| COND. | $\cos u$ | $1-\cos u$ | $u^2\cos u$ | $f(u)$ | $2f(u)$ |
|---|---|---|---|---|---|
| I | .4535 | .5465 | .5487 | .9960 | 1.992 |
| II | .2963 | .7037 | .4779 | 1.472 | 2.945 |
| III | .2442 | .7558 | .4281 | 1.765 | 3.531 |

## MOMENT AMPLIFICATION FACTORS ~ $2f(u)$

### INTEG. STIFF'D PANELS

$$u_I = \frac{24}{2}\left(\frac{2250}{10.5(28{,}580)}\right)^{1/2} = 1.039 \; ; \; u_I^2 = 1.080 \; ; \; u_I\,(\text{DEG}) = 59°32'$$

$$u_{II} = \frac{24}{2}\left(\frac{3000}{10.5(28{,}580)}\right)^{1/2} = 1.200 \; ; \; u_{II}^2 = 1.440 \; ; \; u_{II}\,(\text{DEG}) = 68°45'$$

$$u_{III} = \frac{24}{2}\left(\frac{3000}{9.66(28{,}580)}\right)^{1/2} = 1.251 \; ; \; u_{III}^2 = 1.565 \; ; \; u_{III}\,(\text{DEG}) = 71°41'$$

| COND. | $\cos u$ | $1-\cos u$ | $u^2\cos u$ | $f(u)$ | $2f(u)$ |
|---|---|---|---|---|---|
| I | .5070 | .4930 | .5476 | .9003 | 1.801 |
| II | .3624 | .6376 | .5219 | 1.222 | 2.443 |
| III | .3143 | .6857 | .4919 | 1.394 | 2.788 |



FORM LMSC 362 B-2

## CORR. + SKIN STRUCTURAL PANELS : $l = 24$ in

### SECTION PROPERTIES ~ PER PITCH

SCALE: 2/1

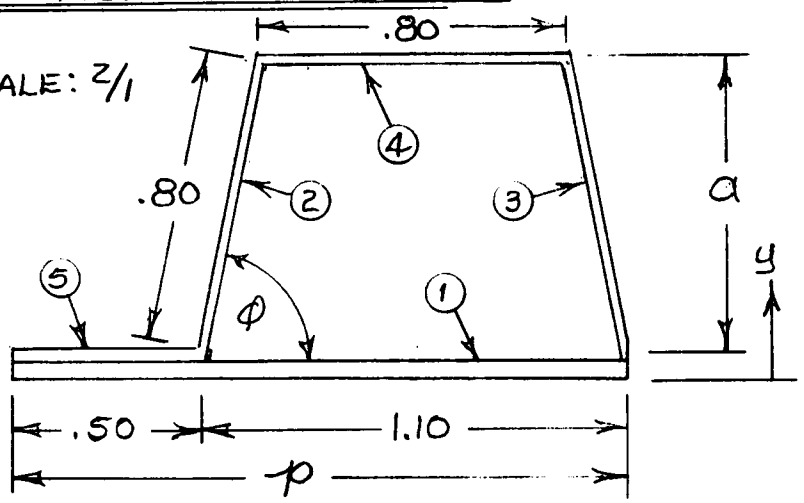


$t_c = .040$ in

$t_s = .051$ in

$\cos\phi = .15/.8 = 0.1875$

$\phi = 79°\,13'$

$\sin\phi = 0.9823$

$a = .8\sin\phi = 0.7858$ in

$p = .50 + 1.10 = 1.60$ in

| ELEM. | A | y | Ay | d | $Ad^2$ | $I_i$ |
|---|---|---|---|---|---|---|
| 1 | .0816 | .0255 | .002081 | .2715 | .006015 | .000018 |
| 2 | .0320 | .4439 | .014205 | .1469 | .000691 | .001647 |
| 3 | .0320 | .4439 | .014205 | .1469 | .000691 | .001647 |
| 4 | .0320 | .8368 | .026778 | .5398 | .009324 | .000004 |
| 5 | .0200 | .0710 | .001420 | .2260 | .001022 | .000003 |
| Σ | .1976 | | .05869 | | .01774 | .003319 |

$\bar{y} = \frac{.05869}{.1976} = 0.2970$ in ; $\bar{t} = \frac{.1976}{1.60} = 0.1235$ in

$C_{MIN} = 0.2970$ in ; $C_{MAX} = .7858 + .051 - .2970 = 0.5398$ in

$I_o = .01774 + .003319 = .02106$ in$^4$

$Z_{OMAX} = \frac{.02106}{.2970} = .07091$ in$^3$ ; $Z_{OMIN} = \frac{.02106}{.5398} = .03901$ in$^3$

### PER INCH of WIDTH:

$\bar{I}_o = \frac{.02106}{1.60} = .01316$ in$^4$/in : NOT ADEQUATE ; SEE NEXT PAGE

$\bar{Z}_{OMAX} = \frac{.07091}{1.60} = .04432$ in$^3$/in

$\bar{Z}_{OMIN} = \frac{.03901}{1.60} = .02438$ in$^3$/in

R.T. $\bar{P}_{CR} = 2602$ lb/in

250° $\bar{P}_{CR} = 2394$ lb/in



FORM LMSC 362 B-2

## CORR. + SKIN STRUCTURAL PANELS

### SECTION PROPERTIES ~ PER PITCH ~ REVISED GEOMETRY

LET $\alpha = 1.00$ & $l_1, l_2$, & $\phi$ CHANGE ACCORDINGLY: REST OF GEOMETRY SAME AS ON p. B4.

$\cot\phi = .15/1 = .1500$ ; $\phi = 81°28'$ ; $\sin\phi = 0.9889$ ; $\cos\phi = 0.1484$

$l_2 = l_3 = 1/\sin\phi = 1.011$ in

| ELEM. | A | y | Ay | d | $Ad^2$ | $I_i$ |
|---|---|---|---|---|---|---|
| 1 | .08160 | .02550 | .002081 | .3553 | .01030 | .000018 |
| 2 | .04044 | .5510 | .02228 | .1702 | .00117 | .003371 |
| 3 | .04044 | .5510 | .02228 | .1702 | .00117 | .003371 |
| 4 | .03200 | 1.051 | .03363 | .6702 | .01437 | .000004 |
| 5 | .02000 | .07100 | .001420 | .3098 | .00192 | .000003 |
| Σ | .2145 | | .08169 | | .02893 | .006767 |

$\bar{y} = \frac{.08169}{.2145} = 0.3808$ in ; $\bar{t} = \frac{.2145}{1.60} = 0.1341$ in

$C_{MIN} = 0.3808$ in ; $C_{MAX} = 1.051 - .3808 = 0.6702$ in

$I_o = .02893 + .006767 = .03570$ in$^4$

$Z_{OMAX} = \frac{.03570}{.3808} = .09375$ in$^3$ ; $Z_{OMIN} = \frac{.03570}{.6702} = .05327$ in$^3$

### PER INCH of WIDTH:

$\bar{I}_o = \frac{.03570}{1.60} = .02231$ in$^4$/in

$\bar{Z}_{OMAX} = \frac{.09375}{1.60} = .05859$ in$^3$/in

$\bar{Z}_{OMIN} = \frac{.05327}{1.60} = .03329$ in$^3$/in



FORM LMSC 362 B-2

## CORR. + SKIN STRUCTURAL PANELS

MATERIAL ~ ALL 7075-T6, WELDBOND CONSTRUCTION
FROM p. 4, PROTOTYPE PANEL ANALYSIS

| | R.T. ~ Ksi | 250°F. ~ Ksi |
|---|---|---|
| $F_{tu}$ | 77 | 63.1 |
| $F_{ty}$ | 67 | 57 |
| $F_{cy}$ | 68 | 60.5 |
| $E_c$ | $10.5 \times 10^3$ | $9.66 \times 10^3$ |

LOADS ~ AREA 2 ~ ALL ULTIMATE VALUES
FROM p. 5, PROTOTYPE PANEL ANALYSIS

| | | |
|---|---|---|
| COND. I (R.T.): | $N_{xT} = 3450$ ppi | $p_B = 4.5$ psi |
| | $N_{xc} = 2250$ ppi | $p_c = 6$ psi |
| COND. II (R.T.): | $N_{xT} = 4050$ ppi | $p_B = 2.85$ psi |
| | $N_{xc} = 3000$ ppi | $p_c = 2.7$ psi |
| COND. III (250°F.): | $N_{xT} = 6000$ ppi | $p_B = 0.75$ psi |
| | $N_{xc} = 3000$ ppi | $p_c = 3$ psi |

ALLOWABLE COLUMN LOADS ~ EULER

$$\bar{P}_{CR} = \frac{\pi^2 E_c \bar{I}_o}{(1-\nu^2)\,\ell^2} = \frac{\pi^2 E_c (.02231)}{.91(24)^2} = \frac{E_c}{2380}$$

AT R.T.:

$$\bar{P}_{CR} = \frac{10{,}500}{2.380} = 4412 \text{ lb/in}\ ;\ \sigma_{CR} = \frac{4412}{.1341} = 32{,}900 \text{ psi}$$

AT 250°F.:

$$\bar{P}_{CR} = \frac{9660}{2.380} = 4059 \text{ lb/in}\ ;\ \sigma_{CR} = \frac{4059}{.1341} = 30{,}270 \text{ psi}$$



FORM LMSC 362 B-2

CORR. + SKIN STRUCTURAL PANELS

MAX. STRESSES ON SECTION ~ ULTIMATE

1. COMPRESSION : COMBINE $N_{\gamma c}$ & $p_B$ ~ BEAM-COLUMN ANALYSIS

$$\sigma_{c_{MAX}} = \frac{N_{\gamma c}}{\bar{t}} + \frac{M_{MAX}}{Z_{o_{MIN}}} = \frac{N_{\gamma c}}{.1341} + \frac{72 p_B 2f(u)}{.03329} = 7.457\, N_{\gamma c} + 2163\, p_B\, 2f(u)$$

COND. I : $\sigma_{c_{I_{MAX}}} = 7.457(2250) + 2163(4.5)(2.314) = 16{,}780 + 22{,}520 = 39{,}300$ psi

COND. II : $\sigma_{c_{II_{MAX}}} = 7.457(3000) + 2163(2.85)(4.049) = 22{,}370 + 24{,}960 = 47{,}330$ psi

COND. III : $\sigma_{c_{III_{MAX}}} = 7.457(3000) + 2163(0.75)(5.475) = 22{,}370 + 8882 = 31{,}250$ psi

2. TENSION : COMBINE $N_{\gamma T}$ & $p_c$ ~ DIRECT SUPERPOSITION

$$\sigma_{T_{MAX}} = \frac{N_{\gamma T}}{\bar{t}} + \frac{M_{MAX}}{Z_{o_{MIN}}} = 7.457\, N_{\gamma T} + 2163\, p_c$$

COND. I : $\sigma_{T_{I_{MAX}}} = 7.457(3450) + 2163(6) = 25{,}730 + 12{,}980 = 38{,}710$ psi

COND. II : $\sigma_{T_{II_{MAX}}} = 7.457(4050) + 2163(2.7) = 30{,}200 + 5840 = 36{,}040$ psi

COND. III : $\sigma_{T_{III_{MAX}}} = 7.457(6000) + 2163(3) = 44{,}740 + 6489 = 51{,}230$ psi

LOCAL BUCKLING STRESSES ~ $\sigma_{cr_\ell}$ ELEMENT ④ (REF: S.M. 80 C)

AT R.T.: $k_\ell = .0816$, $n = 15$, $F_{0.7} = 70$ Ksi } TAB. 2

$\sqrt{K} = 1.90$ (SIMPLY SUPPORTED)

$b/t = .80/.04 = 20$

$(b/t)_e = 20/1.9 = 10.53$

$B = .0816(10.53) = 0.859$

$F/F_{0.7} = 0.95$ (FIG. 2)

$\sigma_{cr_\ell} = .95(70) = 66.5$ Ksi



FORM LMSC 362 B-2

CORR. + SKIN STRUCTURAL PANELS

## MARGINS of SAFETY

1. COMPRESSION ALONE ~ COND. III CRITICAL ; T = 250°F.

$$M.S. = \frac{\bar{P}_{CR}}{N\gamma_c} - 1 = \frac{4059}{3000} - 1 = 1.353 - 1 = \underline{\underline{+0.35}}$$

COLUMN BUCKLING

2. COMBINED TENSION & COLLAPSE PRESSURE ~ COND. III CRITICAL

$$M.S. = \frac{F_{tu}}{\sigma_{T\,III\,MAX}} - 1 = \frac{63.1}{51.23} - 1 = 1.232 - 1 = \underline{\underline{+0.23}}$$

TENS.-ULT.

3. COMBINED COMP. & BURST PRESSURE ~ COND. II CRITICAL

$$M.S. = \frac{\sigma_{CRL}}{\sigma_{C\,II\,MAX}} - 1 = \frac{66.5}{47.33} - 1 = 1.405 - 1 = \underline{\underline{+0.40}}$$

LOCAL BUCKLING



FORM LMSC 362 B-2

## HONEYCOMB STRUCTURAL PANELS : $l = 24$ in

### SECTION PROPERTIES

FULL SCALE

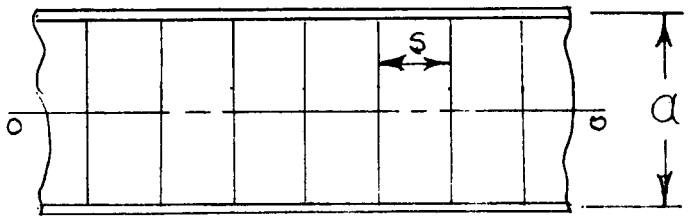


$t_F = .051$ in
$a = 1.0$ in
$s = 0.375$ in
$t_c = .004$ in (5.4 pcf)

$\bar{t} = 2t_F = 2(.051) = 0.1020$ in (THIS $\bar{t}$ NOT FOR WEIGHT)

$\bar{I}_o = t_F a^2/2 = .051(1.0)^2/2 = .02550$ in$^4$/in

$\bar{Z}_o = 2\bar{I}_o/a = 2(.02550)/1 = .05100$ in$^3$/in

LOADS ~ SAME AS ON p.A6, CORR. + SKIN STR. PANELS (AREA 2 LOADS)

MATERIAL ~ FACE SHEETS ~ 7075-T6 : PROPERTIES ON p.A6 CITED ABOVE

ALLOWABLE COLUMN LOADS ~ EULER

$$\bar{P}_{CR} = \frac{\pi^2 E_c \bar{I}_o}{(1-\nu^2)\, l^2} = \frac{\pi^2 E_c (.02550)}{.91(24)^2} = \frac{E_c}{2083}$$

AT R.T.:

$$\bar{P}_{CR} = \frac{10{,}500}{2.083} = 5041 \text{ lb/in} \; ; \; \sigma_{CR} = \frac{5041}{.1020} = 49{,}420 \text{ psi}$$

AT 250°F:

$$\bar{P}_{CR} = \frac{9660}{2.083} = 4638 \text{ lb/in} \; ; \; \sigma_{CR} = \frac{4638}{.1020} = 45{,}470 \text{ psi}$$

FACE SHEET DIMPLING STRESS ~ $F_{CR_D}$

$$F_{CR_D} = \frac{2\eta E_c}{1-\nu^2}(t_F/s)^2 \quad \text{(REF. MIL-HDBK-23A, EQN 4:1)}$$

AT R.T.: $F_{CR_D} = \dfrac{2\eta(10.5\times10^6)(.051)^2}{.91\,(.375)^2} = 427\eta\times10^3$ : NOT A FAILURE MODE FOR THIS PANEL



FORM LMSC 362 B-2

## HONEYCOMB STRUCTURAL PANELS

### MAX. STRESSES ON SECTION ~ ULTIMATE

$$\sigma_{C_{MAX}} = \frac{N_{xc}}{t} + \frac{M_{MAX}}{Z_o} = \frac{N_{xc}}{.1020} + \frac{72 P_{MAX} \cdot 2f(u)}{.05100} = 9.804\, N_{xc} + 1412\, P_{MAX} \cdot 2f(u)$$

$$\sigma_{T_{MAX}} = \frac{N_{xT}}{t} + \frac{M_{MAX}}{Z_o} = \frac{N_{xT}}{.1020} + \frac{72 P_{MAX}}{.05100} = 9.804\, N_{xT} + 1412\, P_{MAX}$$

| | | $\sigma_N$ | $\sigma_P$ | $\sigma_{MAX}$ ~ psi |
|---|---|---|---|---|
| COND. I: | TENS. | +33,820 | +8470 | +42,290 |
| | COMP. | -22,060 | -16,880 | -38,940 |
| COND. II: | TENS. | +39,710 | +4020 | +43,730 |
| | COMP. | -29,410 | -11,850 | -41,260 |
| COND. III: | TENS. | +58,820 | +4240 | +63,060 |
| | COMP. | -29,410 | -14,960 | -44,370 |

### MARGINS of SAFETY ~ COND. III CRITICAL ; T = 250°F.

1. COMPRESSION ALONE

$$M.S. = \frac{\bar{P}_{CR}}{N_{xc}} - 1 = \frac{4638}{3000} - 1 = 1.546 - 1 = \underline{+0.55}$$

COLUMN BUCKLING

2. COMBINED TENSION & PRESSURE

$$M.S. = \frac{F_{tu}}{\sigma_{T\,III\,MAX}} - 1 = \frac{63.1}{63.06} - 1 = 1.001 - 1 = \underline{+0.0}$$

TENS. - ULT.

### UNIT WEIGHT ~ $W_T$ & WEIGHT BAR "t" ~ $t_W$

$$W_T = W_T\,(\text{FACES}) + W_T\,(\text{CORE}) + W_T\,(\text{BOND})$$
$$= (0.1\ lb/in^3)(.1020\ in)(144\ in^2/ft^2) + (5A\ lb/ft^3)(\tfrac{1}{2}\ ft) + 2(0.1\ lb/ft^2)$$
$$= 1.469 + 0.450 + 0.200$$
$$W_T = 2.119\ lb/ft^2$$

$$t_W = \frac{2.119\ lb/ft^2}{(0.1\ lb/in^3)(144\ in^2/ft^2)} = 0.1472\ in$$

: WEIGHT EQUIVALENT AVERAGE THICKNESS IN ALUMINUM



FORM LMSC 362 B-2

INTEG. STIFF'D STRUCTURAL PANELS : $\ell = 24$ in

SECTION PROPERTIES ~ PER PITCH

FULL SCALE

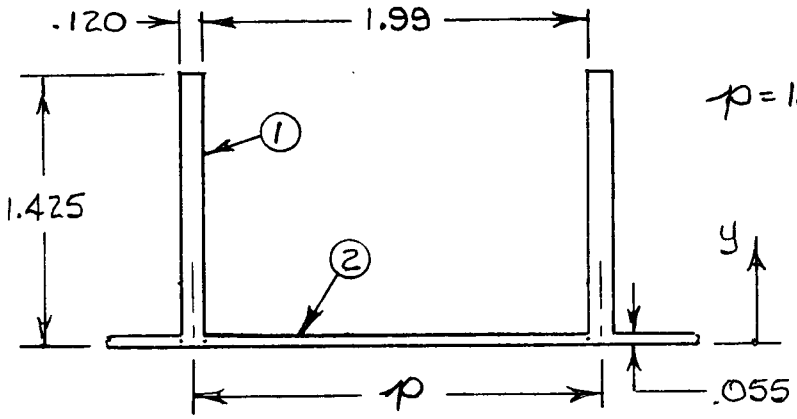


$p = 1.99 + .120 = 2.11$ in

| ELEM. | A | y | Ay | d | $Ad^2$ | $I_i$ |
|---|---|---|---|---|---|---|
| 1 | .1710 | .7125 | .1218 | .2674 | .01223 | .02894 |
| 2 | .1094 | .0275 | .0030 | .4176 | .01910 | .00003 |
| Σ | .2804 | | .1248 | | .03133 | .02897 |

$\bar{y} = \frac{.1248}{.2804} = 0.4451$ in ; $\bar{t} = \frac{.2804}{2.11} = 0.1329$ in

$C_{MIN} = 0.4451$ in ; $C_{MAX} = 1.425 - .4451 = 0.9799$ in

$I_o = .03133 + .02879 = .06030$ in$^4$

$Z_{OMAX} = \frac{.06030}{.4451} = 0.1355$ in$^3$ ; $Z_{OMIN} = \frac{.06030}{.9799} = .06154$ in$^3$

PER INCH of WIDTH :

$\bar{I}_o = \frac{.06030}{2.11} = .02858$ in$^4$/in

$\bar{Z}_{OMAX} = \frac{.1355}{2.11} = .06422$ in$^4$/in

$\bar{Z}_{OMIN} = \frac{.06154}{2.11} = .02917$ in$^4$/in

# INTEG. STIFFENED STRUCTURAL PANELS

LOADS & MATERIAL : ALL AS GIVEN ON p. A6, CORR. + SKIN PANELS

(AREA 2 LOADS ; 7075-T6 MAT'R'L)

## ALLOWABLE COLUMN LOADS ~ EULER

$$\bar{P}_{CR} = \frac{\pi^2 E_c \bar{I}_o}{(1-\nu^2)\,\ell^2} = \frac{\pi^2 E_c (.02858)}{.91(576)} = \frac{E_c}{1858}$$

AT R.T.:

$$\bar{P}_{CR} = \frac{10{,}500}{1.858} = 5651 \text{ lb/in} \; ; \; \sigma_{CR} = \frac{5651}{.1329} = 42{,}520 \text{ psi}$$

AT 250°F:

$$\bar{P}_{CR} = \frac{9660}{1.858} = 5199 \text{ lb/in} \; ; \; \sigma_{CR} = \frac{5199}{.1329} = 39{,}120 \text{ psi}$$

## LOCAL BUCKLING STRESSES ~ $\sigma_{CR_\ell}$

ELEMENT ① : REF. S. TANG REPORT

ASSUME $\alpha = 0.5$ ; THEN $k_c = 1.4$ ; $(t/b)^2 = (.12/1.425)^2 = 1/141.0$

$$\sigma_{CR_\ell} = \frac{k_c \pi^2 E_c}{12(1-\nu^2)}\left(\frac{t}{b}\right)^2 = \frac{1.4\,\pi^2 E_c}{12(.91)(141.0)} = \frac{E_c}{111.4}$$

; NOT A FAILURE MODE ~ THIS SECTION

ELEMENT ② : ASSUME SIMPLE SUPPORTS

$$\sigma_{CR_\ell} = 3.6 E_c \left(\frac{t}{b}\right)^2 = 3.6 E_c \left(\frac{.055}{1.99}\right)^2 = \frac{E_c}{363.6}$$

AT R.T. : $\sigma_{CR_\ell} = \dfrac{10.5 \times 10^6}{363.6} = 28{,}880$ psi

AT 250°F : $\sigma_{CR_\ell} = \dfrac{9.66 \times 10^6}{363.6} = 26{,}570$ psi

# INTEGRALLY STIFFENED STRUCTURAL PANELS

## CRITICAL STRESSES ON SECTION ~ ULTIMATE

1. COMPRESSION ON ELEM. ②: COND. III CRITICAL (COMP. $N_x$ & COLLAPSE $p$)

$$\sigma_{CZ\,MAX} = \frac{N_{xc}}{\bar{t}} + \frac{M_{MAX}}{\bar{Z}_{o\,MAX}} = \frac{3000}{.1329} + \frac{72(3)\cdot Zf(u)}{.06422} = 22{,}570 + 3363\,(2.788)$$

$$\sigma_{CZ\,MAX} = 22{,}570 + 9377 = 31{,}950 \text{ psi}$$

2. TENSION ON ELEM. ①: COND. III CRITICAL (TENS. $N_x$ & COLLAPSE $p$)

$$\sigma_{TI\,MAX} = \frac{N_{xT}}{\bar{t}} + \frac{M_{MAX}}{\bar{Z}_{o\,MIN}} = \frac{6000}{.1329} + \frac{72(3)}{.02917} = 45{,}140 + 7404$$

$$\sigma_{TI\,MAX} = 52{,}540 \text{ psi}$$

## MARGINS of SAFETY ~ COND. III CRITICAL; T = 250 °F.

1. COMPRESSION ALONE

$$M.S. = \frac{\bar{P}_{CR}}{N_{xc}} - 1 = \frac{5199}{3000} - 1 = 1.733 - 1 = \underline{+0.73}$$

COLUMN BUCKLING

2. COMBINED COMPRESSION & COLLAPSE PRESSURE

$$M.S. = \frac{\sigma_{CR\,\ell}}{\sigma_{CZ\,MAX}} - 1 = \frac{26.57}{31.91} - 1 = 0.833 - 1 = \underline{-0.17}^{*}$$

LOCAL BUCKLING

3. COMBINED TENSION & COLLAPSE PRESSURE

$$M.S. = \frac{F_{tu}}{\sigma_{TI\,MAX}} - 1 = \frac{63.1}{52.45} - 1 = 1.203 - 1 = \underline{+0.20}$$

TENS.-ULT.

* THE GEOMETRY SELECTED (p. A11) IS NOT ADEQUATE FOR THE DESIGN LOADS; HOWEVER, THE POINT IS MADE THAT THIS CONFIGURATION IS NOT MORE EFFICIENT THAN THE Z-STIFFENED PANELS.



FORM LMSC 362 B-2

# Appendix B

## STRESS ANALYSIS OF SUBSTRATE FOR PROTOTYPE PANEL No. 1

| Prepared by: A.J. CHINN | Date 9-1-71 | LOCKHEED MISSILES & SPACE COMPANY<br>A GROUP DIVISION OF LOCKHEED AIRCRAFT CORPORATION | Page 81 Temp. Perm. |
|---|---|---|---|
| Checked by: J.R. Ritz | Date 9-13-71 | Title TASK 6: PROTOTYPE PANELS DESIGN & ANALYSIS | Model |
| Approved by: | Date | | Report No. |

Be SUBPANEL #1

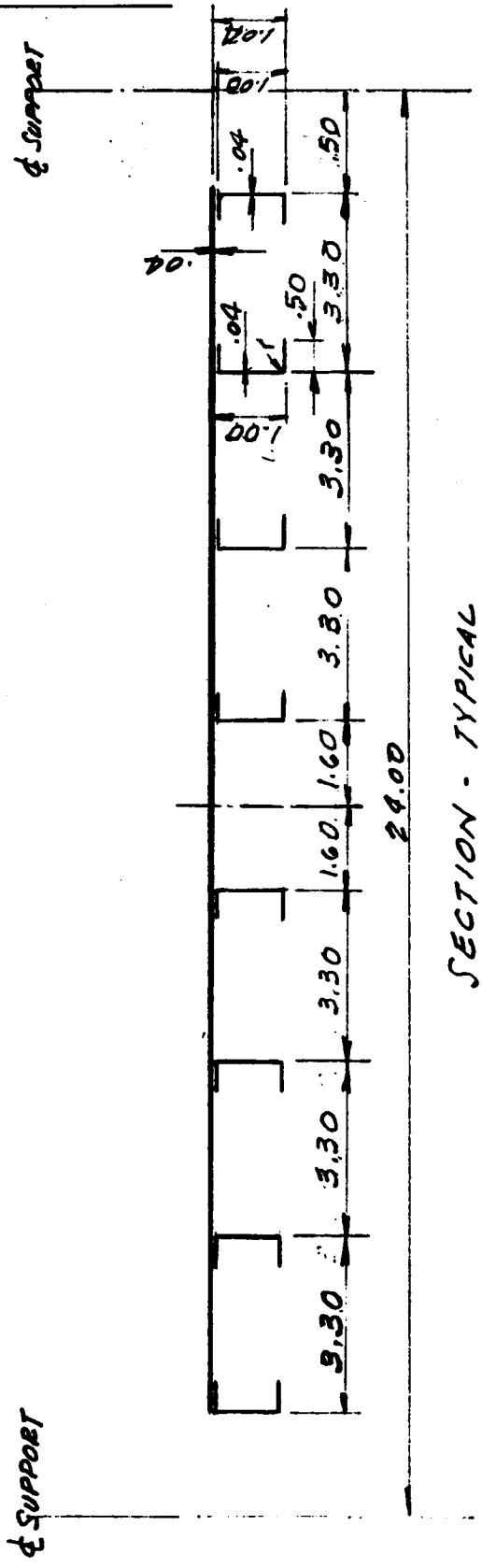


SECTION - TYPICAL

MATERIAL: BERYLLIUM X-ROLLED SHEET 0.003 THICK

BRAZING MAT: B18Ag ALLOY 60Ag-30Cu-10Sn

$r = 5t = 5 \times .040 = .200$

D/N SK 90371

FORM LMSC 362 B-2

Be SUBPANEL #1

THIS PANEL WILL BE DESIGNED FOR PRESSURE ONLY LOADS.

ASCENT $P_{COLLAPSE}$ = 4.0 psi LIMIT @ R.T., 6.0 psi ULT.

$P_{BURST}$ = 3.0 psi LIMIT @ R.T., 4.5 psi ULT.

REENTRY $P_{COLLAPSE}$ = 2.0 psi LIMIT @ 600°F 3.0 psi ULT.

$P_{BURST}$ = 0.5 psi. LIMIT @ 600°F 0.75 psi ULT

BY INSPECTION. ASCENT LOADINGS ARE CRITICAL FOR DESIGN

MATERIAL PROPERTIES.

| | @ R.T. | @ 600°F |
|---|---|---|
| $F_{tu}$ | 75,000 #/IN² | 46,000 #/IN² |
| $F_{cy}$ | 57,800 #/IN² | 43,000 #/IN² |
| $E$ | $42.5 \times 10^6$ #/IN² | $39.3 \times 10^6$ #/IN² |

CRITICAL STRESSES.

$$F_{cr} = K \eta E_c \left(\frac{t}{b}\right)^2$$

FOR FIXED EDGES $K = 6.3$
FOR FREE EDGE $K = 0.385$

$$\eta = \sqrt{\frac{E_T}{E}}$$

REFERENCE

1 BERYLLIUM MECHANICAL PROPERTY DATA AFML. MAR. 67
2 "STRENGTH OF MATERIALS" BY SNANLEY, PAGE 611

Be SUBPANEL #1

FACE SHEET

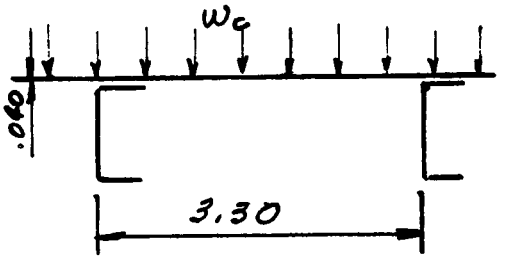


CONSIDER THE FACE SHEET AS CONTINUOUS AND SPANNING OVER A NUMBER OF SUPPORTS.

LOADING = 6.0 #/IN² (ULT.) @ R.T.

FOR CONSERVATIVE REASONS, LET $M = \frac{wl^2}{10}$

$$M = \frac{6.0 \times 3.30^2}{10} = 6.534 \text{ "#/IN}$$

$$f_b = \frac{6M}{t_s^2} = \frac{6 \times 6.534}{.040 \times .040} = 24{,}500 \text{ #/IN}^2$$

$$\frac{F_{cr}}{n} = KE_c\left(\frac{t_s}{b}\right)^2 = 6.3 \times 42.5 \times 10^6 \left(\frac{.040}{3.30}\right)^2 = 39{,}340 \text{ #/IN}^2$$

$$V = \frac{wl}{2} = \frac{6.0 \times 3.30}{2} = 9.90 \text{ #/IN}$$

$$v = \frac{3}{2}\frac{V}{A} = 1.5 \times \frac{9.90}{.040} = 371 \text{ #/IN}^2$$

$$\Delta_{ULT} = \frac{wl^4}{384EI} = \frac{12 \times 6.0 \times 3.30^4}{384 \times 42.5 \times 10^6 \times .04^3} = .0082'' \text{ etc}$$

FROM EM B1-M2-1, ENTITLED, "BERYLLIUM CROSS-ROLLED SHEET DESIGN DATA AT ROOM TEMPERATURE AND 600°F," FIG. 12, THE EFFECT OF INELASTIC BUCKLING REDUCES $F_{cr}$ TO 34,500 #/IN²

$$M.S. = \frac{34{,}500}{24{,}500} - 1 = 0.41$$

Be SUBPANEL #1

STIFFENERS

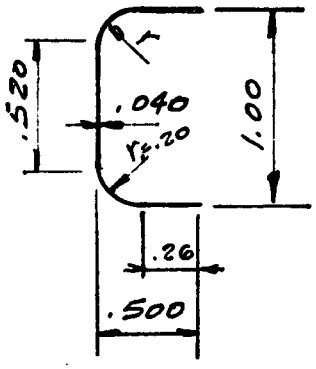


LOADING = +6.0 #/IN² @ R.T.
−4.5 #/IN² @ R.T.

$w_c = 6.0 \times 3.3 = 19.80$ #/IN

$w_b = 4.5 \times 3.3 = 14.85$ #/IN

| b | d | A | y | Ay | y' | A(y')² | $I_o$ | $I_o + A(y')^2$ |
|---|---|---|---|---|---|---|---|---|
| .26 | .040 | .01040 | .020 | .000208 | .480 | .002396 | | |
| .26 | .040 | .01040 | .980 | .010192 | .480 | .002396 | | |
| π × .22 | .040 | .02765 | .500 | .013825 | .400 | .004424 | .000060 | |
| .040 | .520 | .02080 | .500 | .010400 | — | | .000468 | |
| | | .06925 | .500 | .034625 | | | | .009744 ✓ |

FOR COLLAPSE PRESSURE $\quad l = 23''$

$$M = \frac{wl^2}{8} = \frac{19.80 \times 23^2}{8} = 1309 \text{ "\#}$$

$$f_{ULT} = \frac{Mc}{I} = \frac{1309 \times .500}{.009744} = 67{,}170 \text{ \#/IN}^2 \qquad m.s. = +0.12$$

$$\frac{F_{cr}}{n} = 0.385 \times 42.5 \times 10^6 \left(\frac{.040}{.380}\right)^2 = 182{,}000 \text{ \#/IN}^2$$

$$F_{cr} = 53{,}000 \text{ \#/IN}^2$$

FOR BURST PRESSURE

$$f_{ULT} = \frac{4.5}{6.0} \times 67{,}170 = 50{,}380 \text{ \#/IN}^2 \qquad m.s. = +0.05$$

$$f_{yield} = \frac{50{,}380 \div 1.14}{1.5} = 38{,}290 \text{ \#/IN}^2 \qquad m.s. = +0.39$$



FORM LMSC 362 B-2

13e SUBPANEL #1

STIFFENER & FACE SHEET

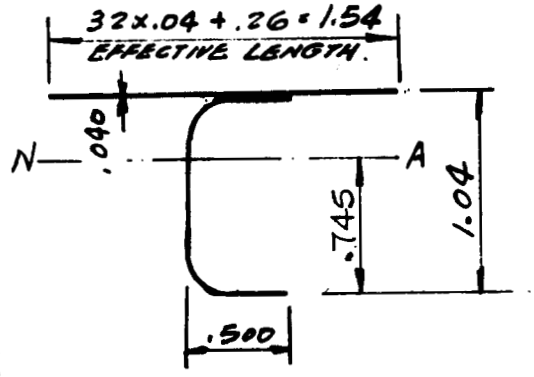


$$\bar{t} = \frac{.06925 + 3.30(.040)}{3.30} = .0610 \text{ in}$$

| | A | y | Ay | y' | A(y')² | $I_o$ | $I_o + A(y')^2$ |
|---|---|---|---|---|---|---|---|
| FACE SHEET 1.54x.04 | .06160 | .520 | .032032 | .275 | .004658 | | |
| STIFFENER | .06925 | 0 | 0 | .245 | .004157 | .009744 | |
| | .13085 | .245 | .032032 | | .008815 | | .01856 ✓ |

FOR COLLAPSE PRESS

$M = 1309$ "# (PAGE 4) $\qquad y_1 = .295 \qquad y_2 = .745$

BENDING STRESSES

$$f_{FACE\ SHEET} = \frac{My_1}{I} = \frac{1309 \times .295}{.01856} = 20{,}810\ \#/IN^2 \text{ COMP. (ULT.)}$$

$$f_{FLANGE} = \frac{My_2}{I} = \frac{1309 \times .745}{.01856} = 52{,}540\ \#/IN^2 \text{ TENSION (ULT.)}$$

M.S. = +0.43

LONGITUDINAL SHEAR AT JOINCTURE

$$V = \frac{wl}{2} = \frac{19.80 \times 23}{2} = 228\ \#$$

$$v = \frac{VQ}{I} = \frac{228 \times .06160 \times .275}{.01856} = 208\ \#/IN \text{ (ULT.)}$$

DEFLECTION FOR LIMIT LOAD, $\quad w = \frac{19.80}{1.5}$

$$\Delta = \frac{5wl^4}{384EI} = \frac{5 \times 19.80 \times 23^4}{1.5 \times 384 \times 42.5 \times 10^6 \times .01856} = 0.061''$$

FOR BURST PRESSURE, $\quad f_{FLANGE} = \frac{4.5}{6.0} \times 52{,}540 = 39{,}400\ \#/IN^2$

M.S. = +0.34



FORM LMSC 362 B-2

Bc SUBPANEL #1

EDGE ANGLE. 1.15 x .95 x .040 Bc.

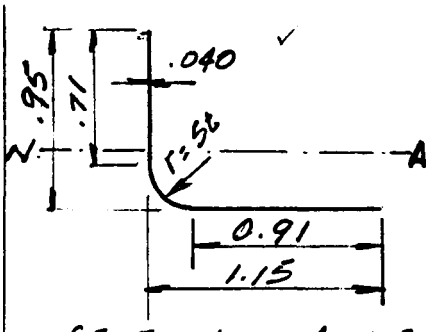


SECTION OF ANGLE

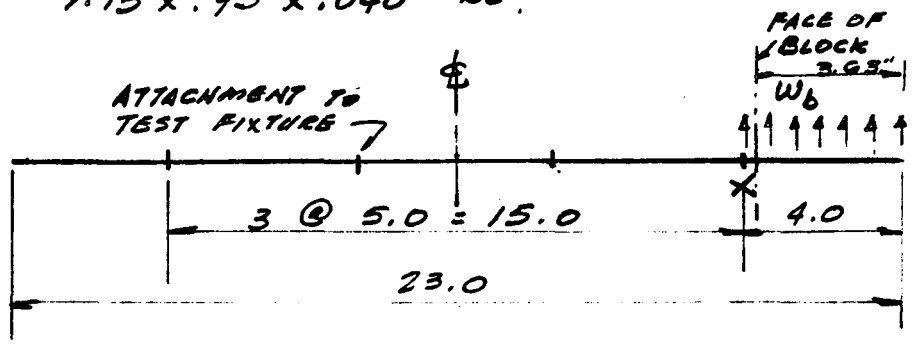


ATTACHMENT LAYOUT AT BOTTOM OF ANGLE

| b | d | A | y | Ay | y' | A(y')² | $I_o$ | $I_o+A(y')^2$ |
|---|---|---|---|---|---|---|---|---|
| 0.910 | 0.040 | .03640 | .020 | .000728 | .222 | .001794 | .000005 | |
| $\frac{\pi}{2}$x.220 | 0.040 | .01382 | .100 | .001382 | .142 | .000279 | .000060 | |
| 0.040 | 0.710 | .02840 | .595 | .016898 | .353 | .003539 | .001193 | |
| | | .078620 | .242 | .019008 | | .005612 | | .006870 |

$w_b = 12 \times 4.5 = 54$ #/IN BURST PRESS (ULT.)

$$M_{\text{FACE OF BLOCK}} = \frac{w_b l^2}{2} = \frac{54 \times 3.63^2}{2} = 356 \text{ "\#}$$

$$f_{\text{BOTTOM FLANGE}} = \frac{My_1}{I} = \frac{356 \times .242}{.00687} = 12{,}530 \text{ \#/IN}^2 \text{ (TENSION)}$$

$$f_{\text{VERT. LEG}} = \frac{My_2}{I} = \frac{356 \times .708}{.00687} = 36{,}690 \text{ \#/IN}^2 \text{ (COMP.)}$$

$$\frac{F_{cr}}{\eta} = 0.385 \times 42.5 \times 10^6 \left(\frac{.040}{.71}\right)^2 = 52{,}000 \text{ \#/IN}^2$$

CORRECTED FOR INELASTIC REDUCTION,

$F_{cr} = 41{,}000$ #/IN² ALLOWED

$$M.S. = \frac{41{,}000}{36{,}690} - 1 = 0.12$$



FORM LMSC 362 B-2

# Appendix C

## STRESS ANALYSIS OF SUBSTRATES

## FOR PROTOTYPE PANEL Nos. 2 THROUGH 4

# TABLE of CONTENTS

1. INTRODUCTION 2

2. DESIGN LOADS ~ SUMMARY 3

3. CONFIGURATION No. 2 ANALYSIS 4

4. CONFIGURATION No. 3 ANALYSIS 11

5. CONFIGURATION No. 4 ANALYSIS 17

6. MAXIMUM STRESSES ~ SUMMARY ~ LINEAR ANALYSIS 24

7. REFERENCES 25

## INTRODUCTION

THE STRUCTURAL PROTOTYPE PANELS, CONFIGURATION NO'S. 2, 3, & 4, WERE OPTIMALLY SIZED FOR THE DESIGN LOAD CONDITIONS BY USE OF THE DIGITAL COMPUTER. THE FOLLOWING ANALYSIS OF THESE PANELS IS, THEREFORE, BASICALLY AN INDEPENDENT CHECK OF THE COMPUTER ANALYSIS. THE PRESSURE LOADS USED IN THIS ANALYSIS ARE, IN MOST CASES, SLIGHTLY LESS THAN THE VALUES WHICH WERE USED IN SIZING THE PANELS; THE SIZING, HOWEVER, HAS NOT BEEN ALTERED.

THE PORTIONS OF THIS WORK WHICH RELATE TO BEARING, FASTENER STRENGTH, AND RIVET SPACING, WERE NOT INCLUDED IN THE COMPUTER ANALYSIS.

THESE PANELS HAVE BEEN FURTHER EVALUATED, AND DEFLECTIONS DETERMINED, UNDER COMBINED PRESSURE & COMPRESSIVE LINE LOAD, BY USE OF THE "BEAM-COLUMN" COMPUTER CODE.



FORM LMSC 362 B-2

| Prepared by: J. R. Ritz | Date 9-29-71 | LOCKHEED MISSILES & SPACE COMPANY<br>A GROUP DIVISION OF LOCKHEED AIRCRAFT CORPORATION | Page C3 |
|---|---|---|---|
| Checked by: E. F. Davis | Date 10-12-71 | Title PROTOTYPE PANELS | Model TPS |
| Approved by: | Date | | Report No. |

DESIGN LOADS ~ SUMMARY (REF. No. 5)

| LOAD COND. | IN PLANE LINE LOAD ~ lb/in | | | | DIFFERENTIAL PRESSURE ~ lb/in² | | | |
|---|---|---|---|---|---|---|---|---|
| | TENSION | | COMPRESSION | | BURST | | COLLAPSE | |
| | LIM. | ULT. | LIM. | ULT. | LIM. | ULT. | LIM. | ULT. |
| **AREA 1 PANELS** | | | | | | | | |
| I | 2400 | 3600 | 2100 | 3150 | 3.0 | 4.5 | 2.0 | 3.0 |
| II | 2700 | 4050 | 4000 | 6000 | 1.5 | 2.25 | 0.9 | 1.35 |
| III | 4000 | 6000 | 2000 | 3000 | 0.5 | 0.75 | 2.0 | 3.0 |
| **AREA 2 PANELS** | | | | | | | | |
| I | 2300 | 3450 | 1500 | 2250 | 3.0 | 4.5 | 4.0 | 6.0 |
| II | 2700 | 4050 | 2000 | 3000 | 1.9 | 2.85 | 1.8 | 2.7 |
| III | 4000 | 6000 | 2000 | 3000 | 0.5 | 0.75 | 2.0 | 3.0 |

NOTES:

1.

| PROTOTYPE PANEL CONFIGURATION No. | LOAD AREA No. | MAX. TEMP. COND. III ~ °F. |
|---|---|---|
| 1 | 2-PRESSURE ONLY | 600 |
| 2 | 2 | 250 |
| 3 | 1 | 250 |
| 4 | 2 | 600 |

2. LOAD CONDITIONS I & II AT ROOM TEMPERATURE

3. LINE LOADS AND PRESSURES ACT IN ANY COMBINATION ON PANEL CONFIGURATIONS 2, 3 & 4

4. FACTOR of SAFETY = 1.5

FORM LMSC 362 B-2

## CONFIGURATION No. 2
## SECTION PROPERTIES

FULL SCALE

D/N SK 90971

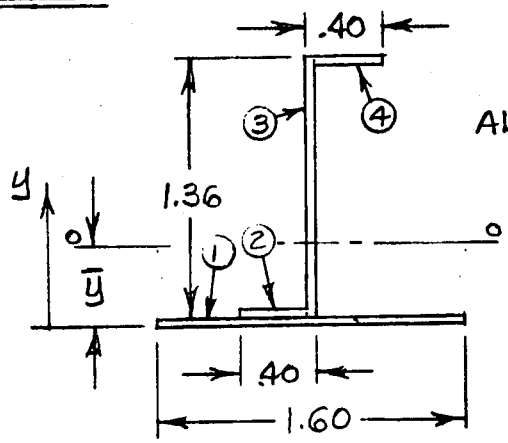


ALL $t = .050$ in

$R = 0.12$ in (MIN.)

$\ell = 24.0$ in

$W_T = 144\,\gamma\,\bar{t}$

$= 144(.101)(.1144)$

$W_T = 1.664$ lb/ft²

| ELEM. | A | y | Ay | d | Ad² | $I_i$ |
|---|---|---|---|---|---|---|
| 1 | .0800 | .025 | .00200 | .3968 | .01260 | .00002 |
| 2 | .0175 | .075 | .00131 | .3468 | .00210 | — |
| 3 | .0680 | .730 | .04964 | .3082 | .00646 | .01048 |
| 4 | .0175 | 1.385 | .02424 | .9632 | .01624 | — |
| Σ | .1830 | | .07719 | | .03740 | .01050 |

$\bar{y} = \frac{.07719}{.1830} = 0.4218$ in ; $\bar{t} = \frac{.1830}{1.60} = 0.1144$ in

$I_o = .03740 + .01050 = .04790$ in⁴ ; $\bar{I}_o = \frac{.04790}{1.60} = .02994$ in⁴/in

$\frac{I_o}{A} = \frac{.04790}{.1830} = 0.2617$ in²

$\rho = (.2617)^{1/2} = 0.5116$ in

$\bar{Z}_{o\,MAX} = .02994/.4218 = .07098$ in³/in

$\bar{Z}_{o\,MIN} = .02994/.9822 = .03048$ in³/in

MATERIAL ~ 7075-T6 - ALUMINUM ALLOY : REF. MIL-HDBK-5A, SECT. 3.2.7

| | R.T. (TAB. 3.2.7.0 (b)) | | 250 °F (5 HRS. EXPOSURE) | |
|---|---|---|---|---|
| $F_{tu}$ = | 77 Ksi | (.82) | 63.1 Ksi | (FIG. 3.2.7.1.1 (a)) |
| $F_{ty}$ = | 67 Ksi | (.85) | 57.0 Ksi | (FIG. 3.2.7.1.1 (b)) |
| $F_{cy}$ = | 68 Ksi | (.89) | 60.5 Ksi | (FIG 3.2.7.1.2 (a)) |
| E = | $10.3 \times 10^3$ Ksi | (.92) | $9.47 \times 10^3$ Ksi | (FIG. 3.2.7.1.4) |
| $E_c$ = | $10.5 \times 10^3$ Ksi | (.92) | $9.66 \times 10^3$ Ksi | (FIG. 3.2.7.1.4) |
| $F_{bru}$ = | 146 Ksi } $\frac{e}{D} = 2$ | (.83) | 121 Ksi | (FIG. 3.2.7.1.3 (a)) |
| $F_{bry}$ = | 107 Ksi } | (.91) | 97.4 Ksi | (FIG. 3.2.7.1.3 (b)) |

$\gamma = 0.101$ lb/in³

FORM LMSC 362 B-2

## CONFIGURATION No. 2

## DESIGN LOADS (AREA 2) (REF. No. 5)

| COND. | $N_x$ ~ ppi | | $p$ ~ psi | |
|---|---|---|---|---|
| | LIMIT | ULT. | LIMIT | ULT. |
| I (R.T.) | 2300<br>-1500 | 3450<br>-2250 | 3.0<br>-4.0 | 4.5<br>-6.0 |
| II (R.T.) | 2700<br>-2000 | 4050<br>-3000 | 1.9<br>-1.8 | 2.85<br>-2.7 |
| III (250°F) | 4000<br>-2000 | 6000<br>-3000 | 0.5<br>-2.0 | 0.75<br>-3.0 |

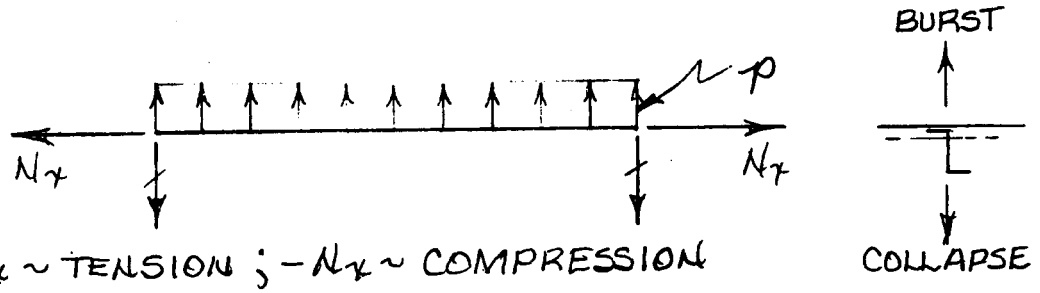


$+N_x$ ~ TENSION ; $-N_x$ ~ COMPRESSION

$+p$ ~ BURST ; $-p$ ~ COLLAPSE

## ALLOW. COLUMN LOADS ~ EULER

$$\bar{P}_{CR} = \frac{\pi^2 E_c \bar{I}_o}{(1-\nu^2)\ell^2} = \frac{\pi^2 E_c (.02994)}{.91(24)^2} = \frac{E_c}{1774}$$

AT R.T.:

$$\bar{P}_{CR} = \frac{10{,}500}{1.774} = 5919 \text{ lb/in}$$

$$\sigma_{CR} = \frac{\bar{P}_{CR}}{\bar{t}} = \frac{5919}{.1144} = 51{,}740 \text{ psi}$$

AT 250° F:

$$\bar{P}_{CR} = \frac{9660}{1.774} = 5445 \text{ lb/in}$$

$$\sigma_{CR} = \frac{5445}{.1144} = 47{,}600 \text{ psi}$$

CONFIGURATION No. 2

MAX. ULTIMATE STRESSES ~ APPLIED

1. COMPRESSIVE $N_x$ & BURST $P$ ~ MAX. $\sigma_c$ ON FREE LEG

REF.: TIMOSHENKO, THEORY of ELASTIC STABILITY, 2ND ED., CHAPTER 1

$$\sigma_{c_{MAX}} = \frac{N_{xc}}{\bar{t}} + \frac{M_{MAX}}{\bar{Z}_{o_{MIN}}}$$

$$M_{MAX} = \frac{P l^2}{8} \cdot \frac{2(1-\cos u)}{u^2 \cos u} = 144 P_B \cdot f(u) \quad \text{(EQN 1-23, REF.)}$$

$$u = \frac{l}{2}\sqrt{\frac{N_{xc}}{E_c \bar{I}_o}} \quad \text{(EQN 1-13, REF.)} \; ; \; f(u) = \frac{1-\cos u}{u^2 \cos u}$$

$$u = \frac{l}{2(I_o \times 10^6)^{1/2}}\left(\frac{N_{xc}}{E_c \times 10^{-6}}\right)^{1/2} = \frac{24}{2(29{,}940)^{1/2}}\left(\frac{N_{xc}}{E_c \times 10^{-6}}\right)^{1/2} = \frac{1}{14.42}\left(\frac{N_{xc}}{E_c \times 10^{-6}}\right)^{1/2}$$

$$u_I = \frac{1}{14.42}\left(\frac{2250}{10.5}\right)^{1/2} = 1.015 \; ; \; u_I^2 = 1.030$$

$$u_{II} = \frac{1}{14.42}\left(\frac{3000}{10.5}\right)^{1/2} = 1.172 \; ; \; u_{II}^2 = 1.374$$

$$u_{III} = \frac{1}{14.42}\left(\frac{3000}{9.66}\right)^{1/2} = 1.222 \; ; \; u_{III}^2 = 1.493$$

| LOAD COND. | $u$ RAD. | $u$ DEG. | $\cos u$ | $1-\cos u$ | $u^2 \cos u$ | $f(u)$ |
|---|---|---|---|---|---|---|
| I | 1.015 | 58°09′ | .5277 | .4723 | .5435 | 0.8690 |
| II | 1.172 | 67°09′ | .3883 | .6117 | .5335 | 1.147 |
| III | 1.222 | 70°01′ | .3418 | .6582 | .5103 | 1.290 |

$$M_{I\,MAX} = 144(4.5)(.8690) = 563.1 \text{ in-lb/in (ULT.)}$$

$$M_{II\,MAX} = 144(2.85)(1.147) = 470.7 \text{ in-lb/in (ULT.)}$$

$$M_{III\,MAX} = 144(0.75)(1.290) = 139.3 \text{ in-lb/in (ULT.)}$$

FORM LMSC 362 B-2

CONFIGURATION No. 2

MAX. ULTIMATE STRESSES ~ APPLIED ~ STIFFENER FREE LEG

1. COMPRESSIVE $N_x$ & BURST $P$ ~ MAX. $\sigma_c$ ON FREE LEG

COND. I: $\sigma_{I\,MAX} = \frac{2250}{.1144} + \frac{563.1}{.03048} = 19{,}670 + 18{,}470 = 38{,}140$ psi (ULT.)

COND. II: $\sigma_{II\,MAX} = \frac{3000}{.1144} + \frac{470.7}{.03048} = 26{,}220 + 15{,}440 = 41{,}660$ psi (ULT.)

COND. III: $\sigma_{III\,MAX} = \frac{3000}{.1144} + \frac{139.3}{.03048} = 26{,}220 + 4570 = 30{,}790$ psi (ULT.)

2. TENSILE $N_x$ & COLLAPSE $P$ ~ MAX. $\sigma_T$ ON FREE LEG

USE DIRECT SUPERPOSITION OF TENSION & BENDING

$$\sigma_{T\,MAX} = \frac{N_{xT}}{t} + \frac{M_{MAX}}{Z_{o\,MIN}} = \frac{N_{xT}}{t} + \frac{P_{MAX}\,l^2}{8 Z_{o\,MIN}} = \frac{N_{xT}}{t} + \frac{72\,P_{MAX}}{Z_{o\,MIN}}$$

COND. I: $\sigma_{I\,MAX} = \frac{3450}{.1144} + \frac{72(6.0)}{.03048} = 30{,}160 + 14{,}170 = 44{,}330$ psi (ULT.)

COND. II: $\sigma_{II\,MAX} = \frac{4050}{.1144} + \frac{72(2.7)}{.03048} = 35{,}400 + 6378 = 41{,}780$ psi (ULT.)

COND. III: $\sigma_{III\,MAX} = \frac{6000}{.1144} + \frac{72(3.0)}{.03048} = 52{,}450 + 7087 = 59{,}540$ psi (ULT.)

ALLOWABLE CRIPPLING STRESSES ~ STIFFENER FREE LEG

REF. STRESS MEMO NO. 126: $b/t = (.40 - .12)/.05 = 5.6$

$F_{cc}$ = 37 (FIG. 12, REF.) (CONSERVATIVE: $t$ IN $b$)

MCF

AT R.T.: $F_{cy}/E_c = 68/10{,}500 = .00648$

$K_m = .0190$ (FIG. 15, REF.)

MCF = .0190 (68) = 1.292

$F_{cc}$ = 1.292 ( 37 ) = 47.8 Ksi

AT 250°F: $F_{cy}/E_c = 60.5/9660 = .00626$

$K_m = .0195$ (FIG. 15, REF.)

MCF = .0195 (60.5) = 1.180

$F_{cc}$ = 1.180 ( 37 ) = 43.7 Ksi

FORM LMSC 362 B-2

CONFIGURATION No. 2

## MARGINS of SAFETY ~ ULTIMATE

### 1. MAX. COMPRESSION ON STIFFENER FREE LEG

$$M.S. = \frac{F_{cc}}{\sigma_{c\,MAX\,(ULT)}} - 1$$

COND. I: $M.S. = \frac{47.8}{38.14} - 1 = 1.253 - 1 =$ **+ 0.25** CRIPPLING-ULT.

COND. II: $M.S. = \frac{47.8}{41.66} - 1 = 1.147 - 1 =$ **+ 0.15** CRIPPLING-ULT.

COND. III: $M.S. = \frac{43.7}{30.79} - 1 = 1.419 - 1 =$ **+ 0.42** CRIPPLING-ULT.

### 2. MAX. TENSION ON STIFFENER FREE LEG

$$M.S. = \frac{F_{tu}}{\sigma_{t\,MAX\,(ULT)}} - 1$$

COND. I: $M.S. = \frac{77}{44.33} - 1 = 1.737 - 1 =$ **+ 0.74** TENS.-ULT.

COND. II: $M.S. = \frac{77}{41.78} - 1 = 1.843 - 1 =$ **+ 0.84** TENS.-ULT.

COND. III: $M.S. = \frac{63.1}{59.54} - 1 = 1.060 - 1 =$ **+ 0.06** TENS.-ULT.

| Prepared by: J. R. Ritz | Date 9-30-71 | LOCKHEED MISSILES & SPACE COMPANY<br>A GROUP DIVISION OF LOCKHEED AIRCRAFT CORPORATION | Page C 9 Temp. Perm. |
|---|---|---|---|
| Checked by: E. F. Davis | Date 10-12-71 | Title PROTOTYPE PANELS DESIGN & ANALYSIS | Model TPS |
| Approved by: | Date | | Report No. |

CONFIGURATION No. 2

MAX. FACE SHEET COMP. STRESSES ~ ULTIMATE

COMBINE COMP. $N_x$ & COLLAPSE $p$

BEAM-COLUMN ANALYSIS (REF. p.6)

$$\sigma_{c_{MAX}} = \frac{N_{xc}}{\bar{t}} + \frac{M_{MAX}}{\bar{Z}_{o_{MAX}}} \; ; \; M_{MAX} = 72\, p_c \cdot 2 f(u)$$

COND. I: $\sigma_{c_{MAX}} = \frac{2250}{.1144} + \frac{72(6)(1.738)}{.07098} = 19{,}670 + 10{,}580 = 30{,}250$ psi (ULT.)

COND. II: $\sigma_{c_{MAX}} = \frac{3000}{.1144} + \frac{72(2.7)(1.294)}{.07098} = 26{,}220 + 3544 = 29{,}760$ psi (ULT.)

COND. III: $\sigma_{c_{MAX}} = \frac{3000}{.1144} + \frac{72(3)(2.580)}{.07098} = 26{,}220 + 7852 = 34{,}070$ psi (ULT.)

FORM LMSC 362 B-2

CONFIGURATION No. 2

BEARING IN STRINGER ENDS: 6 No. 10 JO-BOLTS PER END

MAX. STRINGER LOAD ~ $P_{MAX}$: COND. III CRITICAL (REF. p. 7)

AT 250°F: $P_{MAX} = \sigma_{MAX} A_{STR} = 52{,}450\,(.1030) = 5402$ lb (ULT)

ALLOW. BEARING LOAD ~ PER END

$$A_{br} = 6(.190)(.050) = .05700 \text{ in}^2$$

AT 250°F.: $P_{br_{ALL}} = A_{br} F_{br_u} = .05700\,(121 \times 10^3) = 6897$ lb (ULT.)

MARGIN of SAFETY

$$M.S. = \frac{P_{br_{ALL}}}{P_{MAX}} - 1 = \frac{6897}{5402} - 1 = 1.277 - 1 = \underline{+0.28}$$

BEARING-ULT.

SKIN STABILITY ANALYSIS: COND. III CRITICAL; T = 250°F

MAX. COMP. STRESS, $\sigma_{c_{MAX}} = 34{,}070$ psi (ULT.) (FROM p. 9)

SKIN BUCKLING STRESS ~ $F_{c_{CR}}$; REF. S.M. 80 c

AT R.T.: $k_2 = .0816$; $n = 15$; $F_{0.7} = 70$ Ksi (TAB. II, REF.)

$b/t = 1.60/.050 = 32$ : $\sqrt{K} = 2.51$ (FIG. 3, CASE ⑥, REF.)

$(b/t)_e = 32/2.51 = 12.75$

$B = .0816\,(12.75) = 1.040$

$F/F_{0.7} = 0.84$ (FIG. 2, REF.)

$F_{c_{CR}} = 0.84\,(70) = 58.8$ Ksi

AT 250°F: ASSUME $F_{c_{CR\,250°}} = F_{c_{CR\,R.T.}} \times \frac{E_{c_{RT}}}{E_{c_{250°}}} = 58.8\,(.92) = 54.1$ Ksi (REF. p. 4)

MARGIN of SAFETY

$$M.S. = \frac{F_{c_{CR}}}{\sigma_{c_{MAX}}} - 1 = \frac{54.1}{34.07} - 1 = 1.588 - 1 = \underline{+0.59}$$

BUCKLING-ULT.

FORM LMSC 362 B-2

| Prepared by: J. R. Ritz | Date 9-7-71 | LOCKHEED MISSILES & SPACE COMPANY<br>A GROUP DIVISION OF LOCKHEED AIRCRAFT CORPORATION | Page C 11 Temp. Perm. |
|---|---|---|---|
| Checked by: E. F. Davis | Date 10-12-71 | Title PROTOTYPE PANELS | Model TPS |
| Approved by: | Date | DESIGN & ANALYSIS | Report No. |

## CONFIGURATION No. 3

### SECTION PROPERTIES

FULL SCALE

D/N SK 91071

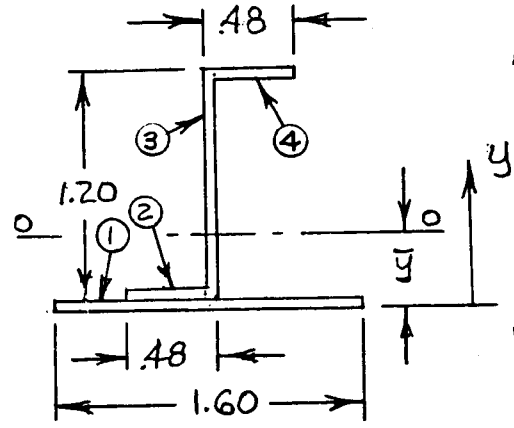


ALL $t = .063$ in

$R = 0.16$ in (MIN.)

$l = 20.0$ in

$W_T = 144(.101)(.1431)$

$W_T = 2.081$ lb/ft$^2$

| ELEM. | A | y | Ay | d | $Ad^2$ | $I_i$ |
|---|---|---|---|---|---|---|
| 1 | .1008 | .0315 | .00318 | .3563 | .01280 | .00003 |
| 2 | .0263 | .0945 | .00249 | .2906 | .00222 | —— |
| 3 | .0756 | .663 | .05012 | .2779 | .00584 | .00907 |
| 4 | .0263 | 1.232 | .03240 | .8469 | .01886 | —— |
| Σ | .2290 | | .08819 | | .03972 | .00910 |

$\bar{y} = \frac{.08819}{.2290} = 0.3851$ in ; $\bar{t} = \frac{.2290}{1.60} = 0.1431$ in

$C_1 = \bar{y} = 0.3851$ in ; $C_2 = 1.263 - \bar{y} = 0.8779$ in

$I_o = .03972 + .00910 = .04882$ in$^4$

$\bar{I}_o = \frac{.04882}{1.60} = .03051$ in$^4$/in

$\bar{Z}_{o\,MAX} = \frac{.03051}{.3851} = .07923$ in$^3$/in

$\bar{Z}_{o\,MIN} = \frac{.03051}{.8779} = .03475$ in$^3$/in

MATERIAL ~ 7075-T6

PROPERTIES GIVEN ON p.4 FOR ROOM TEMP. & 250°F.

FORM LMSC 362 B-2

CONFIGURATION No. 3

DESIGN LOADS (AREA 1) (REF. No. 5)

| COND. | $N_x$ ~ ppi | | $p$ ~ psi | |
|---|---|---|---|---|
| | LIMIT | ULT. | LIMIT | ULT. |
| I (R.T.) | 2400<br>-2100 | 3600<br>-3150 | 3.0<br>-2.0 | 4.5<br>-3.0 |
| II (R.T.) | 2700<br>-4000 | 4050<br>-6000 | 1.5<br>-0.9 | 2.25<br>-1.35 |
| III (250°F) | 4000<br>-2000 | 6000<br>-3000 | 0.5<br>-2.0 | 0.75<br>-3.0 |

SEE p. 2 FOR SIGN CONVENTIONS

ALLOW. COLUMN LOADS ~ EULER (REF. p. 5)

AT R.T.: $\bar{P}_{CR} = \dfrac{\pi^2 (10.5 \times 10^3)(30.51)}{.91(400)} = 8687$ lb/in

$\sigma_{CR} = \dfrac{8687}{.1431} = 60{,}700$ psi

AT 250°F: $\bar{P}_{CR} = .92(8687) = 7905$ lb/in

$\sigma_{CR} = \dfrac{7905}{.1431} = 55{,}240$ psi

ALLOW. CRIPPLING STRESSES ~ STIFFENER FREE LEG

$b = .48 - R - t = .48 - .16 - .063 = .257$ in : $b/t = .257/.063 = 4.08$

$\dfrac{F_{cc}}{MCF} = 47.5$ Ksi (REF. S.M. 126, FIG. 12)

AT R.T.: MCF = 1.292 (FROM p. 4)

$F_{cc} = 1.292(47.5) = 61.4$ Ksi

AT 250°F: MCF = 1.180 (FROM p. 4)

$F_{cc} = 1.180(47.5) = 56.0$ Ksi

## CONFIGURATION No. 3

### MAX. BENDING MOMENTS ~ FOR COMP. $N_x$ & BURST $p$

BEAM-COLUMN ANALYSIS (REF. p. 6)

$$M_{MAX} = \frac{wl^2}{8} \cdot 2f(u) = 50 p_B \cdot 2f(u) \; ; \; f(u) \equiv \frac{1-\cos u}{u^2 \cos u}$$

$$u = \frac{l}{2}\left(\frac{N_{xc}}{E_c \bar{I}_o}\right)^{1/2} = \frac{20}{2} \cdot \frac{1}{(30{,}510)^{1/2}} \cdot \left(\frac{N_{xc}}{E_c \times 10^{-6}}\right)^{1/2} = \frac{1}{17.47}\left(\frac{N_{xc}}{E_c \times 10^{-6}}\right)^{1/2}$$

$$u_I = \frac{1}{17.47}\left(\frac{3150}{10.5}\right)^{1/2} = 0.9914 \; ; \; u_I^2 = 0.9830 \; ; \; u_I(\text{DEG.}) = 56°48'$$

$$u_{II} = \frac{1}{17.47}\left(\frac{6000}{10.5}\right)^{1/2} = 1.368 \; ; \; u_{II}^2 = 1.872 \; ; \; u_{II}(\text{DEG.}) = 78°23'$$

$$u_{III} = \frac{1}{17.47}\left(\frac{3000}{9.66}\right)^{1/2} = 1.009 \; ; \; u_{III}^2 = 1.018 \; ; \; u_{III}(\text{DEG.}) = 57°49'$$

| $u$ | $\cos u$ | $1-\cos u$ | $u^2 \cos u$ | $f(u)$ | $2f(u)$ |
|---|---|---|---|---|---|
| 56°48' | .5476 | .4524 | .5383 | .8404 | 1.681 |
| 78° 23' | .2014 | .7986 | .3770 | 2.118 | 4.237 |
| 57°49' | .5326 | .4674 | .5422 | .8620 | 1.724 |

$$M_{I\,MAX} = 50(4.5)(1.681) = 378.2 \text{ in-lb/in (ULT.)}$$
$$M_{II\,MAX} = 50(2.25)(4.237) = 476.7 \text{ in-lb/in (ULT.)}$$
$$M_{III\,MAX} = 50(0.75)(1.724) = 64.6 \text{ in-lb/in (ULT.)}$$

### MAX. FACE SHEET COMP. STRESSES ~ COMP. $N_x$ & COLLAPSE $p$

$$\sigma_{c_{max}} = \frac{N_{xc}}{t} + \frac{M_{MAX}}{\bar{Z}_{OMAX}} = \frac{N_{xc}}{.1431} + \frac{50 p_c \, 2f(u)}{.07923}$$

COND. I: $\sigma_{c_{I\,MAX}} = \frac{3150}{.1431} + \frac{50(3)(1.681)}{.07923} = 22{,}010 + 3183 = 25{,}190$ psi (ULT)

COND. II: $\sigma_{c_{II\,MAX}} = \frac{6000}{.1431} + \frac{50(1.35)(4.237)}{.07923} = 41{,}930 + 3610 = 45{,}540$ psi (ULT)

COND. III: $\sigma_{c_{III\,MAX}} = \frac{3000}{.1431} + \frac{50(3)(1.724)}{.07923} = 20{,}960 + 3264 = 24{,}220$ psi (ULT)

FORM LMSC 362 B-2

CONFIGURATION No. 3

MAX. ULTIMATE STRESSES ~ APPLIED ~ STIFFENER FREE LEG

1. MAX. COMPRESSIVE STRESSES ~ $\sigma_{c\,max}$ ~ ON FREE LEG

COMBINE COMP. $N_x$ & BURST $p$: BEAM-COLUMN ANALYSIS

$$\sigma_{c\,max} = \frac{N_{xc}}{t} + \frac{M_{max}}{Z_{o\,min}} \quad : M_{max} \text{ FROM p.13}$$

COND. I: $\sigma_{c\,I\,max} = \frac{3150}{.1431} + \frac{378.2}{.03475} = 22{,}010 + 10{,}880 = 32{,}890$ psi (ULT)

COND. II: $\sigma_{c\,II\,max} = \frac{6000}{.1431} + \frac{476.7}{.03475} = 41{,}930 + 13{,}720 = 55{,}650$ psi (ULT)

COND. III: $\sigma_{c\,III\,max} = \frac{3000}{.1431} + \frac{64.6}{.03475} = 20{,}960 + 1859 = 22{,}820$ psi (ULT)

2. MAX. TENSILE STRESSES ~ $\sigma_{T\,max}$ ~ ON FREE LEG

COMBINE TENS. $N_x$ & COLLAPSE $p$: DIRECT SUPERPOSITION

$$\sigma_{T\,max} = \frac{N_{xT}}{t} + \frac{50\,P_{col.}}{Z_{o\,min}}$$

COND. I: $\sigma_{T\,I\,max} = \frac{3600}{.1431} + \frac{50(3.0)}{.03475} = 25{,}160 + 4317 = 29{,}480$ psi (ULT)

COND. II: $\sigma_{T\,II\,max} = \frac{4050}{.1431} + \frac{50(1.35)}{.03475} = 28{,}300 + 1942 = 30{,}240$ psi (ULT)

COND. III: $\sigma_{T\,III\,max} = \frac{6000}{.1431} + \frac{50(3.0)}{.03475} = 41{,}930 + 4317 = 46{,}250$ psi (ULT)

CONFIGURATION No. 3

MARGINS of SAFETY ~ ULTIMATE

1. MAX. COMPRESSION ON STIFFENER FREE LEG

$$M.S. = \frac{F_{cc}}{\sigma_{c\,MAX\,(ULT)}} - 1$$

COND. I: $M.S. = \frac{61.4}{32.89} - 1 = 1.867 - 1 = \underline{+0.87}$ CRIPPLING - ULT.

COND. II: $M.S. = \frac{61.4}{55.65} - 1 = 1.103 - 1 = \underline{+0.10}$ CRIPPLING - ULT.

COND. III: $M.S. = \frac{56.0}{22.82} - 1 = 2.454 - 1 = \underline{+1.5}$ CRIPPLING - ULT.

2. MAX. TENSION ON STIFFENER FREE LEG

$$M.S. = \frac{F_{tu}}{\sigma_{T\,MAX\,(ULT)}} - 1$$

COND. I: $M.S. = \frac{77}{29.48} - 1 = 2.612 - 1 = \underline{+1.6}$ TENS. - ULT.

COND. II: $M.S. = \frac{77}{30.24} - 1 = 2.546 - 1 = \underline{+1.5}$ TENS. - ULT.

COND. III: $M.S. = \frac{63.1}{46.25} - 1 = 1.364 - 1 = \underline{+0.36}$ TENS. - ULT.

FORM LMSC 362 B-2

CONFIGURATION No. 3

BEARING IN STRINGER ENDS

MAX. STRINGER LOAD ~ $P_{MAX}$ : COND. III CRITICAL (REF. p.14)

AT 250°F.: $P_{MAX} = \sigma_{MAX} A_{STR} = 41{,}930(.1282) = 5375$ lb (ULT.)

ALLOW. BEARING LOAD ~ PER END

$$A_{br} = 6(.190)(.063) = .07182 \text{ in}^2$$

AT 250°F.: $P_{br\,ALL} = A_{br} F_{br\,u} = .07182(121 \times 10^3) = 8690$ lb (ULT.)

MARGIN of SAFETY

$$M.S. = \frac{P_{br\,ALL}}{P_{MAX}} - 1 = \frac{8690}{5375} - 1 = 1.617 - 1 = \underline{+0.62}$$

BEARING - ULT.

SKIN STABILITY ANALYSIS: COND. II CRITICAL ; T = R.T.

MAX. COMP. STRESS, $\sigma_{c\,max} = 45{,}540$ psi (ULT) (FROM p. 13)

SKIN BUCKLING STRESS ~ $F_{c\,cr}$ : REF. S.M. 80c

$k_2 = .0816$ ; $n = 15$ ; $F_{0.7} = 70$ Ksi (TAB. II, REF.)
$b/t = 1.60/.063 = 25.4$ : $\sqrt{K} = 2.51$ (FIG. 3, CASE ⑥, REF.)
$(b/t)e = 25.4/2.51 = 10.12$
$B = .0816(10.12) = 0.826$
$F/F_{0.7} = 0.97$ (FIG. 2, REF.)
$F_{c\,cr} = 0.97(70) = 67.9$ Ksi

MARGIN of SAFETY

$$M.S. = \frac{F_{c\,cr}}{\sigma_{c\,max}} - 1 = \frac{67.9}{45.54} - 1 = 1.491 - 1 = \underline{+0.49}$$

BUCKLING - ULT.

FORM LMSC 362 B-2

## CONFIGURATION No. 4
## SECTION PROPERTIES

FULL SCALE

D/N SK 91371

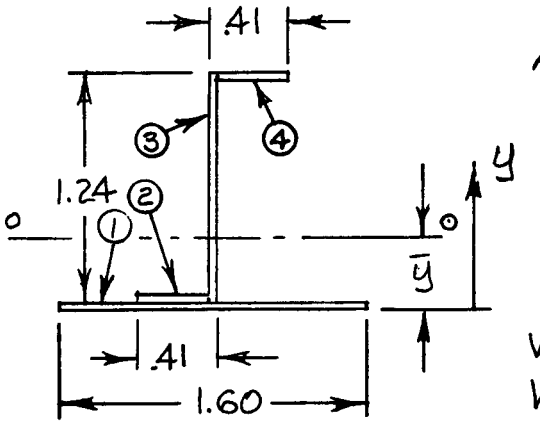


ALL $t = .040$ in
$R = 0.12$ in
$l = 24.0$ in

$W_T = 144(.0895)(.160)$
$W_T = 2.062$ lb/ft²

| ELEM. | A | y | Ay | d | Ad² | $I_i$ |
|---|---|---|---|---|---|---|
| 1 | .0640 | .020 | .00128 | .3540 | .00820 | .00001 |
| 2 | .0148 | .060 | .00089 | .3140 | .00146 | — |
| 3 | .0496 | .660 | .03274 | .2860 | .00406 | .00636 |
| 4 | .0148 | 1.260 | .01865 | .8860 | .01162 | — |
| Σ | .1432 | | .05356 | | .02534 | .00637 |

$\bar{y} = \frac{.05356}{.1432} = 0.3740$ in ; $\bar{t} = \frac{.1432}{1.60} = .08950$ in

$I_o = .03171$ in⁴ ; $\bar{I}_o = .03171/1.60 = .01982$ in⁴/in

$\bar{Z}_{o\,MAX} = .01982/.3740 = .05299$ in³/in ; $\bar{Z}_{o\,MIN} = .01982/.9060 = .02188$ in³/in

MATERIAL ~ 6AL-4V ANNEALED - TITANIUM ALLOY
REF. MIL-HDBK-5A, SECT. 5.4.6

| R.T. (TAB. 5.4.6.1(a)) | | | 600°F | |
|---|---|---|---|---|
| $F_{tu}$ = 134 Ksi | (.74) | | 99.2 Ksi | (FIG. 5.4.6.2.1(a)) |
| $F_{ty}$ = 126 Ksi | (.67) | | 84.4 Ksi | (FIG. 5.4.6.2.1(b)) |
| $F_{cy}$ = 132 Ksi | (.68) | | 89.8 Ksi | (FIG. 5.4.6.2.2(a)) |
| $E$ = 16.0x10³ Ksi | (.82) | | 13.1x10³ Ksi | (FIG. 5.4.6.2.4) |
| $E_c$ = 16.4x10³ Ksi | (.82) | | 13.4x10³ Ksi | (FIG. 5.4.6.2.4) |
| $F_{bru}$ = 252 Ksi | (.75) | $\frac{e}{D}=2$ | 189 Ksi | (FIG. 5.4.6.2.3(a)) |
| $F_{bry}$ = 208 Ksi | (.69) | | 156 Ksi | (FIG. 5.4.6.2.3(b)) |

$\gamma = 0.160$ lb/in³

FORM LMSC 362 B-2

## CONFIGURATION No. 4
## DESIGN LOADS (AREA 2)

SAME DESIGN LOAD CONDITIONS AS FOR CONFIGURATION NO. 2, GIVEN ON p. 5, EXCEPT THAT FOR LOAD CONDITION III, THE MAX. TEMP. IS 600° F.

### ALLOWABLE COLUMN LOADS ~ EULER (REF. p.5)

AT R.T.: $\bar{P}_{CR} = \dfrac{\pi^2 (16.4 \times 10^3)(19.82)}{.91(576)} = 6121$ lb/in

$\sigma_{CR} = \dfrac{6121}{.08950} = 68{,}390$ psi

AT 600° F: $\bar{P}_{CR} = .82(6121) = 5019$ lb/in

$\sigma_{CR} = \dfrac{5019}{.08950} = 56{,}080$ psi

### ALLOWABLE CRIPPLING STRESSES ~ STIFFENER FREE LEG

REF. S.M. 126

$b = .41 - .12 = 0.29$ in; $b/t = .29/.04 = 7.25$ (CONSERVATIVE, t IN b)

$\dfrac{F_{cc}}{MCF} = 29.0$ Ksi (FIG. 12, REF.)

AT R.T.: MCF = 2.234 (TAB. I, REF.)

$F_{cc} = 2.234(29.0) = 64.79$ Ksi

AT 600° F.: MCF = 1.659 (TAB. I, REF.)

$F_{cc} = 1.659(29.0) = 48.11$ Ksi

CONFIGURATION No. 4

MAX. BENDING MOMENTS ~ FOR COMP. $N_x$ & BURST $p$

BEAM-COLUMN ANALYSIS (REF. p. 13)

$$M_{MAX} = \frac{w l^2}{8} \cdot 2f(u) = 72\, p_B \cdot 2f(u); \quad f(u) \equiv \frac{1-\cos u}{u^2 \cos u}$$

$$u = \frac{l}{2}\left(\frac{N_{xc}}{E_c \bar{I}_o}\right)^{1/2} = \frac{24}{2}\,\frac{1}{(19{,}820)^{1/2}}\left(\frac{N_{xc}}{E_c \times 10^{-6}}\right)^{1/2} = \frac{1}{11.73}\left(\frac{N_{xc}}{E_c \times 10^{-6}}\right)^{1/2}$$

$$u_I = \frac{1}{11.73}\left(\frac{2250}{16.4}\right)^{1/2} = 0.9986; \quad u_I^2 = 0.9972; \quad u_I\,(\text{DEG.}) = 57°13'$$

$$u_{II} = \frac{1}{11.73}\left(\frac{3000}{16.4}\right)^{1/2} = 1.153; \quad u_{II}^2 = 1.329; \quad u_{II}\,(\text{DEG}) = 66°04'$$

$$u_{III} = \frac{1}{11.73}\left(\frac{3000}{13.4}\right)^{1/2} = 1.276; \quad u_{III}^2 = 1.628; \quad u_{III}\,(\text{DEG}) = 73°07'$$

| $u$ | $\cos u$ | $1-\cos u$ | $u^2 \cos u$ | $f(u)$ | $2f(u)$ |
|---|---|---|---|---|---|
| 57°13' | .5415 | .4585 | .5400 | .8491 | 1.698 |
| 66°04' | .4057 | .5943 | .5392 | 1.102 | 2.204 |
| 73°07' | .2904 | .7096 | .4728 | 1.501 | 3.002 |

$M_{I\,MAX} = 72(4.5)(1.698) = 550.2$ in-lb/in (ULT.)

$M_{II\,MAX} = 72(2.85)(2.204) = 452.3$ in-lb/in (ULT.)

$M_{III\,MAX} = 72(0.75)(3.002) = 162.1$ in-lb/in (ULT.)

MAX. FACE SHEET COMP. STRESSES ~ COMP. $N_x$ & COLLAPSE $p$

$$\sigma_{c\,MAX} = \frac{N_{xc}}{\bar{t}} + \frac{M_{MAX}}{\bar{Z}_{o\,MAX}} = \frac{N_{xc}}{.08950} + \frac{72\, p_c\, 2f(u)}{.05299}$$

COND. I: $\sigma_{c\,I\,MAX} = \frac{2250}{.08950} + \frac{72(6)(1.698)}{.05299} = 25{,}140 + 13{,}840 = 38{,}980$ psi (ULT.)

COND. II: $\sigma_{c\,II\,MAX} = \frac{3000}{.08950} + \frac{72(3.7)(2.204)}{.05299} = 33{,}520 + 8086 = 41{,}610$ psi (ULT.)

COND. III: $\sigma_{c\,III\,MAX} = \frac{3000}{.08950} + \frac{72(3)(3.002)}{.05299} = 33{,}520 + 12{,}240 = 45{,}760$ psi (ULT.)

FORM LMSC 362 B-2

CONFIGURATION No. 4

MAX. ULTIMATE STRESSES ~ APPLIED ~ STIFFENER FREE LEG

1. MAX. COMPRESSIVE STRESSES ~ $\sigma_{c\,max}$ ~ ON FREE LEG

COMBINE COMP. $N_x$ & BURST $p$ : BEAM-COLUMN ANALYSIS

$$\sigma_{c\,max} = \frac{N_{xc}}{\bar{t}} + \frac{M_{max}}{\bar{Z}_{o\,min}} \quad : M_{max} \text{ FROM p. 19}$$

COND. I: $\sigma_{cI\,max} = \frac{2250}{.08950} + \frac{550.2}{.02188} = 25{,}140 + 25{,}150 = 50{,}290$ psi (ULT)

COND. II: $\sigma_{cII\,max} = \frac{3000}{.08950} + \frac{452.3}{.02188} = 33{,}520 + 20{,}670 = 54{,}190$ psi (ULT)

COND. III: $\sigma_{cIII\,max} = \frac{3000}{.08950} + \frac{162.1}{.02188} = 33{,}520 + 7409 = 40{,}930$ psi (ULT)

2. MAX. TENSILE STRESSES ~ $\sigma_{T\,max}$ ~ ON FREE LEG

COMBINE TENS. $N_x$ & COLLAPSE $p$ : DIRECT SUPERPOSITION

$$\sigma_{T\,max} = \frac{N_{xT}}{\bar{t}} + \frac{M_{max}}{\bar{Z}_{o\,min}} = \frac{N_{xT}}{.08950} + \frac{72\,P_{col.}}{.02188}$$

COND. I: $\sigma_{TI\,max} = \frac{3450}{.08950} + \frac{72(6.0)}{.02188} = 38{,}550 + 19{,}740 = 58{,}290$ psi (ULT)

COND. II: $\sigma_{TII\,max} = \frac{4050}{.08950} + \frac{72(2.7)}{.02188} = 45{,}250 + 8885 = 54{,}130$ psi (ULT)

COND. III: $\sigma_{TIII\,max} = \frac{6000}{.08950} + \frac{72(3.0)}{.02188} = 67{,}040 + 9872 = 76{,}910$ psi (ULT)

FORM LMSC 362 B-2

CONFIGURATION No. 4

MARGINS of SAFETY ~ ULTIMATE

1. MAX. COMPRESSION ON STIFFENER FREE LEG

$$M.S. = \frac{F_{cc}}{\sigma_{c\,MAX}\ (ULT)} - 1$$

COND. I: $M.S. = \frac{64.79}{50.29} - 1 = 1.288 - 1 = +0.29$ CRIPPLING-ULT.

COND. II: $M.S. = \frac{64.79}{54.19} - 1 = 1.196 - 1 = +0.20$ CRIPPLING-ULT.

COND. III: $M.S. = \frac{48.11}{40.93} - 1 = 1.175 - 1 = +0.18$ CRIPPLING-ULT.

2. MAX. TENSION ON STIFFENER FREE LEG

$$M.S. = \frac{F_{tu}}{\sigma_{T\,MAX}\ (ULT)} - 1$$

COND. I: $M.S. = \frac{134}{58.29} - 1 = 2.299 - 1 = +1.3$ TENS.-ULT.

COND. II: $M.S. = \frac{134}{54.13} - 1 = 2.476 - 1 = +1.5$ TENS.-ULT.

COND. III: $M.S. = \frac{99.2}{76.91} - 1 = 1.290 - 1 = +0.29$ TENS.-ULT.

FORM LMSC 362 B-2

# CONFIGURATION No. 4
## FASTENER ANALYSIS

1. INTER-RIVET BUCKLING ~ MAX. ALLOW. SPACING, S

MAX SKIN COMPRESSIVE STRESSES ~ $\sigma_{sc_{MAX}}$ (FROM p. 19)

AT R.T. (COND. II): $\sigma_{sc_{MAX}} = 41{,}610$ psi (ULT)

AT 600°F. (COND. III): $\sigma_{sc_{MAX}} = 45{,}760$ psi (ULT.)

SPACING ~ S : COND. III CRITICAL

$l'/\rho = 54$ (REF. S.M. 83 b, FIG. 29, CURVE ⑤)

$\frac{s}{t} = .577 \frac{l'}{\rho}$ (REF. S.M. 80 C, p.8, NOTE 5)

$S = .577(54)(.04) = 1.25$ in (MAX.) : USE $S = 1.0$ in ; 3/32 MONEL RIVETS

2. BEARING IN STRINGER ENDS ~ SIX No. 10's PER END: JO-BOLTS

MAX. STRINGER LOADS ~ $P_{MAX}$ : COND. III CRITICAL (REF p.20)

AT 600°F: $P_{MAX} = \sigma_{MAX} A_{STR} = 67{,}040(.0792) = 5310$ lb (ULT.)

ALLOW. BEARING LOAD ~ PER END

AT 600°F: $P_{br_{ALL}} = A'_{br} F_{br_u} = 6(.190)(.04)(189 \times 10^3) = 8618$ lb (ULT.)

MARGIN of SAFETY

$$M.S. = \frac{P_{br_{ALL}}}{P_{MAX}} - 1 = \frac{8618}{5310} - 1 = 1.623 - 1 = \underline{\underline{+0.62}}$$

BEARING - ULT.

3. SHEAR ON JO-BOLTS : LS 8892 F6-2, MAT'RL A-286 CRES
D = 3/16 in (REF: PPH, p.1-10.3)

AT R.T.: ALLOW. SINGLE SHEAR (ULT.), $V_{ALL_u} = 2150$ lb (MIL-HDBK-5A, TAB. 8.1.4.2.1(d))

AT 600°F: $V_{ALL_u} = .91(2150) = 1956$ lb (M-H-5A, FIG. 8.1.4.2.1(e))

$$M.S. = \frac{6 V_{ALL_u}}{P_{MAX}} - 1 = \frac{6(1956)}{5310} - 1 = 2.210 - 1 = \underline{\underline{+1.2}}$$

SHEAR - ULT.

FORM LMSC 362 B-2

## CONFIGURATION No. 4

SKIN STABILITY ANALYSIS : COND. III CRITICAL ; T = 600°F

MAX. SKIN COMP. STRESS ~ $\sigma_{SC_{MAX}}$ = 45,760 psi (ULT) (FROM p.19)

SKIN BUCKLING STRESS ~ $F_{CCR}$ REF. S.M. 80 C

AT 600°F : $k_2 = .0820$, $n = 30$, $F_{0.7} = 90.09$ Ksi } TAB II, REF.

$\frac{b}{t} = \frac{1.2}{.04} = 30$

SIMPLE SUPPORT : $\sqrt{K} = 1.90$
CLAMPED : $\sqrt{K} = 2.51$ } FIG. 3, REF.

ASSUME $\sqrt{K} = 1.90$

$(b/t)_e = 30/1.90 = 15.78$

$B = .0820\,(15.78) = 1.292$

$\frac{F}{F_{0.7}} = 0.515$ (FIG. 2, REF.)

$F_{CCR} = 0.515\,(90.09) = 46.40$ Ksi

MARGIN of SAFETY

$$M.S. = \frac{F_{CCR}}{\sigma_{SC_{MAX}}} - 1 = \frac{46.40}{45.76} - 1 = 1.014 - 1 = \underline{+0.01}$$

BUCKLING - ULT.

FORM LMSC 362 B-2

## SUMMARY ~ MAX. PANEL STRESSES

TABLE BASED ON LINEAR ANALYSIS: DIRECT SUPERPOSITION

| CONFIG. | $N_x$ ppi | $p$ psi | $\sigma_N$ psi | $\sigma_p$ psi | $\sigma$ psi | T °F | $\overline{EI}$ lb-in²/in |
|---|---|---|---|---|---|---|---|
| | LOADS & MAX. STRESSES ~ STRINGER | | | | | | |
| 1 | 0 | +4.5 | 0 | -39,410 | -39,410 | R.T. | 239,000 |
| | 0 | -6.0 | 0 | +52,540 | +52,540 | R.T. | 239,000 |
| 2 | -3000 | +2.85 | -26,220 | -6732 | -32,950 | R.T. | 308,400 |
| | +6000 | -3.0 | +52,450 | +7087 | +59,630 | 250 | 283,500 |
| 3 | -6000 | +2.25 | -41,930 | -3237 | -45,170 | R.T. | 314,300 |
| | +6000 | -3.0 | +41,930 | +4317 | +46,250 | 250 | 288,900 |
| 4 | -3000 | +2.85 | -33,520 | -9378 | -42,900 | R.T. | 317,100 |
| | +6000 | -3.0 | +67,040 | +9872 | +76,910 | 600 | 259,600 |
| | LOADS & MAX. STRESSES ~ SKIN | | | | | | |
| 1 | 0 | -6.0 | 0 | -20,810 | -20,810 | R.T. | 239,000 |
| | 0 | +4.5 | 0 | +15,610 | +15,610 | R.T. | 239,000 |
| 2 | -3000 | -3.0 | -26,220 | -3043 | -29,260 | R.T. | 308,400 |
| | +6000 | +0.75 | +52,450 | +761 | +53,300 | 250 | 283,500 |
| 3 | -6000 | -1.35 | -41,930 | -852 | -42,780 | R.T. | 314,300 |
| | +6000 | +0.75 | +41,930 | +473 | +42,400 | 250 | 288,900 |
| 4 | -3000 | -3.0 | -33,520 | -4076 | -37,600 | R.T. | 317,100 |
| | +6000 | +0.75 | +67,040 | +1019 | +68,060 | 250 | 259,600 |

SIGN CONVENTIONS: $+N_x, +\sigma$ TENSION
$-N_x, -\sigma$ COMPRESSION
$+p$ BURST
$-p$ COLLAPSE

ALL $N_x$, $p$, & $\sigma$: ULTIMATE VALUES

FACTOR of SAFETY = 1.5

FORM LMSC 362 B-2

# REFERENCES

1. MIL-HDBK-5A, METALLIC MATERIALS AND ELEMENTS FOR AEROSPACE VEHICLE STRUCTURES, JAN. 1970

2. TIMOSHENKO & GERE, THEORY of ELASTIC STABILITY, 2ND ED., 1961

3. LAC, STRESS MEMO MANUAL

4. LMSC, PREFERRED PARTS HANDBOOK

5. MEMO FROM D. J. TILLIAN, NASA MSC, TO R.D. BUTTRAM, LMSC, "POINT DESIGN REQUIREMENTS FOR 2 ORBITER DESIGN AREAS - REUSABLE SURFACE INSULATION TPS DEVELOPMENT, PHASE 2", DATED 7-21-71.

# Appendix D

# DYNAMIC ANALYSIS OF PROTOTYPE PANEL SUBSTRATES

D1

NASA CONTRACT

# ENGINEERING MEMORANDUM

| | |
|---|---|
| TITLE: DYNAMIC ANALYSIS OF TPS PANELS | EM NO. SSD/451<br>REF: |
| PREPARED BY: A. D. Houston / F. R. Mason<br>CHECKED BY: R. Buttram | DATE: 25 Oct. 1971<br>APPROVAL: |

Refs: (1) U. S. Government Two-Way Memo, dated 7/21/71, "Point Design Requirements for 2 Orbiter TPS Design Areas - Reuseable Surface Insulation TPS Development, Phase 2."

(2) NASA TN-D-451, "Flutter Research on Skin Panels," Kordoes, Tuovilla, and Guy, Sept. 1960.

(3) LMSC/A814091, SS-1106-5522, "Sonic Fatigue Analysis C-5A Program," D. M. Wong, 28 April 1966.

(4) Mc Donnell-Douglas Tech Report AFFDL-TR-67-38, "Design Fabrication, and Test of Aerospace Planes Beryllium Wing Box," March 1967.

(5) Lockheed-California Company, SLM #17, "Structural Life Assurance Manual.

PURPOSE:

To verify by analysis that the four panel designs submitted satisfy the dynamic requirements for sonic fatigue strength and flutter resistence described in Reference (1).

DISCUSSION:

(1) - Panel Flutter Analysis

Two panel flutter modes were examined: complete panel flutter and inter stringer flutter. The experimental data contained in the Reference (2) document was used to demonstrate that the panel flutter requirements of Reference (1) were met.

(a) Complete Panel

The effective stiffness for a stiffened panel is given by:

$$r_{EFF} = \left[12(1-\nu^2)\frac{D_x}{E}\right]^{\frac{1}{3}} \qquad (1)$$

DISCUSSION: (continued)

For all of the four panels examined, the length/width ($\frac{l}{w}$) ratio is approximately 1.0. Hence from Figure 2 of Reference (3), we have:

$$\left(\sqrt{M^2-1}\cdot\frac{E}{q}\right)^{\frac{1}{3}}\frac{L_{EFF}}{\ell} > 0.5 \qquad (2)$$

Substituting from (1)

$$\left[\sqrt{M^2-1}\cdot\frac{E}{q}\cdot 12(1-\nu^2)\frac{D_x}{E}\right]^{\frac{1}{3}}\frac{1}{\ell} > 0.5$$

$$\therefore\ q < \frac{96\sqrt{M^2-1}\,(1-\nu^2)I_x E}{\ell^3}$$

The panel with the lowest value of bending stiffness (Ix) is Panel #1, with a value of 0.01 in.$^3$ Taking Poisson's ratio $\nu$ as 0.3, E = 42 x $10^6$ lb/in$^2$ and length ($\ell$) = 24 inches, $q < 380{,}000\sqrt{M^2-1}$

Clearly, the panels are flutter free in the complete panel bending mode.

(b) Inter Stiffener Panel Flutter

Panel #1 is the most critical of the four panels in this mode, with a l/w ratio of (22.5/3.3) = 6.8. Refering to Figure 2, Reference (2), the following flutter stability criterion applies:

$$\left(\sqrt{M^2-1}\,\frac{E}{q}\right)^{\frac{1}{3}}\frac{t}{\ell} > 0.15$$

$$\therefore\ q < \frac{\sqrt{M^2-1}\,.\,E.t^3}{(.15)^3\ell^3}$$

The panel with the minimum Et3 is panel #4, with a value of 920 lb in. Therefore $q < 3440\sqrt{M^2-1}$ for no flutter. The flutter stability curve for this

FORM LMSC 362 B-2

DISCUSSION: (continued)

mode is plotted in Figure 1, demonstrating that a flutter margin in excess of 1.5 times the maximum dynamic pressure exists at any Mach number along the design trajectories.

(2) - Panel Sonic Fatigue Analysis

The method described in the Reference (3) document was used to evaluate the sonic fatigue characteristics of the four panels. This simplified analysis method developed in Reference (3), provides root mean square stress generated in a panel by acoustic excitation at its fundamental natural vibration mode given by:

$$\sigma = \sigma_o \sqrt{\frac{\pi}{4\delta}} \sqrt{f_n \cdot S_i(f)}$$

where:

| | | |
|---|---|---|
| $\sigma$ | = | rms stress (psi) |
| $\sigma_o$ | = | unit psi stress (psi/psi) |
| $\delta$ | = | damping ratio |
| $f_n$ | = | panel primary natural frequency (Hz) |
| Si(f) | = | pressure power spectral density ($p^2$/Hz) |

From Reference (3),

$\sqrt{f_n S_i(f)}$ = 1/3 octave decibel level + 6.38 decibels

From Reference (1), maximum 1/3 octave level is 150 decibels, therefore

$$\sqrt{f_n \; Si\,(f)} = 150 + 6.38 = 156.38 \text{ decibels}$$
$$\equiv 0.19 \text{ psi}$$

From stress analysis of the panels, the following unit pressure stresses are as shown in Table I, together with computed values of RMS stress assuming $\delta = 0.02$.

TABLE I - RMS STRESSES GENERATED IN PANELS

| Panel | Unit Pressure Stress (psi/psi) $\sigma_o$ | | RMS Stress (Psi) | |
|---|---|---|---|---|
| | | | Stringer | Skin |
| # | Stringer | Skin | | |
| #1 Beryllium | 8800 | 3460 | 10,400 | 4120 |
| #2 7075-T6 | 2360 | 1000 | 2,800 | 1190 |
| #3 7075-T6 | 1440 | 630 | 1,700 | 750 |
| #4 Titanium (6Al 4V) | 3150 | 1330 | 3,750 | 1580 |

Discrete frequency S-N curve fatigue data for 7075-T6 (Aluminum) and 6Al 4V Titanium Alloys were obtained from the Reference (5) document and data for Beryllium sheet from the Reference (4) document. A modified Miner cumulative fatigue damage rule is used and the number of cycles to failure $N_R$ is given by:

$$N_R = \frac{1}{\int_0^\infty \frac{p(x)dx}{N_i}}$$

where: $p(x) = x e^{-\frac{x^2}{2}}$, is the Rayleigh probability distribution of stress peaks, and $x$ = ratio of peak stress to root mean square stress.

For various values of rms stress, the values of $N_R$ were obtained and random S-N curves constructed from the discrete frequency S-N curves. These are shown in Figures 2, 3 and 4. Estimates of the number of cycles of exposure have been based upon the Reference (1) data, which provided an environment history for a particular mission. For one mission the environment was between the maximum value and 20 decibels below the maximum value for a period of 35 seconds. Assuming 100 missions, a safe life margin of 4 times service life, and an average panel natural frequency of 200 Hz, the design life cycles

DISCUSSION: (contained)

($N_D$) are:

$N_D = 4 \times 35 \times 200 \times 100 = 2.8 \times 10^6$ cycles

CONCLUSIONS:

Figure 5 shows induced RMS stress plotted for each panel and each are less than allowable random S-N curve allowables.

Therefore, it is concluded that all four panels have adequate fatigue strength to withstand the Reference (1) design environments.

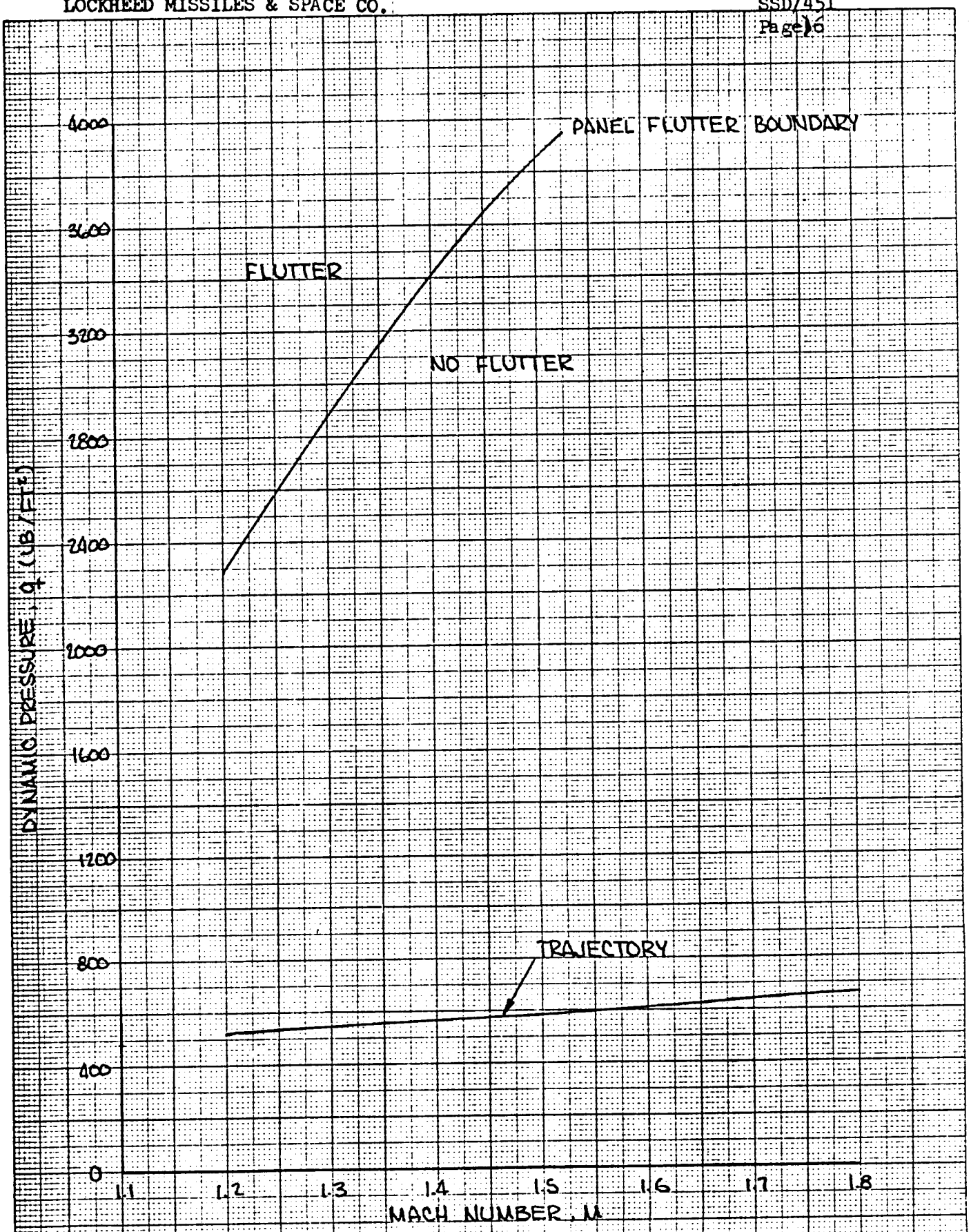


FIGURE 1 PANEL FLUTTER STABILITY VS. MISSION PROFILE



GRAPH PAPER GRAPHIC CONTROLS CORPORATION Buffalo, New York Printed in U.S.A.
SQUARE 10 X 10 TO THE CENTIMETER AS-0014 07

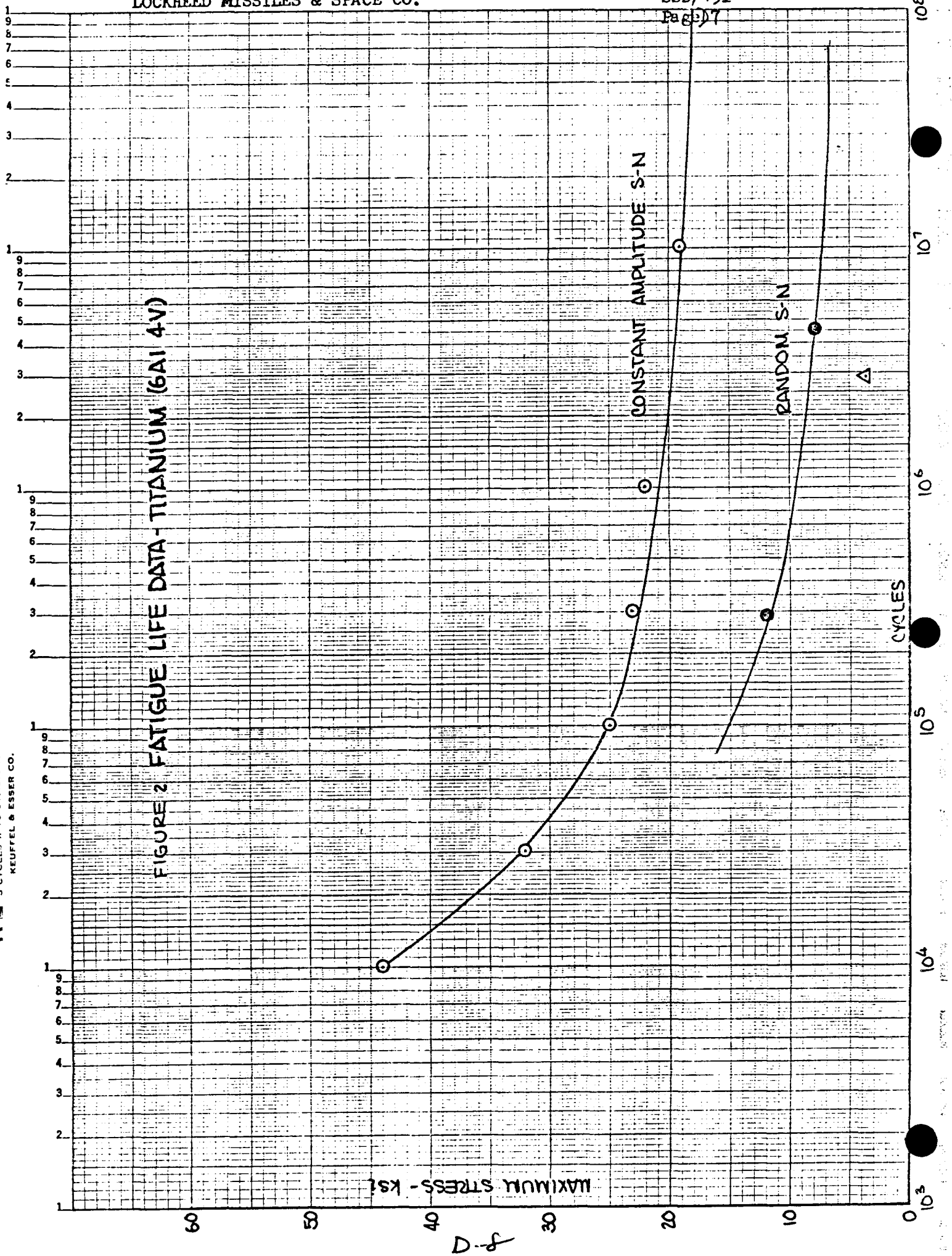


FIGURE 2 FATIGUE LIFE DATA - TITANIUM (6Al 4V)

K&E SEMI-LOGARITHMIC 46 6212
5 CYCLES X 70 DIVISIONS MADE IN U.S.A.
KEUFFEL & ESSER CO.

D-8

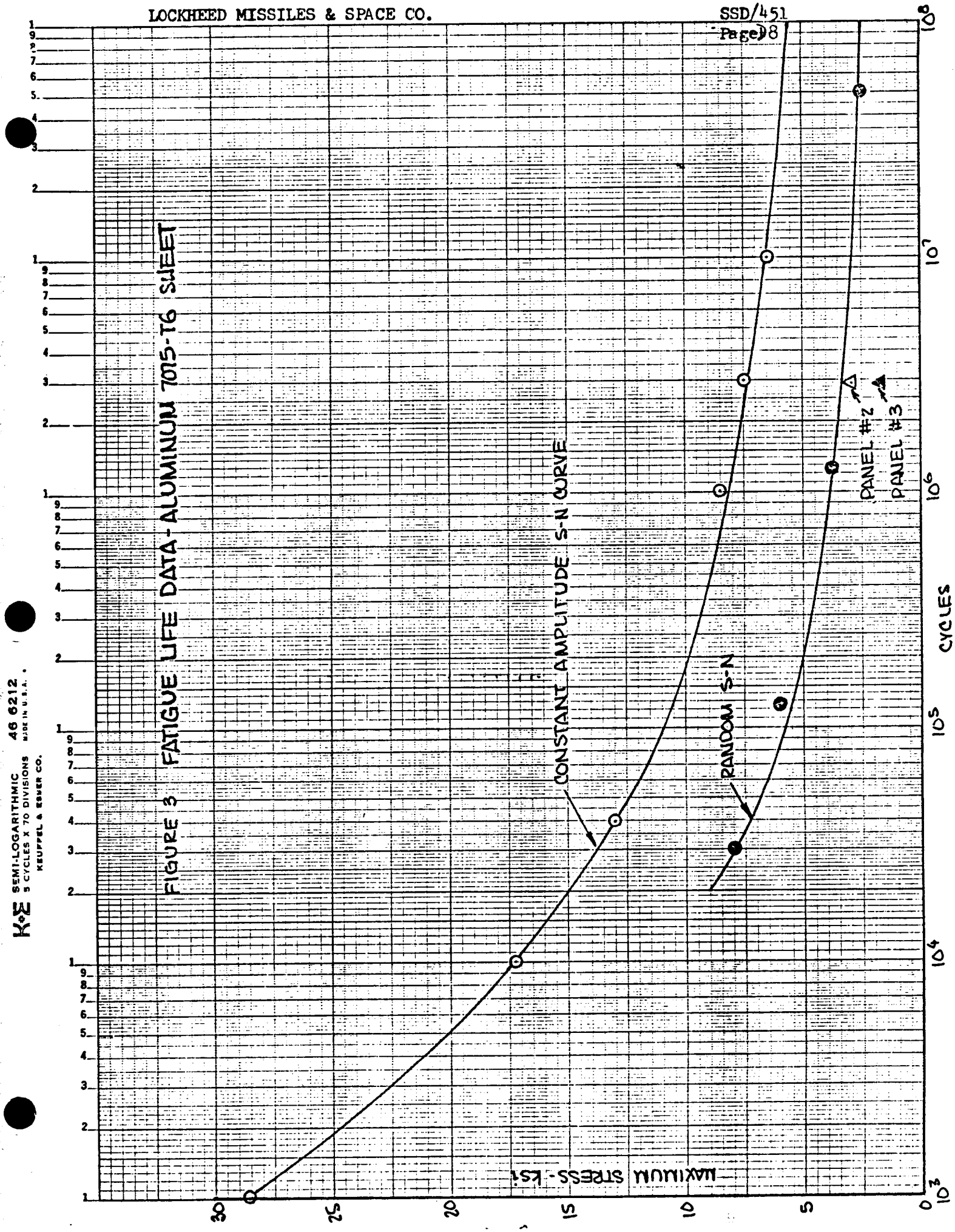
FIGURE 3 FATIGUE LIFE DATA - ALUMINUM 7075-T6 SHEET
CONSTANT AMPLITUDE S-N CURVE
RANDOM S-N
PANEL #2
PANEL #3
MAXIMUM STRESS - ksi
CYCLES
30
25
20
15
10
5
0
$10^3$
$10^4$
$10^5$
$10^6$
$10^7$
$10^8$
K+E SEMI-LOGARITHMIC 46 6212
5 CYCLES X 70 DIVISIONS MADE IN U.S.A.
KEUFFEL & ESSER CO.

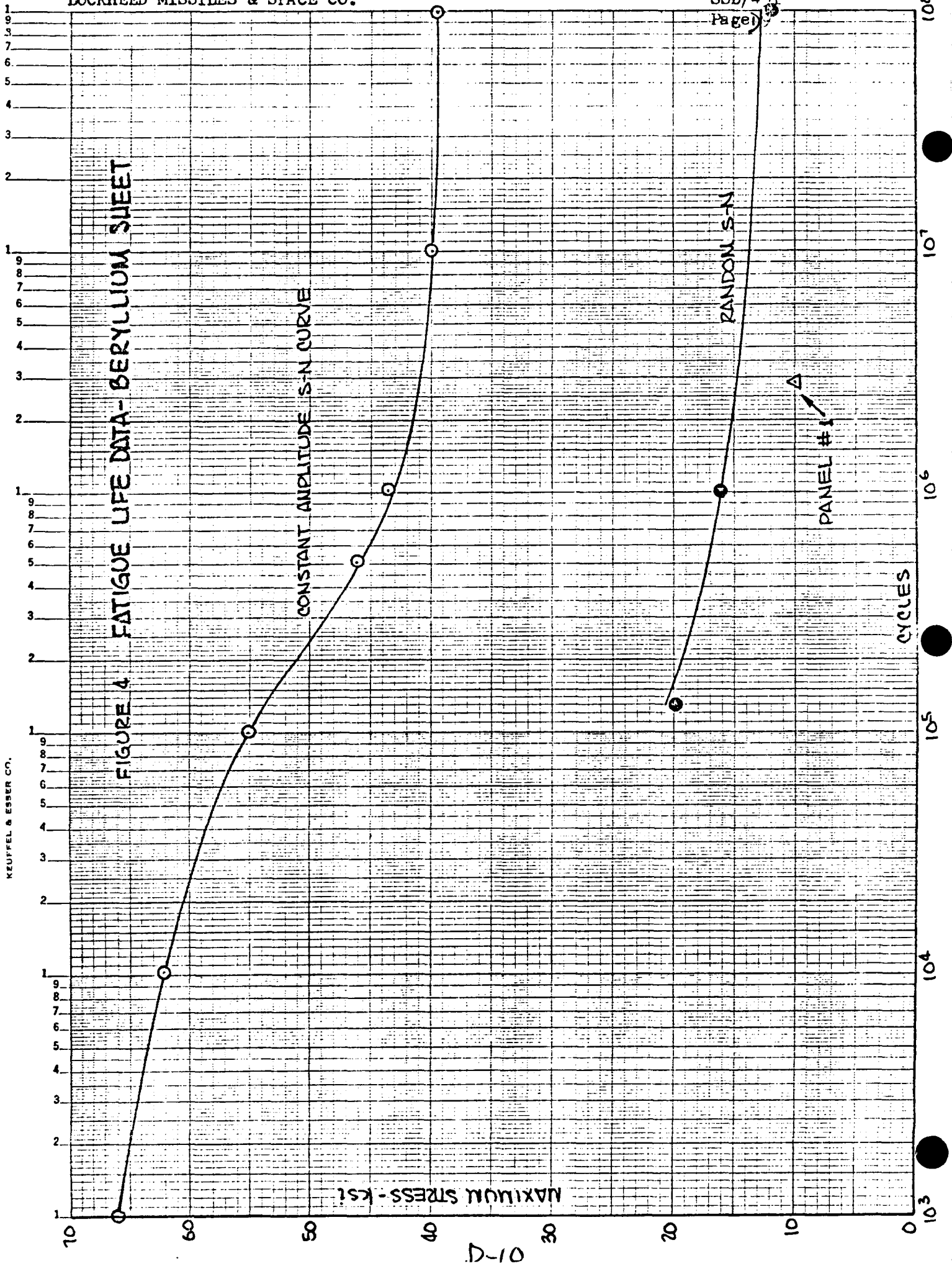
FIGURE 4 FATIGUE LIFE DATA - BERYLLIUM SHEET
CONSTANT AMPLITUDE S-N CURVE
RANDOM S-N
PANEL #1
CYCLES
MAXIMUM STRESS - ksi
70
60
50
40
30
20
10
0
$10^3$
$10^4$
$10^5$
$10^6$
$10^7$
$10^8$
SEMI-LOGARITHMIC 46 6214
5 CYCLES X 70 DIVISIONS MADE IN U.S.A.
KEUFFEL & ESSER CO.

FIGURE 5 RANDOM S-N CURVES VS ACOUSTICALLY INDUCED RMS STRESSES IN PANELS

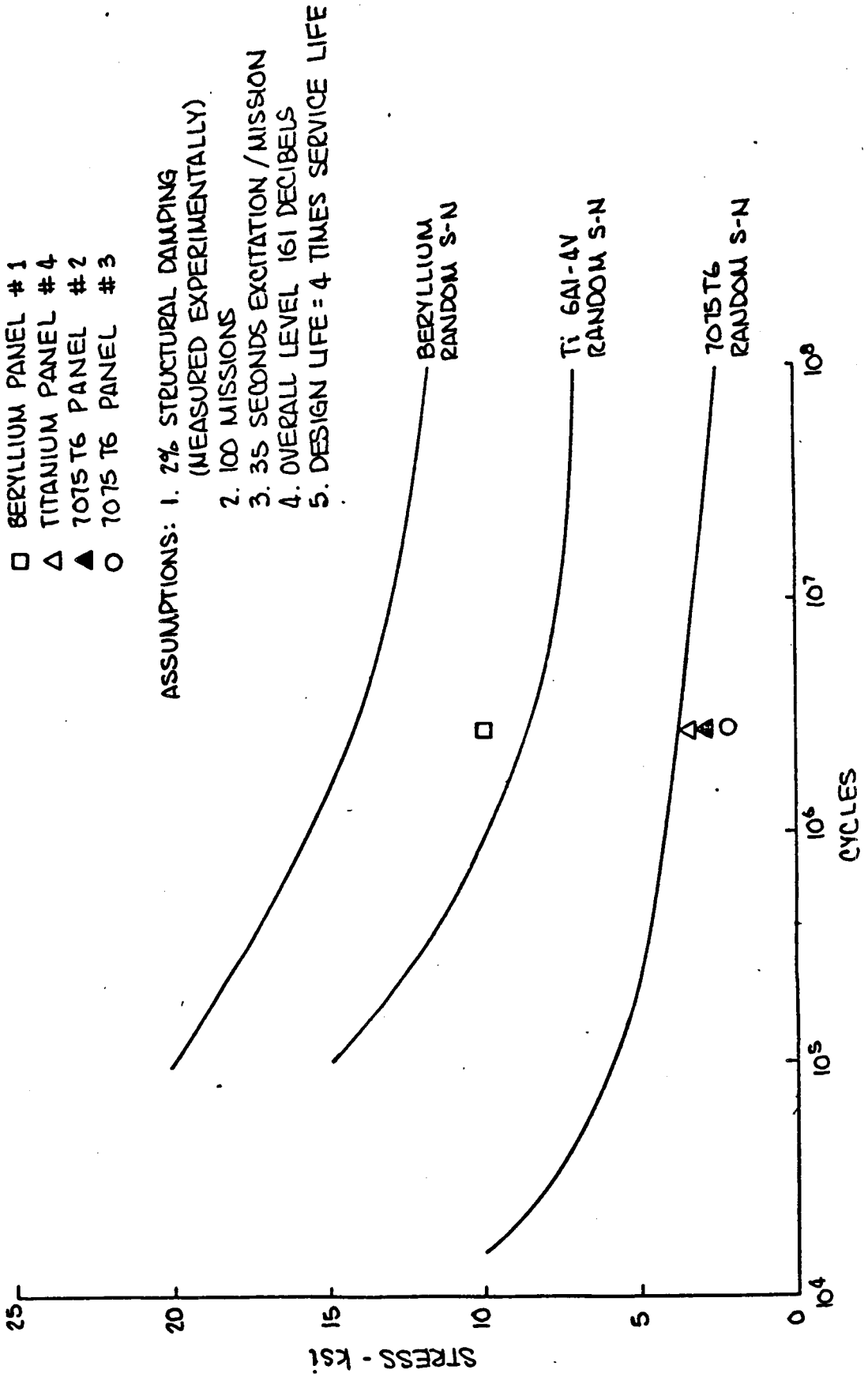

# Appendix E

# VENTING CHARACTERISTICS OF LI-1500 TILES WITH STRAIN ISOLATION

ENGINEERING MEMORANDUM

| TITLE: VENTING CHARACTERISTICS OF LI-1500 TILES WITH STRAIN ISOLATION | EM NO: REF: DATE: 15 October 1971 |
|---|---|
| AUTHORS: R. Diggins | APPROVAL: ENGINEERING SYSTEM ENGRG |

REFERENCES

1. Drawing No. SKJ-205007, "TPS Mechanical Attachment for LI-1500 Tiles With Strain Insulation," 27 September 1971

2. U.S. Government Two-Way Memo, "Point Design Requirements for Two Orbiter TPS Design Areas – Reusable Surface Insulation TPS Development, Phase 2," Tillian to LMSC, 21 July 1971

PURPOSE:

To investigate the venting characteristics of the thermal protection system (TPS) configuration shown on Reference 1. Specifically, as requested, the analysis was performed to determine maximum differential pressures across the TPS tiles, under the assumption that each panel assembly (approximately 10 in. by 30 in.) is hermetically sealed from adjacent panels.

TECHNICAL DISCUSSION:

It has been established that the maximum differential pressures on vented compartments occur during the transonic phase of ascent, rather than during reentry. An ascent venting analysis has been performed, using the digital computer program "VENTRX". In this program, a venting model is set up to describe the volume(s) of air to be vented, orifice areas (external and/or between compartments), and external pressure fields for all external orifices. Sharp-edged, circular orifice flow coefficients are used, as modified to account for the effects of an external velocity field.

The calculated volume of air under each panel assembly is 0.52 cu ft, and the external vent area (in square inches) is 37 times the average gap width (in inches) between TPS tiles. External pressures have been taken from the Area 2 data of Reference 2, and these pressure histories (in envelope form) are shown in Fig. 1. For this analysis, it has been assumed that these pressures (identified as differential pressures in Reference 2), represent the difference between the external surface pressure ($p_o$) and local ambient pressure ($p_\infty$). Ascent venting simulations were run for both the positive and negative pressures shown in Fig. 1, using average gap widths of 0.005 and 0.0025 in. The maximum resultant differential pressures are 0.1 and 0.25 psi, respectively. However, with this venting configuration (individual panels sealed off), since the internal air pressure very nearly follows the external surface pressure, the primary load-carrying structure in "Area 2" must withstand differential pressures similar to (within 1.0 psi) those shown in Fig. 1. Also, the supporting rib structure between adjacent panels must be capable of withstanding up to 8 psi differential in certain locations.

Because high differential pressures are produced by rapid external pressure changes, which are not defined by the pressure envelopes of Fig. 1, an analysis was performed to determine the effects of such changes on maximum differential pressures. In interference regions such as "Area 2," where local surface pressures are affected by the presence of an adjacent body (tank or booster), theoretical techniques during transonic flow are inadequate, and wind-tunnel data are not available to define the maximum rates of change of surface pressures. Therefore, these rates have been analyzed parametrically, using rates of 2 and 4 psi/sec. With each rate, total pressure changes of 4 and 8 psi have been considered. The resulting pressure history for the most severe case (4 psi/sec for 2 sec) is shown in Fig. 2.

The relationship between external, internal, and ambient absolute pressures is shown in Fig. 3, for a gap width of 0.005 in. It is seen that the differential pressure across the thermal-protection surface continues to increase as the external pressure decreases; this is typical for each of the cases examined.

A summary of the maximum differential pressures across the TPS panels is presented in Fig. 4 as a function of gap width, rate of change of external pressure and length of time over which rates are applied. In order to arrive at a maximum differential pressure suitable for design purposes (in lieu of test data), some judgement must be applied. It is considered that 2 psi/sec is a conservative value for change rate; this is approximately twice that used in venting analyses on several SSD programs. Applying this rate for 4 sec reduces the external pressure to less than 1 psi absolute. Thus, the curve noted on Fig. 4 is recommended for use in design analyses. It is emphasized that these pressures apply only for the condition in which it is assumed that each panel assembly is completely sealed from adjacent panels. Should this not be the case, it may be assumed that, for relatively unrestricted flow between panels, the internal pressure (air between TPS and primary structure) will be local ambient ± 1 psi. In that event, the maximum TPS differential pressures (depending on location) will be as given in Fig. 1, plus or minus 1 psi.

## CONCLUSIONS:

Design differential pressures on the TPS panels are relatively low (less than 1 psi for an average gap between tiles greater than 0.005 in.) if the entire surface is constructed such that each panel assembly (approximately 10 in. by 30 in.) is hermetically sealed from adjacent panels. This scheme, however, imposes high differential pressures on primary structure (as much as 5 psi) and on support ribs between panels (as much as 8 psi). In addition, high costs would be incurred in manufacture and testing.

Alternatively, if air flow is allowed between panels, differential pressures on primary structure and TPS support ribs would be reduced to less than 1 psi, while differentials across the TPS surface would be increased to as much as 5 psi in certain areas, possibly requiring structural reinforcement in the form of bonded screen or solid subpanels.

LOCKHEED MISSILES & SPACE COMPANY

SPACE SHUTTLE PROJECT

EM NO.

DATE 15 October 1971

PREPARED BY K. Diggins

PAGE OF

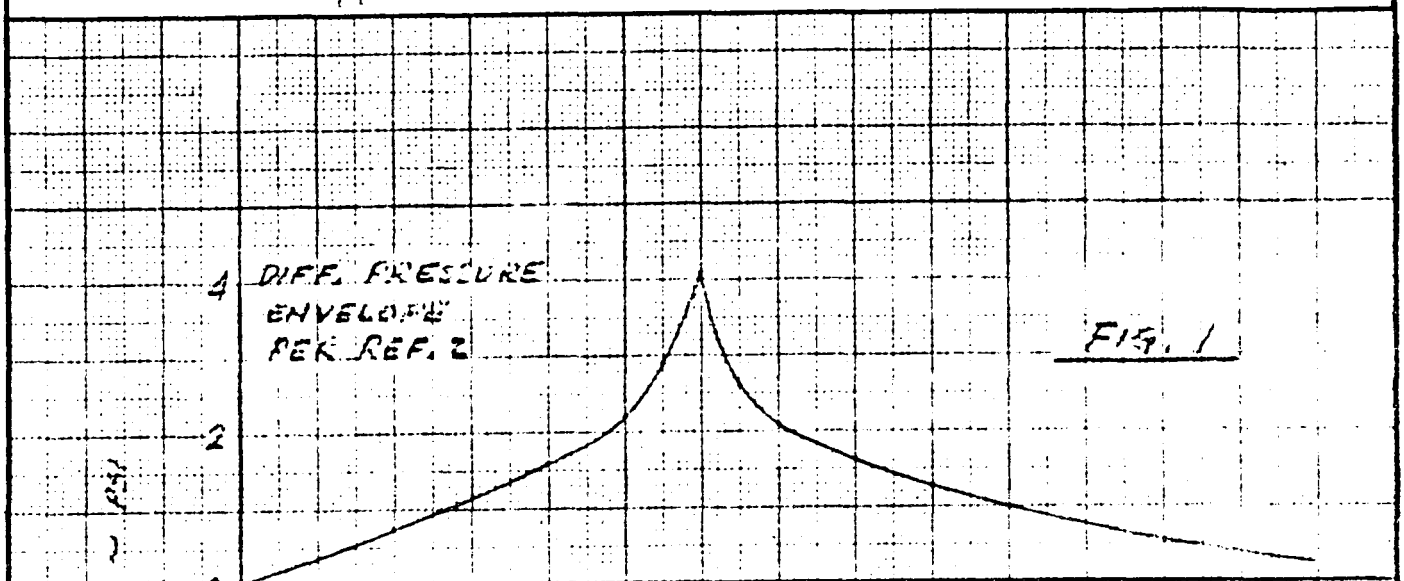


FIG. 1

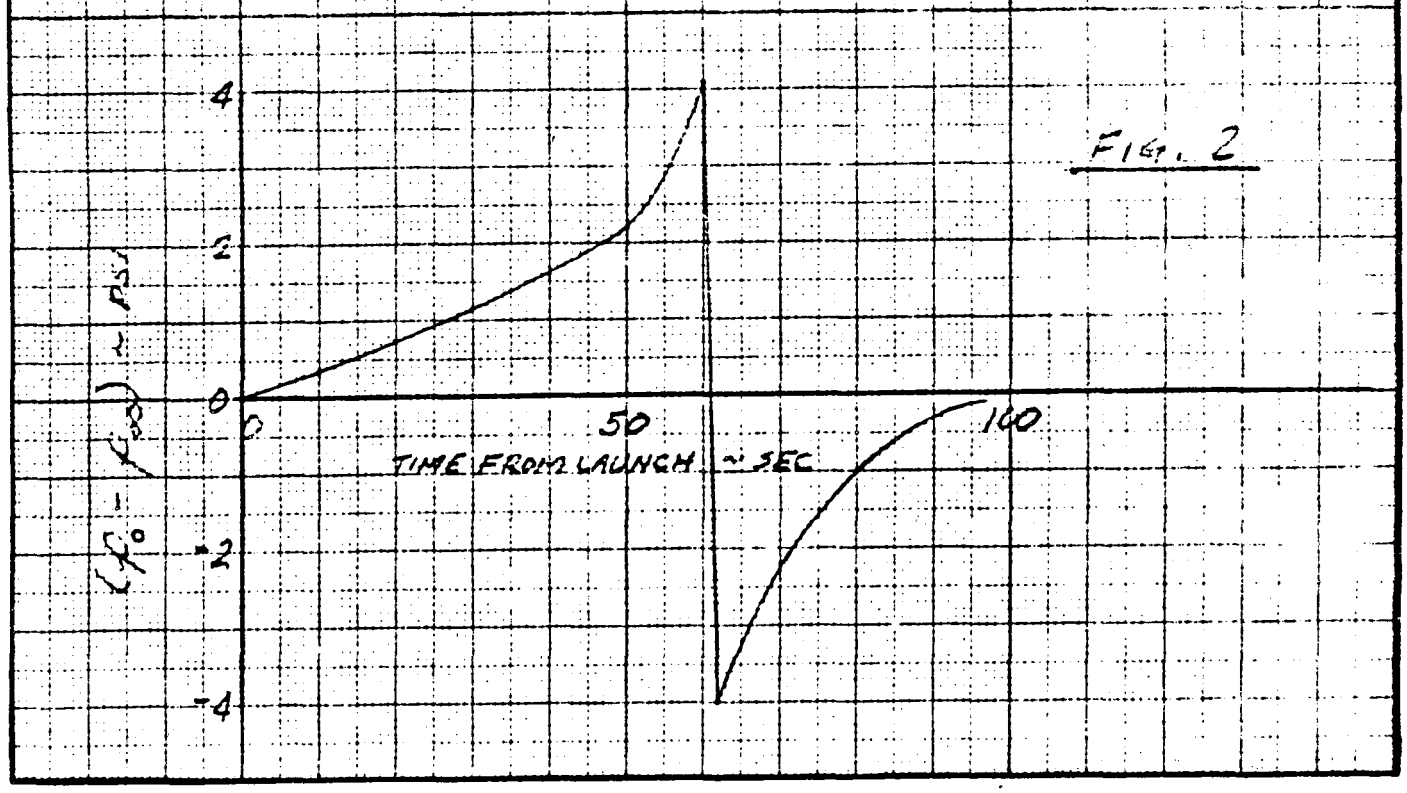


FIG. 2

LOCKHEED MISSILES & SPACE COMPANY

SPACE SHUTTLE PROJECT

EM NO.

DATE 15 October 1971

PREPARED BY L. Diggins

PAGE OF

TYPICAL PRESSURE HISTORIES

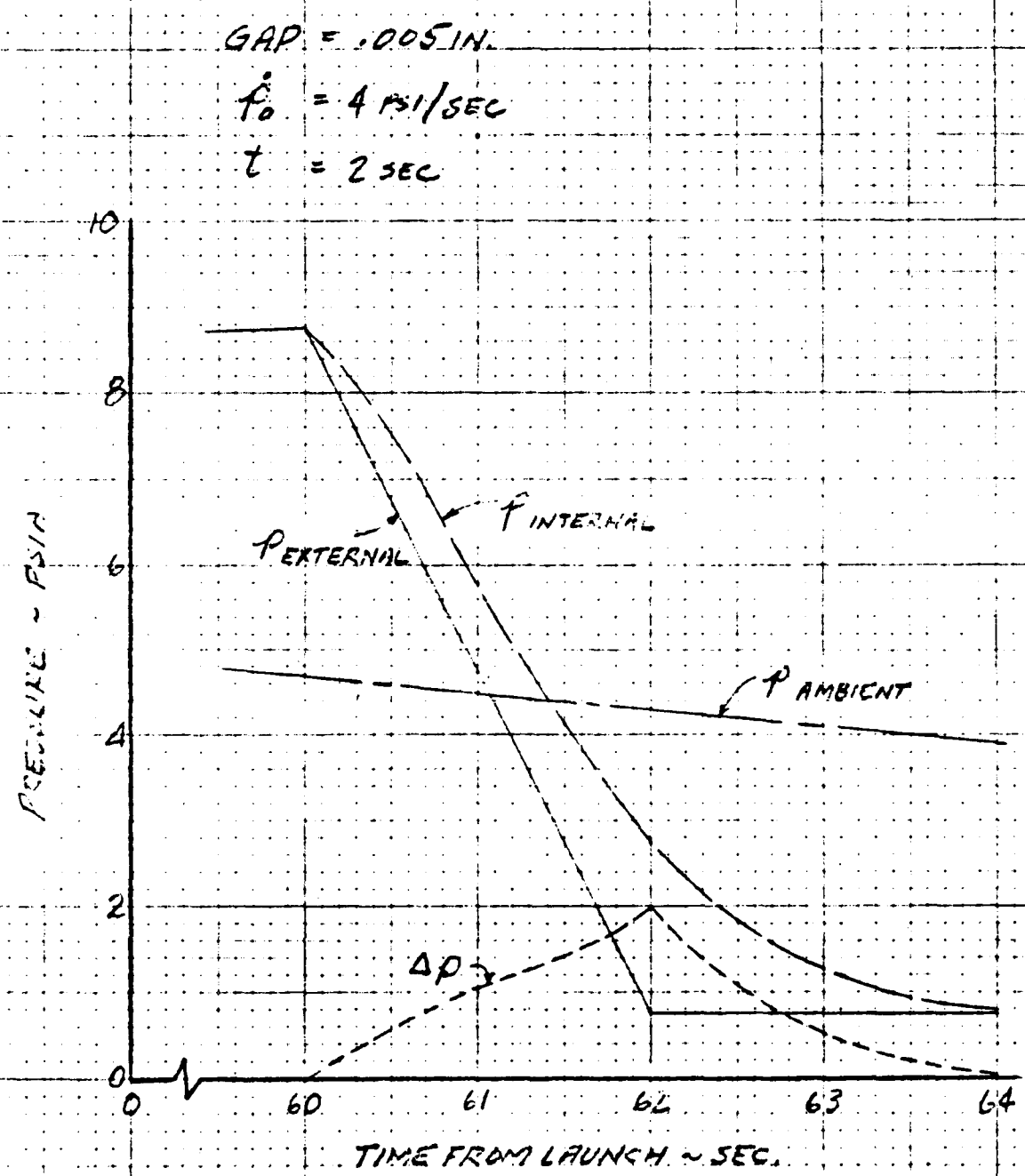


FIG. 3

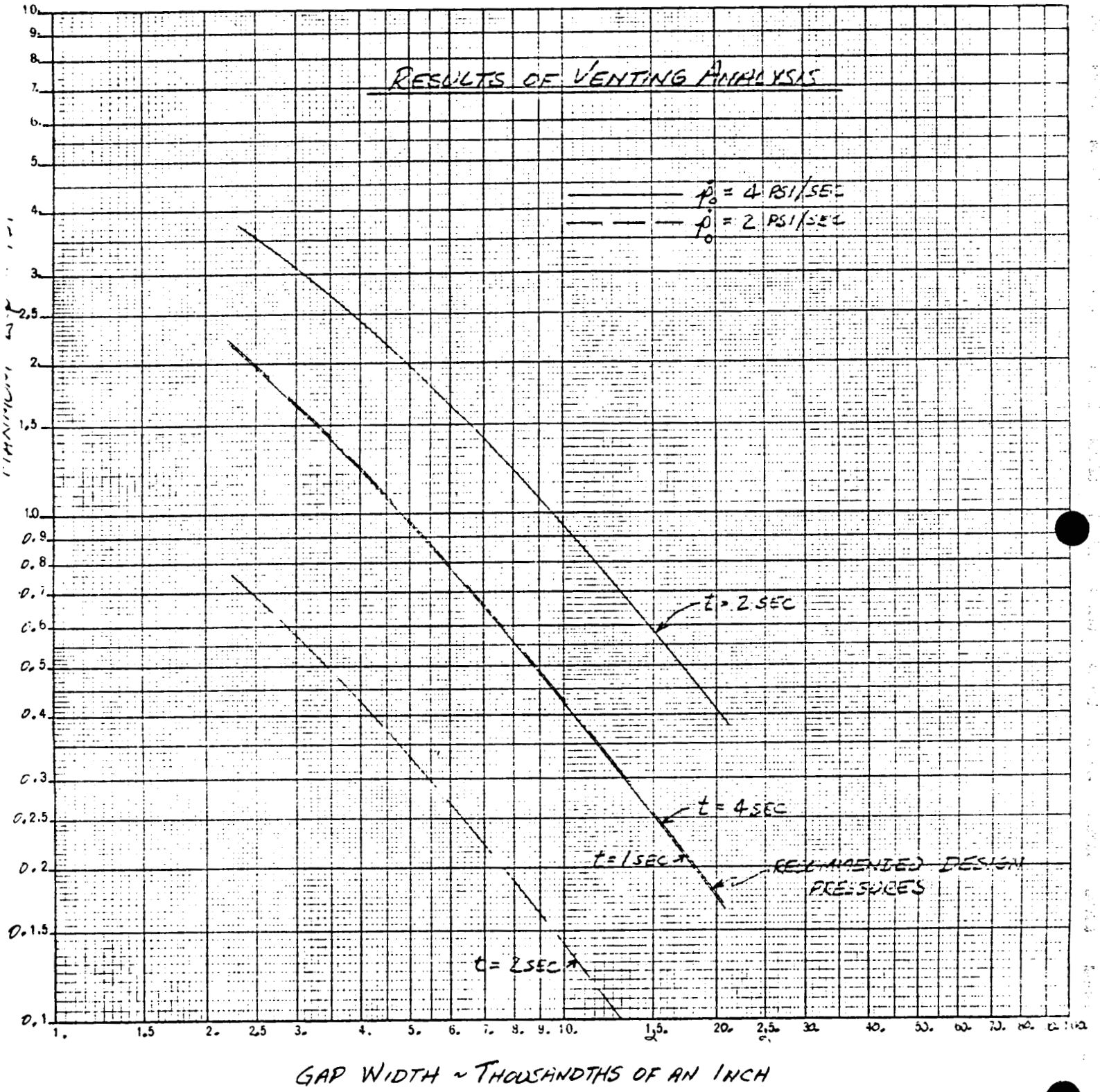


Fig. 4 Results of Venting Analysis

# Appendix F

# ENVIRONMENTAL TEST PLAN

# ENVIRONMENTAL TEST PLAN
# FOR
# LI-1500 SURFACE INSULATION
# TPS FUSELAGE PANELS

Developed By

LOCKHEED MISSILES & SPACE COMPANY

UNDER CONTRACT NAS9-12083

Prepared by:

D. R. Elgin
Task 5 Leader

Approved by:

R. D. Buttram, Project Leader
Contract No. NAS9-12083

CONTENTS


| Section | | Page |
|---|---|---|
| 1 | INTRODUCTION | F-4 |
| 2 | FUSELAGE PANELS | F-6 |
| | 2.1 Beryllium Fuselage Panel Test Setup | F-6 |
| | 2.2 Aluminum and Titanium Fuselage Panel Test Setup | F-17 |
| | 2.3 Fuselage Panel Test Sequence | F-17 |
| | 2.3.1 Beryllium Panel | F-17 |
| | 2.3.1.1 Pressure Loading Tests | F-17 |
| | 2.3.1.2 Radiant Heat Tests | F-18 |
| | 2.3.1.3 Combined Loading and Heating Test | F-20 |
| | 2.3.1.4 Acoustic Test | F-20 |
| | 2.3.1.5 Combined Environmental Tests | F-22 |
| | 2.3.2 Aluminum Panel – Area 2 | F-23 |
| | 2.3.2.1 Axial Load Tests | F-23 |
| | 2.3.2.2 Radiant Heat Tests | F-24 |
| | 2.3.2.3 Combined Loading and Heating Test | F-25 |
| | 2.3.2.4 Acoustic Test | F-25 |
| | 2.3.2.5 Combined Environmental Tests | F-26 |
| | 2.3.3 Aluminum Panel – Area 1 | F-27 |
| | 2.3.4 Titanium Panel | F-29 |

# Section 1
# INTRODUCTION

This test plan outlines the test program to be conducted on the surface insulation thermal protection system (TPS) fuselage panels to be provided by Lockheed Missiles and Space Company under contract NAS9-12083. The objective of the test program is to perform a thermal/structural evaluation on the surface insulation TPS fuselage panels and to demonstrate the feasibility of a surface insulation TPS for application on the Space Shuttle Orbiter Vehicle.

The test panels furnished under the subject contract will be specifically designed for the MSC fixed wing shuttle orbiter vehicle and the panels will be sized and optimized for the nominal environments associated with that particular vehicle.

Four fuselage panels will be furnished by LMSC. One beryllium panel is representative of the subpanel concept. Two aluminum panels and one titanium panel are representative of primary structure. The beryllium subpanel design temperature limit is 600$^{\circ}$F and is representative of structure in Area 2 on the orbiter vehicle lower surface. The aluminum panel design temperature limit of 250$^{\circ}$F occurs in flight during critical load conditions. A maximum temperature of 300$^{\circ}$F occurs after landing. One aluminum panel is designed for Area 1 and the other for Area 2. The titanium panel is designed for a 600$^{\circ}$F temperature limit at the Area 2 location.

The test program consists of subjecting the test panels to sequential and combined environment simulations of ascent acoustic loading, ascent mechanical loading, entry mechanical loading and heating, and cruise mechanical loading.

Since the beryllium subpanel is designed to withstand pressure differential loads instead of primary structure loads, it will be tested under flight differential load conditions. The aluminum and titanium panels are designed to carry primary structure loads with the pressure differential loads of secondary importance. Application of the pressure differential loads in the existing MSC tensile load/radiant heat facility would

require extensive modifications which are not considered justified to perform the panel thermal/structural evaluations. Therefore, it is proposed that the mechanical loads on these panels be confined to tensile loads.

It is intended to subject each of the four panels to a minimum of 25 and a maximum of 100 mission environment simulations.

# Section 2
# FUSELAGE PANELS

The fuselage panels consist of LI-1500 insulation tiles bonded to metallic substrates. The beryllium panel is channel-stiffened, while the aluminum and titanium panels are Z-stiffened. The construction of the panels is shown in Figures 1 through 4. Each panel will be supplied with four platinum - 10 percent rhodium versus platinum thermocouples. The thermocouples are located in the surface coating of the LI-1500 insulation at the center of each tile. Additional thermocouples, deflectometers, strain gages, and accelerometers will be installed at MSC. Suggested instrumentation locations are shown in Figures 5 and 6.

## 2.1 BERYLLIUM FUSELAGE PANEL TEST SETUP

The beryllium fuselage panel will be mounted in a test fixture similar to that used for previous fuselage panel tests described in Reference 1. The panel will remain in the test fixture throughout the complete test program. The panel will be simply supported in the test fixture and sealed to permit evacuation or pressurization of the test fixture box as required to simulate the flight pressure loads. The test fixture will have four chromel alumel thermocouples attached to the four corners for monitoring the temperature during the radiant heating tests to assure that the aluminum test fixture temperature does not exceed 300°F. A pressure control system will also be installed in conjunction with the test fixture to permit control of simulated pressure loads across the fuselage panel. Adequate safety relief valves will be installed on the test fixture to prevent overpressurization or underpressurization of the fixture cavity which would result in failing of the fuselage test panel. A nitrogen purge cooling system will be installed to permit cooling of the panel backface immediately following the radiant heating tests.

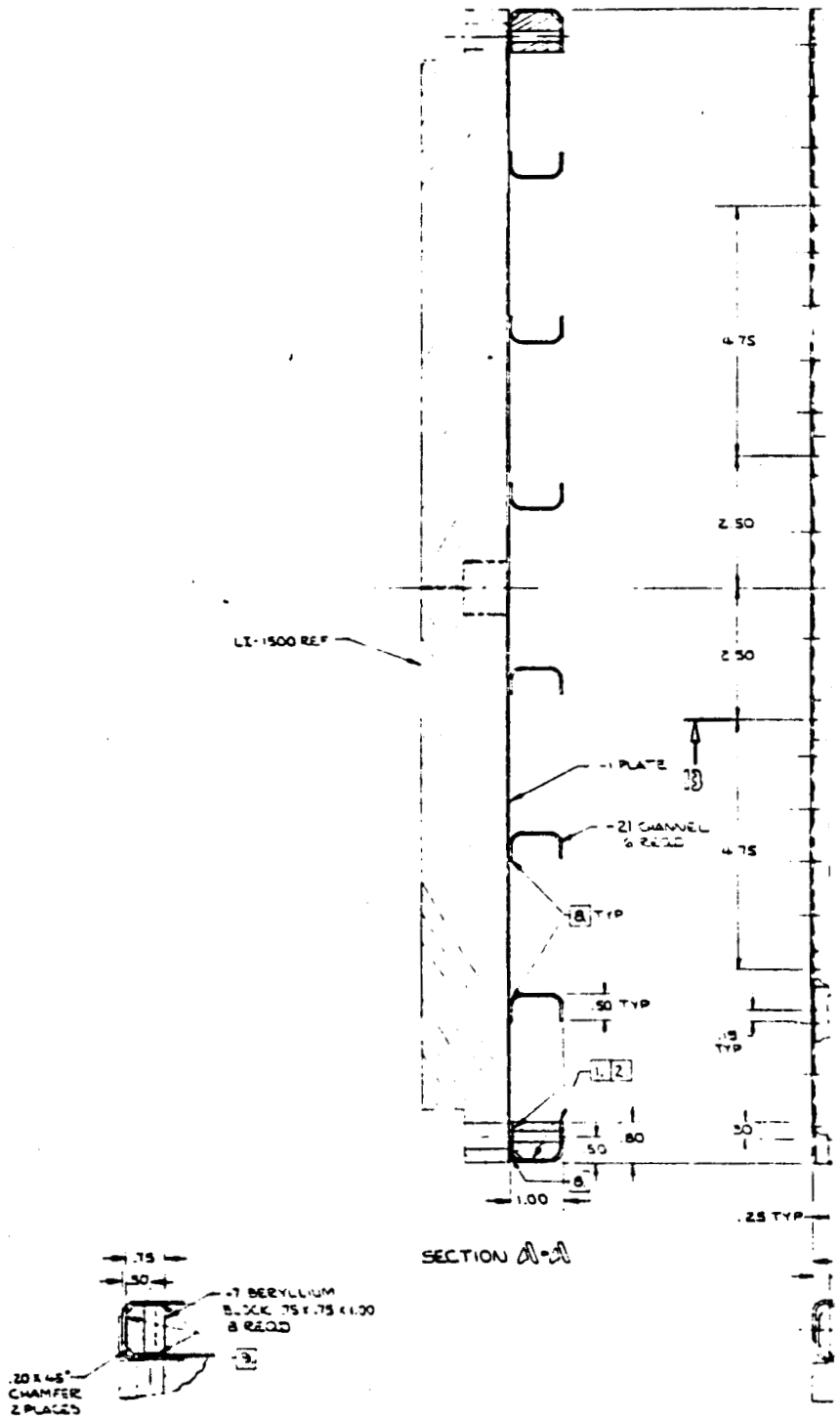
4.75
2.50
2.50
LI-1500 REF
-1 PLATE
B
-21 CHANNEL
6 REQD
4.75
-8 TYP
.50 TYP
.19
TYP
1, 2
.50
.80
.50
-8
1.00
.25 TYP
SECTION A-A
.75
.50
-7 BERYLLIUM
BLOCK .75 X .75 X 1.00
8 REQD
-9
.20 X 45°
CHAMFER
2 PLACES
SECTION B-B
8 PLACES

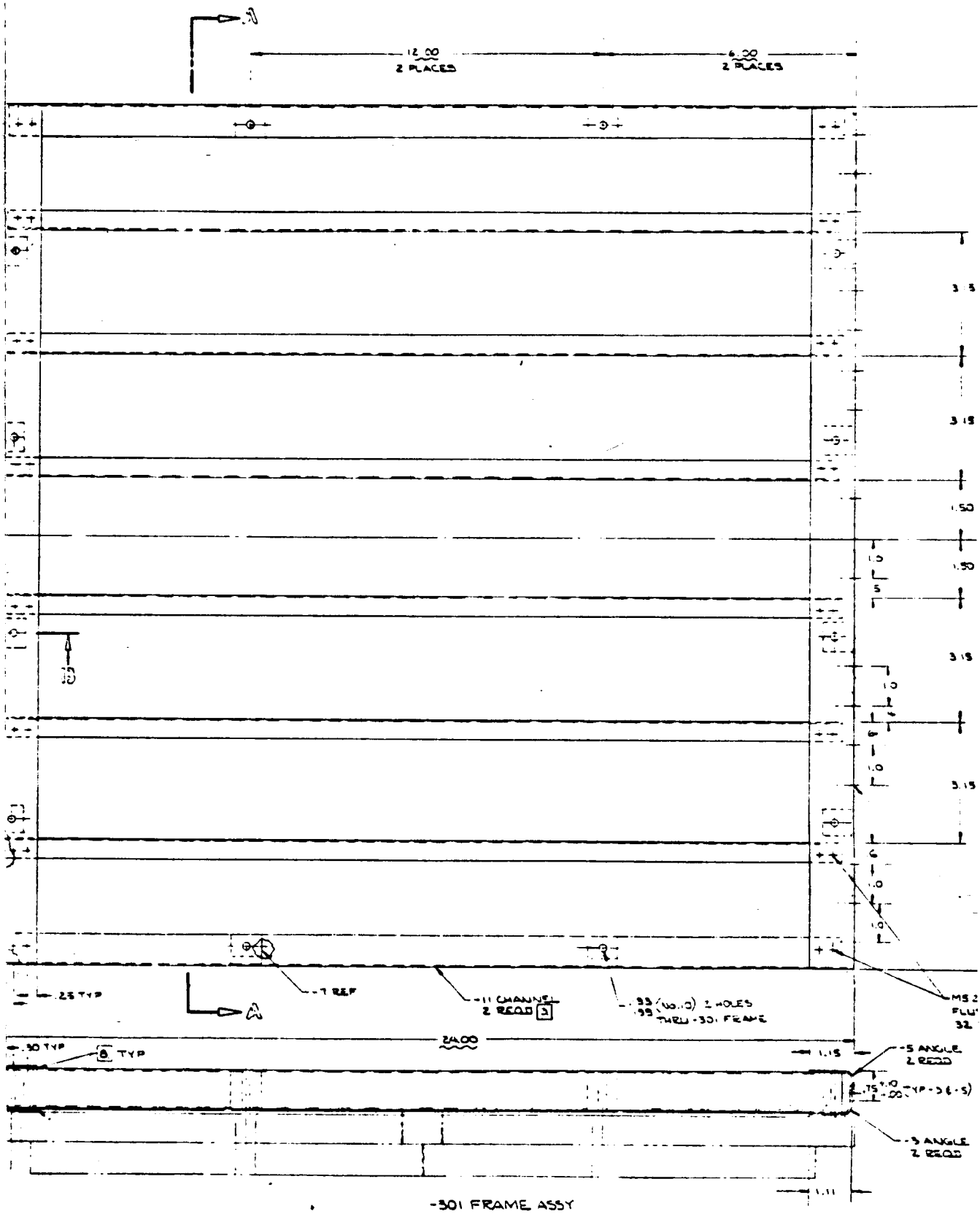


-301 FRAME ASSY

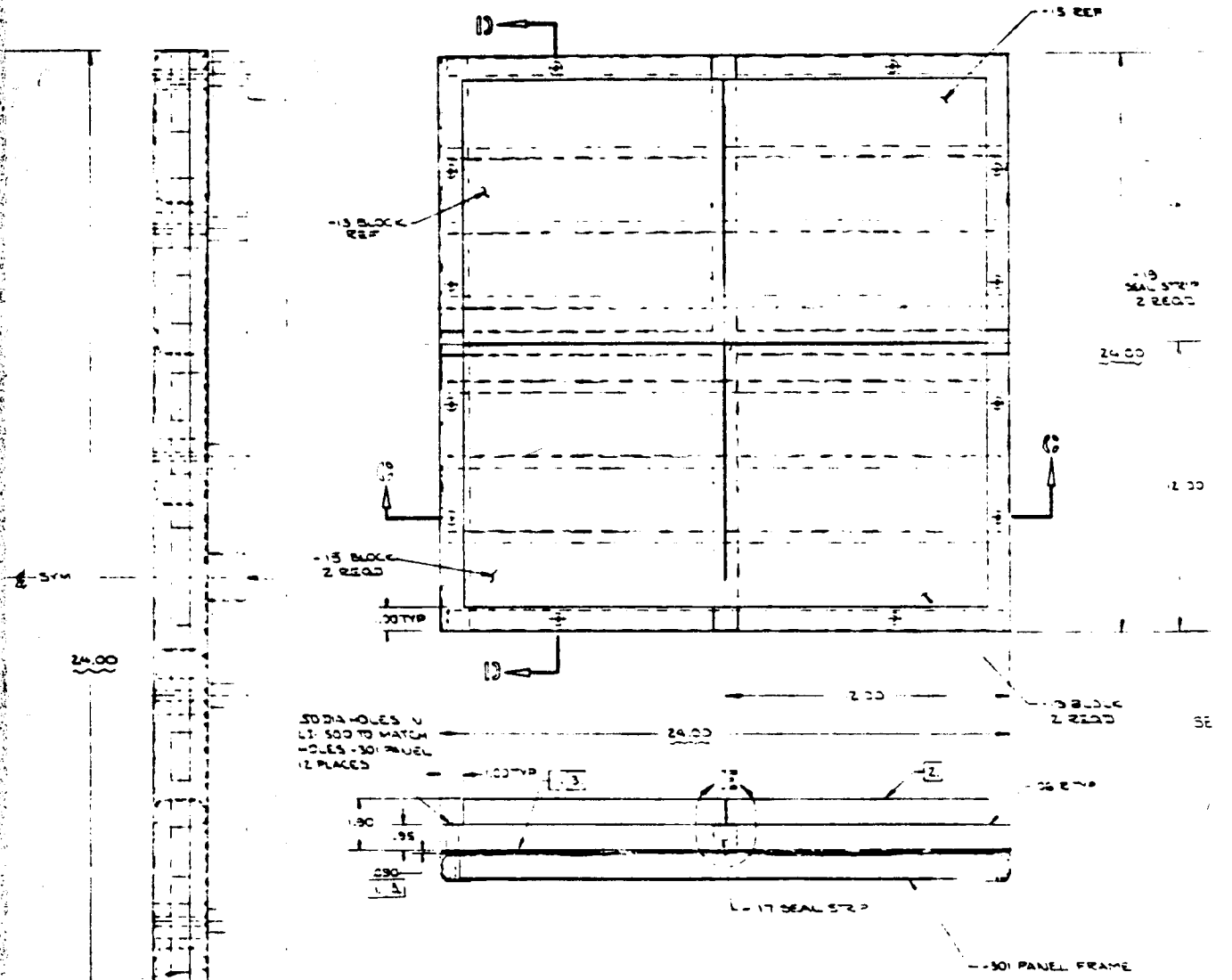


SECTION B-B

PANEL ASSY - 501
SCALE 1/2

9. BON
8. FUR
7. ALL
6. CLE
5. PRI
4. FAB
3. HOL
2. SUR
1. BON PER

NOTES:

| LTR | CHANGE | DATE APPD |
|---|---|---|
| A | LI-1500 THICKNESS WAS 2 [illegible] TILE SIZE WAS 6"x6", REVISED NOTE 2; ADDED DETAIL 'E'. | |

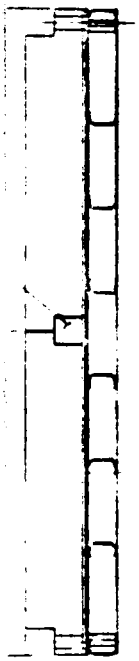

CTION [illegible]-D

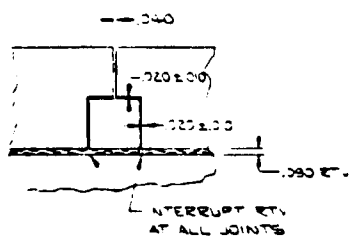


DETAIL [illegible]
SCALE [illegible]
TYP OF ALL JOINTS

FIG 1

PAGE F-7/8

| QTY REQD | QTY REQD | CODE IDENT | PART OR IDENTIFYING NO | NOMENCLATURE OR DESCRIPTION | MATERIAL DESCRIPTION OR NOTE | MATERIAL SPECIFICATION | ZONE | ITEM NO |
|---|---|---|---|---|---|---|---|---|
| 6 | | | -21 | CHANNEL | .040 SHEET BERYLLIUM | | | |
| | 2 | | -19 | SEAL STRIP | LI-1500 | | | |
| | 1 | | -17 | SEAL STRIP | LI-1500 | | | |
| AR | | | | MS20427MS | RIVET, SOLID, FLUSH HEAD | MONEL | | |
| | | | -15 | BLOCK | LI-1500 | | | |
| | 2 | | -13 | BLOCK | LI-1500 | | | |
| 2 | | | -11 | CHANNEL | .040 SHEET BERYLLIUM | | | |
| 6 | | | -9 | SPACER | .75 x .75 SQ BAR BERYLLIUM | | | |
| 8 | | | -7 | SPACER | .75 x .75 SQ BAR BERYLLIUM | | | |
| 2 | | | -5 | ANGLE | .040 SHEET BERYLLIUM | | | |
| 2 | | | -3 | ANGLE | .040 SHEET BERYLLIUM | | | |
| 1 | | | -1 | PLATE | .040 SHEET BERYLLIUM | | | |
| | 1 | | -301 | [illegible] ASSY | | | | |

PARTS LIST

) WITH RTV-560 PER SPEC LAC 30-4455.
JACE BRAZE WITH .003 BRAZE ALLOY BAg 8.
BEND RADII 5 ± MIN
N PER SPEC LAC 0170.
ECT PER SPEC LAC 1001.
JCATE PER LAC PB-92.
GAP BETWEEN PANELS & -301 FRAME TO .030.
FACE COATING .010 THICK ON LI-1500 PER 0042 COATING SYSTEM.
) LI-1500 TO -301 FRAME USING RTV-560 SPEC LAC 30-4455.

INTERPRET DWG PER

NEXT ASSY | USED ON
APPLICATION

UNLESS OTHERWISE SPECIFIED DIM ARE IN INCHES TOLERANCES ON:
FRACTIONS = ± 1/16
DECIMALS: X = ± 1
XX = ± .03
XXX = ± .010
ANGLES = ± 2 DEG

CONTR
CCA/CB

DATE 3-24-71
DR
APPD
APPD
ENGRG
CHK
APPD
APPD

LOCKHEED MISSILES & SPACE COMPANY
A GROUP DIVISION OF LOCKHEED AIRCRAFT CORPORATION
SUNNYVALE CALIFORNIA

THERMAL TEST PANEL
No. 1

SIZE | CODE IDENT | DRAWING NO. SKJ205008 | REV -
SCALE | SHEET

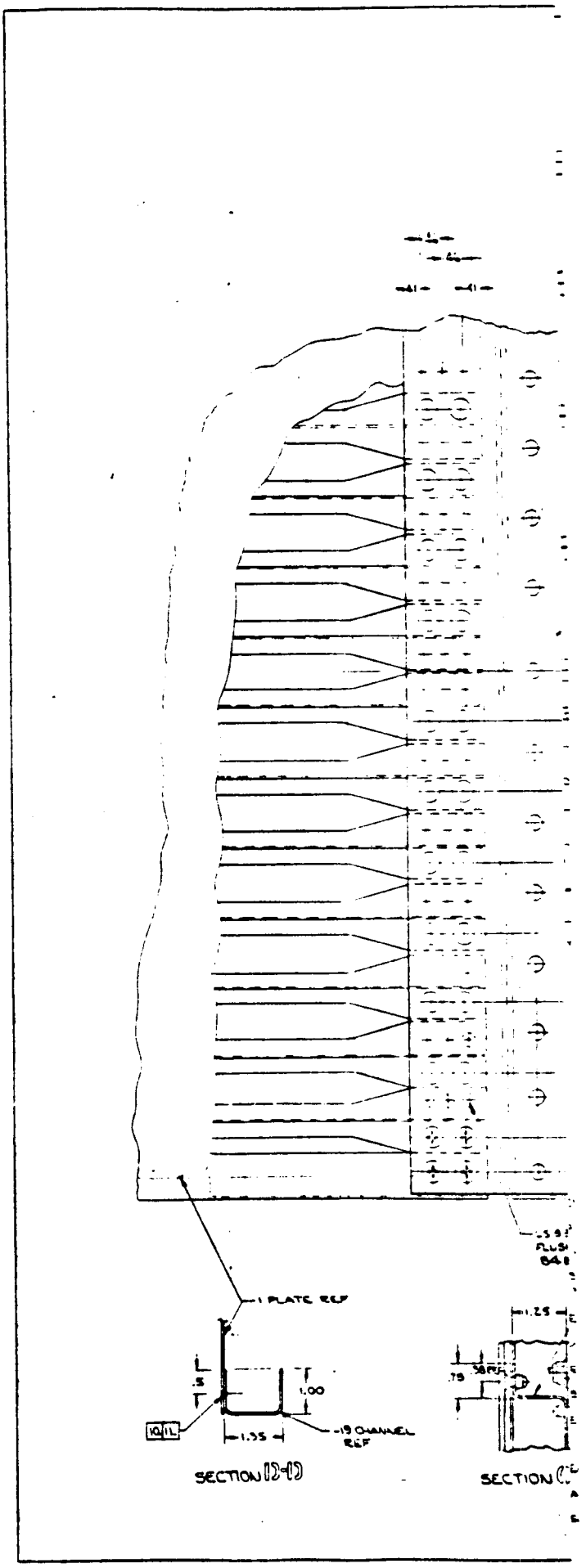

1 PLATE REF
.5
1.00
10/1L
1.35
-19 CHANNEL REF
SECTION D-D
1.25
.75
SECTION

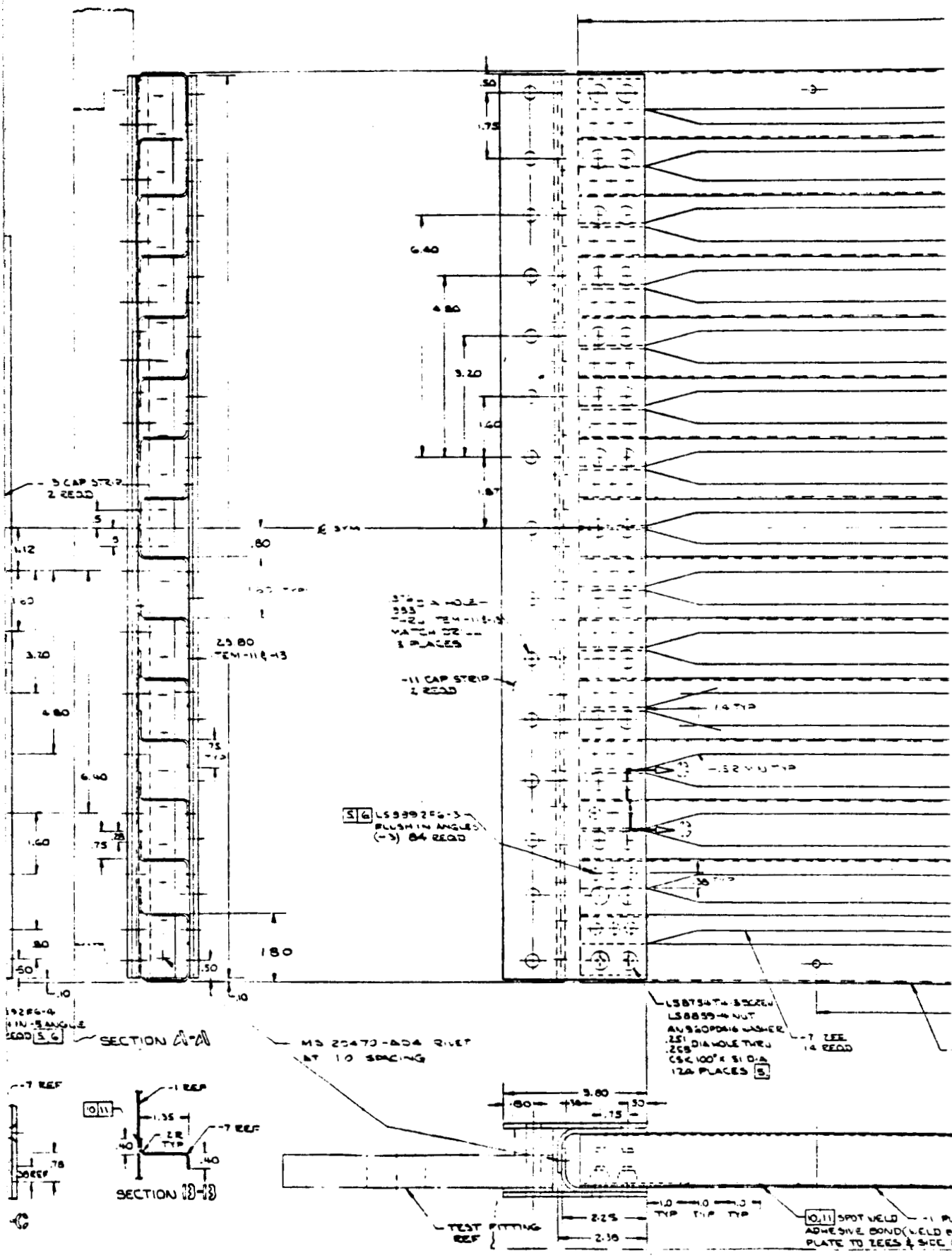

SECTION A-A
SECTION B-B
MS 20470-AD4 RIVET AT 1.0 SPACING
TEST FITTING REF
-11 CAP STRIP 2 REQD
-3 CAP STRIP 2 REQD
LS9392F6-3 FLUSH IN ANGLES (-3) 84 REQD
-7 ZEE 14 REQD
10,11 SPOT WELD

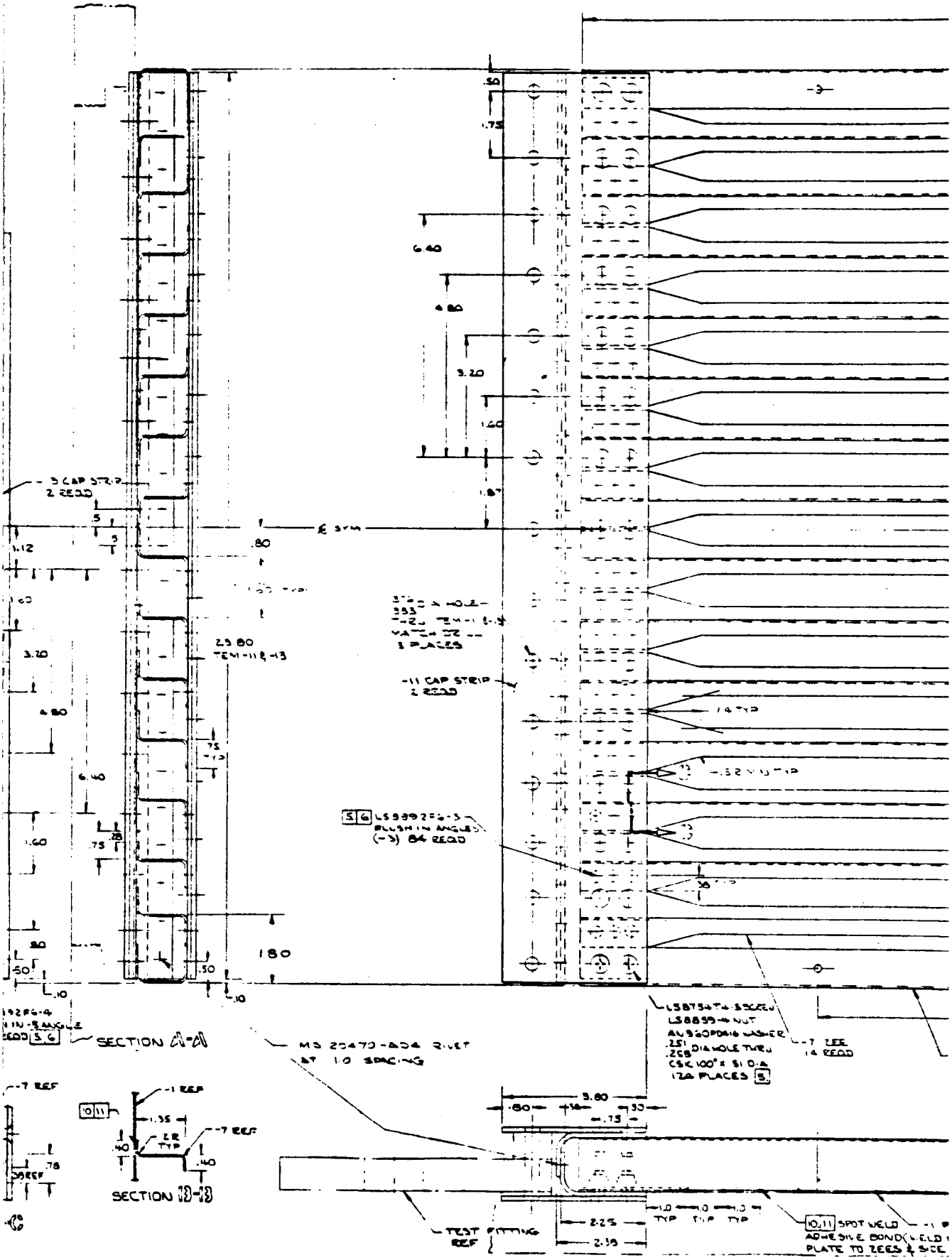

SECTION A-A
SECTION B-B
MS 20470-AD4 RIVET AT 1.0 SPACING
-11 CAP STRIP 2 REQD
-3 CAP STRIP 2 REQD
LS8892F6-3 FLUSH IN ANGLES (-3) 84 REQD
LS8754T4-3 SCREW
LS8859-4 NUT
AN960PD416 WASHER
.251 DIA HOLE THRU
.258 CSK 100° x .51 DIA
124 PLACES 5
-7 ZEE 14 REQD
TEST FITTING REF
10,11 SPOT WELD
ADHESIVE BOND (WELD
PLATE TO ZEES & SIDE

| LTR | CHANGE | DATE | APPD |
|---|---|---|---|
| A | TILE SIZE WAS 4.00 x 4.00 x 3.35 THICK; ADDED NOTE 13 & 14; GAPS REVISED; ADDED DETAIL 5. | | |

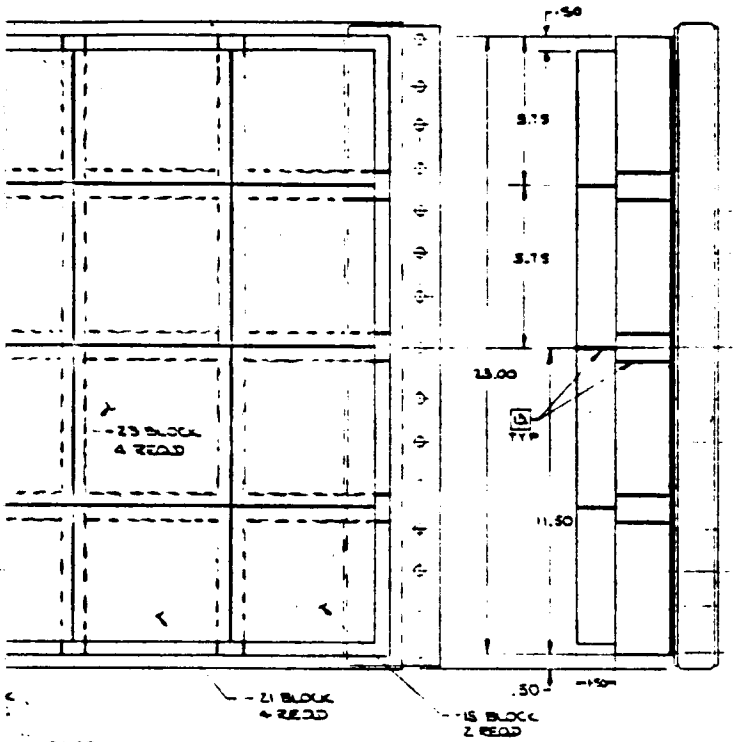


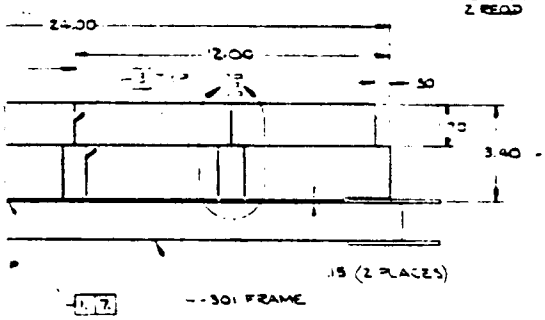


PANEL ASSY -301
SCALE 1/2

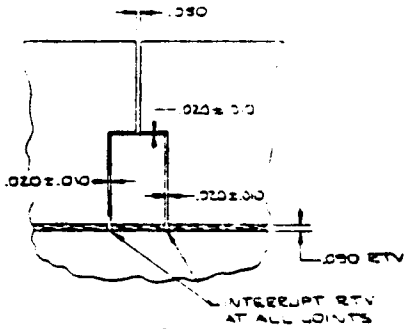


DETAIL 5
TYP OF ALL JOINTS
SCALE 1/1

FIG 2
PAGE F-9/10

| QTY REQD -301 | QTY REQD -50 | CODE IDENT | PART OR IDENTIFYING NO | NOMENCLATURE OR DESCRIPTION | MATERIAL DESCRIPTION OR NOTE | MATERIAL SPECIFICATION | ZONE | ITEM NO |
|---|---|---|---|---|---|---|---|---|
| | 3 | | -21 | SEAL STRIP | LI-1500 | | | |
| | 6 | | -23 | SEAL STRIP | ↓ | | | |
| | 6 | | -27 | SEAL STRIP | | | | |
| | 4 | | -25 | BLOCK | | | | |
| | 4 | | -23 | BLOCK | ↓ | | | |
| | 4 | | -21 | BLOCK | LI-1500 | | | |
| 124 | | | LS8754T4-5 | SCREW | | | | |
| 124 | | | LS8853-4 | NUT | | | | |
| 124 | | | AN960PD4-6 | WASHER | | | | |
| 2 | | | -19 | CHANNEL | .050 SHT AL 7075 T6 3 | | | |
| AR | | | MS20470AD4 | RIVET | | | | |
| 84 | | | LS8892F6-5 | JO-BOLT | | | | |
| 84 | | | LS8892F6-4 | JO-BOLT | | | | |
| | 2 | | -17 | BLOCK | LI-1500 | | | |
| | 2 | | -15 | BLOCK | LI-1500 | | | |
| 2 | | | -13 | CAP STRIP | .125 SHT AL 7075 T6 | | | |
| 2 | | | -11 | CAP STRIP | .125 SHT AL 7075 T6 | | | |
| 28 | | | -9 | CLIP | .050 SHT AL 7075 T6 3 | | | |
| 14 | | | -7 | ZEE | .050 SHT AL 7075 T6 3 | | | |
| 2 | | | -5 | ANGLE | .125 SHT AL 7075 T6 3 | | | |
| 2 | | | -3 | ANGLE | .125 SHT AL 7075 T6 3 | | | |
| 1 | | | -1 | PLATE | .050 SHT AL 7075 T6 | | | |
| | 1 | | -301 | FRAME ASSY | | | | |

PARTS LIST

.0 0 THICK ON LI-1500 PER 0042 COATING SYSTEM.
BLOCKS & SEAL STRIPS TO.
SHALL BE NON ACCUMULATIVE.
E BONDING (WELD BOND) ON 1.0 CENTERS.
TO -1 PLATE. WELD BOND -1 PLATE TO -19 CHANNELS
1557.
LAC 1001.
AC 0170.
LS TO -301 FRAME PER SPEC LAC 50-4436.
PER DESIGN STD DS 40007.
RS PER SPEC LAC 0581.
2 UNLESS OTHERWISE SPECIFIED.
2 FORMING TO TEMPER T6 PER SPEC LAC 521.
C SPEC 1241.
0. HOLD GAP BETWEEN LI-1500 & -301 FRAME TO .090

| INTERPRET DWG PER | | UNLESS OTHERWISE SPECIFIED DIM ARE IN INCHES TOLERANCES ON FRACTIONS = ± 1/16 DECIMALS X = ± .1 XX = ± .03 XXX = ± .010 ANGLES = ± 2 DEG | DATE | LOCKHEED MISSILES & SPACE COMPANY |
|---|---|---|---|---|
| | | | DR | |
| | | | APPD | |
| | | | APPD | |
| | | | ENGRG | |
| | | | CHK | |
| NEXT ASSY | USED ON | CONTR | APPD | SIZE / CODE IDENT / DRAWING NO / REV |
| APPLICATION | | CCA/CEI | APPD | SCALE / SHEET |

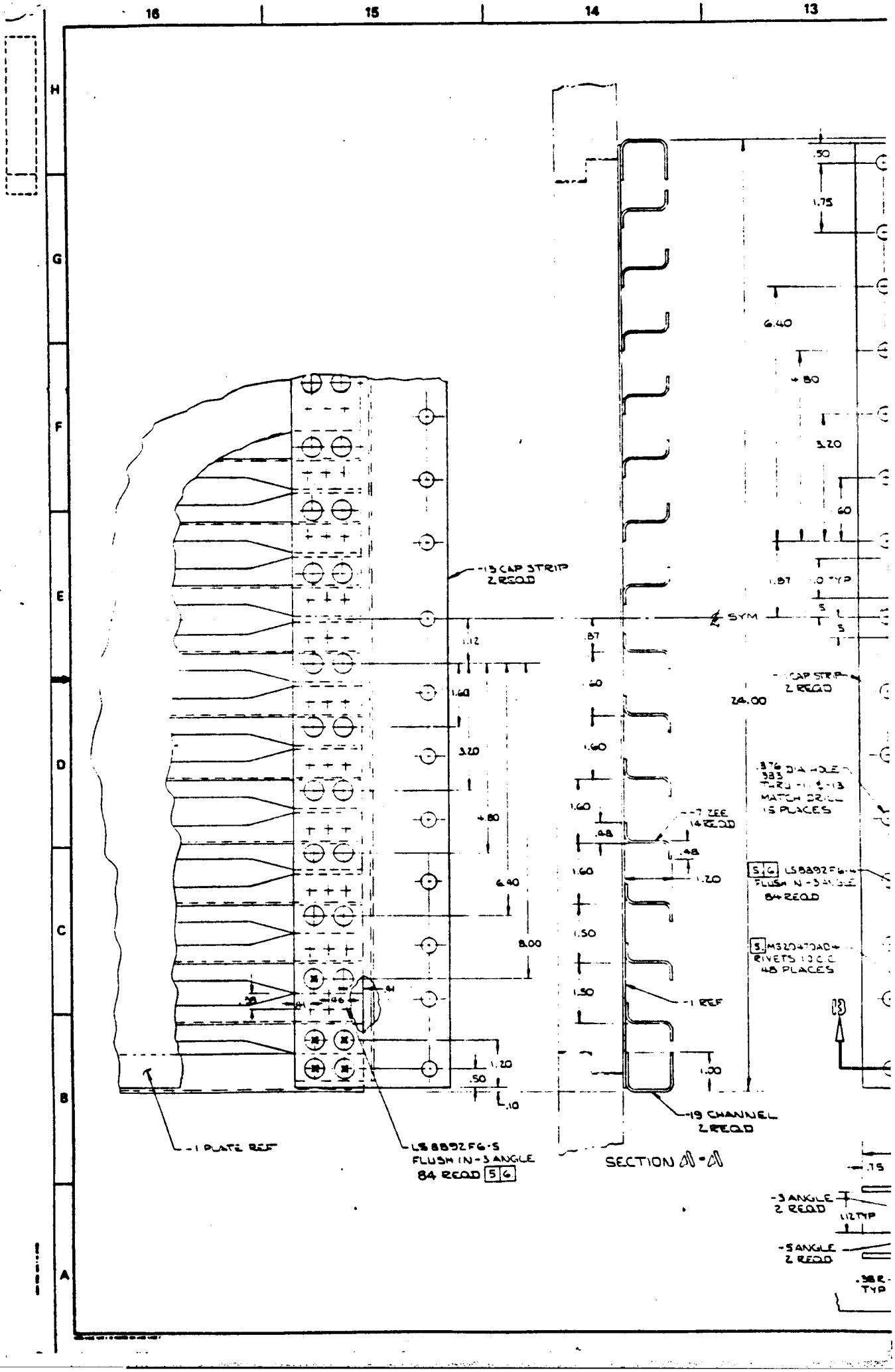

16
15
14
13
H
G
F
E
D
C
B
A
-13 CAP STRIP
2 REQD
SYM
-1 PLATE REF
LS8892F6-5
FLUSH IN-3 ANGLE
84 REQD 5 6
SECTION A-A
-19 CHANNEL
2 REQD
-7 ZEE
14 REQD
-1 REF
24.00
6.40
3.20
1.87
1.12
1.60
4.80
8.00
1.20
.50
.10
1.00
1.50
.48
.87
.60
.50
1.75
.75
-3 ANGLE
2 REQD
-5 ANGLE
2 REQD

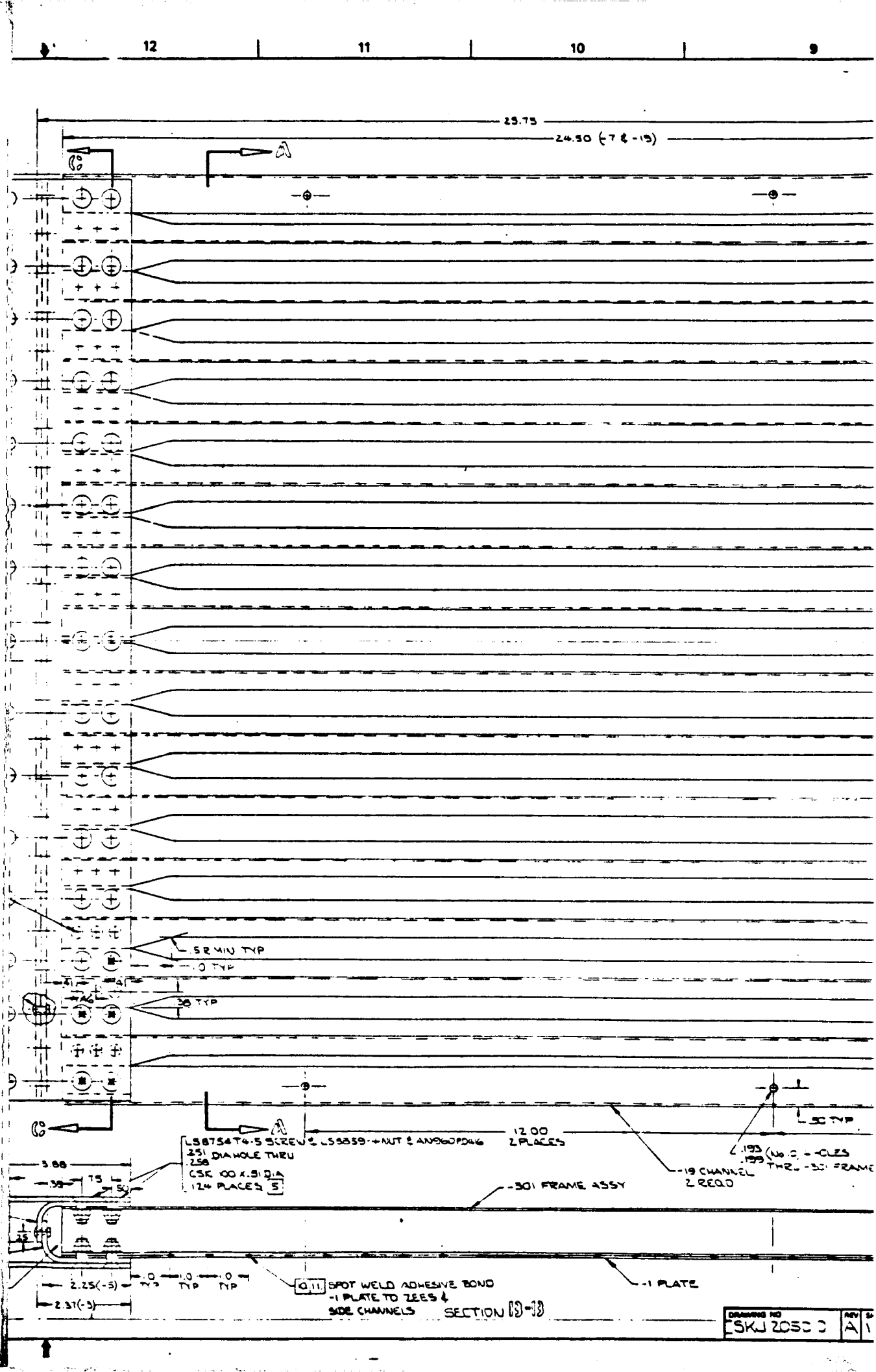

12
11
10
9
25.75
24.50 (-7 & -19)
.5 R MIN TYP
.0 TYP
.38 TYP
.50 TYP
12.00
2 PLACES
LS8754T4-5 SCREW & LS8859-4 NUT & AN960PD416
.251
.258 DIA HOLE THRU
CSK .100 X .51 DIA
.124 PLACES 5
3.88
.75
.50
-19 CHANNEL
2 REQD
-301 FRAME ASSY
2.25(-5)
2.37(-3)
.0 TYP
.0 TYP
.0 TYP
0.11 SPOT WELD ADHESIVE BOND
-1 PLATE TO ZEES &
SIDE CHANNELS
-1 PLATE
SECTION B-B
DRAWING NO
SKJ 2050 0
REV
A

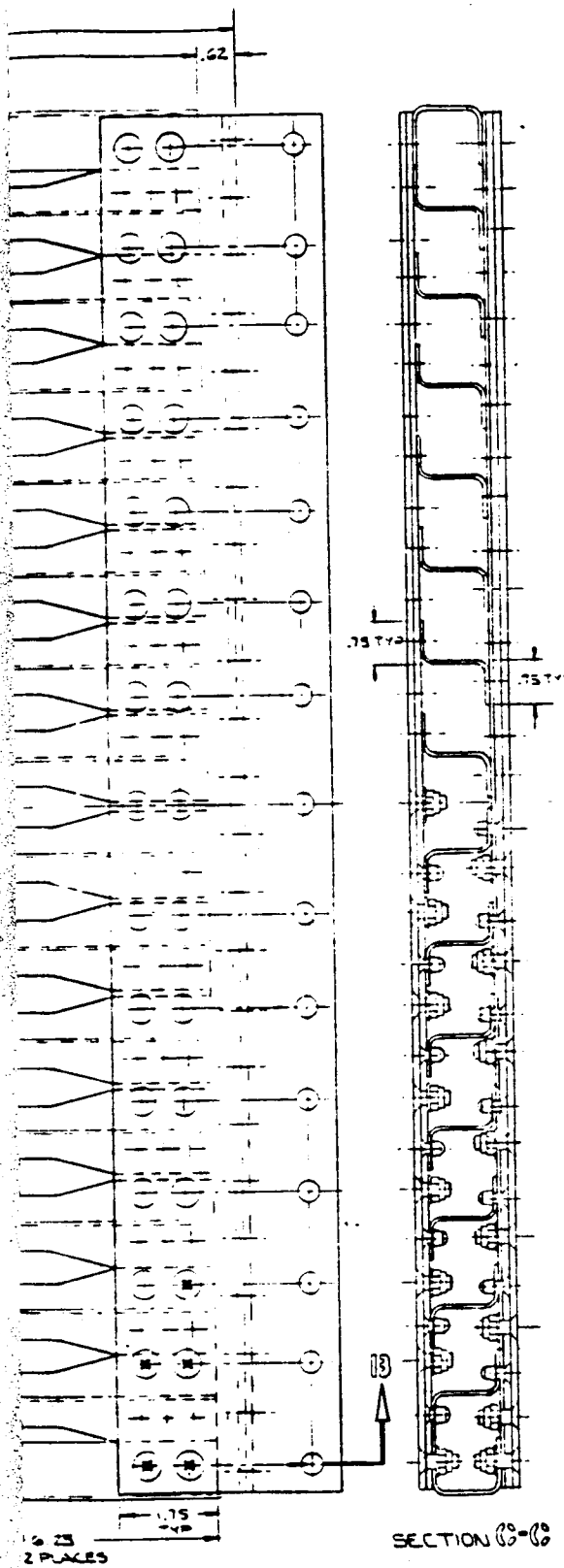


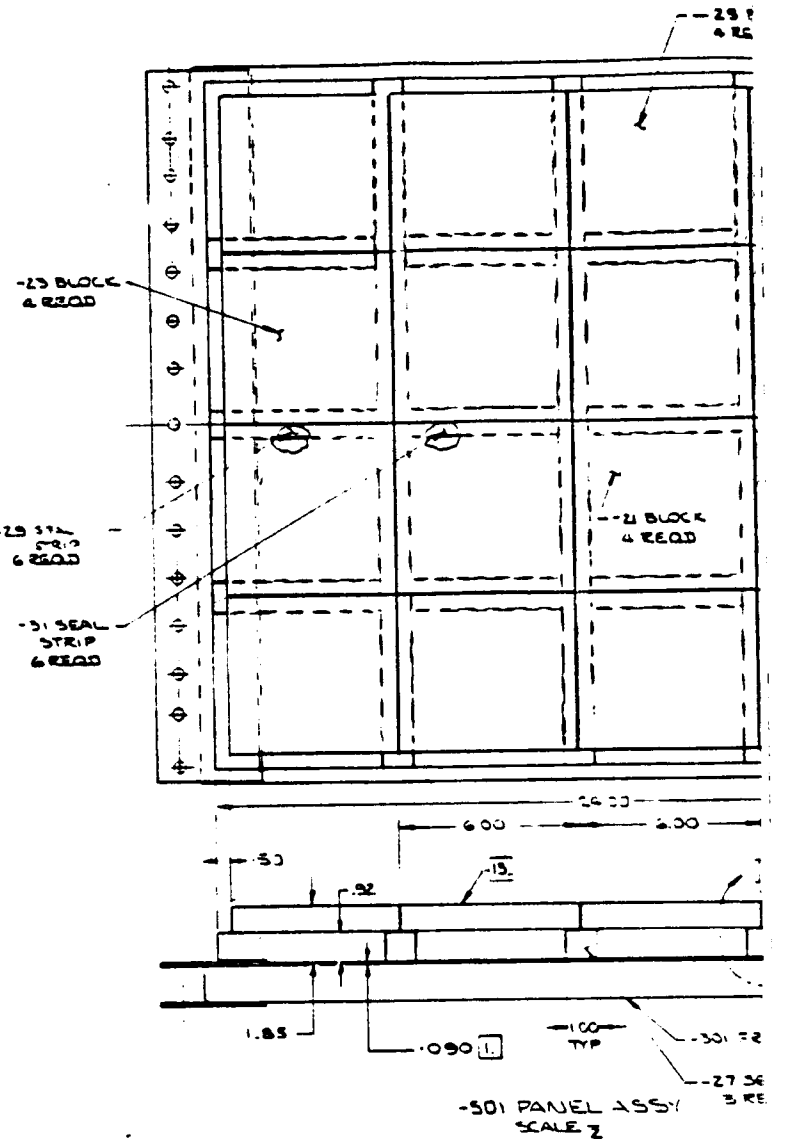


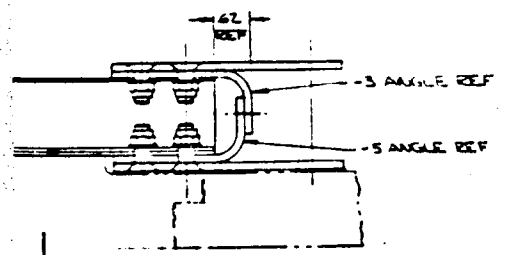


13 SURFACE COATING .010 THICK ON LT-1500 PER CO42 COATING S

12 ALL TOLERANCES SHALL BE NON ACCUMULATIVE.

11 SPOT WELD ADHESIVE BONDING (WELD BOND) ON 1.0 CENTERS.

10 WELD BOND -7 ZEES TO -1 PLATE. WELD BOND -1 PLATE TO -19 CHANNELS PER SPEC LAC X 3857.

9 PROTECT PER SPEC LAC 1001.

8 CLEAN PER SPEC LAC 0170.

7 BOND LT-1500 PANELS TO -301 FRAME PER SPEC LAC 30-4438

6 INSTALL JO-BOLTS PER DESIGN STD DS 40007.

5 INSTALL FASTENERS PER SPEC LAC 0581.

4 ALL BEND RADII .16 UNLESS OTHERWISE NOTED

3 HEAT TREAT AFTER FORMING TO TEMPER T6 PER SPEC LAC 57

2 FABRICATE PER SPEC LAC 1241.

1 BOND USING RTV 560. HOLD GAP TO BETWEEN PARTS TO .090

NOTES.

| REVISIONS | | | | |
|---|---|---|---|---|
| ZONE | LTR | DESCRIPTION | DATE | APVD |
| | A | [illegible] ADDED NOTE 13, ADDED DETAIL B | | |

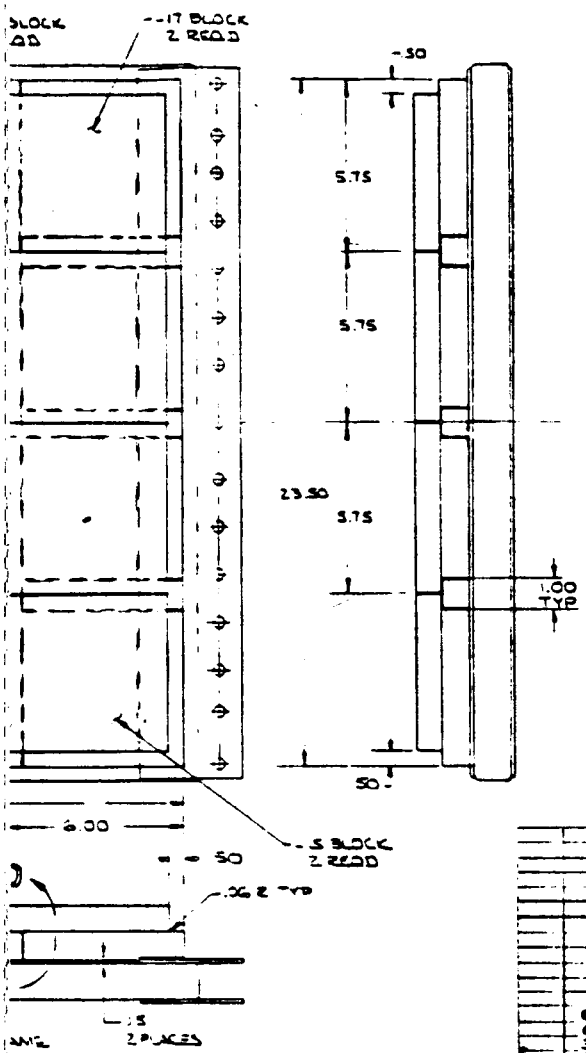


FIG. 3

PAGE F-11/12

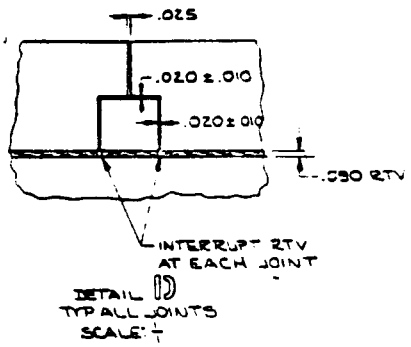


| QTY REQD -301 | QTY REQD -501 | CODE IDENT | PART OR IDENTIFYING NO | NOMENCLATURE OR DESCRIPTION | MATERIAL DESCRIPTION OR NOTE | MATERIAL SPECIFICATION | ZONE | ITEM NO |
|---|---|---|---|---|---|---|---|---|
| | 6 | | -31 | SEAL STRIP | LI-1500 | | | |
| | 6 | | -29 | SEAL STRIP | | | | |
| | 3 | | -27 | SEAL STRIP | | | | |
| | 4 | | -25 | BLOCK | | | | |
| | 4 | | -23 | BLOCK | | | | |
| | 4 | | -21 | BLOCK | LI-1500 3 | | | |
| 2 | | | -19 | CHANNEL | .062 SHT AL 7075-0 3 | | | |
| 124 | | | LS8754T4-5 | SCREW | | | | |
| 124 | | | LS8859-4 | NUT | | | | |
| 124 | | | AN960C416 | WASHER | | | | |
| AR | | | MS20470AD4 | RIVET | | | | |
| 84 | | | LS8892F6-5 | JO-BOLT | | | | |
| 84 | | | LS8892F6-4 | JO-BOLT | | | | |
| | 2 | | -17 | BLOCK | LI-1500 7 | | | |
| | 2 | | -15 | BLOCK | LI-1500 7 | | | |
| 2 | | | -13 | CAP STRIP | .125 SHT AL 7075-T6 | | | |
| 2 | | | -11 | CAP STRIP | .125 SHT AL 7075-T6 | | | |
| 28 | | | -9 | CLIP | .062 SHT AL 7075-0 3 | | | |
| 14 | | | -7 | ZEE | .062 SHT AL 7075-0 | | | |
| 2 | | | -5 | ANGLE | .125 SHT AL 7075-0 | | | |
| 2 | | | -3 | ANGLE | .125 SHT AL 7075-0 3 | | | |
| 1 | | | -1 | PLATE | .062 SHT AL 7075-T6 | | | |
| | 1 | | -301 | FRAME ASSY | | | | |

PARTS LIST

| INTERPRET DWG PER | | UNLESS OTHERWISE SPECIFIED DIM ARE IN INCHES TOLERANCES ON FRACTIONS = ± 1/16 DECIMALS: .X = ± .1 .XX = ± .03 .XXX = ± .010 ANGLES = ± 2 DEG | DATE | LOCKHEED MISSILES & SPACE COMPANY A GROUP DIVISION OF LOCKHEED AIRCRAFT CORPORATION SUNNYVALE, CALIFORNIA |
|---|---|---|---|---|
| | | | DWN | THERMAL TEST PANEL No 3 |
| | | | APVD | |
| | | | APVD | |
| | | | ENGRG | |
| | | | CHKR | |
| NEXT ASSY | USED ON | CONTR | APVD | SIZE J · CODE IDENT · DRAWING NO SKJ205010 · REV A |
| APPLICATION | | CCA/CI/FD | APVD | SCALE · SHEET 1 |

SKJ205010 A

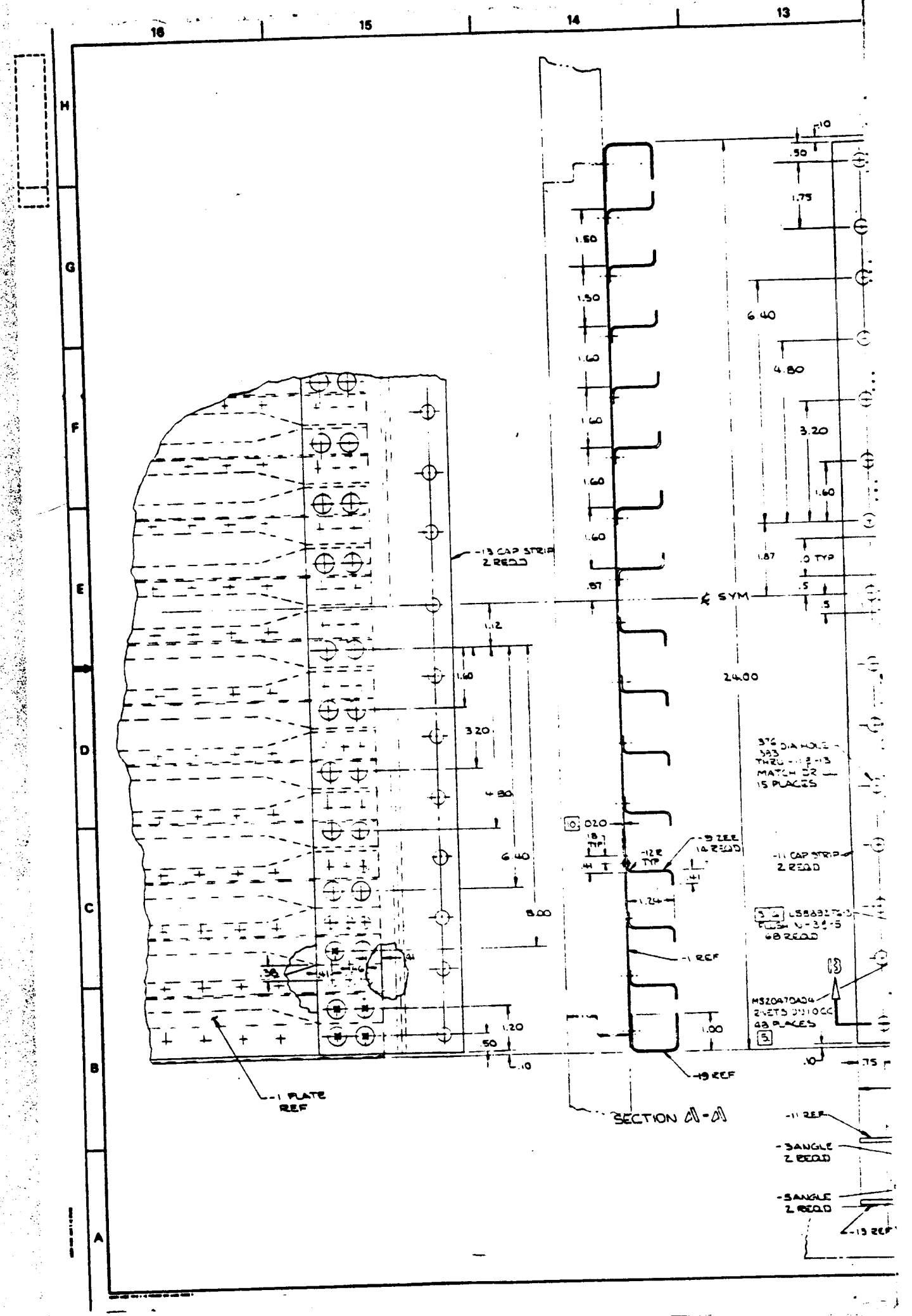

16
15
14
13
H
G
F
E
D
C
B
A
-13 CAP STRIP
2 REQD
℄ SYM
24.00
-1 PLATE
REF
SECTION A-A
-1 REF
-19 REF
-11 CAP STRIP
2 REQD
-11 REF
-3 ANGLE
2 REQD
-3 ANGLE
2 REQD
-13 REF

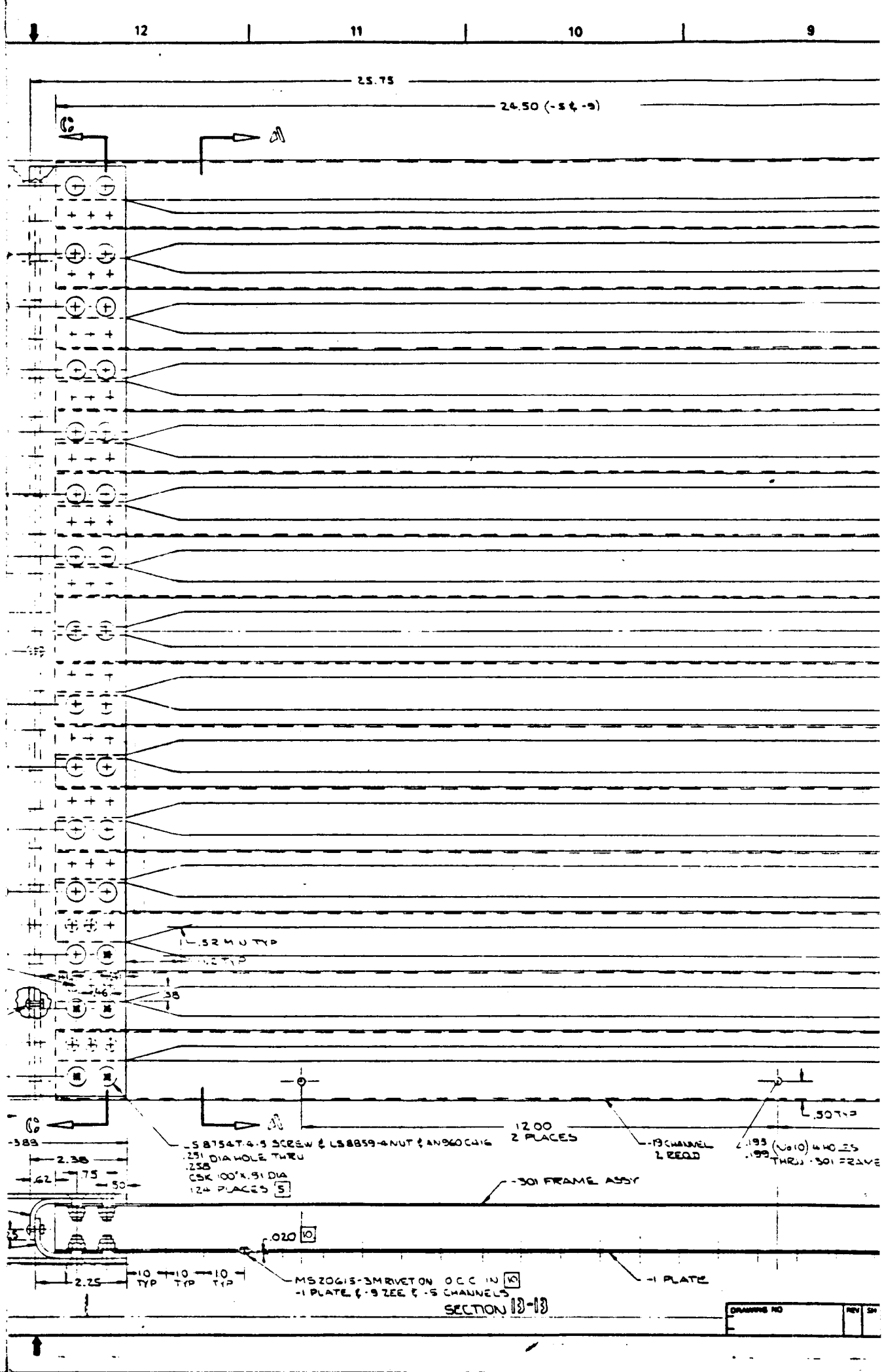
12
11
10
9
25.75
24.50 (-5 & -9)
.52 MIN TYP
.46
.38
12.00
2 PLACES
.50 TYP
-19 CHANNEL
2 REQD
.193 (No 10) 4 HOLES
.199 THRU -301 FRAME
.389
2.38
.62
.75
.50
LS 87547-4-5 SCREW & LS8859-4 NUT & AN960C416
.251 DIA HOLE THRU
.258
CSK .100 X .51 DIA
124 PLACES 5
-301 FRAME ASSY
.020 10
2.25
.10 TYP
.10 TYP
.10 TYP
MS20615-3M RIVET ON O.C.C. IN 10
-1 PLATE & -9 ZEE & -5 CHANNELS
-1 PLATE
SECTION B-B
DRAWING NO
REV
SH

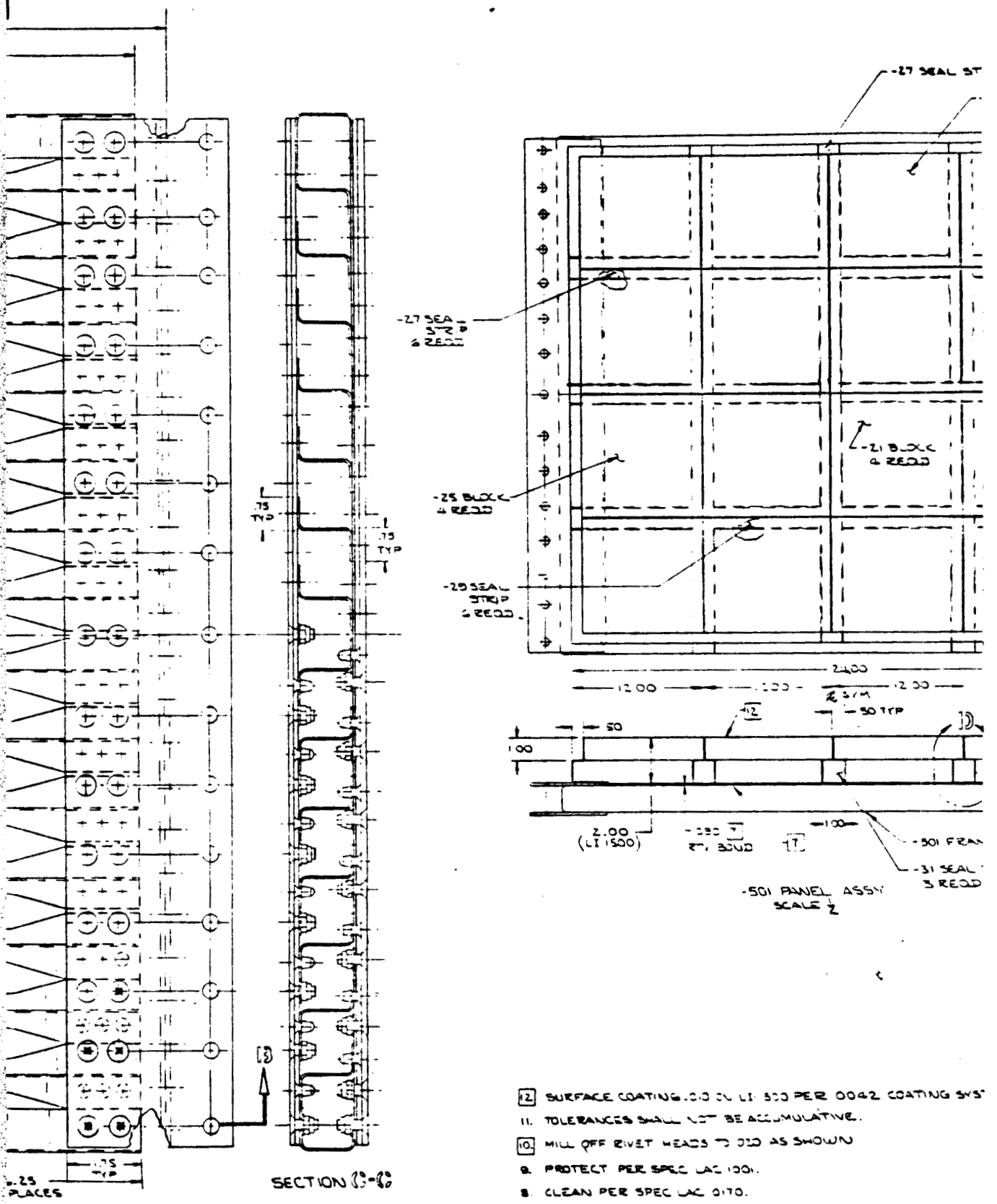


12. SURFACE COATING .010 ON LT 500 PER 0042 COATING SYS
11. TOLERANCES SHALL NOT BE ACCUMULATIVE.
10. MILL OFF RIVET HEADS TO .010 AS SHOWN
9. PROTECT PER SPEC LAC 1001.
8. CLEAN PER SPEC LAC 0170.
7. BOND LT 1600 PANELS TO -501 FRAME PER SPEC LAC 30-44-35 U
6. INSTALL JO-BOLTS PER DESIGN STD DS 40007.
5. INSTALL FASTENERS PER SPEC LAC 0581
4. ALL BOND RADII .12 UNLESS OTHERWISE NOTED.
3. SOLUTION HEAT TREAT & AGE PER PROCESS BULLETIN PB-56 AFTER F
2. FABRICATE PER SPEC LAC 1241.
1. BOND USING RTV 560. HOLD GAP BETWEEN -13 & -15 PANELS TO .0

| ZONE | LTR | REVISIONS DESCRIPTION | DATE | APVD |
|---|---|---|---|---|
| | A | BLOCK SIZE WAS 4 [illegible] X 2.20 THICK; ADDED NOTE 12 & 13 | 8 NOV 71 | |

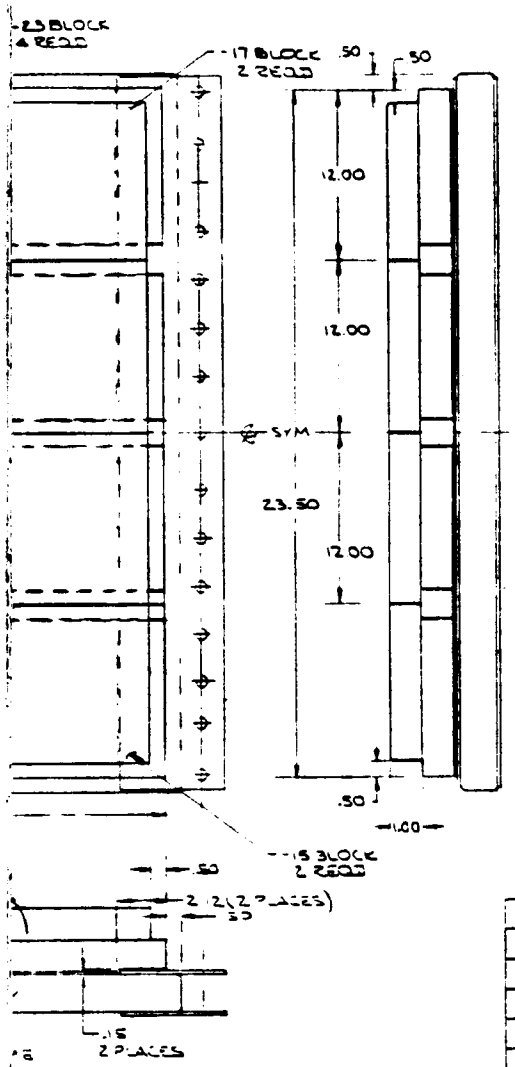


FIG. 4
PAGE F-13/14

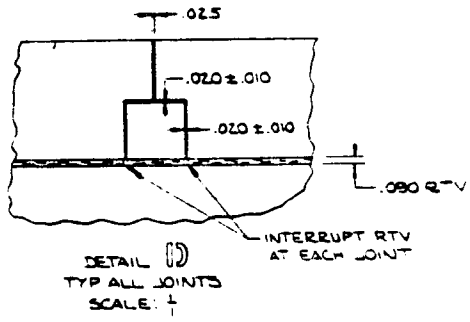


| QTY REQ -301 | QTY REQD -501 | CODE IDENT | PART OR IDENTIFYING NO | NOMENCLATURE OR DESCRIPTION | MATERIAL DESCRIPTION OR NOTE | MATERIAL SPECIFICATION | ZONE | ITEM NO |
|---|---|---|---|---|---|---|---|---|
| | 3 | | -31 | SEAL STRIP | LI-1500 7 | | | |
| | 6 | | -29 | SEAL STRIP | | | | |
| | 6 | | -27 | SEAL STRIP | | | | |
| | 4 | | -25 | BLOCK | | | | |
| | 4 | | -23 | BLOCK | | | | |
| | 4 | | -21 | BLOCK | LI-500 7 | | | |
| AR | | | MS 20615-3M | RIVET | | | | |
| AR | | | MS 20470AD4 | RIVET | | | | |
| 168 | | | LS8392F6-3 | JO-BOLT | | | | |
| 124 | | | LS8754T4-5 | SCREW | | | | |
| 124 | | | LS8359-4 | NUT | | | | |
| 124 | | | AN960C416 | WASHER | | | | |
| 2 | | | -19 | CHANNEL | .040 SHT 6AL-4V | TITANIUM ANNEALED 3 | | |
| | 2 | | -17 | BLOCK | LI-1500 7 | | | |
| | 2 | | -15 | BLOCK | LI-1500 7 | | | |
| 2 | | | -13 | CAP STRIP | .125 SHT 6AL-4V | | | |
| 2 | | | -11 | CAP STRIP | .125 SHT 6AL-4V | | | |
| 28 | | | -9 | CLIP | .040 SHT 6AL-4V | TITANIUM ANNEALED 3 | | |
| 14 | | | -7 | ZEE | .040 SHT 6AL-4V | | | |
| 2 | | | -5 | CHANNEL | .125 SHT 6AL-4V | | | |
| 2 | | | -3 | CHANNEL | .125 SHT 6AL-4V | | | |
| 1 | | | -1 | PLATE | .040 SHT 6AL-4V | TITANIUM ANNEALED 3 | | |
| | 1 | | -301 | FRAME ASSY | | | | |

PARTS LIST

INTERPRET DWG PER

NEXT ASSY | USED ON
APPLICATION

UNLESS OTHERWISE SPECIFIED DIM ARE IN INCHES TOLERANCES ON FRACTIONS = ± 1/16
DECIMALS: X = ± 1
XX = ± .03
XXX = ± .010
ANGLES = ± 2 DEG

CONTR
CCA/CI/FD

DATE
DWN
APVD
APVD
ENGRG
CHKR
APVD
APVD

LOCKHEED MISSILES & SPACE COMPANY
A GROUP DIVISION OF LOCKHEED AIRCRAFT CORPORATION
SUNNYVALE, CALIFORNIA

THERMAL TEST PANEL
No. 4

SIZE J | CODE IDENT | DRAWING NO SKJ205011 | REV A
SCALE 1/1 | SHEET

SKJ205011

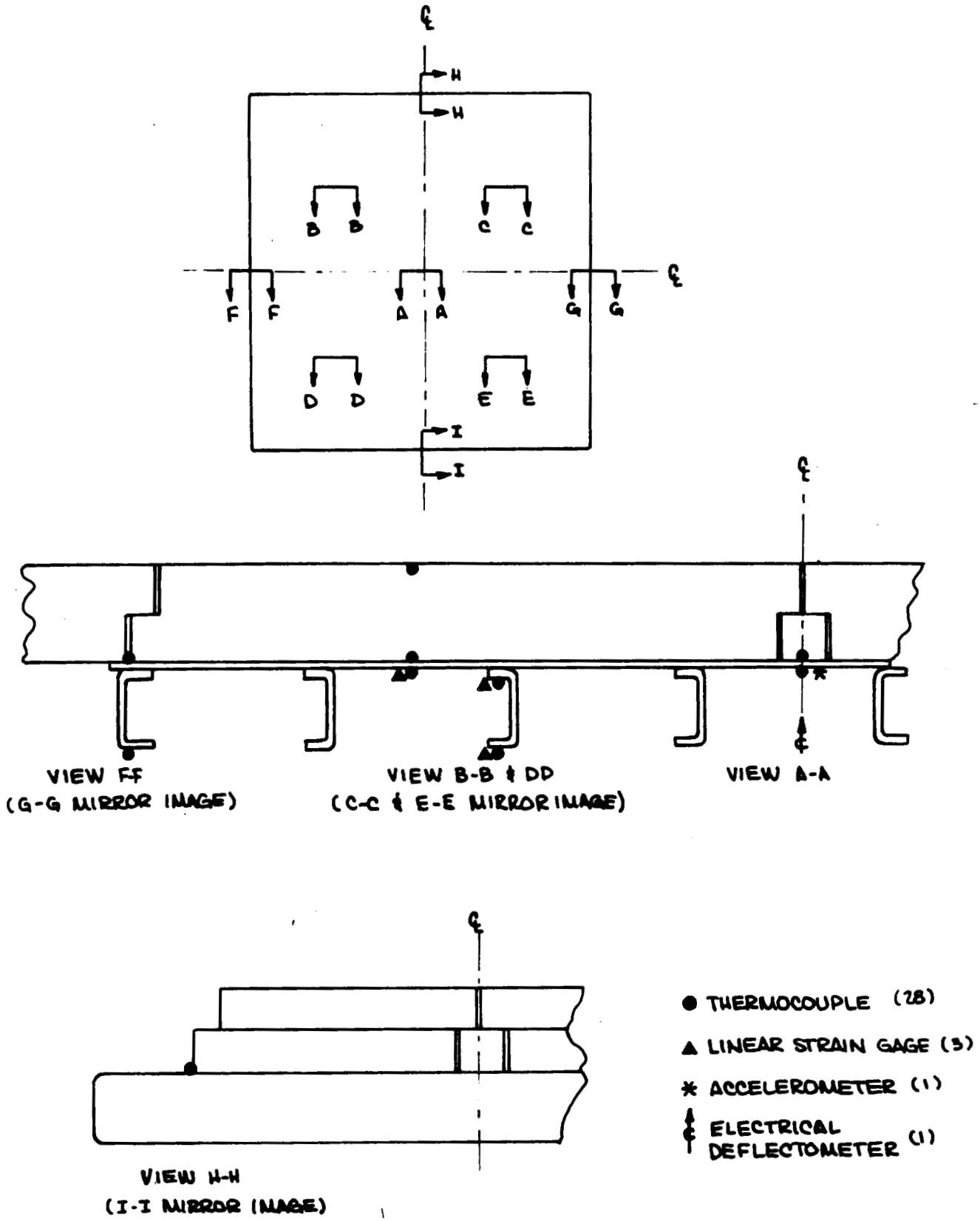


Fig. 5 Beryllium Fuselage Panel Instrumentation

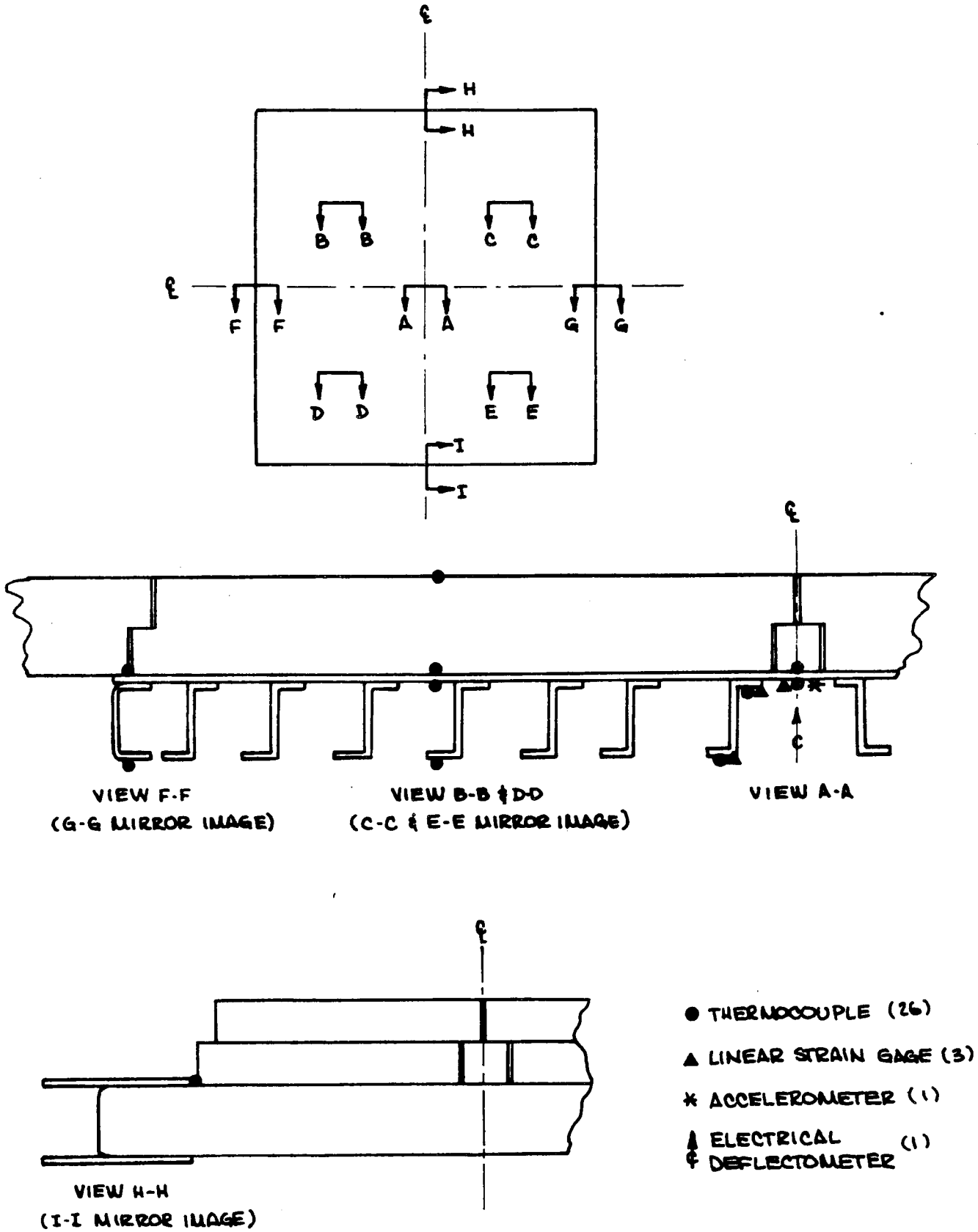


Fig. 6 Aluminum and Titanium Fuselage Panel Instrumentation

## 2.2 ALUMINUM AND TITANIUM FUSELAGE PANEL TEST SETUP

The two aluminum and one titanium panel will be mounted in test fixtures similar to that used for previous wing panel tests described in Reference 1. The panels will remain in their test fixtures throughout the complete test program.

## 2.3 FUSELAGE PANEL TEST SEQUENCE

### 2.3.1 Beryllium Panel

The beryllium fuselage panel will be subjected to an initial series of separate environmental tests to verify the panel design under each environmental condition. The panel will be visually inspected following each of the initial environmental test series. Inspection of both the LI-1500 and beryllium panel will be made after removal of the test fixture base plate. The initial test sequence will consist of the following:

#### 2.3.1.1 Pressure Loading Tests

a. Gradually apply positive differential pressure to 0.5 psi over a 1 minute period.

b. Maintain level for 10 minutes.

c. Reduce differential pressure to zero over a period of 1.5 minutes.

d. Repeat a, b, and c for positive differential pressures of 1.0, 2.0, and 4.0 psi.

e. Remove test fixture base plate, inspect LI-1500 and beryllium panel, and record any changes.

All strain gage, deflectometer, and test fixture pressure data will be recorded during the pressure loading tests.

2.3.1.2 Radiant Heat Tests

a. Increase LI-1500 surface temperature to 1000°F over a period of 500 seconds.

b. Maintain level for 1800 seconds.

c. Decrease LI-1500 surface temperature to ambient over a period of 600 seconds.

d. Allow panel to cool.

e. Inspect insulation surface and record any changes.

f. Increase surface temperature to 1700°F over a period of 500 seconds.

g. Maintain level for 1400 seconds.

h. Decrease LI-1500 surface temperature to ambient over a period of 1000 seconds.

i. Allow panel to cool.

j. Inspect insulation surface and record any changes.

k. Follow the surface temperature history shown in Figure 7.

l. Allow panel to cool.

m. Remove test fixture base plate, inspect LI-1500 and beryllium panel, and record any changes.

During all radiant heat tests the bondline temperature will be limited to 600°F. All thermocouple, strain gage, deflectometer, and test fixture pressure data will be recorded during the radiant heat tests.

The reentry surface temperature histories were obtained from the heat rate histories shown in Reference 2. Shorter duration pulses could be used for the described tests to allow a more rapid progression of the test series. The total heat input to the test panels could still be simulated with a shorter pulse by extending the time at elevated temperatures. The mechanical load histories could be appropriately modified to obtain the desired combination of load and panel temperature.

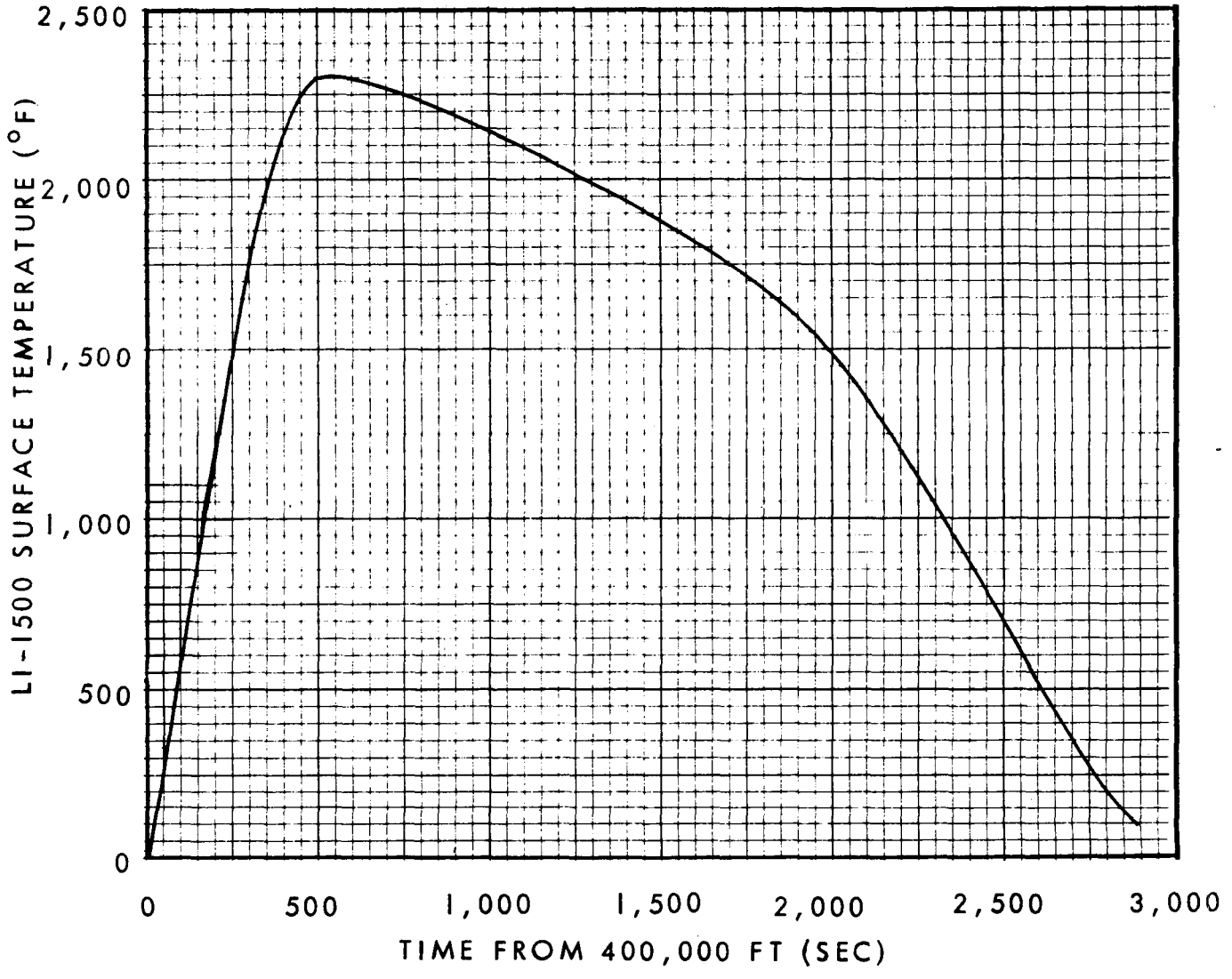


**Fig. 7 Test Temperature Profile – Area 2**

2.3.1.3 Combined Loading and Heating Test

a. Apply radiant heat to LI-1500 surface to obtain the temperature history shown in Figure 7.

b. Gradually apply load to panel to obtain 1.5 psi positive differential pressure at 45 minutes from start of temperature pulse.

c. Maintain 1.5 psi positive differential pressure for 15 minutes.

d. Increase differential pressure to 2.0 psi over a 30 second period.

e. Maintain 2.0 psi positive differential pressure for 1 minute.

f. Reduce differential pressure to zero over a 1 minute period.

g. Allow panel to cool.

h. Remove test fixture base plate, inspect LI-1500 and beryllium panel, and record any changes.

All thermocouple, strain gage, deflectometer, and test fixture pressure data will be recorded during this test.

2.3.1.4 Acoustic Test

a. Expose test panel to the spectrum shown in Figure 8 for a 15 second period.

b. Inspect LI-1500 and beryllium panel after test and record any changes.

The test panel will remain mounted to the test fixture for this test but the fixture back-face panel shall be removed. Data from 6 microphones and 3 accelerometers will be recorded during the test. An initial power spectral density analysis and a 1/3 octave band analysis will be made.

Upon completion of the above initial environmental tests, the fuselage test panels will then be subjected to the following sequence and combination of environmental tests:

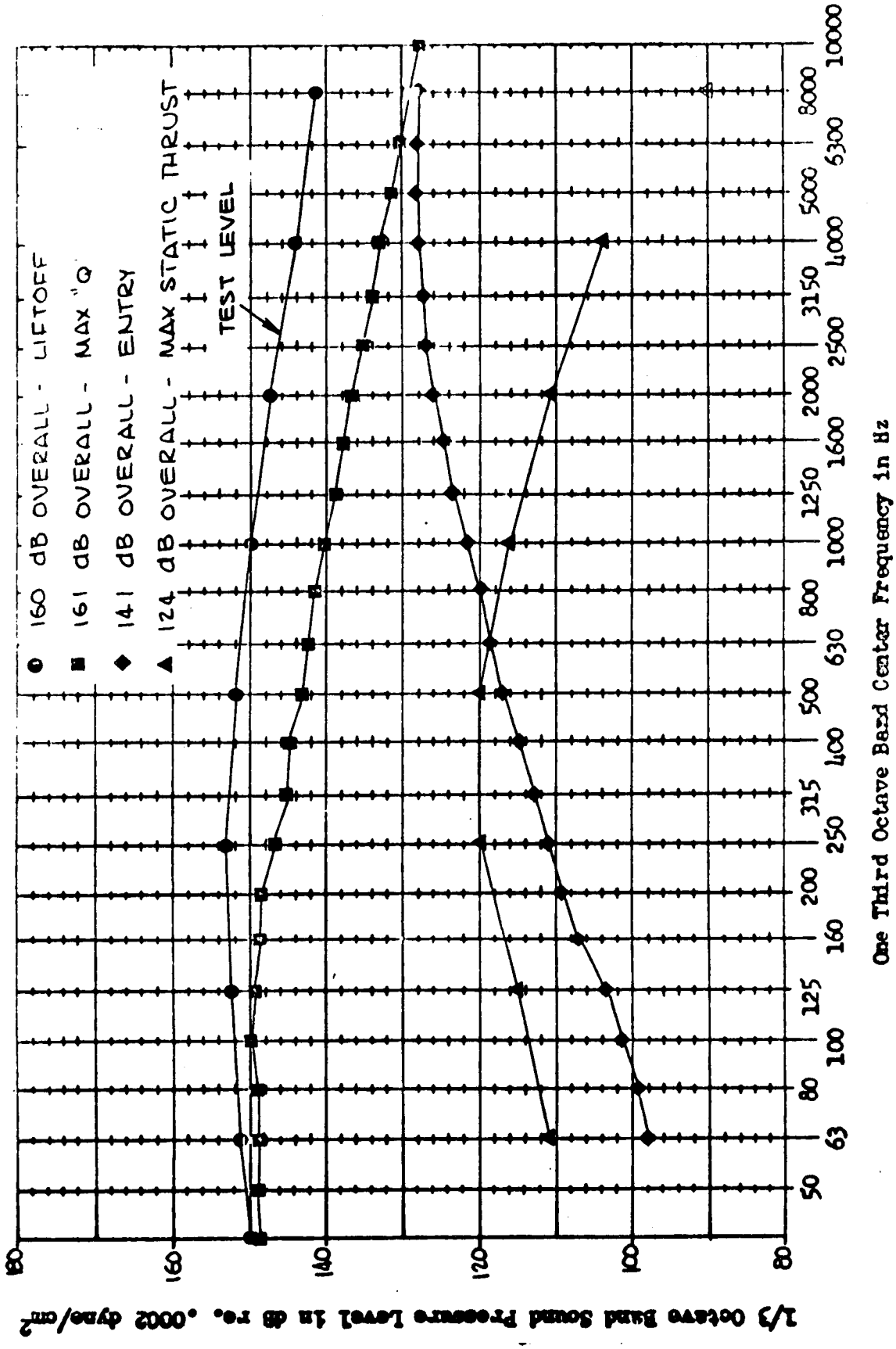


Fig. 8 Acoustic Test Criteria

2.3.1.5 Combined Environmental Tests

a. Gradually apply positive differential pressure to 4.0 psi over a 1 minute period.

b. Reduce differential pressure to zero over a 1.5 minute period.

c. Apply radiant heat to LI-1500 surface to obtain the temperature history shown in Figure 7.

d. Gradually apply load to panel to obtain 1.5 psi positive differential pressure at 45 minutes from start of temperature pulse.

e. Maintain 1.5 psi positive differential pressure for 15 minutes.

f. Increase differential pressure to 2.0 psi over a 30 second period.

g. Maintain 2.0 psi positive differential pressure for 1 minute.

h. Reduce differential pressure to zero over a 1 minute period.

i. Allow panel to cool.

j. Inspect LI-1500 surface and record any changes.

k. Repeat a through j four times.

l. Remove test fixture base plate, inspect LI-1500 and beryllium panel, and record any changes.

All thermocouple, strain gage, test fixture pressure, and deflectometer data will be recorded during these combined radiant heating/pressure loading tests until maximum bondline and beryllium panel temperatures are obtained.

m. Expose test panel to the spectrum shown in Figure 8 for a 75 second period.

n. Inspect LI-1500 and beryllium panel after test and record any changes.

The test panel will remain mounted to the test fixture for this test but the fixture back-face panel will be removed. Data from 3 microphones and 3 accelerometers will be recorded during the tests. A 1/3 octave band analysis will be performed on the microphone data.

o. Repeat c through j (preceding) 10 times.

p. Repeat m and n (preceding) except increase test duration to 150 seconds.

q. Repeat o.

r. Repeat p.

s. Place test panel in vacuum chamber.

t. Pump chamber down to a vacuum of at least $10^{-5}$ Torr.

u. Decrease test panel temperature to $-150^{o}F$.

v. Allow test panel temperature to increase to ambient.

w. Increase chamber pressure to ambient level.

x. Remove panel from chamber, perform visual inspection of LI-1500 and beryllium panel, and record any changes.

y. Repeat a through x 3 times.

2.3.2 Aluminum Panel - Area 2

This panel will be subjected to an initial series of separate environmental tests to verify the panel design under each environmental condition. The panel will be inspected following each of the initial environmental test series. The initial test sequence shall consist of the following:

2.3.2.1 Axial Load Tests

a. Apply axial preload of 1000 lb.

b. Increase load to 18,000 lb over a period of not less than 1 minute.

c. Maintain load for 10 minutes.

d. Reduce load to 1000 lb over a period of not less than 1 minute.

e. Perform visual inspection of panel.

f. Repeat b, c, d, and e for axial loads of 36,000, 72,000 and 144,000 lb.

All strain gage and axial load data shall be recorded during the axial load tests.

2.3.2.2 Radiant Heat Tests

a. Apply axial preload of 1000 lb.

b. Increase LI-1500 surface temperature to 1000°F over a period of 500 seconds.

c. Maintain 1000°F surface temperature for 1800 seconds.

d. Decrease surface temperature to ambient over a period of 600 seconds.

e. Allow panel to cool.

f. Inspect insulation and record any changes.

g. Increase surface temperature to 1700°F over a period of 500 seconds.

h. Maintain 1700°F surface temperature for 1400 seconds.

i. Decrease LI-1500 surface temperature to ambient over a period of 1000 seconds.

j. Allow panel to cool.

k. Inspect insulation and record any changes.

l. Follow the surface temperature pulse shown in Figure 7.

m. Allow panel to cool.

n. Inspect insulation and record any changes.

The bondline temperature will be limited to 250°F during all radiant heat tests. All thermocouple, strain gage and axial load data will be recorded during the radiant heat tests.

2.3.2.3 Combined Loading and Heating Test

a. Apply radiant heat to LI-1500 surface to obtain the temperature history shown in Figure 7.

b. Gradually apply load to panel to obtain an axial load of 50,400 lb at 45 minutes from start of temperature pulse.

c. Maintain 50,400 lb axial load for 10 minutes.

d. Increase load to 97,200 lb over a 30 second period.

e. Maintain 97,200 lb load for 1 minute.

f. Decrease load to 50,400 lb over a 30 second period.

g. At 60 minutes from start of temperature pulse, increase load to 144,000 lb over a 30 second period.

h. Maintain 144,000 lb load for 1 minute.

i. Reduce load to 1000 lb over 1 minute period.

j. Allow panel to cool.

k. Inspect panel and record any changes. All thermocouple, strain gage and axial load data will be recorded during these tests.

2.3.2.4 Acoustic Test

a. Expose test panel to the spectrum shown in Figure 8 for a 15 second period.

b. Inspect panel after test and record any changes.

The same instrumentation and data analysis is required as specified in Section 2.3.1.4 for the fuselage panel tests.

Upon completion of the above environmental tests, the fuselage test panels will then be subjected to the following sequence and combination of environmental tests:

2.3.2.5 Combined Environmental Tests

a. Apply radiant heat to LI-1500 surface to obtain the temperature history shown in Figure 7.

b. Gradually apply load to panel to obtain an axial load of 50,400 lb at 45 minutes from start of temperature pulse.

c. Maintain 50,400 lb axial load for 10 minutes.

d. Increase load to 97,200 lb over a 30 second period.

e. Maintain 97,200 lb load for 1 minute.

f. Decrease load to 50,400 lb over a 30 second period.

g. At 60 minutes from start of temperature pulse, increase load to 144,000 lb over a 30 second period.

h. Maintain 144,000 lb load for 1 minute.

i. Reduce load to 1000 lb over a 1 minute period.

j. Allow panel to cool.

k. Inspect panel and record any changes.

l. Repeat a through k four times.

All thermocouples, strain gages, and axial load data will be recorded during the tests until maximum bondline and aluminum panel temperatures are obtained.

m. Expose test panel to the spectrum shown in Figure 8 for a 75 second period.

n. Inspect panel after test and record any changes.

The same instrumentation and data analysis is required as specified in Section 2.3.1.4 for the fuselage panel tests.

o. Repeat a through k above 10 times.

p. Repeat m and n above except increase test duration to 150 seconds.

q. Repeat o (preceding).

r. Repeat p (preceding).

s. Place test panel in vacuum chamber.

t. Pump chamber down to a vacuum of at least $10^{-5}$ Torr.

u. Decrease test panel temperature to $-150^{\circ}F$.

v. Allow test panel temperature to increase to ambient level.

w. Increase chamber pressure to ambient level.

x. Remove panel from chamber, perform visual inspection of LI-1500 and beryllium panel and record any changes.

y. Repeat a through x three times.

2.3.3 Aluminum Panel - Area 1

Repeat the same test series as described in Section 2.3.2 except for the following changes:

2.3.2.2 1. Apply radiant heat to LI-1500 surface to obtain the temperature history shown in Figure 9.

2.3.2.3 a. Apply radiant heat to LI-1500 surface to obtain the temperature history shown in Figure 9.

b. Gradually apply load to panel to obtain an axial load of 57,600 lb at 45 minutes from start of temperature pulse.

c. Maintain 57,600 lb axial load for 15 minutes.

d. Increase load to 144,000 lb over a 30 second period.

e. Maintain 144,000 lb load for 1 minute.

f. Omit

g. Omit

2.3.2.5 a through g same as above

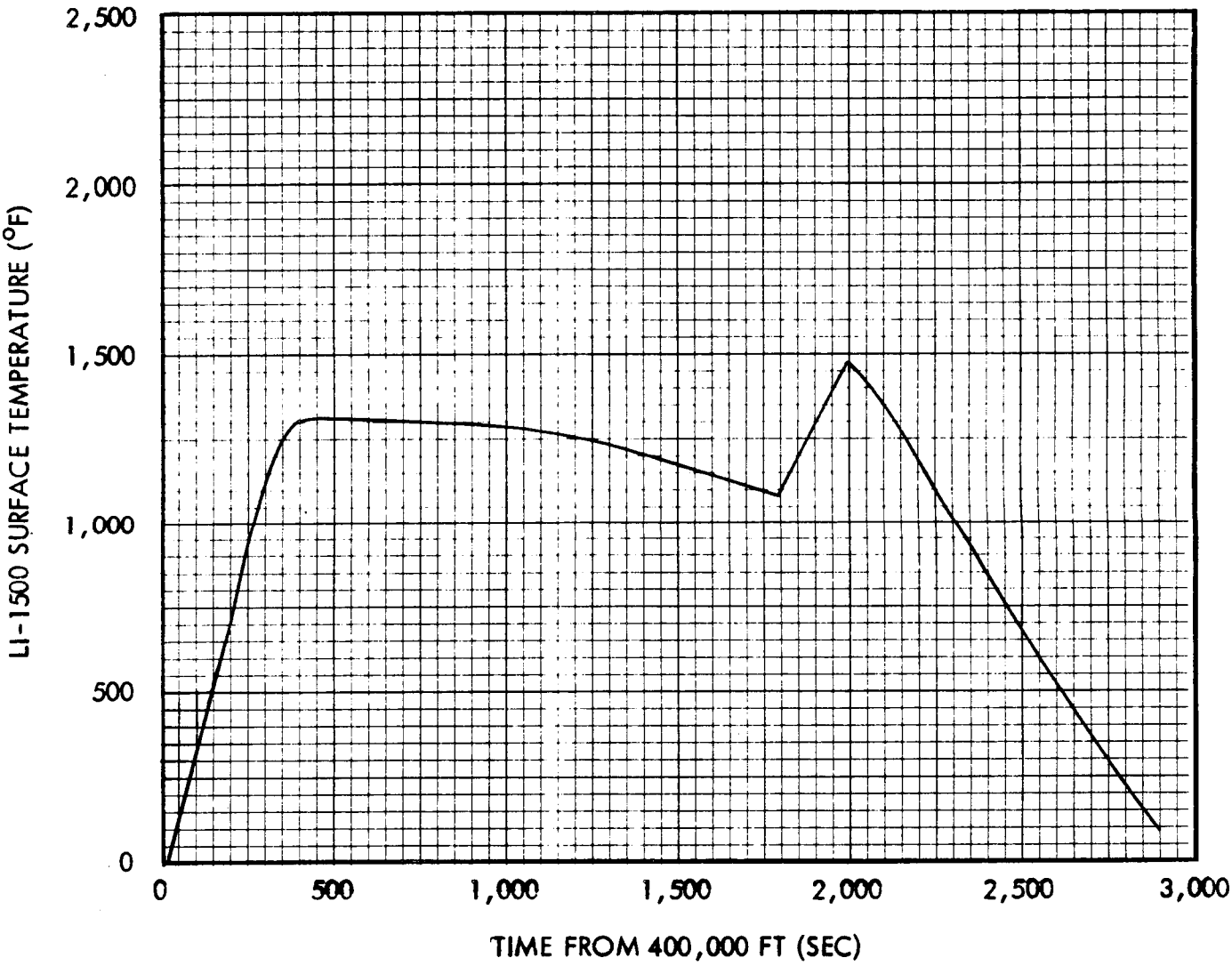


**Fig. 9 Test Temperature Profile - Area 1**

### 2.3.4 Titanium Panel - Area 2

Repeat the same test series as described in Section 2.3.2. The bondline temperature will be limited to 600°F during all radiant heat tests.

## REFERENCES

1. Grimaud, John E. and Murray, Bud, "Environmental Test Plan for Surface Insulation TPS Wing and Fuselage Panels Developed by Lockheed Missiles and Space Co. and McDonnell-Douglas Astronautics Co. Under Contracts NAS9-11222 and NAS9-11221," 17 May 1971
2. Tillian, Donald J., "Point Design Requirements for Two Orbiter TPS Design Areas - Reusable Surface Insulation TPS Development, Phase 2," 7 July 1971

# Appendix G

# NON-DESTRUCTIVE EVALUATION OF LI-1500

# INTERIM STATUS REPORT ON

# PRODUCT ASSURANCE TASKS OF LI-1500 ID PROGRAM

Non-destructive evaluation (NDE) was performed on emissivity coated LI-1500 samples fabricated into the 3-step shape as shown in Figure No. 1. LI-1500 samples, unbonded as well as samples adhesive bonded to a metallic substrate, were examined by various NDE techniques. The two objectives of this NDE of LI-1500 were as follows:

(1) Improvement of the color densitometer method of evaluating X-ray radiographs to determine density variations as well as abnormalities (i.e. cracks, voids, and inclusions) in LI-1500,

(2) Development of NDT methods of detecting causes for catastrophic failure of LI-1500 (i.e. cracks and unbonded areas) by examination of the material from the emissivity coated surface.

## (1) NDE and Process Control of LI-1500 by Color Densitometer Evaluation of X-Ray Radiographs

An X-ray radiograph was made of a series of five LI-1500 blocks, each 3/4" X 3/4" cross sectional area by 2" thick. These blocks of LI-1500 were fabricated for use as physical density standards. The identification of the LI-1500 panels from which each block was obtained, as well as the physical density calculated from weight and micrometer measurements of the standards are as follows:

| LI-1500 PANEL NO. | CALCULATED PHYSICAL DENSITY OF 3/4" X 3/4" X 2" LI-1500 BLOCK |
|---|---|
| 314 | 16.9 lbs/ft.$^3$ |
| 310 | 13.8 lbs/ft.$^3$ |
| 822 | 13.5 lbs/ft.$^3$ |
| 313 | 10.1 lbs/ft.$^3$ |
| 209 | 7.3 lbs/ft.$^3$ |

The radiograph of the five density standards was color enhanced on a Spatial Data Systems, Inc. color densitometer. A correlation was obtained between the physical density of each standard and the color of the standard, as determined by the intensity of grayness in the X-ray radiograph. Evaluation of the radiograph for each density standard indicated that between two and five shades of gray existed for each standard's radiograph. Each shade of gray was reproduced on the color densitometer as a separate color, whose area could be measured by a planimeter. Each color was identified by a numbered switch which could be used to cancel the color from the density standard's radiograph. The area weighted color of each standard's radiograph, as identified by the weighed numbered switches which cancelled all color from the radiograph, was calculated. A correlation was found to exist between the physical density of the standard and the weighted numbered switches (i.e. weighted numbered Data Color black out keys) required to cancel all color from

the standard's radiograph. The mathematical equation for this relationship is

$$K = b\rho^{m} \quad \text{or} \quad \rho = \left(\frac{K}{b}\right)^{1/m}$$

Where:

K = value of the weighted Datacolor key required to cancel color from a given part of a radiograph

$\rho$ = physical density of the area of the color enhanced radiograph cancelled out by K

b = a constant value relating the color densitometer video camera apeture and subject to camera distance with the color analyzer "Set-Up" dial setting (i.e. the range of color covered from maximum density or yellow to minimum density or blue).

m = a constant value determined by the Bright Level and Dark Level dial setting of the color analyzer.

The values of b and m have to be determined from a minimum of two density standards X-rayed with the LI-1500 panel whose density is to be measured. The thickness of the density standards have to be the same as the part being X-rayed whose density is to be measured. This limitation is due to the basic concept of the mechanics of measuring physical density by X-ray techniques. The density of a material is defined as the weight of material/volume of material. An X-ray of LI-1500 at any given point will have varying shades of gray depending on the concentration of silica fiber, binder, and air at that point. The only volume dimension important to the X-ray at the given point is the material thickness. For an X-ray at the given point of LI-1500 being investigated the expression of Density = Weight/Volume becomes concentration of matter/thickness of the material. Upon establishing a constant thickness to the material being X-rayed the density varies with the concentration of matter at the point being examined. The concentration of matter as seen on the X-ray radiograph is shown by variation is shades of gray. It is these same shades of gray which are color enhanced .

Therefore, at any given thickness of material being X-rayed the following relationship exists:

Physical density = concentration of matter being X-rayed = variation of grayness in X-ray radiograph = color identified with each gray shade seen in the radiograph.

Voids introduced into the LI-1500 NDE samples as drill holes were detected in X-ray radiographs of the material. These voids were introduced into the LI-1500 as a set of three drill holes at each of three different locations. The three voids in each set were in the form of drill holes

0.0135" dia. X ½" long, 0.0380" dia. X 1" long and 0.0635" dia. X 1½" long. The drill hole diameters corresponds to Nos. 80, 62 and 52 drill bit diameters. As a result of this test it was determined that a void as small as 0.0380" dia. X 1" long separated from the radiograph by LI-1500 material 1 5/8" thick is detectable on the X-ray radiograph. The void is detectable only when the X-ray is made normal to the surface of the casting, i.e. X-rayed through the material thickness. Radiographs made normal to the thickness of the casting were unsuccessful in detecting voids as large as 0.0635" dia. X 1½" long through only 3/8" thickness of LI-1500 material separating the void and X-ray film.

## 2.0 Development of NDE Methods to Detect Cracks and Unbonded Areas in LI-1500 from Coated Side for Post Flight Inspection.

Several NDE methods were investigated in order to determine the most feasible method of detecting cracks and unbonded LI-1500 areas which could cause catastrophic failure. A second objective of this phase of the investigation was to determine an NDE method for measuring the moisture content of LI-1500. In all cases the NDE method had to be useful when examining the coated 3 step LI-1500 NDE sample adhesive bonded to a metal substrate from the coated side only. This limitation of one side NDE of LI-1500 immediately eliminated X-ray, and neutron radiography of the material. The following NDE methods were investigated for this phase of the program.

2.1 - Microwave
2.2 - Audible Sonic Ringing Test
2.3 - High and Low Frequency Ultrasonic
2.4 - Acoustic Emission Test
2.5 - Laser Holography
2.6 - Laser Vibrascope
2.7 - Infra Red Test (Conventional and Laser Heat Source)

### 2.1 Microwave NDE of LI-1500

Large unbonded areas (½" X 4") between the LI-1500 and metallic substrate were detected by using the reflection method and measuring phase shift at a frequency of 10 GHz. The following data was obtained by reflection of microwaves from the metallic substrate:

| SAMPLE NO. | SUBSTRATE & VOID | PHASE SHIFT AT LI-1500 THICKNESS OF 2" | 1" | ½" | $\alpha$ (ATTENUATION) FOR 2" LI-1500 THICKNESS |
|---|---|---|---|---|---|
| 823-8* | Aluminum with no void in RTV 560 | +175° | +67° | +23° | 13 db |
| 824-7 | Beryllium with ½" X 4" void in RTV 560 | +150° | +62° | +25° | 12 db |
| 823-7 | Titanium with void in RTV 560 | +163° | +56° | +21° | 12 db |

* Sample 823-8 with no void in RTV-560 used as reference standard.

Moisture in LI-1500 was readily detected by microwave reflection techniques at a frequency of 10 GHz on coated, unbonded, LI-1500 sample, no. 824-1. Following is the data on phase shift during microwave NDE due to the addition of water to each step of sample 824-1

| Volume of Water Applied to Step (ml.) | PHASE SHIFT AT LI-1500 STEP THICKNESS OF 1 7/8" | 1" | ½" |
|---|---|---|---|
| 0 | -85° | +74° | +45° |
| 0.25 | - | - | +52° |
| 0.50 | -43° | +15° | - |
| 0.75 | - | + 2° | - |

Other information detected from this microwave NDE of LI-1500 are as follows:

(a) The #0025 emissivity coating does not significantly influence microwave measurements of LI-1500.

(b) The dielectric constant of LI-1500 ($\epsilon r$ = 1.24) is too close to that of air ($\epsilon r$ = 1.00) to detect voids in the material by microwave methods.

## 2.2 Audible Sonic Ringing Test of LI-1500

A sonic test in the audible frequency range of 20 to 20,000 Hz (cycles/sec.) has been developed which shows promise of detecting large cracks in LI-1500. The LI-1500 material is tapped with a calibrated constant force between 5 and 10 gms. The ringing sound emitted by the material when tapped is detected by an

2.2 (Continued)

accelerometer (transducer) placed within ½" of the point where the LI-1500 is tapped. This sound is transmitted to a spectrum analyzer where it is analyzed into its pure frequencies which are in turn reproduced on an oscilloscope. LI-1500 characteristically shows peaks in the range of 2 to 3 KC/sec. LI-1500 with induced major cracks shows peaks in the frequencies exceeding 5 KC/sec.

2.3 High and Low Frequency Ultrasonic NDE of LI-1500

Both low frequency (25 KC/sec. to 1 MC/sec.) and high frequency (1 MC/sec. to 200 MC/sec.) ultrasonic NDE methods failed to detect cracks and voids in LI-1500 samples. Excessive scattering of the sonic wave in LI-1500 and the difficulty of coupling the transducer sensing element to the material make this NDE method unacceptable.

As part of a feasibility study performed for LMSC by Battelle Pacific Northwest Laboratories, Richland, Washington, it was found that the unipolar pulse ultrasonic method was unacceptable. The LI-1500 material is too dead for a signal to penetrate the material and be reflected back to the sensor.

2.4 Acoustic Emission NDE of LI-1500

A second part of the feasibility study performed by Battelle Pacific Northwest Laboratories was acoustic emission testing of LI-1500. LI-1500 samples bonded to a metallic substrate were thermally stressed and a signal was detected on the side opposite the coated side being stressed. Further investigation by Battelle to stress and detect the material's emission from the coated side only was discontinued at the request of the LI-1500 Program Manager's office for the following reasons:

(a) The amount of LI-1500 material requested by Battelle for test purposes is not currently available.

(b) The contract with Battelle for acoustic emission testing would extend into February 1972 or well past the cut-off date of the 1971 ID program.

This method does show promise of detecting cracks and voids in LI-1500.

2.5 Laser Holography NDE of LI-1500

Photos of the interference lines generated during laser holographic testing of LI-1500 were symmetrical. This indicates that

2.5 (Continued)

the flaws introduced into the LI-1500 NDE samples, i.e. lack of adhesive, drilled holes and steel pin, are not revealed by the interference pattern. Investigation of this NDE method is being discontinued.

2.6 Laser Vibrascope NDE of LI-1500

Work has just been commenced on this NDE method of examining LI-1500. No data is available at this time.

2.7 Infra-Red NDE of LI-1500

Infra-red NDE tests were performed on LI-1500 by heating the emissivity coated surface. Due to the low thermal conductivity of LI-1500, defects could not be located at a distance exceeding ½ inch below the surface. This result was determined during a feasibility test conducted by Barnes Engineering, Stamford, Conn., using quartz heating lamps.

Success was achieved in detecting cracks and adhesive voids in LI-1500 by infra red NDE techniques when the LI-1500 sample was heated from the metallic substrate surface. Unfortunately this surface is unavailable for examination if the RSI material is bonded directly to the shuttle.

CONCLUSION:

At this point in the LI-1500 program the following NDE techniques have been proved successful:

(1) In-process control and final inspection of LI-1500 prior to assembling on the vehicle by color densitometer enhanced X-ray radiographs. Physical density, voids and inclusions can be detected by this technique.

(2) Detection of moisture in LI-1500 and unbonded adhesive areas at the RSI/metallic interface by microwave one side NDE techniques as developed by M. H. Jacoby, O/84-35.

(3) Detection of catastrophic cracks in LI-1500 and unbonded areas at the RSI/metallic interface by the audible sonic ringing test one side NDE method as developed by R. F. Walton and R. W. Pfeil, O/75-74.

R. F. Walton
11/9/71

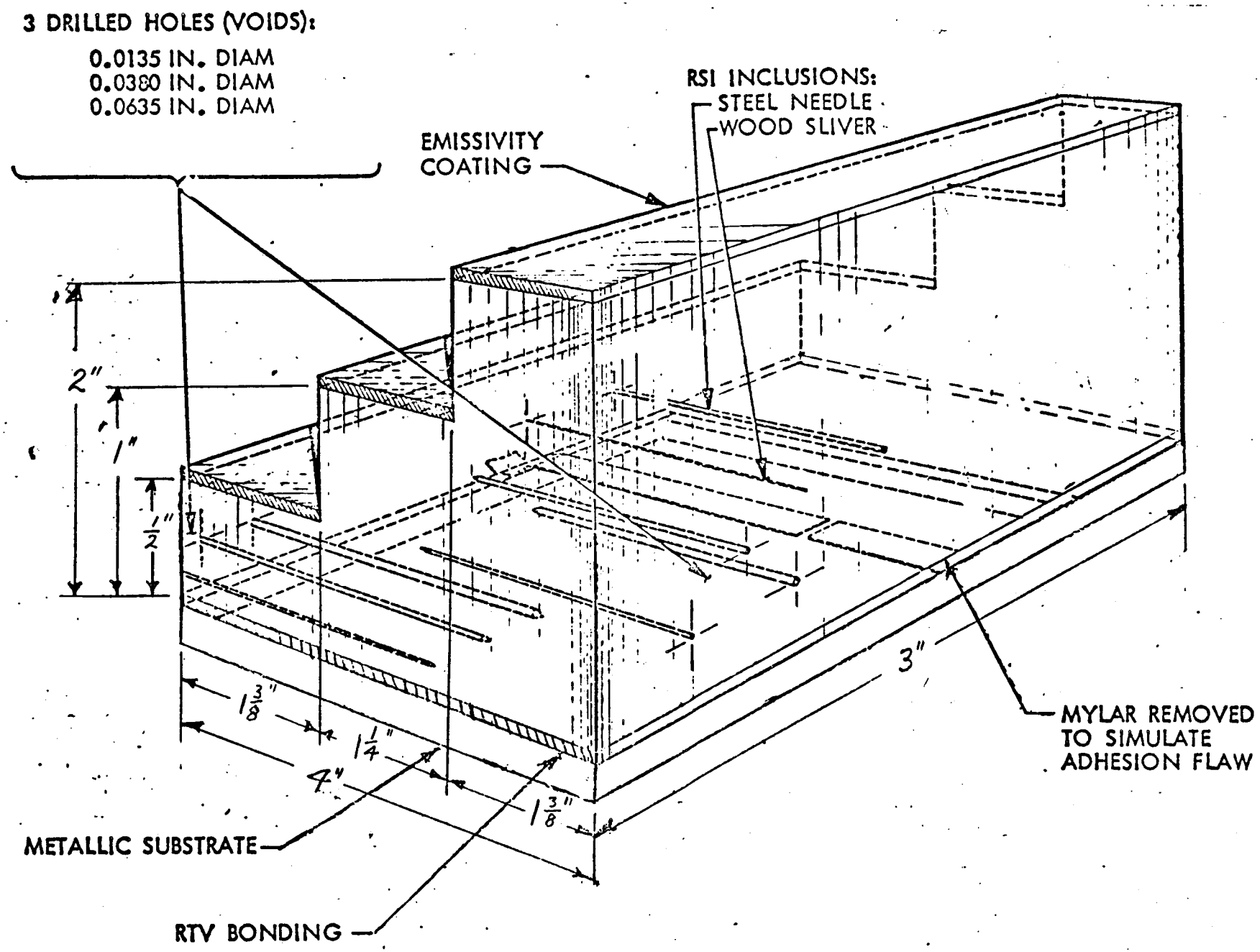
3 DRILLED HOLES (VOIDS):
0.0135 IN. DIAM
0.0380 IN. DIAM
0.0635 IN. DIAM
EMISSIVITY COATING
RSI INCLUSIONS:
STEEL NEEDLE
WOOD SLIVER
2"
1"
1/2"
1 3/8"
1 1/4"
4"
1 3/8"
3"
MYLAR REMOVED TO SIMULATE ADHESION FLAW
METALLIC SUBSTRATE
RTV BONDING

FIG. NO. 1